4.2.4.1 Member of the Public Exposure Pathways

The pathways for MOP release to be used in the PA analyses are presented in Table 4.2-38 and discussed below. Table 4.2-38 also indicates whether detailed dose calculations are included as part of the PA. The scenarios are not assumed to occur until after the 100-year institutional control period ends, during which no active FTF facility maintenance will be conducted. The consumption rates and bioaccumulation factors that are used in conjunction with the pathways are discussed in detail in Section 4.6.

- **Scenario with Well Water as Primary Water Source**

The primary water sources for the MOP release pathways are either a well drilled into the groundwater aquifers or from a GSA stream.

In the groundwater well dose analysis, doses are calculated using water from a well for domestic purposes. The following exposure pathways involving the use of contaminated well water are assumed to occur as presented in Table 4.2-38 and Figure 4.2-27.

- Direct ingestion of well water
- Ingestion of milk and meat from livestock (e.g., dairy and beef cattle) that drink well water
- Ingestion of vegetables grown in garden soil irrigated with well water
- Ingestion of milk and meat from livestock (e.g., dairy and beef cattle) that eat fodder from pasture irrigated with well water
- Ingestion and inhalation of well water while showering

The following exposure pathways involving the use of contaminated surface water (from the applicable stream) for recreational use are assumed to occur:

- Direct irradiation during recreational activities (e.g., swimming, fishing) from stream water
- Dermal contact with stream water during recreational activities (e.g., swimming, fishing)
- Incidental ingestion and inhalation of stream water during recreational activities
- Ingestion of fish from the stream water

Additional exposure pathways could involve releases of radionuclides into the air from the water taken from the well (i.e., volatile radionuclides such as H-3, C-14, I-129). Exposures from the air pathway in this PA:

- Direct plume shine
- Inhalation

There are other secondary and indirect pathways that contribute relatively minor doses to a receptor when compared to direct pathways such as ingestion of milk and meat. These pathways include:

- Inhalation of well water used for irrigation
- Inhalation of dust from the soil that was irrigated with well water
- Ingestion of soil that was irrigated with well water
- Direct radiation exposure from radionuclides deposited on the soil that was irrigated with well water

Figure 4.2-27: Scenario With Well Water As Primary Water Source

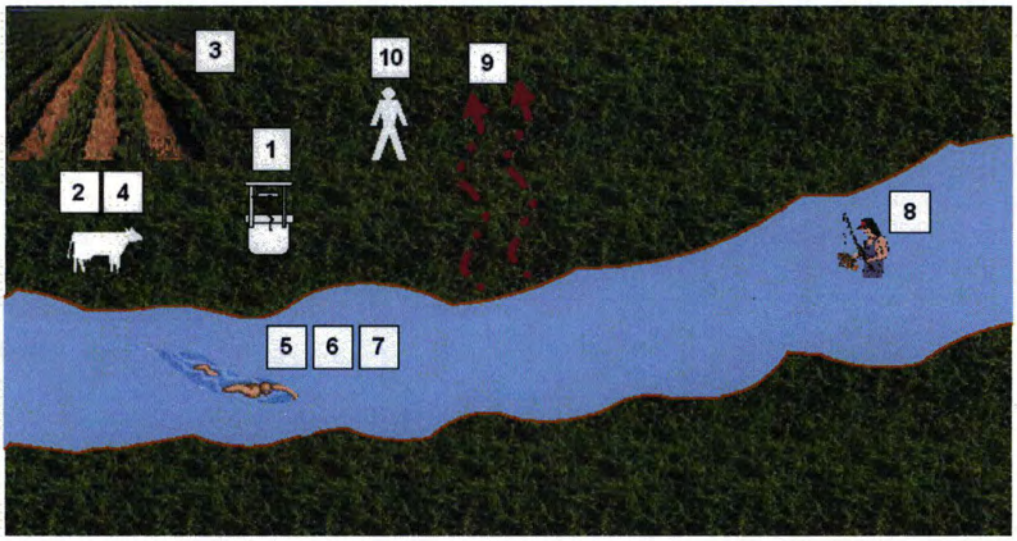

SCENARIO WITH WELL WATER AS PRIMARY WATER SOURCE

1. **Direct ingestion of well water**
2. **Ingestion of milk and meat from livestock (e.g., dairy and beef cattle) that drink well water**
3. **Ingestion of vegetables grown in garden soil irrigated with well water**
4. **Ingestion of milk and meat from livestock (e.g., dairy and beef cattle) that eat fodder from pasture irrigated with well water**
5. **Direct irradiation during recreational activities (e.g., swimming, fishing) from stream water**
6. **Dermal contact with stream water during recreational activities (e.g., swimming, fishing)**
7. **Incidental ingestion and inhalation of stream water during recreational activities**
8. **Ingestion of fish from the stream water**
9. **Direct plume shine**
10. **Inhalation**

➢ **Scenario with Stream Water as Primary Water Source**

In the stream dose analyses, doses are calculated using water from the closest stream (Fourmile Branch or UTR) for domestic and recreational purposes. The following exposure pathways involving the use of surface water (from the applicable stream) are assumed to occur as presented in Table 4.2-38 and Figure 4.2-28.

- Direct ingestion of stream water
- Ingestion of milk and meat from livestock (e.g., dairy and beef cattle) that drink stream water
- Ingestion of vegetables grown in garden soil irrigated with stream water
- Ingestion of milk and meat from livestock (e.g., dairy and beef cattle) that eat fodder from pasture irrigated with stream water
- Ingestion and inhalation of stream water while showering

The following exposure pathways involving the use of contaminated surface water (from the applicable stream) for recreational use are assumed to occur:

- Direct irradiation during recreational activities (e.g., swimming, fishing) from stream water
- Dermal contact with stream water during recreational activities (e.g., swimming, fishing)
- Incidental ingestion and inhalation of stream water during recreational activities
- Ingestion of fish from the stream water

Additional exposure pathways could involve releases of radionuclides into the air from the water taken from the stream (i.e., volatile radionuclides such as H-3, C-14, I-129). Exposures from the air pathway in this PA:

- Direct plume shine
- Inhalation

There are other secondary and indirect pathways that contribute relatively minor doses to a receptor when compared to direct pathways such as ingestion of milk and meat. These pathways include:

- Inhalation of stream water used for irrigation
- Inhalation of dust from the soil that was irrigated with stream water
- Inhalation of gaseous radionuclides released from the soil that was irrigated with stream water
- Ingestion of soil that was irrigated with stream water
- Direct radiation exposure from radionuclides deposited on the soil that was irrigated with stream water

Figure 4.2-28: Dose Analysis Using Stream Water As Primary Water Source Scenario

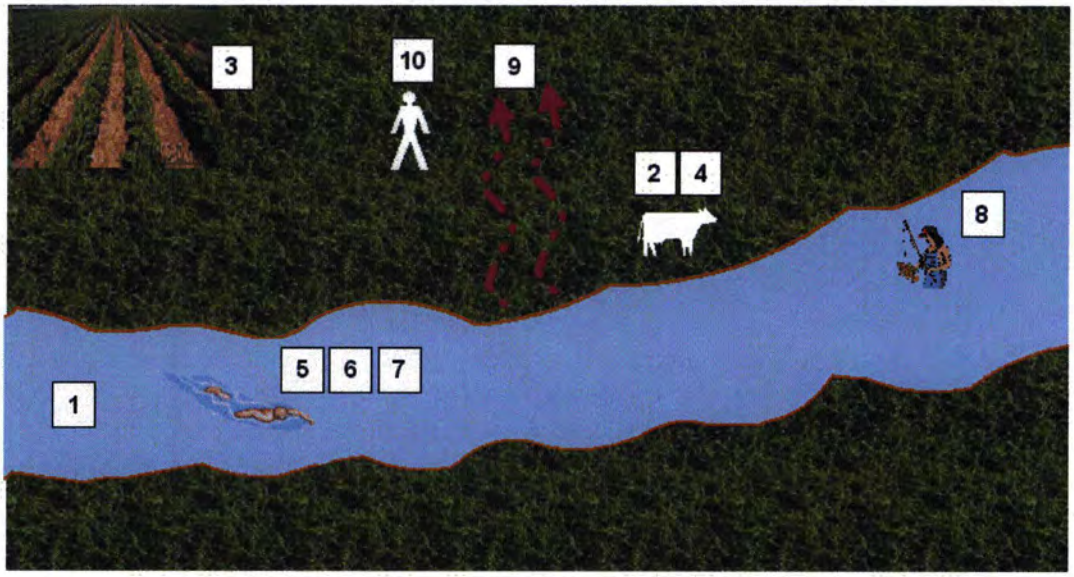

DOSE ANALYSES USING STREAM WATER AS PRIMARY WATER SOURCE

1. **Direct ingestion of water from stream**
2. **Ingestion of milk and meat from livestock (e.g., dairy and beef cattle) that drink stream water**
3. **Ingestion of vegetables grown in garden soil irrigated with stream water**
4. **Ingestion of milk and meat from livestock (e.g., dairy and beef cattle) that eat fodder from pasture irrigated with stream water**
5. **Direct irradiation during recreational activities (e.g., swimming, fishing) from stream water**
6. **Dermal contact with stream water during recreational activities (e.g., swimming, fishing)**
7. **Incidental ingestion and inhalation of stream water during recreational activities**
8. **Ingestion of fish from the stream water**
9. **Direct plume shine**
10. **Inhalation**

⇒ **Basis for Public Release Pathways**

Table 4.2-38 was prepared to provide a list the FTF exposure pathways identified as candidates for detailed analysis. The list of candidates was developed based on a review of SRS PA analyses and NRC documents. [CBU-PIT-2005-00146, NUREG-0782, NUREG-0945, NUREG-1573] Those activities at SRS that could bring humans in contact with stabilized contaminants (e.g., water use, hunting, fishing, recreational activities such a swimming and boating, habitation in dwellings, other unique activities that involve water use or ground disturbance) were considered (with emphasis on local practices), to ensure that any pathways unique to the SRS site were taken into account. The *SRS*

Ecology Environmental Information Document was used as a source of relevant environmental information and conditions at the SRS. [WSRC-TR-2005-00201] For example, the *SRS Ecology Environmental Information Document* was used to identify potential wild game available on site, potential bio-intrusion candidates (flora and fauna), and the potential for the presence of fish and/or shellfish in the creeks bordering the FTF.

Those potential pathways that had quantified analysis are denoted with an "X" for the various receptors. Quantified analysis was not performed for potential pathways denoted with an "O", based on the applicable justifications provided throughout this section. (Table 4.2-38) NUREG-1854 states that transport pathways may be excluded from PA if it can be demonstrated that either there is limited potential for radionuclides to be released into a particular pathway, or the pathway is not viable (e.g., water is not potable). Other pathways were marked as N/A due to the nature of the scenario making them impossible (e.g., a garden that receives 100% of its irrigation water from a well cannot also receive water from a stream).

⇒ **Inputs and Assumptions Related to the Public Release Pathways**

The following assumptions were made regarding the pathways related to the MOP resident scenario using water from a well or stream:

- The stabilized contaminants release mechanisms to the MOP are leaching of stabilized contaminants to the groundwater and volatilization of the stabilized contaminants to the surface. Well drilling is not a release mechanism, since any well drilling associated with the MOP scenarios will be outside the FTF buffer zone, and therefore will not disturb the stabilized contaminants.
- Bio-intrusion and/or erosion are not considered credible mechanisms for significant stabilized contaminant disturbance based on the depth and form of the stabilized contaminant. The stabilized contaminants will be significantly below ground, from at least 10 feet for ancillary equipment to approximately 40 feet for stabilized contaminant tank heels. The stabilized contaminant is contained within stainless steel or carbon steel equipment and will be stabilized and/or grouted as part of tank closure. No mechanism was identified that would result in stabilized contaminant disturbance and dispersal such that the dose to the MOP (outside the FTF buffer zone) would be impacted.
- In the well water as primary water source scenario, well water will be used as a primary potable water source for a residence near the well (e.g., drinking water, showering) and will be used by the resident as a primary water source for agriculture (e.g., irrigation, livestock water).

- In the MOP near a stream scenario, stream water will be used as a primary potable water source for a residence near the stream (e.g., drinking water, showering) and will be used by the resident as a primary water source for agriculture (e.g., irrigation, livestock water).
- In both MOP scenarios, the resident (near the well and/or near a stream) can use a stream for recreational activities (e.g., swimming, fishing).
- Any wild game ingested (deer, wild pigs) would merely offset ingested livestock, and would result in a lower total dose since the livestock raised near FTF would be more affected by FTF stabilized contaminants than transient wild game.
- There are two creeks (UTR and Fourmile Branch) from which ingestion of marine life with significant contamination is possible. These creeks were conservatively assumed to be a source of dietary fish, but shellfish was excluded because UTR and Fourmile Branch are not significant sources of edible shellfish and shellfish play an insignificant role in local diets in relation to other ingested contributors to dose such as livestock, milk, and vegetables (local invertebrate consumption is a total of 2 kg/year). [WSRC-TR-2005-00201, WSRC-STI-2007-00004]
- Since there is no substantive water source readily available at the well site, pathways related to water-related commercial activities were not considered. Based on the relative proximate of a large, natural water source (i.e., the Savannah River), it is not assumed that a man-made body of water would be created at the MOP resident site.
- The dose associated with dermal absorption of radionuclides is considered insignificant because, unlike some chemicals, radionuclides are generally adsorbed into the body very poorly.
- The quantities of water ingested during the relatively short activities of showering (10 min/day) and swimming (8.9 hr/year) are negligibly small and are not addressed independently. The impact of these activities is addressed by the "direct ingestion of well water" pathway (i.e., they are included in the 337 liters of water that is assumed to be ingested every year). [WSRC-STI-2007-00004]

4.2.4.2 Intruder Exposure Pathways

The stabilized contaminant materials after FTF closure will be primarily located in areas protected by significant materials (e.g., grouted waste tanks, DB cell covers and valve box shielding) which are clearly distinguishable from the surrounding soil and make drilling not a practical scenario based on regional drilling practices. Regional drilling conditions are such that a barrier such as the closure cap erosion barrier, tank top, or grout fill are situations that would cause drillers to stop operations and move drilling location. The most vulnerable location for stabilized contaminants is in a transfer line which may be near grade-level prior to closure and are of a small size (typically 3 inch diameter or less) which makes them the most credible stabilized contaminants hit during any intruder drilling operations even though the probability of hitting a transfer line is small due to the small surface area of transfer lines

versus to large FTF footprint. Because 82% of the transfer line length is 3 inch diameter, and only 0.24% is 4 inch diameter and the remainder less than 3 inch diameter, the analysis is performed on 3 inch lines.

The dose pathways for an inadvertent intruder are presented in Table 4.2-39 and discussed below. Table 4.2-39 also indicates whether detailed dose calculations are required. The intruder release scenarios are not assumed to occur until after the 100-year institutional control period ends, during which no active FTF facility maintenance will be conducted.

This scenario is considered conservative because the stainless steel transfer lines maintain their integrity for several hundred years as noted in Section 4.2.3.2.5.

4.2.4.2.1 Intruder Release Scenarios

The consumption rates and bioaccumulation factors that are used in conjunction with the Table 4.2-39 proposed pathways are discussed in detail in Section 4.6.

In order to calculate the dose to an inadvertent intruder, the following intruder scenarios were considered:

- Acute Intruder-Drilling Scenario
- Acute Intruder-Construction Scenario
- Acute Intruder-Discovery Scenario
- Chronic Intruder Agricultural (Post-Drilling) Scenario
- Chronic Intruder-Resident Scenario
- Chronic Intruder-Recreational Hunting Fishing Scenario
- Bio-intrusion Scenario

4.2.4.2.2 Acute Intruder-Drilling Scenario

In this scenario, it is assumed that after the end of active institutional controls, a well is drilled into the waste disposal system. The well is assumed to be used for domestic water use and irrigation. Since no other natural resources have been identified in the FTF, no additional drilling scenarios are considered. In a drilling scenario, an acute intruder is assumed to be the person or persons who install the well and are exposed to drill cuttings during well installation.

The drilling borehole is assumed to penetrate the waste disposal site. This scenario involves stabilized contaminants below the depth of typical construction excavations. The acute drilling scenario assumes that an inadvertent intruder drills a well into a transfer line, but not into a waste tank. Although the probability of hitting a transfer line within the area may be small, it is assumed that this occurs for the drilling scenario. The intruder is exposed to contaminated drill cuttings spread over the ground and contaminated airborne dust.

Exposure of a resident or farmer to drill cuttings left on the land surface after the installation of a well was considered under the intruder-resident scenario or intruder-agricultural scenarios.

The exposure pathways for this acute drilling scenario include (Figure 4.2-29):

- Inhalation of resuspended drill cuttings
- External exposure to the drill cuttings
- Inadvertent drill cuttings ingestion

Figure 4.2-29: Acute Intruder Drilling Scenario

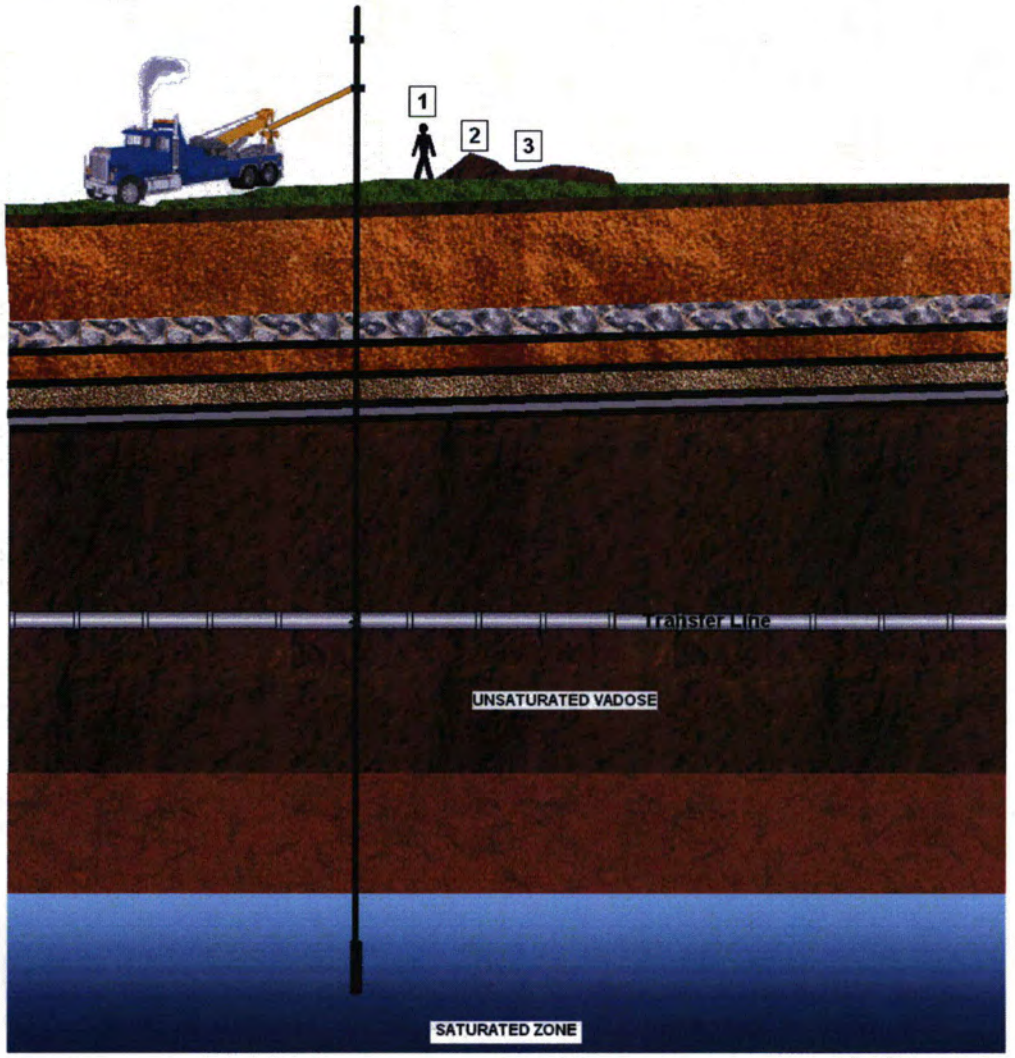

4.2.4.2.3 Acute Intruder-Construction Scenario

In this scenario, it is assumed that after the end of active institutional controls, a construction project begins at the site with associated earthmoving activities. The intruder-construction scenario involves an inadvertent intruder who chooses to excavate or construct a building on the disposal site. The intruder is assumed to dig a basement excavation to a depth of approximately 10 feet. It is assumed that the intruder does not recognize the hazardous nature of the material excavated. During the excavation of the basement, the intruder is exposed to the exhumed stabilized contaminants by inhalation of resuspended contaminated soil and external irradiation from contaminated soil. Due to the disposal depth of the stabilized contaminants in the waste tanks and in ancillary equipment (from at least 10 feet up to approximately 40 feet below the FTF closure cap), the intruder-construction scenario is not considered applicable.

4.2.4.2.4 Acute Intruder-Discovery Scenario

The intruder-discovery scenario is conceptualized as a modification of the intruder-construction scenario. The basis for the intruder-discovery scenario is the same as the intruder-construction scenario except that the exposure time is reduced. The scenario involves the intruder excavating a basement to a depth of approximately 10 feet. The intruder is assumed to recognize that he or she is digging into very unusual soil immediately upon encountering the tank/piping system and leaves the site. Consequently, the exposure time is reduced. Similar to the intruder-construction scenario, the intruder-discovery scenario was not considered for further analysis due to the disposal depth of the stabilized contaminants in the tanks and in ancillary equipment (from at least 10 feet up to approximately 40 feet below the FTF closure cap).

4.2.4.2.5 Chronic Intruder-Agricultural (Post-Drilling) Scenario

In this scenario, it is assumed that after the end of active institutional controls, a farmer lives on, and consumes food crops grown and animals raised on the disposal area. The chronic intruder agriculture (i.e., post-drilling) scenario is an extension of the acute intruder drilling scenario. It is assumed in this scenario that an intruder lives in a building near the well drilled as part of the intruder-drilling scenario and engages in agricultural activities on the contaminated site. Excavation to the surface of the stabilized contaminants in the waste tanks was not considered credible due to its depth of more than 40 feet below the closure cap. Therefore, the intruder-agriculture scenario was retained for the ancillary equipment inventory and specifically a waste transfer line because it is less protected than a DB, valve box or PP which are shielded with thick shield covers of several feet of concrete. The soil used for agricultural purposes is assumed to be contaminated by both drill cuttings and irrigation well water.

The intruder is exposed to (Figure 4.2-30):

- Direct ingestion of well water
- Ingestion and inhalation of well water while showering
- Ingestion of milk and meat from livestock (e.g., dairy and beef cattle) that drink well water
- Ingestion of vegetables grown in garden soil irrigated with well water and containing contaminated drill cuttings
- Ingestion of milk and meat from livestock (e.g., dairy and beef cattle) that eat fodder from pasture irrigated with well water
- Inhalation of well water used for irrigation
- Inhalation of dust from the soil that was irrigated with well water
- Ingestion of soil that was irrigated with well water
- Direct radiation exposure from radionuclides deposited on the soil that was irrigated with well water

The intruder may also be exposed to a release of volatile radionuclides (e.g., H-3, C-14, I-129) from the drill cuttings and contaminated well water. These pathways include:

- Direct plume shine
- Inhalation

Figure 4.2-30: Chronic Intruder Agricultural (Post-Drilling) Scenario

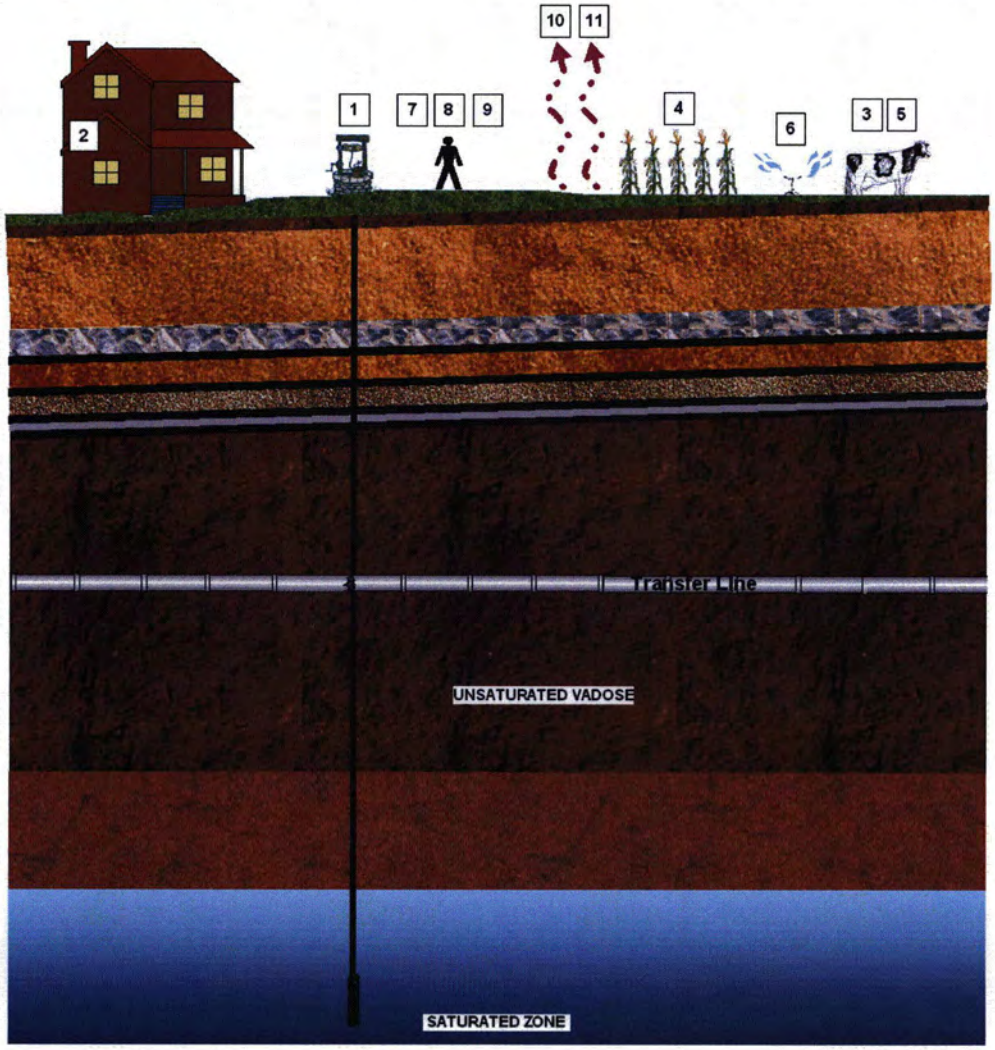

[NOT TO SCALE]

CHRONIC INTRUDER-AGRICULTURAL (POST-DRILLING) SCENARIO

1. Direct ingestion of well water
2. Ingestion and inhalation of well water while showering
3. Ingestion of milk and meat from livestock (e.g., dairy and beef cattle) that drink well water
4. Ingestion of vegetables grown in garden soil irrigated with well water and containing drill cuttings
5. Ingestion of milk and meat from livestock (e.g., dairy and beef cattle) that eat fodder from pasture irrigate with well water and containing drill cuttings
6. Inhalation of well water used for irrigation
7. Inhalation of dust from the soil that was irrigated with well water
8. Ingestion of soil that was irrigated with well water
9. Direct radiation exposure from radionuclides deposited on the soil that was irrigated with well water
10. Direct plume shine
11. Inhalation

4.2.4.2.6 Chronic Intruder-Resident Scenario

In this scenario, it is assumed that after the end of active institutional controls, an intruder (i.e., the resident intruder) inadvertently constructs a house at, and lives on, the waste disposal area. The intruder-resident scenario involves the same pathways as the chronic intruder agriculture (i.e., post-drilling) scenario, with the potential for additional pathways associated with a house constructed over stabilized contaminants. The pathways uniquely associated with construction of a residence over stabilized contaminants were considered insignificant because of the depth of the stabilized contaminants under the closure cap and the shielding provided by the waste tank and ancillary equipment containment shielding. This shielding would reduce the external dose rates to very low levels. Therefore, the intruder- resident scenario will be addressed by the chronic intruder agriculture scenario and does not require unique analysis.

4.2.4.2.7 Chronic Intruder-Recreational Hunting/Fishing Scenario

In this scenario, a hunter/fisher is assumed to inadvertently visit the site, perhaps on a periodic basis, and consumes game and fish taken from the site. Given the significant exposure pathways the inadvertent intruder is considered to experience as part of the intruder agriculture scenario (e.g., use of well water as potable water, ingestion of livestock and vegetables raised using well water. The intruder-recreational scenario is bounded by the chronic intruder agriculture scenario and does not require unique analysis.

4.2.4.2.8 Bio-intrusion Scenario

The bio-intrusion scenario assumes that an intruder moves onto the site but does not excavate into the stabilized contaminants. Rather, radioactivity is brought to the surface by plants through root uptake and by burrowing animals. Bio-intrusion is not considered a credible mechanism for significant stabilized contaminant disturbance, based on the stabilized contaminant depth and form. The stabilized contaminants will be significantly below ground, from at least 10 feet for ancillary equipment to approximately 40 feet for stabilized contaminant tank heels. The stabilized contaminant is contained within closed waste tanks or stainless steel or carbon steel equipment and will be stabilized and/or grouted as part of tank closure. Of the likely burrowing animal residents at SRS, only one burrower, the Florida Harvester Ant, is expected to burrow below 2m, and then, only 5% of its burrows are expected to be that deep. [WSRC-RP-92-1360] Assuming the FTF cover reverts to pine forest in the future, the pine trees could also pose a bio-intrusion risk, with a mature pine having roots from 6 to 12 feet deep. [WSRC-TR-2003-00436] These bio-intrusion depths are not deep enough to reach the principal FTF stabilized contaminant inventory at closure (stabilized contaminant tank heels), and are unlikely to reach any ancillary equipment inventory, which in almost all cases will be more than 12 feet deep. Even if a pine tree root were to reach the ancillary equipment containment, no significant stabilized contaminant dispersal would be anticipated. The amount of contamination excavated from animal burrows or vegetative intrusion is far less than that involved in the agricultural (intruder-drilling) scenarios for drilling a domestic well into the underlying aquifers, therefore, this scenario is bounded by the intruder-drilling scenario for piping due to the concentrated source term in the piping versus any soil

which could be exhumed by animals, and the bio-intrusion scenario does not require further analysis.

4.2.4.2.9 Chronic Intruder-Agricultural Scenario

Table 4.2-39 was prepared to provide a list of all the FTF exposure pathways identified as candidates for detailed analysis. The list of candidates was developed based on a review of SRS PA analyses and NRC documents. [CBU-PIT-2005-00146, NUREG-0782, NUREG-0945, NUREG-1573] Those human activities at SRS that could bring humans in contact with stabilized contaminants (e.g., water use, hunting, fishing, recreational activities such a swimming and boating, habitation in dwellings, other unique activities that involve water use or ground disturbance) were considered (with emphasis on local practices), to ensure that any pathways unique to the SRS site were taken into account. Those potential pathways that had quantitative analysis are denoted with an "X" for the various receptors. Quantitative analysis was not performed for potential pathways denoted with an "O", based on the applicable justifications provided throughout this section. NUREG-1854 states that transport pathways may be excluded from performance analysis if it can be demonstrated that either there is limited potential for radionuclides to be released into a particular pathway, or the pathway is not viable (e.g., water is not potable). Other pathways were excluded due to the nature of the scenario making them impossible (e.g., a garden that receives 100% of its irrigation water from a well can't also receive water from a stream).

The following assumptions were made regarding the pathways related to the intruder scenario using water from a well or stream.

⇒ **Inputs and Assumptions Related to the Intruder Release Pathways**

- The stabilized contaminant release mechanisms to the intruder are well drilling into ancillary equipment, leaching of stabilized contaminants to the groundwater, and volatilization of the stabilized contaminants to the surface. Well drilling into a waste tank is not considered a credible release mechanism, since local practices would cause a well driller to choose a new location before the stabilized contaminant waste tank inventory was disturbed. The local well drillers expect to reach good drinking water aquifers at no more than 150 to 200 feet while drilling through sandy soil (no drilling through high-strength geologic materials). A driller would not expend the effort and equipment damage required to drill through the concrete/grout/steel covering the stabilized contaminant waste tank inventory. Even if the driller did not realize that he had struck a waste tank, and simply thought he had merely hit a layer of high-strength geologic materials, local experience would tell him that moving the drill site a short distance would avoid the impediment. Similarly, well drilling through a transfer line is also unlikely, especially while the line maintains some structural integrity. Nevertheless, as a bounding case for the purposes of this exercise, it has been assumed that a well driller could drill through an intact transfer line immediately after the end of institutional control.

- Well water will be used by the inadvertent intruder as a primary potable water source (e.g., drinking water, showering) and is used as a primary water source for agriculture (e.g., irrigation, livestock water).
- The inadvertent intruder can use a nearby stream for recreational activities (e.g., swimming, fishing).
- Any wild game ingested (deer, wild pigs) would merely offset ingested livestock, and would result in a lower total dose since the livestock raised near FTF would be more affected by FTF stabilized contaminants than transient wild game.
- There are two creeks (UTR and Fourmile Branch) from which ingestion of marine life with significant contamination is possible. These creeks were conservatively assumed to be a source of dietary fish, but shellfish were excluded because UTR and Fourmile Branch are not significant sources of edible shellfish and shellfish play an insignificant role in local diets in relation to other ingested contributors to dose such as livestock, milk, and vegetables. [WSRC-TR-2005-00201, WSRC-STI-2007-00004]
- Since there is no substantive water source readily available at the well site, pathways related to water-related commercial activities were not considered. Based on the relative proximate of a large, natural water source (i.e., the Savannah River), it is not assumed that a man-made body of water would be created at the MOP resident site.
- The showering inhalation and fish ingestion doses were not explicitly included in the intruder dose. These doses were calculated as part of the MOP pathways and their impact on the intruder peak dose is insignificant in comparison to the drill cutting contribution.
- The quantities of water ingested during the relatively short activities of showering (10 min/day) and swimming (8.9 hr/year) are negligibly small and are not be addressed independently. The impact of these activities is addressed by the "direct ingestion of well water" pathway (i.e., they are included in the 337 liters of water that is assumed to be ingested every year). [WSRC-STI-2007-00004]
- The dose associated with dermal absorption of radionuclides is insignificant because, unlike some chemicals, radionuclides are generally adsorbed into the body very poorly. Tritium is an exception to this rule, but tritium is found in such relatively small concentrations in the groundwater that it would not be a significant contributor to dose.

4.3 Modeling Codes

In the process of completing the PA for the FTF, a variety of modeling codes were utilized to perform various media transport, radiological dose and risk assessment calculations for compliance with 10 CFR 61 performance objectives and risk evaluations supporting CERCLA. [http://www.access.gpo.gov/uscode/title42/chapter103_.html] The purpose of this section is to present the modeling codes used and describe the modeling code integration. A brief description is provided for each modeling code, which includes the function of the code, available code manuals or technical documents for the applicable code revision, reasons for selection of the particular code and available QA documentation for the code. The results of the FTF PA will be used during the CERCLA closure process and complement any additional evaluations necessary using existing SGCP modeling methods for residual materials other than those in the waste tanks and ancillary equipment.

4.3.1 Modeling Codes Used

The HELP model is a quasi-two-dimensional water balance model designed to conduct landfill water balance analyses. The HELP model was used to generate water infiltration estimates through the final closure cap for use in PA calculations at the SRS. HELP model infiltration estimates form the input to subsequent flow and contaminant transport models.

4.3.1.1 Hydrologic Evaluation of Landfill Performance (HELP) Model

The HELP model requires the input of weather, soil and design data. It provides estimates of runoff, evapotranspiration, lateral drainage, vertical percolation (i.e., infiltration), hydraulic head and water storage for the evaluation of various landfill designs. United States Army Corps of Engineers (USACE) personnel at the Waterways Experiment Station (WES) in Vicksburg, Mississippi developed the HELP model, under an interagency agreement with the EPA. [EPA-600-R-94-168b] As such, the HELP model is an EPA sanctioned model for conducting landfill water balance analyses. HELP model version 3.07, issued on November 1, 1997, is the latest version of the model and was the version used for the FTF PA calculations. The HELP model was used at SRS during the development of calculations supporting the SPF and is the code used by SGCP during CERCLA closure evaluations. [http://www.access.gpo.gov/uscode/title42/chapter103_.html, CBU-PIT-2005-00146,] While other codes for closure cap infiltration calculations exist, the HELP model is a proven code that is appropriate for use at SRS. It is public domain software available from the WES website at: http://el.erdc.usace.army.mil/products.cfm?Topic=model&Type=landfill EPA and the USACE have provided the following documentation associated with the HELP model:

- A user's guide which provides instructions for HELP model use. [EPA-600-R-94-168a]

Engineering documentation provides information on the source language used to write the code, the hardware necessary to operate the code, data generation methodologies available for use, and the methods of solution. [EPA-600-R-94-168b]

HELP verification test reports exist which compare the model's drainage layer estimates to the results of large-scale physical models and comparing the model's water balance estimates to "field data from a total of 20 landfill cells at seven sites in the United States". [EPA-600-2-87-049, EPA-600-2-87-050]

The *Closure Cap Concept and Infiltration Estimates* report discusses eight water balance and infiltration studies that have been conducted in and around SRS by various organizations, including SRNL, USGS, State University of New York at Brockport, Pennsylvania State University, University of Arizona, and the Desert Research Institute. Findings from eight such studies are reported in Section 3.2.1 and summarized in Section 3.2.2 of the closure cap report. The summary shows that evapotranspiration dominates the water balance distribution of precipitation at the SRS. [WSRC-STI-2007-00184_OUO – Sections 3.2, 3.2.1, 3.2.2]

In summary, additional comparison studies to support HELP appropriateness in humid environments are not needed since the limitations of the software result in conservative infilatration estimates. An action to update the HELP code with more sophisticated software to further enhance PA modeling has been placed on the open items log in WSRC-STI-2007-00184_OUO.

SQAP for the HELP model version used for the FTF PA calculations is documented within Q-SQA-A-00005.

4.3.1.2 PORFLOW

PORFLOW is a commercial Computational Fluid Dynamics (CFD) tool developed by Analytic & Computational Research, Inc., website available at: http://www.acricfd.com/software/porflow/, PORFLOW numerically solves problems involving transient or steady state fluid flow, heat, salinity and mass transport in multi-phase, variably saturated, porous or fractured media with dynamic phase change. PORFLOW was used in FTF PA modeling to calculate fluid flow and contaminant transport in the vadose and saturated zones. PORFLOW transport results were utilized by subsequent modeling codes to calculate radiological doses and perform human health and ecological risk evaluations. PORFLOW flow results were also utilized by GoldSim to conduct contaminant transport via another computational tool. Another use of PORFLOW was to calculate vapor phase radionuclide diffusion to the ground surface from stabilized contaminants material for use in air transport calculations. Figures 4.3-1 and 4.3-2 illustrate the integration of PORFLOW in the modeling efforts and provides additional detail of the integration and steps of PORFLOW calculations for fluid flow and contaminant transport.

PORFLOW options include porous/fractured media may be anisotropic and heterogeneous, arbitrary sources (injection or pumping wells) may be present and, chemical reactions or radioactive decay may take place. PORFLOW accommodates alternate fluid and media property relations and complex and arbitrary boundary conditions. The geometry may be 2D or 3D, Cartesian or Cylindrical and the mesh may be structured or unstructured, giving maximum flexibility to the user. PORFLOW version 6.10.3 was used for PA porous medium flow and transport analyses because its capabilities met program needs, core software functions have been verified through vendor and QA testing, and SRS personnel are experienced in applying PORFLOW in PA analyses. PORFLOW was used at SRS for

calculations supporting the SPF and used by Idaho National Engineering and Environmental Laboratory (INEEL) for analyses supporting closure of the Tank Farm Facility. [CBU-PIT-2005-00146, DOE-ID-10966] For the FTF PA, PORFLOW is an appropriate code because it can accommodate calculations in both the saturated and unsaturated zones and more importantly has the ability to simulate first-order decay and progeny in-growth associated with radionuclide chains, which is necessary for calculations involving radioactive stabilized contaminant disposal.

Analytic & Computational Research, Inc. has provided the following documentation associated with PORFLOW:

- A user's guide (ACRi-2002) which provides instructions for PORFLOW use.
- Validation data for PORFLOW (ACRi-1994).

SQAP for the PORFLOW version used for the FTF PA calculations is covered by WSRC-SQP-A-00028 and G-TR-G-00002.

Design check of the data used for the performance of the PORFLOW modeling is documented in SRT-ESB-2007-00046 and all technical findings have been satisfactorily resolved. The scope of the design check includes:

- Vadose zone flow input,
- Vadose zone transport input, and
- Aquifer transport input.

4.3.1.3 GoldSim

GoldSim is a commercial program developed by GoldSim Technology Group LLC (GTG) that is a user-friendly and highly graphical, Windows-based program for carrying out dynamic, probabilistic simulations of complex systems to support management and decision-making in engineering, science and business.

GoldSim was used to assist in developing uncertainty analyses for the FTF PA and identifying from the parameters modeled in GoldSim the important input parameters in the groundwater transport model. GoldSim utilized the flow field outputs from PORFLOW to perform transport calculations and subsequent dose calculations for evaluation of input parameter importance and calculation uncertainties. GoldSim was also used to evaluate parameter importance while developing the initial model for PORFLOW and provide feedback to the PORFLOW modelers on focus areas requiring additional attention. GoldSim was also used to perform all-pathways and intruder analyses by utilizing the contaminant transport results from PORFLOW to calculate groundwater pathways and inadvertent intruder doses. Figures 4.3-1 and 4.3-2 illustrate the integration of GoldSim in the modeling efforts and provides additional detail of the integration and steps of GoldSim calculations for fluid flow and contaminant transport.

Figure 4.3-1: FTF PA Modeling Code Integration

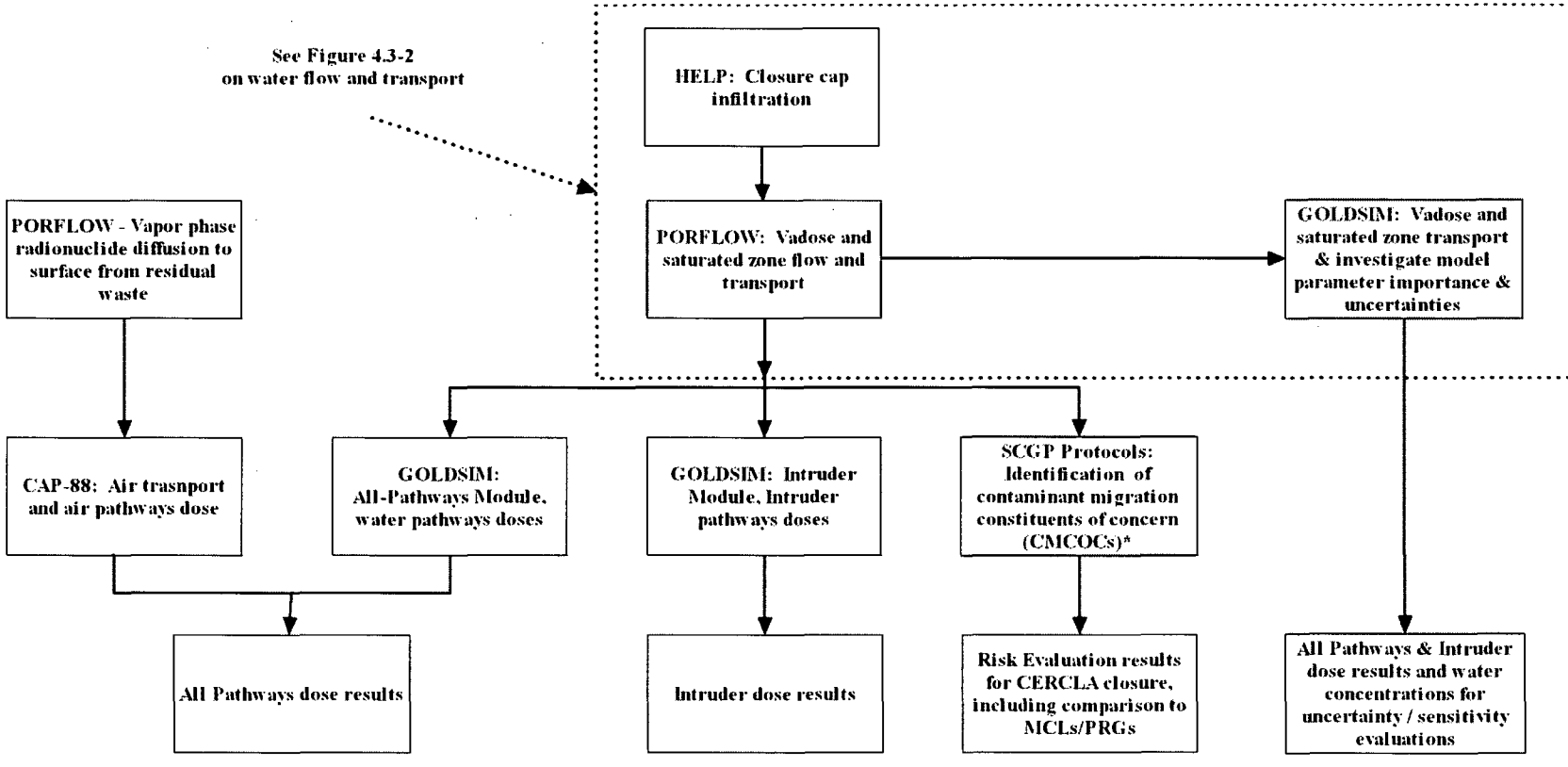

*The SGCP protocols are not a specific computer code and are therefore not discussed here.

Figure 4.3-2: FTF PA Modeling Code Integration – Details of Water Flow and Transport

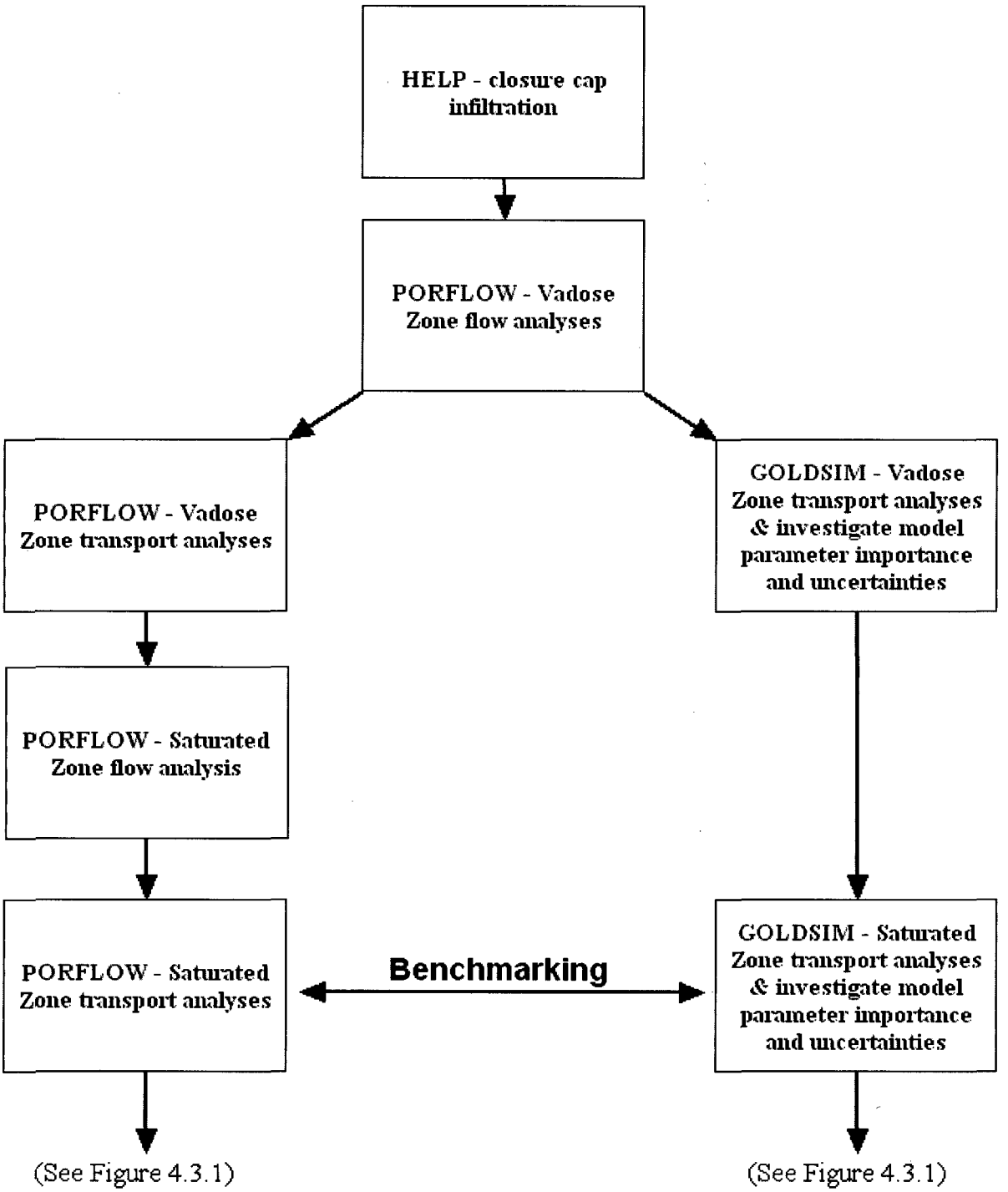

GoldSim was designed to facilitate the construction of large, complex models. The user can build a model of a system in a hierarchical, modular manner, such that the model can evolve and add detail as more knowledge regarding the system is obtained. Other features, such as the ability to manipulate arrays, the ability to "localize" parts of a model, and the ability to assign version numbers to a model which is constantly being modified and improved, further facilitate the construction and management of large models. GoldSim has an extensive internal database of units and conversion factors allowing the user to enter data and display results in any units and/or define customized units. GoldSim ensures dimensional consistency in models and carries out all of the unit conversions internally eliminating the need to carry out (error-prone) unit conversions. The user can dynamically link external programs or spreadsheets directly into a GoldSim model. In addition, GoldSim was specifically designed to support the addition of customized modules (program extensions) to address specialized applications.

GoldSim version 9.60 is used for PA porous medium transport and dose analyses because its capabilities meet program needs, allows for ease of input changes and output visualization and is used by other DOE sites (e.g., Nevada Test Site, Yucca Mountain) and the NRC.

GTG has provided the following documentation associated with GoldSim:

- A user's guide which provides instructions for GoldSim use [GTG-2006a]
- Validation data for GoldSim [GTG-2006b]

SQAP for GoldSim is covered by G-SQA-A-00011.

4.3.1.4 CAP-88

CAP-88 is an EPA code that uses atmospheric dispersion modeling for assessing dose and risk due to radionuclide emissions to the air. CAP-88 was used in the FTF PA to estimate annual dose to Maximally Exposed Individuals (MEI) considering plume and ground gamma-shine, inhalation and foodstuff ingestion pathways using the vapor phase radionuclide diffusion to the surface results from PORFLOW.

CAP-88 was developed by the EPA and is used to demonstrate compliance with 40 CFR 61 *National Emissions Standards for Hazardous Air Pollutants (NESHAPs)*, Subpart H, *National Emission Standards for Emissions of Radionuclides other than Radon from Department of Energy Facilities*. CAP-88 uses a modified Gaussian plume equation to estimate the average dispersion of radionuclides released from up to six sources at the same release location with different release heights. Assessments are done for a circular grid with a radius up to 50 miles. Version 1.0 is still in use today at SRS because prior personal computer versions of CAP-88 do not allow for adjustment of site-specific parameters of significance to SRS and CAP-88 is an accepted model already being used at SRS for NESHAP compliance. CAP-88 was used at SRS during the calculations supporting the SPF, is the code used by SGCP during CERCLA closure evaluations and used by INEEL during the calculations supporting their Tank Farm Facility. [CBU-PIT-2005-00146, DOE-ID-10966]

The following documentation associated with CAP-88 is available:

- A user's manual (CAP-88) which provides instructions for use

SQAP for the CAP-88 version used for the FTF PA calculations is covered by Q-SQP-A-00002.

4.3.2 Software QA and Validation

General WSRC requirements for QA are described in WSRC Manual 1Q *Quality Assurance.* The software QA implementation reports are referenced for the specific software codes in Section 4.3.1. The hierarchy of WSRC documents is described as follows:

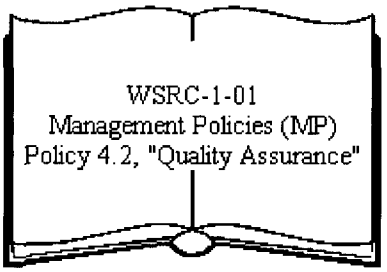

Management Policy (MP) 4.2 contains the WSRC President's policy statement regarding the Company's commitment to provide products and services which meet or exceed the requirements and expectations of our customers. [WSRC 1-01, 4.2] The WSRC QAP is to be implemented in a manner to support implementation of WSRC imperatives of safety, disciplined operations, cost effectiveness, continuous improvement, and teamwork. WSRC has established and implemented an Integrated Safety Management System (ISMS). The QA program is consistent with, and an integral part, of the WSRC ISMS. The policy requires that the program include appropriate procedures to comply with legal, regulatory, contractual, and corporate requirements related to quality. The policy also requires that the WSRC QA program comply with DOE O 414.1B, 10 CFR 830, Subpart A, and the WSRC QAP. [WSRC 1-01, MP 4.2] The QA Program applies in a manner which contributes to the safe, reliable, and environmentally sound operation of the SRS. It incorporates a graded approach commensurate with risk in the definition and application of QA/Quality Control (QC) requirements. The QAP provides for the prevention of errors as well as the detection and correction of deficient conditions and incorporates an assessment process for identifying opportunities for continuous improvement. The focus of quality improvement is to reduce the variability of every process that influences the quality and value of the WSRC products or services.

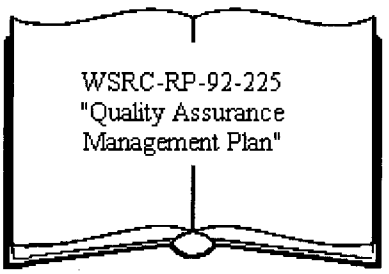

The *WSRC Quality Assurance Management Plan* (QAP) describes the requirements and responsibilities for execution of the WSRC QA Program for implementing DOE O 414.1B, and 10 CFR 830, Subpart A. [WSRC 1-01, MP 4.2] *Quality Assurance Requirements For Nuclear Facility Applications* and other consensus standards are used in the development of the WSRC QAP. [ASME NQA-1-2004, ASME NQA-1a-2005, ASME NQA-1b-2007] The plan has been jointly approved by WSRC and Department of Energy – Savannah River Operations Office (DOE-SR) and serves as the basis for the establishment of the procedures.

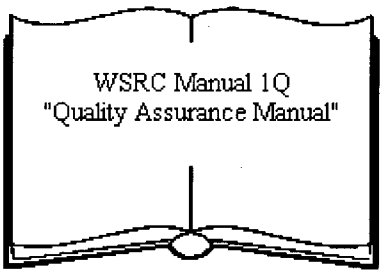

This manual provides the structure and procedures for achieving and verifying the WSRC requirements for quality. The manual consists of a series of QA Procedures which describe applicable QA requirements. Furthermore, WSRC Manual 1Q states:

"The WSRC QA Program has been developed to be responsive to the requirements of DOE O 414.1B, and DOE Safety Rule Title 10 CFR 830, Subpart A. Because of the size and complexity of the SRS and its varied products, services, and missions, the program has been defined in a standard framework of company policy, procedures, and instructions to be used by the implementing organizations to perform quality-related activities. These documents shall, as a minimum, include all of the requirements of WSRC-RP-92-225 criteria for which the implementing organizations have responsibility."

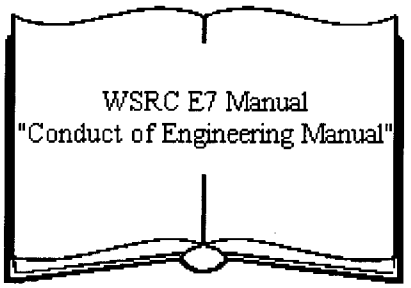

For WSRC, the QA implementing procedure for performing reviews of technical work is found in WSRC E7 Manual, 2.60. The end use of data drives the level of review required. Design Verification, the highest level review, must be performed for work affecting Safety Significant (SS) / Safety Class (SC) systems. Design Check is the next lower level of review and is required for all Production Support (PS) and General Service (GS) design output documents. Because the work associated with the PA and associated documents are not associated with SS or SC systems, the Design Check represents the appropriate level of rigor.

A design checker assures the technical accuracy of the design document by performing the following Design Check activities:

- A mathematical check, if appropriate;
- A review for correct use of technical input, including quality requirements;
- A review of the approach used and reasonableness of the output; and
- An administrative check (page numbers, etc.)

A design checker must meet the following criteria to perform a Design Check:

- Did not participate in the development of the portion of the document being checked;
- Is knowledgeable in the area of the design or analysis for which they review;
- Is capable of performing similar design or analysis activities; and
- Has security clearance for access to sufficient information to perform the Design Check.

Between 2002 and 2004 SRNL developed, piloted and then implemented technical review guidelines incorporating the E7 Manual requirements for performing Design Checks and Design Verification by document review. These guidelines also meet the

requirements for review of Type 2 Calculations contained in WSRC E7 Manual, 2.31. The guidelines provide a flowchart to map the SRNL technical review process, lines of inquiry for performing reviews, a checklist for communicating instructions and best management practices to set a benchmark for management expectations.

Software QA is conducted in accordance with the requirements of the WSRC 1Q Manual through the development and execution of SQAP. This procedure fulfills the requirements of DOE O 414.1.B and 10 CFR 830, Subpart A. The QA plans and processes used by WSRC to verify the inputs and outputs for the different modeling codes used are provided in the code specific descriptions in Section 4.3.1.

4.3.3 Modeling Codes Summary

In conclusion, Figures 4.3-1 and 4.3-2 present the approach to modeling code integration used for the FTF PA. Of extreme importance in the implementation of the modeling integration show in Figures 4.3-1 and 4.3-2 is assurance that the input data to the various codes is verified to be accurate. Documentation of the verification of the model input traced from source documents, to modeling input, and to appropriate sections within this PA has been performed and is described in Appendix H of this document.

4.4 Closure System Modeling

This section describes how the FTF design elements and their associated properties were represented in the computer modeling codes. The closure system conceptual design was an aphysical simplification of the actual FTF system design, which is required for analytical modeling. Certain waste tank features and design elements are by necessity omitted in the conceptual model, and are discussed in Section 4.4.1.

This section also describes how the FTF closure system is expected to behave in the future, and what modeling scenarios are used to depict system behavior over time. Because it is difficult to predict with a high level of certainty just what changes may occur to a closed and grouted waste tank system over the 10,000 year evaluation period, this section describes a range of potential conditions to which a closed waste tank or ancillary system may be subjected. While the baseline analysis (represented through the PORFLOW FTF model) reflected the best estimate of future closure system behavior, the probabilistic analysis (represented through the GoldSim FTF model) considered a variety of possible scenarios. In addition to analyzing differing scenarios in the 10,000 year evaluation period, the transport models were all run to at least 20,000 years for the purposes of determining peak concentrations that occur after the 10,000 year evaluation period.

4.4.1 Individual Waste Tank Modeling

Certain waste tank features and design elements have by necessity been omitted in the conceptual model. The modeling representations are a simplification of the actual physical infrastructure of the waste tanks, which are described in detail in Section 3.2.1. A number of general modeling decisions guidelines were followed for the design representation:

- The intent of the conceptual model was to capture waste tank dimensions and relative material differences for each discrete tank segment.
- Each discrete waste tank segment/area was represented as homogeneous, ignoring interior elements (e.g., rebar, cooling coils) and/or penetrations through the area (e.g., tank risers, transfer lines).
- Minimum segment thicknesses were used in the baseline analysis where an area had variable thickness (e.g., waste tank walls, tank tops).
- Grouting of tank void areas (e.g., waste tank primary, tank annulus, cooling coils) is assumed to have occurred as planned.

4.4.1.1 Type I Tank Modeling

The Type I tank dimensions are presented in Figure 4.4-1. Specific areas where Type I tank modeling decisions of interest are implemented are highlighted below:

- The waste tank basemat segment was based on the basemat thickness and ignores other material layers below the tank (i.e., concrete working slab, grout layer, lean concrete layer, and waterproofing layer).
- The primary liner and annulus liner are explicitly modeled.
- The primary liner and annulus liner assumed thicknesses were based on the minimum thicknesses only.
- The waste tank wall and tank liner penetrations (i.e., transfer lines) were not modeled discretely.
- The waste tank primary cavity or liner was assumed to be filled with grout and was treated as a discrete area.
- The twelve waste tank support columns and cooling coils were not modeled discretely and were included in the tank primary. The waste tank annulus was assumed to be filled with grout and is treated as a discrete area.
- The waste tank roof penetrations (i.e., risers) were not modeled discretely.
- Concrete rebar in the waste tank top, tank walls, and tank basemat was not modeled discretely, such that concrete was considered a homogenous material.
- The waste tank underliner sump was not modeled discretely.

Figure 4.4-1: Typical Type I Tank Modeling Dimensions

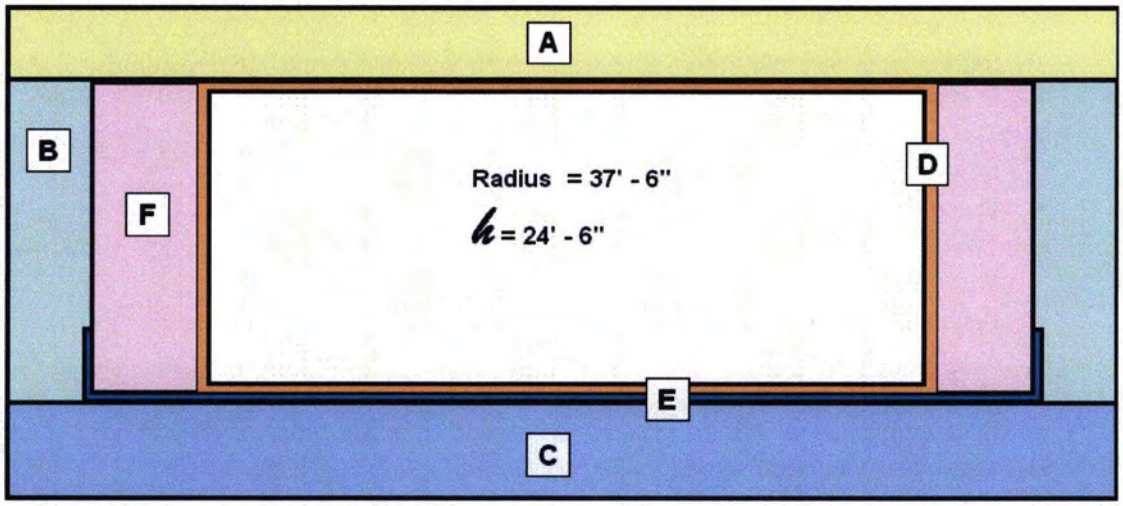

[NOT TO SCALE]

LABEL	THICKNESS	MATERIAL
A Concrete Roof	22"	Concrete (Dupont Spec 3019, Sec. B)
B Concrete Wall	22"	Concrete (Dupont Spec 3019, Sec. B)
C Concrete Basemat	30"	Concrete (Dupont Spec 3019, Sec. B)
D Primary Liner	0.5"	Carbon Steel (ASTM A-285-50T)
E Secondary Liner	5' high and 0.5" thick	Carbon Steel (ASTM A-285-50T)
F Grouted Annulus	30"	Tank Fill Grout

4.4.1.2 Type III and IIIA Tank Modeling

The Type III and Type IIIA tank dimensions are presented in Figures 4.4-2 and 4.4-3. Specific areas where Type III/IIIA tank modeling decisions of interest are implemented are highlighted below:

- The waste tank basemat segment was based on the minimum basemat thickness and ignored the thicker concrete drop panel below the tank center column and other material layers below the tank (i.e., concrete working slab, grout layers). Two inches were subtracted from the Type IIIA basemat thickness to reflect 2 inch leak detection slots cut into the basemat.

- Thermocouple piping running through the waste tank walls and basemat was not modeled discretely.
- The waste tank primary cavity or liner was assumed to be filled with grout and was treated as a discrete area. The waste tank center column, center annulus, ventilation ductwork, and cooling coils were not modeled discretely.
- The waste tank annulus cavity or liner was assumed to be filled with grout and was treated as a discrete area.
- The primary liner and annulus liner are modeled explicitly.
- The primary liner and annulus liner assumed thicknesses were based on the minimum thicknesses only (e.g., extra thickness at knuckle not modeled).
- Penetrations through the waste tank wall and tank liner (i.e., transfer lines) were not modeled discretely.
- The waste tank roof penetrations (i.e., risers) were not modeled discretely.
- Concrete rebar in the waste tank top, tank walls, and tank basemat was not modeled discretely, such that concrete was considered a homogenous material.
- The waste tank underliner sump was not modeled discretely

Figure 4.4-2: Typical Type III Tank Modeling Dimensions

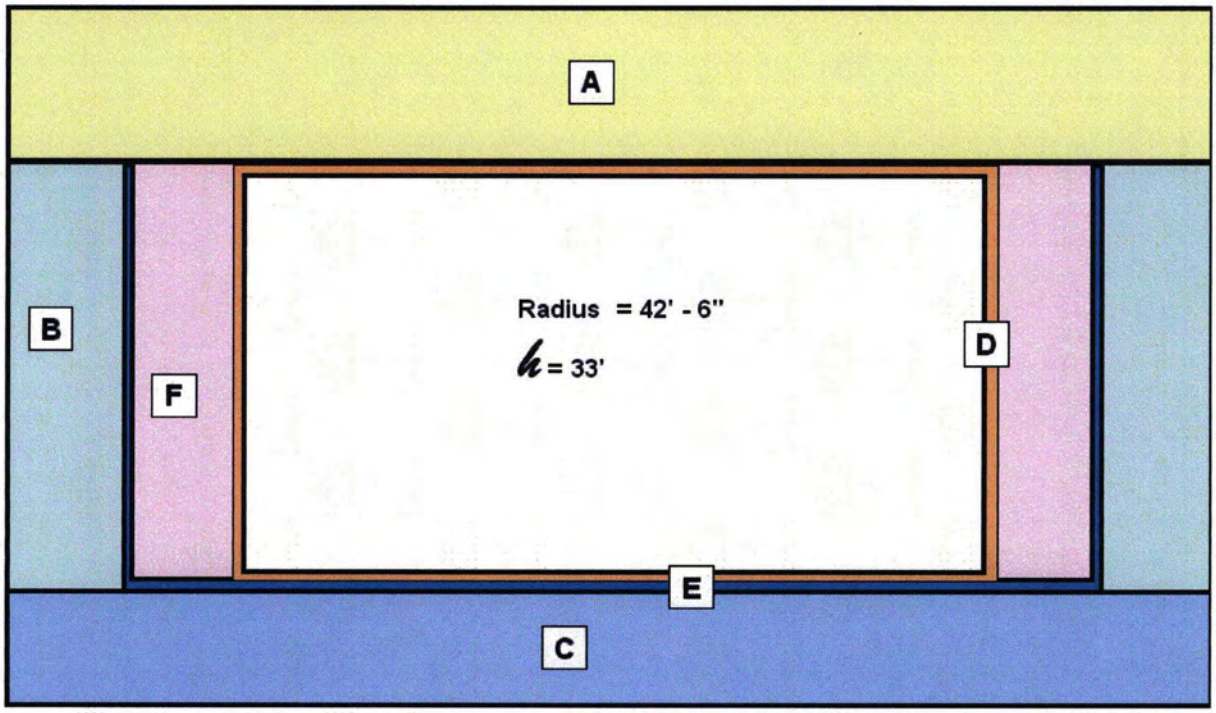

[NOT TO SCALE]

LABEL	THICKNESS	MATERIAL
A Concrete Roof	48"	Class C Concrete
B Concrete Wall	30"	Class C Concrete
C Concrete Basemat	42"	Class C Concrete
D Primary Liner	0.5"	Carbon Steel (ASTM A-516)
E Secondary Liner	3/8"	Carbon Steel (ASTM A-516)
F Grouted Annulus	30"	Tank Fill Grout

Figure 4.4-3: Typical Type IIIA Tank Modeling Dimensions

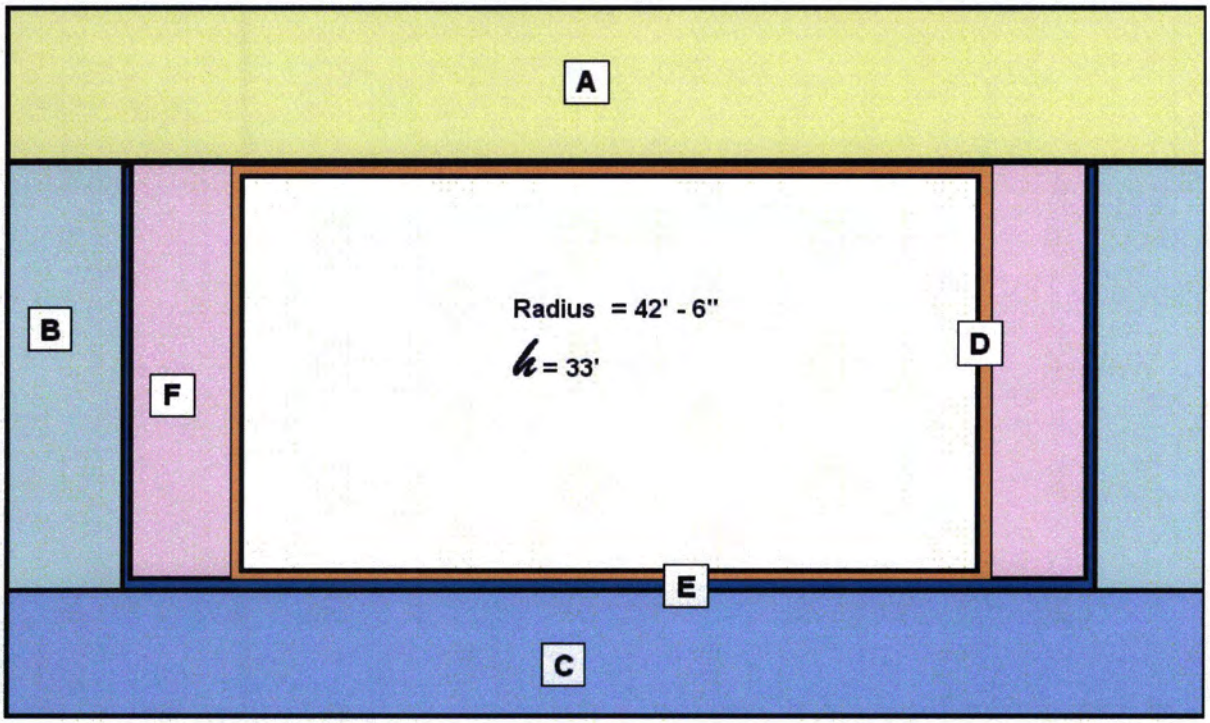

[NOT TO SCALE]

LABEL	THICKNESS	MATERIAL
A Concrete Roof	48"	Class C Concrete
B Concrete Wall	30"	Class C Concrete
C Concrete Basemat	41"	Class C Concrete
D Primary Liner	0.5"	Carbon Steel (Tanks 25 - 28: ASTM A-516) (Tanks 44 - 47: ASTM A-537)
E Secondary Liner	3/8"	Carbon Steel (Tanks 25 - 28: ASTM A-516) (Tanks 44 - 47: ASTM A-537)
F Grouted Annulus	30"	Tank Fill Grout

4.4.1.3 Type IV Tank Modeling

The Type IV tank dimensions are presented in Figure 4.4-4. Specific areas where Type IV tank modeling decisions of interest are implemented are highlighted below:

- The waste tank basemat segment was based on the thickness of the basemat and of the cement topping placed over the basemat. Approximately a tenth of an inch thickness was subtracted to account for the drainage grooves cut into the cement topping. The effective one-tenth inch groove thickness is based grooves being 1.625 inch and covering less than 6% of the waste tank footprint. The waste tank wall footing and the grouted segment between the wall footing and the tank basemat were not modeled discretely.
- The waste tank primary cavity or liner was assumed to be filled with grout and was treated as a discrete modeled area.
- The waste tank primary liner assumed thickness was based on the minimum thicknesses only (e.g., extra thickness at knuckle not modeled).
- The waste tank wall and tank liner penetrations (i.e., transfer lines) were not modeled discretely.
- The waste tank wall thickness was the minimum wall thickness and did not reflect the variable thickness.
- The waste tank roof thickness was the minimum thickness of the dome, and did not reflect the variable thickness of the roof.
- The waste tank roof penetrations (i.e., risers) were not modeled discretely.
- Concrete rebar in the waste tank top and tank basemat was not modeled discretely, such that concrete was considered a homogenous material.
- The waste tank underliner sump was not modeled discretely

Figure 4.4-4: Typical Tank IV Tank Modeling Dimensions

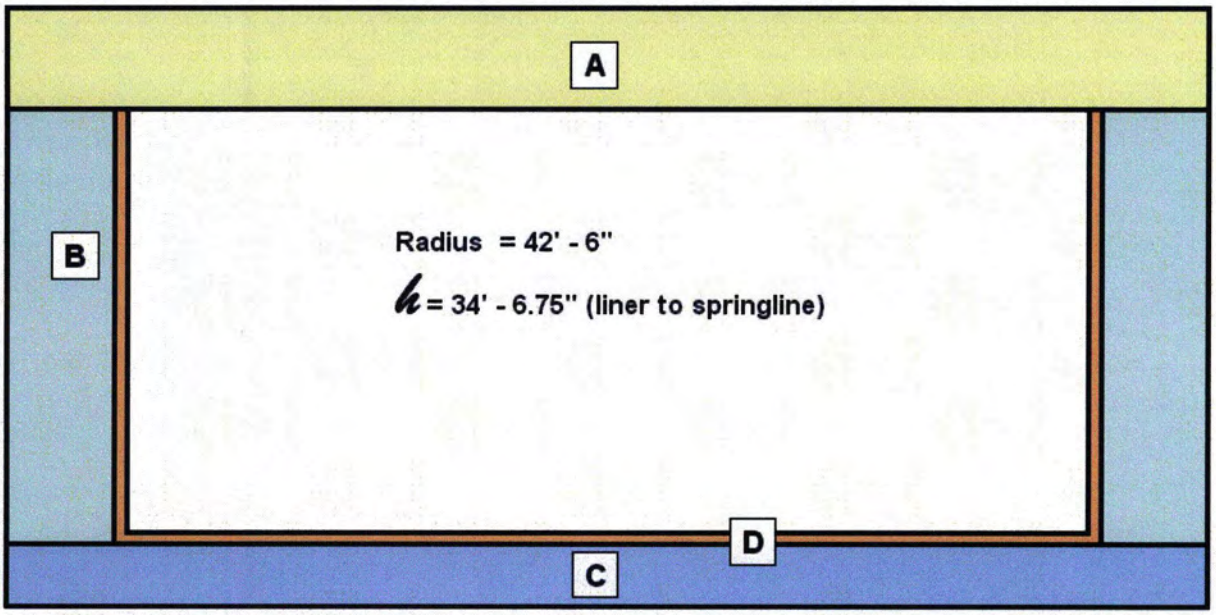

[NOT TO SCALE]

LABEL	THICKNESS	MATERIAL
A Concrete Roof	7"	Class A Concrete
B Concrete Wall	7"	Type I Portland Cement
C Concrete Basemat	6.9025"	Class C Concrete
D Primary Liner	0.375"	Carbon Steel (ASTM A-285-50T)

4.4.2 Systems and Potential Degradation

As noted previously, there are 22 underground waste tanks and eight discrete ancillary systems identified and modeled in the closure of FTF. Each of these systems will initially be placed in a controlled condition at closure (e.g., physically isolated and in most cases filled with grout). However, the waste tanks themselves, the ancillary equipment, and the closure system may degrade over time, eventually releasing contaminants to the environment. The physical and chemical mechanisms that control the release or leaching of residual contamination from the grouted waste tanks are described in Section 4.2.2.

To simulate potential conditions in the FTF closure system over the 10,000 year evaluation period, six waste tank configurations and one ancillary equipment configuration were identified for analysis. While only one configuration (Configuration A) was simulated in the baseline analysis, the six different configurations were considered in the probabilistic analysis. Each configuration starts out with the system closed as planned, with the tanks filled with grout and the closure cap in place. In the time frames discussed, year 0 was taken to be the year during which the FTF is closed.

Tank Configurations A through E start out with the engineered closure cap in place as planned (Tank Configuration F assumed a "soil only" closure cap). In the analysis of configurations A through E, expected degradation of the closure cap materials over time were simulated using the increasing infiltration rates shown in Table 3.2-10. The waste release process described in Section 4.2.2 and the conceptual model material properties described in Section 4.2.3.2 were employed in each waste tank configuration evaluation. The differences between the six waste tank configurations are summarized in Table 4.4-1 and are discussed in detail in the following sections.

Table 4.4-1: Waste Tank Configuration Summary

Case	Closure Cap	Assumed Fast Flow Paths	Degradation of Cementitious Materials	Liner Failure Time	Water Table Level
A	Engineered Closure Cap	None	Degradation curve based on Table 4.2-33	Later failure date (based on Grouted Diff coefficient of E-6 Ca)	No change
B	Engineered Closure Cap	None	Degradation assumed to be a step change at year 501	Later failure date (based on Grouted Diff coefficient of E-6 Ca)	No change
C	Engineered Closure Cap	Channel with no flow impedance through grout	Degradation assumed to be a step change at year 501	Early failure date (based on Grouted Diff coefficient of E-4 Ca)	No change
D	Engineered Closure Cap	Channel with no flow impedance through grout and basemat	Degradation assumed to be a step change at year 501	Early failure date (based on Grouted Diff coefficient of E-4 Ca)	No change
E	Engineered Closure Cap	N/A	Degradation assumed to be a step change at year 501	Early failure date (based on Grouted Diff coefficient of E-4 Ca)	Above CZ
F	Soil Only (16.45 in/yr infiltration)	None	Degradation assumed to be a step change at year 501	Later failure date (based on Grouted Diff coefficient of E-6 Ca)	No change

4.4.2.1 Tank Configuration A

In Tank Configuration A (Figure 4.4-5), the closure cap was in place and no fast flow path exists from outside the waste tank system, through the tank, and exiting the system. In Tank Configuration A, it was assumed that the concrete that makes up the walls, the tank grout, and basemat concrete degrades over time (with these changes simulated by increasing hydraulic conductivity). Degradation of tank cementitious materials (degradation rate and timing) was based on WSRC-STI-2007-00607 and SRS-REG-2007-00027, and can vary dependant on tank type. The timing of the degradation of the tank cementitious materials is detailed in Table 4.2-32 for the various tank types. Closure cap degradation occurs as shown in Table 3.2-9. Configuration A was considered the FTF Base Case for waste tank closure.

Figure 4.4-5: Tank Configuration A

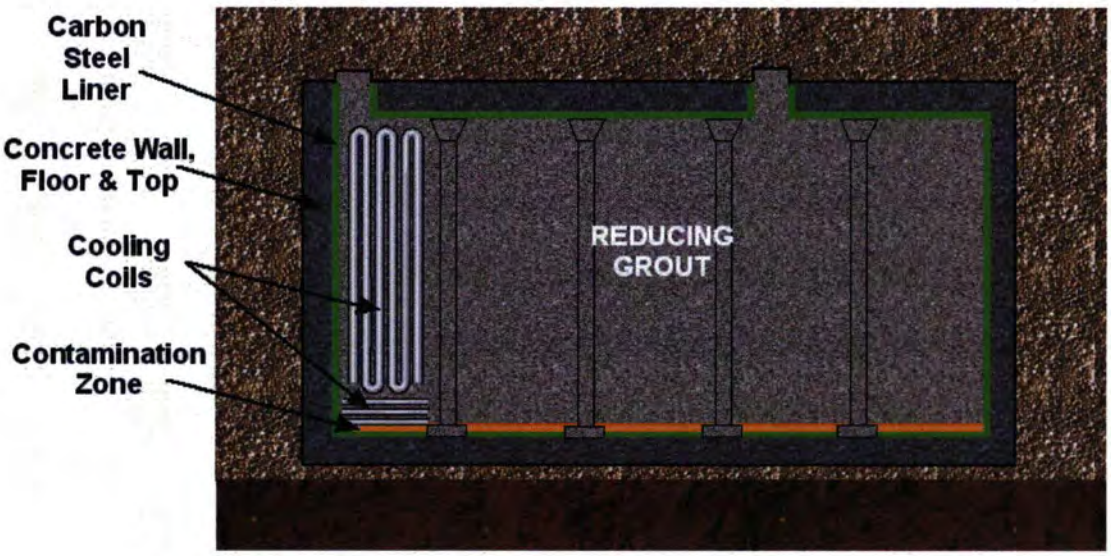

Under Tank Configuration A, the entire steel liner was assumed to be impermeable, with the steel liner in direct contact with intact grout or concrete on all sides. Under these conditions the carbon steel liner was expected to remain impermeable until several thousand years after closure, as shown for the Base Case in Table 4.2-35. After the carbon steel liner fails, it was assumed in Tank Configuration A that contaminants begin to leach from the degraded system, via advection, based on changes to the pH, redox potential, and carbonate concentration of the residual contamination in the floor of the tank system. Individual radionuclide leach rates will vary over time based on solubility and adsorption controls. In this condition, it was assumed that no fast flow exits through the concrete basemat. Rather, contaminants were assumed to be transported through the concrete basemat.

4.4.2.2 Tank Configuration B

Figure 4.4-6 represents Tank Configuration B, a condition where cementitious material degradation is accelerated, with degradation occurring essentially instantaneously at year 500. Concrete degradation could take the form of extensive through-cracking, or shrinkage away from the liner. The grout degradation was not assumed to lead to formation of a fast-flow path through the grout. (i.e., full flow through the grout), but did result in faster flows sooner than in the Base Case.

Figure 4.4-6: Tank Configuration B

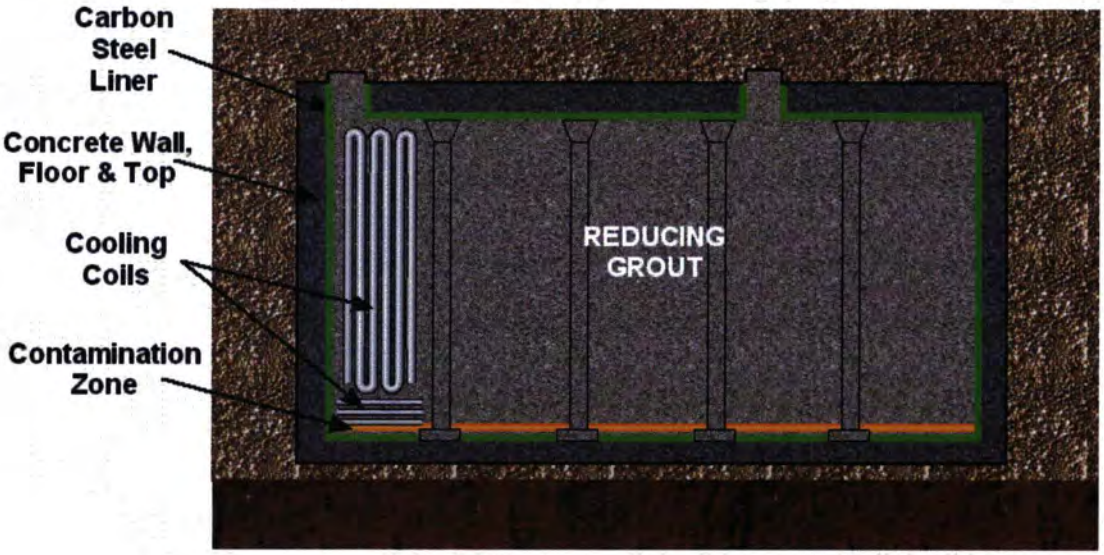

[NOT TO SCALE]

In Tank Configuration B, the closure cap was in place and no fast flow path exists from outside the waste tank system, through the tank, and then exiting the system. The concrete that makes up the walls, the tank grout, and basemat concrete degraded over time (as simulated by increasing hydraulic conductivity). The tank cementitious materials were assumed to begin to degrade at year 500, with degradation occurring essentially instantaneously (full degradation was reached at year 501). Closure cap degradation occurs as shown in Table 3.2-9.

Under Tank Configuration B, the entire steel liner was assumed to be impermeable, with the steel liner in direct contact with intact grout or concrete on all sides. Under these conditions the carbon steel liner was expected to remain impermeable until several thousand years after closure, as shown for the Base Case in Table 4.2-35. After the carbon steel liner fails, it was assumed in Tank Configuration B that contaminants begin to leach from the degraded system, via advection, based on changes to the pH, redox potential, and carbonate concentration of the residual contamination in the floor of the tank system. Individual radionuclide leach rates will vary over time based on solubility and adsorption controls. In

this condition, it was assumed that no fast flow exits through the concrete basemat. Rather, contaminants were assumed to be transported through the concrete basemat.

4.4.2.3 Tank Configuration C

In Tank Configuration C (Figure 4.4-7), the closure cap was in place and it was assumed that a fast flow path exists between the waste tank top and CZ, (e.g., from tank riser through cooling coil) due to incomplete filling with grout during closure. The fast-flow path through the grout was represented in the conceptual design by modeling a channel through the grout with full flow. The concrete that makes up the walls, the tank grout, and basemat concrete degrade over time (as simulated by increasing hydraulic conductivity). The tank cementitious materials were assumed to begin to degrade at year 500, with degradation occurring essentially instantaneously (full degradation is reached at year 501). Closure cap degradation occurs as shown in Table 3.2-9.

Figure 4.4-7: Tank Configuration C

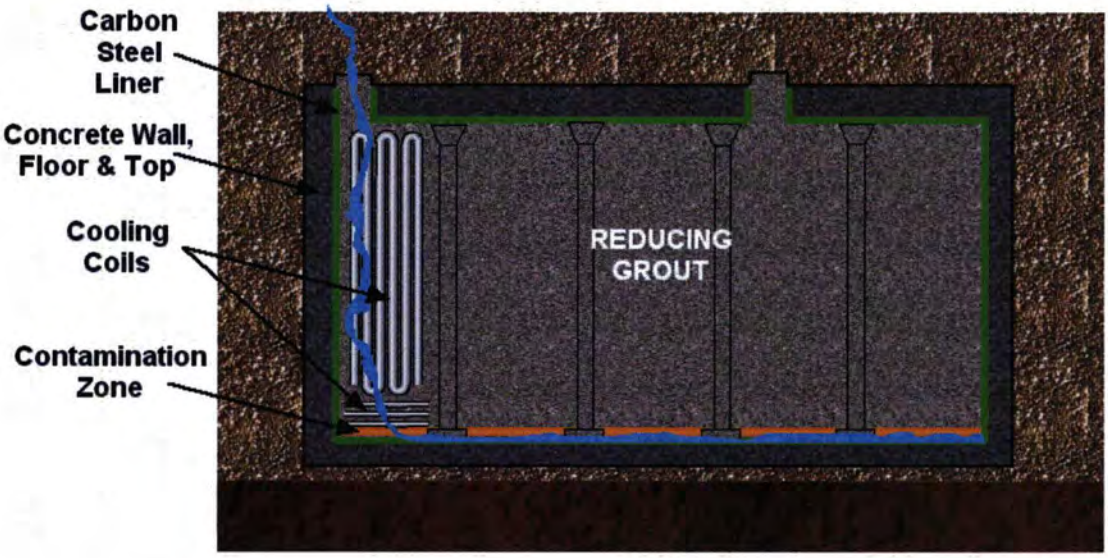

[NOT TO SCALE]

Tank Configuration C assumed no pitting occurs in the carbon steel liner. It is assumed that concrete/grout pore water with relatively high oxygen concentration and low pH is in contact with the steel liner. In this condition, the diffusion coefficients (which control the failure times) are higher than in the Base Case (as shown in Table 4.2-35). Under these conditions the carbon steel liner was expected to remain impermeable until the analyzed failure time (provided in Table 4.2-35) are reached. The analyses were based upon the assumption that carbonation was the most aggressive mechanism of corrosion of the waste tank liner due to the loss of the high pH environment, and that chloride may induce depassivation on the steel surface.

After carbon steel liner failure, it was assumed in Tank Configuration C that contaminants begin to leach from the degraded system, via advection, based on changes to the pH, redox potential, and carbonate concentration of the residual contamination in the floor of the tank system. Individual radionuclide leach rates will vary over time based on solubility and adsorption controls. In Tank Configuration C, it was assumed that no fast flow exits through the concrete basemat. Rather, it was assumed that the basemat has had an increase in permeability based on concrete degradation. Whether the fast flow path is active during any period of time depended on the availability of sufficiently high infiltration through the closure cap.

4.4.2.4 Tank Configuration D

In Tank Configuration D (Figure 4.4-8), the closure cap was in place and it was assumed that a fast flow path exists though the entire closed system (e.g., through a tank riser, through a cooling coil, through the tank fill grout, through pitting in the steel liner, and through the basemat). It was assumed that a fast flow path exists through the concrete/carbon steel roof of the waste tank (e.g., through a riser, due to incomplete filling with grout during closure.). The fast-flow path through the grout and basemat was represented in the conceptual design by modeling a channel through the grout and basemat with full flow. For cementitious material not associated with the fast flow channel, degradation was accelerated over the baseline, with degradation occurring essentially instantaneously at year 500. The concrete that makes up the walls, the tank grout, and basemat concrete degrade over time (as simulated by increasing hydraulic conductivity). The tank cementitious materials were assumed to begin to degrade at year 500, with degradation occurring essentially instantaneously (full degradation is reached at year 501). Closure cap degradation occurs as shown in Table 3.2-9.

Figure 4.4-8: Tank Configuration D

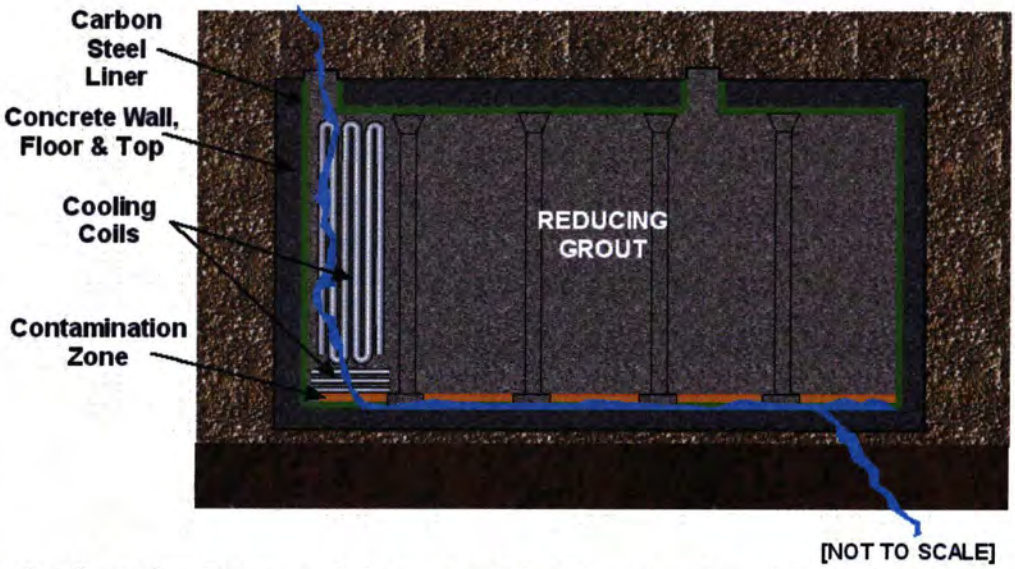

Tank Configuration D assumed that concrete/grout pore water with relatively high oxygen concentration and low pH is in contact with the steel liner. In this condition, the diffusion

coefficients (which control the failure times) are higher than in the Base Case (as shown in Table 4.2-35). Under these conditions the carbon steel liner was expected to remain impermeable until the analyzed failure time (provided in Table 4.2-35) are reached. The analyses were based upon the assumption that carbonation was the most aggressive mechanism of corrosion of the waste tank liner due to the loss of the high pH environment, and that chloride may induce depassivation on the steel surface.

After carbon steel liner failure, it was assumed in Tank Configuration D that contaminants begin to leach from the degraded system, via advection, based on changes to the pH, redox potential, and carbonate concentration of the residual contamination in the floor of the tank system. Individual radionuclide leach rates will vary over time based on solubility and adsorption controls. In Tank Configuration D, it was assumed that a fast flow exits through the concrete basemat. As with Tank Configuration C (Figure 4.4-7), actual flow through the available fast flow path was contingent upon adequate infiltration through the closure cap.

4.4.2.5 Tank Configuration E

In Tank Configuration E (Figure 4.4-9), the closure cap was in place and no fast flow path exists from outside the tank system, through the tank, and then exiting the system, however, this configuration assumed that groundwater is above the tank bottom. (Note that Table 4.2-23 shows the distance from the waste tank working slab bottom to the top of the water table for each tank under existing conditions). The concrete that makes up the walls, the tank grout, and basemat concrete degrade over time (as simulated by increasing hydraulic conductivity). The tank cementitious materials were assumed to begin to degrade at year 500, with degradation occurring essentially instantaneously (full degradation is reached at year 501). Closure cap degradation occurs as shown in Table 3.2-9.

Figure 4.4-9: Tank Configuration E

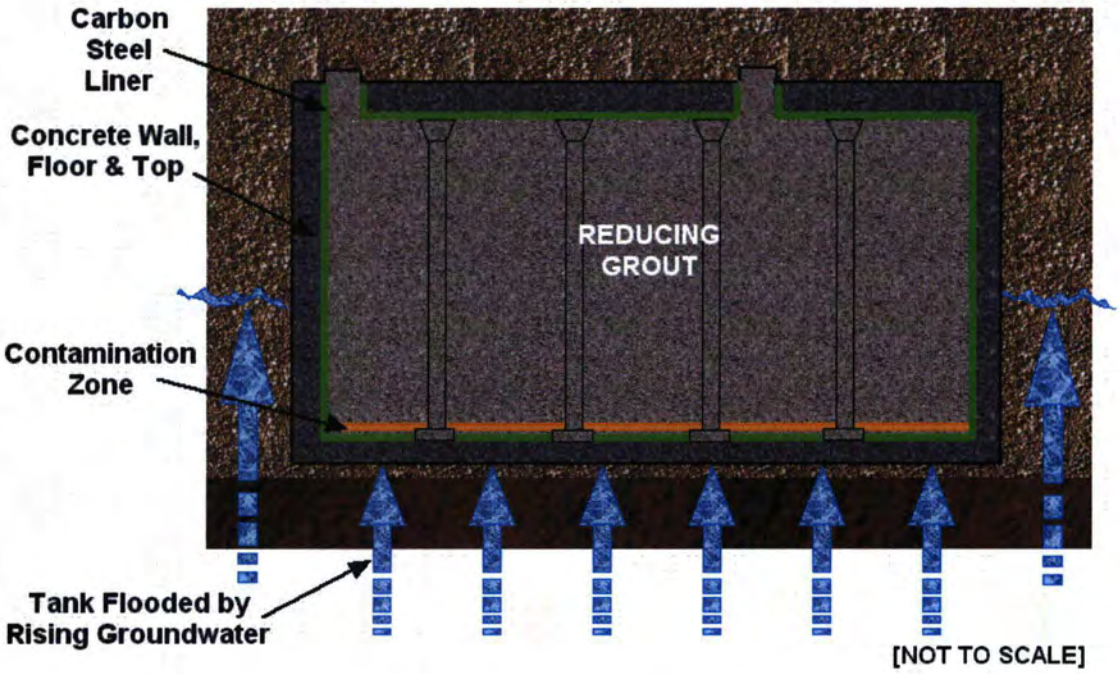

Tank Configuration E assumed that concrete/grout pore water with relatively high oxygen concentration and low pH has been in immediate contact with the steel liner since closure. This configuration assumed the concrete on the outside of the carbon steel liner has degraded to allow groundwater to infiltrate through the concrete to the carbon steel liner. In this condition, the diffusion coefficients (which control the failure times) are higher than in the Base Case, as shown in Table 4.2-35. Under these conditions the carbon steel liner was expected to remain impermeable until the analyzed failure time (provided in Table 4.2-35) were reached. The analyses were based upon the assumption that carbonation was the most aggressive mechanism of corrosion of the waste tank liner due to the loss of the high pH environment, and that chloride may induce depassivation on the steel surface.

After carbon steel liner failure, it was assumed in Tank Configuration E that contaminants begin to leach from the degraded system, via advection and diffusion, based on changes to the pH, redox potential, and carbonate concentration of the residual contamination in the floor of the tank system. Individual radionuclide leach rates will vary over time based on solubility and adsorption controls. Closure cap degradation occurs as shown in Table 3.2-9.

4.4.2.6 Tank Configuration F

Tank Configuration F is exactly the same as Tank Configuration B except that a "soils only" closure cap was assumed to be in place rather than the engineered closure cap that was modeled in the Base Case. The "soil only" closure cap infiltration rate of 16.45 inches per year was held constant over time in Tank Configuration F. [WSRC-STI-2007-00184_OUO, Table 31] The other aspects of this configuration are as described in the Tank Configuration B section.

4.4.2.7 Ancillary Equipment Configuration

In Ancillary Equipment Configuration (Figure 4.4-10), closure cap degradation occurs as shown in Table 3.2-9. The ancillary equipment was located below grade in the FTF (Section 3.2.2 provides additional details of FTF ancillary equipment and its location) and was covered by the closure cap. Modeling consisted of a source geometry of seven separate inventory sources (FPT-1, FPT-2, FPT-3, 242-F, 242-16F, CTS catch tank, and FTF catch tank) and a network of waste transfer lines represented by contaminants distributed over the entire FTF. Any equipment located above grade, such as the portion of one waste line associated with Tank 7, was assumed to have been removed.

Figure 4.4-10: Ancillary Equipment Configuration

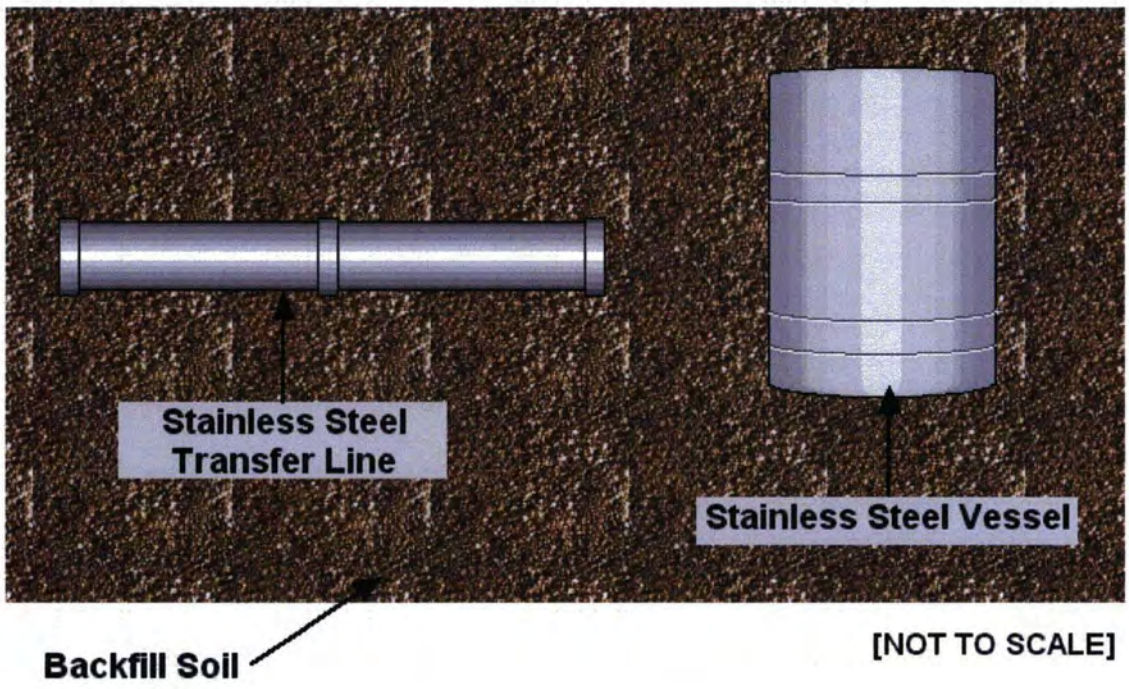

The ancillary equipment was assumed to be completely intact at the time of closure. The contaminant release was assumed to occur when the stainless steel fails. As discussed earlier in Section 4.2.3.2.5, predictions for failure of the stainless steel transfer line core piping were based on the results of a recent study specific to the application of the FTF closure PA. [WSRC-STI-2007-00460] These estimates considered general and localized corrosion mechanisms of the stainless steel exposed to SRS soil conditions for the stainless steel core transfer lines in FTF. The results of this study were incorporated by assuming that the applicable ancillary equipment containment (e.g., pump tank, evaporator pot, and transfer line core pipe) failed and released the associated inventory into the surrounding soil at year 510 (the time of 25% pitting penetration for "in soil" 0.116 inch thick stainless steel). This modeling simplification was considered reasonable for all ancillary equipment containment because in actuality the ancillary equipment containments will not be directly in soil (the pump tanks and evaporator pots are in concrete cells that will be filled with grout and the transfer lines are typically contained within a secondary jacket). Only an insignificant quantity of the FTF transfer lines are carbon steel vs. stainless steel (out of over 45,000 linear feet of pipe there are only three carbon steel lines 145 feet long). This simplification was important for transfer line modeling since the transfer line inventory was not modeled as point sources; rather the transfer line inventory was spread throughout the entire FTF modeling area. More complicated transfer line modeling (e.g., concentrating the transfer line inventory in selected tank farm areas) was determined through scoping analyses to be unnecessary. The line inventory is minor relative to tank inventories. Furthermore, the locations where line concentration would occur (primarily the concrete encasement that runs through the center line of the area where the Type I waste tanks are located) would result in inventory being placed farther away from the peak dose sources (the Type IV and Type III waste tanks), and the 100m point of assessment because of groundwater flow direction.

Once the stainless steel containment for ancillary equipment fails, the source term associated with the ancillary equipment was assumed available for release directly in the backfill soil surrounding the ancillary equipment. No hold up or containment of the source term is assumed to be provided by any of the cementitious materials surrounding the vessels, pits, and waste lines (such as the secondary containment structures). The waste transfer lines were modeled assuming no grout fill of the primary transfer line or jacket. After container failure for ancillary equipment, the flow through the CZ was set equal to the closure cap driven infiltration rate.

For the probabilistic FTF analysis, each piece of ancillary equipment (with the transfer lines being treated as a collective inventory) was assumed to fail independently with the failure time occurring between the time of first pit penetration (116 years) and 100% pitting penetration (approximately 1,000 years). The most probable time of ancillary equipment failure in the probabilistic FTF analysis was assumed to be the time of 25% pitting penetration (510 years).

4.4.3 Evaluation of Integrated System Behavior

Upon the closure of FTF, there is an opportunity for the stabilized contaminants to leach from distinct tank systems and ancillary equipment. The various individual system behaviors that are evaluated have been presented for the Tank Configurations A through E (Figures 4.4-5 through 4.4-9) and the Ancillary Equipment Configuration (Figure 4.4-10). The analysis of the Base Case through the PORFLOW FTF model provided results reflecting the best estimate of closure system behavior. These independent modeling scenarios for the FTF waste tanks and ancillary equipment are melded together in the probabilistic analysis to produce integrated results.

The saturated zone was gridded so that individual tanks and ancillary equipment point sources can be individually resolved. Explicit representation of individual sources enables investigation of potential plume overlap from separate sources. Integrated system behavior, as measured by concentration at exposure points, was simulated by applying contaminant flux transients for chosen tank types and configurations to appropriately located grid cells.

Provided below is a short description of the integrated conceptual model process flow for the closure cap and saturated zone. The integrated conceptual model consists of different segments, some of which were represented by independent sub-models. For example, the waste release model developed different solubility limits for different chemical states; the chemical state used in the model was determined in PORFLOW based on the PORFLOW calculated pore volumes. It should be noted that since the sub-models were developed independently and may have different levels of conservatism, some shared input parameters may have different values from sub-model to sub-model. For example, the diffusion coefficient is different between the concrete degradation evaluation and waste tank liner failure evaluation. While the coefficient in the base case waste tank liner evaluation (Section 4.2.3.2.5) is a more expected value, the concrete degradation evaluation (Section 4.2.3.2.3) chose a very high coefficient to conservatively estimate degradation rates. Emphasis was placed on ensuring that individual sub-models are defensible, and the fact that two model segments may assume different values for the same parameter was not considered significant if the sub-models are valid and defensible.

The model process flow description below describes how each individual model segment is integrated into the entire model and how its behavior is depicted. The Configuration A (base case) and Configuration D (fast flow case) timelines associated with the various model segments for the different tank types are provided in Tables 4.4-2 through 4.4-5.

Table 4.4-2: Type I Waste Tank Process Change Timeline

Change in Model Parameters	Year of Occurrence	
	Configuration A	Configuration D
Concrete (waste tank top, sides, basemat, etc.) starts to degrade hydraulically	1,300	500
Waste tank roof concrete transitions from Oxidized Region II to Oxidized Region III	1,600	1,600
Waste tank grout starts to degrade hydraulically	2,600	500
Concrete fully degraded hydraulically	2,600	501
Closure Cap reaches approximate steady state infiltration rate (11.5 in/yr)	2,625	2,625
Waste tank wall concrete transitions from Oxidized Region II to Oxidized Region III	3,300	15,500
Waste tank annulus concrete transitions from Reducing Region II to Oxidized Region II	5,000	2,200
Waste tank annulus concrete transitions from Oxidized Region II to Oxidized Region III	9,000	20,000
Waset tank basemat concrete transitions from Oxidized Region II to Oxidized Region III	10,000	2,200
Waste tank steel liner fails hydraulically	12,747	1,140
Waste tank grout fully degraded hydraulically	13,000	501
Waste tank grout transitions from Reducing Region II to Oxidized Region II	15,500	3,600
CZ transitions from Reducing Region II to Oxidized Region II	15,500	1,140
Waste tank grout transitions from Oxidized Region II to Oxidized Region III	20,000	15,500
CZ transitions from Oxidized Region II to Oxidized Region III	20,000	1,140

Table 4.4-3: Type III Waste Tank Process Change Timeline

Change in Model Parameters	Year of Occurrence	
	Configuration A	Configuration D
Concrete (waste tank top, sides, basemat, etc) starts to degrade hydraulically	2,500	500
Closure Cap reaches approximate steady state infiltration rate (11.5 in/yr)	2,625	2,625
Waste tank roof concrete transitions from Oxidized Region II to Oxidized Region III	2,800	2,200
Waste tank grout starts to degrade hydraulically	5,000	500
Concrete fully degraded hydraulically	5,000	501
Waste tank wall concrete transitions from Oxidized Region II to Oxidized Region III	7,000	20,000
Waste tank steel liner fails hydraulically	12,751	2,077
Waste tank annulus concrete transitions from Reducing Region II to Oxidized Region II	13,750	5,500
Waste tank basemat concrete transitions from Oxidized Region II to Oxidized Region III	14,250	3,600
Waste tank grout transitions from Reducing Region II to Oxidized Region II	15,500	5,500
CZ transitions from Reducing Region II to Oxidized Region II	15,500	2,077
Waste tank grout fully degraded hydraulically	18,900	501
Waste tank annulus concrete transitions from Oxidized Region II to Oxidized Region III	20,000	20,000
Waste tank grout transitions from Oxidized Region II to Oxidized Region III	20,000	20,000
CZ transitions from Oxidized Region II to Oxidized Region III	20,000	2,077

Table 4.4-4: Type IIIA Waste Tank Process Change Timeline

Change in Model Parameters	Year of Occurrence	
	Configuration A	Configuration D
Concrete (waste tank top, sides, basemat, etc) starts to degrade hydraulically	2,400	500
Closure Cap reaches approximate steady state infiltration rate (11.5 in/yr)	2,625	2,625
Waste tank roof concrete transitions from Oxidized Region II to Oxidized Region III	2,800	2,200
Waste tank grout starts to degrade hydraulically	4,800	500
Concrete fully degraded hydraulically	4,800	501
Waste tank wall concrete transitions from Oxidized Region II to Oxidized Region III	6,000	20,000
Waste tank steel liner fails hydraulically	12,751	2,077
Waste tank annulus concrete transitions from Reducing Region II to Oxidized Region II	13,750	5,500
Waste tank basemat concrete transitions from Oxidized Region II to Oxidized Region III	14,250	3,600
Waste tank grout transitions from Reducing Region II to Oxidized Region II	15,550	5,500
CZ transitions from Reducing Region II to Oxidized Region II	15,550	2,077
Waste tank grout fully degraded hydraulically	18,700	501
Waste tank annulus concrete transitions from Oxidized Region II to Oxidized Region III	20,000	20,000
Waste tank grout transitions from Oxidized Region II to Oxidized Region III	20,000	20,000
CZ transitions from Oxidized Region II to Oxidized Region III	20,000	2,077

Table 4.4-5: Type IV Waste Tank Process Change Timeline

Change in Model Parameters	Year of Occurrence	
	Configuration A	Configuration D
Concrete (waste tank top, sides, basemat, etc) starts to degrade hydraulically	400	500
Waste tank roof concrete transitions from Oxidized Region II to Oxidized Region III	800	1,000
Waste tank grout starts to degrade hydraulically	800	500
Concrete fully degraded hydraulically	800	501
Waste tank wall concrete transitions from Oxidized Region II to Oxidized Region III	600	1,000
Closure Cap reaches approximate steady state infiltration rate (11.5 in/yr)	2,625	2,625
Waste tank steel liner fails hydraulically	3,638	75
Waste tank basemat concrete transitions from Oxidized Region II to Oxidized Region III	4,600	1,000
Waste tank grout transitions from Reducing Region II to Oxidized Region II	10,500	5,500
CZ transitions from Reducing Region II to Oxidized Region II	10,500	400
Waste tank grout transitions from Oxidized Region II to Oxidized Region III	20,000	20,000
CZ transitions from Oxidized Region II to Oxidized Region III	20,000	600
Waste tank grout fully degraded hydraulically	20,000+	501

The Simplified model flow process for a single waste tank is provided below.

4.4.3.1 Closure Cap

A flow rate leaving the closure cap over time is determined in the closure cap sub-model. The infiltration rate into the closure cap top is based on the rainfall rates and the closure cap material properties (which are discussed in detail in Section 4.2.3.2.1). The flow rate out of the cap is calculated using the HELP code, with the closure cap modeled as degrading over time. The flow rate through the closure cap reaches a steady state value at approximately year 2500. Table 3.2-10 provides the time-variant infiltration rates based on the closure cap analysis presented in Section 3.2.4.

4.4.3.2 Waste Tank Top

The flow leaving the closure cap travels to the waste tank, with the flow rate being affected by the concrete tank top. Based on the relative hydraulic properties of the two materials (soil vs. concrete), some flow is directed around the waste tank into the surrounding soil, while some flow travels downward through the concrete. The concrete material properties (which are discussed in detail in Section 4.2.3.2.3) are modeled as changing over time. The only

waste tank top material properties of concern are the hydraulic properties, since the tank top impacts flow but does not retard contaminant transport (contaminant transport is only modeled as occurring near the CZ at the bottom of the tank). The waste tank top hydraulic properties are defined initially and in the fully degraded state, and a cementitious materials degradation analysis was performed to determine the time it would take to reach the fully degraded state (Table 4.2-32). Once the initial and end state times are set, the model assumes linear degradation of the hydraulic properties over time.

4.4.3.3 Waste Tank Top Liner

After passing through the concrete waste tank top, flow leaving the cap travels into the tank grout (for Type IV tanks and Type I/III/IIIA tanks after liner failure), or reaches the top of the tank liner and is deflected away from the tank (for Type I/III/IIIA tanks before liner failure time). The liner failure time was determined by an independent sub-model analysis (described in Section 4.2.3.2.5) for each tank type (the Type IV tanks do not have a top liner). Prior to failure the liner is modeled as being impermeable to both advection and diffusion. After failure, the liner has no further impact in the model.

4.4.3.4 Waste Tank Grout

Water enters the top of the waste tank grout and travels downward to the CZ at the bottom of the tank. The waste tank grout material properties (e.g., hydraulic conductivity, K_ds, which are discussed in detail in Section 4.2.3.2.3) are modeled as changing over time. In some configurations used in the sensitivity analyses (Section 4.4.2), fast flow paths through the grout are modeled resulting in a higher flow rate through the grout. The hydraulic properties are defined initially and in the fully degraded state, and a cementitious materials degradation analysis was performed to determine the time it would take to reach the fully degraded state (Table 4.2-32). Once the initial and end state times are set, the model assumes linear degradation of the grout hydraulic properties over time.

Table 4.2-33, provides K_d values for cementitious materials as a function of aging, with the grout "age" dependent on the pH of the concrete pore water, which in turn is dependent upon the amount of water (number of pore volumes) that has passed through the concrete over time. A description of pore water chemistry modeling is provided in the Section 4.4.3.5.

The grout material properties of principal concern are the hydraulic properties, since the only time the K_d values are a factor in the model are when contaminants move upward from the CZ into the grout. The only time frame in which upward contaminant transfer is significant is for the Type IV tanks, which do not have a top steel liner, so that prior to liner failure, flow into the Type IV tanks may be contained, forcing contaminants to flow upwards into the grout. The contaminant transport is impacted by the K_d values as it moves into and out of the grout. The grout hydraulic properties influence the water flow rate through the waste tank. The earlier the grout degrades, the earlier the flow rate through the waste tank reaches a steady state maximum flow.

4.4.3.5 Contamination Zone

In the model, the waste tank residual inventory is assumed to be contained within a thin layer (i.e., the CZ) at the bottom of the tank. The release rate of contaminants from the CZ is

solubility controlled and is tied to the chemical properties (e.g., Eh, pH) of the tank pore water. The release rate from the CZ is independent of the grout or CZ K_ds. The assumed solubility limit varies depending on waste tank pore water chemistry and the controlling phase of the radionuclide being released. Different solubility limits for different waste tank chemistries were derived for the radionuclides in the CZ (as discussed in Section 4.2.2). Additional emphasis and analysis was placed on those radionuclides shown during initial modeling to have the most impact on peak dose (Pu, Np, U, Tc), including an uncertainty study and development of stochastic distributions for alternative controlling phases (Section 4.2.2.3).

As pore volumes pass through the waste tank, the pH and reducing capability of the grout is affected. The number of pore water volumes passing through the waste tank and the corresponding transitions to different tank chemistry conditions is included in the FTF modeling. As part of the waste release modeling (discussed in detail in Section 4.2.2), the estimated transition times between various chemical phases was calculated for the waste tank pore water. The waste tank pore water chemistry was calculated to change from Region II Reduced conditions (Middle Age Reducing) to Region II Oxidized conditions (Middle Age Oxdizing) after 371 pore volumes have passed through the reducing grout. The change from Region II conditions (Middle Age) to Region III conditions (Old Age) was calculated to occur after 2,063 pore volumes (Table 4.2-1).

4.4.3.6 Tank Liner Sides and Bottom

After leaving the CZ and entering the tank pore water, the tank contaminants do not leave the tank until the tank liner fails. For the Type IV tanks (which do not have a top liner) waste leaving the CZ can migrate into the waste tank grout (based on the grout properties) since it can't flow downward. The liner failure time was determined by analysis for each tank type, with both the primary and secondary liner (where applicable) failing at the same time. While it utilizes many of the same assumptions, the tank liner analyses calculate failure times independent of the flow and transport model. As discussed in Section 4.4.3.3, when the liner fails, it is assumed to fail completely, with the modeled failed liner layer having no further impact in the model.

4.4.3.7 Basemat

After contaminants exit the waste tank liner, they enter the concrete tank basemat located directly below the liner. The waste tank grout material properties (which are discussed in detail in Section 4.2.3.2.3) are modeled as changing over time. The material properties of the concrete impact both the flow rate through the basemat and the K_d value. The hydraulic properties are defined initially and in the fully degraded state, and a cementitious materials degradation analysis was performed to determine the time it would take to reach the fully degraded state (Table 4.2-32). Once the initial and end state times are set, the model assumes linear degradation of the basemat hydraulic properties over time. In some sensitivity configurations, fast flow paths through the basemat are modeled resulting in a higher flow rate through the basemat.

Contaminant transport is retarded by the basemat concrete, with some radionuclides being slowed greatly depending on their K_ds. Table 4.2-33, provides K_d values for cementitious

materials as a function of aging, with the grout "age" dependent on the pH of the concrete pore water, which in turn is dependent upon the amount of water (number of pore water volumes) that has passed through the concrete over time. A description of pore water chemistry modeling is provided in the Section 4.4.3.5. As the waste tank chemistry changes, the concrete transitions from young (Region I) to middle (Region II) to old (Region III), and the associated material properties are modeled as changing.

4.4.3.8 Vadose Zone Beneath the Waste Tank

After contaminants exit the basemat, they enter the vadose zone (e.g., soil) beneath the waste tank, which is discussed in detail in Section 4.2.3.2.2. The vadose zone material properties impact both the flow rate through the soil and the associated K_d values, with both being important to the model. The vadose zone depth below each waste tank can vary depending on the tank involved, as shown in Table 4.2-23. The vadose zone material properties are not modeled as changing over time. In the probabilistic model however, the vadose zone thickness was allowed to vary, which did impact transport time through the soil. The working slabs under waste tank basemats were not explicitly modeled and instead were simply assumed to be soil. Given the thinness of the working slabs relative to the waste tank basemats, as well as the the possibility of cracks in the working slabs, it is appropriate to disregard the working slabs in modeling contaminant transport through the waste tank bottom and basemat into the vadose zone.

4.4.4 Modeling Process

Figure 4.4-11 illustrates the general process followed in implementing the ISCM and presents the three component models and their key inputs.

Some inputs, as indicated by the legend on Figure 4.4-11, involved fixed parameters that do not change over time. These are generally shown on the left side of the figure. The inputs on the right side of the figure do change over time.

As shown in Figure 4.4-11, and as explained previously, six waste tank configurations and one ancillary equipment configuration were used for the probabilistic model runs, which are accomplished using the applicable computer codes identified in Section 4.3. These configurations are analyzed by running the model using different combinations as discussed above. The PORFLOW FTF model was used to simulate the flow behavior for the six configurations. The baseline results are reflected through Tank Configuration A PORFLOW FTF contaminant transport modeling. Sensitivity and uncertainty analyses were also performed using the multiple configurations and variations of the individual parameters modeled as part of a configuration. The GoldSim model used the PORFLOW FTF model flow results and other parameter distributions to provide a range of possible outcomes, and to identify those parameters of most interest.

The Base Case analysis provided baseline contaminant concentrations in groundwater and surface water. The data for radiological contaminants was used in combination with the inputs related to receptor dose shown on Figure 4.4-11 to calculate impacts on various receptors. The data for non-radiological contaminants was used as specified in Section 4.8 to determine the resulting risk.

Figure 4.4-11: Model Process Flow

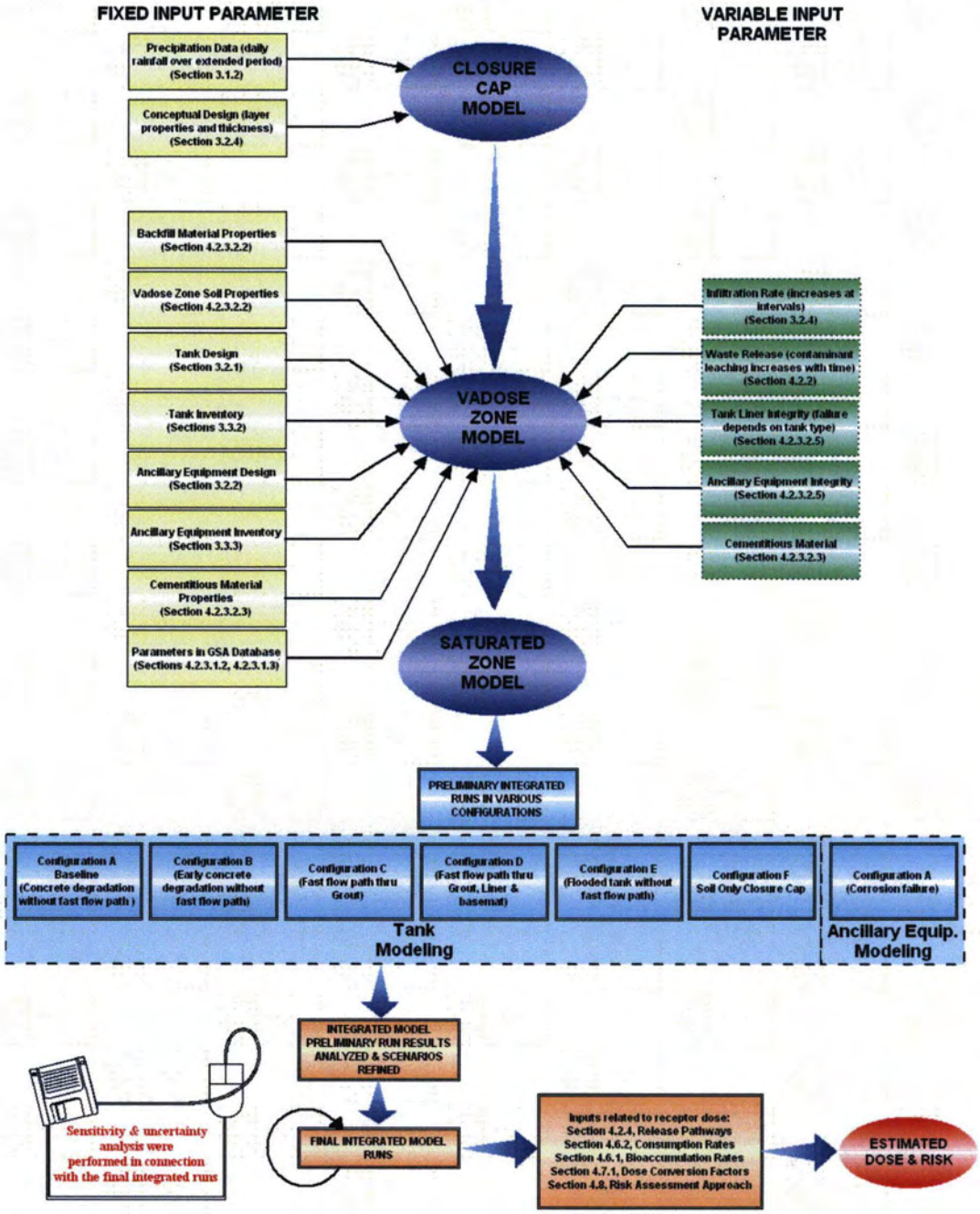

4.4.4.1 PORFLOW Modeling Process

- **Regional (GSA) and Local (FTF) Modeling in PORFLOW**

The PORFLOW computer code was used to model FTF flow for all configurations and transport for the Base Case. Regional (GSA) modeling in PORFLOW was developed using a 200 foot x 200 foot grid, with the primary focus being on seepline concentration (Figure 4.4-12). Most of the groundwater flow paths discharge to UTR, which more deeply incises the terrain in comparison to Fourmile Branch. The abrupt clockwise turn in some pathlines coincides with passage through the Gordon confining unit from the UTR aquifer to the Gordon aquifer. The two aquifers exhibit different flow directions in this area.

Figure 4.4-12: PORFLOW GSA Modeling

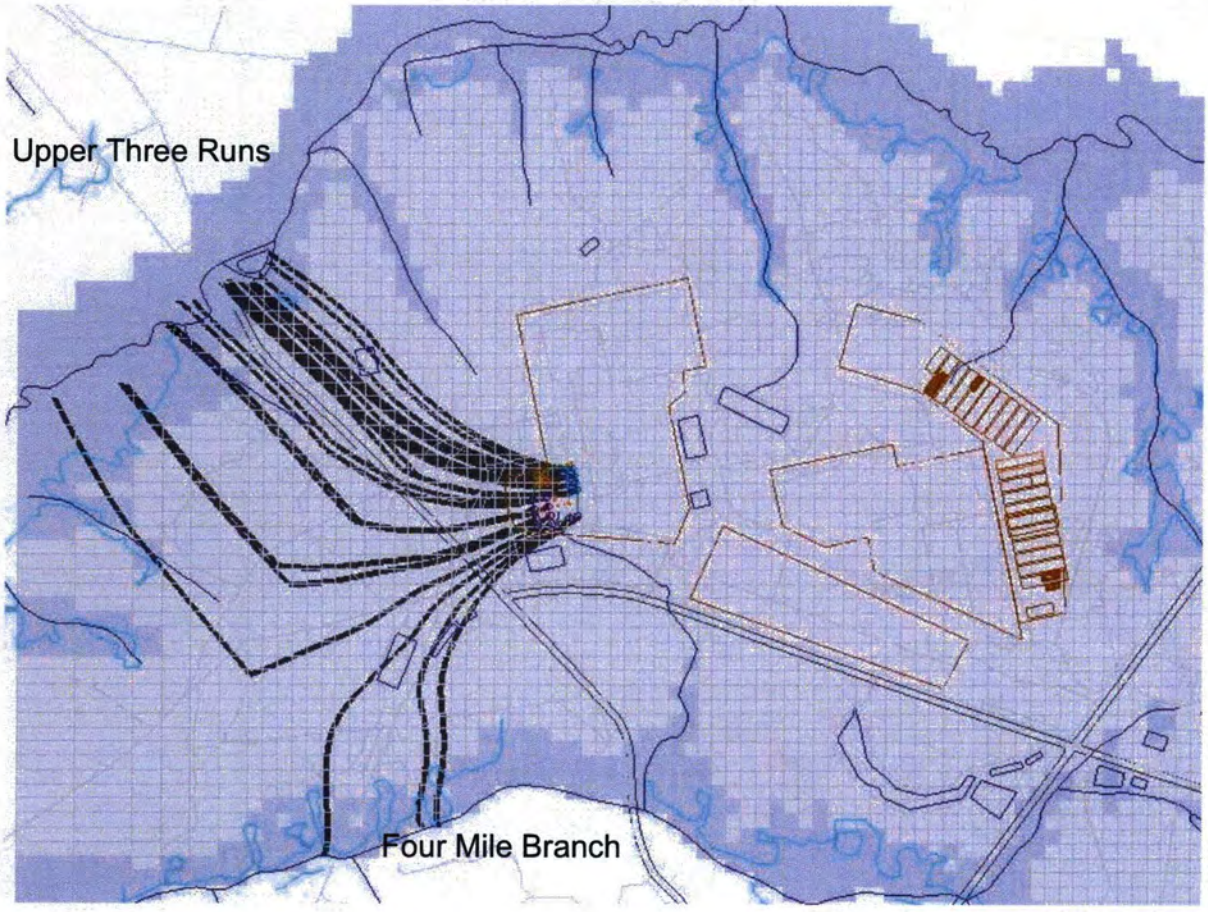

FTF modeling was developed from GSA scale model using a 50 foot x 50 foot grid refinement, with the primary focus being on the 1m and 100m concentrations (Figure 4.4-13). A grid resolution finer than 200 feet x 200 feet is required to avoid excessive numerical dispersion at the 100m scale. The FTF velocity field is generated directly from the coarser scale GSA velocity model using a mass-conserving linear interpolation scheme, rather than a separate flow model requiring its own boundary conditions and properties. This approach ensures strict consistency between the two aquifer flow fields, apart from resolution. The FTF velocity field includes the entire vertical extent of the GSA model within the horizontal confines of the FTF domain. The stream tracers from the FTF waste tanks are shown in Figure 4.4-13. Ten year time markers (red dots) indicate a 10 – 20 year travel time in the saturated zone between waste tanks and the 100m perimeter (grey diamonds). In aquifer transport modeling, hydrodynamic dispersion is represented by longitudinal and transverse dispersivities of 10m and 1m, respectively, which are 10% and 1% of a nominal 100m plume travel distance. Both the GSA and FTF scale models have been shown to preserve mass to adequate tolerances. [WSRC-TR-2004-00106, Q-SQP-G-00003]

Figure 4.4-13: PORFLOW FTF Modeling

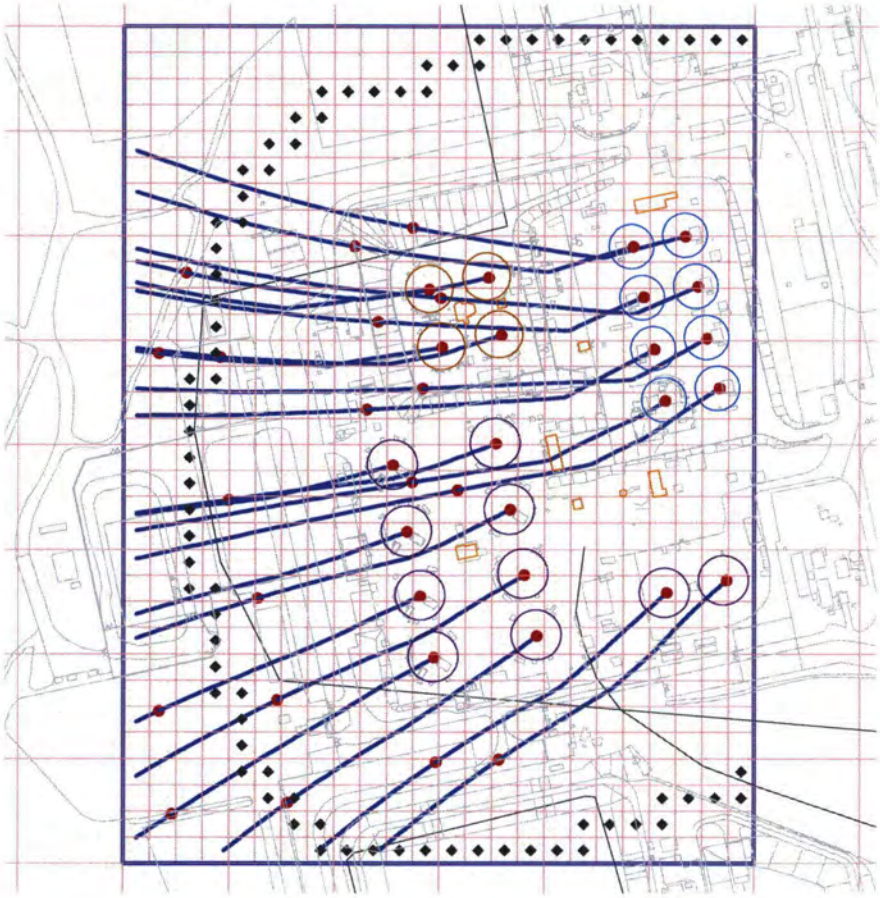

➢ **General Vadose ZoneTank Modeling in PORFLOW**

The waste tanks and surrounding vadose zone soils are modeled in PORFLOW as an axisymmetric, two-dimensional, radial cut (unit radian pie wedge). Up to 20 distinct material zones are used in PORFLOW to represent different materials and to reflect different flow scenarios (e.g., fast flow paths). Approximately 5,000 grid blocks were used to represent each of the four different tank types (grid varies with tank type). A graphic depiction of the PORFLOW grids modeling for the various tank types, including a lower corner detail, is provided in Figures 4.4-14 through 4.4-19 (the Type IIIA tanks are similar to the Type III tanks, so no separate graphic is shown). Figure 4.4-20 shows a portion of the fast flow path (when activated) for a Type IV tank. Tank depth to the vadose zone is modeled as a uniform depth for a particular tank type (i.e., one depth for all Type I tanks) using an average of the values in Table 4.2-23 for the associated tank type. The chosen grid resolution is a compromise between two competing objectives: 1) resolution of thin geometric features (e.g., CZ, liners) and sharp flow field transitions (e.g., ponded water flowing over roof edge), and 2) achieving reasonable computer storage and runtimes. Each grid extends 30 feet beyond the outside radius of a waste tank to represent average conditions. At certain angles, obstructions such as adjacent waste tanks are present at shorter distances. A sensitivity study indicates insignificant impact on water table flux for a grid extending to the shorter half-distance between waste tanks. PORFLOW material properties for native soil utilize Section 4.2.3.2.2 parameters for vadose zone soil and for backfill utilize Section 4.2.3.2.2 parameters for backfill soil. Figures 4.4-21 through 4.4-32 display the flow fields for the various tank types over time. The figures are color coded to show the areas of highest saturation (dark blue) and have arrows which denote the flow magnitude. The figures show how PORFLOW models flow and how flow changes over time, affecting tank changes (e.g., cap degradation, grout degradation, liner failure).

Hydrodynamic dispersion is neglected in vadose transport modeling, because most materials are homogeneous (e.g., concrete) or relatively so (e.g., backfilled soil). Preferential flow pathways through cracks, fractures, or other discrete features are modeled using one of two methods, depending on scale. Small-scale features are implicitly represented as a general increase in saturated hydraulic conductivity within a porous medium formulation. Large-scale features are explicitly represented in a porous medium formulation as discrete zones of high permeability (e.g., sand seam). A porous, rather than fractured, medium approach was considered superior because: 1) smaller scale crack/fracture geometry and other properties have not been defined for the degraded material of interest; 2) the scenarios of interest for the FTF PA can be adequately represented in the simpler porous medium approach.

Figure 4.4-14: PORFLOW Type I Tank Model

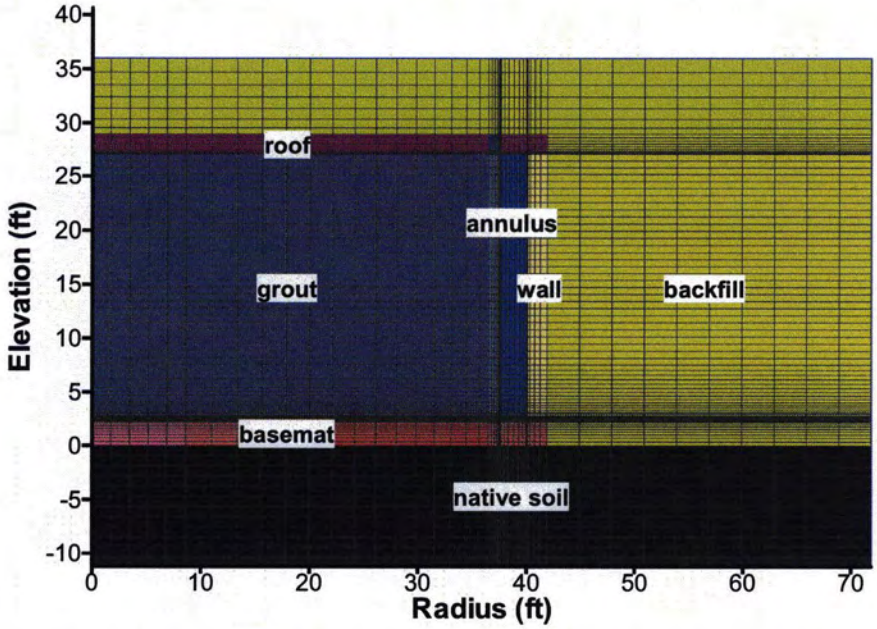

Figure 4.4-15: PORFLOW Type I Tank Model, Lower Corner Details

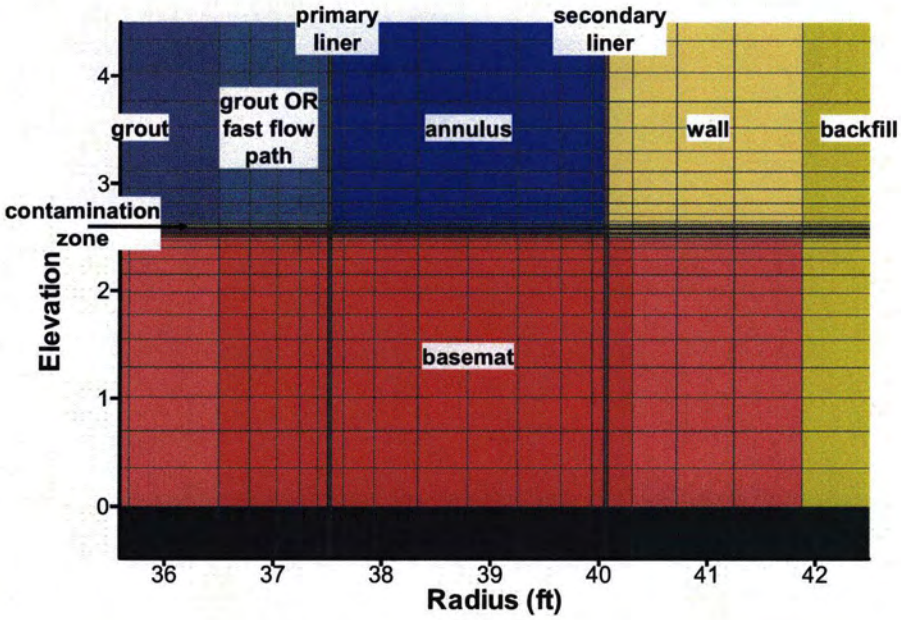

Figure 4.4-16: PORFLOW Type III Tank Model Details

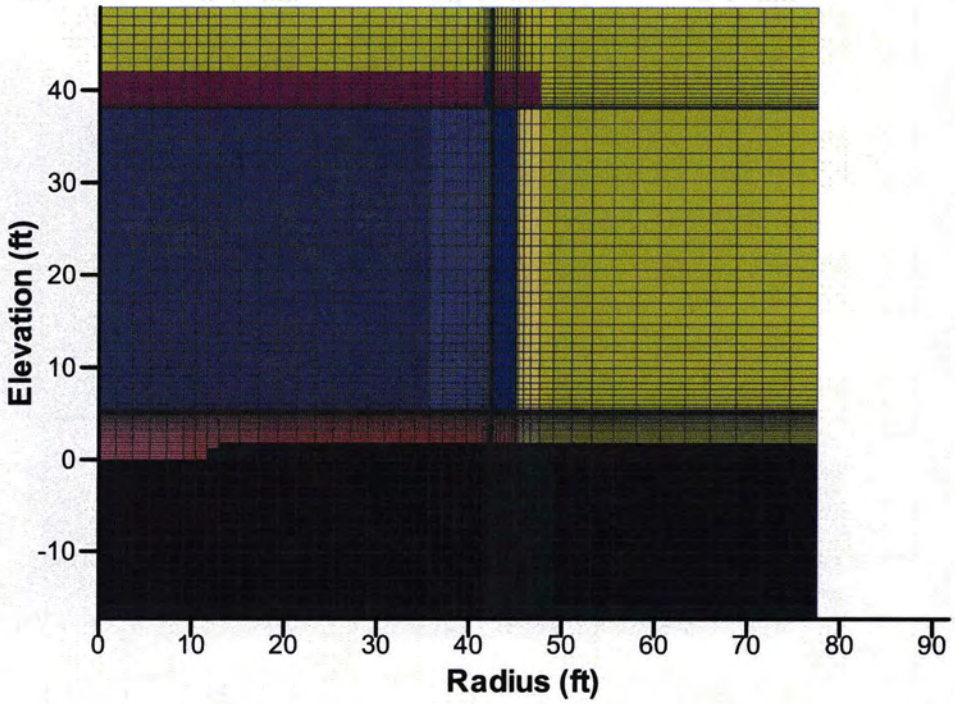

Figure 4.4-17: PORFLOW Type III Tank Model, Lower Corner Details

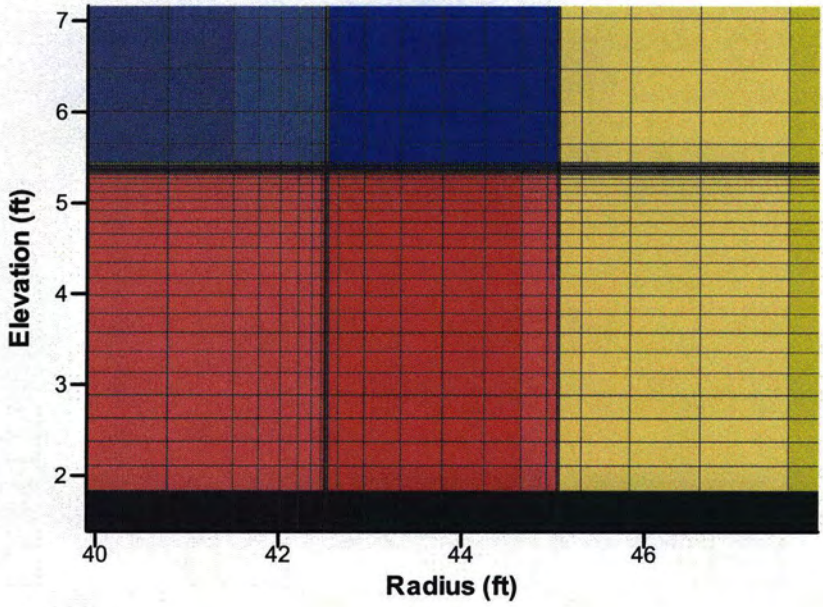

Figure 4.4-18: PORFLOW Type IV Tank Model, Domed Roof Explicitly Modeled

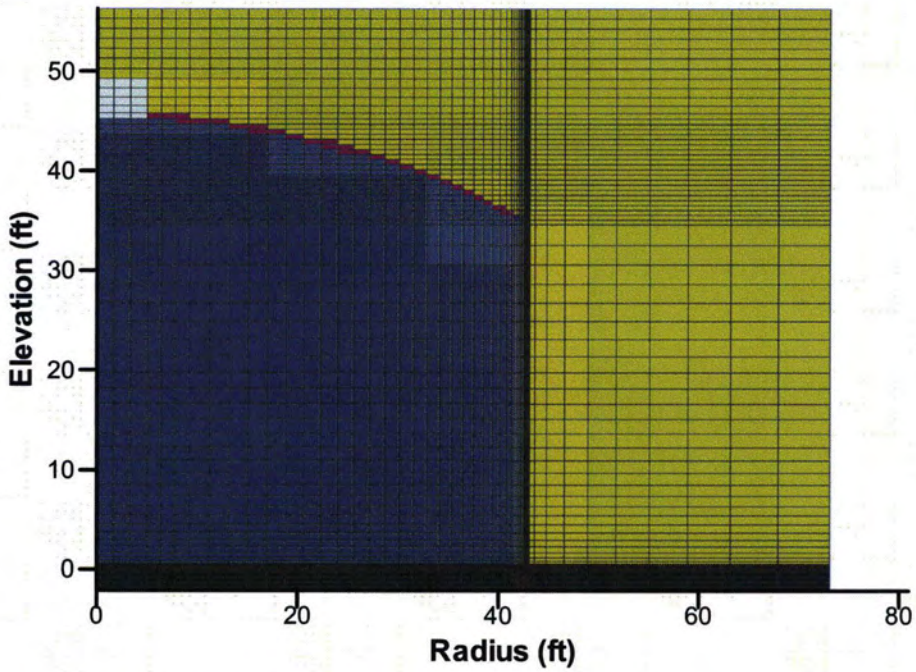

Figure 4.4-19: PORFLOW Type IV Tank Model Lower Corner Detail

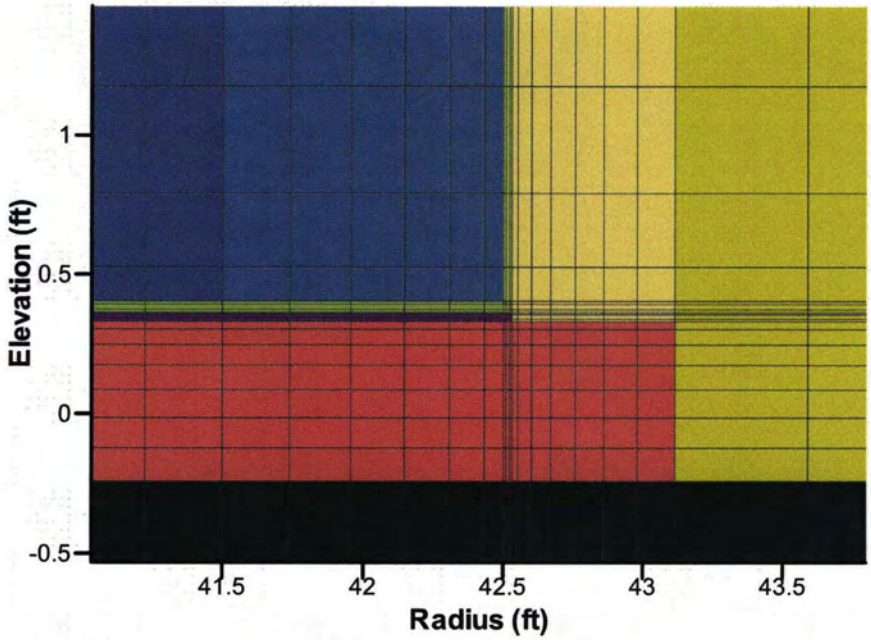

Figure 4.4-20: PORFLOW Type IV Tank Model Tank Top Corner Detail

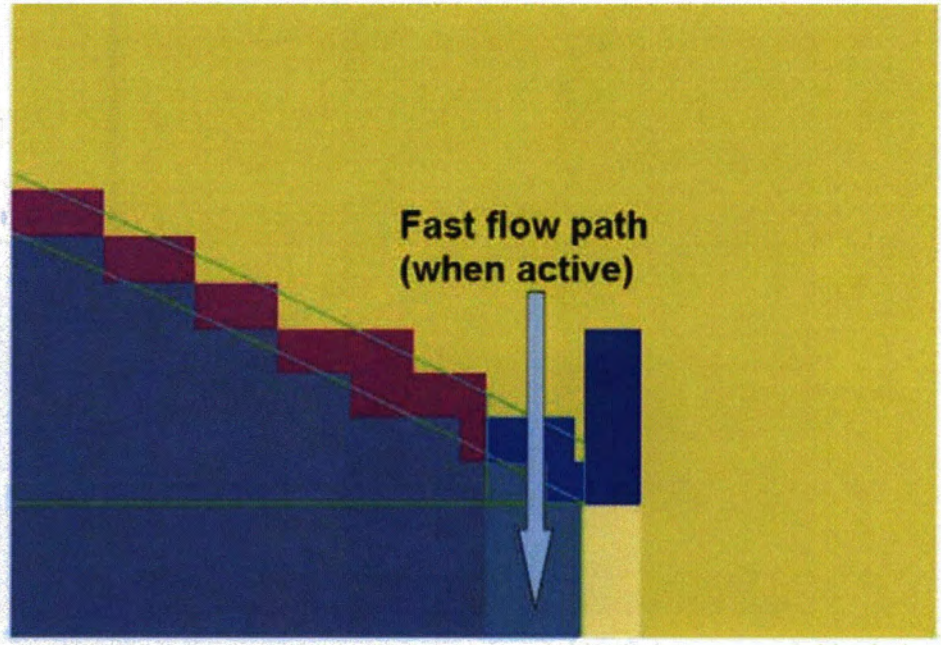

Figure 4.4-21: Type I Tank Flow Field – Year 100

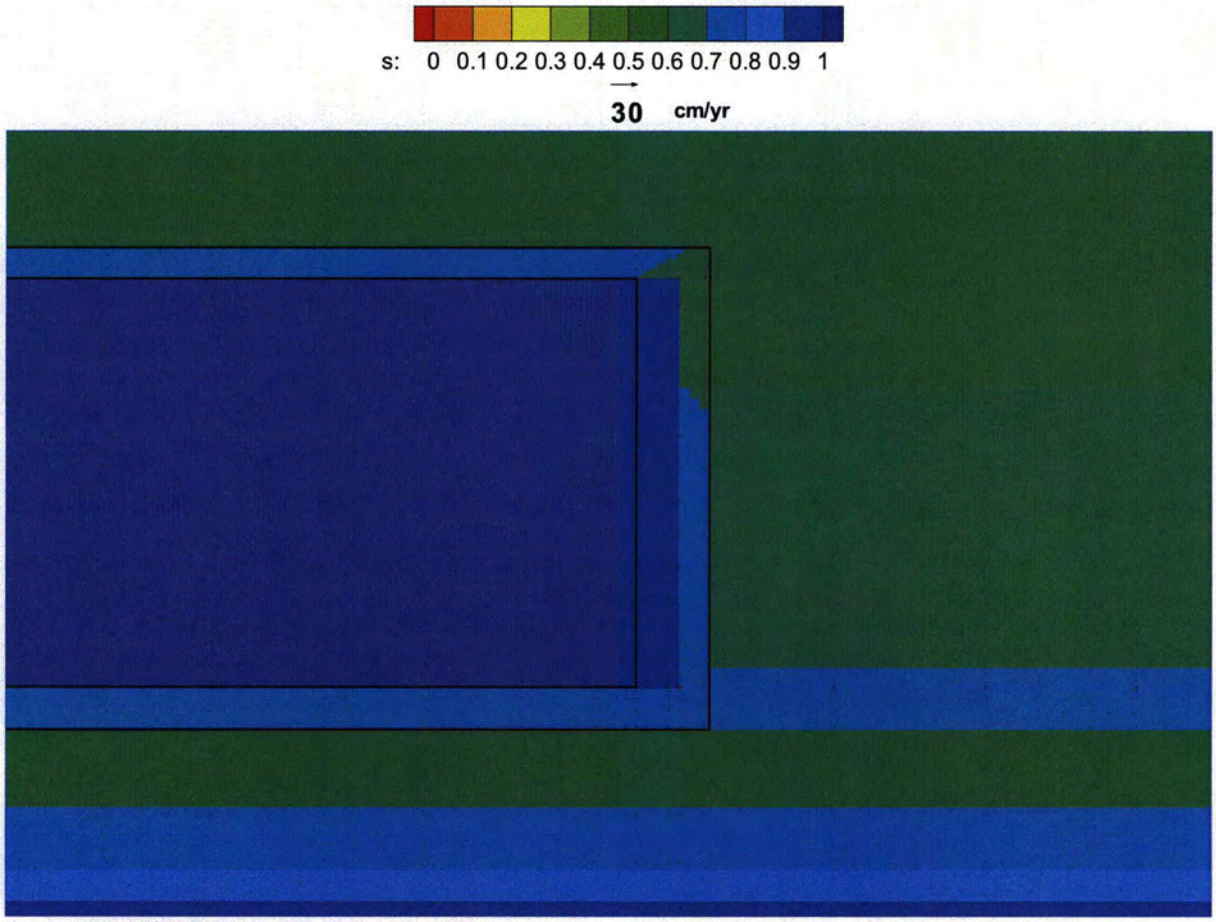

(s: = saturation)

Figure 4.4-22: Type I Tank Flow Field – Year 10,000

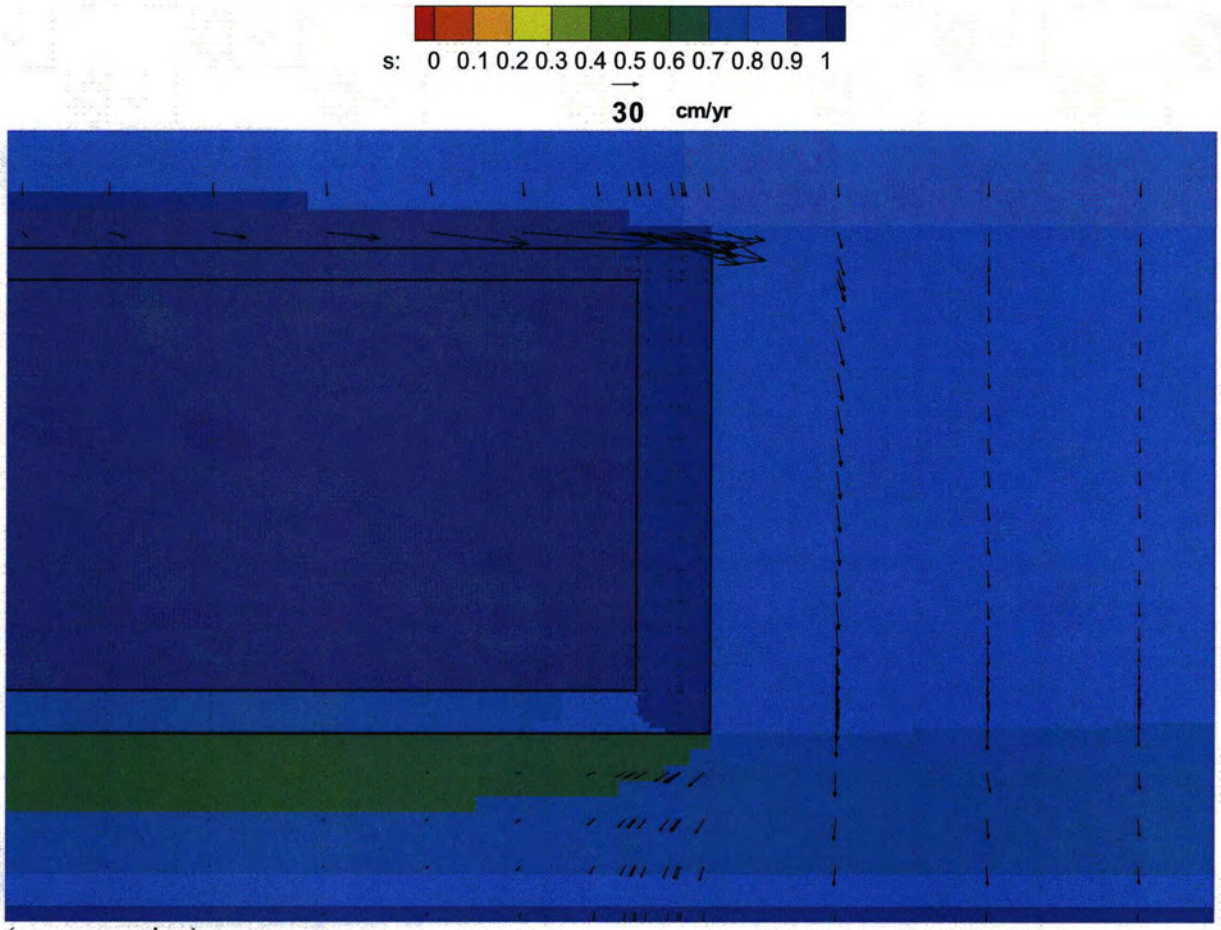

(s: = saturation)

Figure 4.4-23: Type I Tank Flow Field – Immediately Prior to Liner Failure

(s: = saturation)

Figure 4.4-24: Type I Tank Flow Field – Year 20,000

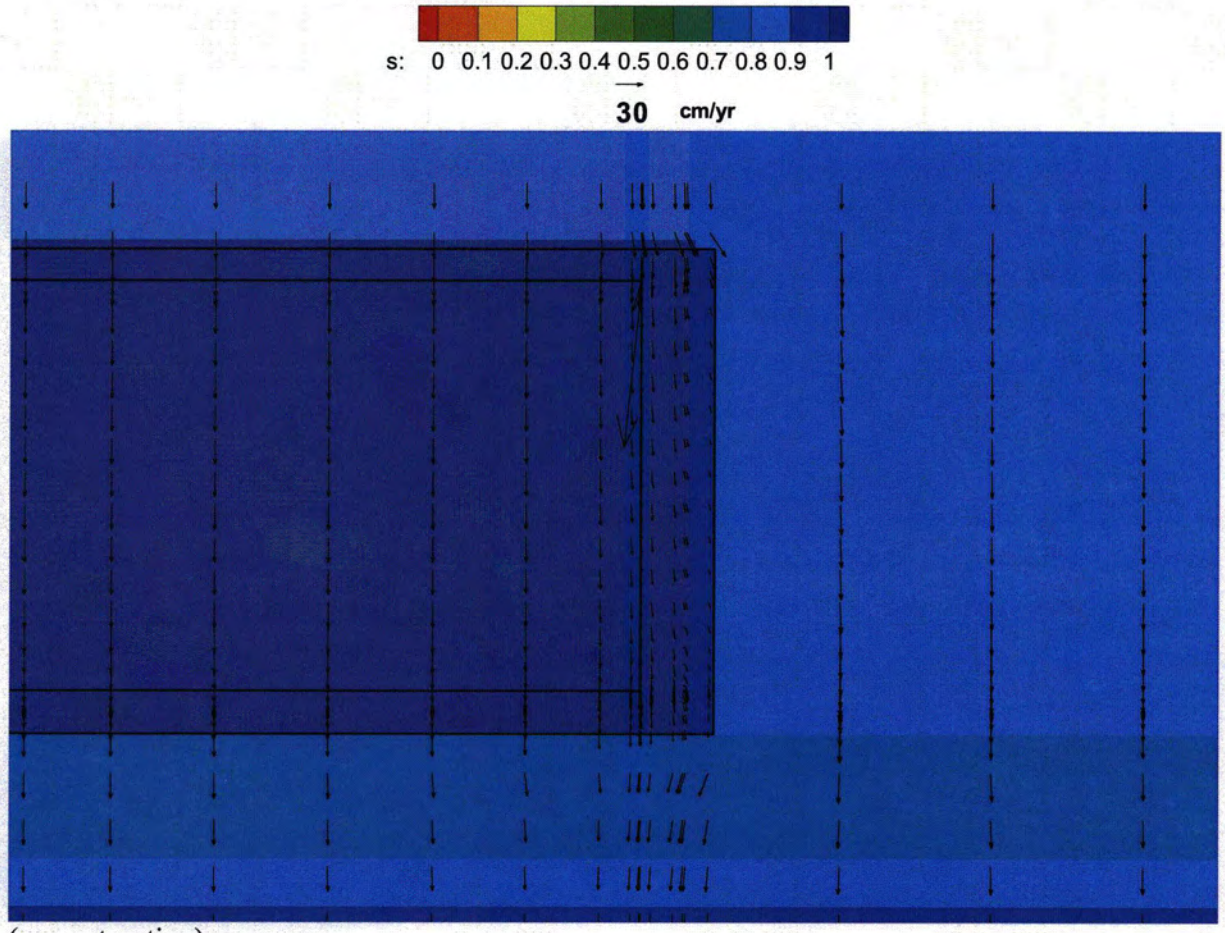

(s: = saturation)

Figure 4.4-25: Type IV Tank Flow Field – Year 100

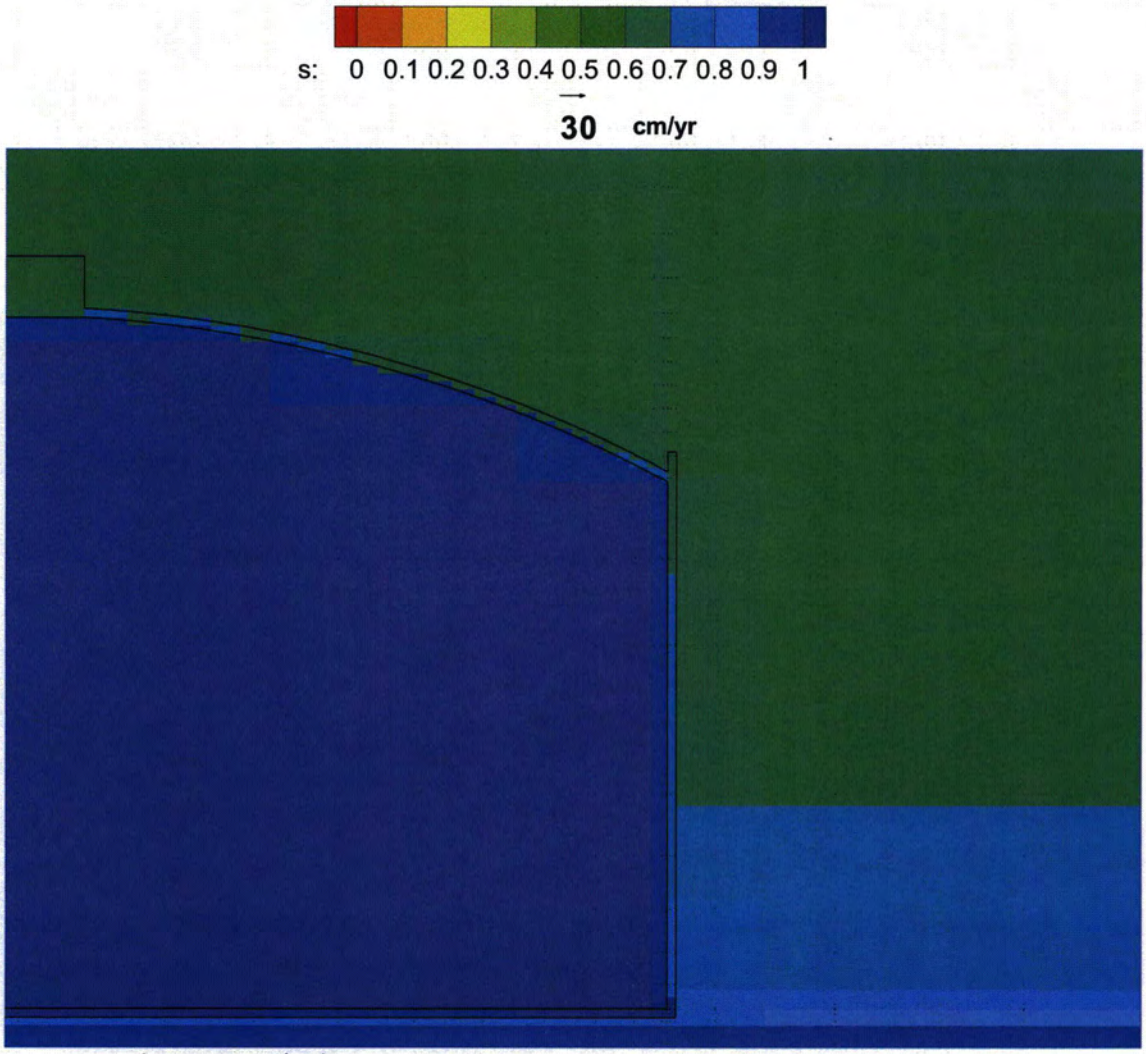

(s: = saturation)

Figure 4.4-26: Type IV Tank Flow Field – Immediately Prior to Liner Failure

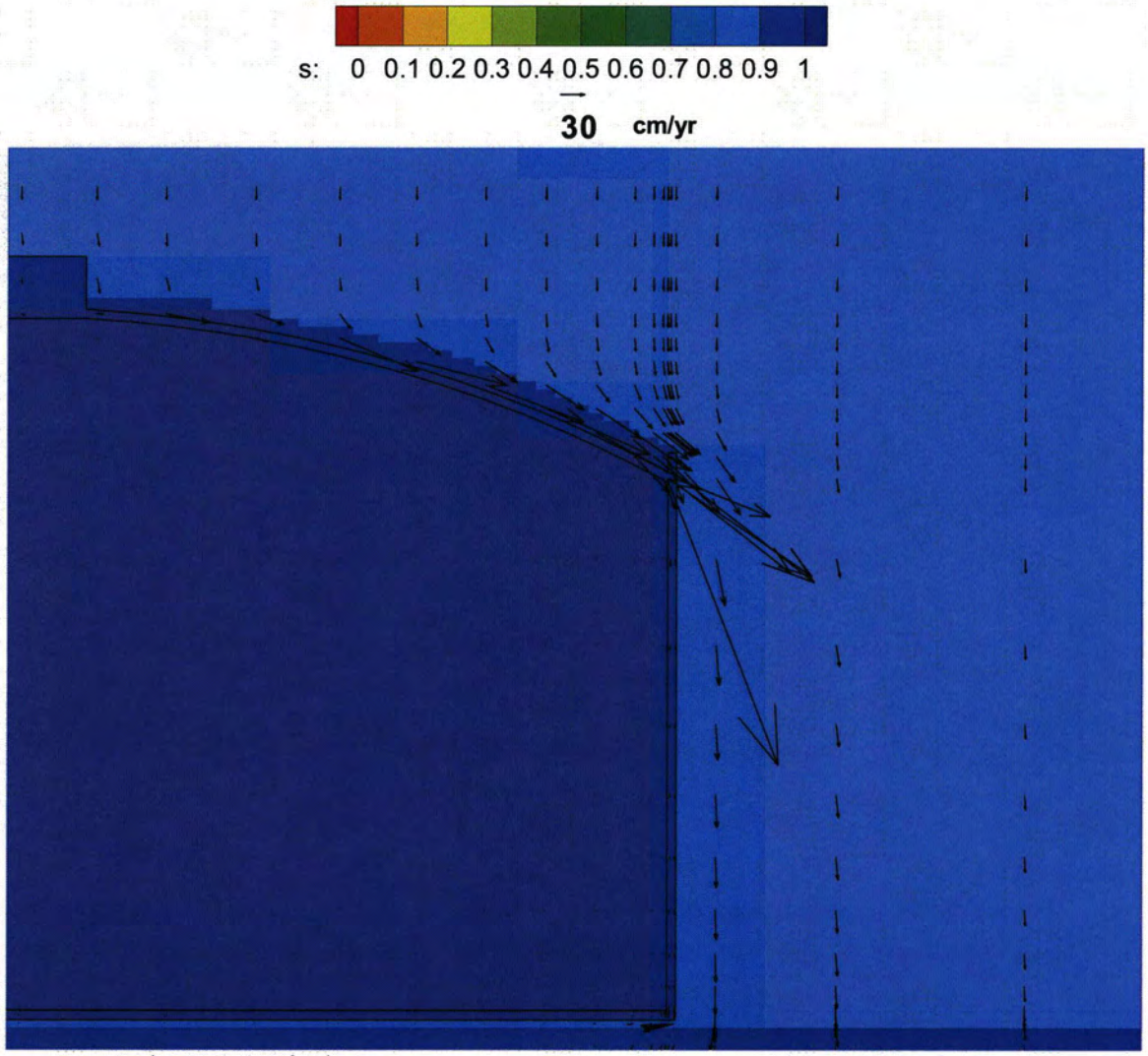

(s: = saturation)

Figure 4.4-27: Type IV Tank Flow Field – Year 10,000

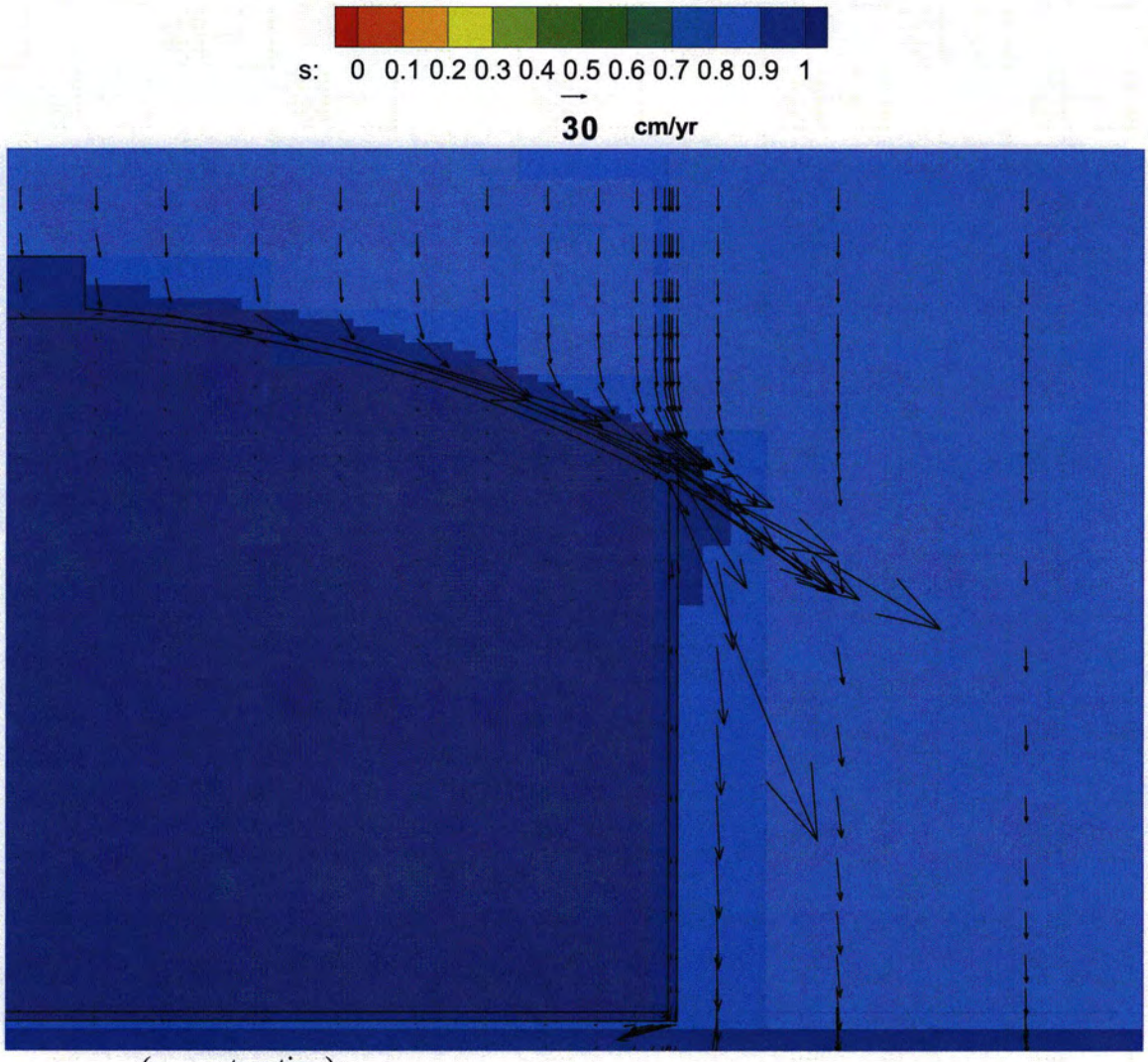

(s: = saturation)

Figure 4.4-28: Type IV Tank Flow Field – Year 20,000

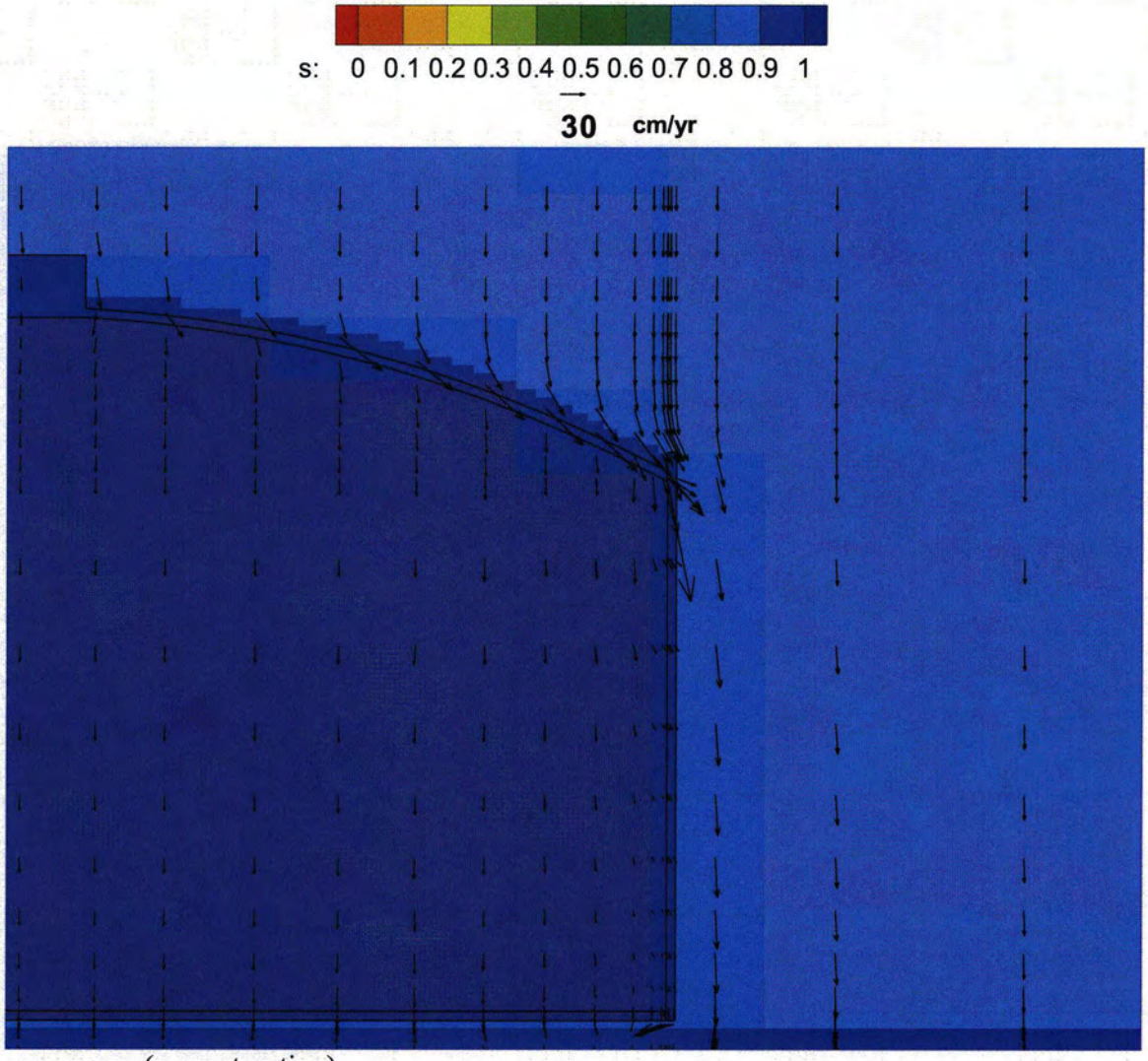

(s: = saturation)

Figure 4.4-29: Type III Tank Flow Field – Year 100

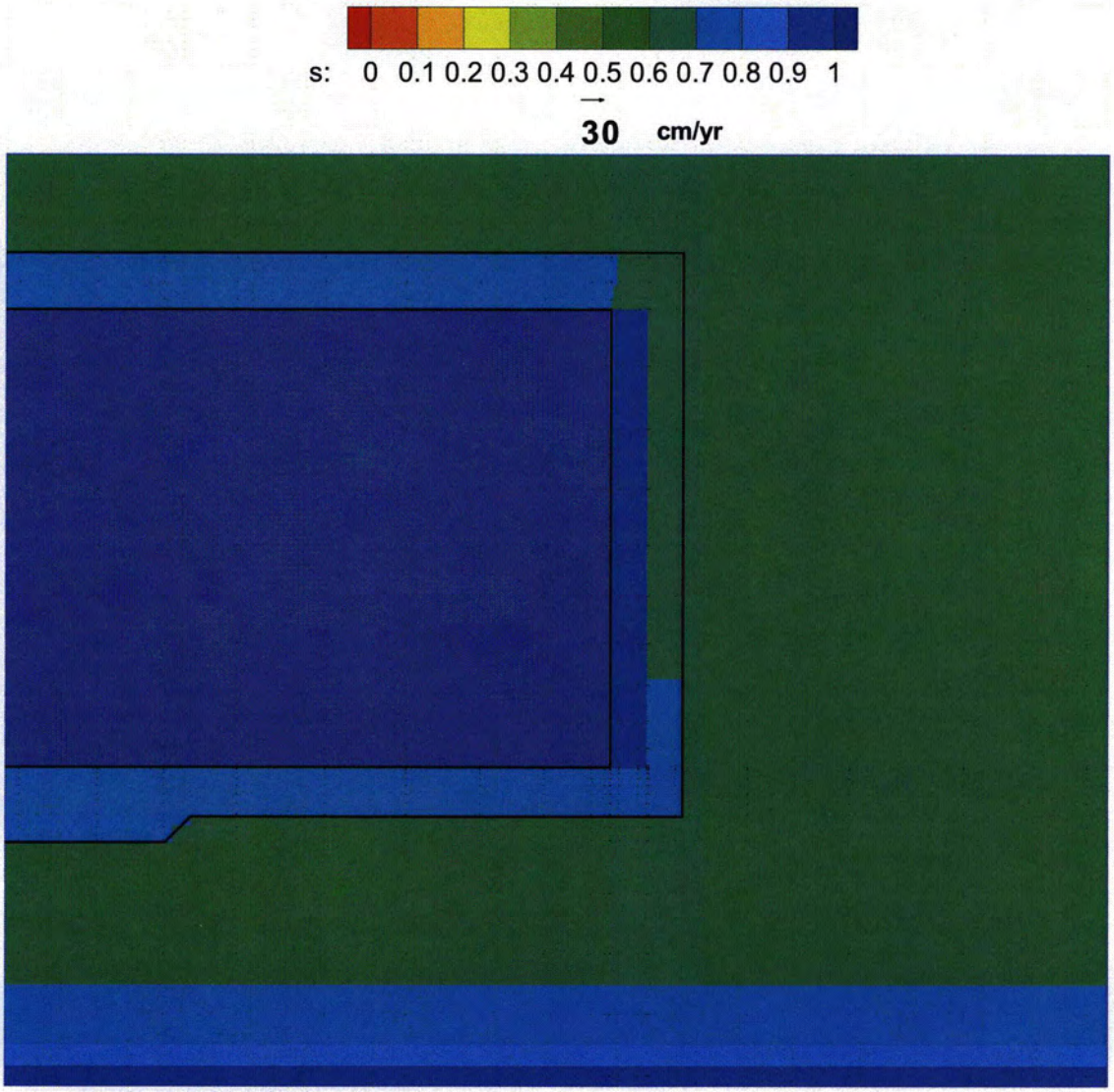

(s: = saturation)

Figure 4.4-30: Type III Tank Flow Field – Year 10,000

(s: = saturation)

Figure 4.4-31: Type III Tank Flow Field – Immediately Prior to Liner Failure

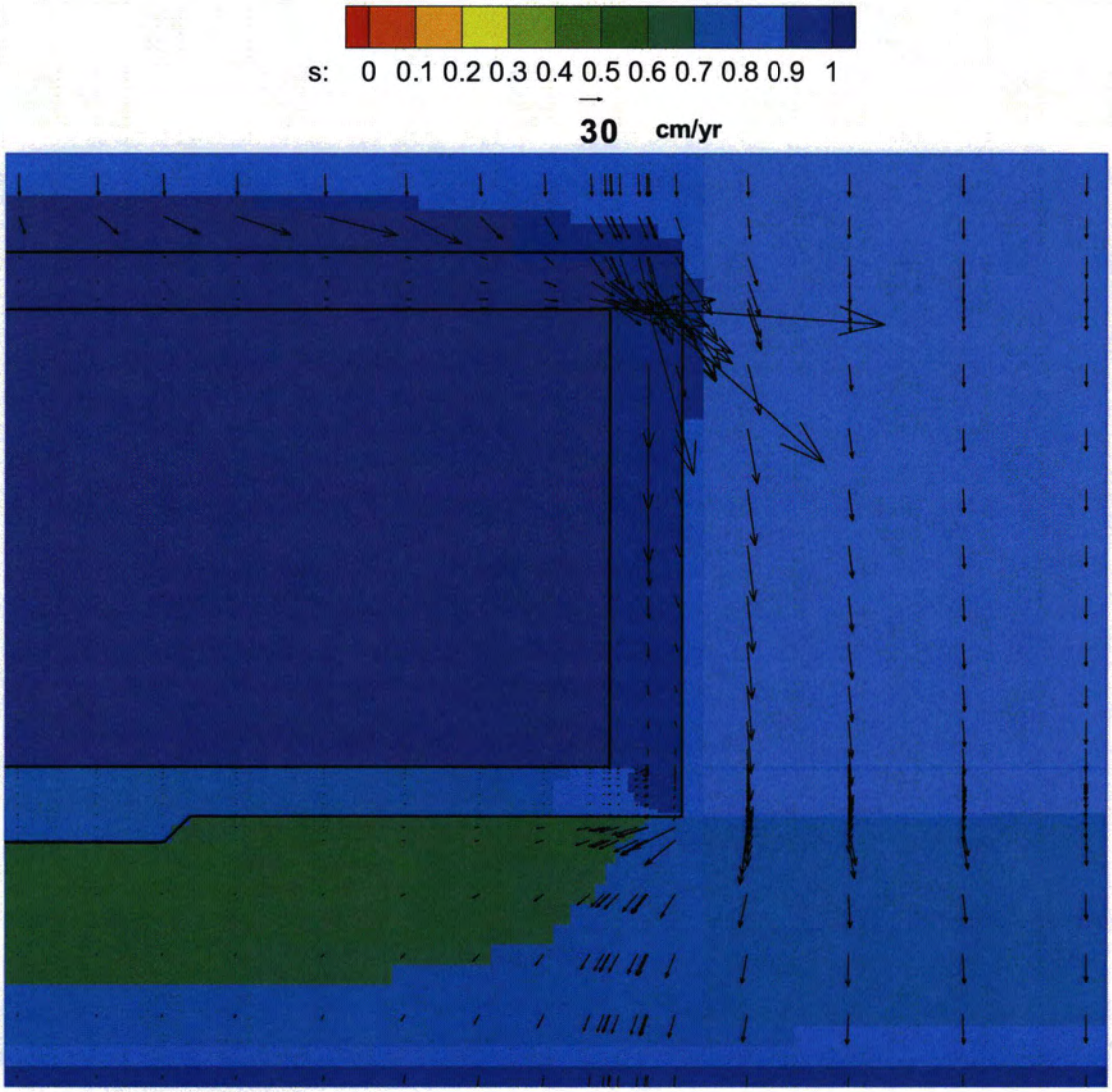

(s: = saturation)

Figure 4.4-32: Type III Tank Flow Field – Year 20,000

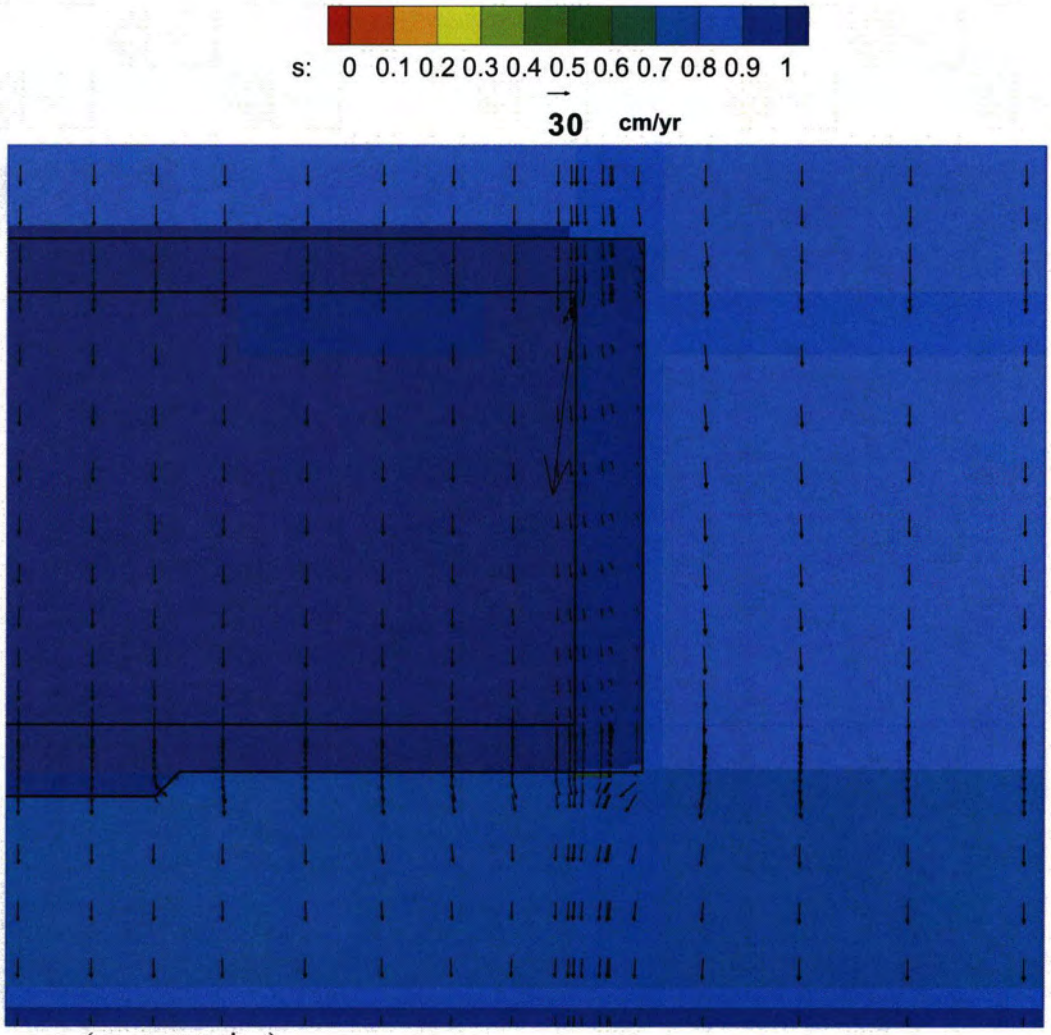

(s: = saturation)

Material properties are independently defined for each grid zone, but are not necessarily different, depending on scenario). Properties are defined as the product of these factors:

- Base value from a materials palette, a time-invariant constant,
- Time-dependent factor #1, intended to represent baseline physical changes,
- Time-dependent factor #2, intended for sensitivity/uncertainty analysis perturbations

The materials palette used in PORFLOW FTF modeling is provided in Table 4.4-6. The latter two factors defining properties can be arbitrary piecewise-linear functions. They are functionally identical, and differ only in intended usage.

Table 4.4-6: PORFLOW Materials Palette

ID_cementitious	Saturated Hydraulic Conductivity. Ks (cm/sec)	Saturated Hydraulic Conductivity. Ks (cm/yr)1	Saturated Hydraulic Conductivity. Ks (cm/sec)	Saturated Hydraulic Conductivity Ks (cm/yr)1	Saturated Effective Diffusion Coeficient De (cm2/sec)	Saturated Effective Diffusion Coeficient De (cm2/yr)2	Effective Porosity (%)	Total Porosity (unitless)	Dry Bulk Density (g/cm3)	Particle Density (g/cm3)
Id 1	Kh_cm/sec 2	Kh_cm/yr 3	Kv_cm/sec 4	Kv_cm/yr 5	De_cm2/sec 6	De_cm2/yr 7	por_% 8	Por 9	rhob_g/cm3 10	rhop_g/cm3 11
UpperVz	6.2E-05	2.0E+03	8.7E-06	2.7E+02	5.3E-06	167.26	39	0.39	1.65	2.70
native_soil	3.3E-04	1.0E+04	9.1E-05	2.9E+03	5.3E-06	167.26	39	0.39	1.62	2.66
OscBefore	1.2E-04	3.8E+03	1.2E-04	3.8E+03	5.3E-06	167.26	46	0.46	1.44	2.65
OscAfter	1.4E-05	4.4E+02	1.4E-05	4.4E+02	4.0E-06	126.23	27	0.27	1.92	2.65
backfill	7.6E-05	2.4E+03	4.1E-05	1.3E+03	5.3E-06	167.26	35	0.35	1.71	2.63
IlvPermeableBackfill	1.4E-03	4.4E+04	7.6E-04	2.4E+04	8.0E-06	252.46	41	0.41	1.56	2.64
SingleVadoseZone	1.9E-04	6.0E+03	3.0E-05	9.5E+02	5.3E-06	167.26	39	0.39	1.63	2.67
Sand	5.0E-04	1.6E+04	2.8E-04	8.8E+03	8.0E-06	252.46	38	0.38	1.65	2.66
ClaySand	8.3E-05	2.6E+03	2.1E-05	6.6E+02	5.3E-06	167.26	37	0.37	1.68	2.67
Clay	2.0E-06	6.3E+01	9.5E-07	3.0E+01	4.0E-06	126.23	43	0.43	1.52	2.67
Gravel	1.5E-01	4.7E+06	1.5E-01	4.7E+06	9.4E-06	296.64	30	0.30	1.82	2.60
basemat	3.5E-08	1.10E+00	3.5E-08	1.10E+00	8.0E-07	25.25	16.8	0.168	2.06	2.51
grout	3.6E-08	1.14E+00	3.6E-08	1.14E+00	8.0E-07	25.25	26.6	0.266	1.81	2.51
wall_roof	3.5E-08	1.10E+00	3.5E-08	1.10E+00	8.0E-07	25.25	16.8	0.168	2.06	2.51
contaminated_zone	3.6E-08	1.14E+00	3.6E-08	1.14E+00	8.0E-07	25.25	26.6	0.266	1.81	2.51
primary_liner	5.0E-15	1.6E-07	5.0E-15	1.6E-07	1.0E-13	3.16E-06	39	0.39	N/A	2.70
secondary_liner	5.0E-15	1.6E-07	5.0E-15	1.6E-07	1.0E-13	3.16E-06	39	0.39	N/A	2.70
primary_vert_liner	5.0E-15	1.6E-07	5.0E-15	1.6E-07	1.0E-13	3.16E-06	39	0.39	N/A	2.70
secondary_vert_liner	5.0E-15	1.6E-07	5.0E-15	1.6E-07	1.0E-13	3.16E-06	39	0.39	N/A	2.70
ff_grout	5.0E-04	1.6E+04	2.8E-04	8.8E+03	8.0E-06	252.46	38	0.38	1.65	2.66
ff_basemat	5.0E-04	1.6E+04	2.8E-04	8.8E+03	8.0E-06	252.46	38	0.38	1.65	2.66
ff_roof	5.0E-04	1.6E+04	2.8E-04	8.8E+03	8.0E-06	252.46	38	0.38	1.65	2.66
ff_p_liner	5.0E-04	1.6E+04	2.8E-04	8.8E+03	8.0E-06	252.46	38	0.38	1.65	2.66
ff_s_liner	5.0E-04	1.6E+04	2.8E-04	8.8E+03	8.0E-06	252.46	38	0.38	1.65	2.66

➢ **Fast Flow Path Modeling in PORFLOW**

PORFLOW was used early in the analysis process to do scoping runs for the various configurations described in Section 4.4.2. To represent the effect of a hypothetical fast flow path through a waste tank (Figure 4.4-33), the PORFLOW model assumed all water being shed from the tank roof was intercepted by a high conductivity vertical leg encircling the tank perimeter just inside the primary liner. Horizontal flow then takes place through the CZ, which is also assigned a large conductivity, with the entire CZ assumed to be contacted by infiltrating water. Contaminant transport was then assumed to take place through a high conductivity center "donut" hole in the waste tank basemat. The hole was sized to allow full flow through the fast flow path and contamination layer in particular. The materials occupying the fast flow zones were assumed to have high conductivity and diffusion coefficient relative to backfilled and native soils, but no adsorption was assumed (i.e., $K_d = 0$ for all radiological and chemical transport).

Figure 4.4-33: PORFLOW Type IV Tank Fast Flow Path Model

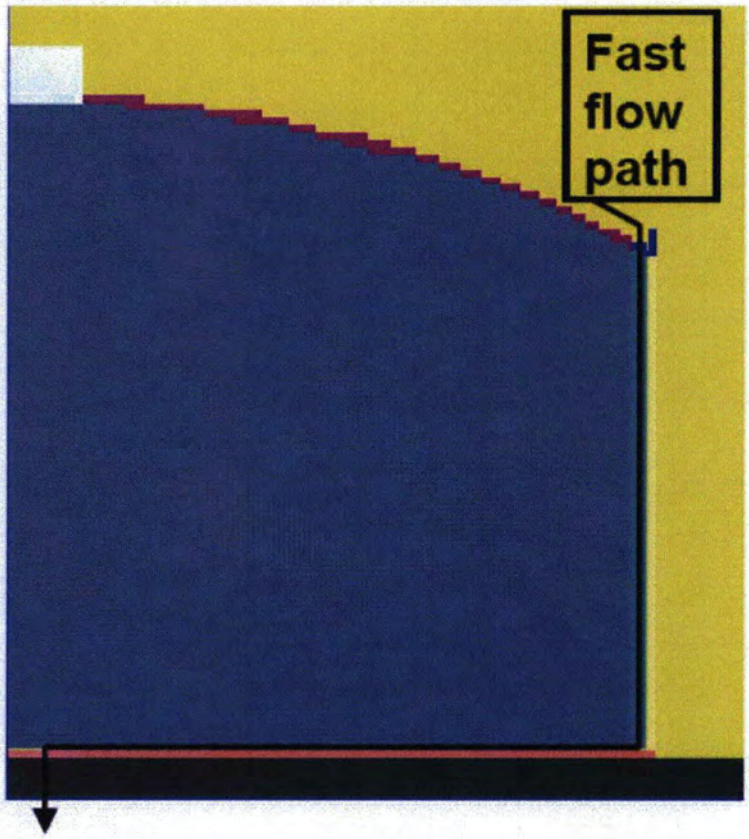

For transport modeling, a fixed time step of one year was chosen for the vadose and saturated zones. The selected step size is a compromise between two competing objectives: 1) resolution of concentration peaks from relatively mobile species that migrate as a pulse, and 2) achieving reasonable computer runtimes. A sensitivity study

using the Base Case indicates good accuracy in general, the exception being nitrate, for which the reported results may be low by roughly one-third. However, nitrate results are well below performance objectives so the modeling bias is acceptable.

➢ **Vadose and Aquifer Model Validation in PORFLOW**

Additional PORFLOW calibration was performed beyond code verification exercises and GSA/FTF model development. Using characterization and monitoring data, aspects of the PORFLOW vadose zone and aquifer models have been validated against independent field data, as identified below. Additional detail can be obtained in the associated references.

Vadose zone

- Soil suction and water content from Vadose Zone Monitoring System (VZMS) in E-Area. [WSRC-STI-2006-00198, Section 5.8]
- Tracer test pore velocity. [WSRC-TR-2007-00283, Section 4.0]
- Tritium migration beneath the E-Area Slit Trenches.

Aquifer

- Surveyed seeplines. [WSRC-TR-2004-00106]
- Pathline comparisons to existing plumes (herein).

The VZMS monitors soil conditions beneath and alongside solid waste disposal trenches in E-Area under uncapped infiltration conditions (Figure 4.4-34). E-Area is located in the GSA Area adjacent to F-Area. Field measurements using tensiometers and neutron probes indicate that soil suction ranges from approximately 50-200 cm, while water content varies between about 0.15 and 0.30. The latter values suggest a water saturation between 35% and 75%. Infiltration over the affected area is estimated to be 30 cm/yr (12 in/yr). Using the "Upper Vadose Zone" and "Lower Vadose Zone" soil properties recommended in WSRC-STI-2006-00198 and adopted for FTF PA modeling, a PORFLOW representation of E-Area conditions produced suction head and saturation values of 83 cm and 91% in the upper vadose zone, and 170 cm and 72% in the lower vadose zone.

A series of field and laboratory tracer experiments have been conducted at SRS under uncapped (normal infiltration) conditions. The PORFLOW model described above produced pore velocities of approximately 34 in/yr and 43 in/yr for the upper and lower vadose zones. Together, the tracer test data indicate a pore velocity of about 45 in/yr for the same infiltration, which is similar to the model similations.

A PORFLOW vadose zone model, similar to that used for FTF PA simulations was compared to tritium concentration data from the VZMS (Figure 4.4-34). Concentration data was grouped according to elevation (high/low) and location (center/edge) relative to a disposal trench (Figure 4.4-35). The concentration data exhibits large variability, as is commonly observed with point measurements (Figure 4.4-36). Being equivalent to a spatial average representation, the PORFLOW predictions do not reflect the data scatter, but do appear to be roughly consistent with the measurement trends.

GSA/PORFLOW model predictions of seeplines bordering the GSA have been compared to field surveys (Figure 4.4-37). The seepline data was not used in model development or calibration. The simulated seepage faces are generally consistent with the field observations.

The GSA contains a number of tritium plumes, typically associated with E-Area solid waste disposal facilities. Being unretarded, tritium is an ideal tracer of groundwater flow. Groundwater pathlines from the GSA/PORFLOW model were compared to an existing tritium plume map to support the E-Area PA. The model pathlines were observed to be consistent with plume trajectory deduced from monitoring well data (Figure 4.4-38). Simulated pathlines have also been compared to F-Area plumes, with good agreement (Figure 4.4-39).

Figure 4.4-34: VZMS Layout and Instrumentation at Slit Trenches 1

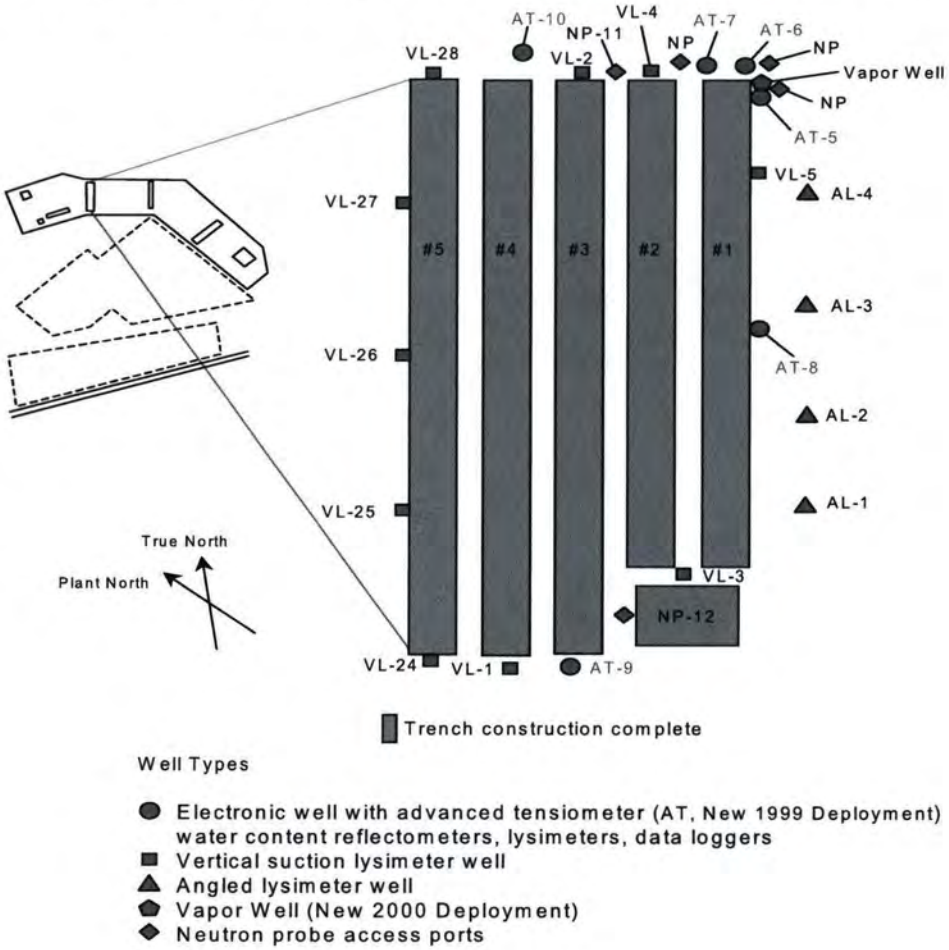

Figure 4.4-35: Basis for PORFLOW Model and VZMS Data Comparison

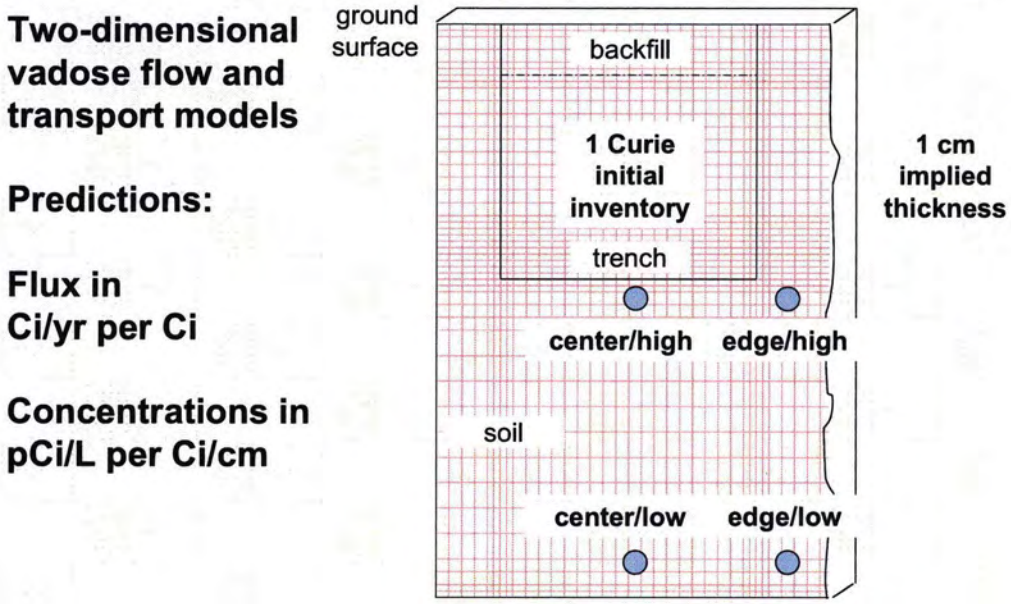

Figure 4.4-36: PORFLOW Model and VZMS Tritium Data Comparison

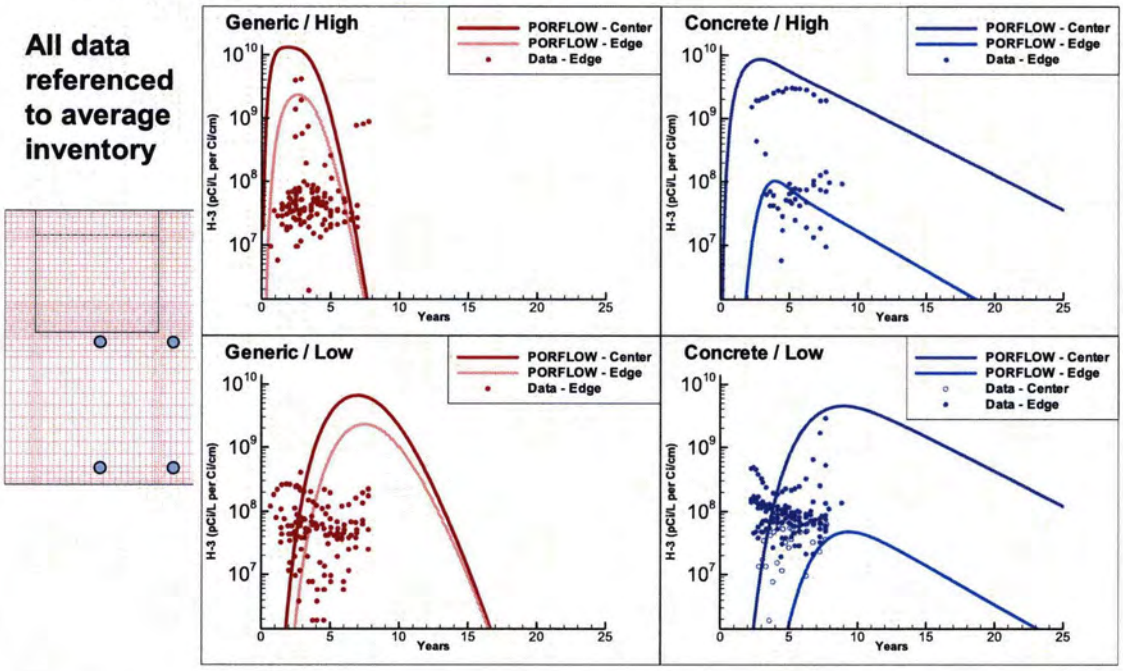

Figure 4.4-37: Surveyed Seeplines Compared to GSA/PORFLOW Model Simulation

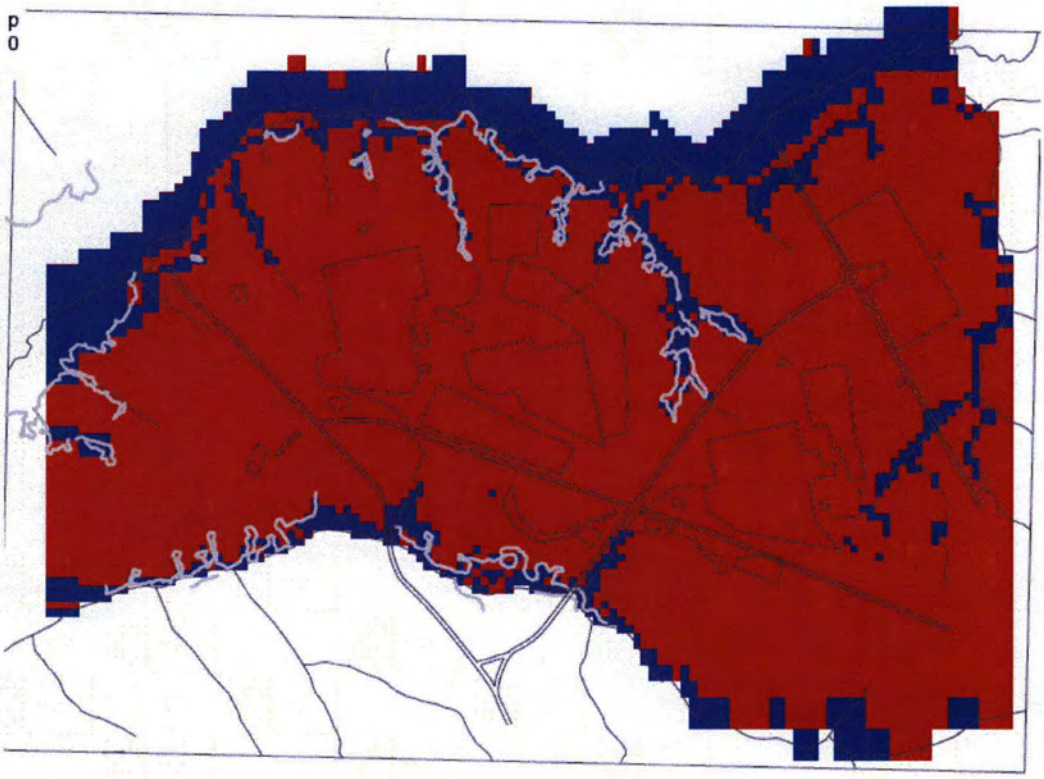

Figure 4.4-38: Comparison of GSA/PORFLOW Groundwater Pathlines to a Tritium Plume Emanating from the E-Area Mixed Waste Management Facility

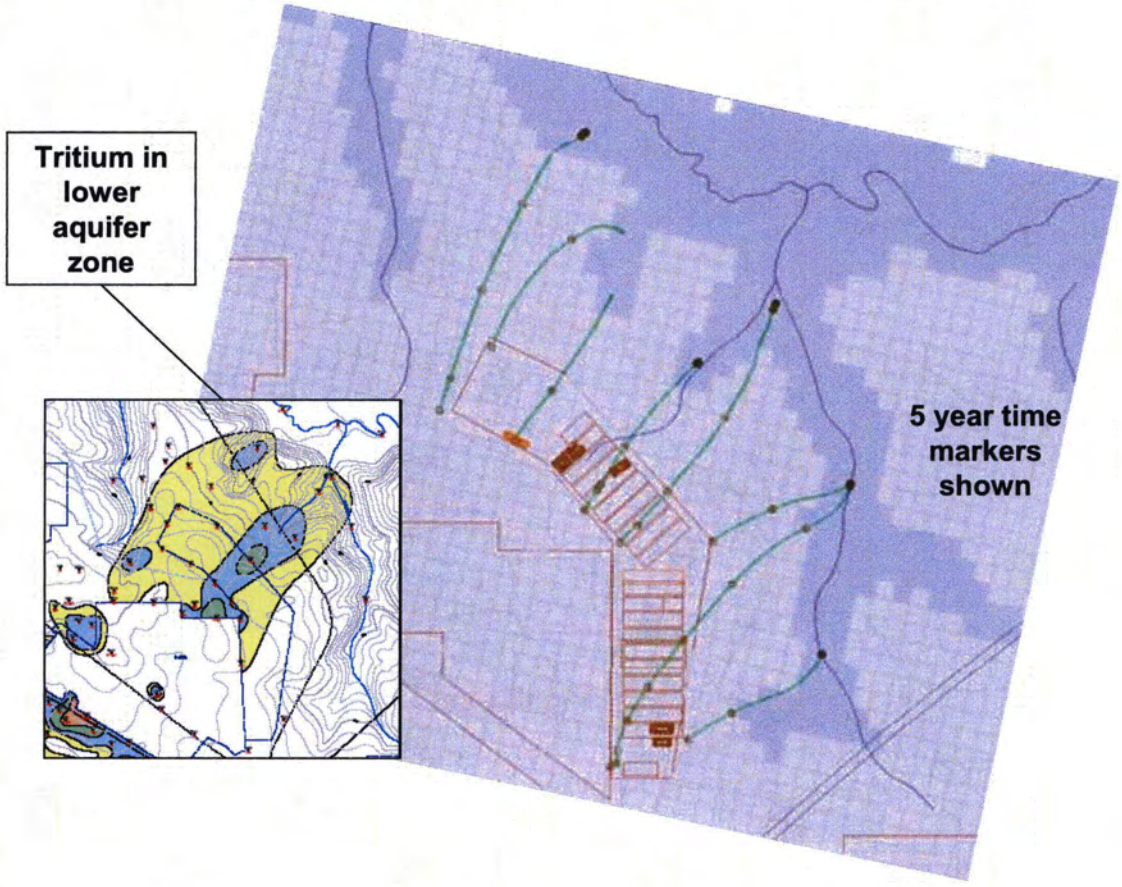

Figure 4.4-39: Comparison of GSA/PORFLOW Groundwater Pathlines to Contaminant Plumes Emanating from F-Area

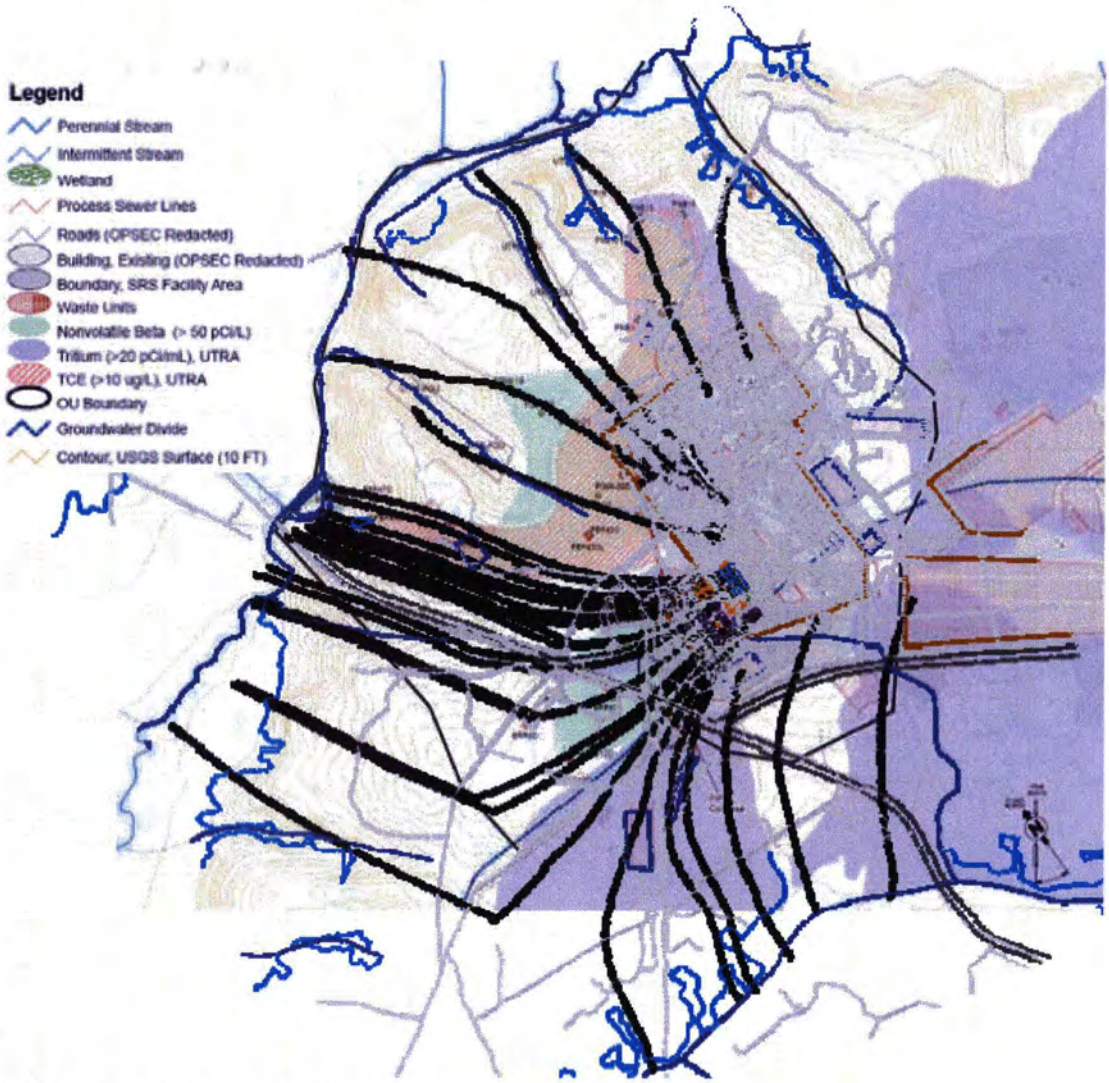

4.4.4.2 GoldSim Modeling Process

In order to address uncertainty and sensitivity of the modeling of the FTF, a probabilistic model was constructed. This model is necessarily simpler than the PORFLOW groundwater model in its environmental transport calculations, but includes additional calculations that cannot be performed in PORFLOW. The GoldSim systems analysis software, developed by GoldSim Technology Group is uniquely suited to probabilistic PA. This program was developed for the task, and incorporates many features that make it particularly useful, such as integrated solutions of physically-based differential equations from radioactive decay and ingrowth to chemical partitioning and diffusion. With its whiteboard-style graphical user interface and a rich toolset of built-in functions and the ability to define expressions governing relationships between model entities, GoldSim allows modelers to quickly build

transparent radiological PA models. The GoldSim model is a one-dimensional model versus a 3-D model (like PORFLOW), so some additional tasks, such as creation of a ring of wells surrounding the FTF (described below) were required during modeling. Validation of the one-dimensional GoldSim model versus the 3-dimensional PORFLOW model is explicitly addressed in the GoldSim benchmarking discussion (Section 5.6.2).

In addition to aiding in uncertainty and sensitivity modeling, a separate model is used to calculate dose results using concentration inputs from PORFLOW (rather than concentrations calculated by the GoldSim FTF model using the FTF rad and non-rad inventories). This "dose calculator" GoldSim model is described in 4.4.4.2.2.

4.4.4.2.1 Vadose Zone Material Properties

This section discusses the GoldSim implementation of the FTF model, and is organized to present the model structure and functionality roughly in the order that the calculations operate. That is, from the definition of model domain, materials, and transport phenomena to the calculation of dose results and their interpretation. This discussion applies to the first released version of the model, "FTF v1.0.gsm".

⇒ **Model Layout and Structure**

Like all GoldSim models, the FTF model is organized hierarchically, with the top level (or GoldSim Container) of the model shown in Figure 4.4-40. Model Containers, represented as yellow boxes, hold major model parts. Several of these do not require detailed explanation of their contents, but are introduced here:

- **SimulationSettings** contain global modeling parameters that control the setup and execution of the model, including switches to enable specific transport phenomena or include or exclude specific sources of contamination.
- **Dashboards** contain the GoldSim Dashboards that aid in model control. A Dashboard is similar to a Windows dialog box, where the user may select settings using graphical controls. The Home Dashboard link at the top of the page takes the user directly to the main Dashboard.
- The **Miscellaneous** container holds various modeling elements that are used throughout the model, mostly for the convenience of the modeler.
- **SensitivityAnalysis** contains the elements necessary to collect information for the sensitivity analysis, including final values of model endpoints (e.g., water concentration at well, or dose to a human receptor) and the values of each input stochastic and modeling switch used for each realization in a probabilistic analysis.

Figure 4.4-40: Top Level of the GoldSim FTF Model

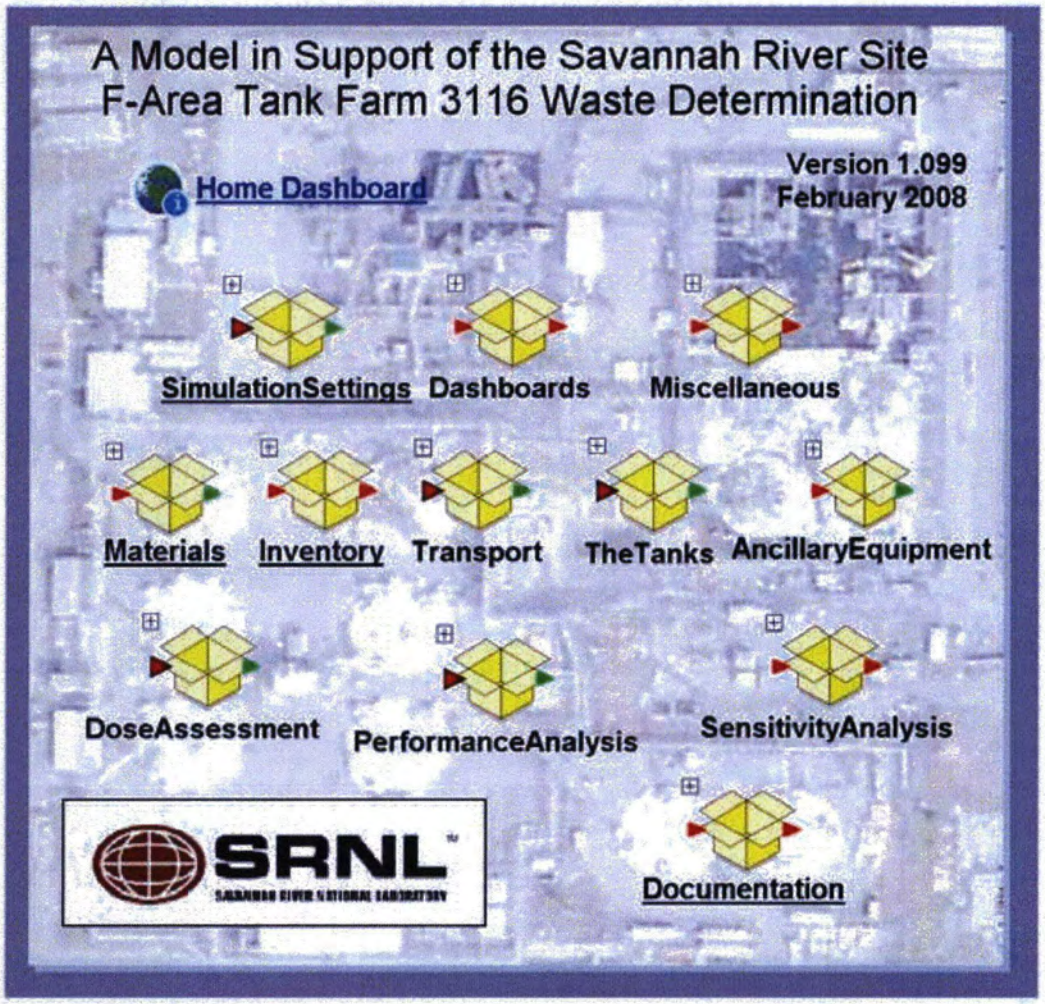

The most interesting containers, hosting the bulk of the model's calculations, are outlined here and are described in greater detail in the following sections.

- **Materials** contains definitions for the list of contaminant Species (radionuclides as well as a few stable contaminants of concern) the definition of Water (including chemical solubilities) and all porous media that are used in the model. Soil/water partition coefficients for the various media (defined as GoldSim Solids) and their variations are part of this definition.
- The **Inventory** container hosts GoldSim Data elements defining Species inventories for each FTF waste tank and piece of ancillary equipment.
- Environmental contaminant transport parameters are defined in the **Transport** container. The FTF model currently considers only advection of water in porous media, be it through the waste, the concrete pads below the bottom of the waste tanks, or the geologic media comprising the unsaturated and saturated zones. This container holds only the definitions of rates and other transport-related parameters, but does not perform transport calculations.
- The FTF contains 22 waste tanks, each defined in its own subcontainer within **TheTanks**. Transport calculations are conducted within each of these subcontainers, starting with the release of contaminants from the layer of waste present at the bottom of each waste tank, following their transport through the concrete pad and geologic media to specific exposure locations where future humans may gain access to the contaminated groundwater.
- The **AncillaryEquipment** container is similarly defined, but instead of waste tanks each subcontainer represents a specific piece or collection of pieces of ancillary equipment, such as evaporators and transfer lines that support operations of the tanks.
- **PerformanceAnalysis** contains a collection of results of interest. Once a simulation is completed, the contents of this container should be examined to evaluate the modeling endpoints (water concentrations and doses) and determine their principal causes, for example, by tracing the results, the user can evaluate which well, radionuclide, exposure pathway, and waste tank is the most significant contributor to a specific endpoint for most users, this will be the most interesting part of the model, and it is discussed in its own section below.

More information on GoldSim fundamentals is available at the website www.goldsim.com.

The GoldSim FTF modeling domain begins at the top of the waste layer and extends to a hypothetical groundwater well located 100m from the FTF boundary. The flow profiles used in the GoldSim FTF model to represent flow through the waste are extracted from the PORFLOW FTF flow model, which allows for changes in the closure cap, tank top, and tank grout to be reflected in the flow used. The model contains all appropriate materials, concrete, soil, etc., as described in detail below. The model is necessarily one-dimensional with downward flow represented in the unsaturated zone and predominantly horizontal flow in the saturated zone. The

unsaturated zone is represented as a column underlying each particular item of equipment (i.e., tank, evaporator, etc.) The transfer lines are represented as the entire FTF area, since they traverse the site.

The water inflow boundary condition, at the boundary of the bottom of the grout mass in the tank and the top of the waste layer, is provided by PORFLOW runs. The PORFLOW output is parsed to select data from approximately 1m under the concrete basemat. Data at that elevation are sampled at five locations and a geometric average of those values is used as the water flow boundary condition through the waste layer. This is consistent with the assumption of continuity through the waste and concrete basemat. This flow is constant downward through the unsaturated zone, though it changes in time as the grout fails hydraulically.

The water flow boundary condition for the saturated zone bulk flow is also provided by the PORFLOW model. A single representative aquifer velocity was chosen. This was a more difficult task than in the unsaturated zone because while the unsaturated zone is essentially a one-dimensional flow (in PORFLOW) the saturated zone is multidimensional. More about this is available in the GoldSim benchmarking discussion (Section 5.6.2). The recharge flow is not considered in the saturated zone flow as GoldSim does not impose a mass balance of materials (water in this case) but only of Species.

A note regarding the mass balance of recharge water entering the saturated zone is in order. Inspection of the flow of water through the GoldSim Cells that represent the aquifer immediately below the waste tank (e.g., in the Container\TheTanks\ Tank01\WasteFootprint) reveals that more water seems to be entering each Cell than leaving. Inflows to each Cell include the regional aquifer flow and recharge from the unsaturated zone within the waste footprint. Outflows include the same aquifer flow, and an implied leakage of excess clean water, representing uncontaminated water below the plume pushed down into the deeper aquifer, driven by infiltration. In essence, the modeled flow is horizontal and constant, with contaminants added from recharge into each Cell. This is preferred to an alternative implementation which could balance the flow by explicitly transferring contaminated water to a sink representing the lower aquifer. This would grossly overestimate vertical dispersion, since each Cell is instantaneously mixed, and would not reflect the conceptual model of a plume of limited thickness.

The GoldSim contaminant transport calculations are, however, perfectly valid in this arrangement, assuming that the contaminant plume is fully mixed over the thickness of the Cells. Further, the Cells are structured so that no contaminants may be transported except within the Cell system. That is, while in reality water must enter and exit any control volume (in this case, the collection of Cells) in equal quantities. This is called the mass balance assumption. GoldSim is designed to assume the volume of water in the Cell is dictated entirely by its Cell definition, paying no attention to competing inflows and outflows. It is up to the modeler to assure that the flows imposed on the Cell are physically correct. In this model, we take advantage of GoldSim's design, which in effect ejects excess (clean) water from the Cell, without

ejecting contaminants. In this scheme, then, all contaminants are retained in the row of Cells, consistent with the conceptual model of a plume of limited depth.

See Figure 4.4-41 for an example of one of the 22 waste tank systems that are modeled independently. Ancillary equipment is modeled similarly. The GoldSim model is constructed so that each waste tank and piece of ancillary equipment may be run separately or in any combination. Even if multiple waste tanks and ancillary equipment are being run, each is independent, with its own inventory, dimensions, and containment failure scenario. Figure 4.4-42 shows the Tank Selector Dashboard. The boxes with integers are where the configuration scenario for each waste tank is defined. GoldSim does not recognize characters, so Configurations A through F are denoted as 1 through 6, 1 being the Base Case Configuration A. When a stochastic run is made, the configuration for each waste tank and piece of equipment is chosen randomly. The checkbox (with an "×") for each tank piece of equipment is used to activate that waste tank or piece of equipment in the model.

Figure 4.4-41: Representative Model of a Tank System

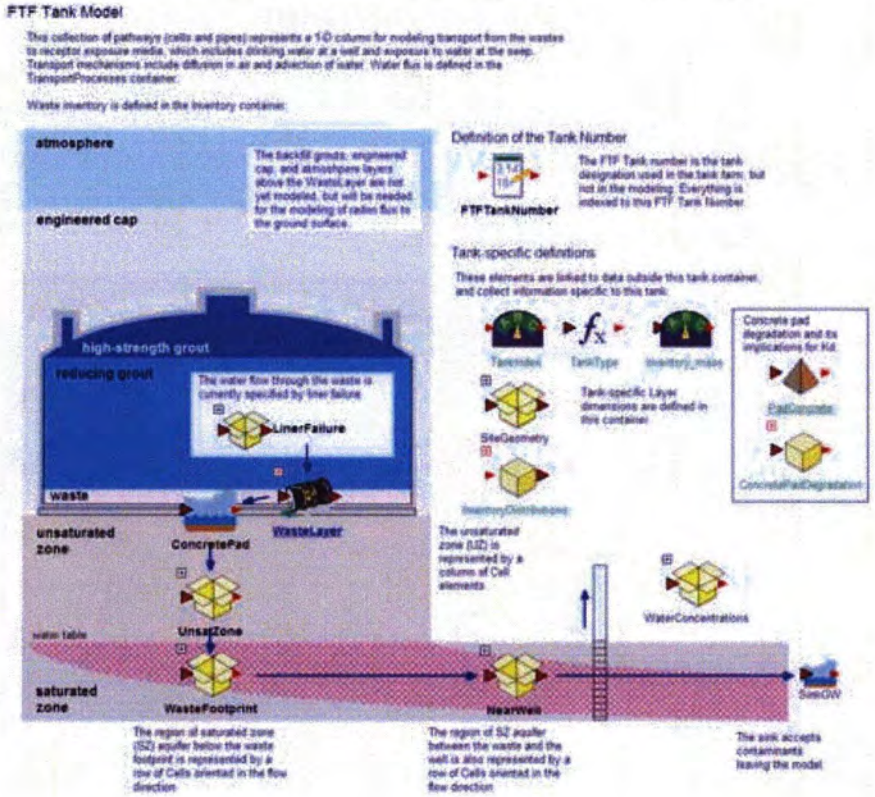

THIS PAGE CONTAINED RESTRICTED RELEASE INFORMATION REDACTED FOR PUBLIC USE

Figure 4.4-42: Tank Selector Dashboard

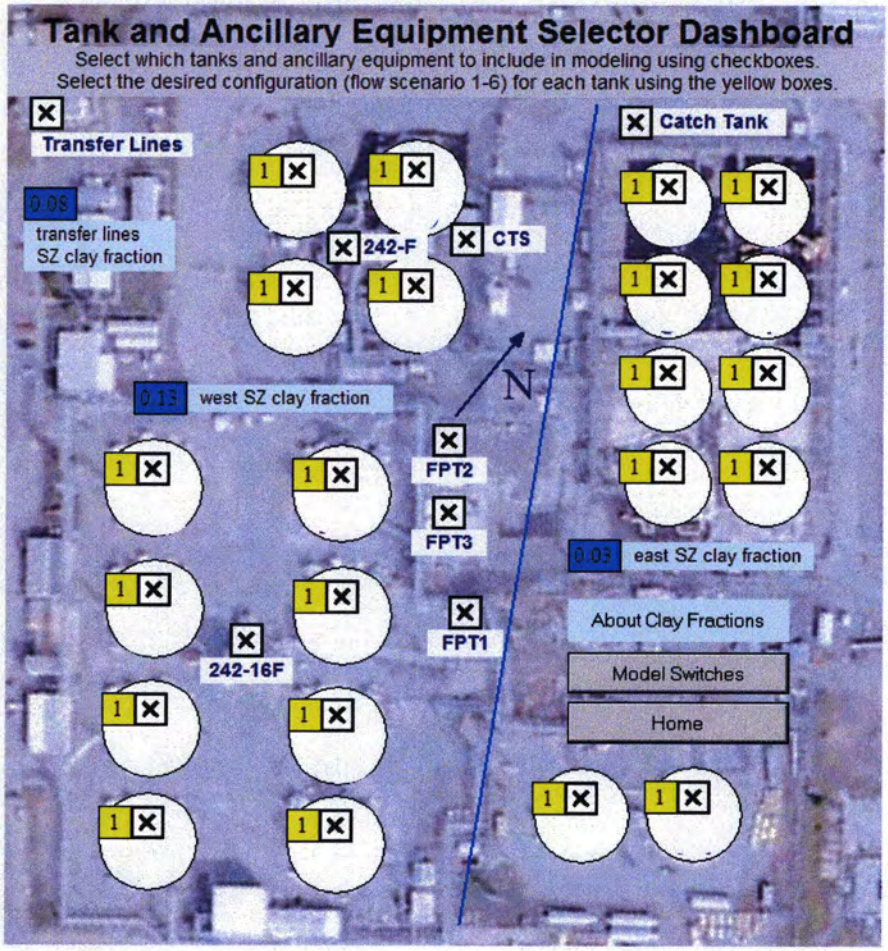

⇒ **Materials and Contaminants**

The Species element in the Materials container (denoted \Materials\Species) defines all chemical species in the model. Radionuclides are given a half-life, and, if appropriate, one or more decay products, which also must be defined in the Species list. In this way, decay chains of any degree of complexity can be constructed. Each defined radioactive Species has a prefix, like "Pb" in "Pb210" that identifies its element. The numeric value that follows, obviously, is the isotope designation. All isotopes (all numbers for a given element) behave the same chemically, sharing soil/water partitioning (K_d) and aqueous solubility limits. A stable form of the same element should be defined using simply the elemental symbol, such as "Pb". Defined this way, it too will share transport geochemical behavior with its radioactive isotopes.

Stable (non-radioactive) Species are defined in this model using a "zz" prefix before the element or radical specification. There is, for example, a stable form of lead, identified as "zzPb". The nitrate radical is "zzNO3". A consequence of this type of definition is that the stable version of lead (or selenium, nickel, or uranium) is not recognized by GoldSim as the same element as the radioactive versions (e.g., Pb210, Se79, Ni63, or U238) and the analysis of fate and transport is therefore independent from the radioactive species.

⇒ **Inventory** A baseline inventory of radionuclides and non-radioactive contaminants was developed for each waste tank and piece of equipment, as discussed in Sections 3.3.2 and 3.3.3. The list of radionuclides used by the GoldSim FTF model for transport modeling is abridged from the list of radionuclides in the FTF PA inventories. Radionuclides with very short half-lives (e.g., less than 5 years) are not separated from their parent and do not have to be included in the list of radionuclides because they will have a negligible effect after transport. Also, GoldSim models daughter products during transport, so that very short lived daughter products (e.g., Ba-137m, Y-90) that are in secular equilibrium with the parent do not have to be explicitly included since they rapidly reach secular equilibrium during transport. The following radionuclides are not included in the GoldSim model initial inventories: Ba-137m, Bk-249, Ce-144, Cm-242, Cs-134, Eu-155, Na-22, Pm-147, Pr-144, Rh-106, Ru-106, Sb-125, Sb-126, Sb-126m, Te-125m, and Y-90. None of these radionuclides are considered "key radionuclides" as discussed in Section 5.2.2. It should be noted that even though these radionuclides are not included in the initial inventory, they are included in dose calculations if present.

The inventory values are assembled into GoldSim data elements for the waste tanks and for the ancillary equipment in the \Inventory container. The user may choose between these baseline inventories or unit inventories for special studies. These selected inventories are multiplied by uncertainty factors 0.01, 0.1, 1 and 10 (each used with equal probability) in each waste tank container during probabilistic simulations. The effect of this is to modify the entire inventory for a given waste tank by the uncertainty factor, rather than individual radionuclides independently.

After the time of failure of the steel waste tank, which depends on the selected failure configuration, the inventory is assumed to be rinse released. That is, all contaminants are no longer subject to any containment, and are free to migrate about the environment set up by the model.

⇒ **Engineered Barriers and Release Mechanisms** The GoldSim FTF model is used to analyze the various waste tank configurations described in Section 4.4.2. The GoldSim FTF model used flow profiles from the PORFLOW FTF model for the various configurations. In this respect all the failure mechanisms for flow are implicitly represented in the GoldSim model by the PORFLOW flows. The only exception to this is the fast flow path which is explicitly represented by a fraction of the flow which bypasses the concrete basemat. The

phenomenon being represented by this is that the fast flow path provides a means for the flow to go through the concrete basemat without interacting with the concrete. In PORFLOW this is represented by a region of no K_ds. By bypassing the concrete basemat, the GoldSim model achieves the same result.

⇒ Waste Layer

A representative waste layer container is shown in Figure 4.4-43. The WasteCell consists of a single layer in which solubility control is used. The local material "Water" defines the solubility for its local WasteCell. The PoreFlushes container is where the dynamic pore flush calculation is performed. The BypassFraction is used to represent the percentage of basemat through which a fast flow path may develop. Waste is considered immediately available for transport.

The pore flushes is based on the volume of pore water in the grout above the waste and the rate at which that pore water is replaced. This is not explicitly modeled, but assuming continuity of flow, the grout water flux is equal to the waste water flux, reflecting the change in pore water chemistry in the waste solubility.

Figure 4.4-43: Representative Model of the Waste Layer within Each Waste Tank

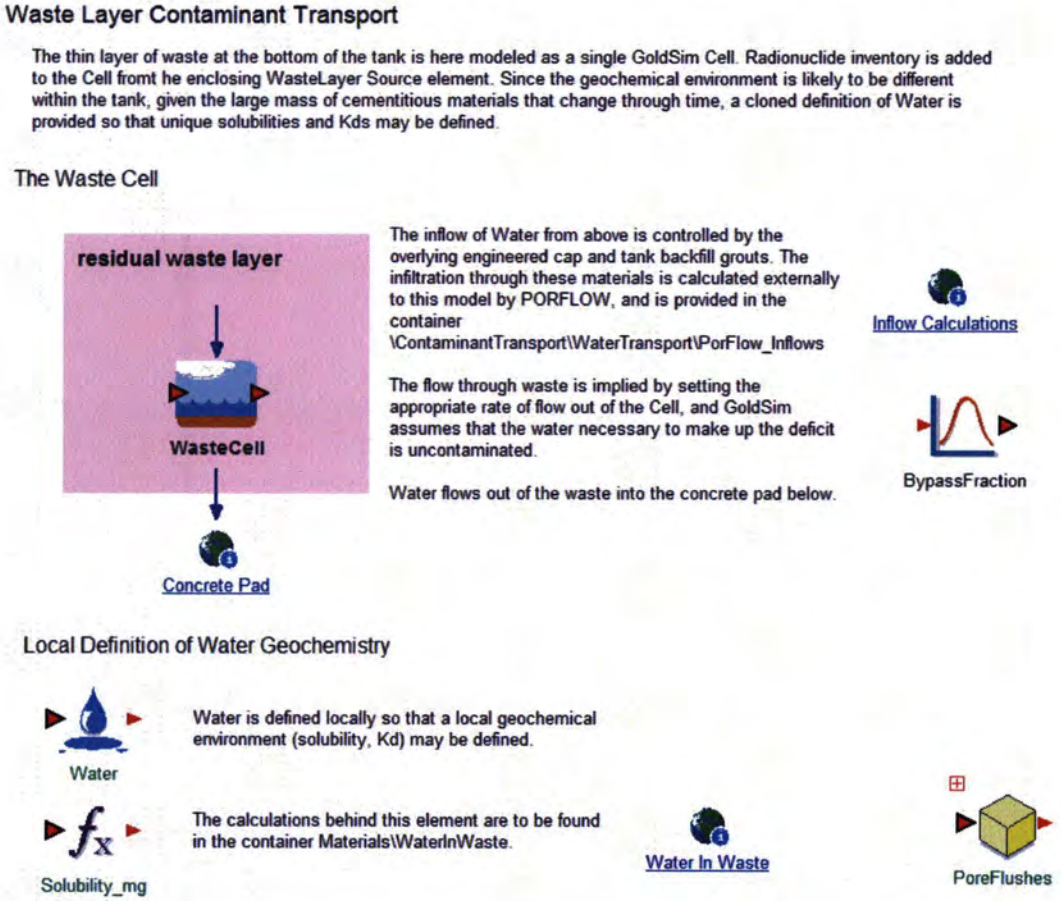

⇒ Environmental Transport Environmental transport is predominantly waterborne. Two controlling geochemical parameters are K_d and solubility. The aqueous solubility of various modeled species in cement pore waters changes as the cement degrades. Solubilities are a property of the GoldSim fluid called Water, and so Water changes in response to degradation of concrete pad underlying the waste. This required a GoldSim manipulation: the separate (yet cloned) definition of Water within each WasteLayer container, connected to an independent locally-defined vector of solubilities (Solubility_mg). The change in the physical and chemical behavior of the concrete occurs after a sufficient number of pore water volumes has passed through the porous medium. As concrete ages chemically, it changes from a geochemically reducing environment to an oxidizing one, and a redefinition of K_d values and solubilities accompanies the change. Note that the waste's solubilities change while the concrete basemat K_d values change.

As the concrete ages physically, its hydraulic characteristics change as well. These changes are handled by calculating the number of pore volumes that have passed through the concrete basemat (in the PoreFlushes container), changing from one type of concrete to another. As the concrete basemat changes type, the water flow changes concurrently, using flow fields calculated previously by the PORFLOW model.

⇒ Dose Calculations In the GoldSim FTF model there are 36 MOP and MCL compliance points evaluated at the 100m boundary, and one evaluated at a location 1m from Tank 17 for the inadvertent intruder). Each of these is discussed below.

⇒ Dose to the MOP Receptor The MOP is assumed to have access to groundwater, by the drilling of a well used for drinking water and other purposes, as close as 100m to the FTF boundary. In order to estimate that location which would provide the highest dose, a line of hypothetical wells is placed along the 100m boundary, and the dose that would be incurred by the MOP is calculated using groundwater from each well. Each well gets contaminant contributions from each waste tank, depending on its proximity to the plume emanating from each tank. Figure 4.4-44 shows the 22 waste tanks, with groundwater streamlines from each (as calculated by the PORFLOW model), and the line of 36 wells. The grid lines and well locations are spaced at 50 feet (15.24m) in order to be consistent with the PORFLOW modeling grid. These well locations were used with a novel application of the GoldSim plume function to assess plume overlap. Each waste tanks streamline has its position relative to the wells calculated. Those positions are then used to calculate each waste tank contribution to each well. These individual contributions to a well are summed up to obtain a total concentration for each contaminant. Once the contaminant concentrations are obtained, the doses are calculated by the pathways described in Sections 4.2.4.1 and 5.4.1, including the ingestion of water, vegetables, beef, milk, and soil, and inhalation of shower and irrigation water. A total dose, the sum of the appropriate pathways, is calculated for each well.

THIS PAGE CONTAINED RESTRICTED RELEASE INFORMATION REDACTED FOR PUBLIC USE

Figure 4.4-44: Hypothetical Well Locations

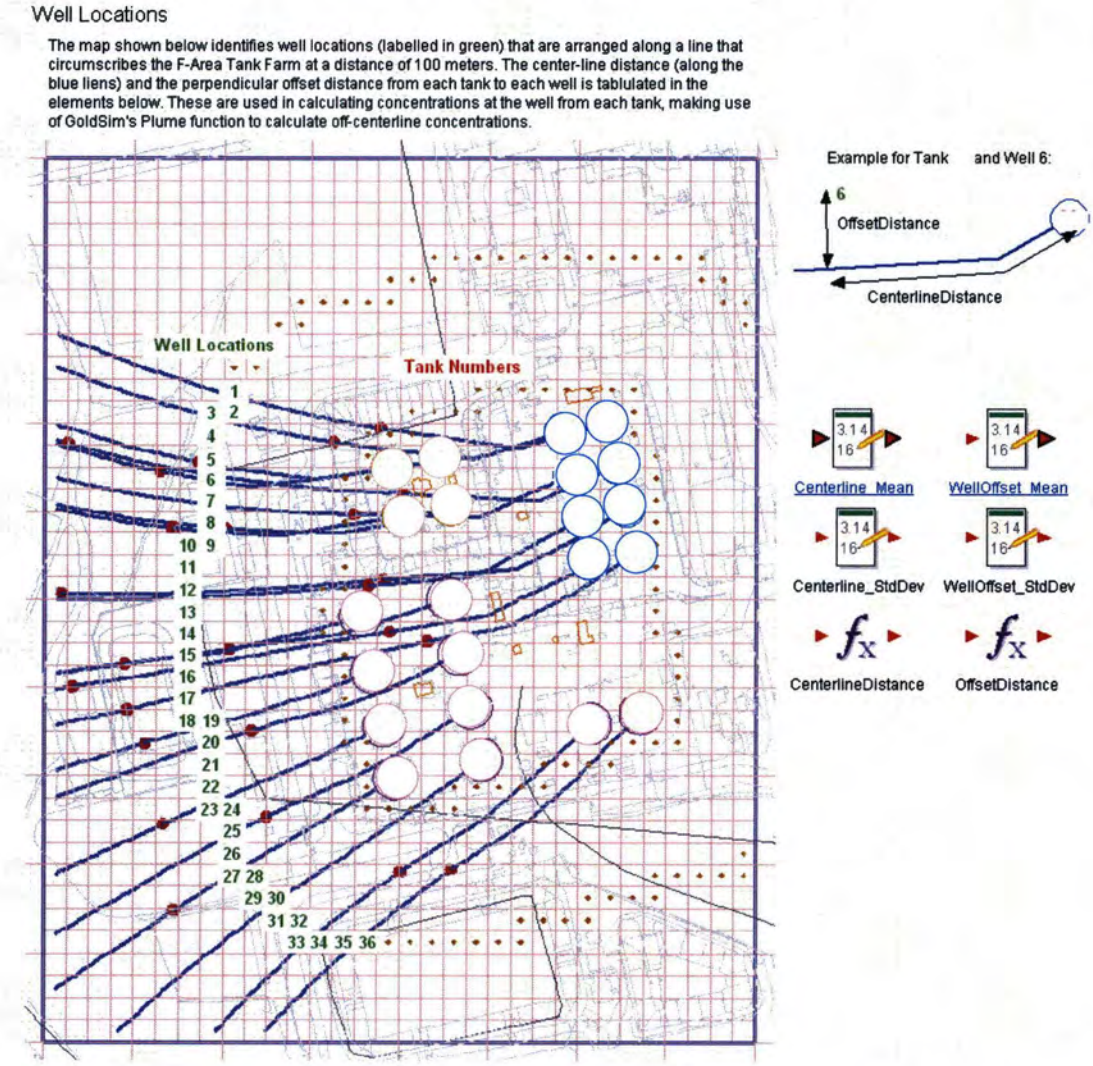

(Depicts a line of hypothetical well locations, placed 100m from the FTF boundary. Blue lines depict groundwater streamlines from each waste tank.)

⇒ **Dose to Inadvertent Intruder Receptor**

Doses to the inadvertent intruder are calculated by the pathways described in Sections 4.2.4.2, 6.2, and 6.3. The 1m well water dose is calculated by using the worst location during the compliance period.

⇒ **Modeling Parameterization** Where possible, model input parameters were defined stochastically so that their influences could be evaluated in the sensitivity analysis. Where the distribution was not well understood, a basic form was assumed, with the idea that if the parameter was identified as sensitive, its input distribution could be refined later. A listing of stochastic parameter definitions is provided in Section 5.6.

⇒ **Modeling Results** The results of modeled simulations are collected into a single high-level container in the FTF model, for the convenience of the user. The PerformanceAnalysis container is organized into subcontainers for doses to the MOP and inadvertent intruder, and water concentrations for comparison to regulatory MCLs. This section discusses the water concentration and dose calculations.

Groundwater concentrations of specific chemical elements, radicals, and compounds are a matter of regulatory concern. The FTF model is set up to estimate aqueous concentrations of specific modeled Species for comparison to MCLs. Such concentrations are evaluated at the same line of wells 100m from the FTF boundary.

4.4.4.2.2 GoldSim Dose Calculator Model Description

The GoldSim dose calculator model is a generic dose calculator in that if the inputs are correctly specified it can be used for any facility. In this case we will be discussing its application to FTF.

The major impetus behind the dose model was to keep it as similar to the FTF model as possible. Figure 4.4-45 shows the model level. Containers not needed for the dose calculation, notably TheTanks, AncillaryEquipment, and Transport have been deleted. The pathways are identical to those described in Section 4.2.4. There are five defined sectors for the 100m well, four defined sectors for the 1m well, and two defined sectors for the seepline. These sectors are shown in Figures 5.2-5 and 5.2.6.

Figure 4.4-45: GoldSim Dose Calculator Model

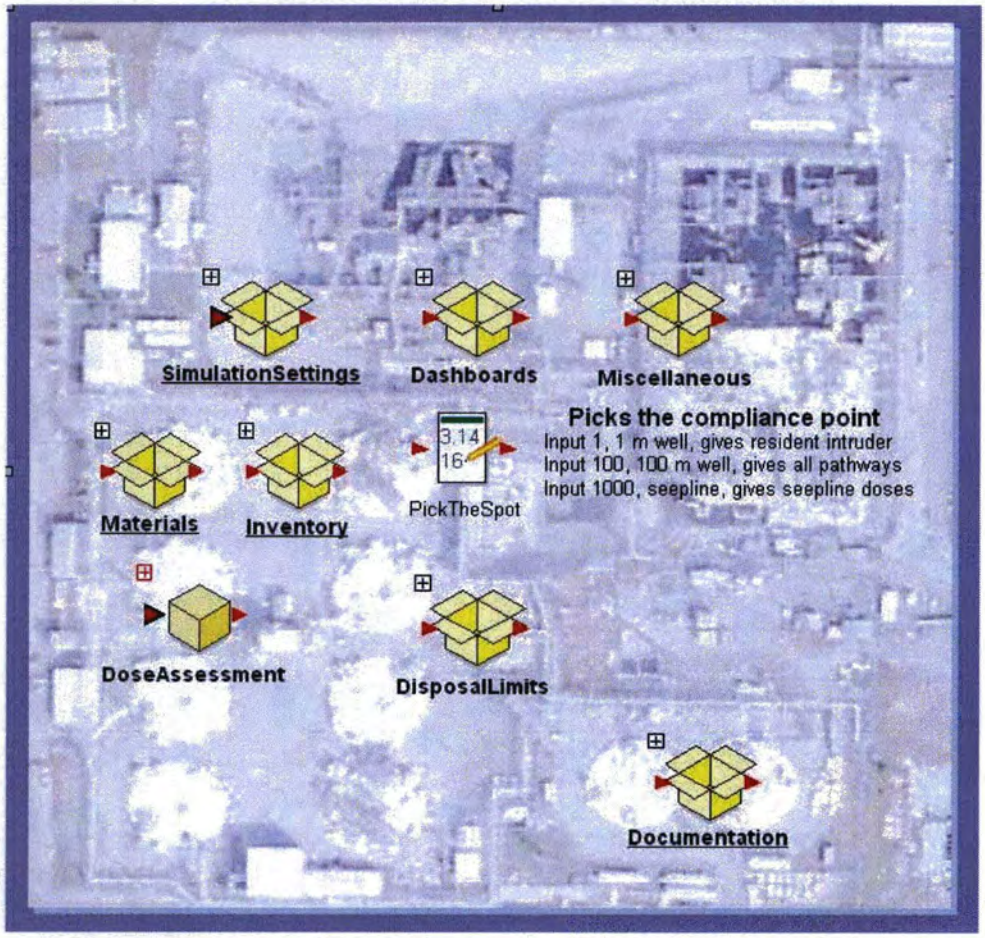

⇒ Input Contaminant Concentrations

The contaminant concentrations used by the standalone model are, for this PA, obtained from the PORFLOW FTF model. Some data manipulation is required as PORFLOW runs each parent radionuclide separately. From each of those runs it creates output concentrations for each region and each aquifer level. Codes were written to coalesce these data into the single input file needed by the GoldSim model.

Since each parent is run individually, if one wishes to obtain the total concentration of a radionuclide which is the daughter of several parents, all parent files must be searched for that daughter. This must then be done for each region and each aquifer. Taking RegionD as an example, the codes generate four final files. Each file is a matrix of concentrations, in mol/L, with indices (Species, Time). Three of the files are for each aquifer and the fourth is the maximum for each radionuclide of the other three. The dose calculation is run using the maximum contaminant file. The seepline concentrations used by the GoldSim model dose calculator is the peak concentrations

calculated by PORFLOW (as discussed in Section 5.4.2), and does not assume any stream dilution.

4.5 Airborne and Radon Analysis

The air and radon pathway analysis was conducted for the 10,000 year post-closure compliance period. The analytical method chosen was a hybrid approach where most parameters were set to their best estimate values (i.e., based on available site-specific measurements or engineering judgment), while other parameters were set to conservative/bounding values. The conceptual PORFLOW transport model used for the air and radon pathway analysis had imbedded within it biases that were intended to be conservative where possible. The conceptual model used for the air and radon pathway analyses were the same and the PORFLOW transport model used for both pathways utilized the same input files.

Of the available four waste tank types, the Type I tank was chosen for this analysis. This analysis did not consider any piping or ancillary equipment associated with the waste tanks. A schematic of the Type I tank is shown in Figure 4.4-1. Of the four tank types, this tank type was selected because it will have the least grout and concrete thickness above the stabilized contaminant zone, which is located at the bottom of the waste tank. Additionally the minimum closure cap thickness over the waste tanks was assumed for conservatism. These assumptions should produce the maximum flux of gaseous radionuclides at the ground surface.

4.5.1 Air and Radon Pathway Conceptual Model

The approach taken focuses primarily on a Base Case where nominal settings for many of the input parameters have been conservatively chosen. The main analysis tool employed was the PORFLOW code which simulates the transport of radionuclide chains (i.e., parents and daughters) in porous media. The flux of radioactive gasses at the land surface above the FTF was evaluated for the closure configuration. [WSRC-STI-2007-00355_OUO] Gaseous radionuclides within the CZ diffuse outward into the air-filled pore space of the overlying materials. Ultimately, some of the radionuclides emanate at the land surface. As such, air is the medium through which they diffuse. It was assumed that fluctuations in atmospheric pressure at the land surface that could induce small pulses of air movement into and out of the shallow soil profile over relatively short periods of time will have a zero net effect when averaged over longer time periods. Thus, advective transport of radionuclides in air-filled soil pores was not considered to be a significant process when compared to the rate of air diffusion.

The closure cap, as described in WSRC-STI-2007-00184_OUO, consists of a top soil layer, an upper backfill layer, an erosion barrier layer, middle backfill layer, lateral drainage layer, a HDPE geomembrane, a GCL, an upper foundation layer, and a lower foundation layer. The HDPE geomembrane and the GCL are excluded from this analysis. By excluding these materials, the baseline air analysis was more conservative as these materials would be expected to significantly reduce gaseous flux at the land surface. The HDPE geomembrane would have very low gaseous diffusion coefficients and the GCL would have very little air-filled porosity, since it would be at or near saturation. The top soil layer and the upper backfill layer were also excluded from the baseline analysis, since they are located above the erosion barrier and are therefore subject to erosion. For the purposes of this analysis, it was

assumed that those components situated below the top of the erosion barrier (soil layers) remain intact for the duration of the simulation.

The Type I tank includes primary and secondary steel liners situated above a layer of basemat concrete as shown in Figure 4.4-1. The top of the waste tank is covered with a concrete roof. For the baseline analysis, the model domain begins at the top surface of the lower primary liner and extends through the stabilized contaminants to the top of the erosion barrier. The baseline model excluded the upper primary steel liner. As with the exclusion of the geomembrane and GCL, this should make the model more conservative because including the steel liner would be expected to significantly reduce gaseous flux at the land surface.

The total thickness of the waste tank, and cover materials (excluding the top soil, upper backfill, geomembrane, GCL, and steel liner) is 36.33 feet (11.07m), with a stabilized contaminant layer thickness of 1.0 feet (0.30m). The stabilized contaminant layer thickness in this model differs from the groundwater model to provide additional conservatism providing a shorter pathway to the surface. Table 4.5-1 lists the individual components of the Type I tank and closure cap included in the analysis. Materials are indicated with the associated thickness of each component, in inches, feet, and meters.

Table 4.5-1: Vertical Layer Sequence and Associated Thickness for FTF Type I Tank and Cover Material

Layer	Thickness (inches)	Thickness (ft)	Thickness (m)
Erosion Barrier	12	1.00	0.3048
Middle Backfill	12	1.00	0.3048
Lateral Drainage	12	1.00	0.3048
Upper Foundation	12	1.00	0.3048
Lower Foundation	72 (minimum)	6.00	1.83
Concrete Roof	22	1.83	0.56
Reducing Grout	282	23.5	7.16
Stabilized Contaminants Layer	12	1.00	0.3048

[Adapted from WSRC-STI-2007-00184_OUO]

4.5.2 Air and Radon Pathway Diffusive Transport Model

A one-dimensional PORFLOW based diffusive transport model was created for the FTF Type I tank Base Case.

The governing equation for mass transport of species *k* in the fluid phase is given by:

$$\frac{\partial C_k}{\partial t} + \frac{\partial}{\partial x_i}(V_i C_k) = \frac{\partial}{\partial x_i}(D_{ij}\frac{\partial C_k}{\partial x_j}) + \gamma_k$$

Where:

C_k	concentration of species *k*, Ci/m^3
V_i	fluid velocity in the i^{th} direction, m/yr
D_{ij}	effective diffusion coefficient for the species, m^2/yr
γ_k	net decay of species *k*, Ci/m^3 yr
i, j	direction index
t	time, yr
x	distance coordinate, m

This equation is solved within PORFLOW to evaluate transient radionuclide transport above the waste tank and to determine gaseous radionuclide flux at the land surface over time. For this analysis, the advection term was disabled within PORFLOW and only the diffusive and net decay terms were evaluated.

The boundary conditions imposed on the entire model domain included:

- No-flux specified for all radionuclides along sides and bottom
  ($\partial C/\partial X = 0$ at x=0, x=1 and $\partial C/\partial Y = 0$ at y=0)
- Species concentration set to 0 at land surface (top of erosion barrier)
  ($C = 0$ at $y=y_{max}$)

These boundary conditions force all of the gaseous radionuclides to move upward from the stabilized contaminant zone to the land surface. In reality, some lateral and downward diffusion occurs in the air-filled pores surrounding the stabilized contaminant zone; hence ignoring this lateral and downward movement has the effect of increasing the flux at the land surface. This introduced some conservatism in the calculated results. Simulations were conducted in transient mode for diffusive transport in air, with results being obtained over the 10,000 year period.

The initial condition imposed on the domain, except for the stabilized contaminant zone, included:

- Species concentration set to 0 at time = 0
  ($C=0$ for $0 \le x \le 1$ at t=0 and $C=0$ for $0 \le y \le y_{max}$ at t=0)

For the air pathway analysis, the initial conditions for the model assumed a 1 Ci inventory of each radionuclide uniformly spread over the stabilized contaminant zone. For the radon pathway analysis, an emanation factor of 0.25 was applied resulting in an initial inventory of

0.25 Ci for each parent radionuclide uniformly spread over the stabilized contaminant zone. The emanation factor for the radon pathway analysis is explained more fully in Section 4.5.6.

4.5.2.1 Grid Construction

The model grid for the waste tank and overlying cover materials was constructed as a node mesh 3 nodes wide by 80 nodes high. This mesh creates a vertical stack of 78 model elements. Figure 4.5-1 shows a schematic of the PORFLOW model grid. The grid extends upward to the top of the erosion barrier, since this is the minimum possible cover thickness that could exist during the simulation period. A set of consistent units was employed in the simulations for length, mass and time, these being meters, grams and years, respectively.

Figure 4.5-1: Schematic of PORFLOW Model Grid for Air and Radon Pathway Analysis

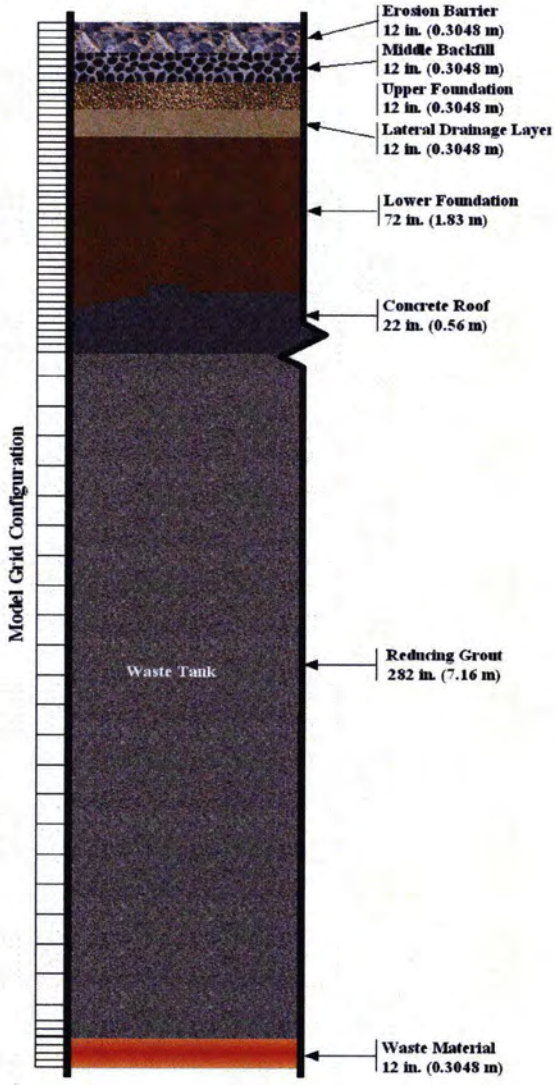

4.5.2.2 Material Zone Properties and Other Input Parameters

Material properties utilized within the one-dimensional numerical model were specified for eight material zones defined within the model domain. Each material zone was assigned values of particle density, total porosity, average saturation, air-filled porosity, air density, and an effective air-diffusion coefficient for each source element or compound. An effective air-diffusion coefficient was used for each radionuclide and material layer. Therefore, tortuosity was assigned a unit value in each material zone. An air fluid density of 1.24E+3 g/m^3 at standard atmospheric conditions was used in the transport simulations. [WSRC-STI-2007-00355_OUO]

The stabilized contaminant layer was assumed to be 1 foot thick and confined to the bottom of the waste tank. The waste tank is to be filled with a reducing grout (OPDEXE-X-P-0-BS) from the existing specification, which is described in Section 3.2.3, and it was assumed that the stabilized contaminant layer would have similar properties. The hydraulic and physical properties of this mix are reported in WSRC-STI-2007-00369. Based on the results of this testing, the stabilized contaminant layer and the reducing grout layer was assigned a particle density of 2.51 g/cm^3 and a total and air-filled porosity of 0.266. The concrete roof layer was assumed to be similar to the basemat surrogate tested and reported in WSRC-STI-2007-00369. This layer was assigned a particle density of 2.51 g/cm^3 and a total and air-filled porosity of 0.168. The stabilized contaminant layer, the reducing grout, and the concrete roof were conservatively assumed to be dry (i.e., total porosity = air-filled porosity).

The foundation layer was divided into the upper and lower foundation layers. [WSRC-STI-2007-00184_OUO] It is anticipated that the lower foundation layer will need to promote drainage of infiltrating water away from and around the waste tanks, requiring a relatively high saturated conductivity such as 1.0E-03 cm/sec. It is anticipated that the upper foundation layer will consist of soil with a moderately low permeability (i.e., $\leq$1.0E-06 cm/sec) produced by blending typical SRS backfill with a small weight percent bentonite. The particle density of the lower and upper foundation layers was assigned that of control compacted backfill from WSRC-STI-2006-00198 (i.e., 2.63 g/cm^3).

The particle density of the middle backfill layer was also assigned that of control compacted backfill from WSRC-STI-2006-00198 (i.e., 2.63 g/cm^3). The lateral drainage layer and erosion barrier layer were assigned a particle density typical of quartz (i.e., 2.65 g/ cm^3).

Infiltration through the closure cap materials over time as the closure cap degraded was evaluated using the HELP model. [WSRC-STI-2007-00184_OUO] Values for total porosity and volumetric moisture content for the closure cap materials and foundation layers were taken from this analysis. These values were used to calculate the average saturation and the air-filled porosity for the closure cap materials. The maximum air-filled porosity for each material layer over the 10,000 year simulation was utilized, since this represented the greatest air filled porosity in which a gas could diffuse.

Table 4.5-2 provides the values of particle density, total porosity, average saturation, and air-filled porosity utilized for all the layers used in the baseline scenario (i.e., waste material layer to the erosion barrier) for the simulation period.

Table 4.5-2: Particle Density, Total Porosity, Average Saturation, and Air-Filled Porosity by Layer for the FTF Type I Tank Baseline Scenario

Layer	Particle Density (g/cm^3)	Total Porosity (fraction)	Average Saturation (fraction)	Air-filled Porosity (fraction)
Erosion barrier layer [1, 3]	2.65	0.150	0.84	0.024
Middle backfill layer [2, 3]	2.63	0.371	0.82	0.067
Upper Foundation layer [2, 3]	2.63	0.35	0.72	0.098
Lateral drainage layer [1, 3]	2.65	0.417	0.61	0.162
Lower Foundation Layer [2, 3]	2.63	0.457	0.28	0.328
Concrete Roof [4, 7]	2.51	0.168	0.00	0.168
Reducing Grout [5, 7]	2.51	0.266	0.00	0.266
Stabilized Contaminant Layer [6, 7]	2.51	0.266	0.00	0.266

1 Particle density assumed to be that typical of quartz. [WSRC-STI-2007-00355_OUO]
2 Values for particle density taken as that of control compacted backfill from WSRC-STI-2007-00184_OUO.
3 Total porosity, average saturation, and air-filled porosity values derived from WSRC-STI-2007-00184_OUO.
4 The concrete roof is assumed to be similar to the basemat surrogate as given by WSRC-STI-2007-00369. Particle density and porosity taken from WSRC-STI-2007-00369.
5 Particle density and porosity of reducing grout taken from WSRC-STI-2007-00369.
6 The stabilized contaminant is assumed to have the properties of reducing grout.
7 The concrete roof, reducing grout, and stabilized contaminant layer are conservatively assumed to be dry; therefore the average saturation is taken as 0 and the air-filled porosity is taken as the total porosity.

4.5.3 Summary of Key Air and Radon Pathway Assumptions

The following are the key air and radon pathway analysis assumptions associated with the FTF baseline scenario:

- The stabilized contaminant layer was represented as a 1 foot layer of material located at the bottom of the waste tank.
- The stabilized contaminant layer was assumed to be dry and to have properties similar to reducing grout.
- Exclusion of the top soil, upper backfill, HDPE geomembrane, GCL, and primary steel liner of the waste tank make the model more conservative.
- The final closure cap as outlined with exclusions was assumed to remain intact for the duration of the simulation.

In this analysis, several conditions introduce conservatism into the calculations. These include:

- The use of boundary conditions that force all of the gaseous radionuclides to move upward from the stabilized contaminant zone to the land surface. In reality, some of the gaseous radionuclides diffuse sideways and downward in the air-filled pores surrounding the stabilized contaminant zone, hence ignoring this has the effect of increasing the flux at the land surface.
- Not taking credit for the removal of radionuclides by pore water moving vertically downward through the model domain. This mechanism would likely remove some dissolved radionuclides, and therefore its omission had the effect of increasing the estimate of instantaneous radionuclide flux at the land surface in simulations conducted as a part of this investigation.
- Exclusion of the HDPE geomembrane, the GCL, and the primary steel liner of the waste tank. Inclusion of these materials in the model would significantly reduce the gaseous flux at the land surface due to their material properties (i.e., low air-filled porosity).
- Exclusion of the cover materials above the erosion barrier (i.e., top soil and upper backfill layers). Excluding these materials shortens the diffusion pathway and could increase the flux at the land surface.
- Assuming the stabilized contaminant layer, the reducing grout, and concrete roof are dry. This makes the air-filled porosity equal to the total porosity. This maximizes diffusive transport through these materials since gaseous flux is through the air-filled porosity.
- Use of the Type I tanks and minimum closure cap thickness.
- Concentrating the entire estimated FTF residual inventory into a 1 foot stabilized contaminant layer in one Type I tank to determine the maximum dose and flux.

4.5.4 Air Pathway Analysis

For the air pathway analysis, a list of radionuclides of interest was chosen based on NCRP-123, atmospheric screening methodology, while accounting for the fact that the radionuclides of concern for the airborne pathway are constrained by the actual waste tank inventory and the limited number of radionuclides susceptible to volatilization. These radionuclides included carbon-14 (C-14), chlorine-36 (Cl-36), iodine-129 (I-129), selenium-79 (Se-79), antimony-125 (Sb-125), tin-126 (Sn-126), tritium (H-3), and technetium-99 (Tc-99). Radon-222 (Rn-222) is addressed separately as required by DOE O 435.1. A summary of the radionuclides and compounds of interest is presented in Table 4.5-3.

Table 4.5-3: Radionuclides and Compounds of Interest for Air and Radon Pathway Analysis

Radionuclide	Half-life[1] (yrs)	Atomic Wt.	Molecular form in gaseous state	Molecular Wt.
C-14	5.70E+03	14	CO_2	45.99
Cl-36	3.01E+05	36	Cl_2	72
I-129	1.57E+07	129	I_2	258
Sb-125	2.76E+00	125	Sb	125
Se-79	2.95E+05	79	Se	79
Sn-126	2.30E+05	126	Sn	126
H-3	1.23E+00	3	H_2	6
Tc-99	2.11E+05	99	Tc	99
Rn-222	1.05E-02	222	Rn	222

[1]2005 Nuclear Wallet Cards [PIT-MISC-0072]

The radionuclides of interest are assumed to be in the gas phase and uniformly distributed through the 1 foot stabilized contaminant layer at the bottom of the waste tank. Certain gaseous radionuclides will not likely remain in the monatomic elemental form. These radionuclides will likely combine with other gaseous elements or form diatomic molecules. The state of existence of each of these radionuclides in the gaseous phase is important in evaluating their transport to the land surface because the diffusion coefficient associated with each is related to its molecular weight.

In this investigation it was assumed that:

- C-14 exists as part of the CO_2 molecule
- Cl-36, H-3 and I-129 exist as diatomic gasses
- Sb-125, Se-79, Sn-126, and Tc-99 exist as monatomic gasses

The effective air diffusion coefficient of each radionuclide or compound within each material zone was determined. A relationship was established between moisture saturation and the radon effective air-diffusion coefficient for various pore sizes of earthen materials. [WSRC-STI-2007-00355_OUO] Using this method, a radon effective air-diffusion coefficient was determined for each material type based upon the average moisture saturation for the material. Subsequently, using Graham's Law, the effective air-diffusion coefficient of each radionuclide or compound evaluated was determined for each material type based on the radon effective air-diffusion coefficient using the following relationship.

$$D = D'\sqrt{\frac{MWT'}{MWT}}$$

Where:

D = the effective diffusion coefficient of the radionuclide of interest (m^2/yr) within the material zone of interest
D' = the effective diffusion coefficient of Rn-222 (m^2/yr) within the material zone of interest
MWT' = the molecular weight of the reference radionuclide (Rn-222)
MWT = the molecular weight of the element or compound of interest

A summary of the radon effective air-diffusion coefficients and the calculated effective air-diffusion coefficients for each radionuclide/compound by material zone are presented in Table 4.5-4.

Table 4.5-4: Effective Air-Diffusion Coefficients for Each Radionuclide/Compound, by Material for FTF Type I Tank and Closure Cap

Radionuclide	Tank Stabilized Contaminants, Reducing Grout, and Concrete Roof Layer (m^2/yr)	Lower Foundation Layer (m^2/yr)	Upper Foundation Layer (m^2/yr)	Lateral Drainage Layer (m^2/yr)	Middle Backfill Layer (m^2/yr)	Erosion Barrier Layer (m^2/yr)
Rn-222	3.470E+02	1.210E+01	2.618E+00	4.194E+00	1.455E+00	1.301E+00
C-14	7.623E+02	2.658E+01	5.752E+00	9.213E+00	3.196E+00	2.858E+00
Cl-36	6.093E+02	2.124E+01	4.597E+00	7.364E+00	2.555E+00	2.284E+00
I-129	3.219E+02	1.122E+01	2.429E+00	3.890E+00	1.350E+00	1.207E+00
Sb-125	4.624E+02	1.612E+01	3.489E+00	5.589E+00	1.939E+00	1.734E+00
Se-79	5.817E+02	2.028E+01	4.389E+00	7.030E+00	2.439E+00	2.181E+00
Sn-126	4.606E+02	1.606E+01	3.475E+00	5.567E+00	1.931E+00	1.727E+00
H-3	2.111E+03	7.359E+01	1.593E+01	2.551E+01	8.850E+00	7.912E+00
Tc-99	5.196E+02	1.812E+01	3.921E+00	6.280E+00	2.179E+00	1.948E+00

Note: The effective diffusion coefficient for Rn-222 was used to determine the effective air diffusion coefficient of each radionuclide/compound based on Graham's Law (Grahams Law states that the rate of diffusion of a gas in inversely proportional to the square root of its molecular weight).

4.5.5 Air Pathway Model Factors for a Unit Curie (Ci)

4.5.5.1 Air Pathway Flux to Ground Surface

Model simulations were conducted to evaluate the peak flux of each radionuclide (other than radon) emanating from the top of the model domain. A unit inventory of 1 Ci was assigned to the FTF Type I tank stabilized contaminant zone for each radionuclide considered in the analysis. Results were output in Ci/yr, consistent with the set of units employed in the model, and are presented for each radionuclide in Figure 4.5-2. The peak fluxes emanating at the land surface are presented Table 4.5-5. The results are reported in this way to facilitate calculation of human exposure at the SRS boundary, at 100m from FTF, and at 1,600m from FTF (i.e., a representative seepline distance).

Figure 4.5-2: Flux at Land Surface for Each Radionuclide

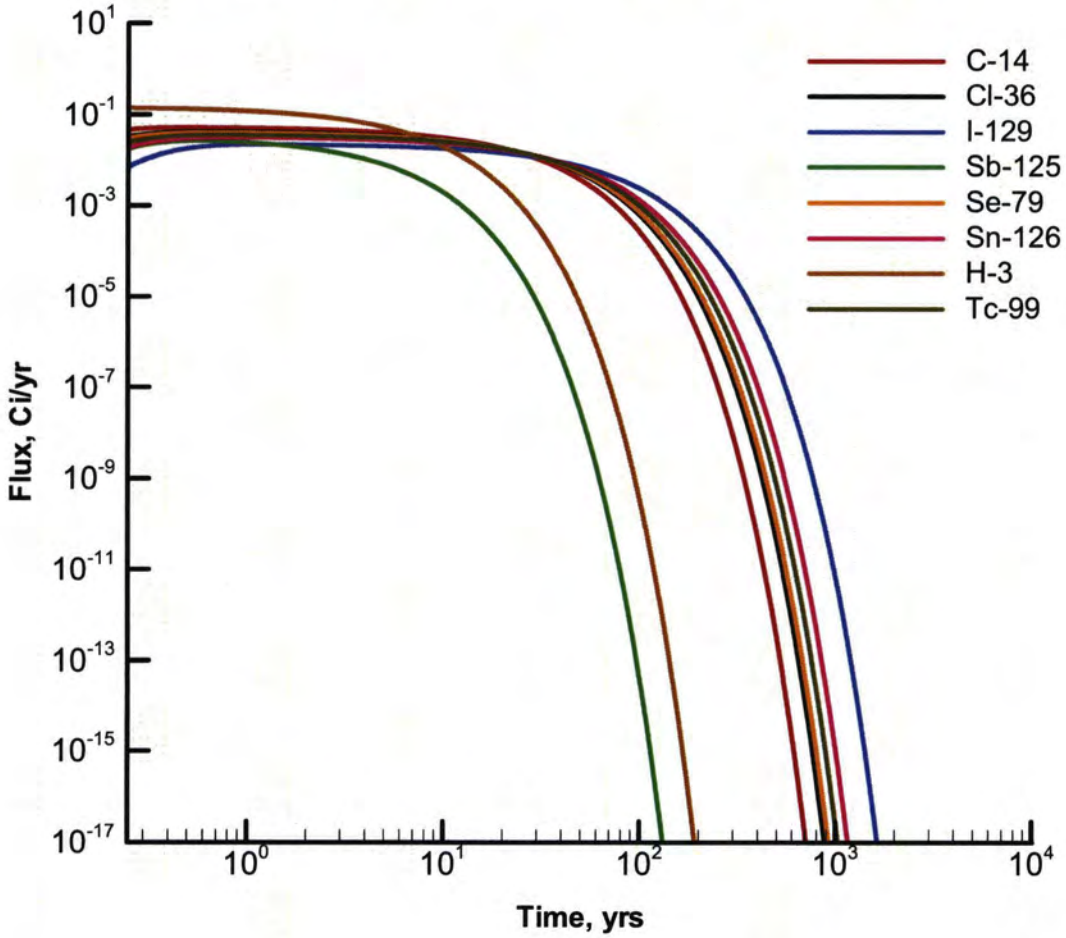

Table 4.5-5: Summary of the Peak Fluxes for Each Radionuclide

Radionuclide	Activity in Residual Waste (Ci)	Peak Flux (Ci/yr/Ci)
C-14	1.0	2.59E-04
Cl-36	1.0	6.07E-04
I-129	1.0	2.38E-03
Sb-125	1.0	3.71E-14
Se-79	1.0	7.02E-04
Sn-126	1.0	1.29E-03
H-3	1.0	3.12E-10
Tc-99	1.0	9.66E-04

4.5.5.2 Air Pathway Dose Calculations

An evaluation was conducted to assess the potential dose to a MEI located at the SRS boundary, at 1,600m from FTF (seepline), and at 100m from FTF. [WSRC-STI-2007-00343] DRFs were calculated for each radionuclide potentially released from the FTF using CAP-88, the EPA model for NESHAP. CAP-88 uses a database of dose and risk factors provided in *Federal Guidance Report 13* for estimating dose and risk, (i.e., factors for lifetime fatal cancer risk). [EPA-402-R-99-001] These dose and risk factors were used for the pathways of ingestion and inhalation intake, ground level air immersion, and ground surface irradiation. DRFs represent the dose to the receptor exposed to 1 Ci of the specified radionuclide potentially released to the atmosphere. For the receptor located at the SRS boundary and at the seepline (1,600m), the distance from the FTF is sufficient for an assumption of a point source. However, the DRFs for the 100m receptor required evaluation of an area source because of the close proximity of FTF to the 100m receptor. For radionuclides not contained within the CAP-88 library (Se-79, Cl-36) atmospheric transport was estimated by assigning surrogates with similar radiological properties. [WSRC-STI-2007-00343] Doses for these radionuclides were estimated by applying their dosimetric properties to the surrogate's relative air concentrations estimated by the model.

Specific SRS 100m DRFs and the calculated exposure levels for the MEI at 100m are presented in Table 4.5-6. Specific SRS 1,600m DRF and the calculated exposure levels for the MEI at 1,600m are presented in Table 4.5-7. Because the DRFs for 100m are calculated from an assumed area source, while the 1,600m DRFs are calculated from an assumed point source, the results show a more conservative estimate at 1,600m which results in a higher estimated dose at 1,600m than at 100m. See WSRC-STI-2007-00343 for details on the estimation of all DRFs.

Table 4.5-6: 100m Dose Release Factors and 100 – 10,000 Year FTF Exposure Levels

Radionuclide	Peak Flux (Ci/yr/Ci)	SRS 100m DRF[1] (mrem/Ci)	Dose to MEI at 100m Boundary[2] (mrem/yr/Ci)
C-14	2.59E-04	2.8E-04	7.2E-08
Cl-36	6.07E-04	2.9E-02	1.7E-05
I-129	2.38E-03	2.0E+01	4.8E-02
Sb-125	3.71E-14	3.9E-01	1.4E-14
Se-79	7.02E-04	3.8E-02	2.7E-05
Sn-126	1.29E-03	1.8E+01	2.3E-02
H-3	3.12E-10	1.3E-02	4.2E-12
Tc-99	9.66E-04	1.1E-01	1.0E-04

[1]WSRC-STI-2007-00343
[2] Dose to MEI at 100m = Peak Flux × Dose Release Factor. [WSRC-STI-2007-00355_OUO]

Table 4.5-7: 1,600m Dose Release Factors and 100 – 10,000 Year FTF Exposure Levels

Radionuclide	Peak Flux (Ci/yr/Ci)	SRS 1,600m DRF[1] (mrem/Ci)	Dose to MEI at 1,600m Boundary[2] (mrem/yr/Ci)
C-14	2.59E-04	2.4E-03	6.2E-07
Cl-36	6.07E-04	6.2E-03	3.7E-06
I-129	2.38E-03	2.3E+00	5.5E-03
Sb-125	3.71E-14	9.7E-02	3.6E-15
Se-79	7.02E-04	9.1E-03	6.4E-06
Sn-126	1.29E-03	4.4E+00	5.7E-03
H-3	3.12E-10	4.9E-05	1.5E-14
Tc-99	9.66E-04	2.6E-02	2.6E-05

[1]From WSRC-STI-2007-00343.
[2]Dose to MEI at 1,600m = Peak Flux × DRF. [WSRC-STI-2007-00355_OUO]

4.5.6 Radon Analysis

The permissible radon flux for DOE facilities is addressed in DOE M 435.1-1, Section IV. P.(c) states the radon flux limitations associated with the development of a disposal facility and maintenance of a PA and the closure of the disposal facility. This requirement is that the release of radon shall be less than an average yearly flux of 20 $pCi/m^2/sec$ at the surface of the disposal facility. The performance objective refers only to radon, and the correct species must be analyzed depending on the characteristics of the residual waste stream. The instantaneous Rn-222 flux at the land surface was evaluated for the simulation period and the maximum flux was then compared to the DOE performance objective.

The potential parent radionuclides that can contribute to the creation of Rn-222 are illustrated in Figure 4.5-3. The diagram indicates the specific decay chains that lead to the formation of Rn-222, as well as the half-lives for each radionuclide. The extremely long half-life of U-238 (4.468E+9 years) cause the other radionuclides higher up on the chain of parents to be of little concern with regard to their potential to contribute significantly to the Rn-222 flux at the land surface over the period of interest. In Figure 4.5-3, the parent radionuclides that were individually evaluated are indicated with the gray shaded area (i.e., beginning with Pu-238 and U-238). Rn-222 generated within the stabilized contaminant zone is in the gaseous phase and diffuses outward from this zone into the air-filled soil pores surrounding the FTF, eventually resulting in some of the radon emanating at the land surface. As such, air is the fluid through which Rn-222 diffuses, although some Rn-222 may dissolve in residual pore water.

The parent radionuclides are assumed to exist in the solid phase and therefore do not migrate upward through the air-filled pore space, although they could be leached and transported downward from the stabilized contaminant zone by pore water movement. This potential downward migration of the parent radionuclides was not considered in the radon analysis.

Decay chains evaluated were U-238→Th-234→Pa-234m→U-234→Th-230→Ra-226→Rn-222 and Pu-238 →U-234→Th-230→Ra-226→Rn-222. Each parent in these chains, except Th-234 and Pa-234m, were simulated separately as the starting point of the decay chain. Th-234 and Pa-234m have extremely short half-lives compared to the other parent radionuclides in these chains. Only a fraction of the Rn-222 generated by the decay of each parent is available for migration away from its source and into open pore space. Since the Rn-222 parent radionuclides exist as oxides or in other crystalline forms, only a fraction of Rn-222 generated by decay of Ra-226 has sufficient energy to migrate away from its original location into adjacent pore space before further decay occurs (3.82 day half-life for Rn-222).

The emanation coefficient is generally defined as the fraction of the total amount of Rn-222 produced by radium decay that escapes from soil particles and enters the pore space of the medium. This is the fraction of the Rn-222 that is available for transport. In the case of the FTF, the parent radionuclides are not embedded in soil but are contained within stabilized contaminants entombed in concrete/grout. Literature values for the Rn-222 emanation factor for these conditions are not available. Studies have shown the emanation factor to vary between 0.02 and 0.7 for various soil types depending primarily on moisture content. Generally, higher emanation factors are associated with higher moisture contents.

Figure 4.5-3: Radioactive Decay Chains Leading to Rn-222

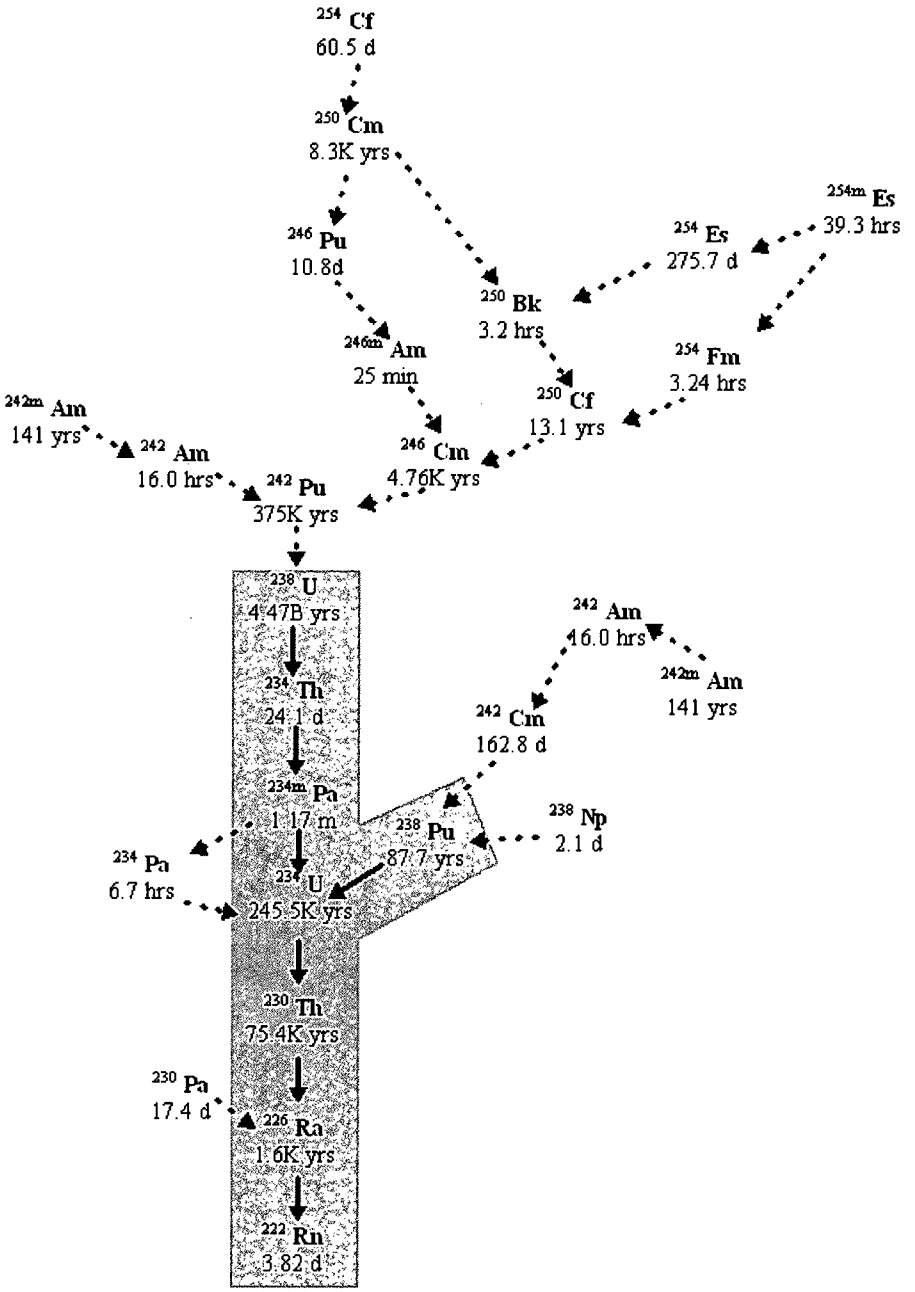

RESidual RADioactivity Computer Software (RESRAD) is a model used to estimate radiation dose and risk from residual radioactive materials. This DOE and NRC approved code, assumes an emanation factor of 0.25 for Rn-222 which is representative of a silty loam soil with low moisture content. For the FTF radon pathway analysis, the RESRAD default emanation factor of 0.25 was chosen recognizing that literature values for residual wastes similar to the FTF are not available. The use of 0.25 should be conservative since the stabilized contaminant is assumed to be dry and emanation factors reported in the literature for drier soils are much lower. [ANL-EAD-4] To account for the emanation factor in the model, an effective source term of 0.25 Ci of parent radionuclide was utilized for each Ci disposed within the facility.

Some radon dissolves in pore water but since diffusion proceeds more slowly in that fluid, air diffusion was the only transport process by which Rn-222 was allowed to reach the land surface of the FTF. This assertion is substantiated in ANL-EAD-4. In that report the effective diffusion coefficient for soil is reported to range from the radon open air diffusion coefficient of 1.0E-5 m^2/sec to that of fully saturated soil, 1.0E-10 m^2/sec. This five order of magnitude difference is consistent with the comparison of water diffusion coefficients to air diffusion coefficients of other common molecular compounds and reported in many references. Thus, the larger volume of water-filled pore space compared to air-filled pore space (maximum of 1 order of magnitude difference) is inconsequential, in terms of the ability of water-dissolved radon to diffuse through water-filled pores as compared to the ability of the same compounds to diffuse as gas in the vapor-filled pore spaces.

The molecular diffusion coefficient of Rn-222 in open air is 347 m^2/yr. [WSRC-STI-2007-00355_OUO] A relationship between moisture saturation and the radon effective air-diffusion coefficient for various pore sizes of earthen materials was established. This method was used to calculate a radon effective air-diffusion coefficient for each material type based upon the average moisture saturation for the material. Tortuosity was assigned a unit value for each material type. A summary of the radon air-diffusion coefficients by material type are presented in Table 4.5-4.

4.5.7 Radon Pathway Model Results

Model simulations were conducted to evaluate the peak instantaneous Rn-222 flux at the land surface for the simulation period of 10,000 years. Model results were output in Ci/m^2/yr per Ci of inventory, consistent with the set of units employed in the model. A graph of these results is shown in Figure 4.5-4, although the units are converted to pCi/m^2/sec per Ci/m^2, which are the units used to define the regulatory flux limit in DOE M 435.1-1. The peak fluxes represent the peak Rn-222 flux per square meter at the land surface for the two time periods and are given in Table 4.5-8.

Figure 4.5-4: Rn-222 Flux at Land Surface Resulting from Unit Source Term

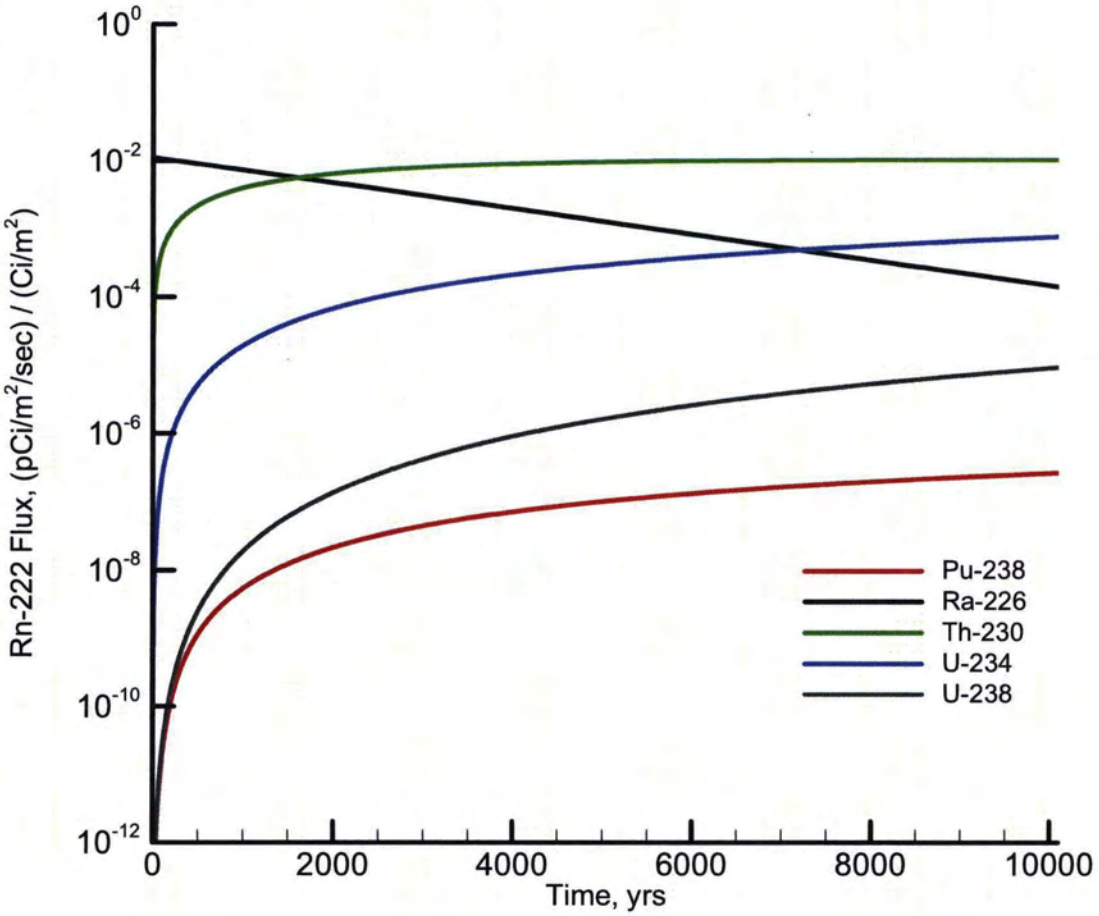

Table 4.5-8: Simulated Peak Instantaneous Rn-222 Flux over 10,000 Years at the Land Surface

Parent Source (1 Ci/m²)	Peak Instantaneous Rn-222 flux at Land Surface (pCi/m²/sec) / (Ci/m²)
Pu-238	2.70E-07
U-238	9.29E-06
U-234	7.68E-04
Th-230	1.03E-02
Ra-226	1.12E-02

4.6 Biotic Pathways

The purpose of this section is to document the Bioaccumulation Factors and Human Health Exposure parameters used in the FTF PA modeling effort. Exposure pathways for the FTF PA are discussed in Section 4.2.4. Bioaccumulation Factors and Human Health Exposure parameters are used to calculate doses for each of the pathways.

4.6.1 Bioaccumulation Factors

For PA analyses at SRS, soil-to-vegetable (also known as soil-to-plant ratios or plant-to-soil ratios), feed-to-milk, feed-to-beef and water-to-fish transfer factors are the bioaccumulation factors considered. Soil-to-vegetable transfer factors determine the fraction of an element that is drawn from the soil into the edible plant. Feed-to-milk transfer factors represent the element fraction transferred from fodder to milk. Feed-to-meat transfer factors represent the element specific fraction transferred from fodder to beef. Water-to-fish transfer factors are the equilibrium ratios between concentration in aquatic foods and concentration in water.

The factors utilized were developed based on comparison to a number of other DOE facilities and generic national/global references to establish relevance of the parameters selected and/or verify the regional differences for the southeastern United States. [WSRC-STI-2007-00004] The values for the parameters are based on expected values along with a range versus estimating an annual dose to the MEI.

4.6.1.1 Bioaccumulation Factor Methodology

A report entitled *Baseline Parameter Update for Human Health Input and Transfer Factors for Radiological Performance Assessments at the Savannah River Site* documents the SRS evaluation and reviews of transfer factors. [WSRC-STI-2007-00004] This report presents additional details on factors utilized in the past and discussion on conversion factors developed for SRS use. This report also established a single bioaccumulation factor parameter source that is up to date with existing data and maintained current via periodic reviews.

In developing the report, a comprehensive literature review was completed and references were updated to include the latest available information. In general, the values from more recent compilations were recommended, rather than those in older publications. The report includes information to establish a range of values for each element which was used to perform uncertainty analysis.

WSRC-STI-2007-00004 recommends updating the factors using site-specific values when available but considers *A Compendium of Transfer Factors for Agricultural and Animal Products* to be the most recent comprehensive evaluation of bioaccumulation factors and recommends this as the secondary source of values if site-specific values are not available. [PNNL-13421]

The hierarchy on document use at SRS for bioaccumulation factors is listed below:

- Site-Specific [WSRC-TR-96-0231, SRT-EST-2003-00134]
- Other site- or regional- specific publications (i.e., CDC-2005)
- PNNL-13421 (This PNNL document has a factor hierarchy of IAEA-364 then NUREG-CR-5512, then NCRP-123
- ORNL-5786 (This ORNL document has a factor hierarchy of 10 CFR 50, Regulatory Guide 1.109 then the TERRA code values.)
- NCRP-123

In PNNL-13421 the hierarchy of documents used to establish transfer factors is IAEA-364 and then NUREG-CR-5512, then NCRP-123. The International Atomic Energy Agency's Technical Report Series #364, *Handbook of Parameter Values for the Prediction of Radionuclide Transfer in Temperate Environments* encompasses a wide variety of plant types and is the result of extensive background investigations. [IAEA-364] It is based on data compiled by the International Union of Radioecologists. *Residual Radioactive Contamination from Decommissioning: Technical Basis for Translating Contamination Levels to Annual Total Effective Dose Equivalent*, NUREG-CR-5512 is frequently referenced because of its large set of data and traceable references.

In general, site-specific values were used without modification where appropriate. When recent generic compilations were used and the differences between the updated value and the currently used value were larger than two orders of magnitude, a geometric mean of the generic updated value and the currently used value was selected for averaging the ratios. *[http://en.wikipedia.org/ wiki/Geometric_mean]*

➢ **Bioaccumulation Parameters** The transfer factors that SRS utilized for the FTF PA appear in Tables 4.6-1 through 4.6-4. The data in these tables were taken from WSRC-STI-2007-00004.

Table 4.6-1: Soil-to-Vegetable Transfer Factors (Unitless)

Atomic No.	Element	Soil-to-Vegetable Transfer Factors			
		Value	Reference	Min.	Max.
89	Ac	6.83E-05	PNNL-13421	6.69E-05	3.50E-03
47	Ag	1.18E-02	PNNL-13421	2.54E-04	1.50E-01
13	Al	1.27E-04	ORNL-5786	1.24E-04	4.00E-03
95	Am	6.83E-05	PNNL-13421	2.15E-06	3.32E-02
18	Ar	0	NUREG-CR-5512	0	0
33	As	1.17E-03	PNNL-13421	1.17E-03	8.00E-02
85	At	2.93E-02	ORNL-5786	2.87E-02	2.00E-01
79	Au	3.51E-03	PNNL-13421	2.50E-04	1.00E-01
5	B	3.90E-01	ORNL-5786	1.00E-02	4.00E+00
56	Ba	2.93E-03	PNNL-13421	2.87E-03	4.00E-02
4	Be	2.93E-04	PNNL-13421	2.87E-04	4.00E-03
83	Bi	9.75E-02	PNNL-13421	9.56E-04	1.00E-01
97	Bk	1.00E-03	NCRP-123	5.90E-05	1.00E-03
35	Br	2.93E-01	PNNL-13421	2.93E-01	7.60E-01
6	C	1.37E-01	PNNL-13421	1.37E-01	5.50E+00
20	Ca	6.83E-02	PNNL-13421	6.69E-02	5.00E-01
48	Cd	2.93E-02	PNNL-13421	2.87E-02	5.00E-01
58	Ce	3.90E-03	PNNL-13421	7.65E-04	3.00E-02
98	Cf	6.83E-05	PNNL-13421	6.50E-06	1.00E-02
17	Cl	1.37E+01	PNNL-13421	3.00E-01	7.00E+01
96	Cm	8.39E-05	PNNL-13421	2.15E-06	2.50E-03
27	Co	1.31E-02	PNNL-13421	1.34E-03	2.34E-01
24	Cr	8.78E-04	PNNL-13421	2.50E-04	1.00E-02
55	Cs	9.00E-01	WSRC-TR-96-0231	2.15E-04	9.00E-01
29	Cu	4.88E-02	PNNL-13421	4.88E-02	1.30E-01
66	Dy	3.90E-03	PNNL-13421	7.80E-04	3.90E-03
68	Er	3.90E-03	PNNL-13421	7.80E-04	3.90E-03
99	Es	1.00E-03	NCRP-123	5.90E-05	1.00E-03
63	Eu	3.90E-03	PNNL-13421	7.65E-04	4.00E-03
9	F	1.17E-03	PNNL-13421	1.17E-03	2.00E-02
26	Fe	9.75E-03	PNNL-13421	1.91E-04	9.75E-03
100	Fm	2.00E-03	NCRP-123	2.00E-03	2.00E-03
87	Fr	5.85E-03	ORNL-5786	5.73E-03	3.00E-02
31	Ga	7.80E-05	PNNL-13421	7.65E-05	3.00E-03
64	Gd	3.90E-03	PNNL-13421	7.65E-04	4.00E-03

Table 4.6-1: Soil-to-Vegetable Transfer Factors (Unitless) (Continued)

Atomic No.	Element	Soil-to-Vegetable Transfer Factors			
		Value	Reference	Min.	Max.
32	Ge	1.56E-02	ORNL-5786	1.53E-02	4.00E-01
1	H	4.80E+00	10 CFR 50, Reg. Guide 1.109	0	6.92E+00
108	Ha	2.00E-03	NCRP-123	2.00E-03	2.00E-03
2	He	0	NCRP-123	0	0
72	Hf	1.95E-04	PNNL-13421	1.00E-04	3.00E-03
80	Hg	3.90E-02	PNNL-13421	3.82E-02	3.80E-01
67	Ho	3.90E-03	PNNL-13421	7.65E-04	4.00E-03
53	I	7.80E-03	PNNL-13421	6.63E-05	5.00E-02
49	In	7.80E-05	PNNL-13421	7.65E-05	3.00E-03
77	Ir	2.93E-03	PNNL-13421	2.87E-03	3.00E-02
19	K	1.07E-01	PNNL-13421	1.05E-01	5.50E-01
36	Kr	0	NUREG-CR-5512	0	0
57	La	6.83E-05	PNNL-13421	6.83E-05	2.50E-03
3	Li	7.80E-04	ORNL-5786	7.80E-04	1.71E-03
103	Lr	2.00E-03	NCRP-123	2.00E-03	2.00E-03
71	Lu	7.80E-04	ORNL-5786	7.65E-04	2.50E-03
101	Md	2.00E-03	NCRP-123	2.00E-03	2.00E-03
12	Mg	1.07E-01	PNNL-13421	3.00E-02	2.35E-01
25	Mn	3.90E-02	PNNL-13421	9.56E-03	3.00E-01
42	Mo	1.56E-01	PNNL-13421	1.15E-02	8.00E-01
7	N	3.50E-01	PNNL-13421	9.56E-03	1.28E+01
11	Na	5.85E-02	PNNL-13421	1.05E-02	3.00E-01
41	Nb	4.88E-03	PNNL-13421	9.56E-04	1.70E-02
60	Nd	3.90E-03	PNNL-13421	7.80E-04	3.90E-03
10	Ne	0	NCRP-123	0	0
28	Ni	1.17E-02	PNNL-13421	3.51E-03	3.51E-01
102	No	2.00E-03	NCRP-123	2.00E-03	2.00E-03
93	Np	2.54E-03	PNNL-13421	1.38E-04	2.73E-02
8	O	6.00E-01	NCRP-123	6.00E-01	6.00E-01
76	Os	6.83E-04	PNNL-13421	6.83E-04	3.00E-02
15	P	6.83E-01	PNNL-13421	6.69E-01	3.50E+00
91	Pa	4.18E-04	PNNL-13421	4.78E-05	1.00E-02
82	Pb	1.17E-03	PNNL-13421	2.54E-05	1.00E-02
46	Pd	7.80E-03	PNNL-13421	7.65E-03	1.00E-01
61	Pm	3.90E-03	PNNL-13421	7.65E-04	4.00E-03
84	Po	1.37E-03	PNNL-13421	7.65E-05	7.00E-03
59	Pr	3.90E-03	PNNL-13421	7.65E-04	3.90E-03
78	Pt	4.88E-03	ORNL-5786	4.78E-03	1.00E-01

Table 4.6-1: Soil-to-Vegetable Transfer Factors (Unitless) (Continued)

Atomic No.	Element	Soil-to-Vegetable Transfer Factors			
		Value	Reference	Min.	Max.
94	Pu	2.15E-04	PNNL-13421	7.41E-07	1.09E-02
88	Ra	4.64E-03	PNNL-13421	3.90E-04	4.00E-02
37	Rb	1.76E-01	PNNL-13421	1.34E-02	9.00E-01
75	Re	1.29E+00	PNNL-13421	6.83E-02	2.10E+02
104	Rf	3.00E-03	NCRP-123	3.00E-03	3.00E-03
45	Rh	7.80E-03	PNNL-13421	7.65E-03	1.30E+01
86	Rn	0	NUREG-CR-5512	0	0
44	Ru	7.80E-03	PNNL-13421	3.82E-03	5.00E-02
16	S	2.93E-01	PNNL-13421	2.87E-01	6.42E-01
51	Sb	2.49E-03	PNNL-13421	2.15E-05	1.30E-02
21	Sc	1.95E-04	PNNL-13421	1.91E-04	2.00E-03
34	Se	5.14E-02	PNNL-13421	4.78E-03	1.30E+00
14	Si	1.37E-02	PNNL-13421	1.34E-02	8.80E-02
62	Sm	3.90E-03	PNNL-13421	7.65E-04	4.00E-03
50	Sn	1.17E-03	PNNL-13421	1.15E-03	3.00E-01
38	Sr	9.75E-02	PNNL-13421	1.70E-02	2.73E+00
73	Ta	4.88E-03	PNNL-13421	4.78E-04	2.00E-02
65	Tb	3.90E-03	PNNL-13421	7.80E-04	3.90E-03
43	Tc	4.68E-02	PNNL-13421	4.68E-02	5.46E+00
52	Te	1.20E-02	PNNL-13421	7.65E-04	1.30E+00
90	Th	6.44E-05	PNNL-13421	5.85E-06	4.20E-03
22	Ti	5.85E-04	ORNL-5786	1.00E-04	3.00E-03
81	Tl	7.80E-05	PNNL-13421	7.65E-05	2.00E-01
69	Tm	7.80E-04	ORNL-5786	7.80E-04	2.00E-03
92	U	2.34E-03	PNNL-13421	2.73E-04	2.73E-02
23	V	5.85E-04	ORNL-5786	5.73E-04	3.00E-03
74	W	5.00E-02	PNNL-13421	1.91E-03	8.00E-01
54	Xe	0	NUREG-CR-5512	0	0
39	Y	1.95E-03	PNNL-13421	1.15E-03	3.00E-01
70	Yb	7.80E-04	ORNL-5786	7.80E-04	2.00E-03
30	Zn	6.83E-02	PNNL-13421	6.83E-02	2.34E+00
40	Zr	1.95E-04	PNNL-13421	9.56E-05	1.00E-03

[WSRC-STI-2007-00004, Table B-1]

Table 4.6-2: Feed-to-Milk Transfer Factors (d/L)

Atomic No.	Element	Feed-to-Milk Transfer Factors			
		Factor	Reference	Min.	Max.
89	Ac	2.00E-05	PNNL-13421	2.00E-06	2.06E-05
47	Ag	1.58E-03	PNNL-13421	5.00E-05	5.00E-02
13	Al	2.06E-04	ORNL-5786	2.00E-04	2.06E-04
95	Am	1.50E-06	PNNL-13421	4.00E-07	5.00E-06
33	As	6.00E-05	PNNL-13421	6.00E-05	1.00E-04
85	At	1.03E-02	ORNL-5786	1.00E-02	1.03E-02
79	Au	5.50E-06	PNNL-13421	5.00E-06	1.00E-05
5	B	1.55E-03	ORNL-5786	1.50E-03	3.00E-03
56	Ba	4.80E-04	PNNL-13421	3.50E-04	8.00E-03
4	Be	9.00E-07	PNNL-13421	9.00E-07	2.00E-06
83	Bi	5.00E-04	PNNL-13421	5.00E-04	1.00E-03
97	Bk	2.00E-06	NCRP-123	4.00E-07	2.00E-06
35	Br	2.00E-02	PNNL-13421	2.00E-02	2.06E-02
6	C	1.20E-02	10 CFR 50, Reg. Guide 1.109	1.05E-02	1.20E-02
20	Ca	3.00E-03	PNNL-13421	3.00E-03	1.03E-02
48	Cd	1.00E-03	PNNL-13421	1.20E-04	2.00E-03
58	Ce	3.00E-05	PNNL-13421	2.00E-05	1.00E-04
98	Cf	1.50E-06	PNNL-13421	7.50E-07	2.00E-06
17	Cl	1.70E-02	PNNL-13421	1.50E-02	2.00E-02
96	Cm	2.00E-05	PNNL-13421	2.00E-06	2.06E-05
27	Co	3.00E-04	PNNL-13421	3.00E-04	2.06E-03
24	Cr	1.00E-05	PNNL-13421	1.00E-05	2.20E-03
55	Cs	7.90E-03	PNNL-13421	7.00E-03	1.20E-02
29	Cu	2.00E-03	PNNL-13421	1.50E-03	1.40E-02
66	Dy	3.00E-05	PNNL-13421	2.00E-05	6.00E-05
68	Er	3.00E-05	PNNL-13421	2.00E-05	6.00E-05
99	Es	2.00E-06	NCRP-123	4.00E-07	2.00E-06
63	Eu	3.00E-05	PNNL-13421	2.00E-05	6.00E-05
9	F	1.00E-03	PNNL-13421	1.00E-03	7.00E-03
26	Fe	3.00E-05	PNNL-13421	3.00E-05	1.20E-03
87	Fr	2.06E-02	ORNL-5786	8.00E-03	2.06E-02
31	Ga	5.00E-05	PNNL-13421	1.00E-05	5.15E-05
64	Gd	3.00E-05	PNNL-13421	2.00E-05	6.00E-05
32	Ge	7.21E-02	ORNL-5786	1.00E-02	7.21E-02
1	H	1.50E-02	PNNL-13421	0	1.50E-02
105	Ha	5.00E-06	NCRP-123	5.00E-06	5.00E-06
2	He	0	NCRP-123	0	0

Table 4.6-2: Feed-to-Milk Transfer Factors (d/L) (Continued)

Atomic No.	Element	Feed-to-Milk Transfer Factors			
		Factor	Reference	Min.	Max.
72	Hf	5.50E-07	PNNL-13421	5.50E-07	2.50E-05
80	Hg	4.70E-04	PNNL-13421	4.50E-04	5.00E-04
67	Ho	3.00E-05	PNNL-13421	2.00E-05	6.00E-05
53	I	9.00E-03	PNNL-13421	6.00E-03	1.20E-02
49	In	2.00E-04	PNNL-13421	1.00E-04	2.00E-04
77	Ir	2.00E-06	PNNL-13421	2.00E-06	2.06E-06
19	K	7.20E-03	PNNL-13421	7.00E-03	7.21E-03
57	La	2.00E-05	PNNL-13421	5.00E-06	6.00E-05
3	Li	2.06E-02	ORNL-5786	2.06E-02	5.00E-02
103	Lr	5.00E-06	NCRP-123	5.00E-06	5.00E-06
71	Lu	2.06E-05	ORNL-5786	2.00E-05	6.00E-05
101	Md	5.00E-06	NCRP-123	5.00E-06	5.00E-06
12	Mg	3.90E-03	PNNL-13421	3.90E-03	8.00E-03
25	Mn	3.00E-05	PNNL-13421	3.00E-05	3.61E-04
42	Mo	1.70E-03	PNNL-13421	1.50E-03	7.50E-03
7	N	2.50E-02	PNNL-13421	1.00E-02	2.58E-02
11	Na	1.60E-02	PNNL-13421	1.60E-02	4.00E-02
41	Nb	3.20E-05	PNNL-13421	4.10E-07	2.06E-02
60	Nd	3.00E-05	PNNL-13421	5.00E-06	6.00E-05
28	Ni	1.60E-02	PNNL-13421	1.00E-03	2.00E-02
102	No	5.00E-06	NCRP-123	5.00E-06	5.00E-06
93	Np	5.00E-06	PNNL-13421	5.00E-06	1.00E-05
76	Os	5.00E-03	PNNL-13421	1.00E-04	3.50E+00
15	P	1.60E-02	PNNL-13421	1.50E-02	2.50E-02
91	Pa	5.00E-06	PNNL-13421	5.00E-06	5.15E-06
82	Pb	2.60E-04	PNNL-13421	2.50E-04	3.00E-04
46	Pd	1.00E-02	PNNL-13421	1.00E-04	1.03E-02
61	Pm	3.00E-05	PNNL-13421	2.00E-05	6.00E-05
84	Po	3.40E-04	PNNL-13421	3.40E-04	4.00E-04
59	Pr	3.00E-05	PNNL-13421	5.00E-06	6.00E-05
78	Pt	5.15E-03	ORNL-5786	1.00E-04	5.15E-03
94	Pu	1.10E-06	PNNL-13421	1.00E-07	2.00E-06
88	Ra	1.30E-03	PNNL-13421	4.50E-04	1.30E-03
37	Rb	1.20E-02	PNNL-13421	1.00E-02	3.00E-02
75	Re	1.50E-03	PNNL-13421	1.40E-04	2.00E-03
104	Rf	2.00E-05	NCRP-123	2.00E-05	2.00E-05
45	Rh	1.00E-02	PNNL-13421	5.00E-04	1.03E-02
86	Rn	0	NCRP-123	0	0

Table 4.6-2: Feed-to-Milk Transfer Factors (d/L) (Continued)

Atomic No.	Element	Feed-to-Milk Transfer Factors			
		Factor	Reference	Min.	Max.
44	Ru	3.30E-06	PNNL-13421	6.00E-07	2.00E-05
16	S	1.60E-02	PNNL-13421	1.50E-02	2.00E-02
51	Sb	2.50E-05	PNNL-13421	2.50E-05	1.50E-03
21	Sc	5.00E-06	PNNL-13421	5.00E-06	6.00E-05
34	Se	4.00E-03	PNNL-13421	4.00E-03	4.50E-02
14	Si	2.00E-05	PNNL-13421	2.00E-05	2.06E-05
62	Sm	3.00E-05	PNNL-13421	5.00E-06	6.00E-05
50	Sn	1.00E-03	PNNL-13421	1.00E-03	2.50E-03
38	Sr	2.80E-03	PNNL-13421	8.00E-04	2.80E-03
73	Ta	4.10E-07	PNNL-13421	4.10E-07	5.00E-06
65	Tb	3.00E-05	PNNL-13421	2.00E-05	6.00E-05
43	Tc	1.87E-03	PNNL-13421	2.30E-05	2.50E-02
52	Te	4.50E-04	PNNL-13421	2.00E-04	1.00E-03
90	Th	5.00E-06	PNNL-13421	5.00E-06	5.15E-06
22	Ti	7.53E-05	ORNL-5786	5.50E-07	1.03E-02
81	Tl	2.00E-03	PNNL-13421	1.00E-03	1.00E-02
69	Tm	2.06E-05	ORNL-5786	2.06E-05	6.00E-05
92	U	4.00E-04	PNNL-13421	4.00E-04	6.18E-04
23	V	2.06E-05	ORNL-5786	2.00E-05	5.00E-04
74	W	3.00E-04	PNNL-13421	3.00E-04	5.00E-04
39	Y	2.00E-05	PNNL-13421	1.00E-05	2.00E-03
70	Yb	2.06E-05	ORNL-5786	2.06E-05	6.00E-05
30	Zn	1.00E-02	PNNL-13421	1.00E-02	3.90E-02
40	Zr	5.50E-07	PNNL-13421	5.50E-07	3.09E-05

[WSRC-STI-2007-00004, Table B-2]

Table 4.6-3: Feed-to-Meat Transfer Factors (d/kg)

Atomic No.	Element	Feed-to-Meat Transfer Factors			
		Value	Reference	Min.	Max.
89	Ac	4.00E-04	PNNL-13421	2.00E-05	4.00E-04
47	Ag	3.00E-03	PNNL-13421	3.00E-03	1.70E-02
13	Al	1.50E-03	ORNL-5786	5.00E-04	1.50E-03
95	Am	4.00E-05	PNNL-13421	3.50E-06	2.00E-04
33	As	2.00E-03	PNNL-13421	1.50E-03	2.00E-02
85	At	1.00E-02	ORNL-5786	1.00E-02	1.00E-02
79	Au	5.00E-03	PNNL-13421	2.00E-04	8.00E-03
5	B	8.00E-04	ORNL-5786	8.00E-04	8.00E-04
56	Ba	2.00E-04	PNNL-13421	1.50E-04	3.00E-02
4	Be	1.00E-03	PNNL-13421	1.00E-03	5.00E-03
83	Bi	4.00E-04	PNNL-13421	4.00E-04	2.00E-03
97	Bk	2.50E-05	NCRP-123	2.00E-05	4.00E-05
35	Br	2.50E-02	PNNL-13421	2.00E-02	5.00E-02
6	C	3.10E-02	10 CFR 50, Reg. Guide 1.109	3.10E-02	4.89E-02
20	Ca	2.00E-03	PNNL-13421	7.00E-04	2.00E-03
48	Cd	4.00E-04	PNNL-13421	4.00E-04	1.00E-03
58	Ce	2.00E-05	PNNL-13421	2.00E-05	1.20E-03
98	Cf	4.00E-05	PNNL-13421	4.00E-05	5.00E-03
17	Cl	2.00E-02	PNNL-13421	2.00E-02	8.00E-02
96	Cm	4.00E-05	PNNL-13421	3.50E-06	2.00E-04
27	Co	1.00E-02	PNNL-13421	1.00E-02	3.00E-02
24	Cr	9.00E-03	PNNL-13421	2.40E-03	3.00E-02
55	Cs	5.00E-02	PNNL-13421	4.00E-03	5.00E-02
29	Cu	9.00E-03	PNNL-13421	8.00E-03	1.00E-02
66	Dy	2.00E-05	PNNL-13421	2.00E-05	5.50E-03
68	Er	2.00E-05	PNNL-13421	2.00E-05	4.00E-03
99	Es	2.50E-05	NCRP-123	2.00E-05	2.50E-05
63	Eu	2.00E-05	PNNL-13421	2.00E-05	5.00E-03
9	F	1.50E-01	PNNL-13421	2.00E-02	1.50E-01
26	Fe	2.00E-02	PNNL-13421	2.00E-02	4.00E-02
100	Fm	2.00E-04	NCRP-123	2.00E-04	2.00E-04
87	Fr	2.50E-03	ORNL-5786	2.50E-03	3.00E-02
31	Ga	5.00E-04	PNNL-13421	3.00E-04	5.00E-04
64	Gd	2.00E-05	PNNL-13421	2.00E-05	3.50E-03
32	Ge	7.00E-01	ORNL-5786	2.00E-01	7.00E-01
1	H		Not Used in Model	0	1.20E-02
105	Ha	5.00E-06	NCRP-123	5.00E-06	5.00E-06
72	Hf	3.16E-05	PNNL-13421	1.00E-06	1.00E-03

Table 4.6-3: Feed-to-Meat Transfer Factors (d/kg) (Continued)

Atomic No.	Element	Feed-to-Meat Transfer Factors			
		Value	Reference	Min.	Max.
80	Hg	2.50E-01	PNNL-13421	1.00E-02	2.50E-01
67	Ho	3.00E-04	PNNL-13421	2.00E-05	4.50E-03
53	I	4.00E-02	PNNL-13421	2.90E-03	4.00E-02
49	In	8.00E-03	PNNL-13421	4.00E-03	8.00E-03
77	Ir	1.50E-03	PNNL-13421	1.50E-03	2.00E-03
19	K	2.00E-02	PNNL-13421	2.00E-02	2.00E-02
57	La	2.00E-03	PNNL-13421	2.00E-04	2.00E-03
3	Li	1.00E-02	ORNL-5786	1.00E-02	2.00E-02
103	Lr	2.00E-04	NCRP-123	2.00E-04	2.00E-04
71	Lu	4.50E-03	ORNL-5786	2.00E-03	4.50E-03
12	Mg	2.00E-02	PNNL-13421	3.00E-03	2.00E-02
25	Mn	5.00E-04	PNNL-13421	4.00E-04	1.00E-03
42	Mo	1.00E-03	PNNL-13421	1.00E-03	8.00E-03
7	N	7.50E-02	PNNL-13421	1.00E-02	7.50E-02
11	Na	8.00E-02	PNNL-13421	3.00E-02	8.00E-02
41	Nb	2.90E-04	PNNL-13421	3.00E-07	2.80E-01
60	Nd	2.00E-05	PNNL-13421	2.00E-05	3.30E-03
28	Ni	5.00E-03	PNNL-13421	5.00E-03	5.30E-02
102	No	2.00E-04	NCRP-123	2.00E-04	2.00E-04
93	Np	1.00E-03	PNNL-13421	5.50E-05	1.00E-03
76	Os	4.00E-01	PNNL-13421	2.00E-03	4.00E-01
15	P	5.00E-02	PNNL-13421	4.60E-02	2.00E-01
91	Pa	4.47E-04	PNNL-13421	5.00E-06	5.00E-03
82	Pb	4.00E-04	PNNL-13421	3.00E-04	8.00E-04
46	Pd	4.00E-03	PNNL-13421	2.00E-04	4.00E-03
61	Pm	2.00E-05	PNNL-13421	2.00E-05	5.00E-03
84	Po	5.00E-03	PNNL-13421	9.50E-05	5.00E-03
59	Pr	2.00E-05	PNNL-13421	2.00E-05	4.70E-03
78	Pt	4.00E-03	ORNL-5786	2.00E-04	4.00E-03
94	Pu	1.00E-05	PNNL-13421	5.00E-07	1.00E-04
88	Ra	9.00E-04	PNNL-13421	2.50E-04	1.00E-03
37	Rb	1.00E-02	PNNL-13421	1.00E-02	3.10E-02
75	Re	8.00E-03	PNNL-13421	1.00E-04	1.00E-02
45	Rh	2.00E-03	PNNL-13421	1.00E-03	2.00E-03
86	Rn	0	NCRP-123	0	0
44	Ru	5.00E-02	PNNL-13421	2.00E-03	4.00E-01
16	S	2.00E-01	PNNL-13421	1.00E-01	2.00E-01
51	Sb	1.00E-03	PNNL-13421	4.00E-05	4.00E-03
21	Sc	1.50E-02	PNNL-13421	2.00E-03	1.50E-02

Table 4.6-3: Feed-to-Meat Transfer Factors (d/kg) (Continued)

Atomic No.	Element	Feed-to-Meat Transfer Factors			
		Value	Reference	Min.	Max.
34	Se	1.50E-02	PNNL-13421	1.50E-02	1.00E-01
14	Si	4.00E-05	PNNL-13421	4.00E-05	3.00E-04
62	Sm	3.16E-04	PNNL-13421	2.00E-05	5.00E-03
50	Sn	8.00E-02	PNNL-13421	1.00E-02	8.00E-02
38	Sr	8.00E-03	PNNL-13421	3.00E-04	1.00E-02
73	Ta	1.34E-05	PNNL-13421	3.00E-07	6.00E-04
65	Tb	2.00E-05	PNNL-13421	2.00E-05	4.50E-03
43	Tc	6.32E-03	PNNL-13421	1.00E-04	4.00E-01
52	Te	7.00E-03	PNNL-13421	7.00E-03	7.70E-02
90	Th	4.00E-05	PNNL-13421	6.00E-06	2.00E-04
22	Ti	1.73E-04	ORNL-5786	1.00E-06	3.00E-02
81	Tl	4.00E-02	PNNL-13421	2.00E-03	4.00E-02
69	Tm	4.50E-03	ORNL-5786	2.00E-03	4.50E-03
92	U	3.00E-04	PNNL-13421	2.00E-04	8.00E-04
23	V	2.50E-03	ORNL-5786	2.50E-03	1.00E-02
74	W	4.00E-02	PNNL-13421	1.30E-03	4.50E-02
39	Y	1.00E-03	PNNL-13421	3.00E-04	8.00E-03
70	Yb	4.00E-03	ORNL-5786	2.00E-03	4.00E-03
30	Zn	1.00E-01	PNNL-13421	3.00E-02	1.00E-01
40	Zr	1.84E-04	PNNL-13421	1.00E-06	3.40E-02

[WSRC-STI-2007-00004, Table B-3]

Table 4.6-4: Water-to-Fish Bioaccumulation Factors (L/kg)

Atomic No.	Element	Water-to-Fish Bioaccumulation Factors			
		Value	Reference	Min.	Max.
89	Ac	2.50E+01	PNNL-13421	1.50E+01	2.50E+01
47	Ag	5.00E+00	PNNL-13421	2.30E+00	5.00E+00
13	Al	5.00E+02	NCRP-123	1.00E+01	5.00E+02
95	Am	3.00E+01	PNNL-13421	2.10E+01	2.40E+03
33	As	1.70E+03	PNNL-13421	1.00E+02	1.70E+03
85	At	1.50E+01	NCRP-123	1.50E+01	1.50E+01
79	Au	3.30E+01	PNNL-13421	3.30E+01	3.50E+01
56	Ba	4.00E+00	PNNL-13421	4.00E+00	2.00E+02
4	Be	1.00E+02	PNNL-13421	2.00E+00	1.00E+02
83	Bi	1.50E+01	PNNL-13421	1.00E+01	1.50E+01
97	Bk	2.50E+01	NCRP-123	2.50E+01	2.50E+01
35	Br	4.00E+02	PNNL-13421	4.00E+02	4.20E+02
6	C	5.00E+04	PNNL-13421	4.60E+03	5.00E+04
20	Ca	4.00E+01	PNNL-13421	4.00E+01	1.00E+03
48	Cd	2.00E+02	PNNL-13421	2.00E+02	2.00E+02
58	Ce	3.00E+01	PNNL-13421	1.00E+00	5.00E+02
98	Cf	2.50E+01	PNNL-13421	2.50E+01	2.50E+01
17	Cl	5.00E+01	PNNL-13421	5.00E+01	1.00E+03
96	Cm	3.00E+01	PNNL-13421	2.10E+01	2.50E+02
27	Co	3.00E+02	PNNL-13421	5.00E+01	3.30E+02
24	Cr	4.00E+00	PNNL-13421	4.00E+00	2.00E+02
55	Cs	3.00E+03	SRT-EST-2003-00134	2.00E+03	4.70E+03
29	Cu	2.00E+02	PNNL-13421	5.00E+01	2.00E+02
66	Dy	3.00E+01	PNNL-13421	3.00E+01	3.00E+01
68	Er	3.00E+01	PNNL-13421	3.00E+01	3.00E+01
99	Es	2.50E+01	NCRP-123	1.00E+01	2.50E+01
63	Eu	3.00E+01	PNNL-13421	2.50E+01	5.00E+01
9	F	1.00E+01	PNNL-13421	1.00E+01	1.00E+01
26	Fe	2.00E+02	PNNL-13421	1.00E+02	2.00E+03
87	Fr	3.00E+01	NCRP-123	3.00E+01	3.00E+01
31	Ga	4.00E+02	PNNL-13421	3.33E+02	4.00E+02
64	Gd	3.00E+01	PNNL-13421	2.50E+01	3.00E+01
32	Ge	4.00E+03	NCRP-123	3.33E+03	4.00E+03
2	He	1.00E+00	PNNL-13421	1.00E+00	1.00E+00
1	H	1.00E+00	NCRP-123	9.00E-01	1.00E+00
72	Hf	3.00E+02	PNNL-13421	3.33E+00	3.00E+02
80	Hg	1.00E+03	PNNL-13421	1.00E+03	1.00E+03
67	Ho	3.00E+01	PNNL-13421	2.50E+01	3.00E+01
53	I	4.00E+01	PNNL-13421	1.50E+01	5.00E+02

Table 4.6-4: Water-to-Fish Bioaccumulation Factors (L/kg) (Continued)

Atomic No.	Element	Water-to-Fish Bioaccumulation Factors			
		Value	Reference	Min.	Max.
49	In	1.00E+04	PNNL-13421	1.00E+04	1.00E+05
77	Ir	1.00E+01	PNNL-13421	1.00E+01	1.00E+01
19	K	1.00E+03	PNNL-13421	1.00E+03	1.00E+04
57	La	3.00E+01	PNNL-13421	2.50E+01	3.00E+01
71	Lu	2.50E+01	NCRP-123	2.50E+01	2.50E+01
12	Mg	5.00E+01	PNNL-13421	5.00E+01	5.00E+01
25	Mn	4.00E+02	PNNL-13421	1.00E+02	4.00E+02
42	Mo	1.00E+01	PNNL-13421	1.00E+01	1.00E+01
7	N	2.00E+05	PNNL-13421	1.50E+05	2.00E+05
11	Na	2.00E+01	PNNL-13421	8.00E+00	1.00E+02
41	Nb	3.00E+02	PNNL-13421	2.00E+02	3.00E+04
60	Nd	3.00E+01	PNNL-13421	2.50E+01	1.00E+02
28	Ni	1.00E+02	PNNL-13421	1.00E+02	1.00E+02
93	Np	2.10E+01	PNNL-13421	1.00E+01	2.50E+02
8	O	1.00E+00	PNNL-13421	1.00E+00	1.00E+00
76	Os	1.00E+03	PNNL-13421	1.00E+01	1.00E+05
15	P	5.00E+04	PNNL-13421	1.50E+03	1.00E+05
91	Pa	1.00E+01	PNNL-13421	1.00E+01	1.13E+01
82	Pb	3.00E+02	PNNL-13421	1.00E+02	3.00E+02
46	Pd	1.00E+01	PNNL-13421	1.00E+01	1.00E+01
61	Pm	3.00E+01	PNNL-13421	2.50E+01	3.00E+01
84	Po	5.00E+01	PNNL-13421	5.00E+01	5.00E+02
59	Pr	3.00E+01	PNNL-13421	2.50E+01	1.00E+02
78	Pt	3.50E+01	NCRP-123	3.50E+01	1.00E+02
94	Pu	3.00E+01	PNNL-13421	3.50E+00	4.70E+03
88	Ra	5.00E+01	PNNL-13421	5.00E+01	7.00E+01
37	Rb	2.00E+03	PNNL-13421	2.00E+03	2.00E+03
75	Re	1.20E+02	PNNL-13421	1.19E+02	1.20E+04
45	Rh	1.00E+01	PNNL-13421	1.00E+01	1.00E+01
45	Rn	0	NCRP-123	0	5.70E+01
44	Ru	1.00E+02	PNNL-13421	1.00E+01	1.00E+02
16	S	8.00E+02	PNNL-13421	7.50E+02	1.00E+03
51	Sb	1.00E+02	PNNL-13421	1.00E+00	2.00E+02
21	Sc	1.00E+02	PNNL-13421	1.00E+02	1.00E+02
34	Se	1.70E+02	PNNL-13421	1.70E+02	2.00E+02
14	Si	2.00E+01	PNNL-13421	2.50E+00	2.00E+01
62	Sm	3.00E+01	PNNL-13421	2.50E+01	3.00E+01
50	Sn	3.00E+03	PNNL-13421	3.00E+03	3.00E+03
38	Sr	6.00E+01	PNNL-13421	3.00E+01	5.01E+02

Table 4.6-4: Water-to-Fish Bioaccumulation Factors (L/kg) (Continued)

Atomic No.	Element	Water-to-Fish Bioaccumulation Factors			
		Value	Reference	Min.	Max.
73	Ta	3.00E+02	PNNL-13421	1.00E+02	3.00E+04
65	Tb	3.00E+01	PNNL-13421	2.50E+01	3.00E+01
43	Tc	2.00E+01	PNNL-13421	1.50E+01	2.00E+01
52	Te	4.00E+02	PNNL-13421	4.00E+02	4.00E+02
90	Th	1.00E+02	PNNL-13421	3.00E+01	1.00E+02
22	Ti	1.00E+03	NCRP-123	1.00E+03	1.00E+03
81	Tl	1.00E+04	PNNL-13421	1.00E+04	1.00E+04
92	U	1.00E+01	PNNL-13421	2.00E+00	5.00E+01
23	V	2.00E+02	NCRP-123	1.00E+01	2.00E+02
74	W	1.00E+01	PNNL-13421	1.00E+01	1.20E+03
39	Y	3.00E+01	PNNL-13421	2.50E+01	3.00E+01
30	Zn	3.50E+02	PNNL-13421	3.50E+02	2.50E+03
40	Zr	3.00E+02	PNNL-13421	3.30E+00	3.00E+02

[WSRC-STI-2007-00004, Table B-4]

4.6.2 Human Health Exposure Parameters (Consumption Rates)

This section documents the Human Health Exposure parameters (i.e., consumption rates) used in the FTF PA modeling effort. The parameters utilized were compared to a number of other DOE facilities and generic national references to establish relevance of the parameters selected and/or verify the regional differences for the southeastern United States. The values for the parameters recommended were based on expected values along with a range for these values versus estimating an annual dose to the MEI. The consumption rates that SRS utilized for the FTF PA appear in Tables 4.6-5 through 4.6-7. The data in these tables were taken from WSRC-STI-2007-00004.

4.6.2.1 Human Health Exposure Parameters Methodology

A report entitled *Baseline Parameter Update for Human Health Input and Transfer Factors for Radiological Performance Assessments at the Savannah River Site* documents the results of the SRS evaluation and reviews of consumption rates. [WSRC-STI-2007-00004] Refer to this report for additional discussion on parameters such as water ingestion rates, crop yields, garden fractions and sizes along with soil exposure times. This report established a single Human Health Exposure parameters source that is up to date with existing data and maintained current via periodic reviews.

In developing the report, a comprehensive literature review was completed and references were updated to include the latest available information. In general, the values from more recent compilations were recommended, rather than those in older publications. This report includes information to establish a range of values for each parameter which were used to perform uncertainty analysis.

A hierarchy of data sources was established to select values for human health exposure parameters. The utilization of site-specific values from the most recent and comprehensive references are given priority. Values promulgated by national or international organizations were used as representative of the SRS area practices in the absence of site-specific values. The *Risk-Based Screening of Radionuclide Releases from the Savannah River Site* was used as a source to validate the receptor practices in the areas surrounding SRS. [CDC-2005] The values given for the parameters are given as expected values, together with an observed range.

Site-specific information is available for most of the human health exposure parameters required to estimate doses. *Land and Water-Use Characteristics in the Vicinity of the Savannah River Site* and *Site-Specific Parameter Values for the Nuclear Regulatory Commission's Food Pathway Dose Model*, surveyed county agents in South Carolina and Georgia and compiled county-specific statistics on land and water use within a 50-mile radius of SRS. [WSRC-RP-91-17, ISSN: 0017-9078 - Volume 62, Page 136] When these reports do not provide site-specific information for physical parameters and consumption rates, global data are used. [WSRC-RP-91-17, ISSN 0017-9078 - Volume 62, Page 136] Documents ANL-EAD-4 and ANL-EAIS-8 provide data for use in RESRAD, a NRC and DOE supported dose model, based on literature review of standard values and publications. The EPA report *Exposure Factors Handbook* summarizes and recommends human health exposure parameter data for human exposure to environmental contaminants based on studies published through August 30, 1997. [EPA-600-P-95-002] NUREG-CR-5512 provides generic and site-specific human health data for estimating dose from exposure to residual radioactive contamination.

The general hierarchy of the global data use is listed below:

- Site-Specific [WSRC-RP-91-17, ISSN 0017-9078, Volume 62, Page 136]
- Other site- or regional- specific publications [CDC-2005]
- EPA Exposure Factors Handbook [EPA-600-P-95-002]
- RESRAD Version 6 [ANL-EAD-4, ANL-EAIS-8]
- NUREG-CR-5512

Table 4.6-5: Crop Exposure Times and Productivity

Parameter	Value		Reference	Min	Max
Pasture exposure time to irrigation (days)	30		10 CFR 50, Reg. Guide 1.109	30	90
Vegetable crop exposure times to irrigation(days)	70		WSRC-RP-91-17	60	90
Soil exposure time period to irrigation (days) (Buildup time in soil)	183		Scenario-specific	60	365
Productivity					
Pasture grass (kg/m^2)	1.8		WSRC-RP-91-17	0.7	2
Agricultural (veg/produce) (kg/m^2)	0.7		WSRC-RP-91-17	0.5	4
Vegetable crop yield (kg/m^2)	0.7		WSRC-RP-91-17	0.2	4
Fraction of Foodstuff Produced Locally	**All-Pathway**	**Intruder**			
Vegetables	0.173	0.308	EPA-600-P-95-002	0	0.5
Meat	0.306	0.319	EPA-600-P-95-002	0	0.5
Milk	0.207	0.254	EPA-600-P-95-002	0	0.5
Dilution Factor for mixing of stabilized contaminants in vegetable garden					
Agricultural Scenario	0.2		NUREG-CR-3620	0.2	0.2
Post-Drilling Scenario	0.02		WSRC-RP-94-0218	0.002	0.02

[Based on WSRC-STI-2007-00004, Table 3-1]

Table 4.6-6: Physical Parameters

Parameter	Value	Reference	Min	Max
Areal density of soil (kg/m^2)	240	WSRC-RP-93-1174	180	270
Soil Density (kg/m^3)	1,600	WSRC-TR-93-304	1,350	1,600
Atmospheric mass loading of soil (kg/m^3)				
while working in garden	1.00E-07	WSRC-RP-94-0218	1.0E-09	3.0E-07
while residing in home	1.00E-08	WSRC-RP-94-0218	1.0E-09	3.0E-08
Depth of garden (cm)	15	WSRC-TR-93-304	15	61
Garden irrigation rate ($L/d/m^2$)	3.6*	WSRC-RP-93-1174	2.08	5.5
Fraction of the year that crops are irrigated	0.2	Estimated (70/365)**	0.2	0.25
Crop weathering constant (L/d)	0.0495	10 CFR 50, Reg. Guide 1.109	0.03	0.0495
Fractional retention of deposition on leaves	0.25	10 CFR 50, Reg. Guide 1.109	0.2	0.25
Area of garden for family of four (m^2)	100	Based on Section 3.3 estimate from WSRC-STI-2007-00004	100	1,000

[Based on WSRC-STI-2007-00004, Table 3-2]

*Based on an assumption of 1 in/wk = 0.36 cm/d. For a 1 m^2 area, 0.36 cm/d x 10,000 cm^2/m^2 x 1L/1000 cm^3=3.6 $L/d/m^2$.

**Based on literature validation of estimated 70 days of irrigation in growing season of total year.

Table 4.6-7: Individual Exposure Times and Consumption Rates

Parameter	Recommendation			
	Value	Reference	Min	Max
Breathing rate (m^3/year)	5,548	EPA-600-P-95-002	1,267	11,600
Consumption Rate				
Soil (kg/year)	0.0365	EPA-600-P-95-002	0.0008	0.05
Leafy vegetable (kg/year)	21	ISSN 0017-9078	18	43
Other vegetable (kg/year)	163	ISSN 0017-9078	90	276
Meat (kg/year)	43	ISSN 0017-9078	26	81
Finfish (kg/year)	9	ISSN 0017-9078	2.2	19
Seafood (kg/year)	0	ISSN 0017-9078	0	5
Milk (L/year)	120	ISSN 0017-9078	73.7	230
Water (L/year)	337	EPA-822-R-00-001	184	730
Fodder-Beef cattle (kg/day)	36	WSRC-RP-91-17	27	50
Fodder-Milk cattle (kg/day)	52	WSRC-RP-91-17	36	55
Fraction of milk-cow intake from pasture	0.56	ISSN 0017-9078	0.05	1
Fraction of beef-cow intake from pasture	0.75	ISSN 0017-9078	0.05	1
Water (beef cow) (L/day)	28	WSRC-RP-93-1174	28	50
Water (milk cow) (L/day)	50	WSRC-RP-93-1174	50	60
Exposure Time				
Shoreline (hour/years)	23	WSRC-RP-91-17	11	35
Swimming (hours/year)	8.9	WSRC-RP-91-17	8.9	13
Boating (hours/year)	21	WSRC-RP-91-17	9.1	21
Showering (minutes/day)	10	EPA-600-P-95-002	10	30
Fraction of year working in garden	0.01	NUREG-CR-1759	0.01	0.08
Fraction of year residing in home	0.7	EPA-600-P-95-002	0.3	0.7
Fraction of time cattle on pasture (per year)	1	WSRC-RP-91-17	0.75	1
Transport (days)				
Vegetables	6	ANL-EAD-4	6	14
Feed-milk-man transport time	3	WSRC-RP-91-17	1	4
Time from slaughter to consumption	6	WSRC-RP-91-17	6	20

[Based on WSRC-STI-2007-00004, Table 4-1]

4.7 Dose Analysis

Over time, the mobile contaminants in the FTF waste tanks and ancillary equipment will gradually migrate downward through unsaturated soil to the hydrogeologic units comprising the shallow aquifer underlying the FTF. Some contaminants will be transported by groundwater through the aquifers to the outcrops at Fourmile Branch and UTR. Upon reaching the surface water, the contaminants could be present at the seepline, in sediments at the bottom of streams, and at the shoreline. Human receptors could be exposed to contaminants through various pathways associated with the aquifers and surface water as described in Section 4.2.4.

The potential dose to MOP via the air pathway was also evaluated as described in Section 4.5.

4.7.1 Dose Conversion Factors

The purpose of this section is to present the set of DCFs used in dose calculations for the FTF PA modeling effort. A comprehensive list of DCFs was prepared and included in Table4.7-1, even though only a subset of the values listed was actually utilized in the PA modeling.

Radiation doses to humans may result from internal intake of radionuclides by inhalation or ingestion or from external exposure to radionuclides present in the environment. Dose assessment at SRS is carried out by considering radionuclide concentrations in environmental media, factoring in human exposure conditions, and performing the conversion of exposure to dose. For internal exposure, radionuclide activity intake is calculated by combining the radioactivity concentration in environmental media (e.g., food, soil, air, and water) with the amount of environmental medium taken into the body. Then, using internal DCFs, radionuclide intake is converted into dose. To assess exposure from external sources, SRS uses external DCFs that convert radionuclide concentrations in environmental media to doses for the duration of exposure. Only internal DCFs for adults were utilized in the FTF PA.

4.7.1.1 Internal DCFs

Previous SRS PA analyses utilized the DCFs from EPA Federal Guidance Report 11, published in 1988. [EPA-520-1-88-020] The International Commission on Radiological Protection (ICRP) published new DCFs based upon updated dosimetric models in ICRP Publication 72 in 1996. [ICRP-72] The DOE has begun using the ICRP models for occupational exposure internal dose assessments at different sites including SRS and they are also used for SRS safety basis calculations. Safety Basis Documents, as defined in 10 CFR 830, Subpart B, are the DSA and hazard controls that provide reasonable assurance that a DOE nuclear facility can be operated safely in a manner that adequately protects workers, the public, and the environment. [10 CFR 830]

The DCFs are converted to standard units for input into the calculations by multiplying the ICRP 72 DCFs by 3.7E+06 (Sv/Bq x 3.7E+6 = rem/μCi). [ICRP-72] The internal DCFs in rem/μCi are presented in Table 4.7-1 for the various radionuclides. For inhalation DCFs, the most likely lung absorption type from Table 2 of ICRP-72 was used if available, and if not available, the most conservative type was assumed.

Because the ICRP data is the most recent data available and is based on the most recent dosimetric models, the ICRP 72 DCFs are used for this FTF PA analysis. [ICRP-72]

4.7.1.2 External DCFs

External DCFs for uniformly distributed contamination at an infinite depth with no shielding and at 15 cm are taken from EPA Federal Guidance Report 12. [EPA-402-R-93-081] The external DCFs in EPA-402-R-93-081 represent the dose rate per unit of activity of soil contaminated at various depths, reported in SI units (Sv/s per Bq/m^3). The DCFs are converted to standard units for input into PA calculations by multiplying the Federal Guidance Report No. 12 DCF by 1.168E+14 ((rem/yr per $\mu Ci/m^3$) / (Sv/s per Bq/m^3)) [EPA-402-R-93-081] External DCFs in rem/yr per $\mu Ci/m^3$ are presented in Table 4.7-1 for various radionuclides.

Table 4.7-1: Internal and External Dose Conversion Factors

Radionuclide	Internal DCFs (rem/μCi)		External DCFs (rem/yr per $\mu Ci/m^3$)		
	Ingestion	Inhalation	Infinite Depth	15 cm	Water Immersion
Ac-225	8.88E-02	3.15E+01	3.98E-05	3.90E-05	1.88E-04
Ac-227	4.07E+00	2.04E+03	3.10E-07	3.06E-07	1.52E-06
Ac-228	1.59E-03	9.25E-02	3.74E-03	3.22E-03	1.21E-02
Al-26	1.30E-02	7.40E-02	1.09E-02	9.03E-03	3.43E-02
Am-241	7.40E-01	1.55E+02	2.73E-05	2.73E-05	2.20E-04
Am-242	1.11E-03	6.29E-02	3.12E-05	3.12E-05	1.61E-04
Am-242m	7.03E-01	1.37E+02	1.06E-06	1.05E-06	8.50E-06
Am-243	7.40E-01	1.52E+02	8.88E-05	8.88E-05	5.77E-04
Ar-39	--	--	5.40E-07	5.31E-07	2.06E-06
At-217	--	--	1.11E-06	1.01E-06	3.76E-06
At-218	--	--	3.65E-06	3.65E-06	3.21E-05
Ba-133	5.55E-03	1.15E-02	1.24E-03	1.15E-03	4.57E-03
Ba-137m	--	--	2.25E-03	2.00E-03	7.31E-03
Bi-210	4.81E-03	3.44E-01	2.25E-06	2.17E-06	7.39E-06
Bi-211	--	--	1.60E-04	1.49E-04	5.66E-04
Bi-212	9.62E-04	1.15E-01	7.32E-04	6.26E-04	2.34E-03
Bi-213	7.40E-04	1.11E-01	4.79E-04	4.38E-04	1.62E-03
Bi-214	4.07E-04	5.18E-02	6.13E-03	5.09E-03	1.94E-02
Bk-249	3.59E-03	5.92E-01	2.91E-09	2.90E-09	1.89E-08
C-14	2.15E-03	7.40E-03	8.41E-09	8.41E-09	5.13E-08
Ca-41	7.03E-04	3.52E-04	--	--	--
Cd-113m	8.51E-02	4.07E-01	4.05E-07	3.99E-07	1.57E-06
Ce-144	1.92E-02	1.33E-01	4.49E-05	4.44E-5	2.23E-04
Cf-249	1.30E+00	2.59E+02	1.16E-03	1.07E-03	4.03E-03
Cf-250	5.92E-01	1.26E+02	7.40E-08	7.40E-08	1.24E-06
Cf-251	1.33E+00	2.63E+02	3.29E-04	3.22E-04	1.45E-03
Cf-252	3.33E-01	7.40E+01	1.10E-07	1.10E-07	1.38E-06

Table 4.7-1: Internal and External Dose Conversion Factors (Continued)

Radionuclide	Internal DCFs (rem/μCi)		External DCFs (rem/yr per μCi/m^3)		
	Ingestion	Inhalation	Infinite Depth	15 cm	Water Immersion
Cl-36	3.44E-03	2.70E-02	1.50E-06	1.42E-06	5.23E-06
Cm-242	4.44E-02	1.92E+01	1.07E-07	1.06E-07	1.55E-06
Cm-243	5.55E-01	1.15E+02	3.64E-04	3.53E-04	1.52E-03
Cm-244	4.44E-01	9.99E+01	7.87E-08	7.87E-08	1.34E-06
Cm-245	7.77E-01	1.55E+02	2.13E-04	2.10E-04	1.03E-03
Cm-246	7.77E-01	1.55E+02	7.26E-08	7.26E-08	1.23E-06
Cm-247	7.03E-01	1.44E+02	1.11E-03	1.03E-03	3.82E-03
Cm-248	2.85E+00	5.55E+02	5.49E-08	5.49E-08	9.30E-07
Co-60	1.26E-02	3.70E-02	1.01E-02	8.47E-03	3.20E-02
Cs-134	7.03E-02	2.44E-02	5.92E-03	5.22E-03	1.92E-02
Cs-135	7.40E-03	2.55E-03	2.39E-08	2.40E-08	1.28E-07
Cs-137	4.81E-02	1.70E-02	4.70E-07	4.60E-07	1.74E-06
Eu-152	5.18E-03	1.55E-01	4.38E-03	3.76E-03	1.44E-02
Eu-154	7.40E-03	1.96E-01	4.80E-03	4.11E-03	1.55E-02
Eu-155	1.18E-03	2.55E-02	1.14E-04	1.14E-04	6.55E-04
Fr-221	--	--	9.60E-05	9.23E-05	3.76E-04
Fr-223	8.88E-03	3.29E-03	1.24E-04	1.18E-04	5.97E-04
Gd-152	1.52E-01	7.03E+01	--	--	--
H-3	6.66E-05	1.67E-04	--	--	--
I-129	4.07E-01	1.33E-01	8.10E-06	8.10E-06	1.04E-04
K-40	2.29E-02	7.77E-03	6.51E-04	5.34E-04	2.03E-03
Kr-85	--	--	8.94E-06	8.14E-06	2.98E-05
Mo-93	1.15E-02	2.18E-03	3.69E-07	3.69E-07	6.91E-06
Na-22	1.18E-02	4.81E-03	8.55E-03	7.37E-03	2.74E-02
Nb-93m	4.44E-04	1.89E-03	6.50E-08	6.50E-08	1.21E-06
Nb-94	6.29E-03	4.07E-02	6.05E-03	5.29E-03	1.95E-02
Ni-59	2.33E-04	4.81E-04	--	--	--
Ni-63	5.55E-04	1.78E-03	--	--	--
Np-237	4.07E-01	8.51E+01	4.87E-05	4.86E-05	2.71E-04
Np-238	3.37E-03	7.77E-03	2.15E-03	1.84E-03	6.88E-03
Np-239	2.96E-03	3.44E-03	4.71E-04	4.56E-04	1.99E-03
Np-240	3.03E-04	3.15E-04	4.83E-03	4.26E-03	1.60E-02
Np-240m	--	--	1.26E-03	1.11E-03	4.10E-03
Pa-231	2.63E+00	5.18E+02	1.19E-04	1.12E-04	4.42E-04
Pa-233	3.22E-03	1.44E-02	6.38E-04	6.03E-04	2.39E-03
Pa-234	1.89E-03	1.48E-03	7.22E-03	6.28E-03	2.37E-02
Pa-234m	--	--	5.61E-05	4.90E-05	1.78E-04

Table 4.7-1: Internal and External Dose Conversion Factors (Continued)

Radionuclide	Internal DCFs (rem/μCi)		External DCFs (rem/yr per μCi/m^3)		
	Ingestion	Inhalation	Infinite Depth	15 cm	Water Immersion
Pb-209	2.11E-04	2.07E-04	4.83E-07	4.76E-07	1.83E-06
Pb-210	2.55E+00	4.07E+00	1.53E-06	1.53E-06	1.53E-05
Pb-211	6.66E-04	4.07E-02	1.91E-04	1.70E-04	6.32E-04
Pb-212	2.22E-02	6.29E-01	4.40E-04	4.23E-04	1.78E-03
Pb-214	5.18E-04	5.18E-02	8.39E-04	7.83E-04	3.03E-03
Pd-107	1.37E-04	2.18E-03	--	--	--
Pm-147	9.62E-04	1.85E-02	3.13E-08	3.12E-08	1.64E-07
Po-210	4.44E+00	1.22E+01	3.27E-08	2.86E-08	1.05E-07
Po-211	--	--	2.98E-05	2.62E-05	9.66E-05
Po-212	--	--	--	--	--
Po-213	--	--	--	--	--
Po-214	--	--	3.21E-07	2.80E-07	1.03E-06
Po-215	--	--	6.35E-07	5.82E-07	2.15E-06
Po-216	--	--	6.52E-08	5.69E-08	2.10E-07
Po-218	--	--	3.53E-08	3.07E-08	1.13E-07
Pr-144	1.85E-04	6.66E-05	1.58E-04	1.32E-04	4.85E-04
Pu-238	8.51E-01	1.70E+02	9.46E-08	9.43E-08	1.33E-06
Pu-239	9.25E-01	1.85E+02	1.85E-07	1.78E-07	1.12E-06
Pu-240	9.25E-01	1.85E+02	9.17E-08	9.16E-08	1.30E-06
Pu-241	1.78E-02	3.33E+00	3.69E-09	3.68E-09	1.89E-08
Pu-242	8.88E-01	1.78E+02	8.00E-08	8.00E-08	1.09E-06
Pu-243	3.15E-04	3.07E-04	4.98E-05	4.90E-05	2.70E-04
Pu-244	8.88E-01	1.74E+02	4.72E-08	4.72E-08	8.13E-07
Ra-223	3.70E-01	2.74E+01	3.77E-04	3.62E-04	1.58E-03
Ra-224	2.41E-01	1.11E+01	3.20E-05	3.06E-05	1.20E-04
Ra-225	3.66E-01	2.33E+01	6.89E-06	6.89E-06	7.58E-05
Ra-226	1.04E+00	1.30E+01	1.99E-05	1.93E-05	8.12E-05
Ra-228	2.55E+00	9.62E+00	--	--	--
Rb-87	5.55E-03	1.85E-03	8.81E-08	8.78E-08	4.13E-07
Re-188	5.18E-03	2.00E-03	2.01E-04	1.83E-04	7.31E-04
Rh-106	--	--	8.07E-04	7.18E-4	2.62E-3
Rn-219	--	--	1.93E-04	1.80E-04	6.83E-04
Rn-220	--	--	1.44E-06	1.28E-06	4.71E-06
Rn-222	--	--	1.47E-06	1.33E-06	4.86E-06
Ru-106	2.59E-02	1.04E-01	--	--	--
S-35	4.81E-04	5.18E-03	9.31E-09	9.31E-09	5.54E-08
Sb-125	4.07E-03	1.78E-02	1.53E-03	1.38E-03	5.13E-03

Table 4.7-1: Internal and External Dose Conversion Factors (Continued)

Radionuclide	Internal DCFs (rem/μCi)		External DCFs (rem/yr per μCi/m^3)		
	Ingestion	Inhalation	Infinite Depth	15 cm	Water Immersion
Sb-126	8.88E-03	1.04E-02	1.07E-02	9.50E-03	3.49E-02
Sb-126m	1.33E-04	7.03E-05	5.82E-03	5.19E-03	1.90E-02
Sc-46	5.55E-03	2.52E-02	7.93E-03	6.77E-03	2.52E-02
Se-79	1.07E-02	4.07E-03	1.16E-08	1.16E-08	6.93E-08
Sm-151	3.63E-04	1.48E-02	6.15E-10	6.15E-10	9.93E-09
Sn-121	8.51E-04	8.51E-04	1.23E-07	1.21E-07	5.37E-07
Sn-121m	1.41E-03	1.67E-02	1.23E-06	1.23E-06	1.65E-05
Sn-126	1.74E-02	1.04E-01	9.22E-05	9.22E-05	5.56E-04
Sr-90	1.04E-01	1.33E-01	4.40E-07	4.34E-07	1.71E-06
Tc-99	2.37E-03	1.48E-02	7.85E-08	7.82E-08	3.67E-07
Te-125m	3.22E-03	1.26E-02	9.47E-06	9.46E-06	1.24E-04
Th-227	3.26E-02	3.70E+01	3.26E-04	3.10E-04	1.25E-03
Th-228	2.66E-01	1.48E+02	4.96E-06	4.87E-06	2.39E-05
Th-229	1.81E+00	2.63E+02	2.01E-04	1.99E-04	1.00E-03
Th-230	7.77E-01	5.18E+01	7.56E-07	7.46E-07	4.60E-06
Th-231	1.26E-03	1.22E-03	2.28E-05	2.27E-05	1.38E-04
Th-232	8.51E-01	9.25E+01	3.26E-07	3.25E-07	2.32E-06
Th-234	1.26E-02	2.85E-02	1.51E-05	1.51E-05	8.92E-05
Tl-207	--	--	1.24E-05	1.11E-05	3.95E-05
Tl-208	--	--	1.44E-02	1.13E-02	4.49E-02
Tl-209	--	--	8.08E-03	6.76E-03	2.59E-02
U-232	1.22E+00	2.89E+01	5.64E-07	5.57E-07	3.76E-06
U-233	1.89E-01	1.33E+01	8.74E-07	8.46E-07	4.25E-06
U-234	1.81E-01	1.30E+01	2.51E-07	2.50E-07	2.04E-06
U-235	1.74E-01	1.15E+01	4.51E-04	4.38E-04	1.86E-03
U-236	1.74E-01	1.18E+01	1.34E-07	1.33E-07	1.35E-06
U-238	1.67E-01	1.07E+01	6.45E-08	6.45E-08	9.29E-07
U-240	4.07E-03	1.96E-03	8.90E-07	8.90E-07	1.06E-05
W-181	2.81E-04	9.99E-05	4.78E-05	4.78E-05	3.76E-04
W-185	1.63E-03	4.44E-04	2.71E-07	2.69E-07	1.30E-06
W-188	7.77E-03	2.11E-03	6.05E-06	5.75E-06	2.31E-05
Y-90	9.99E-03	5.55E-03	1.50E-05	1.40E-05	4.24E-05
Zr-93	4.07E-03	3.70E-02	--	--	--

4.7.2 Member of the Public Dose Analysis

Two distinct release scenarios were analyzed to assess the potential MOP doses associated with the FTF. The difference in the scenarios was the primary water source, with one being a well drilled into the groundwater aquifers and the other being an FTF stream. The MOP dose pathways used in the PA analyses are discussed in detail in Section 4.2.4.1.

The consumption rates and bioaccumulation factors that are used in conjunction with the proposed pathways are discussed in detail in Section 4.6.

4.7.3 Intruder Dose Analysis

Two distinct release scenarios were analyzed to assess the potential intruder doses associated with the FTF. The intruder scenarios of concern are the Acute Intruder-Drilling Scenario and the Chronic Intruder Agricultural (Post-Drilling) Scenario. The intruder dose pathways used in the PA analyses are discussed in detail in Section 4.2.4.2.

The consumption rates and bioaccumulation factors that are used in conjunction with the proposed pathways are discussed in detail in Section 4.6.

4.7.4 Analysis Approach

The MOP and intruder exposure scenarios were analyzed for FTF to provide results to demonstrate compliance with the performance criteria. The analysis provides not only the maximum projected dose and time of occurrence, but also the dominant pathway contributing to the dose and the radionuclides responsible for the maximum dose.

The groundwater and surface water concentrations and resulting human health impacts are calculated for the Base Case using the PORFLOW computer code. The analysis approaches used for FTF are based upon the radionuclide inventories (Sections 3.3.2 and 3.3.3), stabilized contaminant release mechanisms (Section 4.2.2), and radionuclide transport models (Section 4.2.3) as described previously in this document.

4.8 RCRA/CERCLA Risk Evaluation

Protocols have been developed, with approval of SCDHEC and the EPA, to support the SRS SGCP remediation activities. [ERD-AG-003] The protocols provide instructions for the development of conceptual site models used in the RCRA Facility Investigation and CERCLA Remedial Investigation (RI) process. These same protocols were used to evaluate the potential for adverse affects associated with exposure to constituents present at the FTF in the stabilized contaminants. The evaluation implemented a streamlined approach that uses standardized lookup tables to estimate risk. The evaluation estimated the risk potential in the absence of institutional controls at this site and provided a basis for determining whether or not remedial action is necessary. Groundwater concentrations at the FTF were compared to the SDWA MCL. In the absence of MCLs, groundwater concentrations were compared to calculated PRGs.

PRGs are risk-based tools used to evaluate and clean up contaminated sites. The use of PRGs to evaluate risk/hazard is a simple and accepted method; however this method does not replace the current Constituent of Potential Concern (COPC) identification process which considers the residential soil PRGs in the initial screening step.

The EPA Region 9 Table is the source of PRGs for nonradiological constituents; it combines current EPA toxicity values with standard exposure factors to estimate contaminant concentrations in environmental media (soil, air, and water) that the agency considers protective of humans (including sensitive groups), over a lifetime. Region 9 PRG concentrations are based on direct contact pathways for which generally accepted methods, models, and assumptions have been developed (i.e., quantitative ingestion, dermal contact, and inhalation factors) for specific land use conditions. More detailed information can be found at the EPA Region 9 website: www.epa.gov/region09/waste/sfund/prg/index.htm

The EPA does not publish radiological values in a standardized table as they do nonradiological PRGs. However, the agency has issued updated guidance on calculation methods used for determining radionuclide activity screening levels. EPA's Superfund radionuclide PRG website provides a database tool with which to derive risk-based PRGs calculated using default parameters and the latest toxicity values. The database tool also allows the user to modify input parameters to create site-specific PRGs. The PRGs for radiological constituents are identified in calculation K-CLC-G-00077. The EPA website provides specific details regarding use of the database tool to calculate the PRGs. [http://epa-prgs.ornl.gov/radionuclides/]

4.8.1 Integrated Site Conceptual Model

The ISCM for FTF (Figure 4.8-1) depicts the understanding of the site and focuses on identifying potential contaminant migration from the sources to potential receptors. The ISCM identifies potential sources of contamination, release mechanisms, media of concern, exposure routes, and potential receptors. For the purposes of the ISCM, the surface soil interval is defined as the 0 to 0.3m (0 to 1 feet) interval and is evaluated for human and ecological exposure. The subsurface soil interval is the 0.3 to 1.2m (1 to 4 feet) interval and is evaluated for ecological exposure. The deep soil interval (>1.2m) is defined on a subunit specific basis and is evaluated for Principal Threat Source Material (PTSM) (future excavation scenario) and contaminant migration potential. The approved risk evaluation approach used in the RCRA Facility Investigation and CERCLA RI process differs slightly from the general analysis approach used calculating the PA dose results in Sections 5 and 6, such that there will be some differences between the risk analysis release scenarios (shown in Figure 4.8-1), and the dose analysis pathways and scenarios (Section 4.2.4).

Initially, the ISCM provides a representation of the source of contamination and how it was released into the environment. It also includes potential release mechanisms and exposure routes based on existing understanding of the nature and extent of contamination. For this evaluation, because the FTF will remain operational while the individual waste tanks are closed, only the stabilized contamination in the waste tanks is considered. Final closure of the FTF will include the evaluation of potential surface soil contamination.

Figure 4.8-1: Integrated Conceptual Site Model for FTF

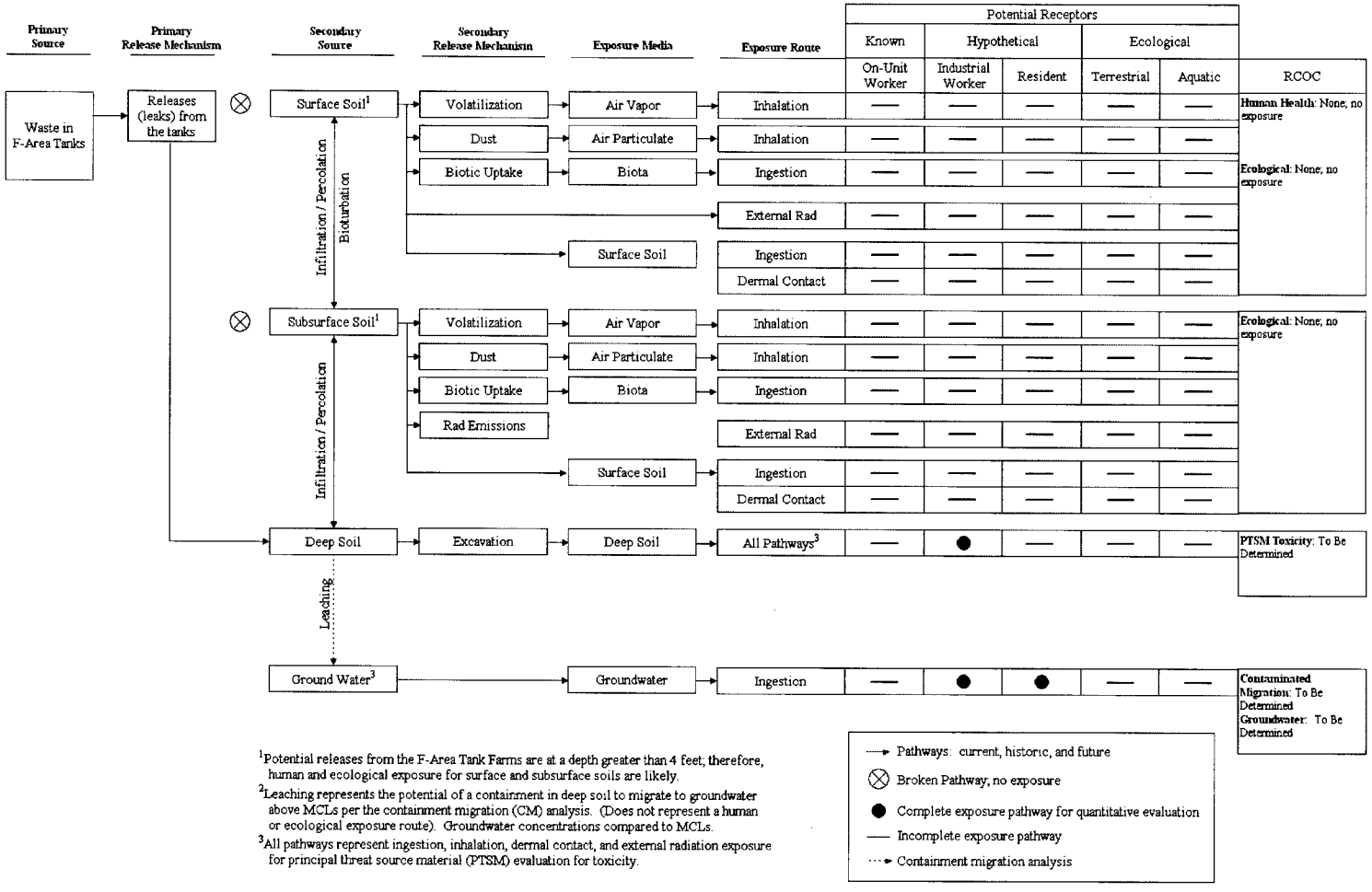

4.8.1.1 Primary Source of Contamination

The primary source of contamination was the stabilized contaminants in the FTF waste tanks and ancillary equipment. Contaminants may be released from primary sources through the following mechanisms:

- Release of contaminants (migration) from the waste tanks and ancillary equipment

4.8.1.2 Secondary Sources of Contamination

Environmental media impacted by the release of primary source contamination becomes a secondary source. After grouting waste tanks and ancillary equipment, at least 10 feet of material will be placed as backfill. Potential releases from the FTF are then at depths greater than (1.2m); therefore human and ecological exposure for surface or subsurface soils is unlikely (incomplete pathway). Secondary sources include the following:

- Deep soils beneath the waste tanks; and
- Groundwater

Environmental media may serve as both a contaminant reservoir, via chemical bonding and biotic uptake, and/or secondary release mechanism of contaminants. Secondary release mechanisms include the following:

- Leaching of constituents from deep soils to groundwater; and
- Excavation of deep soils

4.8.1.3 Exposure Pathways (Media)

Contact with contaminated environmental media creates exposure pathways for human receptors. Potential exposure media include the following:

- Excavation of deep soil

4.8.1.4 Exposure Routes

Potential exposure routes for human receptors may include the following:

- Ingestion of excavated soil;
- Inhalation of air vapor and particulates from excavated soil;
- Dermal contact with excavated soil; and
- External radiation exposure from radiological constituents in excavated soil.

4.8.1.5 Receptors

Potential releases from the FTF are at a depth greater than 1.2m (4 feet); therefore, the standard human and ecological receptor scenarios do not apply. A future industrial worker scenario is considered for deep soils at the PTSM toxicity threshold to take into account potential exposure through excavation.

4.8.2 Risk Assessment

The risk assessment for the FTF closure follows the SGCP protocols for human health and ecological risk assessments. [ERD-AG-003] Based on available characterization data and estimated volume of residual material expected to remain in each of the waste tanks and

ancillary equipment, the chemical and radiological inventory used for PA modeling has been calculated for FTF as discussed in Section 3.3. Modeling was conducted to determine the peak concentrations of the non-radiological and radiological contaminants in the groundwater over the next 10,000 years. When each waste tank is closed, analysis will be performed to compare the actual residual inventory versus the calculated values used in the modeling.

4.8.2.1 Human Health Risk Assessment

SGCP protocols call for evaluation of surface soils from 0 to 1 foot in depth for exposure to a future industrial worker. Some of the ancillary equipment may currently be within the 0 to 1 foot depth. However, since the waste tanks and ancillary equipment will be stabilized and covered with at least 10 feet of backfill, there will be no pathway for future industrial worker exposure. Therefore, no human health risk assessment was required.

4.8.2.2 Ecological Risk Assessment

SGCP protocols call for evaluation of surface soils from 0 to 4 feet for ecological exposure. Some of the ancillary equipment may currently be within the 0 to 4 foot depth. However, since the waste tanks and ancillary equipment will be stabilized and covered with at least 10 feet of backfill, there will be no pathway for ecological exposure. Therefore, no ecological risk assessment was required.

4.8.2.3 Principal Threat Source Materials

PTSM are those materials that include or contain hazardous substances, pollutants or contaminants that act as a reservoir for migration of contamination to groundwater, surface water or air, or that act as a source for direct exposure. [OSWER 9380.3-06FS] Source characterizations are necessary to determine whether the source(s) can be designated as PTSM, Low-Level Threat Source Material (LLTSM), or non-hazardous materials.

The closed FTF waste tanks and ancillary equipment are, by the above definition, PTSM. The waste tanks and the residue remaining in the tanks will be stabilized and then covered as part of tank closure. This approach is consistent with SGCP remediation of reactor seepage basins which contained contaminated soils determined to be PTSM.

4.8.2.4 Contaminant Migration Constituents of Concern

Contaminant Migration Constituents of Concern (CMCOCs) were identified through a system that is consistent with both the SGCP protocols and the PA. CMCOCs were identified by modeling the release of contaminants and their travel through the vadose zone. The same model utilized in the PA to meet 10 CFR 61 requirements is used as the basis of the CMCOC evaluation. Any contaminants that are modeled to reach the water table are compared to MCL or PRG or other appropriate standards in cases where the constituent does not have an MCL. Any constituents that are predicted to exceed these standards in the groundwater directly beneath FTF are identified as CMCOCs. CMCOCs are often addressed by the placement of a low permeability cap such as is planned for the FTF closure. [www.epa.gov/region09/waste/sfund/prg/index.html] Risk Assessment modeling results are discussed in detail in Section 5.7.

5.0 RESULTS OF ANALYSIS

The purpose of this section is to present the results for the analyses described in Section 4 of this PA.

Section 5.1 presents the Source Term results. The purpose of this section is to present the stabilized contaminant release rates for key radionuclides.

Section 5.2 presents peak groundwater concentrations for the radionuclides and chemicals discussed in Section 4.2.1. Maximum groundwater concentrations for multiple exposure points are provided:

1. 100m from the FTF.
2. At the UTR and Fourmile Branch seeplines.

Section 5.3 presents the Air Pathway and Radon release results.

Section 5.4 presents individual Biotic Pathway formulas used to calculate the doses to MOP.

Section 5.5 presents the MOP Dose Analysis.

Section 5.6 presents the Sensitivity and Uncertainty Analysis.

Section 5.7 presents the Risk Analysis.

Section 5.8 presents the As Low As Reasonably Achievable (ALARA) Analysis.

5.1 Source Term (Analysis Results)

This purpose of this section is to present the peak stabilized contaminant release rates from the FTF waste tanks and ancillary equipment. The release rates (fluxes) were calculated using the PORFLOW FTF baseline model presented in Section 4.4. The flux from the FTF waste tanks and ancillary equipment were calculated at two locations:

1. Exiting the inventory source containment.
2. Entering the upper aquifer below the associated inventory source.

It should be noted that the flux exiting the inventory source containment is different than the flux leaving the CZ since a radionuclide can leave the CZ and still be held up in the containment. This fact can lead to peaks associated with containment (e.g., liner) failure since the source material that left the CZ is collected in the containment and then released simultaneously when the containment fails.

In the analysis, the release of radionuclides from the waste tanks was controlled in most cases by solubility, which will vary with pH, and can vary with redox potential as well. All chemicals and some radionuclides are modeled as being released instantaneously from the CZ. In addition to solubility, the stabilized contaminant release rate for waste tanks was also impacted by the water flow through the tank, which varied by tank type and changed over time as the hydraulic properties of the tank materials changed. The flux from the applicable containment (e.g., transfer line wall, pump tank wall, evaporator pot wall) was less complicated for the ancillary equipment,

because the entire waste inventory was released instantaneously from the ancillary source location when the containment failed. After a contaminant had left its applicable containment, the basemat retardation (for waste tanks only) and soil retardation impacted the contaminant's transport rate into the aquifers.

Table 5.1-1 presents the peak flux (in Ci/yr) from the containment for any FTF source (tank or ancillary equipment) for the key radionuclides. The determination of the key radionuclides, radionuclides with peak individual water ingestion doses (assuming 337 L/yr ingestion) greater than 0.005 mrem/yr is discussed in Section 5.2.2. Appendix A.1 of this document contains data curves showing the flux (Ci/year) leaving the associated containment for the individual waste tanks and ancillary equipment out to 20,000 years. The flux is provided for all radionuclides and chemicals.

Table 5.1-1: Peak Fluxes Exiting Containment Out to 10,000 and 20,000 Years

Radionuclide	Peak FTF Flux in 10,000 Years (Ci/yr)	Source of Peak Flux	Year Largest Flux in 10,000 Years Occurs	Peak FTF Flux in 20,000 Years (Ci/yr)	Source of Peak Flux	Year Largest Flux in 20,000 Years Occurs
C-14	9.67E-05	Transfer Lines	511	9.67E-05	Transfer Lines	511
Np-237	1.46E-05	Tank 18	6,001	1.44E-01	Tank 34	15,501
Pa-231	6.58E-08	Tank 18	3,639	1.49E-07	Tank 34	12,752
Pb-210	2.17E-06	Tank 18	3,639	1.55E-04	Tank 34	12,752
Pu-239	1.29E-04	242-3F	2,501	1.29E-04	242-3F	2,501
Pu-240	2.84E-05	242-3F	2,001	3.17E-05	Type III	12,754
Pu-242	3.11E-07	Tanks 17, 18, 19	9,601	4.34E-07	Tank 6	12,700
Ra-226	9.91E-06	Tank 18	3,640	7.51E-04	Tank 34	12,753
Tc-99	4.02E-02	242-3F	511	4.02E-02	242-3F	511
Th-229	3.76E-05	Tank 18	3,639	3.76E-05	Tank 18	3,639
Th-230	1.49E-06	Tank 18	3,639	4.26E-05	Tank 34	12,752
U-233	1.68E-04	Tank 18	5,401	1.68E-04	Tank 18	5,401
U-234	8.98E-05	Tank 18	4,402	9.44E-05	Tank 34	15,501
U-236	2.30E-06	Tank 18	5,401	2.50E-06	Tank 34	15,501
U-238	6.51E-07	Transfer Lines	4,631	6.51E-07	Transfer Lines	4,631

Table 5.1-2 presents the peak flux (Ci/yr) entering the upper aquifer for any FTF source (waste tank or ancillary equipment) for the key radionuclides. Appendix A.2 of this document contains data curves showing the waste flux (Ci/year) entering the upper aquifer for the individual waste tanks and ancillary equipment out to 20,000 years. The flux is provided for all radionuclides and chemicals.

Table 5.1-2: Peak Fluxes Entering Upper Aquifer Out to 10,000 and 20,000 Years

Radionuclide	Peak FTF Flux in 10,000 Years (Ci/yr)	Source of Peak Flux	Year Largest Flux in 10,000 Years Occurs	Peak FTF Flux in 20,000 Years (Ci/yr)	Source of Peak Flux	Year Largest Flux in 20,000 Years Occurs
C-14	6.29E-05	Tank 19	3,746	6.29E-05	Tank 19	3,746
Np-237	1.52E-05	Tank 18	6,009	1.75E-04	Tank 34	17,326
Pa-231	8.34E-08	Tank 18	6,001	1.47E-07	Tank 34	16,094
Pb-210	2.24E-08	Transfer Lines	1,501	3.11E-07	Tank 34	13,846
Pu-239	4.13E-06	Tanks 17, 18, 19, 20	9,997	6.45E-05	242-3F	19,999
Pu-240	1.22E-05	Tanks 17, 18, 19, 20	9,998	1.50E-05	Tanks 17, 18, 19	11,229
Pu-242	2.88E-07	Tanks 17, 18, 19, 20	9,997	3.44E-07	Tanks 17, 18, 19	11,141
Ra-226	8.52E-06	Transfer Lines	1,501	1.20E-04	Tank 34	13,807
Tc-99	1.31E-02	Transfer Lines	580	1.31E-02	Transfer Lines	580
Th-229	1.48E-05	Tank 18	10,000	1.69E-05	Tank 18	10,512
Th-230	9.83E-07	Tank 18	10,000	1.43E-06	Tank 18	12,001
U-233	1.36E-04	Tank 18	7,001	1.36E-04	Tank 18	7,001
U-234	5.40E-05	Tank 18	7,001	5.40E-05	Tank 18	7,001
U-236	2.27E-06	Tank 18	7,001	2.27E-06	Tank 18	7,001
U-238	5.13E-08	Transfer Lines	10,000	6.29E-07	Transfer Lines	15,666

5.2 Environmental Transport of Radionuclides

The purpose of this section is to present the groundwater concentrations for all of the radionuclides and chemicals discussed in the source term screening section of the PA (Section 4.2.1). Maximum groundwater concentrations are presented for two exposure points:

1. 100m from the FTF
2. At the seeplines (UTR and Fourmile Branch)

Results are presented for the three distinct aquifers modeled (UTR-UZ, the UTR-LZ, and the Gordon aquifer).

The groundwater concentrations at 100m and at the seepline were calculated using the PORFLOW FTF model for the Base Case discussed in Section 4.4.2.1. A summary of several key parameters used in the baseline PORFLOW FTF modeling configuration are provided in Table 5.2-1

Table 5.2-1: Baseline Configuration

FTF Parameter	Baseline
Radiological Inventory	Table 3.3-2
Chemical Inventory	Table 3.3-3
Solubilities (reduced and oxidized)	Table 4.2-10
Vadose K_d values	Table 4.2-29
Cementitious K_d values	Table 4.2-33
Cementitious Material Degradation Times	Table 4.2-32
Type I Basemat thickness (inches)	30
Type III Basemat thickness (inches)	42
Type IIIA Basemat thickness (inches)	41
Type IV Basemat thickness (inches)	6.9025
Bypass Fraction (% Basemat with $K_d = 0$, Represents fast flow path in GoldSim)	0%
Tank configuration	Configuration A (Section 4.4.2.1)
Vadose Zone Thickness	Table 4.2-23
Type I Tank Liner failure (year)	12,747
Type III/IIIA Tank Liner failure (year)	12,751
Type IV Tank Liner failure (year)	3,638
Ancillary Equipment containment failure (year)	510
Chemical Transition of tank grout from Reduced to Oxidized (pore volumes)	371
Chemical Transition of tank grout from Region II to Region III (pore volumes)	2,063

The uncertainties and sensitivities associated with the Base Case is discussed in detail in Section 5.6.

5.2.1 Groundwater Concentrations at 100m

The 100m groundwater concentrations were calculated using the PORFLOW FTF model, which divides the area around FTF into computational cells. The green band in Figure 5.2-1 shows the boundary for FTF. The blue dots in Figure 5.2-1 show the 100m distance from FTF. Figure 5.2-2 illustrates the contaminant flow from the waste tanks. Since contaminant transport is not via a straight line, but rather by the applicable aquifers, the actual travel distance to reach 100m from the FTF boundary is greater than 100m for some sources. Table 5.2-2 shows the approximate distances a contaminant has to travel from each waste tank to reach a point 100m from the FTF boundary in the direction of the flow. The groundwater

concentrations at 100m is assumed to be the highest concentration in the area 100m or farther from the FTF. This assumption is supported by Figures 5.2-3 and 5.2-4, which present the plume that would result from a continuous (non-depleting) source of tracer (no decay, nor sorption). These figures show that the contaminant plumes leaving the FTF clearly get less intense as you move away and downward. The groundwater arrangement around the FTF is such that concentrations would only decrease at greater distances from the inventory sources.

Figure 5.2-1: 100m Distance from FTF

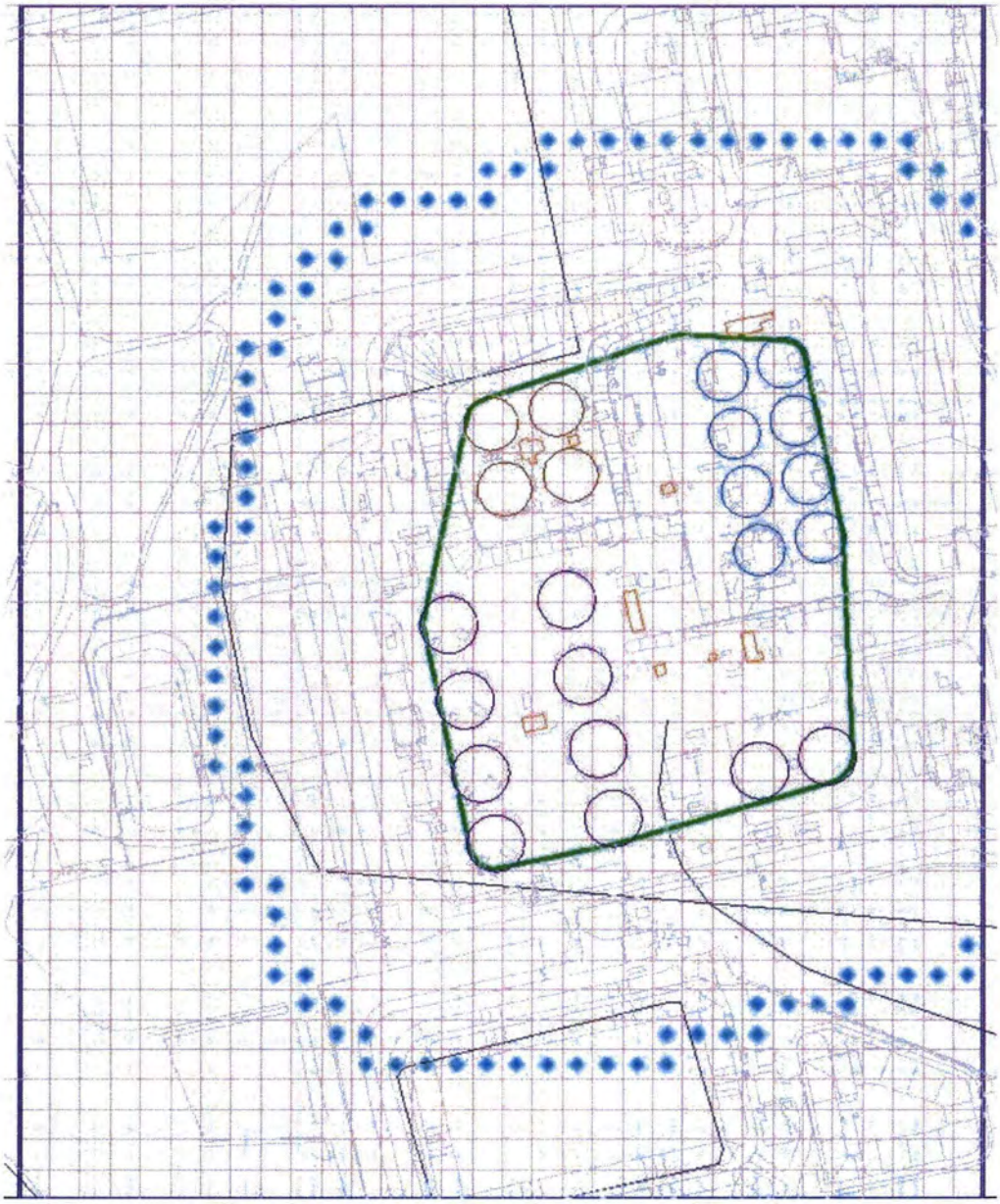

Figure 5.2-2: Stream Tracers from FTF

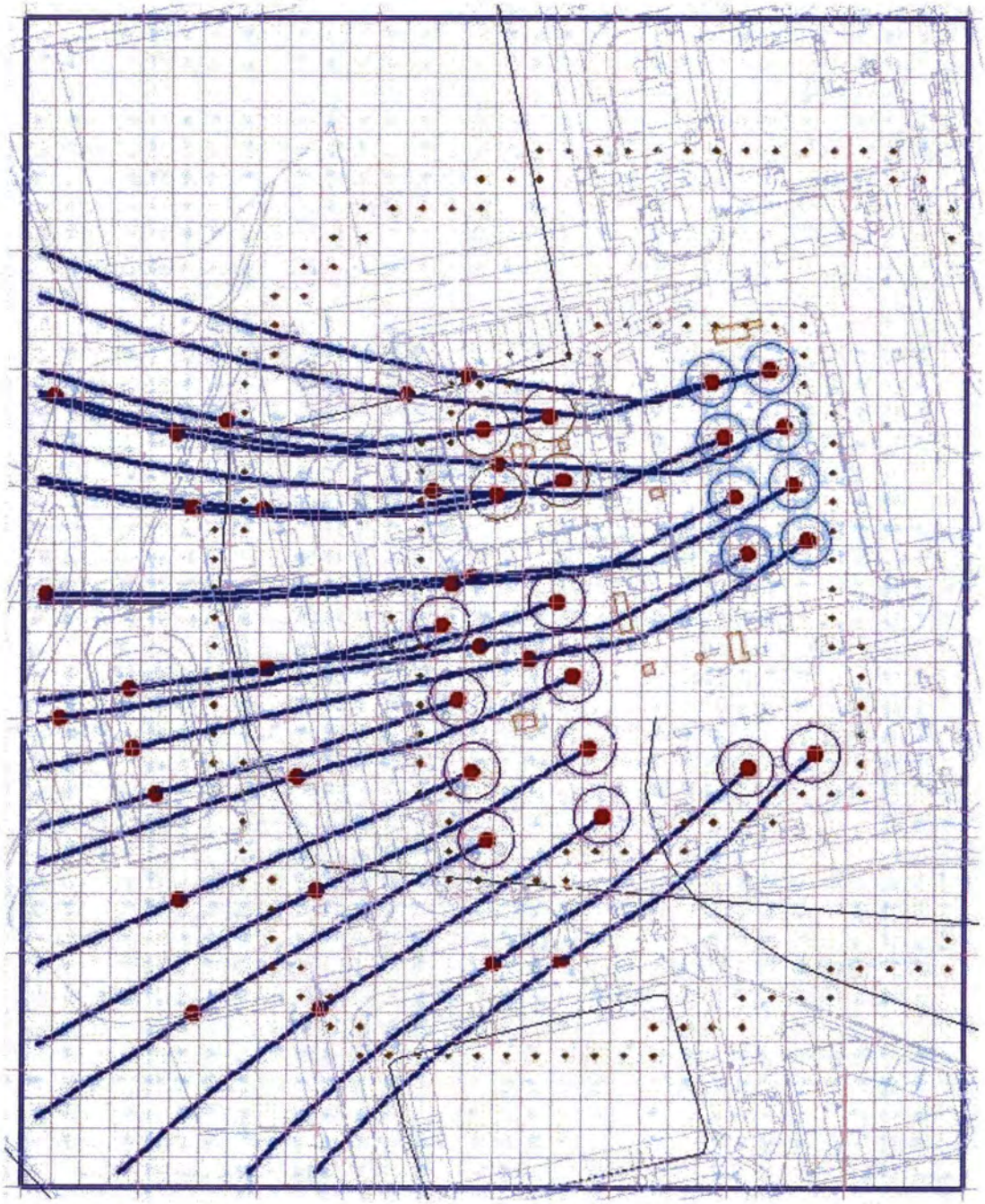

Table 5.2-2: Approximate Aquifer Travel Distance to the FTF 100m Boundary

Tank	Approximate Distance to 100m Boundary (Meters)
1	224
2	248
3	244
4	274
5	264
6	300
7	274
8	310
17	112
18	132
19	127
20	152
25	183
26	173
27	178
28	160
33	244
34	244
44	112
45	104
46	112
47	119

Figure 5.2-3: Contaminant Plume Leaving FTF – Aerial View

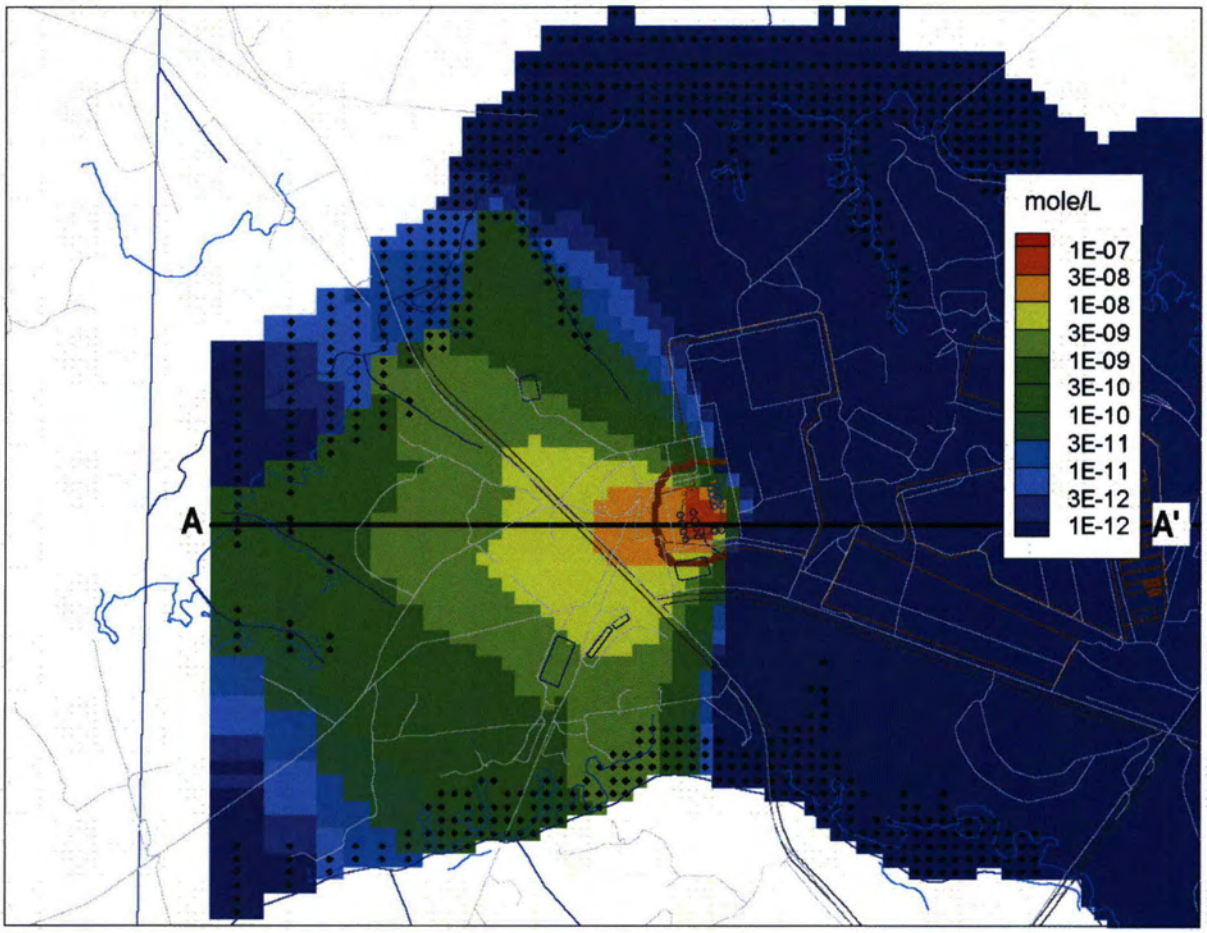

Figure 5.2-4: Contaminant Plume Leaving FTF – Cross Sectional View

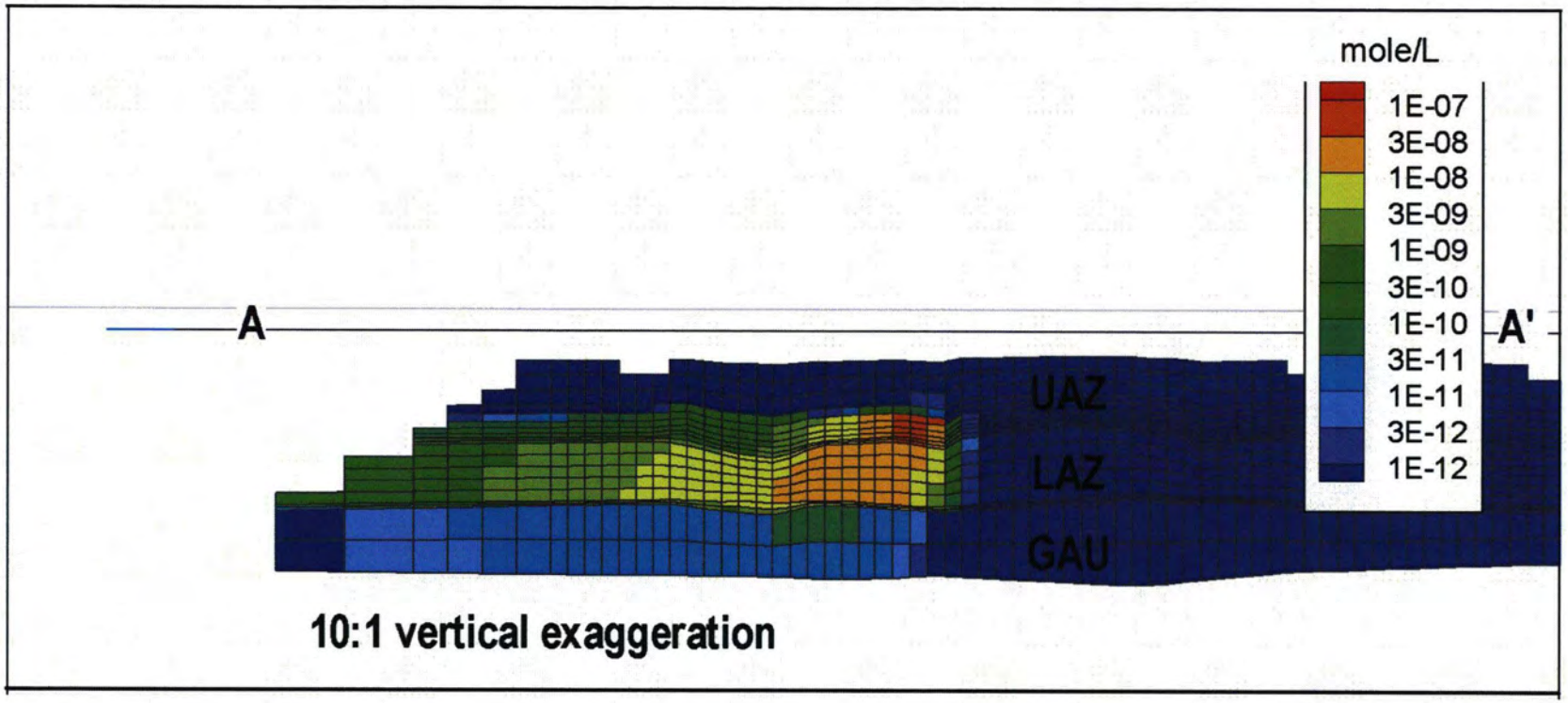

The PORFLOW 100m concentrations are calculated for five sectors (Sectors A – E) as shown on Figure 5.2-5. The peak concentration values for the 100m results are recorded for the three aquifer depths of concern (i.e., UTR-UZ, UTR-LZ, and Gordon Aquifer). The concentration for each aquifer represents peak concentration in any vertical computational mesh within the aquifer. The mesh vertical thicknesses (heights) in the computational model are less than 10 feet in the UTR-UZ, and less than 15 feet in the UTR-LZ. No well screen averaging was used in determining the concentrations for dose calculations because the typical well screen length of 20 feet is approximate to the computational mesh height. Dividing the results into sectors was necessary to allow the large amount of concentration data to be stored from PORFLOW and used by the GoldSim dose calculator model, but also allowed variability in peak concentration for different areas of the FTF to be more easily evaluated. The five sectors are analyzed for each radionuclide and chemical to find the maximum groundwater concentrations at 100m from the FTF. The PORFLOW 1m concentrations are calculated for four sectors (Sector 1A – 1D), as shown in Figure 5.2-5. Using the sectors to determine the highest groundwater concentrations causes the calculated peak doses to be higher than they actually are, since the peak concentrations are determined for each radionuclide independent of the location within the sector.

Figure 5.2-5: PORFLOW FTF 1m and 100m Model Evaluation Sectors

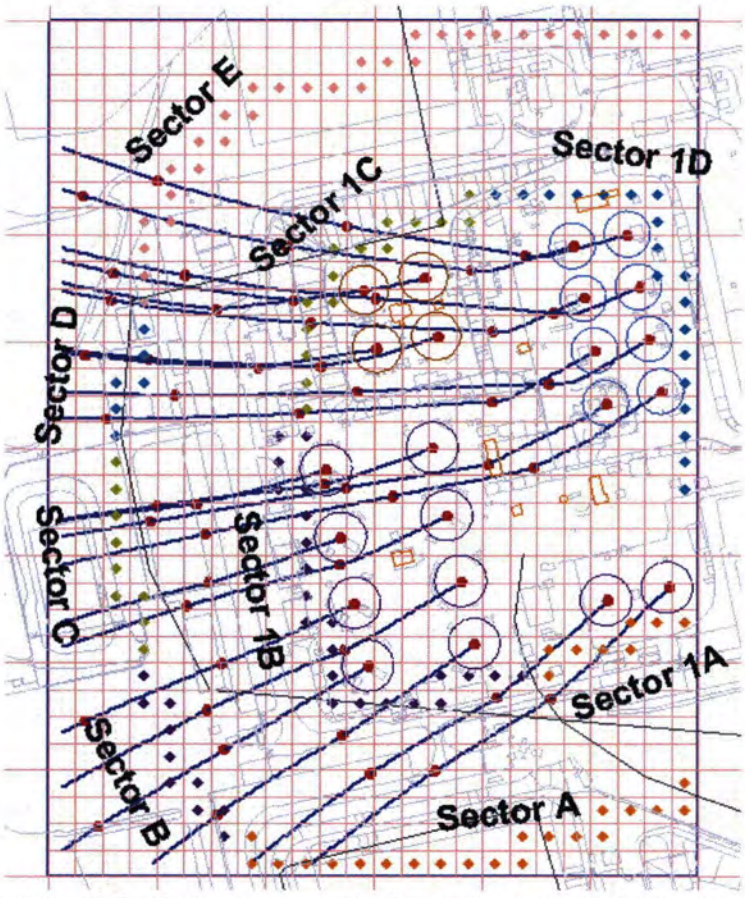

Note: The individual sectors are indicated by unique diamond colors.

Tables 5.2-3 through 5.2-5 present the peak 100m radionuclide concentrations within the 10,000 year evaluation period for the three aquifers. These radionuclide concentrations reflect the peak concentrations for each radionuclide in the highest sector. These values are conservatively high for the radionuclides present in multiple decay chains because the totals are simply the sum of the individual peaks within that sector for a given radionuclide, without regard to time or location. For example, if Pb-210 were present as a daughter product in six decay chains, those six concentrations would all be added (along with the parent Pb-210) together to arrive at a single Pb-210 concentration for that sector event, though the peaks for six daughters might have occurred at different times and at different locations within the sector. Tables 5.2-6 through 5.2-8 show the peak 100m chemical concentrations within the 10,000 year evaluation period for the three aquifers. The chemical concentrations also reflect the peak concentrations for the highest sector. Tables 5.2-3 through 5.2-8 also list the MCL for each constituent. The total alpha MCL includes Ra-226 but does not include radon or uranium. The radium MCL includes both Ra-226 and Ra-228 [SCDHEC R61-58]

Table 5.2-3: Radiological 100m Concentrations for UTR-UZ

Radionuclide	Maximum Contamination Limit (MCL) (pCi/L)	Sector A		Sector B		Sector C		Sector D		Sector E	
		Concentration (pCi/L)	Year Peak Contribution Occurs	Concentration (pCi/L)	Year Peak Contribution Occurs	Concentration (pCi/L)	Year Peak Contribution Occurs	Concentration (pCi/L)	Year Peak Contribution Occurs	Concentration (pCi/L)	Year Peak Contribution Occurs
Ac-227	N/A	3.35E-08	1,804	5.76E-08	1,800	3.62E-07	6,118	5.82E-06	6,112	7.85E-06	6,110
Al-26	N/A	2.43E-29	10,000	8.97E-27	10,000	9.49E-16	10,000	1.02E-09	10,000	3.11E-12	10,000
Am-241	Total α	<1.0E-30	10,000	4.31E-29	10,000	1.10E-18	10,000	4.83E-13	10,000	2.62E-12	10,000
Am-242m	Total α	<1.0E-30	9,692	<1.0E-30	9,950	<1.0E-30	8,540	8.82E-27	7,606	2.12E-29	8,024
Am-243	Total α	3.80E-30	10,000	2.27E-30	10,000	5.72E-20	10,000	2.20E-14	10,000	1.49E-14	10,000
Ba-137m	N/A	*	*	*	*	*	*	*	*	*	*
Bk-249	2,000	*	*	*	*	*	*	*	*	*	*
C-14	2,000	4.64E-01	564	7.95E-01	562	1.27E+00	3,760	1.04E+01	3,758	4.33E+00	3,758
Ce-144	30	*	*	*	*	*	*	*	*	*	*
Cf-249	Total α	<1.0E-30	10,000	<1.0E-30	10,000	<1.0E-30	10,000	<1.0E-30	10,000	<1.0E-30	10,000
Cm-242	Total α	*	*	*	*	*	*	*	*	*	*
Cm-243	Total α	<1.0E-30	1,904	<1.0E-30	1,908	<1.0E-30	1,624	<1.0E-30	1,424	<1.0E-30	1,494
Cm-244	Total α	<1.0E-30	1,344	<1.0E-30	1,352	<1.0E-30	1,174	<1.0E-30	1,050	<1.0E-30	1,088
Cm-245	Total α	<1.0E-30	10,000	<1.0E-30	10,000	1.15E-21	10,000	4.06E-16	10,000	5.82E-16	10,000
Cm-247	Total α	<1.0E-30	10,000	<1.0E-30	10,000	<1.0E-30	10,000	2.86E-26	10,000	2.03E-26	10,000
Cm-248	Total α	<1.0E-30	10,000	<1.0E-30	10,000	<1.0E-30	10,000	6.47E-27	10,000	4.60E-27	10,000
Co-60	100	<1.0E-30	384	<1.0E-30	432	<1.0E-30	190	<1.0E-30	164	<1.0E-30	164
Cs-134	80	*	*	*	*	*	*	*	*	*	*
Cs-135	900	8.00E-04	9,004	1.37E-03	8,796	3.95E-03	6,252	3.27E-02	5,648	3.46E-02	5,626
Cs-137	200	4.96E-29	2,076	7.62E-26	1,376	6.00E-19	1,160	3.06E-15	1,006	7.33E-17	1,052
Eu-152	200	*	*	*	*	*	*	*	*	*	*
Eu-154	60	*	*	*	*	*	*	*	*	*	*
Eu-155	600	*	*	*	*	*	*	*	*	*	*
Gd-152	N/A	<1.0E-30	10,000	<1.0E-30	10,000	1.03E-28	10,000	3.63E-23	10,000	2.78E-23	10,000

Table 5.2-3: Radiological 100m Concentrations for UTR-UZ (Continued)

Radionuclide	Maximum Contamination Limit (MCL) (pCi/L)	Sector A		Sector B		Sector C		Sector D		Sector E	
		Concentration (pCi/L)	Year Peak Contribution Occurs	Concentration (pCi/L)	Year Peak Contribution Occurs	Concentration (pCi/L)	Year Peak Contribution Occurs	Concentration (pCi/L)	Year Peak Contribution Occurs	Concentration (pCi/L)	Year Peak Contribution Occurs
H-3	20,000	1.76E-12	558	3.17E-12	558	2.04E-11	208	2.21E-09	202	3.38E-09	202
I-129	1	3.10E-04	584	5.30E-04	584	7.77E-04	3,794	6.06E-03	3,792	1.33E-03	3,792
Na-22	400	*	*	*	*	*	*	*	*	*	*
Nb-94	N/A	4.29E-01	564	7.35E-01	562	7.14E-01	560	6.40E-01	560	3.90E-01	560
Ni-59	300	5.82E-01	2,066	9.94E-01	2,036	1.72E+00	7,370	1.68E+01	7,292	1.74E+01	7,286
Ni-63	50	5.19E-04	1,504	1.09E-03	1,474	1.21E-03	1,434	1.01E-03	1,480	3.26E-03	1,208
Np-237	Total α	5.73E-02	1,606	9.80E-02	1,602	9.73E-02	1,596	1.52E+00	6,056	2.16E+00	6,058
Pa-231	Total α	4.41E-05	1,772	7.58E-05	1,768	4.79E-04	6,066	7.70E-03	6,060	1.04E-02	6,058
Pb-210	N/A	1.67E-04	1,708	2.89E-04	1,694	3.34E-04	1,662	1.49E-03	10,000	1.89E-03	10,000
Pm-147	600	*	*	*	*	*	*	*	*	*	*
Pr-144	N/A	*	*	*	*	*	*	*	*	*	*
Pu-238	Total α	<1.0E-30	5,260	<1.0E-30	7,962	3.30E-26	7,218	1.80E-21	6,668	2.67E-23	6,884
Pu-239	Total α	1.45E-07	10,000	4.20E-09	10,000	2.21E-05	10,000	1.08E-02	10,000	1.37E-02	10,000
Pu-240	Total α	2.47E-08	10,000	7.28E-10	10,000	5.10E-05	10,000	2.72E-02	10,000	3.76E-02	10,000
Pu-241	300	<1.0E-30	10,000	2.90E-31	10,000	5.96E-21	10,000	1.95E-15	10,000	2.81E-15	10,000
Pu-242	Total α	5.75E-10	10,000	1.70E-11	10,000	1.62E-06	10,000	8.24E-04	10,000	1.02E-03	10,000
Pu-244	Total α	2.75E-13	10,000	1.16E-14	10,000	6.90E-09	10,000	3.22E-06	10,000	6.29E-07	10,000
Ra-226	Total α/Ra	6.40E-02	1,686	1.11E-01	1,672	1.28E-01	1,642	5.72E-01	10,000	7.25E-01	10,000
Ra-228	Total Ra	9.85E-14	10,000	9.04E-14	10,000	8.83E-10	10,000	8.31E-08	10,000	1.51E-07	10,000
Rh-106	N/A	*	*	*	*	*	*	*	*	*	*
Ru-106	30	*	*	*	*	*	*	*	*	*	*
Sb-125	300	*	*	*	*	*	*	*	*	*	*
Sb-126	N/A	*	*	*	*	*	*	*	*	*	*
Sb-126m	N/A	*	*	*	*	*	*	*	*	*	*

Table 5.2-3: Radiological 100m Concentrations for UTR-UZ (Continued)

Radionuclide	Maximum Contamination Limit (MCL) (pCi/L)	Sector A		Sector B		Sector C		Sector D		Sector E	
		Concentration (pCi/L)	Year Peak Contribution Occurs	Concentration (pCi/L)	Year Peak Contribution Occurs	Concentration (pCi/L)	Year Peak Contribution Occurs	Concentration (pCi/L)	Year Peak Contribution Occurs	Concentration (pCi/L)	Year Peak Contribution Occurs
Se-79	N/A	6.32E-24	10,000	3.47E-21	10,000	1.43E-11	10,000	1.38E-06	10,000	2.47E-06	10,000
Sm-147	N/A	<1.0E-30	10,000	<1.0E-30	10,000	5.41E-24	10,000	1.93E-18	10,000	1.96E-18	10,000
Sm-151	1,000	<1.0E-30	6,688	<1.0E-30	4,574	<1.0E-30	3,666	<1.0E-30	3,056	<1.0E-30	3,274
Sn-126	N/A	<1.0E-30	10,000	<1.0E-30	10,000	1.54E-19	10,000	1.63E-12	10,000	2.14E-12	10,000
Sr-90	8	9.89E-10	1,108	3.06E-09	1,084	1.41E-08	1,026	7.09E-09	1,048	1.24E-07	990
Tc-99	900	1.07E+02	598	1.83E+02	596	1.77E+02	594	4.20E+02	586	3.38E+02	584
Te-125m	600	*	*	*	*	*	*	*	*	*	*
Th-228	Total α	5.71E-16	10,000	5.24E-16	10,000	5.12E-12	10,000	4.83E-10	10,000	8.77E-10	10,000
Th-229	Total α	1.76E-07	10,000	2.77E-07	10,000	1.37E-03	10,000	1.15E-01	10,000	6.03E-02	10,000
Th-230	Total α	2.84E-09	10,000	1.38E-09	10,000	6.94E-06	10,000	1.43E-03	10,000	3.94E-03	10,000
Th-232	Total α	2.86E-16	10,000	1.38E-16	10,000	2.86E-12	10,000	3.37E-10	10,000	6.16E-10	10,000
U-232	Total U**	<1.0E-30	4,280	<1.0E-30	3,006	1.59E-30	2,430	7.18E-26	2,030	1.03E-25	2,024
U-233	Total U**	3.56E-06	10,000	4.90E-06	10,000	8.68E-02	10,000	4.29E+00	10,000	2.75E+00	10,000
U-234	Total U**	1.95E-06	10,000	1.49E-06	10,000	4.54E-03	10,000	6.77E-01	10,000	1.59E+00	10,000
U-235	Total U**	1.91E-08	10,000	1.46E-08	10,000	5.42E-05	10,000	4.41E-03	10,000	6.07E-03	10,000
U-236	Total U**	3.70E-08	10,000	2.86E-08	10,000	3.41E-04	10,000	2.67E-02	10,000	4.93E-02	10,000
U-238	Total U**	9.10E-07	10,000	6.85E-07	10,000	1.48E-05	10,000	5.28E-04	10,000	5.65E-04	10,000
Y-90	30	*	*	*	*	*	*	*	*	*	*
Total alpha	15	1.21E-01	1,686	2.09E-01	1,672	2.27E-01	1,642	2.25E+00	6,056	3.01E+00	6,058
Total Ra	5	6.40E-02	1,686	1.1E-01	1,672	1.28E-01	1,642	5.72E-01	10,000	7.25E-01	10,000
Sum of beta/gamma MCL fractions		1.2.E-01	598	2.1.E-01	596	2.0.E-01	594	5.3.E-01	586	4.4.E-01	584

* Short-lived radionuclides decayed prior to liner failure. PORFLOW does not track short-lived radionuclides during transport modeling, but the DCFs do include the equilibrium progeny.

** Total uranium is evaluated in Table 5.2-6.

Table 5.2-4: Radiological 100m Concentrations for UTR-LZ

Radionuclide	Maximum Contamination Limit (MCL) (pCi/L)	Sector A		Sector B		Sector C		Sector D		Sector E	
		Concentration (pCi/L)	Year Peak Contribution Occurs	Concentration (pCi/L)	Year Peak Contribution Occurs	Concentration (pCi/L)	Year Peak Contribution Occurs	Concentration (pCi/L)	Year Peak Contribution Occurs	Concentration (pCi/L)	Year Peak Contribution Occurs
Ac-227	N/A	4.78E-08	10,000	9.17E-08	10,000	2.81E-07	10,000	4.44E-06	6,114	9.16E-06	10,000
Al-26	N/A	<1.0E-30	10,000	<1.0E-30	10,000	9.99E-20	10,000	1.81E-13	10,000	2.97E-15	10,000
Am-241	Total α	<1.0E-30	10,000	<1.0E-30	10,000	2.62E-22	10,000	3.04E-16	10,000	3.42E-15	10,000
Am-242m	Total α	<1.0E-30	10,000	<1.0E-30	10,000	<1.0E-30	9,348	<1.0E-30	8,512	<1.0E-30	8,694
Am-243	Total α	<1.0E-30	10,000	<1.0E-30	10,000	1.37E-23	10,000	1.01E-17	10,000	2.01E-17	10,000
Ba-137m	N/A	*	*	*	*	*	*	*	*	*	*
Bk-249	2,000	*	*	*	*	*	*	*	*	*	*
C-14	2,000	5.00E-01	564	9.27E-01	564	9.65E-01	564	9.26E+00	3,758	5.66E+00	3,760
Ce-144	30	*	*	*	*	*	*	*	*	*	*
Cf-249	Total α	<1.0E-30	10,000	<1.0E-30	10,000	<1.0E-30	10,000	<1.0E-30	10,000	<1.0E-30	10,000
Cm-242	Total α	*	*	*	*	*	*	*	*	*	*
Cm-243	Total α	<1.0E-30	2,066	<1.0E-30	2,122	<1.0E-30	1,846	<1.0E-30	1,652	<1.0E-30	1,690
Cm-244	Total α	<1.0E-30	1,460	<1.0E-30	1,492	<1.0E-30	1,318	<1.0E-30	1,196	<1.0E-30	1,216
Cm-245	Total α	<1.0E-30	10,000	<1.0E-30	10,000	2.90E-25	10,000	2.04E-19	10,000	8.09E-19	10,000
Cm-247	Total α	<1.0E-30	10,000	<1.0E-30	10,000	<1.0E-30	10,000	1.43E-29	10,000	2.88E-29	10,000
Cm-248	Total α	<1.0E-30	10,000	<1.0E-30	10,000	<1.0E-30	10,000	3.23E-30	10,000	6.54E-30	10,000
Co-60	100	*	*	*	*	*	*	*	*	*	*
Cs-134	80	*	*	*	*	*	*	*	*	*	*
Cs-135	900	8.72E-04	9,224	1.64E-03	9,308	3.01E-03	6,820	2.49E-02	6,114	3.05E-02	6,052
Cs-137	200	<1.0E-30	1,538	9.26E-28	1,476	5.70E-21	1,256	3.64E-17	1,114	2.49E-18	1,150
Eu-152	200	*	*	*	*	*	*	*	*	*	*
Eu-154	60	*	*	*	*	*	*	*	*	*	*
Eu-155	600	*	*	*	*	*	*	*	*	*	*
Gd-152	N/A	<1.0E-30	10,000	<1.0E-30	10,000	<1.0E-30	10,000	1.81E-26	10,000	3.95E-26	10,000

Table 5.2-4: Radiological 100m Concentrations for UTR-LZ (Continued)

Radionuclide	Maximum Contamination Limit (MCL) (pCi/L)	Sector A		Sector B		Sector C		Sector D		Sector E	
		Concentration (pCi/L)	Year Peak Contribution Occurs	Concentration (pCi/L)	Year Peak Contribution Occurs	Concentration (pCi/L)	Year Peak Contribution Occurs	Concentration (pCi/L)	Year Peak Contribution Occurs	Concentration (pCi/L)	Year Peak Contribution Occurs
H-3	20,000	1.62E-12	562	3.10E-12	560	9.91E-12	210	1.07E-09	204	2.16E-09	204
I-129	1	3.38E-04	586	6.37E-04	586	6.59E-04	586	5.53E-03	3,792	2.41E-03	3,792
Na-22	400	*	*	*	*	*	*	*	*	*	*
Nb-94	N/A	4.62E-01	564	8.57E-01	564	8.92E-01	564	8.39E-01	564	7.05E-01	564
Ni-59	300	6.34E-01	2,102	1.19E+00	2,118	1.23E+00	2,102	1.39E+01	7,336	1.72E+01	7,334
Ni-63	50	2.92E-04	1,580	6.94E-04	1,532	9.88E-04	1,358	6.72E-04	1,556	3.16E-03	1,274
Np-237	Total α	6.25E-02	1,610	1.18E-01	1,610	1.23E-01	1,608	1.03E+00	6,064	2.30E+00	6,062
Pa-231	Total α	4.81E-05	1,776	9.19E-05	1,778	3.58E-04	6,076	5.88E-03	6,062	1.17E-02	6,060
Pb-210	N/A	1.79E-04	1,724	3.38E-04	1,728	3.87E-04	1,718	1.22E-03	10,000	2.28E-03	10,000
Pm-147	600	*	*	*	*	*	*	*	*	*	*
Pr-144	N/A	*	*	*	*	*	*	*	*	*	*
Pu-238	Total α	<1.0E-30	5,616	<1.0E-30	8,304	6.81E-29	7,576	3.73E-24	7,102	1.54E-25	7,218
Pu-239	Total α	1.69E-09	10,000	8.21E-11	10,000	6.14E-07	10,000	6.94E-04	10,000	1.09E-03	10,000
Pu-240	Total α	2.87E-10	10,000	1.45E-11	10,000	1.27E-06	10,000	1.71E-03	10,000	3.00E-03	10,000
Pu-241	300	<1.0E-30	10,000	<1.0E-30	10,000	1.60E-24	10,000	1.04E-18	10,000	4.09E-18	10,000
Pu-242	Total α	6.67E-12	10,000	3.41E-13	10,000	4.07E-08	10,000	5.33E-05	10,000	8.12E-05	10,000
Pu-244	Total α	3.20E-15	10,000	2.22E-16	10,000	1.73E-10	10,000	2.18E-07	10,000	5.91E-08	10,000
Ra-226	Total α/Ra	6.88E-02	1,700	1.30E-01	1,702	1.48E-01	1,692	4.68E-01	10,000	8.71E-01	10,000
Ra-228	Total Ra	3.95E-15	10,000	5.68E-15	10,000	8.09E-11	10,000	1.60E-08	10,000	4.25E-08	10,000
Rh-106	N/A	*	*	*	*	*	*	*	*	*	*
Ru-106	30	*	*	*	*	*	*	*	*	*	*
Sb-125	300	*	*	*	*	*	*	*	*	*	*
Sb-126	N/A	*	*	*	*	*	*	*	*	*	*
Sb-126m	N/A	*	*	*	*	*	*	*	*	*	*

Table 5.2-4: Radiological 100m Concentrations for UTR-LZ (Continued)

Radionuclide	Maximum Contamination Limit (MCL) (pCi/L)	Sector A		Sector B		Sector C		Sector D		Sector E	
		Concentration (pCi/L)	Year Peak Contribution Occurs	Concentration (pCi/L)	Year Peak Contribution Occurs	Concentration (pCi/L)	Year Peak Contribution Occurs	Concentration (pCi/L)	Year Peak Contribution Occurs	Concentration (pCi/L)	Year Peak Contribution Occurs
Se-79	N/A	9.90E-28	10,000	1.25E-24	10,000	8.93E-15	10,000	2.08E-09	10,000	7.78E-09	10,000
Sm-147	N/A	<1.0E-30	10,000	<1.0E-30	10,000	1.36E-27	10,000	9.57E-22	10,000	2.70E-21	10,000
Sm-151	1,000	<1.0E-30	4,882	<1.0E-30	5,058	<1.0E-30	4,244	<1.0E-30	3,688	<1.0E-30	3,802
Sn-126	N/A	<1.0E-30	10,000	<1.0E-30	10,000	2.17E-24	10,000	3.05E-17	10,000	2.33E-16	10,000
Sr-90	8	3.42E-10	1,144	1.68E-09	1,118	1.01E-08	1,062	1.99E-09	1,082	6.62E-08	1,026
Tc-99	900	1.16E+02	598	2.16E+02	600	2.29E+02	598	4.85E+02	590	5.69E+02	588
Te-125m	600	*	*	*	*	*	*	*	*	*	*
Th-228	Total α	2.29E-17	10,000	3.29E-17	10,000	4.69E-13	10,000	9.28E-11	10,000	2.46E-10	10,000
Th-229	Total α	6.99E-07	10,000	1.32E-06	10,000	1.07E-04	10,000	2.34E-02	10,000	1.52E-02	10,000
Th-230	Total α	9.22E-11	10,000	6.11E-11	10,000	5.00E-07	10,000	2.00E-04	10,000	9.23E-04	10,000
Th-232	Total α	9.15E-18	10,000	6.61E-18	10,000	2.07E-13	10,000	5.59E-11	10,000	1.45E-10	10,000
U-232	Total U**	<1.0E-30	4,556	<1.0E-30	3,270	<1.0E-30	2,704	1.76E-28	2,340	4.39E-28	2,272
U-233	Total U**	1.27E-05	10,000	2.39E-05	10,000	8.63E-03	10,000	1.25E+00	10,000	9.54E-01	10,000
U-234	Total U**	7.91E-08	10,000	7.46E-08	10,000	4.15E-04	10,000	1.24E-01	10,000	5.28E-01	10,000
U-235	Total U**	7.71E-10	10,000	7.31E-10	10,000	4.85E-06	10,000	9.56E-04	10,000	1.65E-03	10,000
U-236	Total U**	1.47E-09	10,000	1.49E-09	10,000	3.16E-05	10,000	5.93E-03	10,000	1.61E-02	10,000
U-238	Total U**	3.68E-08	10,000	3.41E-08	10,000	3.04E-06	10,000	1.15E-04	10,000	1.46E-04	10,000
Y-90	30	*	*	*	*	*	*	*	*	*	*
Total alpha	15	1.31E-01	1610	2.48E-01	1702	2.71E-01	1,692	1.53E+00	10,000	3.20E+00	6,062
Total Ra	5	6.88E-02	1,700	1.30E-01	1,702	1.48E-01	1,692	4.68E-01	10,000	8.71E-01	10,000
Sum of beta/gamma MCL fractions		1.3.E-01	598	2.5.E-01	600	2.6.E-01	598	6.0.E-01	590	6.9.E-01	588

* Short-lived radionuclides decayed prior to liner failure. PORFLOW does not track short-lived radionuclides during transport modeling, but the DCFs do include the equilibrium progeny.

** Total uranium is evaluated in Table 5.2-7.

Table 5.2-5: Radiological 100m Concentrations for Gordon Aquifer

Radionuclide	Maximum Contamination Limit (MCL) (pCi/L)	Sector A		Sector B		Sector C		Sector D		Sector E	
		Concentration (pCi/L)	Year Peak Contribution Occurs	Concentration (pCi/L)	Year Peak Contribution Occurs	Concentration (pCi/L)	Year Peak Contribution Occurs	Concentration (pCi/L)	Year Peak Contribution Occurs	Concentration (pCi/L)	Year Peak Contribution Occurs
Ac-227	N/A	3.61E-12	10,000	1.94E-11	10,000	4.38E-11	10,000	3.30E-10	10,000	1.10E-09	10,000
Al-26	N/A	<1.0E-30	10,000	<1.0E-30	10,000	<1.0E-30	10,000	4.54E-27	10,000	1.30E-27	10,000
Am-241	Total α	<1.0E-30	10,000	<1.0E-30	10,000	<1.0E-30	10,000	1.02E-30	10,000	1.43E-29	10,000
Am-242m	Total α	<1.0E-30	10,000	<1.0E-30	10,000	<1.0E-30	10,000	<1.0E-30	9,800	<1.0E-30	9,782
Am-243	Total α	<1.0E-30	10,000	<1.0E-30	10,000	<1.0E-30	10,000	<1.0E-30	10,000	<1.0E-30	10,000
Ba-137m	N/A	*	*	*	*	*	*	*	*	*	*
Bk-249	2,000	*	*	*	*	*	*	*	*	*	*
C-14	2,000	4.12E-05	614	2.28E-04	614	3.79E-04	614	3.55E-03	3,898	4.88E-03	3,900
Ce-144	30	*	*	*	*	*	*	*	*	*	*
Cf-249	Total α	<1.0E-30	10,000	<1.0E-30	10,000	<1.0E-30	10,000	<1.0E-30	10,000	<1.0E-30	10,000
Cm-242	Total α	*	*	*	*	*	*	*	*	*	*
Cm-243	Total α	<1.0E-30	2,364	<1.0E-30	2,416	<1.0E-30	2,138	<1.0E-30	1,940	<1.0E-30	1,942
Cm-244	Total α	<1.0E-30	1,644	<1.0E-30	1,676	<1.0E-30	1,500	<1.0E-30	1,380	<1.0E-30	1,352
Cm-245	Total α	<1.0E-30	10,000	<1.0E-30	10,000	<1.0E-30	10,000	<1.0E-30	10,000	<1.0E-30	10,000
Cm-247	Total α	<1.0E-30	10,000	<1.0E-30	10,000	<1.0E-30	10,000	<1.0E-30	10,000	<1.0E-30	10,000
Cm-248	Total α	<1.0E-30	10,000	<1.0E-30	10,000	<1.0E-30	10,000	<1.0E-30	10,000	<1.0E-30	10,000
Co-60	100	*	*	*	*	*	*	*	*	*	*
Cs-134	80	*	*	*	*	*	*	*	*	*	*
Cs-135	900	1.35E-09	10,000	7.52E-09	10,000	1.54E-08	10,000	5.20E-08	10,000	8.59E-08	10,000
Cs-137	200	<1.0E-30	1,730	<1.0E-30	1,654	<1.0E-30	1,442	2.66E-28	1,318	1.95E-28	1,332
Eu-152	200	*	*	*	*	*	*	*	*	*	*
Eu-154	60	*	*	*	*	*	*	*	*	*	*
Eu-155	600	*	*	*	*	*	*	*	*	*	*
Gd-152	N/A	<1.0E-30	10,000	<1.0E-30	10,000	<1.0E-30	10,000	<1.0E-30	10,000	<1.0E-30	10,000

Table 5.2-5: Radiological 100m Concentrations for Gordon Aquifer (Continued)

Radionuclide	Maximum Contamination Limit (MCL) (pCi/L)	Sector A		Sector B		Sector C		Sector D		Sector E	
		Concentration (pCi/L)	Year Peak Contribution Occurs	Concentration (pCi/L)	Year Peak Contribution Occurs	Concentration (pCi/L)	Year Peak Contribution Occurs	Concentration (pCi/L)	Year Peak Contribution Occurs	Concentration (pCi/L)	Year Peak Contribution Occurs
H-3	20,000	2.67E-17	580	1.45E-16	190	5.06E-16	188	1.20E-14	226	5.15E-14	226
I-129	1	2.41E-08	734	1.33E-07	732	2.22E-07	732	1.24E-06	4,092	1.36E-06	4,094
Na-22	400	*	*	*	*	*	*	*	*	*	*
Nb-94	N/A	3.83E-05	614	2.12E-04	614	3.52E-04	614	3.83E-04	614	3.82E-04	614
Ni-59	300	1.58E-05	6,528	8.77E-05	6,472	1.78E-04	10,000	1.07E-03	10,000	1.96E-03	10,000
Ni-63	50	5.14E-11	1,886	3.09E-10	1,852	7.08E-10	1,734	7.11E-10	1,772	1.74E-09	1,500
Np-237	Total α	1.69E-06	6,988	9.38E-06	6,888	1.65E-05	7,212	6.19E-05	10,000	2.20E-04	10,000
Pa-231	Total α	4.45E-09	10,000	2.49E-08	10,000	5.62E-08	10,000	4.15E-07	10,000	1.42E-06	10,000
Pb-210	N/A	5.16E-09	10,000	2.86E-08	10,000	4.93E-08	10,000	9.64E-08	10,000	2.50E-07	10,000
Pm-147	600	*	*	*	*	*	*	*	*	*	*
Pr-144	N/A	*	*	*	*	*	*	*	*	*	*
Pu-238	Total α	<1.0E-30	6,328	<1.0E-30	8,930	<1.0E-30	8,234	6.12E-38	7,812	<1.0E-30	7,876
Pu-239	Total α	1.59E-22	10,000	1.25E-22	10,000	1.15E-18	10,000	2.76E-15	10,000	7.25E-15	10,000
Pu-240	Total α	2.71E-23	10,000	2.16E-23	10,000	1.46E-18	10,000	6.64E-15	10,000	1.98E-14	10,000
Pu-241	300	<1.0E-30	10,000	<1.0E-30	10,000	<1.0E-30	10,000	2.74E-33	10,000	<1.0E-30	10,000
Pu-242	Total α	6.31E-25	10,000	5.04E-25	10,000	4.64E-20	10,000	2.11E-16	10,000	5.47E-16	10,000
Pu-244	Total α	3.02E-28	10,000	2.72E-28	10,000	1.87E-22	10,000	6.42E-19	10,000	6.01E-19	10,000
Ra-226	Total α/Ra	1.97E-06	9,980	1.09E-05	9,970	1.88E-05	9,982	3.69E-05	10,000	9.58E-05	10,000
Ra-228	Total Ra	6.38E-25	10,000	6.33E-24	10,000	1.17E-19	10,000	9.12E-17	10,000	5.70E-16	10,000
Rh-106	N/A	*	*	*	*	*	*	*	*	*	*
Ru-106	30	*	*	*	*	*	*	*	*	*	*
Sb-125	300	*	*	*	*	*	*	*	*	*	*
Sb-126	N/A	*	*	*	*	*	*	*	*	*	*
Sb-126m	N/A	*	*	*	*	*	*	*	*	*	*

Table 5.2-5: Radiological 100m Concentrations for Gordon Aquifer (Continued)

Radionuclide	Maximum Contamination Limit (MCL) (pCi/L)	Sector A		Sector B		Sector C		Sector D		Sector E	
		Concentration (pCi/L)	Year Peak Contribution Occurs	Concentration (pCi/L)	Year Peak Contribution Occurs	Concentration (pCi/L)	Year Peak Contribution Occurs	Concentration (pCi/L)	Year Peak Contribution Occurs	Concentration (pCi/L)	Year Peak Contribution Occurs
Se-79	N/A	<1.0E-30	10,000	<1.0E-30	10,000	3.18E-27	10,000	1.93E-21	10,000	1.18E-20	10,000
Sm-147	N/A	<1.0E-30	118	<1.0E-30	128	<1.0E-30	148	<1.0E-30	10,000	<1.0E-30	10,000
Sm-151	1,000	<1.0E-30	5,774	<1.0E-30	5,920	<1.0E-30	5,108	<1.0E-30	4,546	<1.0E-30	4,542
Sn-126	N/A	<1.0E-30	10,000	<1.0E-30	10,000	<1.0E-30	10,000	<1.0E-30	10,000	<1.0E-30	10,000
Sr-90	8	1.40E-17	1,240	1.47E-16	1,220	1.47E-15	1,154	1.51E-15	1,144	1.23E-14	1,088
Tc-99	900	9.19E-03	680	5.10E-02	680	8.53E-02	680	1.09E-01	678	1.34E-01	678
Te-125m	600	*	*	*	*	*	*	*	*	*	*
Th-228	Total α	3.69E-27	10,000	3.66E-26	10,000	6.74E-22	10,000	5.28E-19	10,000	3.30E-18	10,000
Th-229	Total α	3.18E-10	10,000	1.82E-09	10,000	2.81E-09	10,000	4.60E-09	10,000	9.02E-09	10,000
Th-230	Total α	2.15E-20	10,000	9.88E-20	10,000	9.41E-16	10,000	1.19E-12	10,000	1.23E-11	10,000
Th-232	Total α	2.09E-27	10,000	1.02E-26	10,000	3.75E-22	10,000	3.62E-19	10,000	1.83E-18	10,000
U-232	Total U**	<1.0E-30	5,108	<1.0E-30	3,750	<1.0E-30	3,210	<1.0E-30	2,874	<1.0E-30	2,814
U-233	Total U**	6.24E-09	10,000	3.22E-08	10,000	5.05E-08	10,000	1.23E-07	10,000	2.88E-08	10,000
U-234	Total U**	3.02E-17	10,000	1.56E-16	10,000	1.23E-12	10,000	1.26E-09	10,000	1.21E-08	10,000
U-235	Total U**	2.93E-19	10,000	1.52E-18	10,000	1.38E-14	10,000	1.12E-11	10,000	3.42E-11	10,000
U-236	Total U**	5.45E-19	10,000	3.03E-18	10,000	9.09E-14	10,000	6.99E-11	10,000	3.42E-10	10,000
U-238	Total U**	1.41E-17	10,000	7.10E-17	10,000	4.02E-14	10,000	1.46E-12	10,000	6.81E-12	10,000
Y-90	30	*	*	*	*	*	*	*	*	*	*
Total Alpha	15	3.66E-06	9980	2.03E-05	9,970	3.54E-05	9,982	9.92E-05	10,000	3.17E-04	10,000
Total Ra	5	1.97E-06	9,980	1.09E-05	9,970	1.88E-05	9,982	3.69E-05	10,000	9.58E-05	10,000
Sum of beta/gamma MCL fractions		1.0.E-05	680	5.7.E-05	680	9.6.E-05	680	1.3.E-04	678	1.6.E-04	678

* Short-lived radionuclides decayed prior to liner failure. PORFLOW does not track short-lived radionuclides during transport modeling, but the DCFs do include the equilibrium progeny.

** Total uranium is evaluated in Table 5.2-8.

Table 5.2-6: Chemical 100m Concentrations for UTR-UZ

Chemical	Maximum Contamination Limit (MCL) (µg/L)	Sector A		Sector B		Sector C		Sector D		Sector E	
		Concentration (µg/L)	Year Peak Contribution Occurs	Concentration (µg/L)	Year Peak Contribution Occurs	Concentration (µg/L)	Year Peak Contribution Occurs	Concentration (µg/L)	Year Peak Contribution Occurs	Concentration (µg/L)	Year Peak Contribution Occurs
Ag	N/A	5.96E-04	8,906	1.14E-03	8,520	5.03E-02	6,696	6.12E-01	5,844	7.37E-01	5,700
As	1.00E+01	8.17E-06	10,000	1.92E-05	10,000	6.06E-03	9,796	5.14E-02	8,520	6.82E-03	9,092
Ba	2.00E+03	5.39E-03	1,714	9.39E-03	1,690	5.16E-02	5,028	4.03E-01	4,954	3.36E-01	4,918
Cd	5.00E+00	2.30E-02	1,414	3.94E-02	1,394	3.82E-02	1,380	7.29E-01	7,242	1.04E+00	7,248
Cr	1.00E+02	8.71E-03	1,416	1.53E-02	1,408	4.41E-02	4,804	3.86E-01	4,752	2.94E-01	4,748
Cu	N/A	6.47E-04	6,346	1.14E-03	6,238	3.04E-02	6,218	4.08E-01	5,520	5.02E-01	5,404
F	N/A	8.60E-02	564	1.48E-01	562	1.92E+00	3,844	1.20E+01	3,840	1.88E+00	3,840
Fe	N/A	6.57E-06	10,000	4.47E-06	10,000	5.54E-03	10,000	1.14E+00	10,000	2.04E+00	10,000
Hg	2.00E+00	6.16E-23	10,000	4.13E-20	10,000	3.45E-11	10,000	1.19E-06	10,000	1.07E-06	10,000
Mn	N/A	1.29E-02	5,252	2.31E-02	5,652	8.94E-01	5,294	1.26E+01	5,130	1.61E+01	5,102
N	1.00E+04	3.31E+00	564	5.73E+00	562	7.34E+01	3,658	5.69E+02	3,654	2.09E+01	3,654
Ni	N/A	2.99E-01	2,068	5.11E-01	2,038	4.90E-01	2,008	4.43E-01	1,878	2.91E-01	1,668
Pb	1.50E+01	<1.0E-30	10,000	5.83E-29	10,000	5.03E-17	10,000	1.96E-10	10,000	1.96E-10	10,000
Sb	6.00E+00	<1.0E-30	10,000	<1.0E-30	10,000	9.68E-28	10,000	1.04E-17	10,000	5.79E-15	10,000
Se	5.00E+00	3.99E-24	10,000	2.69E-21	10,000	1.11E-11	10,000	1.06E-06	10,000	2.66E-09	10,000
U	3.00E+01	2.98E-06	10,000	2.24E-06	10,000	4.65E-05	10,000	1.57E-03	10,000	1.69E-03	10,000
V	N/A	1.54E-05	578	1.32E-04	578	5.94E-03	562	1.01E-01	558	8.15E-02	558
Zn	N/A	3.02E-04	10,000	6.37E-04	10,000	2.64E-02	9,436	3.81E-01	7,972	4.81E-01	7,730

Table 5.2-7: Chemical 100m Concentrations for UTR-LZ

Chemical	Maximum Contamination Limit (MCL) (µg/L)	Sector A		Sector B		Sector C		Sector D		Sector E	
		Concentration (µg/L)	Year Peak Contribution Occurs	Concentration (µg/L)	Year Peak Contribution Occurs	Concentration (µg/L)	Year Peak Contribution Occurs	Concentration (µg/L)	Year Peak Contribution Occurs	Concentration (µg/L)	Year Peak Contribution Occurs
Ag	N/A	6.46E-04	9,218	1.42E-03	9,002	3.52E-02	7,278	4.54E-01	6,386	5.60E-01	6,252
As	1.00E+01	3.68E-06	10,000	1.04E-05	10,000	3.24E-03	10,000	4.26E-02	9,440	1.56E-02	9,942
Ba	2.00E+03	5.84E-03	1,736	1.11E-02	1,728	3.95E-02	5,074	3.63E-01	4,982	3.58E-01	4,962
Cd	5.00E+00	2.50E-02	1,434	4.64E-02	1,442	4.81E-02	1,432	4.83E-01	7,276	1.02E+00	7,260
Cr	1.00E+02	9.46E-03	1,438	1.82E-02	1,448	3.05E-02	4,844	3.21E-01	4,788	2.92E-01	4,788
Cu	N/A	6.72E-04	7,136	1.34E-03	7,288	2.17E-02	6,704	2.97E-01	5,970	3.87E-01	5,864
F	N/A	9.27E-02	564	1.72E-01	564	1.50E+00	3,846	1.23E+01	3,842	5.85E+00	3,842
Fe	N/A	2.62E-07	10,000	2.26E-07	10,000	2.89E-04	10,000	1.40E-01	10,000	2.87E-01	10,000
Hg	2.00E+00	2.03E-26	10,000	3.17E-23	10,000	4.78E-14	10,000	4.01E-09	10,000	6.69E-09	10,000
Mn	N/A	1.41E-02	5,336	3.01E-02	5,730	6.20E-01	5,428	9.42E+00	5,248	1.44E+01	5,220
N	1.00E+04	3.59E+00	564	6.68E+00	564	4.79E+01	3,660	5.15E+02	3,656	1.56E+02	3,658
Ni	N/A	3.26E-01	2,104	6.10E-01	2,118	6.32E-01	2,102	5.95E-01	2,098	4.99E-01	2,050
Pb	1.50E+01	<1.0E-30	10,000	<1.0E-30	10,000	1.49E-21	10,000	1.01E-14	10,000	5.02E-14	10,000
Sb	6.00E+00	<1.0E-30	10,000	<1.0E-30	10,000	<1.0E-30	10,000	4.16E-22	10,000	3.94E-19	10,000
Se	5.00E+00	6.38E-28	10,000	9.71E-25	10,000	6.93E-15	10,000	1.59E-09	10,000	4.12E-11	10,000
U	3.00E+01	1.21E-07	10,000	1.12E-07	10,000	9.76E-06	10,000	3.41E-04	10,000	4.40E-04	10,000
V	N/A	1.44E-05	580	1.43E-04	578	4.53E-03	564	1.03E-01	560	1.36E-01	560
Zn	N/A	1.36E-04	10,000	3.58E-04	10,000	1.82E-02	10,000	2.70E-01	8,900	3.60E-01	8,662

Table 5.2-8: Chemical 100m Concentrations for Gordon Aquifer

Chemical	Maximum Contamination Limit (MCL) (µg/L)	Sector A		Sector B		Sector C		Sector D		Sector E	
		Concentration (µg/L)	Year Peak Contribution Occurs	Concentration (µg/L)	Year Peak Contribution Occurs	Concentration (µg/L)	Year Peak Contribution Occurs	Concentration (µg/L)	Year Peak Contribution Occurs	Concentration (µg/L)	Year Peak Contribution Occurs
Ag	N/A	1.46E-09	10,000	8.57E-09	10,000	1.11E-07	10,000	1.86E-06	10,000	3.23E-06	10,000
As	1.00E+01	2.38E-13	10,000	1.80E-12	10,000	2.98E-10	10,000	1.98E-08	10,000	2.03E-08	10,000
Ba	2.00E+03	1.76E-07	4,354	9.79E-07	4,314	5.32E-06	10,000	6.94E-05	10,000	8.67E-05	10,000
Cd	5.00E+00	8.41E-07	3,044	4.66E-06	3,024	7.76E-06	3,036	9.29E-05	10,000	4.00E-04	10,000
Cr	1.00E+02	3.17E-07	3,044	1.77E-06	3,024	5.34E-06	9,118	7.08E-05	9,780	1.06E-04	9,844
Cu	N/A	1.16E-08	10,000	6.51E-08	10,000	3.47E-07	10,000	4.37E-06	10,000	8.50E-06	10,000
F	N/A	7.69E-06	614	4.25E-05	614	5.52E-04	4,002	6.97E-03	3,996	7.63E-03	3,996
Fe	N/A	5.47E-17	10,000	2.71E-16	10,000	3.00E-13	10,000	2.84E-10	10,000	9.45E-10	10,000
Hg	2.00E+00	7.71E-40	10,000	<1.0E-30	10,000	5.07E-26	10,000	9.50E-21	10,000	3.08E-20	10,000
Mn	N/A	1.23E-07	10,000	7.05E-07	10,000	1.92E-06	10,000	1.56E-05	10,000	3.58E-05	10,000
N	1.00E+04	2.99E-04	614	1.65E-03	614	3.07E-03	3,718	4.74E-02	3,716	4.89E-02	3,716
Ni	N/A	8.47E-06	6,762	4.69E-05	6,686	7.81E-05	6,736	8.52E-05	6,768	8.82E-05	6,902
Pb	1.50E+01	<1.0E-30	10,000	<1.0E-30	10,000	<1.0E-30	10,000	7.26E-30	10,000	6.60E-29	10,000
Sb	6.00E+00	<1.0E-30	10,000	<1.0E-30	10,000	<1.0E-30	10,000	2.15E-37	10,000	<1.0E-30	10,000
Se	5.00E+00	<1.0E-30	10,000	<1.0E-30	10,000	2.46E-27	10,000	9.58E-22	10,000	3.77E-22	10,000
U	3.00E+01	4.60E-17	10,000	2.32E-16	10,000	1.31E-13	10,000	4.34E-12	10,000	3.86E-11	10,000
V	N/A	7.83E-10	628	1.81E-08	626	2.86E-07	612	7.47E-06	610	1.70E-05	612
Zn	N/A	8.79E-12	10,000	6.65E-11	10,000	3.41E-09	10,000	2.09E-07	10,000	4.94E-07	10,000

The 100m radionuclide and chemical concentration curves (for 20,000 years) associated with the five sectors and three aquifers for the Base Case, as described in Section 4.4.2.1, are captured in Appendix B.

- Appendix B.1 – 100m Radiological and Chemical Concentrations at the UTR-UZ (Sectors A through E).
- Appendix B.2 – 100m Radiological and Chemical Concentrations at the UTR-LZ (Sectors A through E).
- Appendix B.3 - 100m Radiological and Chemical Concentrations at the Gordon Aquifer (Sectors A through E).

To support further and varied investigation of key radionuclides (e.g., individual waste tank contributions, peak beyond the 10,000 year evaluation period), additional 100m groundwater concentrations were calculated using the PORFLOW FTF model. Appendix D contains 40,000 year curves for the 100m radionuclide concentrations for all of FTF (waste tank and ancillary inventories). Appendix E contains 20,000 year data curves for the 100m radionuclide concentrations for selected FTF sources (Tanks 1, 2, 3, 4, 5, 6, 7, 8, 17, 18, 19, 20, 33, 34 and waste transfer lines). These Base Case concentration results are for key radionuclides only and are presented from the three aquifers of concern (UTR-UZ, UTR-LZ and Gordon Aquifer) for Sectors A through E.

5.2.2 Key Radionuclide Determination

The purpose of this section is to present the methodology used in determining which radionuclides were most significant and to document which radionuclides would be considered "key". While all radionuclides identified in the FTF tank inventory (Section 3.3.2) were included in 100m groundwater modeling efforts, narrowing the catalog of radionuclides down to a "key" radionuclide list allowed the analysis to concentrate on the few radionuclides which posed the highest risk and concentrated modeling efforts on the areas of greatest concern (e.g., only key radionuclides were included in the PORFLOW seepline modeling runs). The key radionuclides were determined based on the peak 100m groundwater concentration listed in Section 5.2.1. Any radionuclide with a peak individual water ingestion dose (assuming 337 L/yr ingestion) greater than 0.005 mrem/yr was considered a key radionuclide. The screening conclusions are provided in Table 5.2-9. The resulting key radionuclides are C-14, Np-237, Pa-231, Pb-210, Pu-239, Pu-240, Pu-242, Ra-226, Tc-99, Th-229, Th-230, U-233, U-234, U-236, and U-238. Although U-238 does not contribute >.005 mrem/yr, it remains in the analysis due to its decay contribution to other key radionuclides. The 0.005 mrem/yr screening threshold was considered sufficiently low that no radionuclides that were screened out would contribute appreciably to the peak dose results, even accounting for cumulative pathway effects. This was supported by the fact that the total water ingestion dose contribution at 100m for all the non-key radionuclides was less than 0.01 mrem/yr.

Table 5.2-9: Determination of Key Radionuclides

Radionuclide	Peak 100m Concentration in 20,000 years (pCi/L)	Ingestion Dose Conversion Factor (rem/μCi)	**Ingestion Dose (mrem/yr)
Ac-227	7.90E-06	4.07E+00	1.08E-05
Al-26	6.39E-04	1.30E-02	2.80E-06
Am-241	3.84E-11	7.40E-01	9.58E-12
Am-242m	8.82E-27	7.03E-01	2.09E-27
Am-243	6.73E-09	7.40E-01	1.68E-09
Ba-137m	*	*	*
Bk-249	<1.0E-30	3.59E-03	<1.0E-30
C-14	1.04E+01	2.15E-03	7.54E-03
Ce-144	<1.0E-30	1.92E-02	<1.0E-30
Cf-249	<1.0E-30	1.30E+00	<1.0E-30
Cm-242	<1.0E-30	4.44E-02	<1.0E-30
Cm-243	<1.0E-30	5.55E-01	<1.0E-30
Cm-244	<1.0E-30	4.44E-01	<1.0E-30
Cm-245	2.89E-11	7.77E-01	7.56E-12
Cm-247	1.74E-20	7.03E-01	4.12E-21
Cm-248	3.88E-21	2.85E+00	3.73E-21
Co-60	*	*	*
Cs-134	*	*	*
Cs-135	3.74E-01	7.40E-03	9.34E-04
Cs-137	3.06E-15	4.81E-02	4.97E-17
Eu-152	*	*	*
Eu-154	*	*	*
Eu-155	*	*	*
Gd-152	2.39E-17	1.52E-01	1.22E-18
H-3	3.38E-09	6.66E-05	7.58E-14
I-129	2.21E-02	4.07E-01	3.03E-03
Na-22	*	*	*
Nb-94	7.35E-01	6.29E-03	1.56E-03
Ni-59	1.74E+01	2.33E-04	1.36E-03
Ni-63	3.26E-03	5.55E-04	6.09E-07
Np-237	7.19E+00	4.07E-01	9.86E-01
Pa-231	1.05E-02	2.63E+00	9.31E-03
Pb-210	1.68E-02	2.55E+00	1.44E-02
Pm-147	*	*	*
Pr-144	*	*	*
Pu-238	1.80E-21	8.51E-01	5.17E-22
Pu-239	7.27E-01	9.25E-01	2.27E-01

Table 5.2-9: Determination of Key Radionuclides (Continued)

Radionuclide	Peak 100m Concentration in 20,000 years (pCi/L)	Ingestion Dose Conversion Factor (rem/μCi)	**Ingestion Dose (mrem/yr)
Pu-240	1.35E+00	9.25E-01	4.21E-01
Pu-241	1.22E-10	1.78E-02	7.29E-13
Pu-242	5.94E-02	8.88E-01	1.78E-02
Pu-244	1.64E-04	8.88E-01	4.92E-05
Ra-226	6.44E+00	1.04E+00	2.26E+00
Ra-228	1.87E-06	2.55E+00	1.61E-06
Rh-106m	*	*	*
Ru-106	*	*	*
Sb-125	*	*	*
Sb-126	*	*	*
Sb-126m	*	*	*
Se-79	2.18E-02	1.07E-02	7.86E-05
Sm-147	2.88E-13	1.78E-01	1.72E-14
Sm-151	<1.0E-30	3.63E-04	<1.0E-30
Sn-126	1.43E-05	1.15E-02	5.55E-08
Sr-90	1.24E-07	1.04E-01	4.36E-09
Tc-99	4.20E+02	2.37E-03	3.36E-01
Te-125m	*	*	*
Th-228	1.09E-08	2.66E-01	9.77E-10
Th-229	6.42E-01	1.81E+00	3.92E-01
Th-230	4.56E-02	7.77E-01	1.19E-02
Th-232	1.06E-08	8.51E-01	3.04E-09
U-232	1.03E-25	1.22E+00	4.25E-26
U-233	6.57E+00	1.89E-01	4.18E-01
U-234	2.99E+00	1.81E-01	1.82E-01
U-235	1.90E-02	1.74E-01	1.11E-03
U-236	1.17E-01	1.74E-01	6.86E-03
U-238	1.04E-02	1.67E-01	5.85E-04
Y-90	*	*	*

*Short-lived radionuclides decayed prior to liner failure. PORFLOW does not track short-lived radionuclides during transport modeling, but the DCFs do include the equilibrium progeny.

**Calculation of ingestion dose calculated in pCi/L x 10^{-6} x rem/μCi x 337 L/yr x 1,000 mrem/rem.

5.2.3 Groundwater Concentrations at the Seeplines

The seepline groundwater concentrations were calculated using the PORFLOW FTF model, which grids the GSA surrounding FTF. Figure 5.2-6 shows the FTF seeplines (UTR-UZ, UTR-LZ and Fourmile Branch) in relation to the FTF. The PORFLOW seepline concentrations are provided for two sectors (UTR and Fourmile Branch) and five aquifers (three for UTR and two for Fourmile Branch) as shown on Figure 5.2-6. The peak concentration values for the seepline results were recorded for the three aquifer depths of concern (i.e., UTR-UZ, UTR-LZ and Gordon Aquifer). Dividing the results into sectors allows variability in peak concentration for different areas of the FTF to be more easily seen. The five aquifers were analyzed for each radionuclide to find the maximum groundwater concentrations at each seepline.

Tables 5.2-10 (UTR) and 5.2-11 (Fourmile Branch) show the peak seepline radionuclide concentrations in the 10,000 year evaluation period and out to 20,000 years. These radionuclide concentrations reflect the peak concentrations for each radionuclide in the highest sector. These values are conservatively high for the radionuclides present in multiple decay chains because the totals are simply the sum the individual peaks within that sector for a given radionuclide, without regard to time or location.

Appendix C contains data curves showing the far field (i.e., seepline) radionuclide concentrations (key radionuclides only for 20,000 years) for all of FTF (tank and ancillary inventories) for the Base Case.

Figure 5.2-6: PORFLOW FTF Seepline Evaluation Sectors

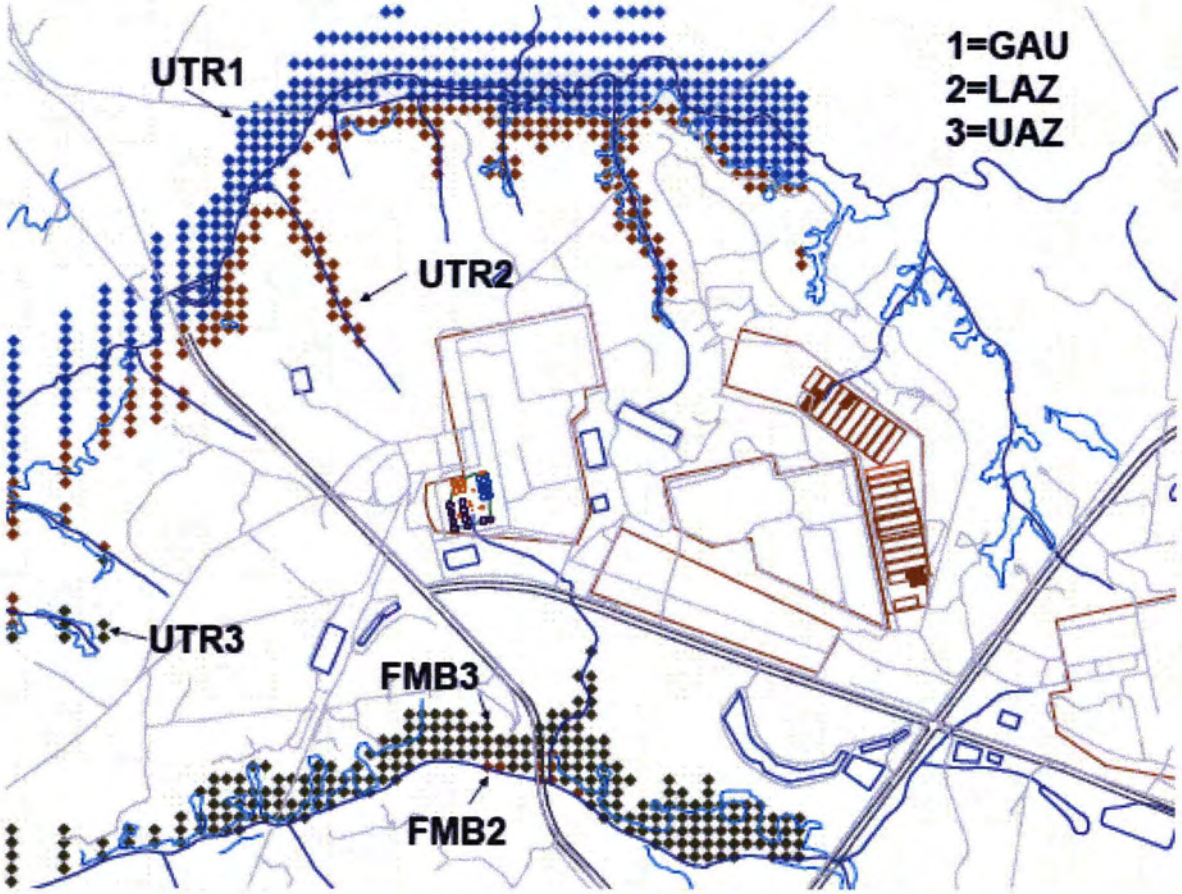

Note: GAU = Gordon Aquifer
LAZ = UTR-LZ
UAZ = UTR-UZ

Table 5.2-10: Upper Three Runs Seepline Key Radionuclide Concentrations

Radionuclide	Peak Seepline Concentration in 10,000 Yrs (pCi/L)	Location of Largest Contributor (Sector)	Year Largest Contribution in 10,000 Years Occurs	Peak Seepline Concentration in 20,000 Yrs (pCi/L)	Location of Largest Contributor (Sector)	Year Largest Contribution in 20,000 Years Occurs
C-14	2.11E-01	UTR-LZ	3,788	2.11E-01	UTR-LZ	3,788
Np-237	5.24E-02	UTR-LZ	6,176	1.41E-01	UTR-LZ	17,532
Pa-231	2.84E-04	UTR-LZ	6,172	4.53E-04	UTR-LZ	15,220
Pb-210	4.31E-05	UTR-LZ	10,000	3.73E-04	UTR-LZ	14,282
Pu-239	3.92E-15	UTR-LZ	10,000	2.97E-06	UTR-LZ	20,000
Pu-240	7.22E-15	UTR-LZ	10,000	2.79E-06	UTR-LZ	20,000
Pu-242	2.27E-16	UTR-LZ	10,000	2.20E-07	UTR-LZ	20,000
Ra-226	1.65E-02	UTR-LZ	10,000	1.43E-01	UTR-LZ	14,248
Tc-99	1.56E+01	UTR-LZ	630	1.56E+01	UTR-LZ	630
Th-229	1.64E-07	UTR-LZ	10,000	7.24E-05	UTR-LZ	20,000
Th-230	1.96E-13	UTR-LZ	10,000	3.61E-06	UTR-LZ	20,000
U-233	2.61E-06	UTR-LZ	10,000	2.08E-03	UTR-LZ	20,000
U-234	2.79E-10	UTR-LZ	10,000	9.28E-04	UTR-LZ	20,000
U-236	9.15E-12	UTR-LZ	10,000	3.84E-05	UTR-LZ	20,000
U-238	1.24E-12	UTR-LZ	10,000	2.92E-06	UTR-LZ	20,000

Table 5.2-11: Fourmile Branch Seepline Key Radionuclide Concentrations

Radionuclide	Peak Seepline Concentration in 10,000 Yrs (pCi/L)	Location of Largest Contributor (Sector)	Year Largest Contribution in 10,000 Years Occurs	Peak Seepline Concentration in 20,000 Yrs (pCi/L)	Location of Largest Contributor (Sector)	Year Largest Contribution in 20,000 Years Occurs
C-14	6.09E-02	UTR-UZ	586	6.09E-02	UTR-UZ	586
Np-237	9.52E-03	UTR-UZ	1,704	9.05E-01	UTR-UZ	17,448
Pa-231	1.43E-05	UTR-UZ	6,200	1.07E-03	UTR-UZ	16,210
Pb-210	2.06E-05	UTR-UZ	10,000	1.77E-03	UTR-UZ	14,500
Pu-239	1.02E-12	UTR-UZ	10,000	3.35E-06	UTR-UZ	20,000
Pu-240	2.31E-13	UTR-UZ	10,000	5.36E-07	UTR-UZ	20,000
Pu-242	5.91E-15	UTR-UZ	10,000	3.80E-08	UTR-UZ	20,000
Ra-226	7.92E-03	UTR-UZ	10,000	6.78E-01	UTR-UZ	14,466
Tc-99	1.52E+01	UTR-UZ	630	1.52E+01	UTR-UZ	630
Th-229	2.60E-08	UTR-UZ	10,000	7.54E-06	UTR-UZ	20,000
Th-230	2.35E-13	UTR-UZ	10,000	7.90E-08	UTR-UZ	20,000
U-233	2.41E-07	UTR-UZ	10,000	1.60E-04	UTR-UZ	20,000
U-234	2.52E-10	UTR-UZ	10,000	1.65E-05	UTR-UZ	20,000
U-236	1.30E-11	UTR-UZ	10,000	9.23E-07	UTR-UZ	20,000
U-238	6.27E-11	UTR-UZ	10,000	2.17E-06	UTR-UZ	20,000

5.3 Air Pathway and Radon Analysis

Section 4.5 describes the method used to conservatively bound the dose from airborne radionuclides. The results in that section provided a dose to MEI per Ci of inventory. The total waste tank and ancillary equipment inventory of selected potentially airborne isotopes, as described in Section 3.3 is summarized in Table 5.3-1. Specific SRS 100m DRFs and the calculated exposure levels for the 100 to 10,000 year MEI at 100m are presented in Table 5.3-2. Specific SRS 1,600m (seepline) DRFs and the calculated exposure levels for the 10,000 year MEI at 1,600m are presented in Table 5.3-3. Because the DRFs for 100m are calculated from an assumed area source, while the 1,600m DRFs are calculated from an assumed point source, the results reflect a conservative estimate at 1,600m, which results in a higher estimated dose at 1,600m than at 100m for C-14. See WSRC-STI-2007-00343 for details on the estimation of all DRFs.

The dose to the MEI at 100m and 1,600m are 0.14 mrem/yr and 0.035 mrem/yr respectively. For the air pathway, the flux of eight radionuclides was modeled. Each of these radionuclides reached peak flux within the first year of simulation, as shown in Figure 4.5-2. Since the flux is steadily decreasing at the end of the 100-year institutional control period, it can be assumed that would also be the time of the maximum dose. For the radon pathway, the Rn-222 flux resulted from five radionuclides: Pu-238, Ra-226, Th-230, U-234, and U-238. As shown in Figure 4.5-4, with the exception of Ra-226, the peak flux of Rn-222 occurs at the end of the simulation period (10,100 years). This is due to the long half-life for each of the parent radionuclides. For Ra-226, the peak flux of Rn-222 occurs within the first year of the simulation. The peak dose of radon for the performance period is assumed to be at 10,000 years. These results are highly conservative because the entire inventory is assumed to be concentrated in a 1 foot layer in a Type I tank. Section 4.5.3 describes other factors contributing to the conservative nature of the results.

Table 5.3-1: Summary of Total FTF Inventory of Gaseous Radionuclides

	H-3 (Ci)	C-14 (Ci)	I-129 (Ci)	Sb-125 (Ci)	Se-79 (Ci)	Sn-126 (Ci)	Tc-99 (Ci)
All Waste Tanks	6.70E+00	7.44E-02	2.71E-04	1.16E+01	3.15E+00	5.88E+00	5.75E+01
Transfer Lines	1.12E-01	1.51E-03	2.51E-06	1.45E-01	3.00E-02	5.62E-02	5.30E-01
FPT-1	1.53E-04	7.97E-06	1.33E-08	7.65E-04	1.59E-04	2.97E-04	2.81E-03
FPT-2	1.53E-04	7.97E-06	1.33E-08	7.65E-04	1.59E-04	2.97E-04	2.81E-03
FPT-3	1.53E-04	7.97E-06	1.33E-08	7.65E-04	1.59E-04	2.97E-04	2.81E-03
FTF Catch Tank	8.64E-04	3.84E-05	7.15E-08	1.45E-04	8.67E-04	1.61E-03	1.50E-02
242-3F CTS	6.66E-02	NE	NE	NE	1.77E-06	NE	1.10E-01
Evaporator Vessel 242-F	NE	NE	NE	NE	7.70E-09	NE	1.28E-03
Evaporator Vessel 242-16F	NE	NE	NE	NE	7.70E-09	NE	1.28E-03
Total FTF Inventory	**6.88E+00**	**7.60E-02**	**2.74E-04**	**1.17E+01**	**3.18E+00**	**5.94E+00**	**5.82E+01**

NE = Not Estimated

Table 5.3-2: 100m DRFs and 10,000 Year FTF Dose

Radionuclide	Peak Flux (Ci/yr/Ci)	SRS 100m DRF[1] (mrem/Ci)	Dose to MEI at 100m Boundary[2] (mrem/yr/Ci)	FTF Inventory (Ci)	Dose to MEI at 100m Boundary (mrem/yr)
C-14	2.59E-04	2.8E-04	7.2E-08	7.60E-02	5.5E-09
I-129	2.38E-03	2.0E+01	4.8E-02	2.74E-04	1.3E-05
Sb-125	3.71E-14	3.9E-01	1.4E-14	1.17E+01	1.6E-13
Se-79	7.02E-04	3.8E-02	2.7E-05	3.18E+00	8.6E-05
Sn-126	1.29E-03	1.8E+01	2.3E-02	5.94E+00	1.4E-01
H-3	3.12E-10	1.3E-02	4.2E-12	6.88E+00	2.9E-11
Tc-99	9.66E-04	1.1E-01	1.0E-04	5.82E+01	5.8E-03
Total Dose					**1.4E-1**

[1]From WSRC-STI-2007-00343
[2] Dose to MEI = Peak Flux × DRF

Table 5.3-3: 1,600m DRFs and 10,000 Year FTF Dose

Radionuclide	Peak Flux (Ci/yr/Ci)	SRS 1,600m DRF[1] (mrem/Ci)	Dose to MEI at 1,600m Boundary[2] (mrem/yr/Ci)	FTF Inventory (Ci)	Dose to MEI at 1,600m Boundary (mrem/yr)
C-14	2.59E-04	2.4E-03	6.2E-07	7.60E-02	4.7E-08
I-129	2.38E-03	2.3E+00	5.5E-03	2.74E-04	1.5E-06
Sb-125	3.71E-14	9.7E-02	3.6E-15	1.17E+01	4.2E-14
Se-79	7.02E-04	9.1E-03	6.4E-06	3.18E+00	2.0E-05
Sn-126	1.29E-03	4.4E+00	5.7E-03	5.94E+00	3.4E-02
H-3	3.12E-10	4.9E-05	1.5E-14	6.88E+00	1.1E-13
Tc-99	9.66E-04	2.6E-02	2.6E-05	5.82E+01	1.5E-03
Total Dose					**3.5E-02**

[1]From WSRC-STI-2007-00343
[2]Dose to MEI = Peak Flux × DRF

The instantaneous flux is found by multiplying the peak flux by the total inventory divided by the total area in the FTF. The total inventory of isotopes contributing to the radon flux is summarized in Table 5.3-4. The inventory of Th-230 and Ra-226 in the CTS and evaporator vessels, while not detected in analysis, is known to be present because they are daughter products of other isotopes present. However, the inventory of the CTS and evaporator vessels is much less than that of the waste tanks so it is assumed insignificant to this analysis.

Table 5.3-4: Summary of Total FTF Inventory of Isotopes Producing Rn-222

Inventory Location	Pu-238 (Ci)	U-238 (Ci)	U-234 (Ci)	Th-230 (Ci)	Ra-226 (Ci)
Total Waste Tank	2.47E+02	3.04E-01	4.23E-01	3.41E-01	3.44E-01
Transfer Lines	6.49E+00	4.95E-03	8.46E-03	5.06E-03	5.10E-03
FPT-1	3.43E-02	2.62E-05	4.48E-05	2.68E-05	2.70E-05
FPT-2	3.43E-02	2.62E-05	4.48E-05	2.68E-05	2.70E-05
FPT-3	3.43E-02	2.62E-05	4.48E-05	2.68E-05	2.70E-05
FTF Catch Tank	1.04E-01	8.99E-05	8.99E-05	1.30E-04	1.31E-04
242-3F CTS	9.17E-01	3.92E-04	2.09E-03	N/A	N/A
242-F Evaporator	4.72E-03	7.50E-06	7.08E-06	N/A	N/A
242-16F Evaporator	4.72E-03	7.50E-06	7.08E-06	N/A	N/A
Total FTF Inventory	**2.55E+02**	**3.10E-01**	**4.34E-01**	**3.46E-01**	**3.49E-01**

As shown in Table 5.3-5, the peak instantaneous radon flux using the entire FTF inventory as described in Section 3.3, is 9.3E-08 $pCi/m^2/sec$.

Table 5.3-5: Peak Instantaneous Rn-222 Flux at Land Surface

Parent Source	FTF Inventory (Ci)	FTF Inventory (Ci/m^2) [1]	Peak Instantaneous Rn-222 flux at Land Surface	
			($pCi/m^2/sec$) / (Ci/m^2)	($pCi/m^2/sec$)
Pu-238	2.55E+02	4.09E-03	2.7E-07	8.3E-10
U-238	3.10E-01	3.74E-06	9.3E-06	3.5E-11
U-234	4.34E-01	3.47E-05	7.7E-04	4.0E-09
Th-230	3.46E-01	4.19E-06	1.0E-02	4.3E-08
Ra-226	3.49E-01	4.21E-06	1.1E-02	4.6E-08
Total				**9.3E-08**

[1] Total area of FTF is 82,910 m^2

5.4 Biotic Pathways

The MOP exposure pathways are discussed in detail in Section 4.2.4.1. The FTF MOP scenario with 100m well water as a primary water source is graphically represented in Figure 4.2-27. The FTF MOP scenario with stream water as a primary water source is graphically represented in Figure 4.2-28. Provided below are the individual elements of the MOP biotic pathways that were identified for analysis and inclusion in the two MOP scenarios. The GoldSim computer code was used to calculate doses following the dose formulas provided below and utilizing the PORFLOW calculated 100m and seepline concentrations as inputs. Unless otherwise noted, formulas were based on those used in LADTAP model, report WSRC-STI-2006-00123, or in the PA for Idaho Tank Farm, document DOE-ID-10966. While these documents were used as guides for the formulas, ultimately the basis for all the formulas can be traced to 10 CFR 50, Reg. Guide 1.109.

5.4.1 Member of the Public at the 100m Well Dose Pathways

The MOP exposure pathways detailed below are used in calculating the dose to the MOP receptor with 100m well water as a primary water source. All transfers times are assumed negligible due to the half lives of the radionuclides and the long term analysis of the PA. Unit conversions are not explicitly stated in the equations, but are coded into GoldSim.

5.4.1.1 Member of the Public at the 100m Well Ingestion Dose Pathways

Ingestion of Water

The drinking water exposure route assumes the receptor uses a well located 100m from the tank farm tanks as a drinking water source. The incidental ingestion of water from showering and during recreational activities is assumed to be negligible when compared to ingestion of drinking water. The dose from consumption of drinking water is calculated using the following formula.

$$D = C_{GW} \times U_W \times DCF$$

where:

D	=	dose from 1 year's consumption of contaminated media; in this equation, groundwater (rem/year)
C_{GW}	=	radionuclide concentration in groundwater from a well (pCi/L)
U_W	=	human consumption rate of water (L/year), Table 4.6-7
DCF	=	ingestion dose conversion factor (rem/μCi), Table 4.7-1

Ingestion of Beef and Milk

The beef and dairy exposure route assumes cattle drink contaminated stock water and the receptor in turn consumes the contaminated beef and milk from the cattle. Beef and milk are treated separately. The dose is calculated using the following formula.

Beef:

$$D = T_B \times \left(FF_B \times C_f \times Q_{FB} + C_{GW} \times Q_{WB}\right) \times DCF \times U_B \times F_B$$

Milk:

$$D = T_M \times \left(FF_M \times C_f \times Q_{FM} + C_{GW} \times Q_{WM}\right) \times DCF \times U_M \times F_M$$

where:

T_B	=	beef transfer coefficient (d/kg), Table 4.6-3
T_m	=	milk transfer coefficient (d/L), Table 4.6-2
FF_i	=	beef or milk cattle intake fraction from irrigated field/pasture, Table 4.6-7
C_f	=	radionuclide concentration in fodder (pCi/kg)
Q_{Fi}	=	consumption rate of fodder by beef or milk cattle (Kg/d), Table 4.6-7
C_{GW}	=	radionuclide concentration in groundwater from a well (pCi/L)
Q_{Wi}	=	consumption rate of water by beef or milk cattle (L/d), Table 4.6-7
DCF	=	ingestion dose conversion factor (rem/μCi), Table 4.7-1
U_B	=	human consumption rate of beef (kg/year), Table 4.6-7
U_M	=	human consumption rate of milk (L/year), Table 4.6-7
F_B	=	fraction of beef produced locally (unitless), Table 4.6-5
F_M	=	fraction of milk produced locally (unitless), Table 4.6-5

Ingestion of Vegetables

The dose to humans from ingestion of contaminated leafy vegetables and produce is calculated assuming two contamination routes: (1) direct deposition of contaminated irrigation water on plants and (2) deposition of contaminated irrigation water on soil followed by root uptake by plants. Leafy vegetables and produce are treated separately. The dose is calculated using:

$$D = C_{GW} \times I \times (LEAF + ROOT) \times DCF \times (U_{LV} + U_{OV} \times k) \times FV \times e^{-\lambda_i t_t}$$

$$LEAF = \frac{r \times (1 - e^{-\lambda_e t_V})}{Y_V \times \lambda}$$

$$ROOT = \frac{T_{StV} \times (1 - e^{-\lambda_i t_b})}{\rho_S \times \lambda_i}$$

$$\lambda_e = \lambda_i + \lambda_w$$

where:

C_{GW}	=	radionuclide concentration in groundwater from a well (pCi/L)
I	=	irrigation rate (L/m^2-d), Table 4.6-6
$LEAF$	=	radionuclide concentration in the vegetable's leaves (m^{2}d/kg)
$ROOT$	=	radionuclide concentration in the vegetable's roots (m^{2}d/kg)
DCF	=	ingestion dose conversion factor (rem/μCi), Table 4.7-1
U_{LV}	=	human consumption rate of leafy vegetables (kg/year), Table 4.6-7
U_{OV}	=	human consumption rate of other vegetables (produce) (kg/year), Table 4.6-7
k	=	fraction retention of deposition on leaves (unitless) [1]
FV	=	fraction of leafy vegetables and produce produced locally (unitless), Table 4.6-5
r	=	fraction of material deposited on leaves that is retained (unitless), Table 4.6-6
λ_e	=	weathering and radiological decay constant (1/d)
λ_w	=	weathering decay constant (0.0495/d)
t_V	=	time vegetables are exposed to irrigation (d), Table 4.6-5
Y_V	=	vegetation production yield (kg/m^2), Table 4.6-5
T_{StV}	=	soil to vegetable ratio (unitless), Table 4.6-1
ρ_S	=	surface soil density (kg/m^2), Table 4.6-6
t_b	=	buildup time of radionuclides in soil, Table 4.6-1
λ_i	=	radiological decay constant (ln2/half life of radionuclide i – 1/d)
t_t	=	transport time (d), assumed to be zero

Ingestion of Fish

The fish exposure route assumes fish are caught from a stream contaminated from the aquifer, diluted, and the receptor in turn consumes the contaminated fish. The dose is calculated using the following formula.

$$D = C_S \times U_F \times T_F \times DCF$$

where:

C_S	=	radionuclide concentration in groundwater at the seepline (pCi/L)
U_F	=	human consumption rate of finfish (kg/year), Table 4.6-7
T_F	=	fish bioaccumulation factor (L/kg), ,Table 4.6-4
DCF	=	ingestion dose conversion factor (rem/μCi), ,Table 4.7-1

Ingestion of Soil

The soil ingestion exposure route assumes soil is irrigated with groundwater from a 100m well and the receptor in turn consumes the contaminated soil. For simplicity and conservatism, the soil ingested is assumed to be groundwater. This formula was derived following the approach of the previous pathway calculations. The dose is calculated using the following formula.

$$\frac{D = C_{GW} \times DCF \times U_D}{\rho_W}$$

where:

C_{GW}	=	radionuclide concentration in groundwater from a well (pCi/L)
DCF	=	ingestion dose conversion factor (rem/μCi), Table 4.7-1
U_D	=	human consumption rate of dirt (kg/year), Table 4.6-7
ρ_W	=	density of water (g/ml)

5.4.1.2 Member of the Public at the 100m Well Direct Exposure Dose Pathways

Direct Exposure from Irrigated Soil

The irrigated soil direct exposure route assumes soil is irrigated with groundwater from a 100m well and the receptor in turn is exposed during time spent caring for a garden. The dose is calculated using the following formula.

$$D = C_D \times F_G \times DCF$$

where:

C_D = radionuclide concentration in irrigated soil (pCi/m^3)

DCF = external dose conversion factor, 15cm (rem/yr per μCi/m^3), Table 4.7-1

F_G = fraction of time spent in garden (unitless), Table 4.6-7

Direct Exposure from Swimming

The swimming direct exposure route assumes the receptor receives dose from swimming in a stream contaminated from the aquifer. The dose is calculated using the following formula.

$$D = GF_S \times t_S \times C_{SW} \times DCF$$

where:

DCF = external dose conversion factor, water immersion (rem/yr per μCi/m^3), Table 4.7-1

GF_S = swimming geometry factor (unitless) ,[1]

t_S = time per year spent swimming (hr/yr),, Table 4.6-7

C_{SW} = radionuclide concentration in water from the stream (undiluted aquifer) (pCi/L) ,

Direct Exposure from Fishing/Boating

The fishing/boating direct exposure route assumes the receptor receives dose from fishing or boating in a stream contaminated from the aquifer. The dose is calculated using the following formula.

$$D = GF_B \times t_B \times C_{SW} \times DCF$$

where:

DCF = external dose conversion factor, 15 cm (rem/yr per μCi/m^3), Table 4.7-1

GF_B = boating geometry factor (unitless), ,[0.5]

t_B = time per year spent boating (hr/yr), Table 4.6-7

C_{SW} = radionuclide concentration in water from the stream (undiluted aquifer) (pCi/L)

5.4.1.3 Member of the Public at the 100m Well Inhalation Dose Pathways

Inhalation during Irrigation

The irrigation inhalation exposure route assumes soil is irrigated with groundwater from a 100m well and the receptor in turn is exposed by breathing while the garden is irrigated but only during time spent caring for a garden. For simplicity and conservatism, the source material is the moisture contained within the air with equal concentrations as the groundwater. No resistance to vaporization (i.e., vapor pressure) was used. This formula was derived following the approach of the previous pathway calculations. The dose is calculated using the following formula.

$$D = \frac{C_{GW} \times DCF \times U_A \times F_G \times C_{WA}}{\rho_W}$$

where:

C_{GW}	=	radionuclide concentration in groundwater from a well (pCi/L)
DCF	=	inhalation dose conversion factor (rem/μCi), Table 4.7-1
U_A	=	air intake (m^3/yr), Table 4.6-7
F_G	=	fraction of time spent in garden exposed to soil irrigated with contaminated ground water (unitless), Table 4.6-7
C_{WA}	=	water contained in air at ambient conditions, (g/m^3) [10 g/m^3]
ρ_W	=	water density (g/ml)

Inhalation during Showering

The showering inhalation exposure route assumes the receptor is exposed by breathing humid air within the shower. The source of water for the shower is a well 100m from the tank farm. For simplicity and conservatism, the source material is the moisture contained within the air with equal concentrations as the groundwater. No resistance to vaporization (i.e., vapor pressure) was used, adding to the conservatism. For example, heavy elements would be greatly influenced by this assumption because they would be less likely to volatize. This formula was derived following the approach of the previous pathway calculations. The dose is calculated using the following formula.

$$D = \frac{C_{GW} \times DCF \times U_A \times t_S \times C_{WS}}{\rho_W}$$

where:

C_{GW}	=	radionuclide concentration in groundwater from a well (pCi/L)
DCF	=	inhalation dose conversion factor (rem/μCi), Table 4.7-1
U_A	=	air intake (m^3/yr), Table 4.6-7
t_S	=	time spent in shower (min), Table 4.6-7 GoldSim uses fraction of time [0.0069 = 10 min/day
C_{WS}	=	water contained in air at shower conditions, (g/m^3) [41 g/m^3]
ρ_W	=	water density (g/ml)

Inhalation of Dust from Irrigated Soil

The irrigation soil inhalation exposure route assumes soil is irrigated with groundwater from a 100m well and the receptor is exposed by breathing dust during time spent caring for a garden. This formula was derived following the approach of the previous pathway calculations. The dose is calculated using the following formula.

$$D = \frac{U_A \times L_{SiA} \times C_D \times DCF \times F_G}{\rho_{SS}}$$

where:

U_A	=	air intake (m3/yr), Table 4.6-7
L_{SiA}	=	soil loading in air while working in a garden (kg/m^3), Table 4.6-6
C_D	=	radionuclide concentration in soil irrigated with water from a well (pCi/m3)
DCF	=	inhalation dose conversion factor (rem/μCi), Table 4.7-1
F_G	=	fraction of time spent in garden exposed to soil irrigated with contaminated ground water (unitless), Table 4.6-7
ρ_{SS}	=	density of sandy soil (g/cm3)

Inhalation During Swimming

The swimming inhalation exposure route assumes a stream contaminated from the aquifer and the receptor inhales saturated air. For simplicity and conservatism, the amount of moisture contained in the inhaled air assumed to be groundwater. The dose is calculated using the following formula.

$$D = \frac{U_A \times GF_S \times t_S \times C_{SW} \times DCF \times C_{WiA}}{\rho_W}$$

where:

U_A	=	air intake (m^3/yr), Table 4.6-7
GF_S	=	swimming geometry factor (unitless) ,[1]
t_S	=	time per year spent swimming (hr/yr), ,Table 4.6-7
C_{SW}	=	radionuclide concentration in water from the stream (undiluted aquifer) (pCi/L)
DCF	=	inhalation dose conversion factor (rem/μCi), Table 4.7-1
C_{WA}	=	water contained in air at ambient conditions, (g/m3) [10 g/m^3]
ρ_W	=	water density (g/ml)

5.4.2 Member of the Public at the Stream Dose Pathways

The MOP exposure pathways detailed below are used in calculating the dose to the MOP receptor with stream water as a primary water source. The stream concentrations used in the dose calculations are the peak aquifer concentrations (as discussed in Section 5.2.3), and conservatively assume no stream dilution. All transfer times are assumed negligible due to the half lives of the radionuclides and the long term analysis of the PA. Unit conversions are not explicitly stated in the equations, but are coded into GoldSim.

5.4.2.1 Member of the Public at the Stream Ingestion Dose Pathways

Ingestion of Water

The drinking water exposure route assumes the receptor uses a well located at the seepline, undiluted, as a drinking water source. The incidental ingestion of water from showering and during recreational activities is assumed to be negligible when compared to ingestion of drinking water. The dose from consumption of drinking water is calculated using the following formula.

$$D = C_{SLW} \times U_W \times DCF$$

where:

D	=	dose from 1 year's consumption of contaminated media; in this equation, groundwater (rem/year)
C_{SLW}	=	radionuclide concentration in water from the seepline aquifer (undiluted) (pCi/L)
U_W	=	human consumption rate of water (L/year) – Table 4.6-7
DCF	=	ingestion dose conversion factor (rem/μCi) Table 4.7-1

Ingestion of Beef and Milk

The beef and dairy exposure route assumes cattle drink contaminated stream water and the receptor in turn consumes the contaminated beef and milk from the cattle. Beef and milk are treated separately. The dose is calculated using the following formula.

Beef:

$$D = T_B \times \left(FF_B \times C_f \times Q_{FB} + C_{SW} \times Q_{WB}\right) \times DCF \times U_B \times F_B$$

Milk:

$$D = T_M \times \left(FF_M \times C_f \times Q_{FM} + C_{SW} \times Q_{WM}\right) \times DCF \times U_M \times F_M$$

where:

T_B	=	beef transfer coefficient (d/kg), Table 4.6-3
T_m	=	milk transfer coefficient (d/L), Table 4.6-2
FF_i	=	beef or milk cattle intake fraction from irrigated field/pasture,Table 4.6-7
C_f	=	radionuclide concentration in fodder (pCi/kg)
Q_{Fi}	=	consumption rate of fodder by beef or milk cattle (kg/d), Table 4.6-7
C_{SW}	=	radionuclide concentration in water from the stream (undiluted aquifer) (pCi/L)
Q_W	=	consumption rate of water by beef or milk cattle (L/d), Table 4.6-7
DCF	=	ingestion dose conversion factor (rem/μCi), Table 4.7-1
U_B	=	human consumption rate of beef (kg/year), Table 4.6-7
U_M	=	human consumption rate of milk (L/year), Table 4.6-7
F_B	=	fraction of beef produced locally (unitless), Table 4.6-5
F_M	=	fraction of milk produced locally (unitless), Table 4.6-5.

Ingestion of Vegetables

The dose to humans from ingestion of contaminated leafy vegetables and produce is calculated assuming two contamination routes: (1) direct deposition of contaminated irrigation water on plants and (2) deposition of contaminated irrigation water on soil followed by root uptake by plants. Leafy vegetables and produce are treated separately. The dose is calculated using:

$$D = C_{GW} \times I \times (LEAF + ROOT) \times DCF \times (U_{LV} + U_{OV} \times k) \times FV \times e^{-\lambda_i t_t}$$

$$LEAF = \frac{r \times \left(1 - e^{-\lambda_e t_V}\right)}{Y_V \times \lambda}$$

$$ROOT = \frac{T_{StV} \times \left(1 - e^{-\lambda_i t_b}\right)}{\rho_S \times \lambda_i}$$

$$\lambda_e = \lambda_i + \lambda_w$$

where:

C_{SW}	=	radionuclide concentration in groundwater from a well (pCi/L)
I	=	irrigation rate (L/m^2-d), Table 4.6-6
$LEAF$	=	radionuclide concentration in the vegetable's leaves (m^{2}d/kg)
$ROOT$	=	radionuclide concentration in the vegetable's roots (m^{2}d/kg)
DCF	=	ingestion dose conversion factor (rem/μCi), Table 4.7-1
U_{LV}	=	human consumption rate of leafy vegetables (kg/year), Table 4.6-7
U_{OV}	=	human consumption rate of other vegetables (produce) (kg/year), Table 4.6-7
k	=	fraction retention of deposition on leaves (unitless) [1]
FV	=	fraction of leafy vegetables and produce produced locally (unitless), Table 4.6-5
r	=	fraction of material deposited on leaves that is retained (unitless), Table 4.6-6
λ_e	=	weathering and radiological decay constant (1/d)
λ_w	=	weathering decay constant (0.0495/d)
t_V	=	time vegetables are exposed to irrigation (d), Table 4.6-5
Y_V	=	vegetation production yield (kg/m^2)], Table 4.6-5
T_{StV}	=	soil to vegetable ratio (unitless), Table 4.6-1
ρ_S	=	surface soil density (kg/m^2), Table 4.6-6
t_b	=	buildup time of radionuclides in soil, Table 4.6-1
λ_i	=	radiological decay constant (ln2/half life of radionuclide i – 1/d)
t_t	=	transport time (d), assumed to be zero

Ingestion of Fish

The fish exposure route assumes fish are caught from a stream contaminated from the aquifer, and the receptor in turn consumes the contaminated fish. The dose is calculated using the following formula.

$$D = C_{SW} \times U_F \times T_F \times DCF$$

where:

C_{SW}	=	radionuclide concentration in water from the stream (undiluted aquifer) (pCi/L)
U_F	=	human consumption rate of finfish (kg/year), Table 4.6-7
T_F	=	fish bioaccumulation factor (L/kg), Table 4.6-4
DCF	=	ingestion dose conversion factor (rem/μCi), Table 4.7-1

Ingestion of Soil

The soil ingestion exposure route assumes soil is irrigated with groundwater from a stream contaminated from the aquifer, and the receptor in turn consumes the contaminated soil. For simplicity and conservatism, the soil ingested is assumed to be groundwater. This formula was derived following the approach of the previous pathway calculations. The dose is calculated using the following formula.

$$\frac{D = C_{SW} \times DCF \times U_D}{\rho_W}$$

where:

C_{SW}	=	radionuclide concentration in water from the stream (undiluted aquifer) (pCi/L)
DCF	=	ingestion dose conversion factor (rem/μCi), Table 4.7-1
U_D	=	human consumption rate of dirt (kg/year), Table 4.6-7
ρ_W	=	density of water (g/ml)

5.4.2.2 Member of the Public at the Stream Direct Exposure Dose Pathways

Direct Exposure from Irrigated Soil

The irrigated soil direct exposure route assumes soil is irrigated with groundwater from a stream contaminated from the aquifer, diluted, and the receptor in turn is exposed during time spent caring for a garden. The dose is calculated using the following formula.

$$D = C_D \times F_G \times DCF$$

where:

C_D = radionuclide concentration in irrigated soil (pCi/m^3)

DCF = external dose conversion factor, 15cm (rem/yr per μCi/m^3), Table 4.7-1

F_G = fraction of time spent in garden (unitless), Table 4.6-7

Direct Exposure from Swimming

The swimming direct exposure route assumes the receptor receives dose from swimming in a stream contaminated from the aquifer. The dose is calculated using the following formula.

$$D = GF_S \times t_S \times C_{SW} \times DCF$$

where:

DCF = external dose conversion factor, water immersion (rem/yr per μCi/m^3), Table 4.7-1

GF_S = swimming geometry factor (unitless) [1]

t_S = time per year spent swimming (hr/yr), Table 4.6-7

C_{SW} = radionuclide concentration in water from the stream (undiluted aquifer) (pCi/L)

Direct Exposure from Fishing/Boating

The fishing/boating direct exposure route assumes the receptor receives dose from fishing or boating in a stream contaminated from the aquifer. The dose is calculated using the following formula.

$$D = GF_B \times t_B \times C_{SW} \times DCF$$

where:

DCF = external dose conversion factor, 15 cm (rem/yr per μCi/m^3), Table 4.7-1

GF_B = boating geometry factor (unitless) [0.5]

t_B = time per year spent boating (hr/yr), Table 4.6-7

C_{SW} = radionuclide concentration in water from the stream (undiluted aquifer) (pCi/L)

5.4.2.3 Member of the Public at the Stream Inhalation Dose Pathways

Inhalation during Irrigation

The irrigation inhalation exposure route assumes soil is irrigated with groundwater from a stream contaminated from the aquifer, and the receptor in turn is exposed by breathing while the garden is irrigated but only during time spent caring for a garden. For simplicity and conservatism, the source material is the moisture contained within the air with equal concentrations as the groundwater. This formula was derived following the approach of the previous pathway calculations.

$$D = \frac{C_{SLW} \times DCF \times U_A \times F_G \times C_{WA}}{\rho_W}$$

where:

C_{SLW}	=	radionuclide concentration in water from the seepline aquifer (undiluted) (pCi/L)
DCF	=	inhalation dose conversion factor (rem/μCi), Table 4.7-1
U_A	=	air intake (m^3/yr), Table 4.6-7
F_G	=	fraction of time spent in garden exposed to soil irrigated with water from the seepline aquifer (unitless), Table 4.6-7
C_{WA}	=	water contained in air at ambient conditions, (g/m^3) [10 g/m^3]
ρ_W	=	water density (g/ml)

Inhalation during Showering

The showering inhalation exposure route assumes receptor exposed by breathing humid air within the shower. The source of water for the shower is a stream contaminated from the aquifer. For simplicity and conservatism, the source material is the moisture contained within the air with equal concentrations as the aquifer. No resistance to vaporization (i.e., vapor pressure) was used, adding to the conservatism. For example, heavy elements would be greatly influenced by this assumption because they would be less likely to volatize. This formula was derived following the approach of the previous pathway calculations. The dose is calculated using the following formula.

$$D = \frac{C_{SLW} \times DCF \times U_A \times t_S \times C_{WS}}{\rho_W}$$

where:

C_{SLW} = radionuclide concentration in water from the seepline aquifer (undiluted) (pCi/L)

DCF = inhalation dose conversion factor (rem/μCi), Table 4.7-1

U_A = air intake (m^3/yr), Table 4.6-7

t_S = time spent in shower (min), Table 4.6-7
GoldSim uses fraction of time [0.0069 = 10 min/day

C_{WS} = water contained in air at shower conditions, (g/m^3) [41 g/m^3]

ρ_W = water density (g/ml)

Inhalation of Dust from Irrigated Soil

The irrigation soil inhalation exposure route assumes soil is irrigated with groundwater from a stream contaminated from the aquifer, and the receptor in turn is exposed by breathing dust during time spent caring for a garden. This formula was derived following the approach of the previous pathway calculations. The dose is calculated using the following formula.

$$D = \frac{U_A \times L_{SiA} \times CSW \times DCF \times F_G}{\rho_{SS}}$$

where:

U_A = air intake (m^3/yr), Table 4.6-7

L_{SiA} = soil loading in air while working in a garden (kg/m^3), Table 4.6-6

C_{SW} = radionuclide concentration in water from the stream (undiluted aquifer) (pCi/L)

DCF = inhalation dose conversion factor (rem/μCi), Table 4.7-1

F_G = fraction of time spent in garden exposed to soil irrigated with contaminated ground water (unitless), Table 4.6-7

ρ_{SS} = density of sandy soil (g/cm^3)

Inhalation during Swimming

The swimming inhalation exposure route assumes a stream contaminated from the aquifer and the receptor inhales saturated air. For simplicity and conservatism, the amount of moisture contained in the inhaled air assumed to be stream water. This formula was derived following the approach of the previous pathway calculations. The dose is calculated using the following formula.

$$D = \frac{U_A \times GF_S \times t_S \times C_{SW} \times DCF \times C_{WiA}}{\rho_W}$$

where:

U_A	=	air intake (m^3/yr) Table 4.6-7
GF_S	=	swimming geometry factor (unitless) [1]
t_S	=	time per year spent swimming (hr/yr), Table 4.6-7
C_{SW}	=	radionuclide concentration in water from the stream (undiluted aquifer) (pCi/L)
DCF	=	inhalation dose conversion factor (rem/μCi), Table 4.7-1
C_{WA}	=	water contained in air at ambient conditions, (g/m^3) [10 g/m^3]
ρ_W	=	water density (g/ml)

5.5 Dose Analysis

The peak total doses are calculated utilizing the pathways identified in Section 5.4 for (a) the MOP at the 100m well and (b) the MOP at applicable streams (either UTR or Fourmile Branch). The peak total doses are calculated using the MCLs identified in Section 5.2. A peak dose is identified for the 10,000 year performance period. In addition, a peak dose associated with the key radionuclides is calculated through 40,000 years (40,000 years was set as the end point because the total doses were shown to be in decline after that point).

5.5.1 Member of the Public at 100m Groundwater Pathway Dose Results

The groundwater pathway peak doses for the five 100m sectors are calculated using the peak concentration for each radionuclide in the Sector (a discussion of how peak concentrations are determined by sector is provided in Section 5.2). These groundwater pathway peak doses are the total dose associated with all the individual 100m well pathways identified in Section 5.4.

5.5.1.1 Member of the Public 100m Peak Annual Groundwater Pathway Dose

Table 5.5-1 shows a comparison of the 100m peak groundwater pathway doses for the different 100m sectors within both 10,000 and 20,000 years. In calculating the peak groundwater pathway dose, the highest radionuclide concentration within the vertical computational meshes is used from each of the three distinct aquifers modeled (UTR-UZ, UTR-LZ, and the Gordon aquifer).

The highest peak groundwater pathway dose in the 10,000 year performance period is associated with Sector E. Sector E is the Sector associated most closely with the Type IV tanks, which are the tanks whose liners are modeled as failing earlier than any other tank type (and within the 10,000 year performance period).

Figure 5.5-1 shows the peak doses to the 100m MOP receptor over time during the performance period (10,000 years) for the five 100m sectors. The highest 100m MOP groundwater pathway peak dose in the 10,000 year evaluation period is a 1.26 mrem/yr dose at year 10,000. Figure 5.5-2 shows the 100m MOP receptor doses within 20,000 years for the five 100m sectors.

Table 5.5-1: Member of the Public at 100m Peak Groundwater Pathways Dose by Sector

Sector	Highest Peak Dose in 10,000 Years	Highest Peak Dose in 20,000 Years
A	**0.20 mrem/yr (year 594)** Principal Pathways: Water Ingestion (46%) Fish Ingestion (26%) Vegetable Ingestion (21%) Principal Radionuclide: Tc-99 (72%)	**4.1 mrem/yr (year 17,390)** Principal Pathways: Water Ingestion (44%) Vegetable Ingestion (20%) Principal Radionuclide: Ra-226 (39%) Np-237 (60%)
B	**0.32 mrem/yr (year 598)** Principal Pathways: Water Ingestion (53%) Vegetable Ingestion (24%) Principal Radionuclide: Tc-99 (83%)	**3.9 mrem/yr (year 14,134)** Principal Pathways: Water Ingestion (61%) Vegetable Ingestion (27%) Principal Radionuclide: Ra-226 (98%)
C	**0.33 mrem/yr (year 596)** Principal Pathways: Water Ingestion (55%) Vegetable Ingestion (25%) Principal Radionuclide: Tc-99 (87%)	**2.2 mrem/yr (year 13,776)** Principal Pathways: Water Ingestion (61%) Vegetable Ingestion (28%) Principal Radionuclide: Ra-226 (89%)
D	**1.2 mrem/yr (year 10,000)** Principal Pathways: Water Ingestion (52%) Vegetable Ingestion (23%) Principal Radionuclides: U-233 (43%) Ra-226 (23%)	**5.9 mrem/yr (year 13,712)** Principal Pathways: Water Ingestion (53%) Vegetable Ingestion (25%) Principal Radionuclides: Ra-226 (51%) Th-229 (14%)
E	**1.3 mrem/yr (year 10,000)** Principal Pathways: Water Ingestion (53%) Vegetable Ingestion (24%) Principal Radionuclide: Ra-226 (36%) U-233 (27%)	**5.6 mrem/yr (year 13,722)** Principal Pathways: Water Ingestion (53%) Vegetable Ingestion (25%) Principal Radionuclides: Ra-226 (45%) U-233 (14%)

Note: Sectors illustrated in Figure 5.2-5

Provided below is a discussion of the peaks that appear in Figures 5.5-1 and 5.5-2. The discussion also relies upon information from Figures 5.5-3 and 5.5-4 relating to the individual radionuclide contributors to the groundwater pathway doses.

- The peaks prior to year 3,600 are associated with ancillary equipment releases, in particular the transfer lines, which are distributed throughout the FTF and therefore affect all sectors. The timing of the ancillary equipment peaks is fairly consistent for all sectors, with the magnitude of the peak varying depending on what ancillary equipment other than the transfer lines are contributing to the peak (i.e., Sectors D and E have more inventory sources, such as the CTS tank and catch tank nearby). The ancillary equipment releases start around the time its containment fails (at year 510). In contrast to the waste tanks (where solubility control was modeled as controlling waste release), the ancillary equipment releases were modeled as instantaneous, so the entire inventory in each ancillary equipment location is available for release at year 510.
- The peaks near year 580 are associated with Tc-99 from the ancillary equipment. The Tc-99 travels quickly (K_d in soil 0.1 mL/g) to the 100m boundary after the ancillary equipment containment fails (at year 510). The entire Tc-99 inventory in all ancillary equipment location is available for transport beginning at year 510 and can contribute to a single peak soon thereafter. The largest ancillary equipment Tc-99 inventories are in the transfer lines (0.53 Ci) and CTS tank (0.11 Ci).
- The peaks near year 725 are associated with Np-237 from the ancillary equipment. The Np-237 travels relatively quickly (K_d in soil 0.6 mL/g), but does not travel as quickly as the Tc-99 due to soil retardation being greater for Np, so the peak associated with Np-237 is later and less acute. The largest ancillary equipment Np-237 inventories are in the transfer lines (2.79E-03 Ci) and CTS tank (4.74E-04 Ci). The transfer lines (2.07 Ci) and CTS tank (1.01 Ci) also have the largest inventories of Am-241, which is a parent of Np-237.
- The peaks near year 1,800 are associated with Ra-226 from the ancillary equipment and also the tail end of the Np-237 release from the ancillary equipment. The Ra-226 itself travels fairly quickly through the soil (K_d in soil 5 mL/g), but it lags behind the Np-237 because it is being released primarly as a daughter product of U-238 not as a part of an initial inventory. There is an initial peak associated with the Ra-226 produced in the tank via ingrowth from U-238. After that initial peak, the RA-226 release is tied to the steady state U-238 release and therefore levels off. Since it is a daughter product, its initial travel time is tied to its parent and U-238 has a higher than average K_d (K_d in soil 200 mL/g). The Ra-226 peak is therefore tied to the release and travel of the U-238. The transfer lines and CTS tank have the largest inventories of U-238.
- The peaks between years 3,600 and 12,700 are tied primarily to releases from the Type IV tanks. The peaks after year 12,700 are tied to the tail end of releases from the Type IV tanks and the start of releases from the Type I and III/IIIA tanks. The Type IV tank liners are considered to fail at approximately year 3,600 while the Type I and III/IIIA tanks don't fail until approximately year 12,700. The releases from the waste tank CZs are potentially solubility limited, such that release fluxes from tank

liners may vary by radionuclide dependant on its individual solubility controlled release rate from the CZ.

- The peaks near year 3,600 are associated with C-14 from the Type IV tanks. The C-14 contributes to dose almost immediately through fish ingestion at the stream because it travels extremely quickly (K_d in basemat $\leq$ 20 mL/g, K_d in soil = 0.0 mL/g) and has a very high water to fish accumulation factor (50,000 L/kg). The largest Type IV tank C-14 inventories are in Tank 18 (0.028 Ci) and Tank 19 (0.014 Ci).
- The Sector D and E doses between approximately year 4,000 and 10,000 have a significant Ra-226 contribution. As discussed previously, the Ra-226 contribution is tied to the release and travel of U-238, but once the U-238 is released from the Type IV tanks the Ra-226 travels faster and can reach the 100m boundary before its parent. The Ra-226 contribution starts ramping up almost as soon as the Type IV tank liners fail and steadily increases as more U-238 is released. As expected, there is an initial peak associated with the Ra-226 inventory produced through ingrowth. Since Uranium has a higher than average K_d (K_d in soil 200 mL/g), the associated quantity of Ra-226 released tend to increase slowly. The largest Type IV tank U-238 inventories (the parent and principal source of the Ra-226) are in Tank 18 (0.049 Ci) and Tank 19 (0.011 Ci). The Ra-226 inventories in the Type IV tanks are insignificant.
- There is dose spike for Sectors D and E at approximately year 13,750 associated with Ra-226. There is also dose spike for Sectors A and B at approximately year 14,000 associated with Ra-226. These dose peaks are tied to the liner failure dates (~ year 12,700) for the Type I and Type III/IIIA tanks (it should be noted that all the tanks for a given tank type are assumed to fail in the same year). These peaks are associated with the U-238 and its daughter Ra-226 being release from the tank liner. The spike is twice the magnitude of the steady state release due to the Ra-226 ingrowth inside the tank liners for 12,700 years prior to liner failure. There is a lag time between the release from the liner and the peak date as the Ra-226 travels though the Type I and Type III/IIIA tank basemats. The concrete basemats have a relatively low K_d for Ra (basemat K_d 70 -100 mL/g) but are thick (30 inches for the Type I tanks and 41 - 42 inches for the Type III/IIIA tanks). The lag time is slightly longer for Sectors A and B because the primary sources of U-238 (Tanks 33 and 34) are farther from the 100m boundary (~250m) than the Type I tanks. The largest Type I tank U-238 inventories are in Tank 6 (0.017 Ci), Tank 5 (0.014 Ci), and Tank 1 (0.011 Ci). Tanks 1, 5, and 6 also have the largest Ra-226 inventories for the Type I tanks. The largest Type III/IIIA tank U-238 inventories are in Tank 33 (0.079 Ci) and Tank 34 (0.088 Ci). Tanks 1, 5, and 6 also have the largest Ra-226 inventories for the Type I tanks.
- The Sector D and E peaks near year 6,000 are associated with Np-237 and Ra-226 from the Type IV tanks. These peaks don't show up in Sectors A – C because theses sectors see very little of the plume spread from the Type IV tanks. The timing of the peak near year 6,000 is due to Np-237, which peaks at this time and then rapidly falls off (Figure 5.5-3). The Np-237 doesn't begin to contribute to the dose until around year 5,600, but after it appears it spikes rapidly until it peaks near year 6,000. The solubility of Np-237 is relative high, and the Np-237 is released from the CZ

comparatively quickly. The delay between the Type IV tank liner failure date (near year 3,600) and the appearance of Np-237 can be attributed to the basemat K_d for Np, which starts at 5,000 mL/g for the basemat. Once the Np-237 travels through the basemat, it doesn't take as long for the peak to be reached since the Np soil K_d is much lower (soil K_d 0.6 mL/g). The largest Type IV tank Np-237 inventories are in Tank 18 (0.038 Ci) and Tank 17 (0.014 Ci). Tank 18 also has 18.6 Ci of Am-241, which is a parent of Np-237.

- The Sector D and E peaks at year 10,000 are associated with Ra-226 as explained previously, but also with relatively slow moving radionuclides that are just reaching the 100m boundary at year 10,000. The radionuclides that were released from the Type IV tanks but that are starting to be seen at year 10,000 include Pu-239, Pu-240, U-233, U-234, and Th-229. Release from the CZ for all of these radionuclides is subject to solubility control, which tends to flatten their associated peaks. In addition Pu, U, and Th all have relatively high K_d values for both the basemat and soil, which explains why they don't show up for some time after the Type IV tank liner failure date and why their associated peaks are relatively flat.
- The Sector A and B peaks at year 16,000 and 17,500 are associated with Np-237 from the Type III tanks (Tanks 33 and 34). Np-237 (and its parent Am-241) are released from the Type III tanks after tank liner failure and the first peak is driven by the release of inventory built up over time through Np-237 ingrowth (from Am-241). This Np-237 peak levels of near year 16,000 as a steady state release is reached and then ramps up again beginning near year 16,700 as the impact of the solubility change (to oxidized Region II) makes its way to the 100m boundary. As mentioned previously, the solubility of Np-237 is relative high, especially once the pore water is oxidized at approximately year 15,500 (2.2E-05 for oxidized Region II) such that the Np-237 is released from the CZ rapidly. The Np-237 inventories in Tank 33 and Tank 34 are 0.025 Ci and 0.068 Ci respectively. The Am-241 inventories in Tank 33 and Tank 34 are 63 Ci and 1590 Ci respectively. The Tank 34 Am-241 is a significant source of Np-237.
- Sector C mirrors the dose profiles from the other sectors in many ways but always with a smaller magnitude dose. Sector C is nearest to the Type IIIA tanks, which fail at the same time as the Type III tanks but do not have the inventory of key radionuclides that the Type III tanks have.

Figure 5.5-1: Member of the Public at 100m Peak Groundwater Pathway Dose Results within 10,000 Years for the Five 100m Sectors

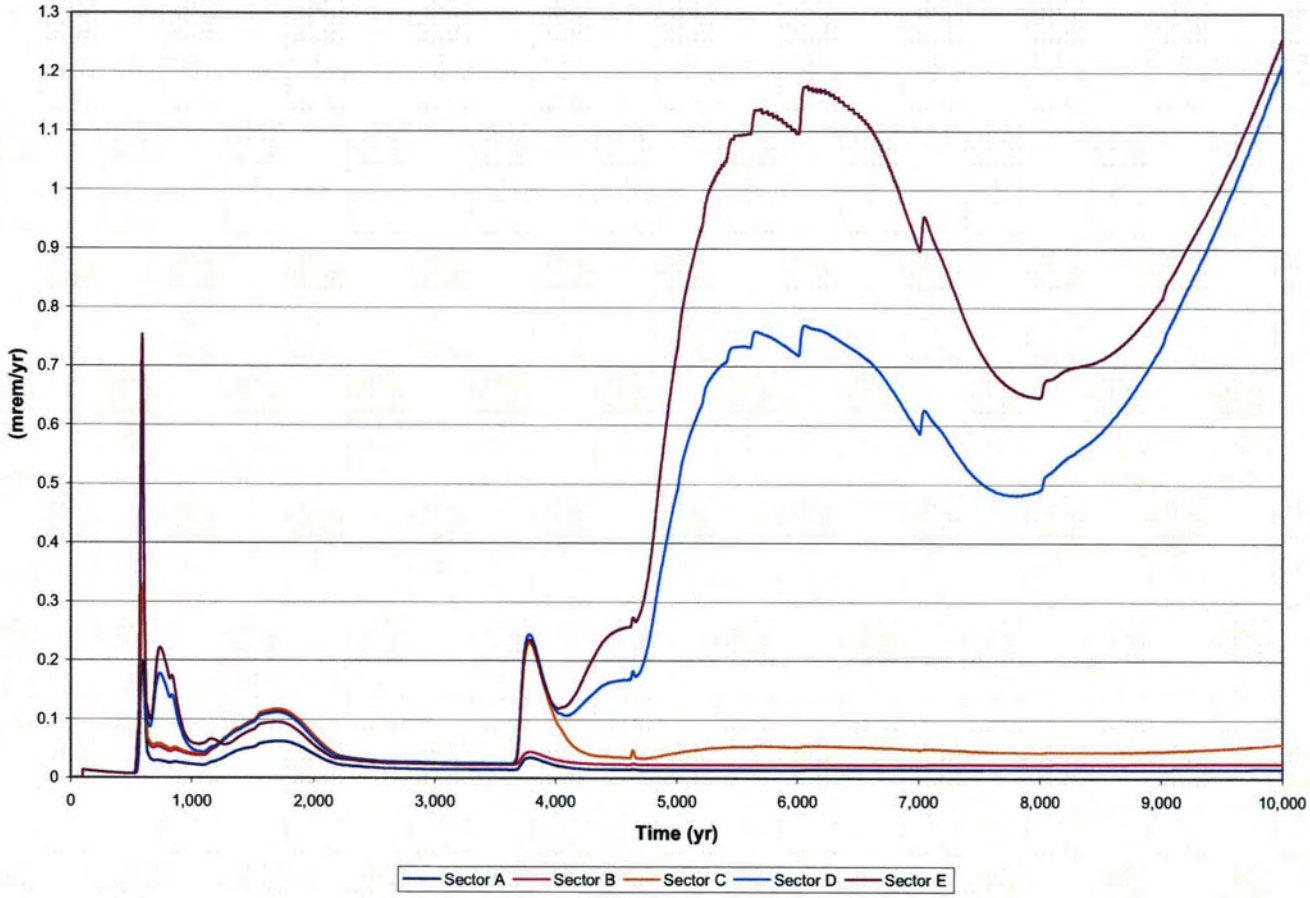

Figure 5.5-2: Member of the Public at 100m Peak Groundwater Pathway Dose Results within 20,000 Years for the Five 100m Sectors

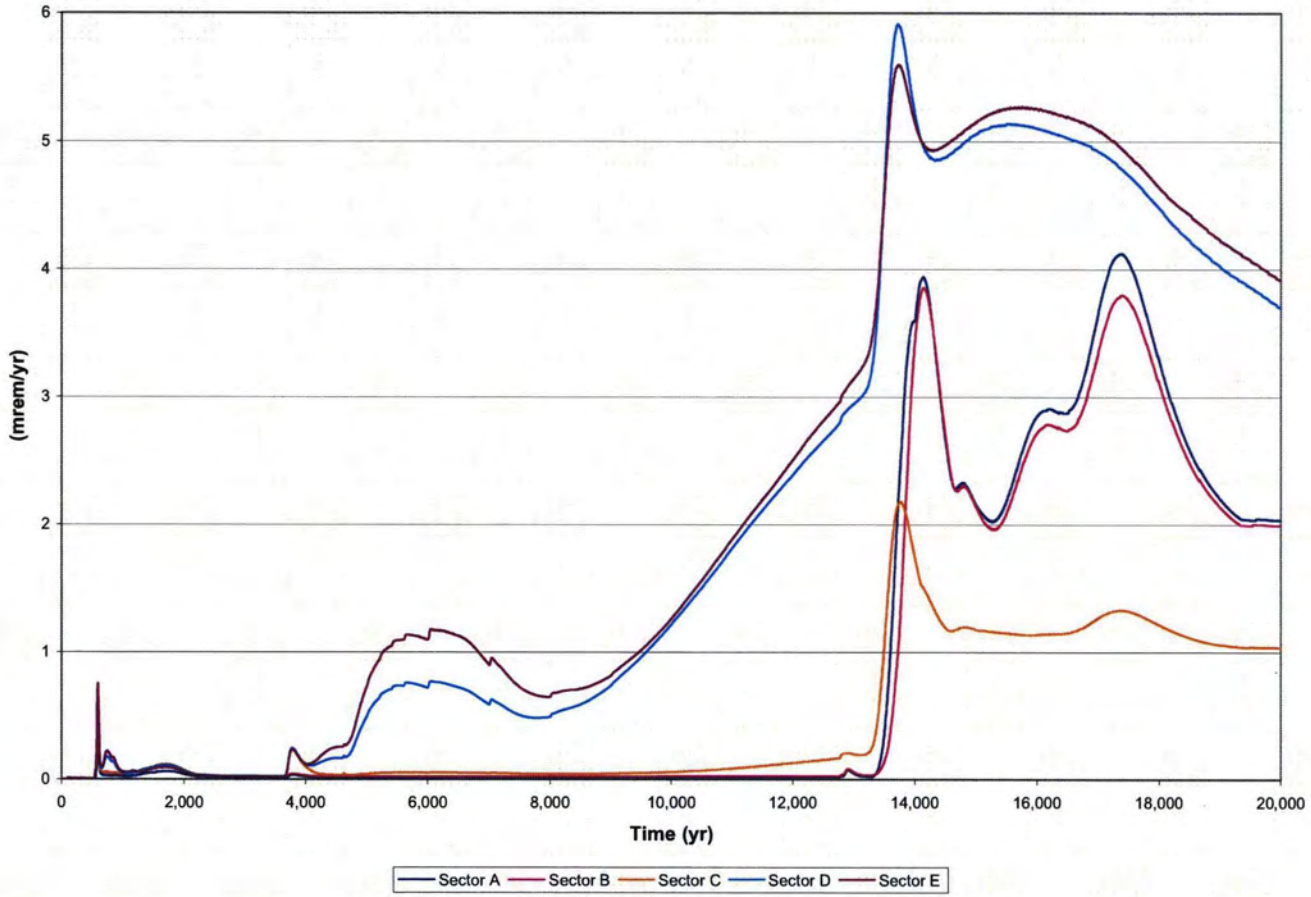

5.5.1.2 Individual Radionuclide Contributions to the MOP 100m Peak Annual Groundwater Pathway Dose

Figures 5.5-3 and 5.5-4 show the relative contribution from the key radionuclides to the Sector E 100m groundwater pathway dose over time (10,000 and 20,000 years respectively). Table 5.5-2 shows the relative contribution from the key radionuclides to the 1.26 mrem/yr peak groundwater pathway dose. The peak groundwater pathway dose to the MOP at 100m during the 10,000 years evaluation period is primarily associated with Ra-226 (37%) and U-233 (26%). The top contributors (>5% contribution) to the MOP at 100m peak groundwater pathway dose are Ra-226, U-233, U-234, Np-237, and Th-229.

Figure 5.5-3: Individual Radionuclide Contributors to the Sector E 100m Peak Groundwater Pathway Dose, 10,000 years

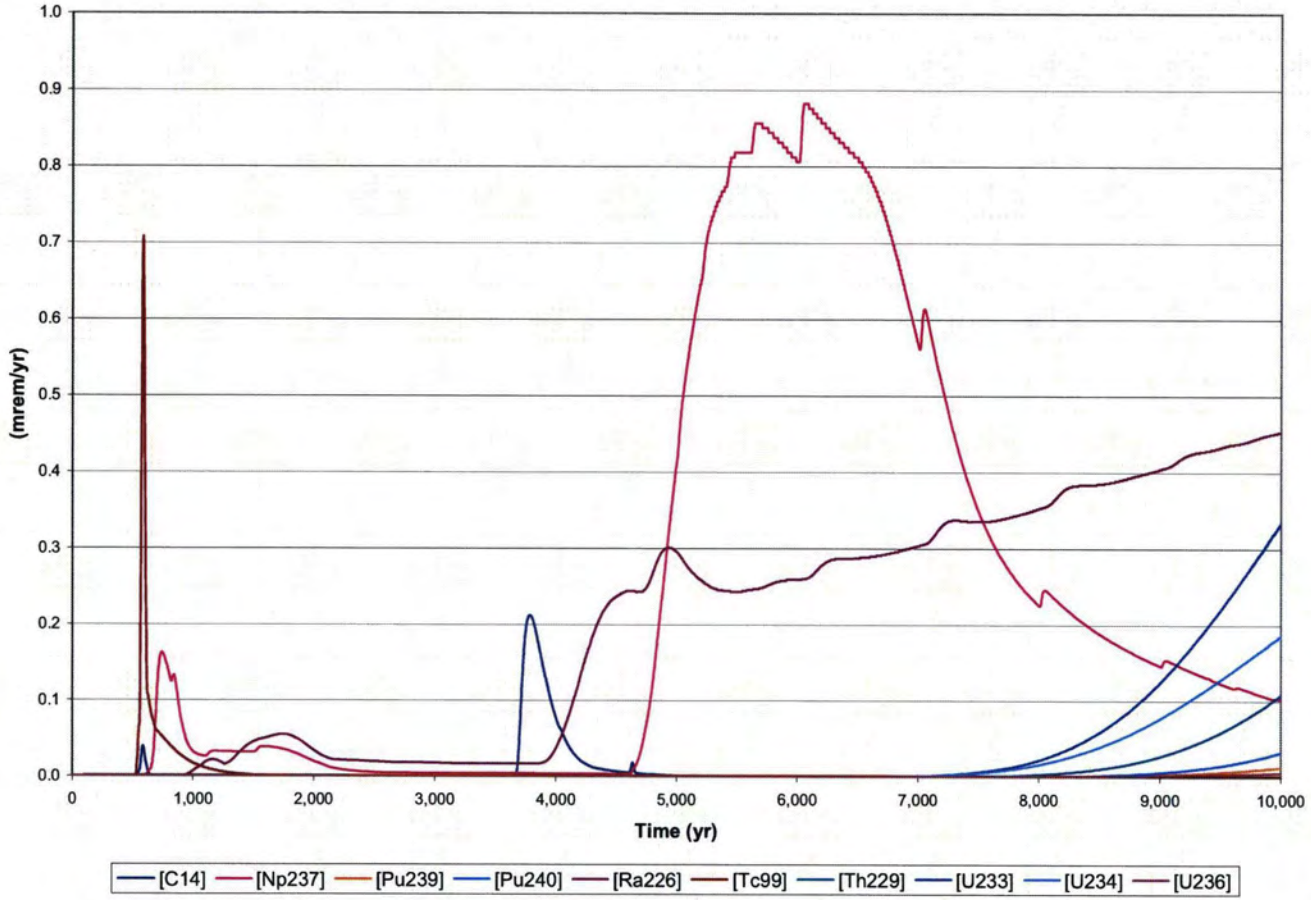

Figure 5.5-4: Individual Radionuclide Contributors to the Sector E 100m Peak Groundwater Pathway Dose, 20,000 years

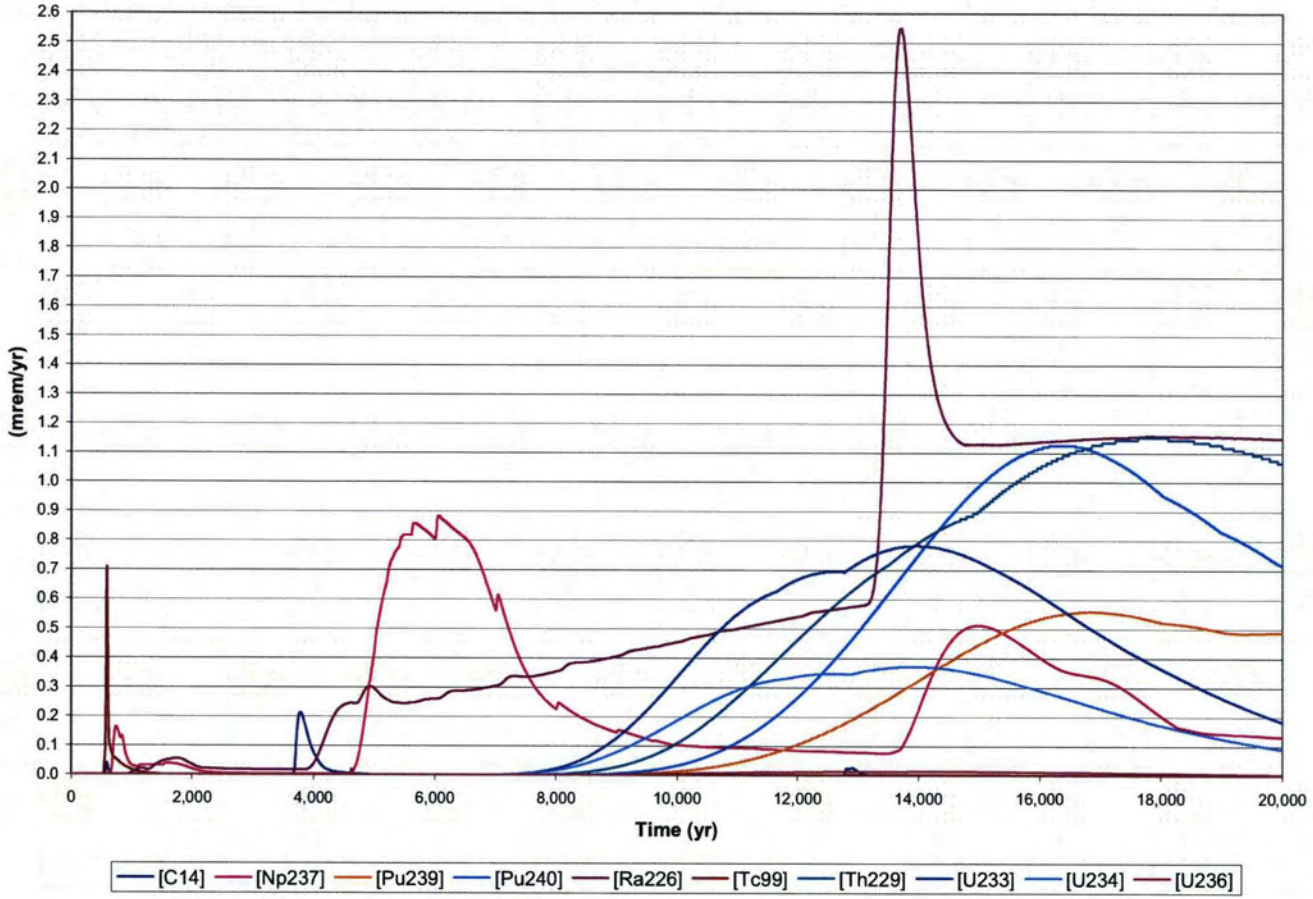

Table 5.5-2: Member of the Public at 100m Peak Groundwater Pathway Dose Individual Radionuclide Contributions at Year 10,000 (Peak Year)

Radionuclide	Contribution to Sector E Peak dose at year 10,000 (mrem/yr)	Percentage of Total Peak Dose (%)
C-14	<0.01	0%
Np-237	0.10	8%
Pa-231	0.02	2%
Pb-210	<0.01	0%
Pu-239	0.01	1%
Pu-240	0.03	3%
Pu-242	<0.01	0%
Ra-226	0.45	37%
Tc-99	<0.01	0%
Th-229	0.11	8%
Th-230	<0.01	0%
U-233	0.33	26%
U-234	0.19	15%
U-236	0.01	0%
U-238	<0.01	0%
Total	**1.26**	**100%**

5.5.1.3 Individual Tank Contributions to MOP 100m Peak Annual Groundwater Pathway Dose

Table 5.5-3 shows the relative contributions from those waste sources (Tanks 17 through 20 and the transfer lines) which will contribute to the Sector E 100m MOP groundwater pathway dose at 10,000 years (the year of the peak dose). Tanks 1 through 8 and Tanks 33 and 34 were excluded because the liners for these tanks are not expected to fail within 10,000 years. Tanks 25 through 28 and 44 through 47, and the other ancillary equipment were excluded from individual analysis because they have a relatively insignificant residual inventory for the key radionuclides. Tank 18 is the primary contributor (~83%) to the 100m Peak Groundwater Pathway Dose in Section E at year 10,000. Appendix E contains the 100m radionuclide concentration curves (20,000 years) for Tanks 1 through 8, Tanks 17 through 20, Tanks 33, 34 and the transfer lines.

Table 5.5-3: Member of the Public at 100m Peak Groundwater Pathway Dose Individual Source Contributions at Year 10,000 (Peak Year) for Sector E

Waste Source	Contribution to Sector E Peak Dose at year 10,000 (mrem/yr)	Percentage of Total Peak Dose (%)
Tank 17	0.10	8%
Tank 18	1.05	83%
Tank 19	0.06	5%
Tank 20	0.01	1%
Transfer Lines	0.03	2%
Other Sources	<0.01	<1%
TOTAL	**1.26**	**~100%**

5.5.1.4 Individual Pathway Contributions to MOP 100m Peak Annual Groundwater Pathway Dose

As stated previously, the total peak groundwater pathway dose results are the summation of the doses associated with all the individual 100m well pathways identified in Section 5.4. Table 5.5-4 shows the relative contributions from the individual groundwater pathways to the Sector E 100m MOP receptor dose at 10,000 years (the year of the peak dose). The primary contributors are water ingestion (53% of peak dose) and vegetable ingestion (24% of peak dose).

Table 5.5-4: Member of the Public at 100m Peak Dose Individual Groundwater Pathway Contributions for Sector E

Pathway	Associated Contribution at year 10,000 (mrem/yr)	Percentage of Total Peak Dose (%)	Principal Radionuclide Pathway Dose (%)
Water Ingestion	0.67	52.8	Ra-226 (43%)
Vegetable Ingestion	0.30	23.7	Ra-226 (43%)
Shower Inhalation	0.21	16.6	U-233 (29%)
Garden Inhalation	0.069	5.4	U-233 (29%)
Finfish Ingestion	0.010	0.8	Ra-226 (91%)
Milk Ingestion	0.007	0.6	Ra-226 (76%)
Beef Ingestion	0.002	<1	Ra-226 (66%)
TOTAL	**1.26**	**100**	

Table 5.5-5 shows a comparison of the 100m peak water ingestion doses for the different 100m sectors within both 10,000 and 20,000 years. The peak water ingestion doses for Sectors A through C occur relatively quickly (year 598) because they are associated with ancillary equipment (whose secondary containment is assumed to be breached at year 510) rather than the waste tanks, which is the case for Sectors D and E. Figure 5.5-5 shows the water ingestion doses to the 100m MOP receptor over time during the performance period (10,000 years) for the five 100m sectors. The highest 100m MOP water ingestion dose in the 10,000 year evaluation period is a 0.66 mrem/yr dose in Sector E at year 10,000. Figure 5.5-6 shows the 100m MOP receptor water ingestion doses within 20,000 years for the five 100m sectors. Figures 5.5-7 and 5.5-8 show the vegetable ingestion doses to the 100m MOP receptor for the five 100m sectors within 10,000 and 20,000 years respectively.

Table 5.5-5: Member of the Public at 100m Peak Water Ingestion Doses by Sector

Sector	Peak Water Ingestion Dose in 10,000 years (mrem/yr)	Principal Radionuclide	Peak Water Ingestion Dose in 20,000 years (mrem/yr	Principal Radionuclide
A	0.093 (year 598)	Tc-99 (~99%)	2.4 (year 14,132)	Ra-226 (99%)
B	0.17 (year 598)	Tc-99 (~99%)	2.4 (year 14,134)	Ra-226 (99%)
C	0.18 (year 598)	Tc-99 (~99%)	1.3 (year 13,776)	Ra-226 (92%)
D	0.63 (year 10,000)	U-233 (45%)	3.2 (year 13,712)	Ra-226 (58%)
E	0.67 (year 10,000)	Ra-226 (43%)	3.0 (year 13,722)	Ra-226 (55%)

Figure 5.5-5: Member of the Public at 100m Peak Water Ingestion Dose Results within 10,000 Years for the Five 100m Sectors

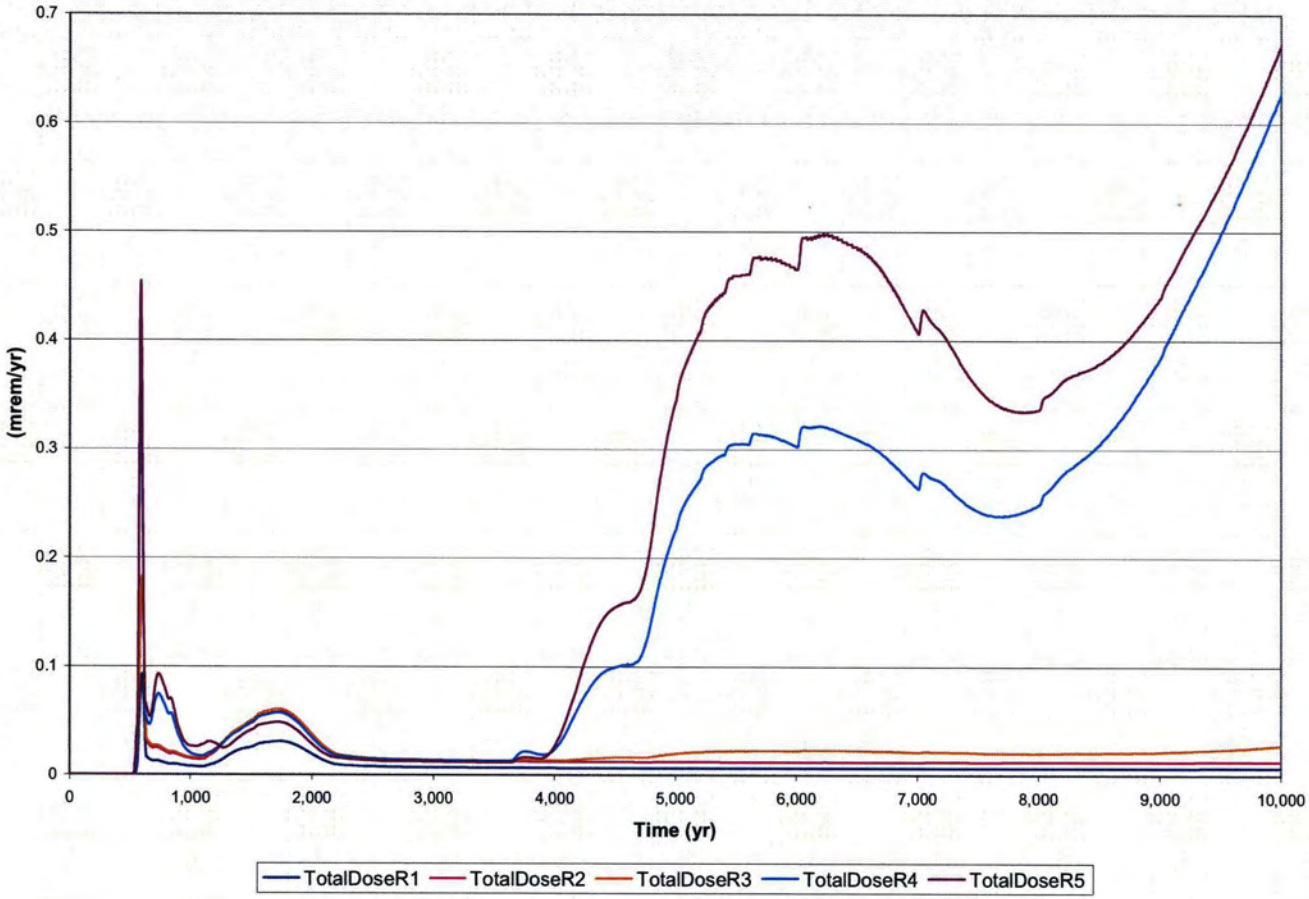

Figure 5.5-6: Member of the Public at 100m Peak Water Ingestion Dose Results within 20,000 Years for the Five 100m Sectors

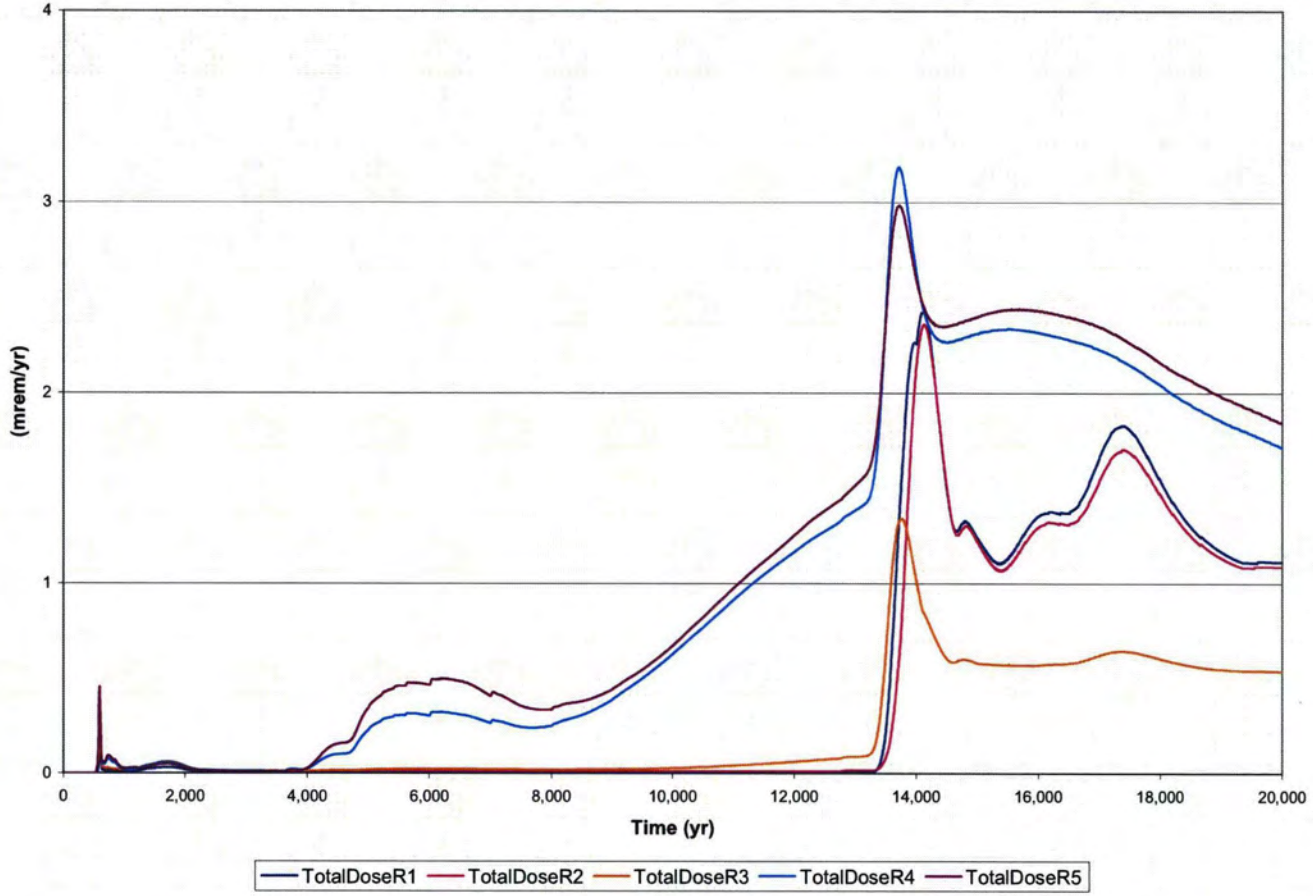

Figure 5.5-7: Member of the Public at 100m Peak Vegetable Ingestion Dose Results within 10,000 Years for the Five 100m Sectors

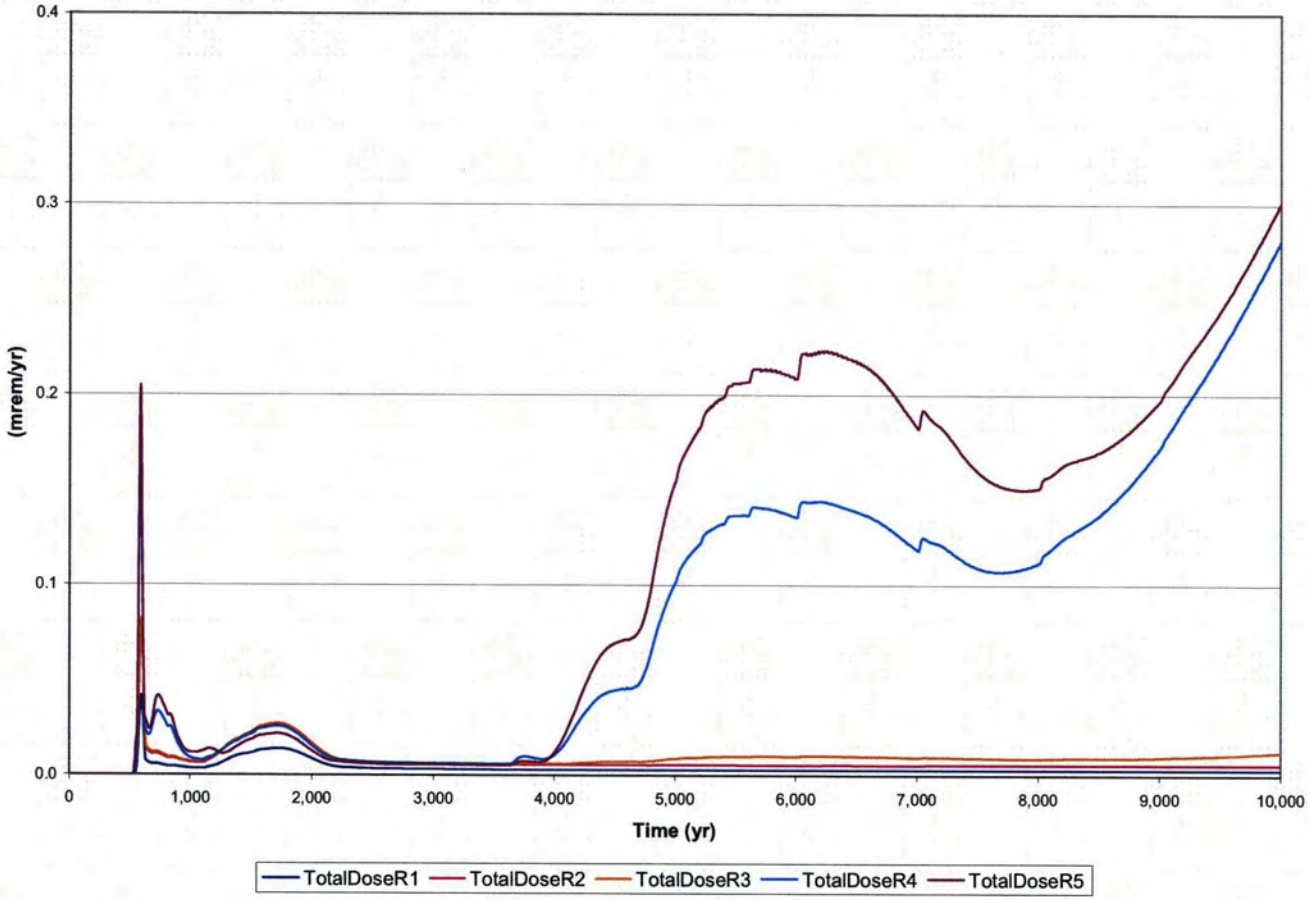

Figure 5.5-8: Member of the Public at 100m Peak Vegetable Ingestion Dose Results within 20,000 Years for the Five 100m Sectors

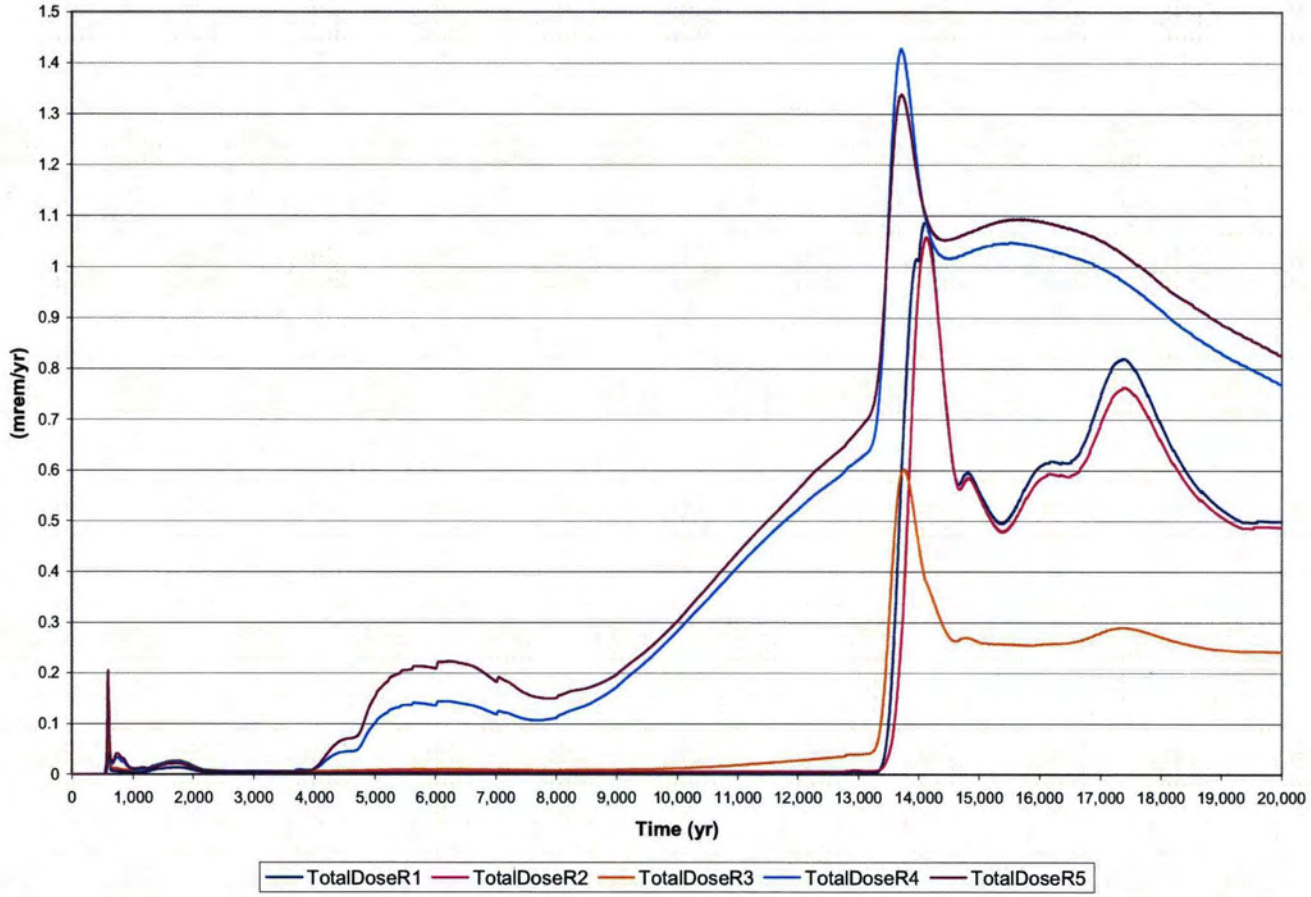

5.5.1.5 Member of the Public 100m Peak Annual Groundwater Pathway Dose Results for 40,000 years

The peak groundwater pathway doses associated with the key radionuclides are calculated for 40,000 years in order that the dose behavior well past the performance period can be evaluated (Appendix D contains 40,000 year curves for the 100m radionuclide concentrations for all of FTF). These peak groundwater pathway doses are the total dose associated with all the individual MOP 100m pathways identified in Section 5.4. Figure 5.5-9 shows the peak 100m groundwater pathway doses over time for 40,000 years for the five 100m sectors. It is evident from Figure 5.5-9 that the groundwater pathway doses associated with the key dose contributors in Sector E are all declining by year 40,000. The peak dose is approximately 335 mrem at year 28,496, and is associated with Pu-239 (94% of the dose).

Figure 5.5-9: Member of the Public at 100m Peak Groundwater Pathway Dose Results within 40,000 Years for Sector E

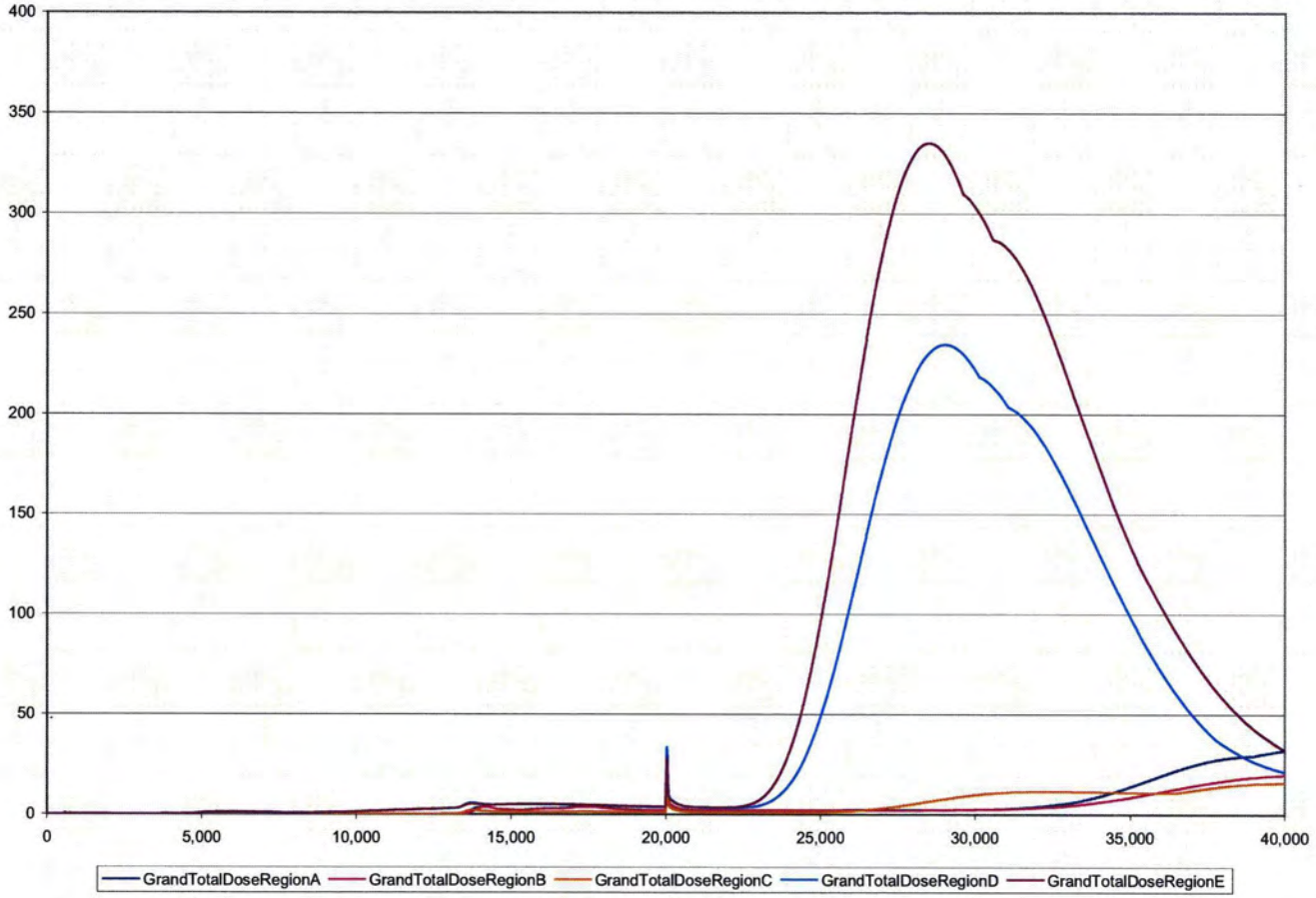

5.5.2 Member of the Public at Stream Groundwater Pathway Dose Results

The peak groundwater pathway doses for two stream sectors (Sector A - Fourmile Branch, and Sector B – UTR) are calculated using the highest concentration for each radionuclide in the sector (a discussion of how peak concentrations are determined by sector is provided in Section 5.2). In calculating the peak groundwater pathway dose, the highest radionuclide concentration is used from each of the distinct aquifers modeled (the UTR-UZ, UTR-LZ, and the Gordon Aquifer) for the two sectors. The concentration for each aquifer represents peak concentration in any vertical computational mesh within the aquifer. The mesh vertical thicknesses (heights) in the computational model are less than 10 feet in the UTR-UZ, and less than 15 feet in the UTR-LZ. No well screen averaging was used in determining the concentrations for dose calculations because the typical well screen length of 20 feet is approximate to the computational mesh height. These peak groundwater pathway doses are the total dose associated with all the individual MOP stream pathways identified in Section 5.4.

5.5.2.1 Member of the Public at Stream Peak Annual Dose

Table 5.5-6 shows a comparison of the MOP stream peak groundwater pathway doses for the two sectors. The highest peak groundwater pathway dose in the 10,000 year performance period is associated with UTR (Sector B). Figure 5.5-10 shows the peak groundwater pathway doses over time during the performance period (10,000 years) for the two streams of concern (UTR and Fourmile Branch). The highest MOP at the stream peak groundwater pathway dose in the 10,000 year evaluation period is a 0.21 mrem/yr groundwater pathway dose at year 3,788. Figure 5.5-11 shows the peak groundwater pathway stream doses within 20,000 years for both sectors.

Table 5.5-6: Member of the Public at Stream Peak Groundwater Pathway Doses by Sector

Sector	Highest Peak Dose in 10,000 Years	Highest Peak Dose in 20,000 Years
Fourmile Branch	**0.07 mrem/yr (year 586)** Principal Pathway: Finfish Ingestion (86%) Principal Radionuclide: C-14 (85%)	**0.72 mrem/yr (year 14,468)** Principal Pathway: Finfish Ingestion (46%) Principal Radionuclide: Ra-226 (97%)
UTR	**0.21 mrem/yr (year 3,788)** Principal Pathway: Finfish Ingestion (98%) Principal Radionuclide: C-14 (98%)	**0.21 mrem/yr (year 3,788)** Principal Pathway: Finfish Ingestion (98%) Principal Radionuclide: C-14 (98%)

Figures 5.5-12 and 5.5-13 show the relative contribution from the key radionuclides to the groundwater pathway MOP dose at the stream within 20,000 years (Sector A - Fourmile Branch, and Sector B – UTR, respectively).

Figure 5.5-10: Member of the Public at Stream Peak Groundwater Pathway Dose Results within 10,000 Years for the Two Stream Sectors

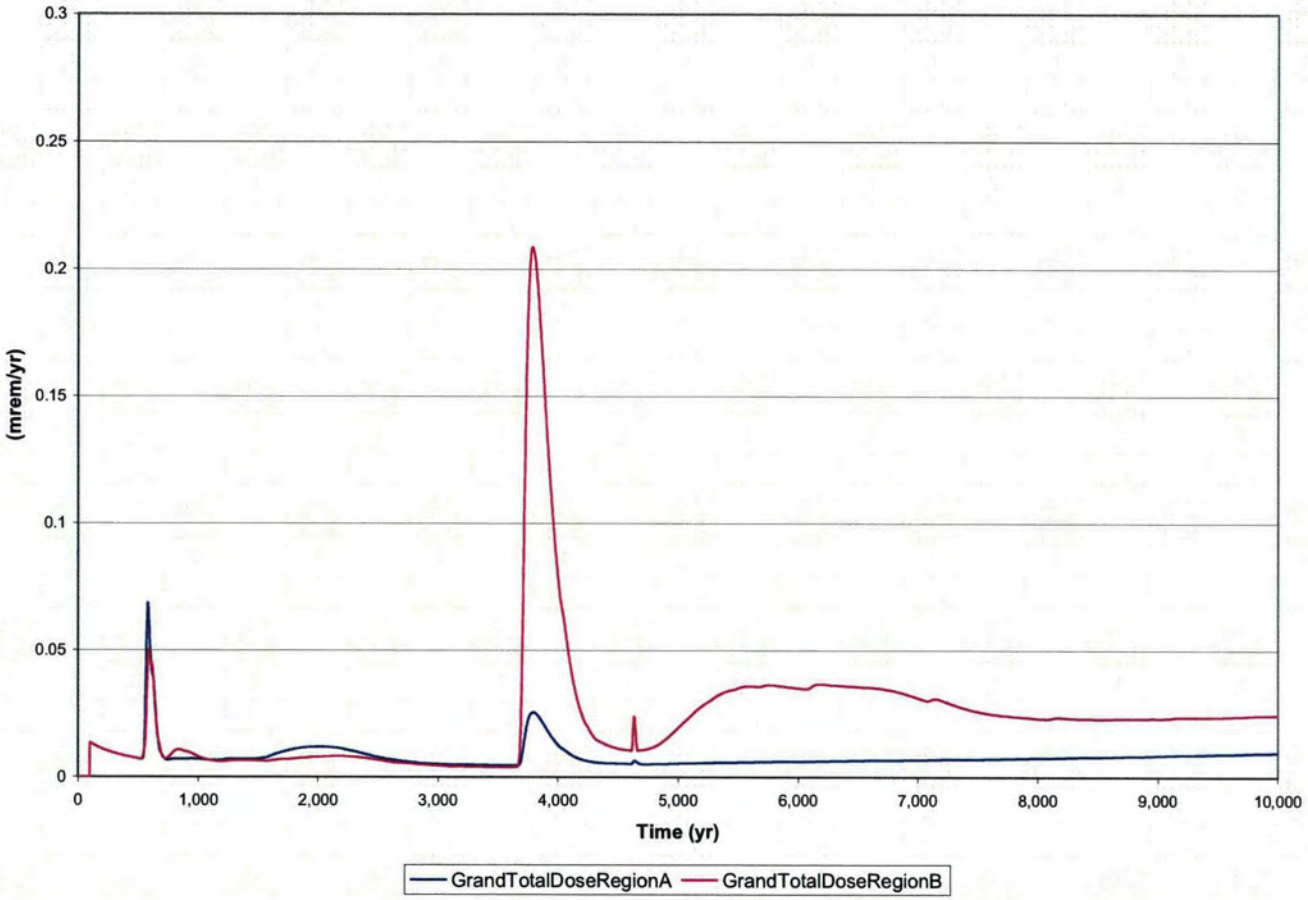

Figure 5.5-11: Member of the Public at Stream Peak Groundwater Pathway Dose Results within 20,000 Years for the Two Stream Sectors

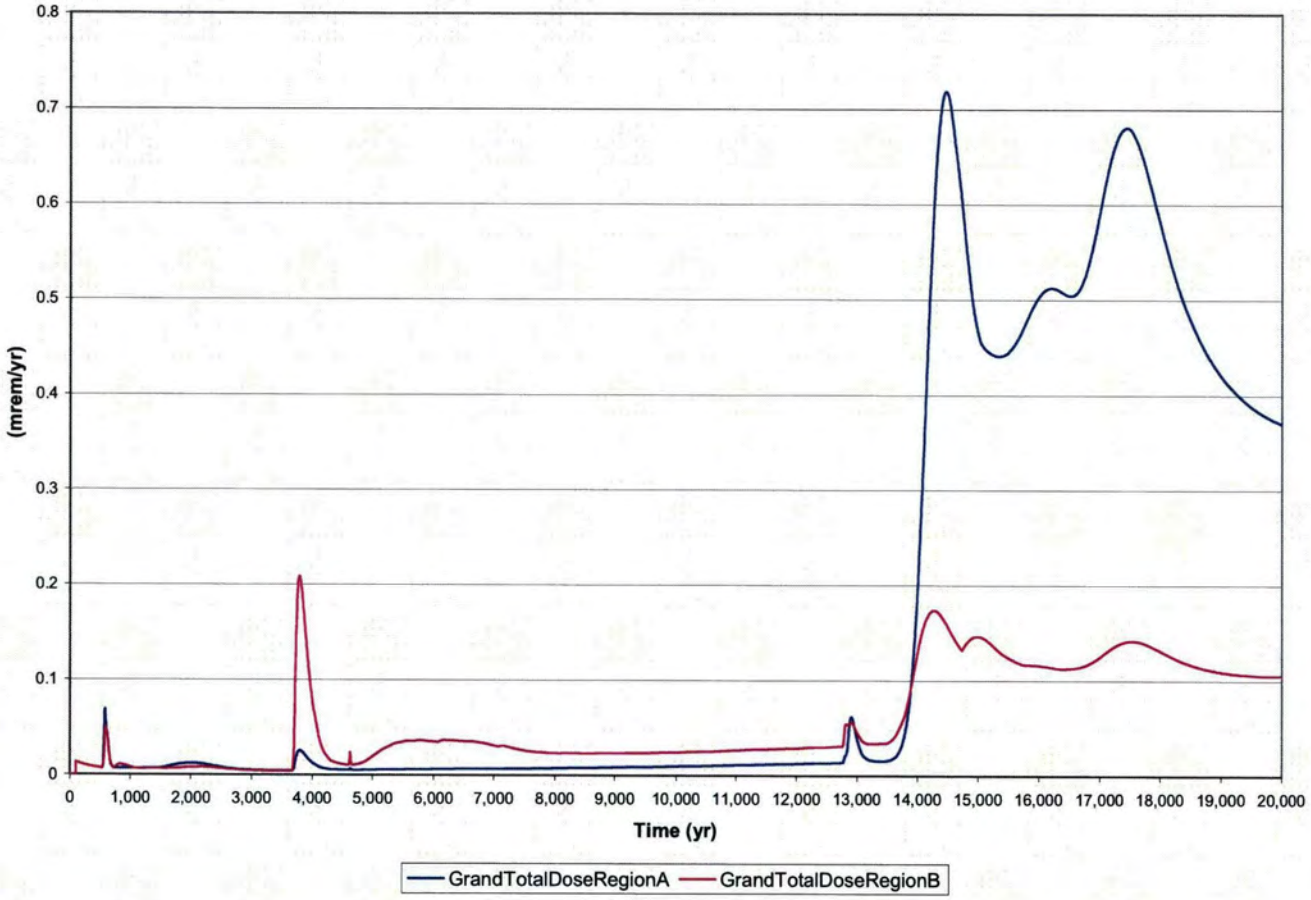

Figure 5.5-12: Individual Radionuclide Contributors to the Fourmile Branch (Sector A) Groundwater Pathway Dose, 20,000 Years

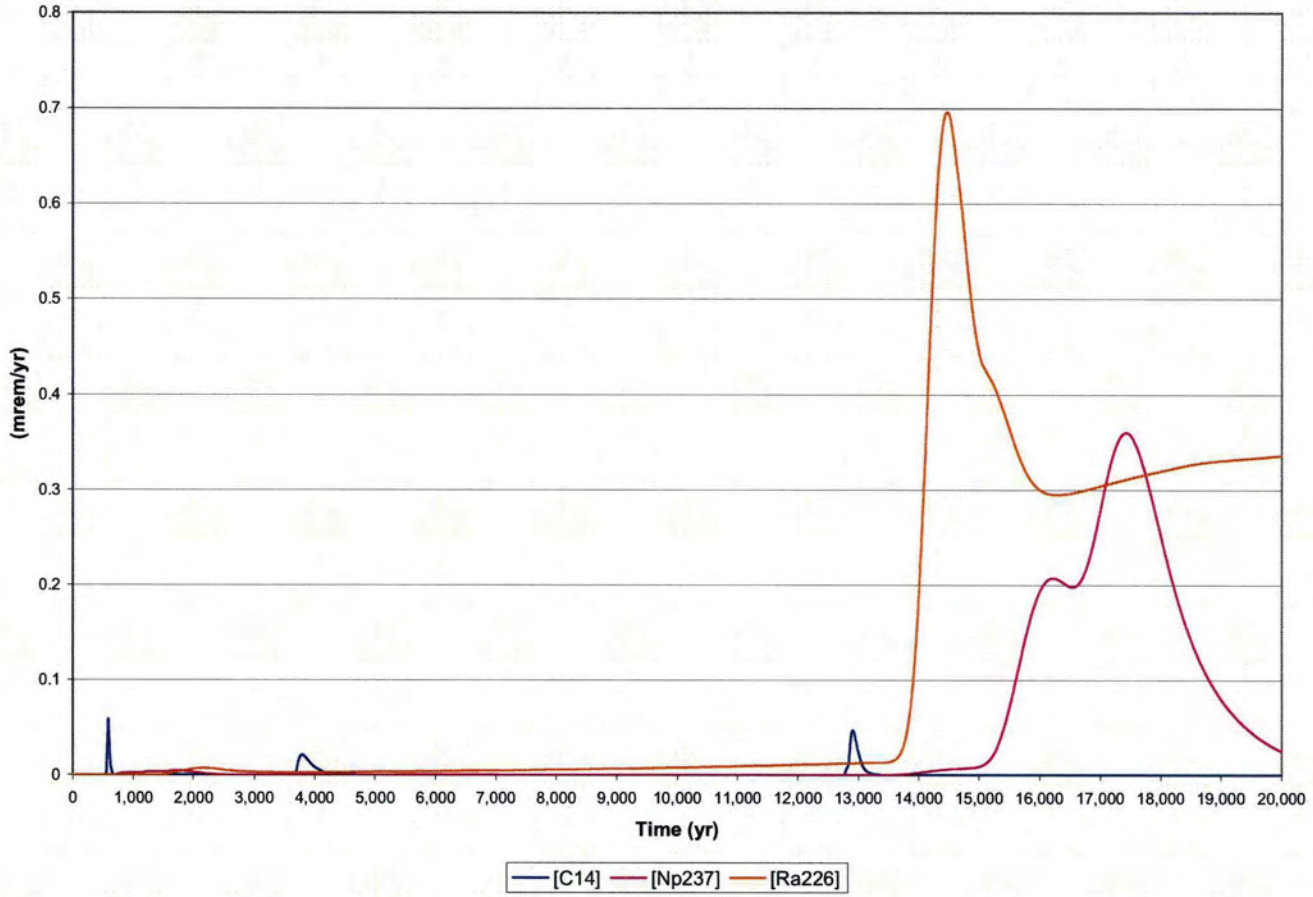

Figure 5.5-13: Individual Radionuclide Contributors to the Upper Three Runs (Sector B) Groundwater Pathway Dose, 20,000 Years

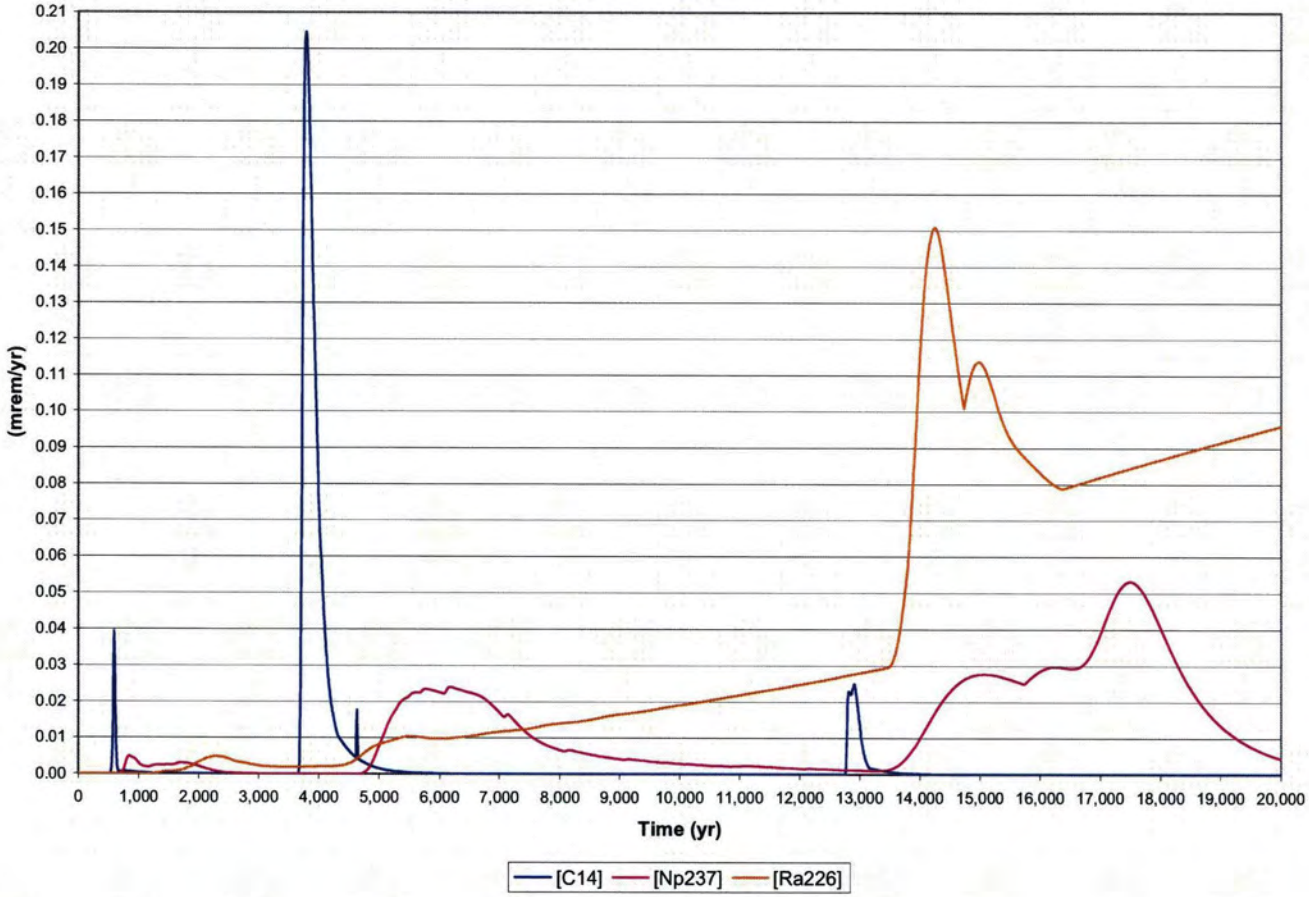

5.5.2.2 Member of the Public at Stream Individual Pathway Contributors

Table 5.5-7 shows the relative contributions from the individual groundwater pathways to the Sector B (UTR) MOP receptor dose at 3,788 years (the year of the peak Sector B dose). The primary contributor (98% of the peak dose) to the UTR peak is fish ingestion, which is due to the large C-14 peak at year 3,788 (Figure 5.5-12). Table 5.5-8 shows the relative contributions from the individual groundwater pathways to the Sector A (Fourmile Branch) MOP receptor dose at 14,468 years (the year of the peak Sector A dose). The primary contributors are finfish ingestion (46% of peak dose) and water ingestion (33% of peak dose).

Table 5.5-7: Member of the Public at Stream Peak Dose Individual Groundwater Pathway Contributions for Sector B (UTR)

Pathway	Associated Contribution at year 3,788 (mrem/yr)	Total Peak Dose (%)	Principal Radionuclide Pathway Dose (%)
Finfish Ingestion	0.205	99	C-14 (99%)
All Others	0.002	1	- - -
Total	**0.207**	**100**	

Table 5.5-8: Member of the Public at Stream Peak Dose Individual Groundwater Pathway Contributions for Sector A (Fourmile Branch)

Pathway	Associated Contribution at year 14,468 (mrem/yr)	Total Peak Dose (%)	Principal Radionuclide Pathway Dose (%)
Finfish Ingestion	0.34	47	Ra-226 (96%)
Water Ingestion	0.25	34	Ra-226 (99%)
Vegetable Irrigation	0.11	15	Ra-226 (99%)
All Others	0.02	4	- - -
Total	**0.72**	**100**	

5.5.3 Member of the Public All-Pathway Dose Results

The purpose of this section is to present the total all-pathway peak doses for both the MOP at 100m and the MOP at the stream. The total all-pathway doses include both the groundwater and air pathway contributors.

5.5.3.1 Member of the Public at 100m Peak Annual All-Pathway Dose

The peak all pathway annual dose for the MOP at 100m is calculated using the highest 100m groundwater pathway dose results during the 10,000 year performance period (from Section 5.5.1) in combination with the air pathway results (from Section 5.4). The peak all pathway annual dose for the MOP is 1.4 mrem/yr and is associated with Sector E. The breakdown of the individual dose contributors is provided in Table 5.5-9.

Table 5.5-9: Member of the Public at 100m Peak Annual All-Pathway Dose Contributors

Pathway	Associated Contribution at year 10,000 (mrem/yr)	Percentage of Total Peak Dose (%)	Principal Radionuclide Pathway Dose (%)
Water Ingestion	0.67	48	Ra-226 (43%)
Vegetable Ingestion	0.30	21	Ra-226 (43%)
Shower Inhalation	0.21	14	U-233 (29%)
Garden Inhalation	0.069	5	U-233 (29%)
Finfish Ingestion	0.010	1	Ra-226 (91%)
Milk Ingestion	0.007	<1	Ra-226 (76%)
Beef Ingestion	0.002	<1	Ra-226 (66%)
Air Pathway	0.14	10	Sn-126 (~100%)
Total	**1.40**	**100**	

5.5.3.2 Member of the Public at Stream Peak Annual All-Pathway Dose

The peak all-pathway annual dose for the MOP at the stream is calculated using the highest stream groundwater pathway dose results during the 10,000 year performance period (from Section 5.5.2.1) in combination with the air pathway results (from Section 5.4). The peak all-pathway annual dose for the MOP within 10,000 year is 0.25 mrem/yr and is associated with UTR. The breakdown of the individual dose contributors is provided in Table 5.5-10.

Table 5.5-10: Member of the Public at Stream Peak Annual All-Pathway Dose Individual Groundwater Pathway Contributions

Pathway	Associated Contribution at Year 3,788 (mrem/yr)	Percentage of Total Peak Dose (%)	Principal Radionuclide Pathway Dose (%)
Finfish Ingestion	0.20	82	C-14 (99%)
Air Pathway	0.035	14	Sn-126 (97%)
All Others	0.01	4	- - -
Total	**0.25**	**100**	

5.6 Sensitivity and Uncertainty Analysis

The purpose of the sensitivity and uncertainty section is to consider the effects of uncertainties in the conceptual models used and sensitivities in the parameters used in the mathematical models. This evaluation was conducted for analyses related to MOP as well as those related to inadvertent intruders. These evaluations focused on key uncertainties and key sensitivities identified during modeling. The sensitivity and uncertainty analyses were primarily performed using a probabilistic model (i.e., the GoldSim FTF model), as discussed in Sections 5.6.1 through 5.6.6. As described in Section 5.6.7, some additional single parameter sensitivity analyses were performed through deterministic modeling using both PORFLOW and GoldSim models.

The probabilistic model allows for variability of multiple parameters simultaneously, so concurrent effect of changes in the model can be analyzed, and the potential impact of changes can be assessed. This assessment allows for identification of parameters that are only of significance when varied simultaneously with another parameter. The deterministic model single parameter analysis provides a method to evaluate parametric effects in isolation, so the importance of the uncertainty around a parameter of concern can be more effectively evaluated. Using both probabilistic and deterministic models for sensitivity analysis versus a single approach provides additional information concerning which parameters are of most importance to the FTF model.

5.6.1 Sensitivity and Uncertainty Analysis using Probablistic Modeling

The objective of these analyses was to investigate uncertainties that are inherent in conceptual models, mathematical models, and related data and assumptions to help confirm that the Base Case modeling provides reasonable results.

5.6.1.1 GoldSim FTF Model

In order to address uncertainty and sensitivity of the modeling of the FTF, a probabilistic model was constructed. This model is necessarily simpler than the PORFLOW groundwater model in its environmental transport calculations, but includes additional calculations that cannot be performed in PORFLOW. The GoldSim FTF model is described in detailed in Section 4.4.4.2.

The probabilistic model, written using the GoldSim systems analysis software, accepts uncertainty and variability in the input parameters, the values of which can be defined using probability distributions. If a given model input (e.g., the porosity of sandy soil) is given a distribution, or range of values, then this distribution is sampled in the collection of Monte Carlo runs that constitutes a probabilistic analysis. The collective uncertainty of all stochastic (probabilistic) inputs is reflected in the range and distribution of modeled results, such as water concentrations or dose to hypothetical future human receptors. If a given input parameter is given no range of input values, that is, if it is defined deterministically, then it contributes nothing to the overall uncertainty in the results. In the real world, there are few parameters that have zero uncertainty. An example of a parameter without a defined range is the half-life of radionuclides.

Before probabilistic modeling became computationally feasible, the traditional approach to PA modeling was to assume extreme yet discrete values for parameters whose values were

not well known. Practitioners attempted to build what were termed "conservative" models, wherein values would be deliberately chosen to make the result worse, e.g., increasing the dose to a human receptor. This approach is problematic for two reasons: 1) the resulting model was often so far removed from reality that it provided little useful information, and 2) the attempt to determine what a conservative value might be for a given parameter was frustrated by the fact that what may be "conservative" for one exposure pathway may not be for another. Parameterizing the model with realistic input distributions avoids the problem of false conservatism, and produces results that are based on our state of knowledge.

The probabilistic model allows evaluation of the degree of uncertainty in the PA and its role in evaluating results. The results of the uncertainty analysis of this model are discussed in Section 5.6.4. Adopting a probabilistic approach also allows analysts to determine which model input parameters are the most significant to the results. This is done through sensitivity analysis, which identifies covariance between model inputs and results. Section 5.6.6 discusses the sensitivity analysis performed for the FTF model.

A benchmarking of the environmental transport calculations within a deterministic version of the GoldSim FTF model and those performed by the PORFLOW model is discussed in Section 5.6.2.

5.6.1.2 GoldSim FTF Model Assumptions

The minimum evaluation distance from the FTF was determined for the GoldSim FTF model by using Figure 5.2-2, which shows the 100m distance from FTF along the applicable stream tracers. Using this figure it was possible to determine the actual transport distance required to reach the "100m from the FTF" distance (Table 5.2-1 presents these distances).

The inventory used for GoldSim FTF stochastic analysis is a slightly abridged version of the inventory used for the Base Case simulations performed using the PORFLOW FTF model. The following radionuclides are not explicitly included in the initial GoldSim inventory: Ba-137m, Bk-249, Ce-144, Cm-242, Cs-134, Eu-155, Na-22, Pm-147, Pr-144, Rh-106, Ru-106, Sb-125, Sb-126, Sb-126m, Te-125m, and Y-90. These radionuclides are not included for various reasons (e.g., short half-life, no DCF) and all of these radionuclides have been shown to have an insignificant contribution to dose (as demonstrated in Section 5.2.1).

Since the GoldSim FTF model did not include explicit stream concentration analysis, in instances where the stochastic analysis required a stream concentration to calculate a dose pathway (e.g., fishing at the stream), a value of 5% of the associated 100m concentration was used. The 5% value is reasonably conservative based on the fact that the peak stream concentration is on average less than 5% of the associated peak 100m concentration (Appendix F.1) and the fact that the water used in the stream pathways would be subject to stream dilution, which is not accounted for when the raw seepline concentration from PORFLOW is used.

5.6.2 GoldSim Benchmarking

5.6.2.1 Benchmarking Between the GoldSim and PORFLOW Models

The probabilistic model of FTF using the GoldSim systems analysis software is described in Section 4.4. In order for the probabilistic results of this model to be compared to the results

of the PORFLOW FTF model, obtaining a sufficient degree of agreement between the two models is appropriate. Calibration of the PORFLOW model is addressed in Section 4.4.4.1. Ideally, the results of a deterministic Base Case assessment using the PORFLOW model could be mimicked by a similar run in the GoldSim model. Deterministic results from both models should be comparable for the various configurations and scenarios developed in the conceptual configuration model as well. Benchmarking of the two models for a Base Case scenario (for selected waste tanks and radionuclides) has achieved the degree of agreement illustrated by the figures within this section. The term "benchmarking" has been chosen, rather than "calibration", since this process establishes a point from which comparisons can be made rather than attempting to ensure that all results for the two models are identical for all configurations. Only the Base Case configuration was evaluated.

Challenges in achieving the benchmarking comparisons include:

- the abstraction from a site conceptual model to different computer modeling platforms,
- fundamental differences in modeling platforms, and
- differences in model approach (i.e., 2-D and 3-D process model *vs* a one-dimensional system model).

The following sections describe the procedure used to benchmark the GoldSim FTF model to the PORFLOW FTF model. There were two main parts to the benchmarking effort, generic changes to the models to align them, and the specific changes made to the GoldSim model to mimic the PORFLOW model.

5.6.2.2 Background

Baseline groundwater modeling is carried out using the PORFLOW modeling software, a 3-D finite difference porous media flow and transport program. For performing a comprehensive evaluation of uncertainty and sensitivity, the PORFLOW FTF model is not optimum, since such an analysis requires the execution, integration, and analysis of more information than can be handled practically using a large process model such as PORFLOW. The PORFLOW model could be used for analysis of single parameter changes, but is not designed to model a large number of varying configurations. For this reason, uncertainty and sensitivity analysis for the FTF PA is performed using the GoldSim systems analysis software, which is designed to perform probabilistic analysis of abstracted (greatly simplified) systems. As part of this approach, a benchmarking is required to demonstrate that the PORFLOW FTF model and the GoldSim FTF model are performing essentially the same calculations and producing comparable results. This is difficult, since the 3-D complexity of the PORFLOW model is a challenge to abstract into the much simpler systems-based modeling used by GoldSim.

5.6.2.3 Initial Benchmarking

Early benchmarking efforts identified some inconsistencies between the models which have since been addressed. The key effect on the benchmarking was the GoldSim implementation of the PORFLOW saturated zone apparent bulk density. In the PORFLOW model the bulk density was adjusted to account for the removal of the clay lens masses. The dry bulk

density of the sandy soil medium in the GoldSim model was not modeled consistently with the PORFLOW definition. A large improvement in the comparisons was seen when the GoldSim value was adjusted to match the PORFLOW value. The precise changes made to the GoldSim model as a result of the benchmarking process are summarized in more detail below.

To improve alignment of the water fluxes, the solubility of Pa in the water was changed from infinite to a very small value (1.0E-12 mol/L). A small but finite value was necessary in order to account for the manner in which the solubility was treated by PORFLOW. Although the input value was K_d=0mL/g, PORFLOW assumes a linear isotherm for the parent which leads to an implied solubility limit for the daughter product.

The second GoldSim model modification was performed to improve alignment of concentrations at Well 6. These adjustments, described below in greater detail, could be considered calibration steps:

- ClayeySoil was added to the GoldSim saturated zone transport Cells.
- The ratio of model scale to longitudinal dispersivity was modified.

The PORFLOW model includes, in its saturated zone transport pathway, more than just GoldSim's simple row of Cells with SandySoil (a solid medium defined in the GoldSim model). In particular, the porous media in PORFLOW include regions of both sandy and clayey soil. Since these media have different adsorption characteristics (as expressed in different soil/water K_ds), some accounting must be made for the presence of both materials in the saturated zone transport path. By adding clayey soil, some retardation is added in its most general sense. The solution was to add some of the medium ClayeySoil to the saturated zone transport Cells in the GoldSim model, so that the clayey K_ds would have some influence on the transport. The fraction of ClayeySoil (with the remainder being SandySoil) present in these Cells was used as a calibration parameter. Further, since Tank 17 is only about 100m from Well 6 (along with other waste tanks in the western half of the tank farm) and Tank 1 and the other eastern waste tanks are about twice that distance, the two sets of tanks were calibrated separately. An additional ClayeySoil fraction was added for the transfer lines across FTF with an intermediate value chosen. The GoldSim model tank selector dashboard shows the specific benchmarking factors added. (Figure 4.4-42)

Dispersivity accounts for the degree to which a contaminant plume spreads as it travels through a porous medium. In general, a plume will spread longitudinally (parallel to the direction of flow), laterally (transverse to the direction of flow, in the horizontal plane), and vertically (perpendicular to the direction of flow). Dispersivity of plumes in the real world are difficult to characterize and are generally based on detailed mapping of discrete plumes which is very difficult in the SRS GSA due to the numerous co-located facilities. Another complicating factor is that numerical approximations to contaminant transport create their own dispersion through discretization of the modeling domain and mathematical mixing within discrete cells. This numerical dispersion occurs in the GoldSim one-dimensional approximation and the PORFLOW 3-D modeling. In the GoldSim model, the longitudinal migration along a one-dimensional flow path is subject to longitudinal numerical dispersion between cells, and an instantaneous dispersion of the plume to the cell width and height.

Superposed on that concentration is a GoldSim plume function which adds dispersivities to the calculated result. These additional dispersivities were modified slightly to improve alignment between the two models.

In summary, the initial benchmarking showed there was an issue with numerical dispersion with the GoldSim model. The GoldSim model results showed a faster transport than the PORFLOW model. The transport time was essentially unaffected by changing the flow velocity. From this, it was apparent that it must be numerical dispersion. By increasing the number of mixing cells in GoldSim to more closely match the PORFLOW discretization, the timing of the arrival of radionuclides was consistent between the two models. This will be discussed in more detail in the following section.

5.6.2.4 Benchmarking Process

The benchmarking process was accomplished in distinct phases. Each phase requires comparison of the timing of the radionuclides at the evaluation point (e.g., at the saturated zone or at the 100m well). Once the timing was deemed reasonable, the concentration magnitudes at the evaluation point were aligned. Six tanks were used for benchmarking, Tanks 17, 18, 1, 3, 5, and 34. These tanks were selected based on physical location, a representation of each of the tank types found in FTF, and because early scoping runs showed these waste tanks to be significant dose contributors. Table 5.6-1 provides a summary of the characteristics of each of the selected waste tanks.

Table 5.6-1: Benchmarked Tank Characteristics

Tank	Type	Distance to Water Table (ft)	Distance to 100m Evaluation Location (m)	PORFLOW Evaluation Sector
1	I	13.5	224	E
3	I	12.1	244	E
5	I	10.6	264	D
17	IV	2.5	112	E
18	IV	2.1	132	E
34	III	17.1	244	A

The benchmarking was carried out in two phases. The first phase was to benchmark the flux from the unsaturated zone to the saturated zone. The second phase was to benchmark the concentrations of radionuclides at the 100m well. The first phase was essentially complete when the PORFLOW and GoldSim runs were initially made. The two models showed very similar results with the inputs aligned. The majority of the benchmarking effort was allocated to aligning the saturated zone results.

It should be noted that the two different implementations of the conceptual model for the unsaturated zone produced very similar results. The similar results provide added confidence that the results are an acceptable representation of the ISCM. Using two separate models is a true benchmarking of the implementation of the ISCM, and verifies the models via independent calculations showing the same behavior.

Four radionuclides (Tc-99, Np-237, U-238, and Pu-239), and their progeny were chosen for the benchmarking due to scoping results indicating they are major contributors to the all-pathways dose. Figure 5.6-1 shows the preliminary results that are a comparison of the two models before any benchmarking adjustments were made (but after the model inputs were made consistent). As shown in Figure 5.6-1, there was a disparity with both the timing and magnitude of the peaks.

Figure 5.6-1: Preliminary Results

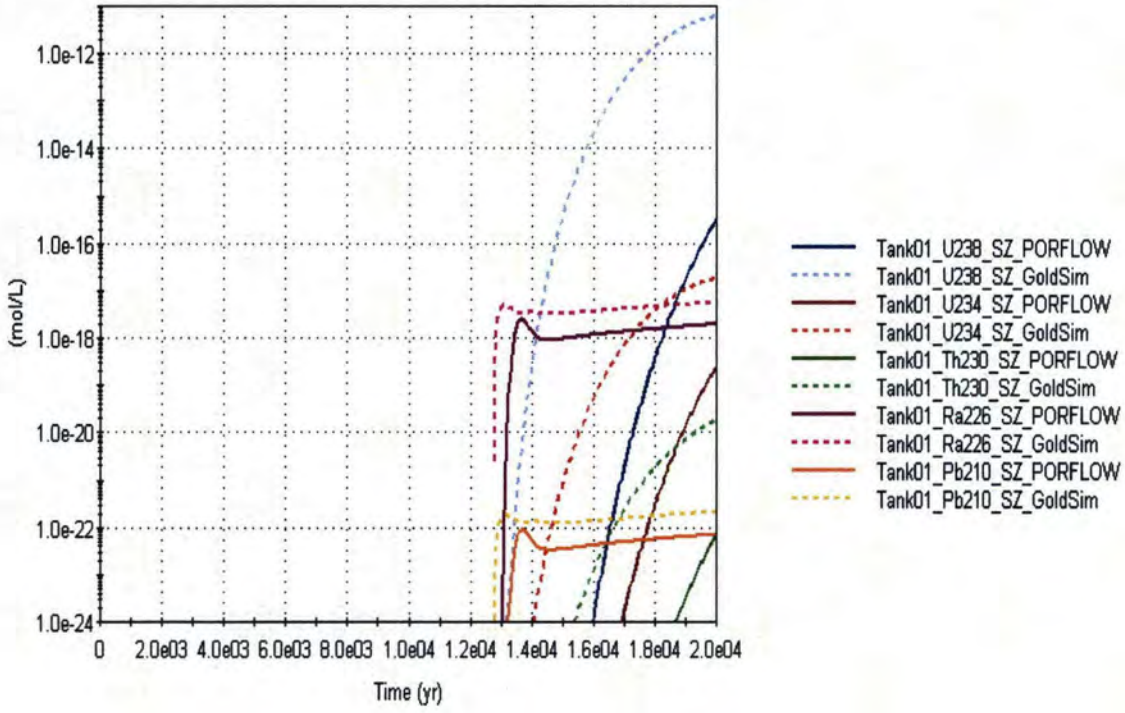

➢ **Peak Timing**

As noted above, the major correction in peak timing was accomplished by eliminating the numerical dispersion in the GoldSim model. The timing was then fine-tuned by varying the saturated zone velocity. As presented in Section 4.4.4.1, the flowstreams from the waste tanks are neither linear nor in the same x-y plane. These effects can be accounted for by varying GoldSim's one-dimensional velocity.

The first step in adjusting the peak timing was to examine the behavior of Tc-99, which was chosen because it is a non-sorbing radionuclide. If the arrival times in the two models coincided, then the saturated zone velocities are consistently represented. This was accomplished for the six representative tanks.

The next step was to use a sorbing radionuclide. Initial runs showed earlier peaks than expected. It was believed that since the PORFLOW model was modeling the clay layers separating the aquifers then the clay should have a delaying affect on the arrival time of peaks. Therefore, the GoldSim model was modified to include a mixture of clay and sand. The Pu-239 series runs were informative in that the plutonium peak moved

substantially while the uranium peak did not move. The value of the K_d for plutonium changes from 270 ml/g in sand to 5,900 ml/g in clay, uranium varies from 200 ml/g in sand to 300 ml/g in clay. This showed that it was not a K_d effect, rather the numerical dispersion of the GoldSim model.

Once the numerical dispersion issue was addressed, the peaks of the sorbing radionuclide fell into reasonable agreement with the PORFLOW peaks using the same velocities as determined by the Tc-99 comparisons. This is another indication that the ISCM is giving consistent results when modeled by two independent models.

- **Peak Magnitude** The peak values were adjusted by applying a benchmarking factor to the GoldSim plume function. The plume function is an analytical solution of plume spreading based on several factors. These factors are based on literature values, not site-specific information. The benchmarking factor is applied to account for the site-specific data as reflected in the PORFLOW results.

As before, Tc-99 (the non-sorbing radionuclide), was the first to be benchmarked. After the benchmarking factor was applied for Tc-99, the other radionuclides were run and no additional adjustments were necessary. Figure 5.6-2 shows the improved benchmarking for the Pu-239 decay chain.

Figure 5.6-2: Improved Benchmarking

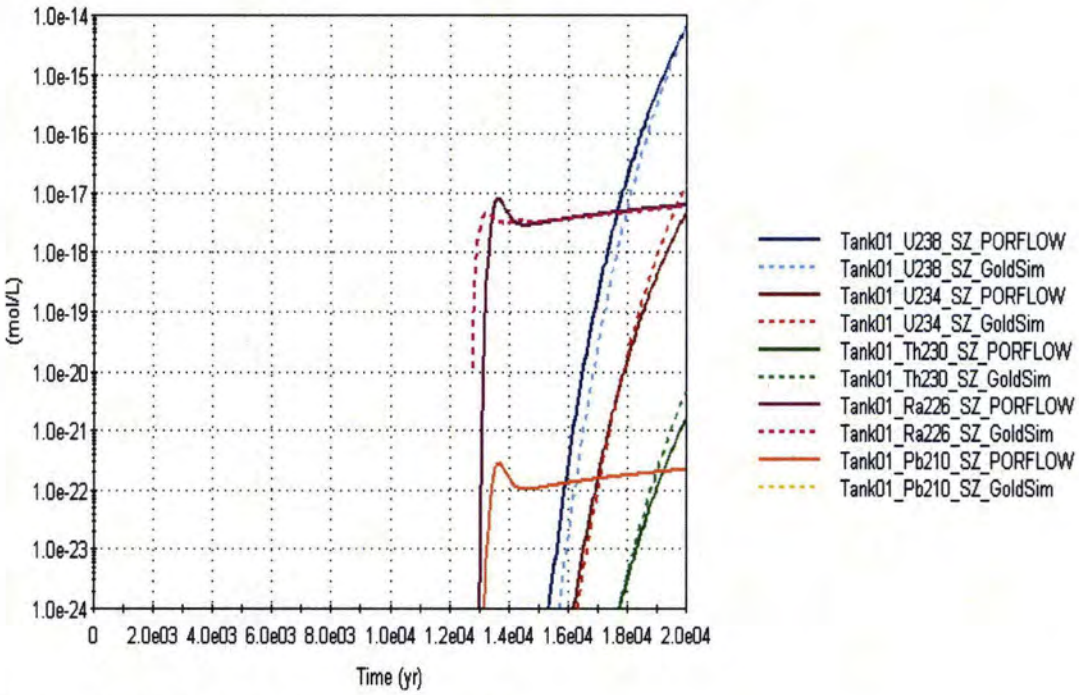

5.6.2.5 PORFLOW Solubility Control

During benchmarking it was determined that PORFLOW does not implement solubility controls for multiple isotopes of the same element. Each isotope of an element is treated independently so that they do not add up to an elemental solubility limit. This is true of the case shown in Figure 5.6-3, where two uranium isotopes, U-238 and U-234 appear in the same decay chain. It is also true with the basic implementation of the PORFLOW model where each isotope is run independently (as a parent). For instance, each plutonium isotope is run as a parent in different simulations. Therefore, the amount of plutonium in solution is based on the single parent when in fact is should be based on the total amount of plutonium in the inventory (Note that this is an issue only if applying solubility controls to the PORFLOW calculation). At the end of this section it will be demonstrated that for the FTF analyses this implementation of the solubility control by PORFLOW is conservative.

Figure 5.6-3: Original Comparison

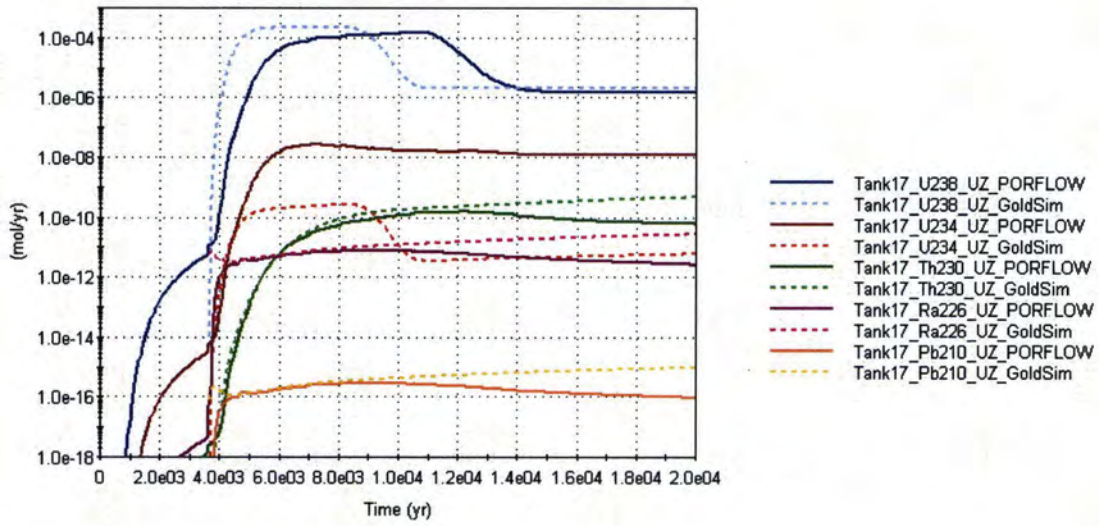

Figure 5.6-3 presents the original comparison of the PORFLOW and GoldSim FTF results. The GoldSim U-234 line has a profile similar to its parent, U-238. This is not the case with the PORFLOW curves. This difference in U-234 behavior raised a question as to why the curves were so different. Review of the PORFLOW inputs revealed that U-234 and U-238 had the same values for their independent solubility limits. Rather than treating the isotopes as the same element they were treated independently, therefore, the solubility limit was essentially doubled. At the present no means has been discovered to implement elemental solubility limits in the current version of PORFLOW.

Figure 5.6-4 shows a comparison in which the GoldSim U-234 solubility limit is specified to be independent of U-238. The GoldSim and PORFLOW U-234 curves essentially overlay. This validates that independent solubilities are used in PORFLOW.

Figure 5.6-4: Modified GoldSim U-234 Solubility

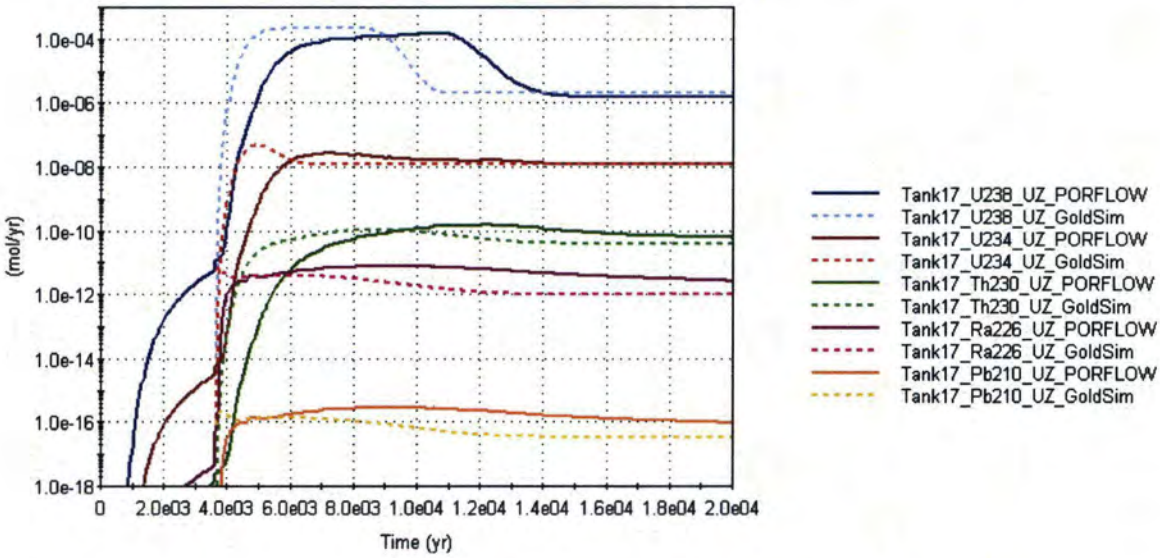

This analysis demonstrates that the PORFLOW FTF model differs from actual expected behavior in the way it addresses solubility control. By running each parent individually, the solubility effects are not apparent. In addition to the uranium isotopes, other radionuclides that could potentially be effected most are the plutonium and thorium isotopes. Even though the solubility control in the PORFLOW FTF model is not elemental, the model results are still valid for use since the solubility control method used allowed more of the contaminant into solution, causing peak doses to occur sooner and with higher peaks. To verify this, two GoldSim model cases were run. Using Configuration A, and a representative waste tank inventory, one case was run with no isotopes, (i.e., every radionuclide has its own, independent solubility limit), and compared it to the run where the solubility limits were run per element.

Figure 5.6-5 shows the effect of the different solubility implementations on the total all-pathways dose. As expected, the independent solubility implementation results in a higher dose. The first peak, around 5,000 years, is driven primarily by Tc-99 which is the lone isotope of that element in the model, hence, the same peak for both implementations. The later peaks come from uranium and plutonium parents, of which there are multiple isotopes.

Figure 5.6-5: Elemental versus Independent Solubility

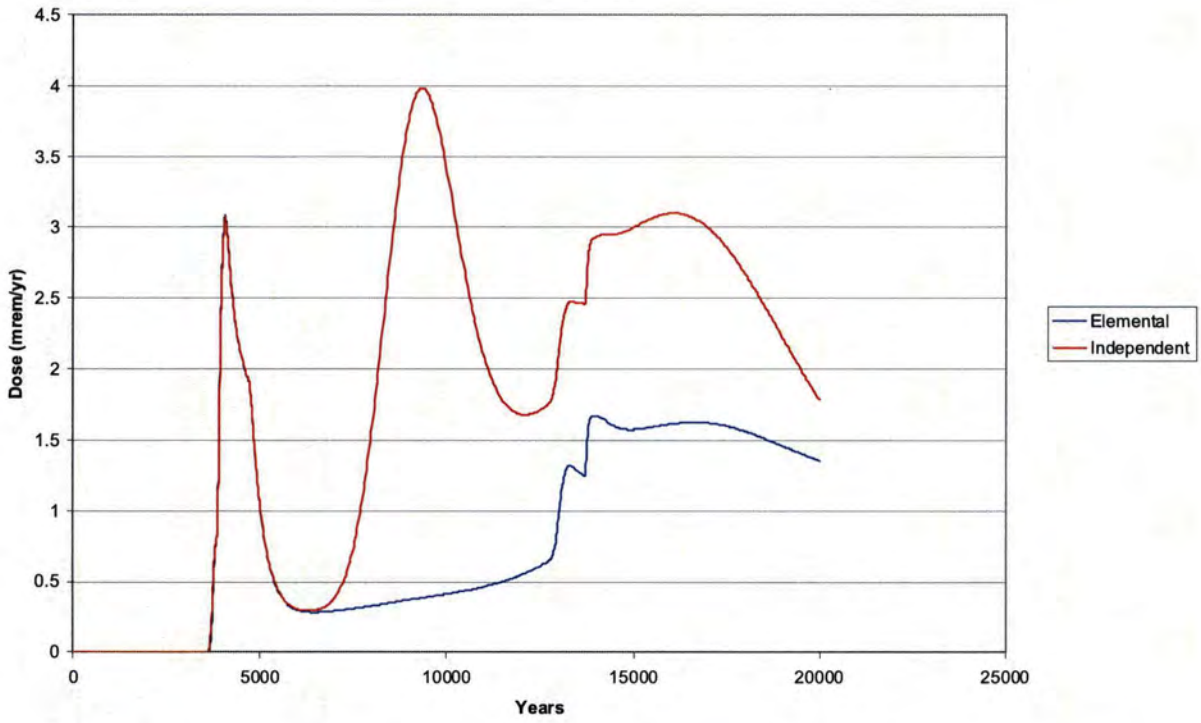

5.6.2.6 Differences Between the PORFLOW FTF and GoldSim FTF Models

Due to inherent differences between the 3-D PORFLOW model and one-dimensional GoldSim model, it was expected that the complete agreement between the models would not be achieved during the benchmarking process. Two areas where model differences remain are detailed below.

- **Movement Upward Into The Grout in the FTF PORFLOW Model**

Figure 5.6-6 presents the comparison of the Np-237 decay chain of Type IV tanks for both models. Type IV tanks are unique in that they have no "solid" roof. When the concrete is assumed to fail, water can begin infiltrating into the tanks grout. According to the PORFLOW model, that water allows for some of the waste to migrate up into the reducing grout, which has a high K_d relative to the waste reducing region solubility limit. As a result, the PORFLOW model shows a slower release of the Np-237 than the GoldSim model. The GoldSim model begins at the waste layer, therefore it does not model this phenomenon. This difference causes the GoldSim FTF model to allow radionuclides to release earlier than would be expected, since their movement into the grout is not modeled.

Figure 5.6-6: Np-237 Comparison for Type IV Tanks

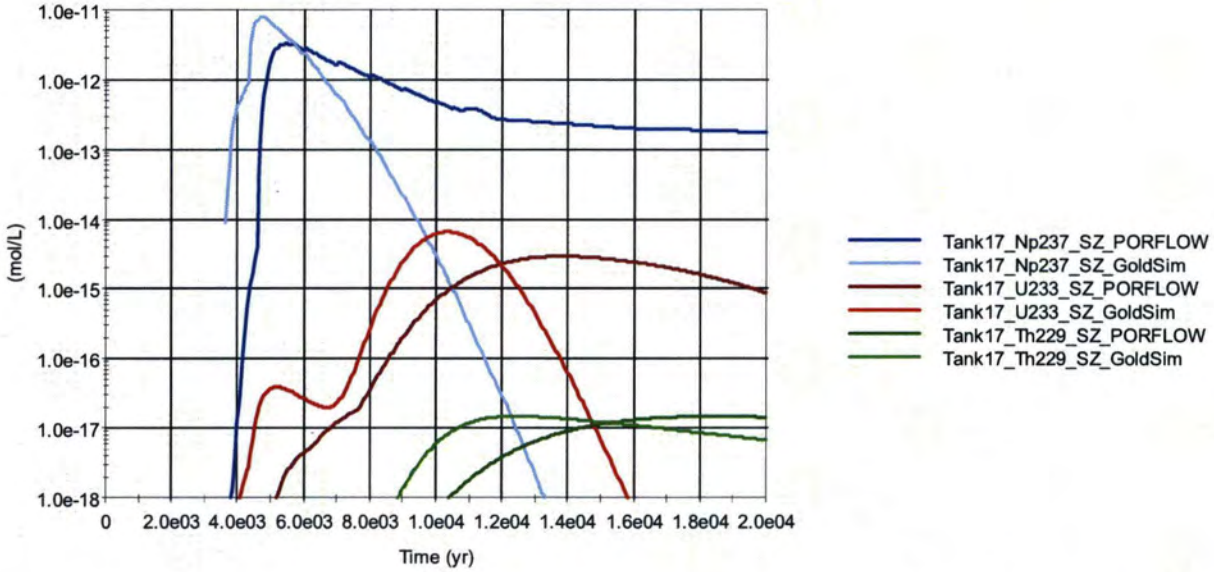

Figure 5.6-7 presents the comparison of Tc-99 curves for both models. While the models agree well, there is the question of the spike which appears in the GoldSim run but not the PORFLOW run. The spike in the GoldSim run is caused by a delay in the transition from reducing to oxidizing pore water by several time steps. This delay does not occur in the PORFLOW run. It is believed that the difference is due to the GoldSim model calculating the transition point explicitly during the run, while in the PORFLOW run it is inferred from a previous analysis and adjusted to fit into one of the model's time periods. Note that this peak occurs for all tank types. As presented in Figure 5.6-3, the difference in solubility transition timing has an insignificant impact on the peaks, and this difference is further minimized by the fact that the FTF probabilistic model considers a range of solubility transition times.

Figure 5.6-7: Tc-99 Comparison

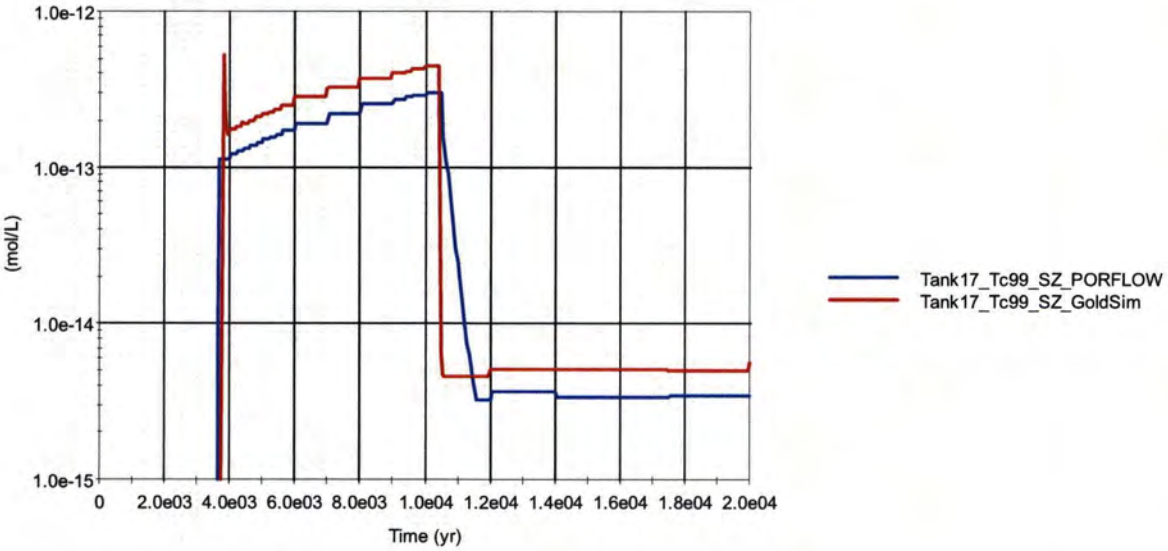

5.6.2.7 Benchmarking Results

Following are the results for the six tanks benchmarked. The results are shown for the saturated zone only, as that is what drives the dose calculation. Note that many of these results are in the distant future and that the concentrations are fractions to thousands of atoms per liter.

Tanks 1, 3, and 5 (Figures 5.6-8, 5.6-9 and Figure 5.6-10, respectively) are quite similar in behavior. Tanks 1 and 3 results are practically identical. Tank 5 is different from the other two, in that its flowstream is into a different PORFLOW region. In order for Tank 5 to be benchmarked, its parameters were altered from the other two tanks. While the Tank 5 curves do not match exactly, they are quite close considering the uncertainty in the calculation.

Tanks 17 and 18 (Figures 5.6-11 and 5.6-12) present the Np-237 behavior. Both of these tanks flow into the same PORFLOW region as Tanks 1 and 3, but since they are much closer to the 100m well, they have different benchmarking parameters.

Tank 34 (Figure 5.6-13) is the final tank to be benchmarked, it flows into a different region than the other five tanks, and therefore has its own set of benchmarking parameters.

Figure 5.6-8: Tank 1 Benchmarking Results

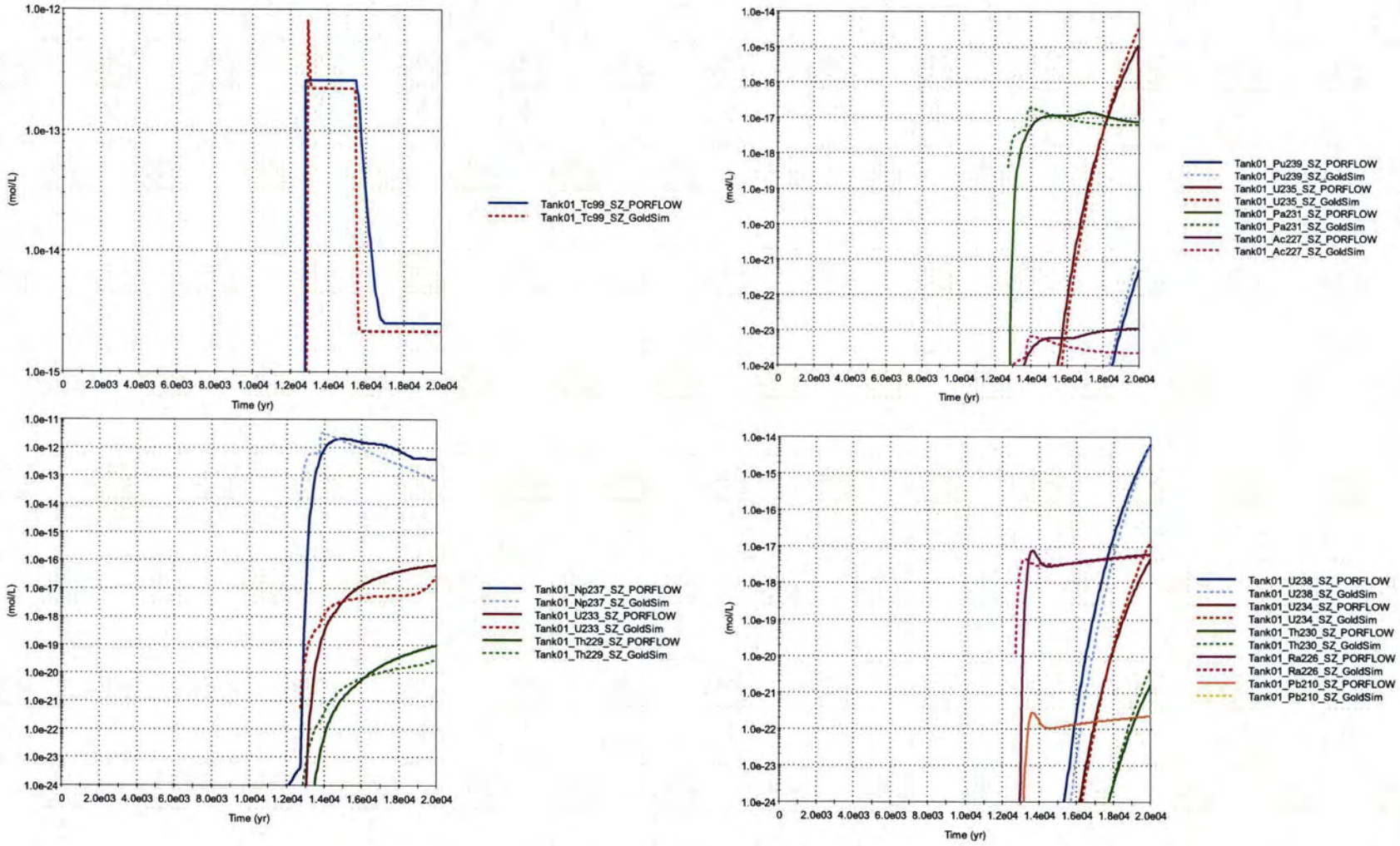

Figure 5.6-9: Tank 3 Benchmarking Results

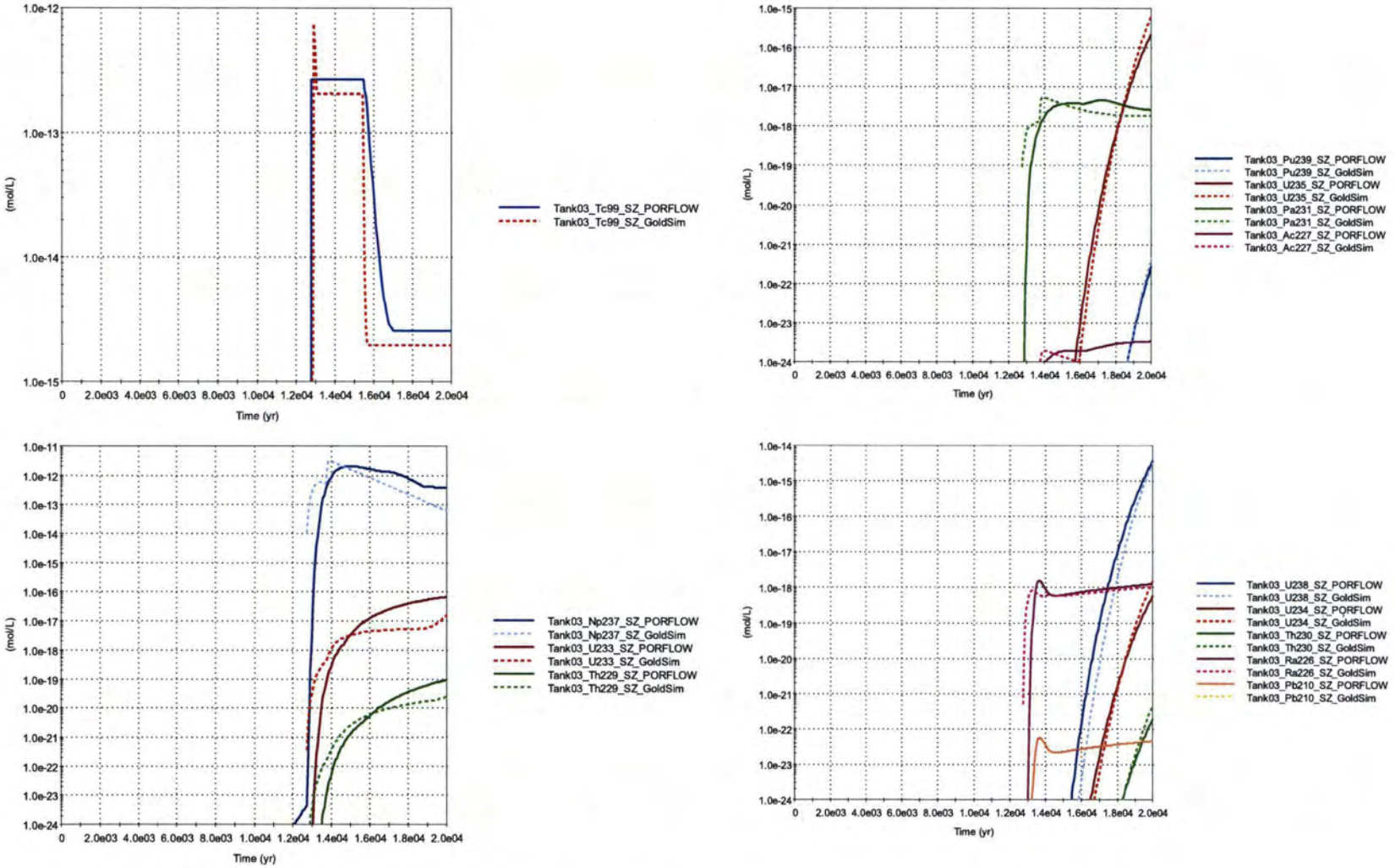

Figure 5.6-10: Tank 5 Benchmarking Results

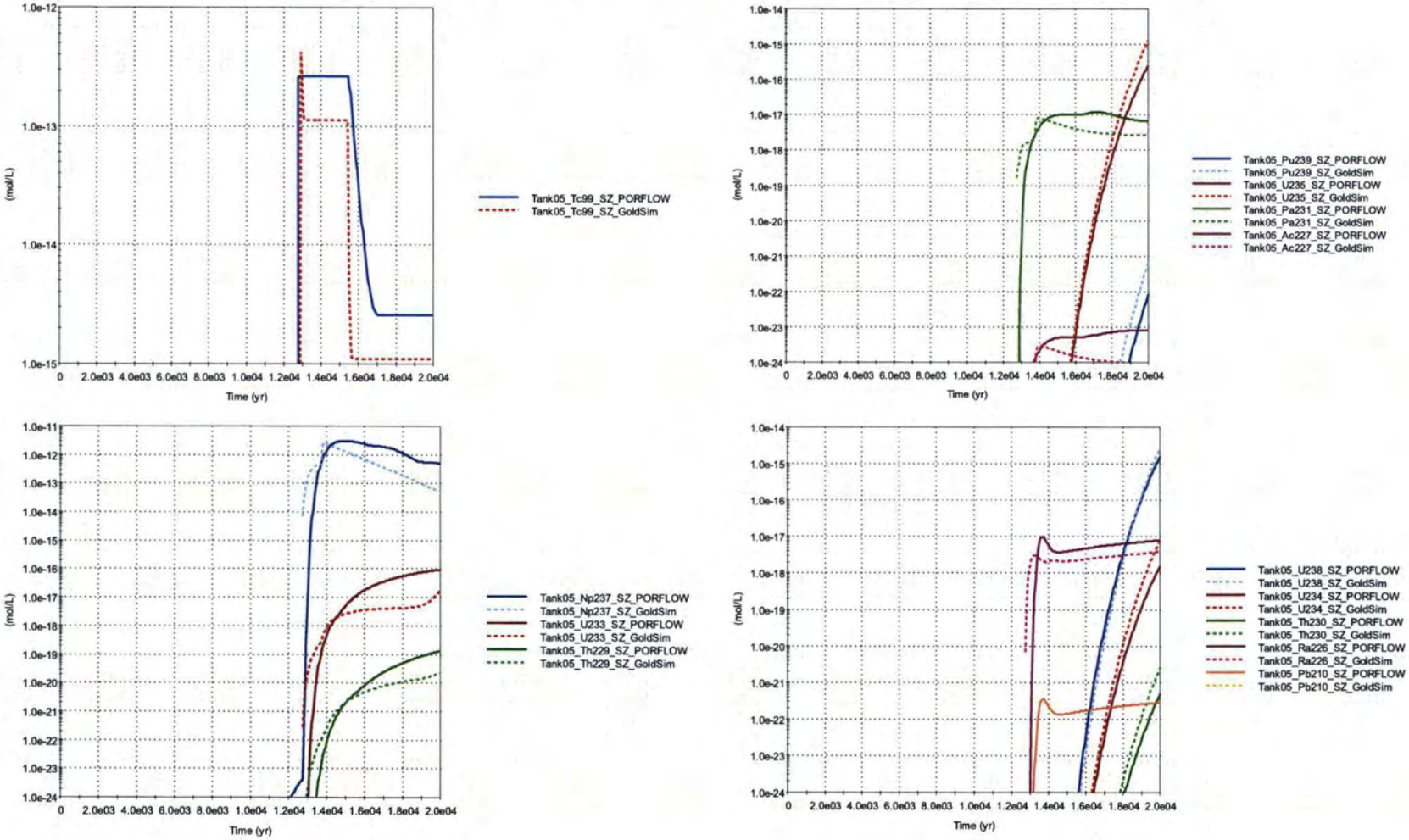

Figure 5.6-11: Tank 17 Benchmarking Results

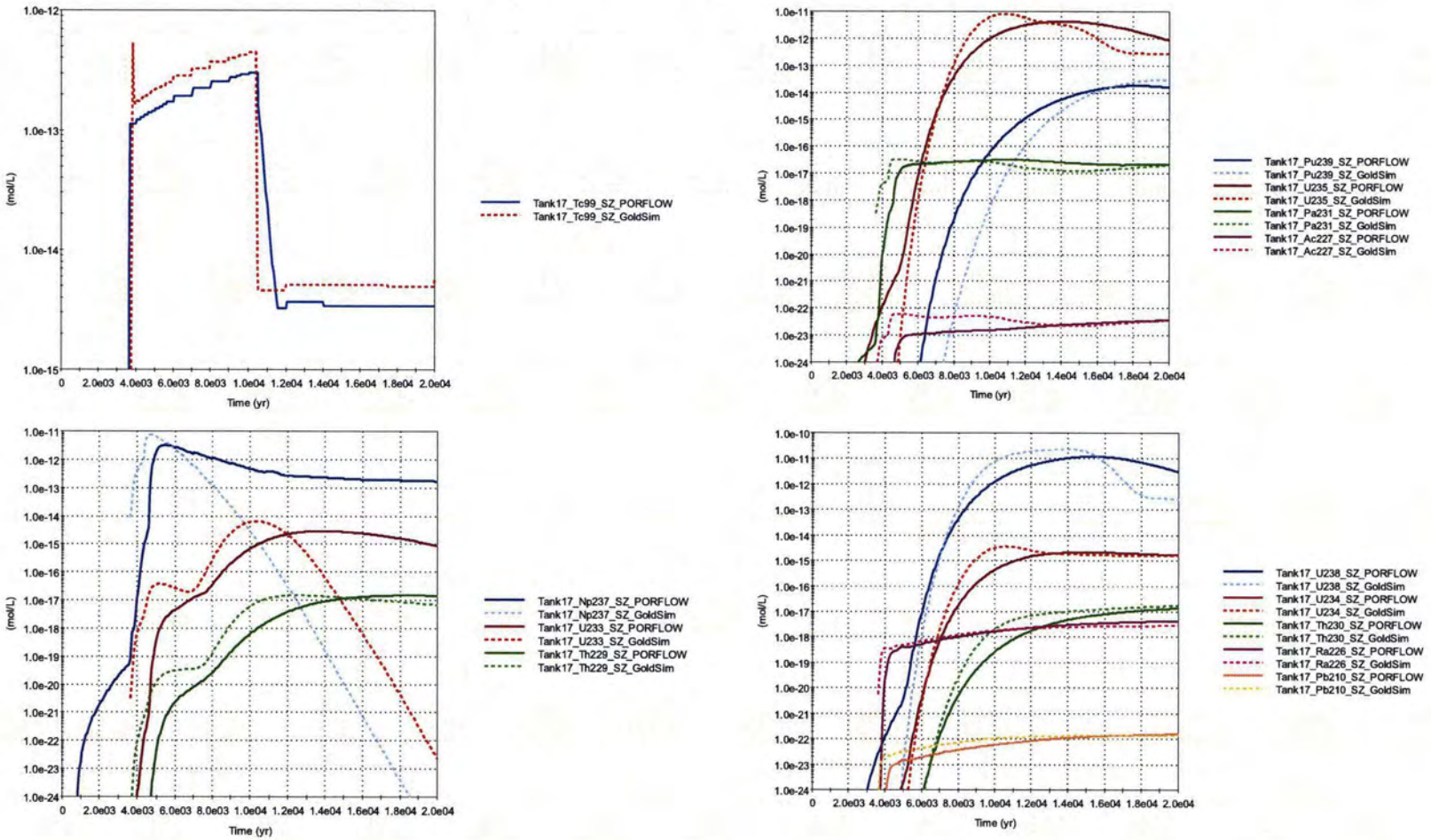

Figure 5.6-12: Tank 18 Benchmarking Results

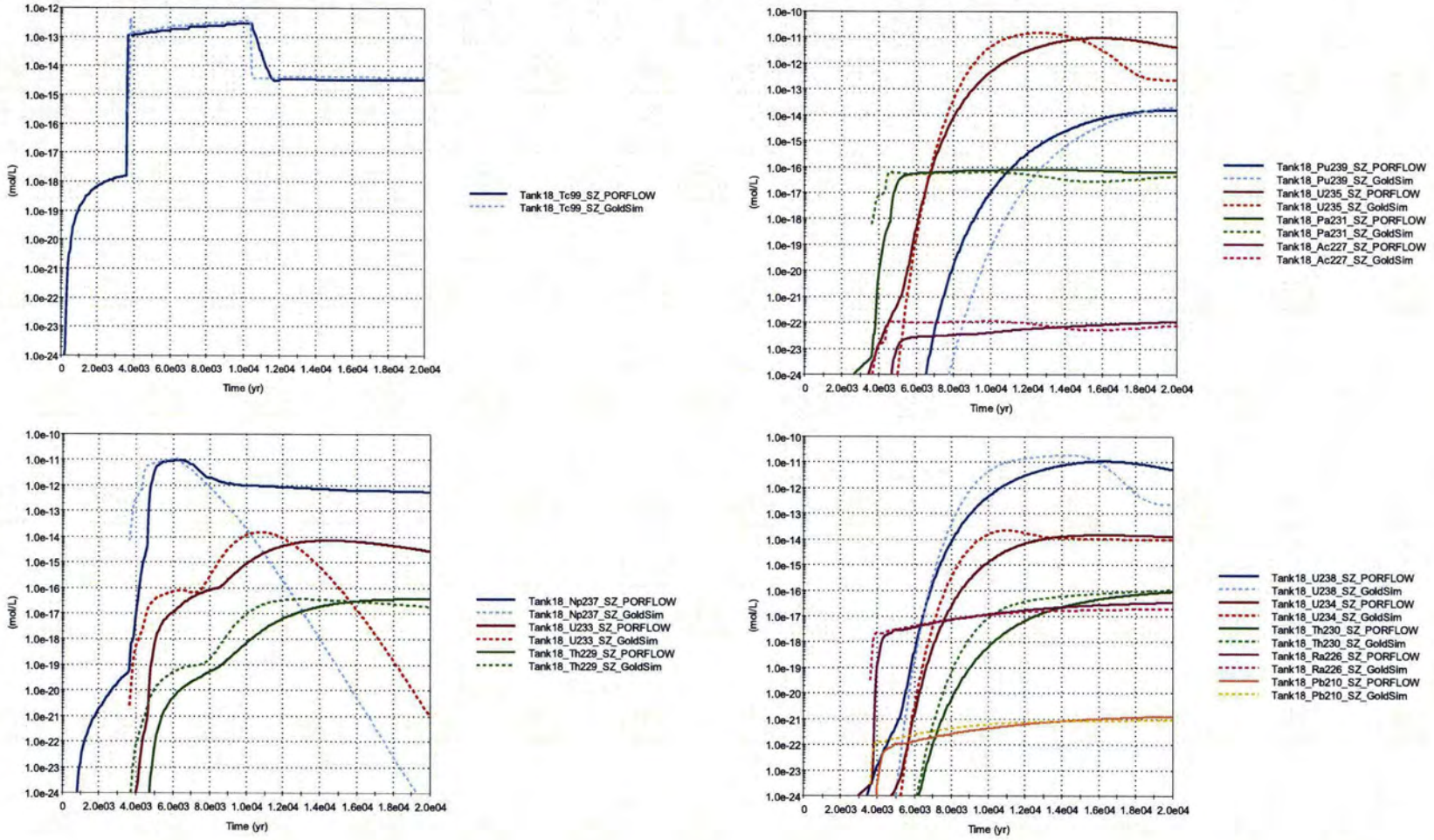

Figure 5.6-13: Tank 34 Benchmarking Results

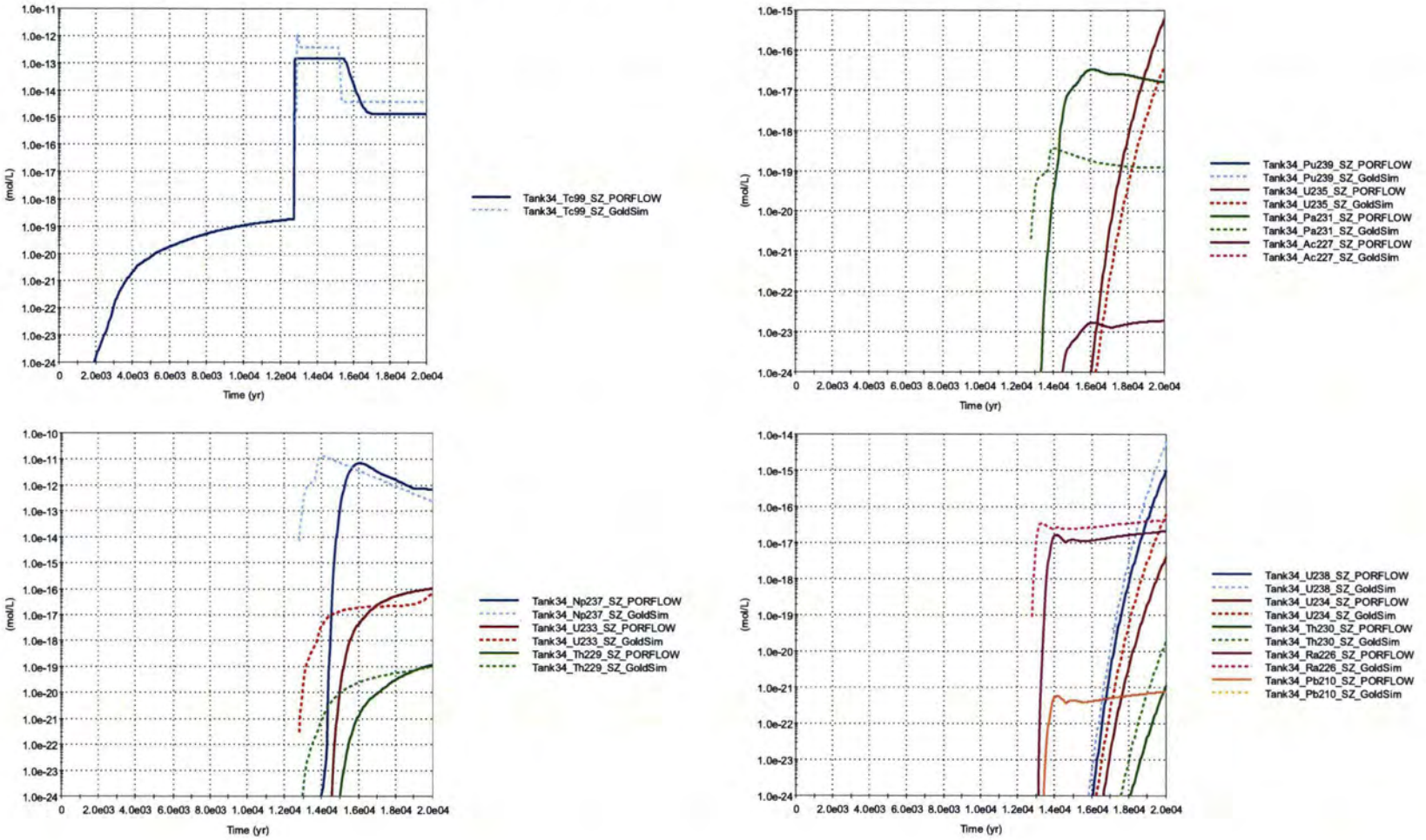

The benchmarking parameters obtained for the individual tanks were applied to groups of tanks based on several criteria, including: distance to the assessment point and PORFLOW region. The results of the benchmarking show that the FTF ISCM results of a multi-dimensional model can be abstracted into a one-dimensional model. The flow fields calculated by PORFLOW are essentially one dimensional in the unsaturated zone and slightly less so in the saturated zone.

In conclusion, the benchmarking provides assurance that the parametric insights revealed through a sensitivity analysis of the GoldSim FTF model are representative of similar parametric insights true in the PORFLOW FTF model. The goal of the benchmarking was to demonstrate a general agreement between overall system behaviors for the two models to provide confidence that the results of the GoldSim FTF model sensitivity and uncertainty analysis could be related to the baseline FTF analysis, which used the PORFLOW FTF model.

5.6.3 Parameters Evaluated in the FTF Probablistic Model

The parameters selected for evaluation in the stochastic analyses were based on modeling experience informed by bases for the selected values and available generic and site-specific data to evaluate the most sensitive parameters. A thorough discussion of the parameters evaluated and the ranges considered is provided in the following discussion.

5.6.3.1 Waste Tank and Ancillary Equipment Configurations

As discussed in Section 4.4.2, six different tank configurations are considered. The scenarios differ based on whether a closure cap or fast flow paths are present, assumptions associated with time of liner failure and cementitious material degradation, and if the water table rises above the CZ. The differences between the six cases are summarized in Table 5.6-2. Depending on the tank type, different probabilities are assumed for each of the potential scenarios (Table 5.6-3). Discrete distributions are chosen using engineering judgment informed by tank design specifics. The tank design differences that informed the probability choices are listed below:

- The fast flow path cases (Configuration C and D) probabilities are much lower than the non-fast flow path cases in general because cracks are not anticipated to occur in the cementitious materials. Any degradation of the cementitious materials that does occur is expected to result in small cracks (which causes increased flow through hydraulic conductivity changes) rather than void spaces. If void spaces develop, it is probable they get filled by material migrating downward from the materials above the void space (e.g., as the cementitious materials degrade). Cracks causing increased flow through hydraulic conductivity changes are modeled independently of the fast flow path cases. In addition, the possibility that fast flow paths might form in the basemat was simulated independently in the GoldSim FTF model through a "Bypass Fraction" (Section 5.6.3.6).

- The "soil only" closure cap configuration (Configuration F), probability is less than the probability associated with Configurations A through E which utilize the engineered closure cap because a closure cap will be in place and will provide some flow retardation. Configuration F reflects the small potential that the closure cap will not perform as designed. Currently, the presumed CERCLA include a closure cap. [http://www.access.gpo.gov/uscode/title42/chapter103_.html]
- Type IV rising aquifer case (Configuration E) probability is higher than other tank types because the Type IV tanks are closer to the water table.
- Type IV fast flow path in the grout case (Configuration C) probability is lower than other tank types because the Type IV tanks do not have cooling coils.
- Type IV fast flow path in the basemat case (Configuration D) probability is higher than the grout fast flow path case (Configuration C) probability because the Type IV tank basemat is relatively thin and has drainage channels which lead to a drain (that is planned to be grouted) at the center of the tank. If the center drain is improperly grouted there is a greater chance of a fast flow path developing though the basemat.
- Type III/IIIA fast flow path in the basemat case (Configuration D) probability is lower than for Type I tanks because the Type I tanks are of an older design. It is assumed that better materials of construction and improved engineering practices for the new Type III/IIIA tanks would provide greater confidence in basemat construction since there is approximately a 20-year difference between the timeframe the different tank types were built.

Table 5.6-2: Tank Scenarios

Configuration	Closure Cap	Liner Failure Date	Fast flow paths	Cementitious Materials Degradation	Water Table
A	Present	Later failure (based on grouted diffusion coefficient of E-6 Ca/O2)	None	Degradation curve based on WSRC-STI-2007-00607	No change
B	Present	Later failure (based on grouted diffusion coefficient of E-6 Ca/O2)	None	Step change at year 501	No change
C	Present	Early failure (based on grouted diffusion coefficient of E-4 Ca)	Channel with no flow impedance through grout (no fast flow path through basemat)	Step change at year 501	No change
D	Present	Early failure (based on grouted diffusion coefficient of E-4 Ca)	Channel with no flow impedance through grout and basemat	Step change at year 501	No change
E	Present	Early failure (based on grouted diffusion coefficient of E-4 Ca)	N/A	Step change at year 501	Above CZ
F	Soil Only (16.45 in/yr)	Later failure (based on grouted diffusion coefficient of E-6 Ca/O2)	None	Step change at year 501	No change

Table 5.6-3: Configuration Probability by Tank Type

Configuration	Probability by Tank Type (a)		
	Type I	Type III/IIIA	Type IV
A	58.25%	60%	54%
B	28%	30%	26%
C	5%	2.5%	1.25%
D	2.5%	1.25%	2.5%
E	5%	5%	15%
F	1.25%	1.25%	1.25%

(a) Discrete distribution chosen using engineering judgment informed by tank specifics. For example Type IV rising aquifer (Configuration E) probability higher based on closeness to water table.

Since the GoldSim FTF model is used only to model contaminant transport, flow profiles over time are calculated for each of the six configurations using the PORFLOW FTF model, as shown in Figures 5.6-14 though 5.6-19. The PORFLOW FTF model flow results are simplified into a one-dimensional steady state flow through the CZ to allow use in the GoldSim FTF model. Having different flow profiles for different cases is the method by which uncertainties in parameters affecting flow (e.g., liner failure date, closure cap infiltration rate, cementitious materials degradation time, water table level) are incorporated into the sensitivity/uncertainty analysis.

Figure 5.6-14: Configuration A Flow Profile

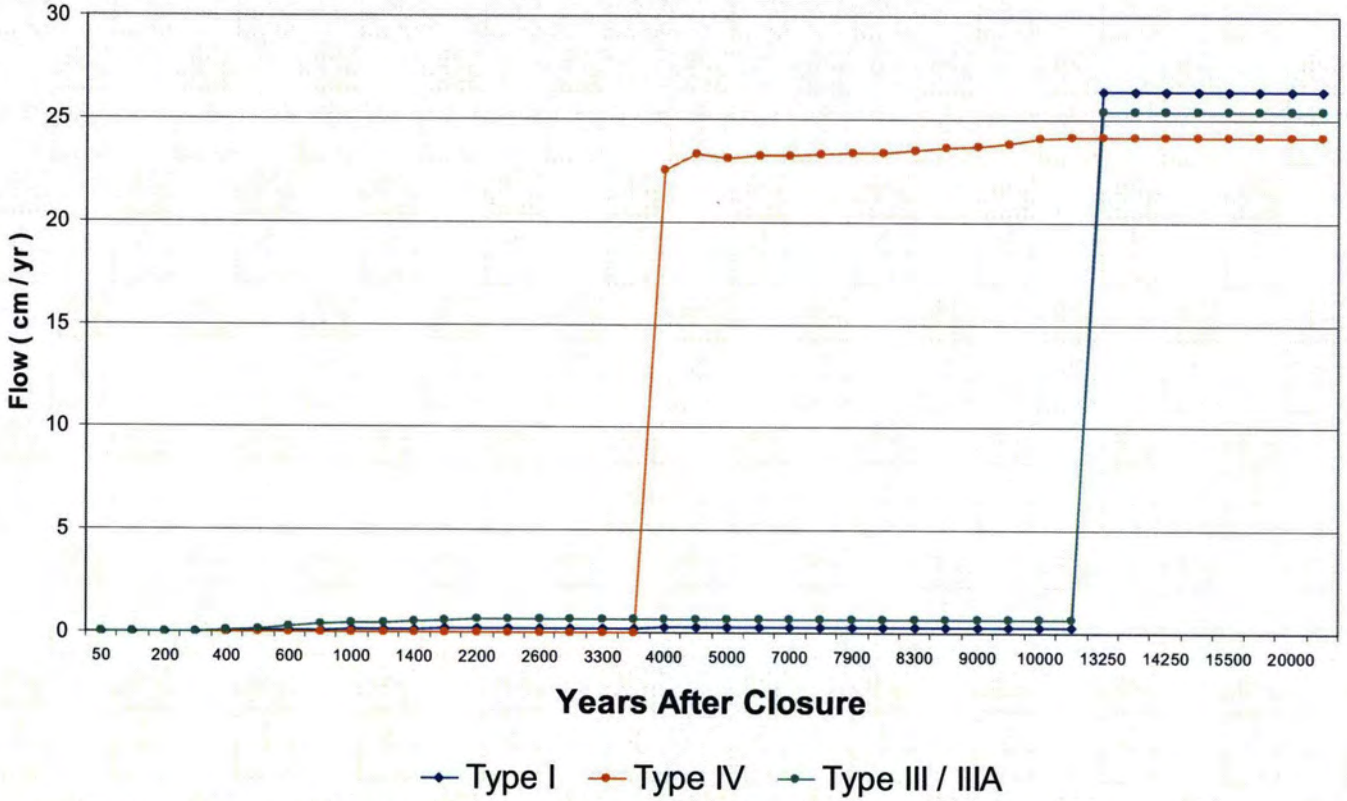

Configuration A: No initial fast flow condition exists, contaminants remain in the CZ until liner failure occurs (3,638 years for Type IV: 12,747 years for Type I; and 12,751 years for Type III/IIIA) and the degradation of the basemat begins at 400 years, 2,600 years, and 4,800 years for Type IV, I, and III/IIIA, respectively. Complete degradation of the basemat is assumed at 63,800 years, 13,000 years, and 18,700 years for Type IV, I, and III/IIIA, respectively.

Figure 5.6-15: Configuration B Flow Profile

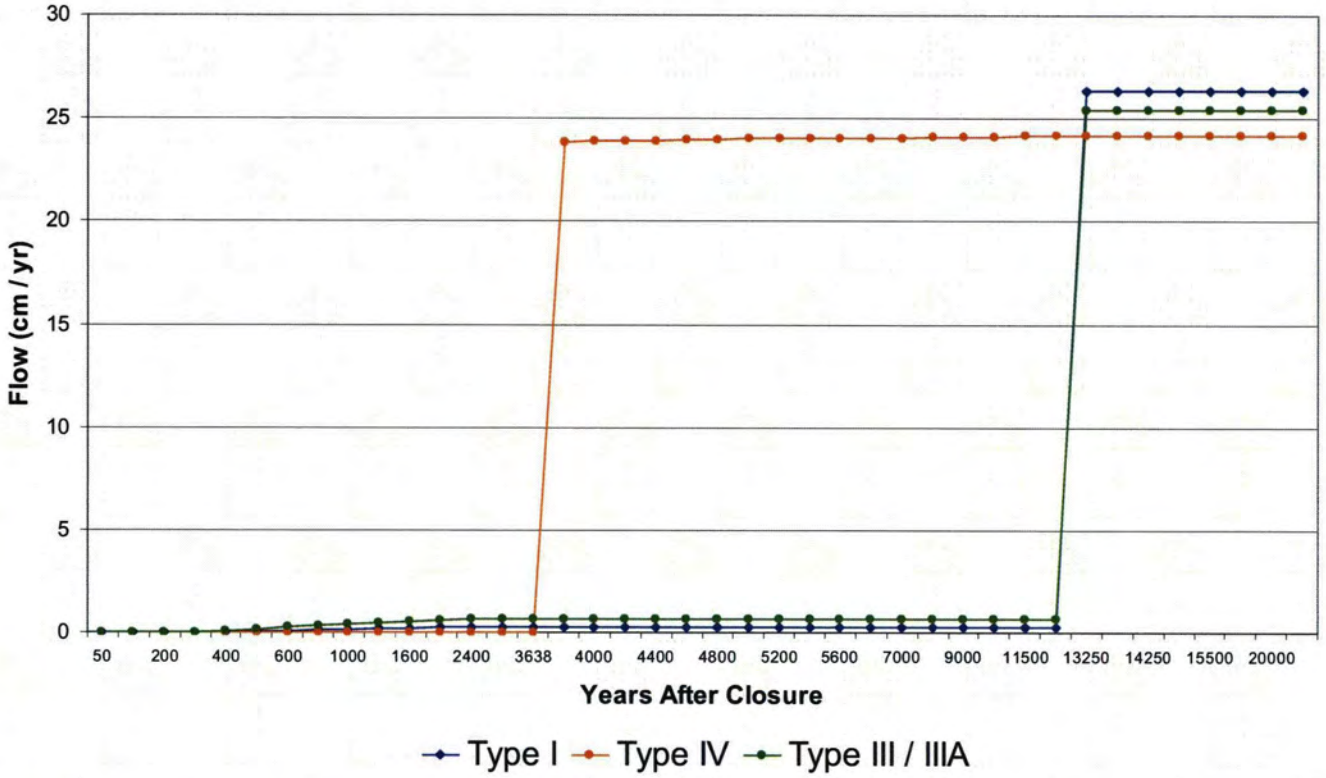

Configuration B: No fast flow condition exists, contaminants remain in the CZ until liner failure occurs (3,638 years for Type IV: 12,747 years for Type I; and 12,751 years for Type III/IIIA) and complete degradation of the basemat occurs at 501 years for all waste tanks.

Figure 5.6-16: Configuration C Flow Profile

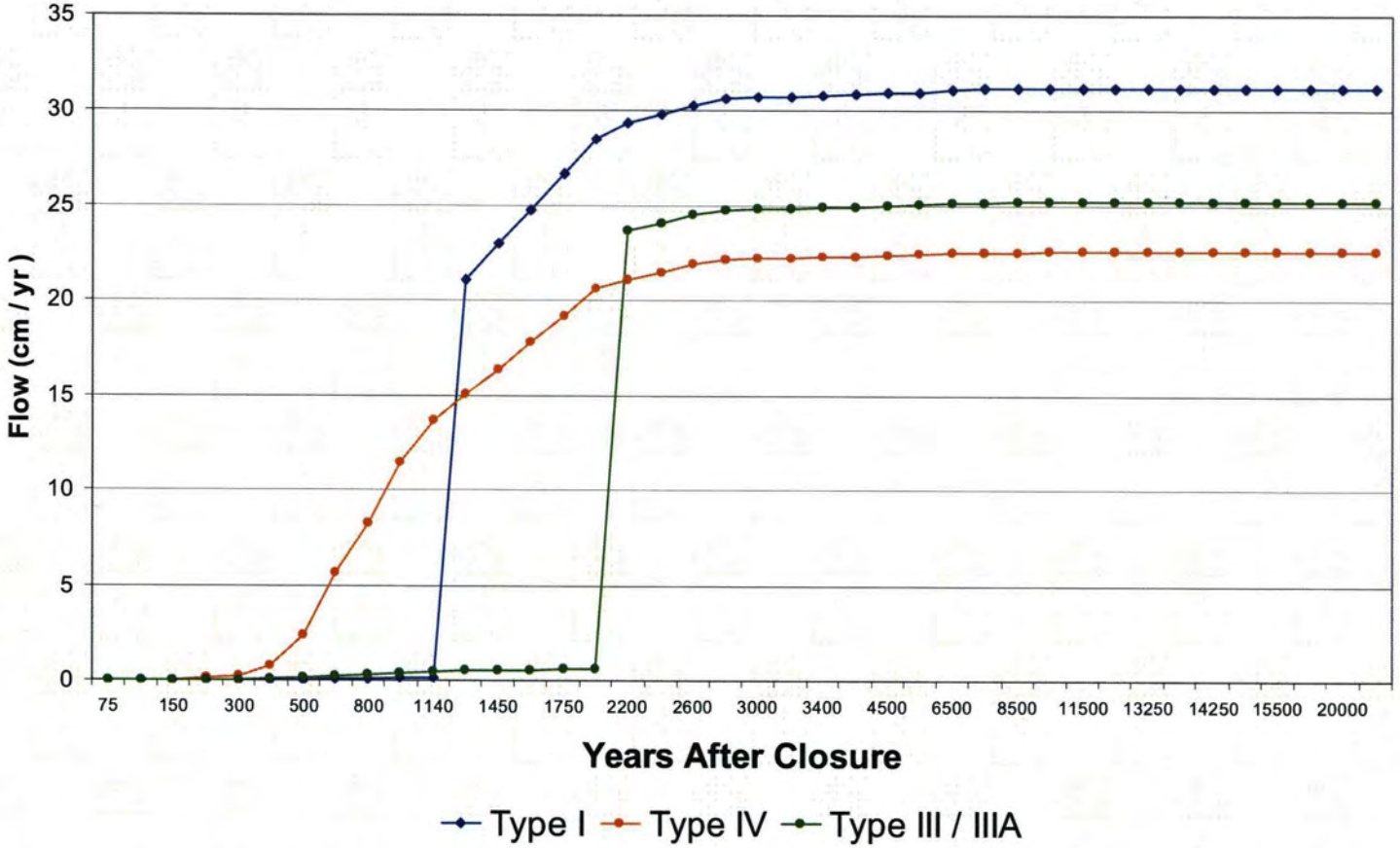

Configuration C: Fast flow condition exists in fill grout, contaminants remain in the CZ until liner failure occurs (75 years for Type IV: 1,140 years for Type I; and 2,077 years for Type III/IIIA) and complete degradation of the basemat occurs at 501 years for all waste tanks.

Figure 5.6-17: Configuration D Flow Profile

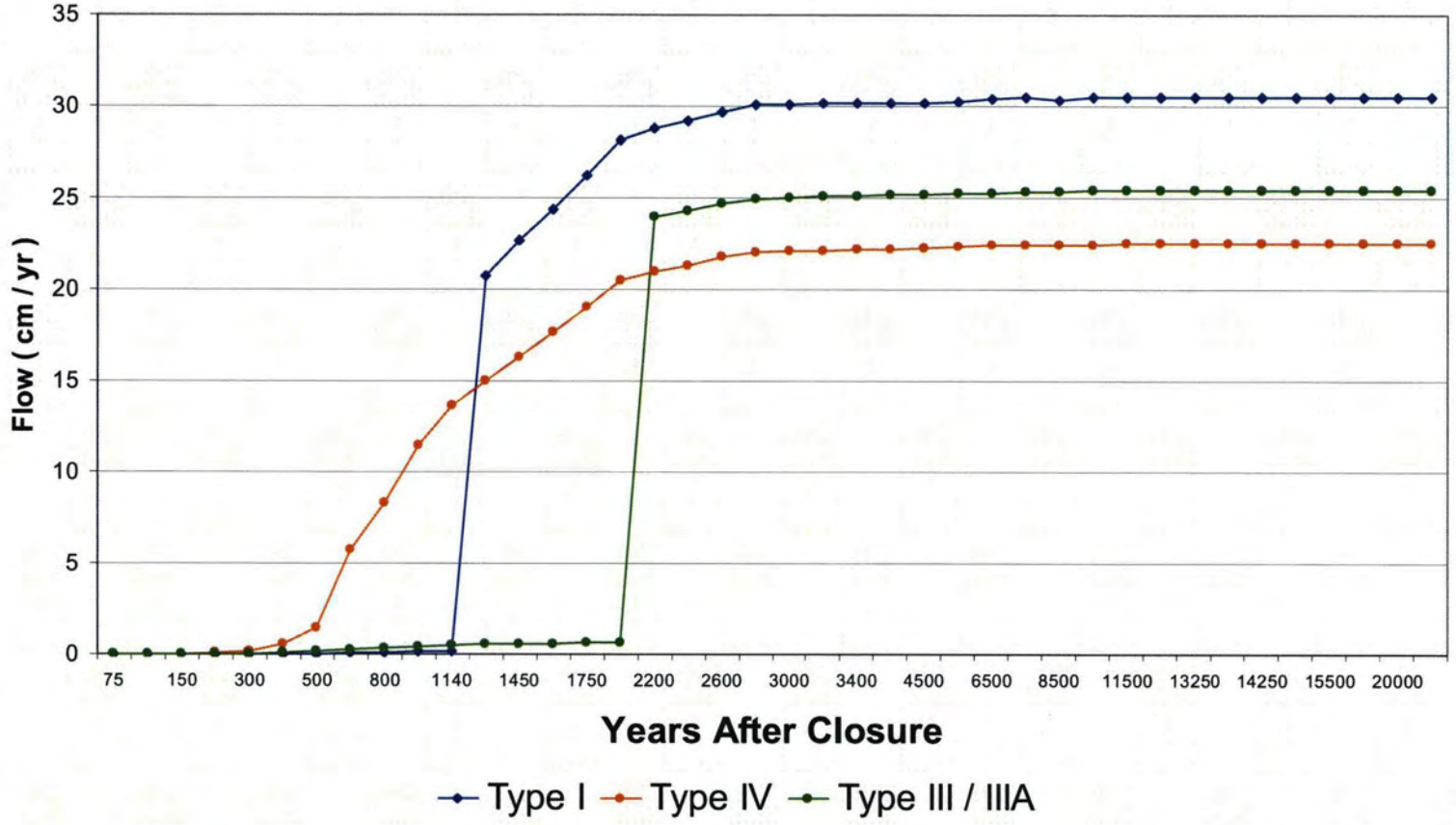

Configuration D: Fast flow condition exists in fill grout and basemat, contaminants remain in the CZ until liner failure occurs (75 years for Type IV: 1,140 years for Type I; and 2,077 years for Type III/IIIA) and complete degradation of the basemat occurs at 501 years for all waste tanks.

Figure 5.6-18: Configuration E Flow Profile

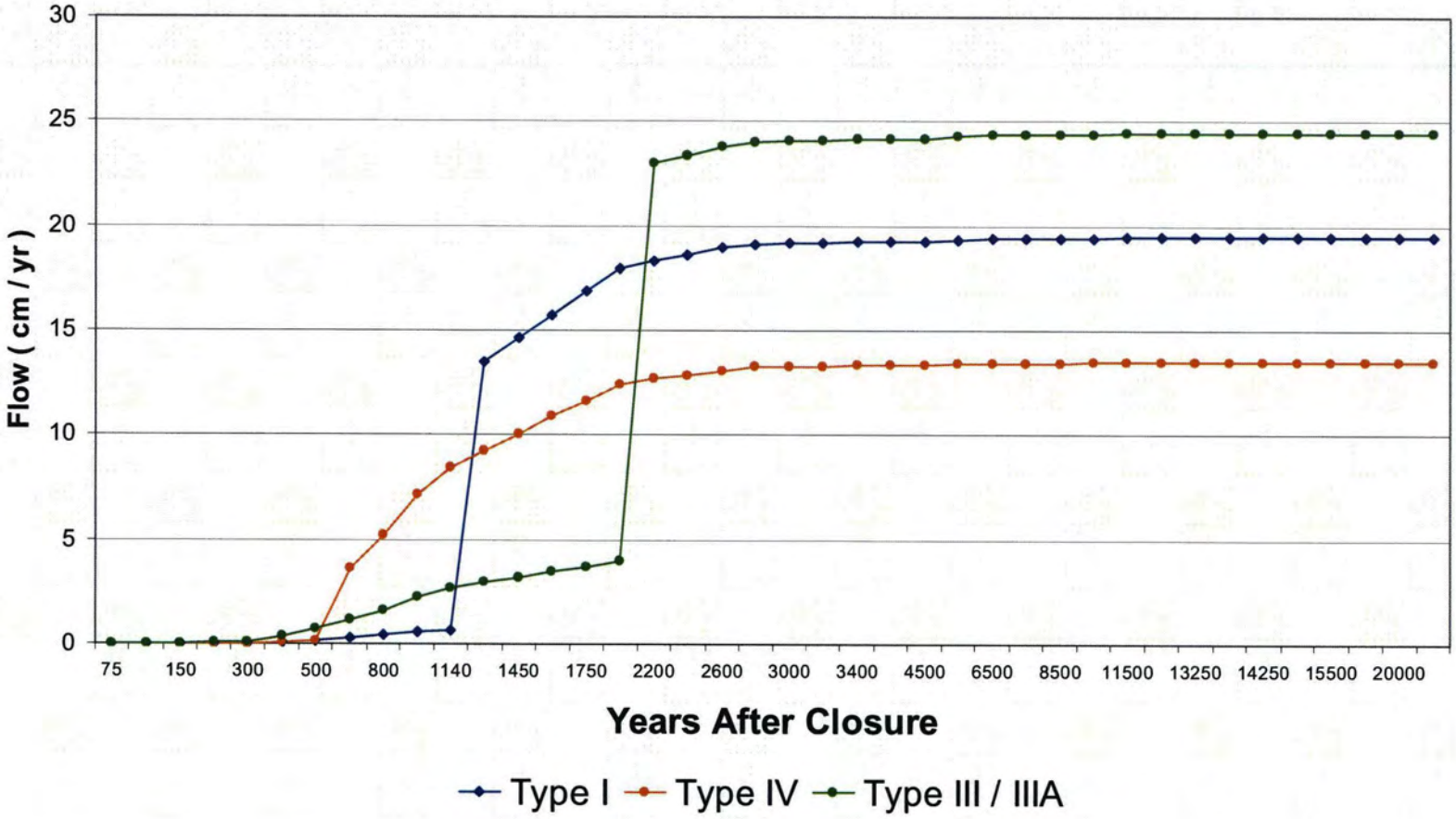

Configuration E: No fast flow conditions exist; however, the water table rises to a level above the tank bottom thus steel degradation starts at time of closure and complete degradation of the basemat occurs at 501 years for all waste tanks.

Figure 5.6-19: Configuration F Flow Profile

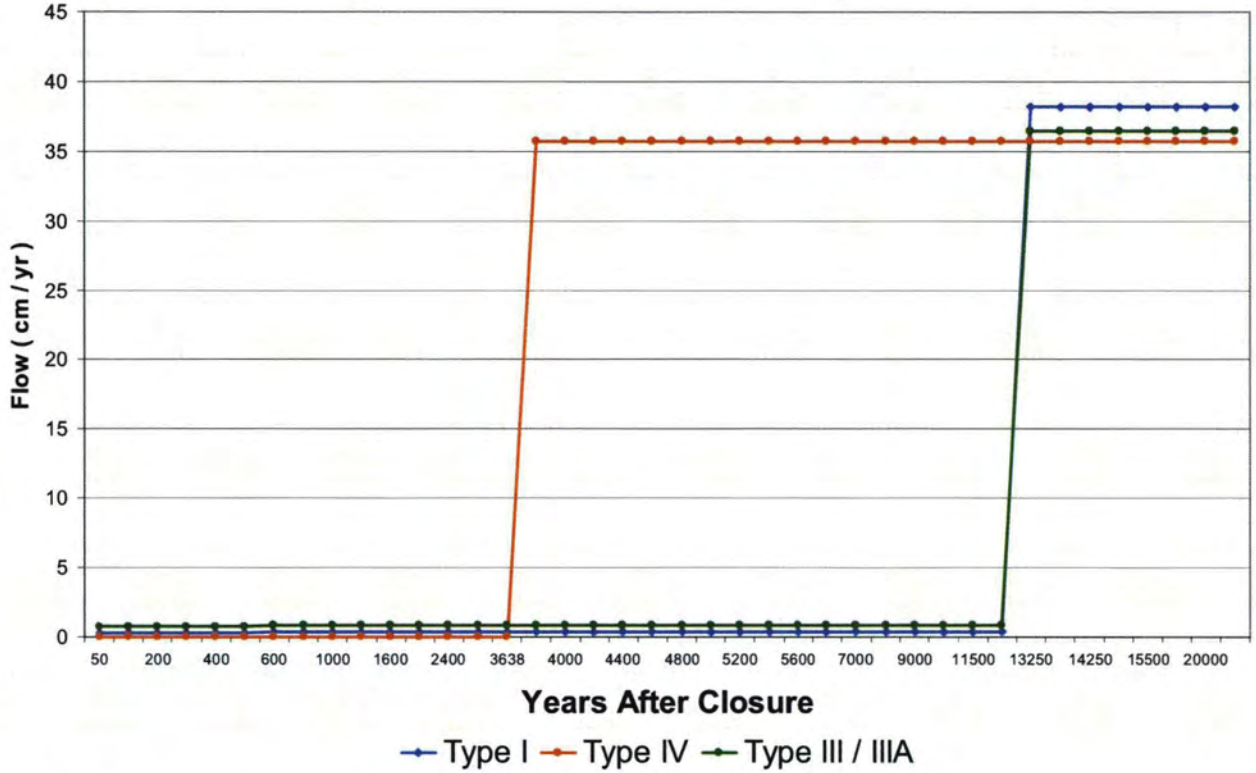

Configuration F: Like Configuration B except with a "Soils Only" closure cap. The FTF ancillary equipment consists of seven separate point sources (FPT-1, FPT-2, FPT-3, 242-F, 242-16F, CTS tank, and FTF catch tank) and a network of waste transfer lines represented by waste distributed over the entire FTF. As discussed in Section 4.4.2, only one ancillary equipment scenarios was analyzed. Each individual piece of ancillary equipment is modeled as source in a completely intact steel containment at the time of closure. The contaminant release is assumed to occur when the stainless steel fails. A single flow profile over time is calculated for ancillary equipment modeling. The impact of liner failure date on both tank and ancillary equipment contaminant transport was addressed independently of flow through the liner failure stochastic.

5.6.3.2 Radiological and Chemical Inventory

The waste tank and ancillary equipment inventories in the GoldSim FTF model control the total amount of contaminants available for release. Sections 3.3 and 4.2.1 describe the bases for estimates of residual radiological and chemical inventory in the FTF waste tanks and ancillary equipment. The baseline inventory used for each radionuclide and chemical is listed in Table 3.3-2 and Table 3.3-3. In the probabilistic analyses of this parameter, the inventories of each radionuclide and chemical were increased to one order of magnitude above baseline inventory and decreased to two orders of magnitude below the baseline inventory. These ranges are based on data from radionuclide predictions and actual sample results for Tanks 5, 18, and 19, displayed in Figure 3.3-3. An explanation as to why the predicted values are generally over-estimated and a general discussion of the uncertainties associated with inventory estimation are provided in more detail in Section 3.3.2.4.

The discrete distribution used for radiological and chemical inventory sensitivity analysis is shown in Table 5.6-4.

Table 5.6-4: Inventory Multipliers

Value (a)	Probability
0.01	0.25
0.1	0.25
1	0.25
10	0.25

(a) These values will be multiplied by the baseline inventories from Table 3.3-2 and Table 3.3-3 to account for radiological and chemical inventory uncertainty.

5.6.3.3 Solubilities

The waste solubility values in the GoldSim FTF model control contaminant release, with different solubility values resulting in different release rates. Table 4.2-10 (from Section 4.2.2) shows baseline solubility values and controlling phases for all of the elements of interest at each of the chemical states of interest. For plutonium, technetium and uranium, the solubility values listed correspond to Fe co-precipitation (discussed in detail in Section 4.2.2) as the controlling mechanism. As discussed in Section 4.2.2, there are uncertainties in the calculation of the solubilities. Much of the uncertainty is because of unknowns related to the CZ and how the conditions it will experience will evolve with time. Uncertainty in implementation of the solubility conceptual model was managed to a large extent through conservatism in modeling assumptions. As discussed in Section 4.2.2, uncertainty in choice of the solubility controlling phase (which is the largest uncertainty in calculating solubilities) was addressed primarily through conservatism in choice of the controlling phase. For those radionuclides which have in the past been of most concern (plutonium, uranium, neptunium, and technetium), distributions were assigned for Region II conditions (Reducing and Oxidizing). Tables 4.2-13 and 4.2-14 show distribution for different phases for plutonium, uranium, neptunium, and technetium, where the probabilities are weighted to account for the possibility of different phases. In addition, the possibility of Fe co-precipitation controlling

was factored into the plutonium, technetium, and uranium probabilities. The probabilities chosen are based on observations in the literature, thermodynamic stability, etc.

5.6.3.4 K_d Values

The tank basemats and soil under the FTF in the GoldSim FTF model retard contaminant transport, with their effectiveness tied to the assigned K_d values (which will vary for different elements). Tables 4.2-29 and 4.2-33 show baseline K_d values for all of the elements of interest at each of the chemical states of interest (e.g., different Reducing/Oxidizing Regions). Distributions for the K_d values used in the FTF GoldSim modeling are based on the approach described in SRNL-SCS-2007-00011. This report documents lognormal fits of groundwater distributional parameters for selected elements. The distribution selection is predicated on whether the applicable K_d value is less than or greater than 1,000. The bounds of the distributions are calculated by dividing the expected value by 3.3 for the lower bound, and multiplying by 3.3 for the upper bound if the expected K_d is greater than 1,000 mg/L. The factor is 1.9 if the expected K_d is less than 1,000 mg/L.

5.6.3.5 Basemat Thickness

The basemat thickness in the GoldSim FTF model retards contaminant transport, with its effectiveness related to the basemat K_d values and the basemat thickness. Section 4.4.1 shows the design dimensions used in baseline modeling for the various tank types, including concrete basemat thickness. Section 3.2.1 provides design details for the various tank types, including details regarding the concrete basemat designs. The basemat thickness specified on construction drawings is used as the most likely basemat thickness, with other design details used to determine a probable maximum and minimum thickness of basemat concrete. A triangular distribution using these maximum, minimum and the most likely value as the peak was utilized for basemat thickness in the stochastic analysis. The design details used in determining the various thicknesses are described below for each tank type.

- **Type IV Tank Concrete Floor Thickness** As described in Section 3.2, Type IV waste tanks basemat was specified to be four inches thick with a tolerance of plus 0.5 inch and minus 0.5 inch. A three inch cement topping was then poured over the basemat and given a float and trowel finish having a maximum tolerance of plus or minus 0.125 inch from a true level. Drainage channels, 1.625 inches deep and approximately 3.5 inches wide (3.625 inches at the top and 3.125 inches at the bottom, for use in leak detection were formed in the basemat's three inch deep cement topping. The drainage channels cover less than six percent of the total foundation area.

Thickness calculations:

Minimum at channel location thickness - 5 inches (3.75 + 2.875 – 1.625)
Minimum w/o channel – 6.625 inches (3.75 + 2.875)
Median at channel location - 5.375 inches (3 + 4 – 1.625)
Median w/o channel – 7 inches (3 + 4)
Maximum at channel location – 6 inches (4.5 + 3.125 – 1.625)
Maximum w/o channel – 7.625 inches (4.5 + 3.125)

Modeling Values Used:

	Inches	Basis
Most likely	6.9025	Weighted median (0.06 (5.375) + 0.94 (7))
Minimum	6.5275	Weighted minimum (0.06 (5) + 0.94 (6.625))
Maximum	7.5275	Weighted minimum (0.06 (6) + 0.94 (7.625))
Mean	6.9858	Based on triangular distribution

➢ **Type I Tank Concrete Floor Thickness**

As described in Section 3.2, the working slab for a Type I tank is 4 inches thick. The working slab assumed tolerance is plus 0.5 inch and minus 0.5 inch based on requirement Spec 3019 requirement of no visual variance in concrete level. A 1.5 feet thick layer of tank plaster and membrane waterproofing sits above the working slab. A 30 inch reinforced concrete base (i.e., the basemat) sits on top of the working slab. The basemat assumed tolerance is plus 1 inch and minus 1 inch based on requirement Spec 3019 requirement of no visual variance in concrete level. A 3 inch layer of grout sits on top of the basemat, and the primary container sits above the grout.

Modeling Values Used:

	Inches	Basis
Most likely	30	30 inch basemat
Minimum	29	30 inch basemat – 1 inch tolerance on basemat
Maximum	40	4 inch working slab + 0.5 inch tolerance on working slab + 1.5 inch plaster + 30 inch basemat + 1 inch tolerance on basemat + 3 inch grout layer
Mean	33	Based on triangular distribution

➢ **Type III Tank Concrete Floor Thickness**

As described in Section 3.2, Type III tanks have a 4 inch working slab. The Type III tank basemat, made of reinforced concrete, has a 3 foot - 6 inch minimum thickness (5 foot - 4 inches at drop panel at tank center). The concrete finish shall have a tolerance of 0.125 inches per 10 feet per standard Specification SB-10-U. The basemats in Type III tanks do not have leak detection slots.

Modeling Values Used:

	Inches	Basis
Most likely	42	42 inch basemat (ignore drop panel)
Minimum	41.5	42 inch basemat – 0.5 inch tolerance on basemat
Maximum	46.5	4 inch working slab + 42 inch basemat + 0.5 inch tolerance on basemat (ignore drop panel)
Mean	43.3	Based on triangular distribution

- **Type IIIA Tank Concrete Floor Thickness** As described in Section 3.2, Type IIIA tanks have a 4 inch working slab. The Type IIIA tank basemat has a 3 foot - 7 inch minimum thickness (6 feet - 4 inches at drop panel at tank center). The concrete finish shall have a tolerance of 0.125 inch per 10 feet per standard Specification SB-10-U. A grid of two inch deep interconnected radial channels is grooved into the concrete basemat upon which the secondary liner rests.

Modeling Values Used:

	Inches	Basis
Most likely	41	43 inch basemat – 2 inch drainage channels (ignore drop panel)
Minimum	40.5	43 inch basemat – 2 inch drainage channels – 0.5 inch tolerance on basemat
Maximum	45.5	4 inch working slab + 43 inch basemat – 2 inch drainage channels + 0.5 inch tolerance on basemat (ignore drop panel)
Mean	42.3	Based on triangular distribution

5.6.3.6 Basemat Fast Flow

In order to reflect the possibility that fast flow paths might form in the basemat, a "Bypass Fraction" was simulated in the GoldSim FTF model. The bypass fraction allowed a percentage of the basemat to have no retardation (K_d = 0 for all elements). The bypass fraction was represented by a triangular distribution based on engineering judgment, with 0% being set as the most likely value and the upper bound set at 10%. This judgment is based on the fact that cracking in the basemat might possibly lead to some void spaces forming all the way through the basemat, but it was judged much more likely that the cracking would tend to be self-sealing and would not create full channels. Assuming a full 10% of the basemat was replaced by a void space that had no retardation effect was conservative.

5.6.3.7 Tank and Ancillary Equipment Containment Failure Dates

The containment failure dates in the GoldSim FTF model control initial contaminant release from the associated location (tank or ancillary equipment) and to limit the number of pore volume passing through the tank grout (by restricting flow though the tank grout). Table 4.2-35 shows the deterministic (i.e., single value) and probabilistic (i.e., distribution) values that are used to determine liner failure during modeling. The results corresponding to the reasonably bounding diffusion rates (1.0E-6 cm2/sec) were utilized for the modeling cases where there were no fast flow paths through the cementitious materials (Configurations A, B

and F). The results corresponding to the maximum evaluated diffusion rates (1.0E-4 cm2/sec) were utilized for fast flow case modeling (Configurations C and D) and for the rising aquifer modeling case (Configuration E), where the loss of reducing capability for the cementitious materials might be expected to occur sooner. The waste tank liner failure distributions used for the various tank types and cases are taken directly from the probabilistic analysis presented in WSRC-STI-2007-00061.

Each piece of ancillary equipment (with the transfer lines being treated as a collective inventory) is assumed in the model to fail independently, with the failure time occurring between the time of first pit penetration (116 years) and 100% pitting penetration (approximately 1,000 years). The most probable time of ancillary equipment failure in the probabilistic FTF analysis was assumed to be the time of 25% pitting penetration (510 years). A triangular distribution using these maximum and minimum and the most likely value as the peak was utilized for ancillary equipment containment failure in the stochastic analysis. More details concerning ancillary equipment containment failure are described in Section 4.2.3.2 and WSRC-STI-2007-00460.

The diffusion rates utilized for all cases are considered bounding (i.e., faster than are typically reported.

5.6.3.8 Transition Times between Chemical States

The "Transition Times between Chemical States" in the GoldSim FTF model determine how many pore water volumes are required to pass through the waste tank before the grout transitions to a different tank chemistry. As part of the waste release modeling (discussed in detail in Section 4.2.2), the estimated transition times between various chemical phases was calculated for the waste tank pore water. The waste tank pore water chemistry was calculated to change from Region II Reducing conditions to Region II Oxidizing conditions after 371 pore volumes pass through the reducing grout. The change from Region II conditions to Region III conditions was calculated to occur after 2,063 pore volumes (Table 4.2-1). [ISSN 1019-0643, WSRC-STI-2007-00544] A triangular distribution using these calculated values (which are used as the most likely values in the baseline) as a peak is utilized in the stochastic analysis for analyzing the "Transition Times between Chemical States". The maximum and minimum values chosen for the distribution for the first transition were "482" and "260". The maximum and minimum values chosen for distribution of the second transition were "3,095" and "1,032". The 30% and 50% variation provided by these values was judged reasonable to provide a distribution that showed the effects of uncertainty without overwhelming the sensitivity analysis.

5.6.3.9 FTF Lower Vadose Zone Thickness

The lower vadose zone in the GoldSim FTF model retards contaminant transport, with its effectiveness related to the soil K_d values and the vadose zone thickness. Table 4.2-23 shows the values used in the baseline analysis for thickness of the lower vadose zone beneath each of the waste tanks. A minimum and maximum variation from this most likely thickness was developed based on WSRC-TR-2005-00131, which concluded that the maximum water table elevation rise at the Saltstone Disposal Facility (SDF) would be 12 feet, and the fact that the closure cap over the entire FTF will tend to cause a localized water table drop during the life

of the closure cap. A triangular distribution using these maximum, minimum and the most likely value as the peak was utilized for ancillary equipment containment failure in the stochastic analysis. The FTF lower vadose zone thickness distribution values are presented in Table 5.6-5.

Table 5.6-5: FTF Lower Vadose Zone Thickness Distribution

Tank Type	Tank Number	Most Likely Lower Vadose Zone Thickness; feet (Base Case)	Minimum Lower Vadose Zone Thickness; feet (a)	Maximum Lower Vadose Zone Thickness; feet
I	1	13.5	1.5	25.5
	2	13.1	1.1	25.1
	3	12.1	0.1	24.1
	4	11.7	0.1	23.7
	5	10.6	0.1	22.6
	6	10.2	0.1	22.2
	7	9.4	0.1	21.4
	8	9	0.1	21
IV	17	2.5	0.1	14.5
	18	2.1	0.1	14.1
	19	1.7	0.1	13.7
	20	1.2	0.1	13.2
III	33	17.4	5.4	29.4
	34	17.1	5.1	29.1
IIIA	25	18.1	6.1	30.1
	26	19.5	7.5	31.5
	27	19.6	7.6	31.6
	28	18.4	6.4	30.4
	44	18.3	6.3	30.3
	45	19.8	7.8	31.8
	46	19.9	7.9	31.9
	47	18.5	6.5	39.5

(a) a minimum thickness of soil was used for modeling purposes.

5.6.3.10 Well Depth

As discussed in the exposure pathways section of this PA (Section 4.2.4), well water may be used as a primary potable water source for a future residence near the well (e.g., drinking water, showering) and may be used by the resident as a primary water source for agriculture (e.g., irrigation, livestock water). The hypothetical impacts to the receptor can be highly dependent on which aquifer the water is drawn from. SRS-REG-2007-00029 examines available on-site and off-site well drilling data, as well as information from regional commercial well drillers to determine probabilities associated with a future resident using a particular aquifer.

Based on the information obtained, SRS-REG-2007-00029 concludes that a well drilled by a professional driller would have a high probability of being located in the Gordon aquifer or deeper. There is a possibility that the MOP receptor would choose to drill his own well and would only drill down as far as necessary to meet some short term minimum flow need (e.g., 10 gpm from the UTR-UZ), however this probability is considered reasonably small. Combining the percentages of the wells drilled in each depth range both onsite and offsite, it is reasonable to apply the probabilities in Table 5.6-6 when estimating well depths for well drilling scenarios within the GSA.

Table 5.6-6: Probability of Well Driller Exposure from Each Aquifer

Aquifer (Depth)	% of Total in GSA
UTR-UZ (less than 109 feet)	13%
UTR-LZ (109-170 feet)	44%
Gordon Aquifer (170 feet and lower)	43%

The GoldSim FTF model corresponds to a single aquifer (UTR-UZ) and was benchmarked with the PORFLOW FTF model accordingly. To simulate the probability that a potential well driller (MOP or intruder) might drill into a lower aquifer (UTR-LZ or the Gordon Aquifer), the well depth probabilities in Table 5.6-6 were used as a stochastic in the GoldSim FTF model. To reflect that a well at a different drill depth might have contaminant concentrations different than the single aquifer (UTR-UZ) represented by the GoldSim FTF model, Table 5.6-6 provides the relationships between the contaminant concentrations in the three aquifers of interest. The percentages in Table 5.6-7 are based on a comparison of the 100m peak nitrogen concentrations in the three aquifer zones (from the PORFLOW FTF model). The UTR-UZ and UTR-LZ concentrations are similar because the aquitard that separates them (the "tan clay" layer) is a relatively ineffective flow barrier. In contrast, the aquitard that separates the Gordon Aquifer (the "green clay" layer) is very effective and there is very little downward flow into the Gordon Aquifer relatively to lateral flow along the UTR-LZ aquifer. The calculations showing that the assumed aquifer ratios (i.e., 100/100/5) are reasonably conservative are based on PORFLOW peak 100m concentrations at the various aquifers (Appendix F.2).

Table 5.6-7: Contaminant Transfer Ratios between Aquifers

Aquifer	Contaminant Concentration % in Relation to UTR-UZ	Calculation used for Basis
UTR-UZ	100%	Not Applicable
UTR-LZ	100%	Peak Concentration UTR-LZ/ Peak Concentration UTR-UZ
Gordon Aquifer	5%	Peak Concentration Gordon Aquifer/ Peak Concentration UTR-UZ

5.6.3.11 Bioaccumulation Factors and Human Health Exposure Parameters

The Bioaccumulation Factors (Section 4.6.1) and Human Health Exposure (Section 4.6.2) parameters have various functions in the GoldSim FTF model, but they all assist in some way in calculating doses for the exposure pathways. The baseline values and stochastic distributions used for various Bioaccumulation Factors and Human Health Exposure parameters are provided in Tables 5.6-8 through 5.6-10. For the transfer factors in Tables 4.6-1 through 4.6-4, only the most likely value was used in the stochastic analysis (no distributions were created for these values).

Table 5.6-8: Crop Exposure Time and Productivity Stochastics

Parameter	Baseline	Minimum	Maximum	Distribution Used
Pasture exposure time to irrigation	30 days	30 days	90 days	Normal
Vegetable crop exposure times to irrigation(days)[(1)]	70 days	60 days	90 days	Normal
Soil exposure time period to irrigation (Buildup time in soil)	183 days	60 days	365 days	Triangular
Vegetable Crop Yield Productivity	0.7 kg/m^2	0.2 kg/m^2	4 kg/m^2	Normal
MOP Fraction of Vegetables Produced Locally	0.173	0	0.5	Triangular
MOP Fraction of Meat Produced Locally	0.306	0	1	Triangular
MOP Fraction of Milk Produced Locally	0.207	0	1	Triangular
Intruder Fraction of Vegetables Produced Locally	0.308	0	0.5	Triangular
Intruder Fraction of Meat Produced Locally	0.319	0	1	Triangular
Intruder Fraction of Milk Produced Locally	0.254	0	1	Triangular

[(1)] average growing time for above ground vegetables.

Table 5.6-9: Pathway Physical Parameter Stochastics

Parameter	Baseline	Minimum	Maximum	Distribution Used
Areal Density of Soil	240 kg/m2	180 kg/m2	270 kg/m2	Normal
Atmospheric Mass Loading of Soil	1.0E-07 kg/m3	1.0E-09 kg/m3	3.0E-07 kg/m3	Triangular
Depth of Garden	15 cm	15 cm	61 cm	Triangular
Garden Irrigation Rate	3.6 L/d/m2	2.08 L/d/m2	5.5 L/d/m2	Triangular
Fraction of Year Garden Irrigated	0.2	0.2	0.25	Triangular
Crop Weathering Constant	0.0495 L/d	0.03 L/d	0.0495 L/d	Triangular
Fractional Retention of Deposition on Leaves	0.25	0.2	0.25	Triangular
Garden Size	100 m2	100 m2	1000 m2	Triangular
Annual Breathing Rate	5,548 m3/yr	1,267 m3/yr	11,600 m3/yr	Normal

Table 5.6-10: Consumption Rate, Pathway Exposure Time and Transport Stochastics

Consumption Rate Parameters	Baseline	Minimum	Maximum	Distribution Used
Annual Soil Consumption	0.0365 kg/yr	0.0008 kg/yr	0.05 kg/yr	Triangular
Annual Leafy Veggie Consumption	21 kg/yr	18 kg/yr	43 kg/yr	Lognormal
Annual Other Veggie Consumption	163 kg/yr	90 kg/yr	276 kg/yr	Lognormal
Annual Beef Consumption	43 kg/yr	26 kg/yr	81 kg/yr	Lognormal
Annual Finfish Food Consumption	9 kg/yr	2.2kg/yr	19 kg/yr	Triangular
Annual Milk Consumption	120 L/yr	73.7 L/yr	230 L/yr	Lognormal
Water Consumption Rate	337 L/yr	184 L/yr	730 L/yr (2 L/day)	Triangular
Fodder Beef Cow Consumption	36 kg/day	27 kg/day	50 kg/day	Lognormal
Fodder Milk Cow Consumption	52 kg/day	36 kg/day	55 kg/day	Lognormal
Fraction of Beef Cow intake from pasture	0.75	0.5	1	Triangular
Fraction of Milk Cow intake from pasture	0.56	0.5	1	Triangular
Water Beef Cow Consumption	28 L/day	28 L/day	50 L/day	Triangular
Water Milk Cow Consumption	50 L/day	50 L/day	60 L/day	Triangular
Exposure Time Parameters				
Shoreline Exposure Time	23 hr/yr	11 hr/yr	35 hr/yr	Triangular
Swimming Exposure Time	8.9 hr/yr	8.9 hr/yr	13 hr/yr	Triangular
Boating Exposure Time	21 hr/yr	9.1 hr/yr	21 hr/yr	Triangular
Showering Exposure Time	10 min/day	10 min/day	30 min/day	Triangular
Fraction of Year In Garden	0.01 /yr	0.01 /yr	0.08 /yr	Triangular
Fraction of Year In Home	0.7 /yr	0.3 /yr	0.7 /yr	Triangular
Fraction of Year Cattle In Pasture	1 /yr	1 /yr	1 /yr	Normal
Transport				
Vegetable Transport Time	6 days	6 days	14 days	Normal
Feed-Milk-Man Transport Time	3 days	1 days	4 days	Lognormal
Time from Slaughter to Consumption	6 days	6 days	20 days	Lognormal

Where available, site-specific distribution information, obtained from WSRC-STI-2007-00004 was used in determing the stochastic range to be evaluated. Where no specific guidance was available, a triangular distribution using maximum, minimum and most-likely values from WSRC-STI-2007-00004 is utilized in the stochastic analysis. The most likely value is the recommended value from WSRC-STI-2007-00004, and is used as the distribution peak. For cases where site-specific distribution data was not available, it was judged reasonable to use the maximum and minimum values from WSRC-STI-2007-00004. Although they may not be site-specific and have not been weighted for the purpose of the stochastic analysis, they provide a wide range of possible outcomes and are therefore better able to identify parameters of potential concern.

Additional background information regarding a few parameters of interest are provided below.

- **Drinking Water Ingestion**

Ingestion of water is a key usage factor for the all-pathway and inadvertent intruder analyses. The rate of contaminated water consumption can vary by exposure scenario based on assumed access to the water supply. For the inadvertent intruder where the contaminated water is expected to come from a well an assumption can be made that water from the well is only used for cooking. Likewise, for the all-pathway analyses the assumption could be made that total water intake comes from the community water supply. However, in the absence of site and/or regional specific surveys, national estimates are appropriate.

The RESRAD 511 L/yr (1.4 L/day) average water ingestion rate updated for use in the all-pathway analysis is based on EPA surveys published in the early 1990s. [ANL-EAD-4] The 730 L/yr (2 L/day) water ingestion rates for the inadvertent intruder are taken from *Site-Specific Parameter Values for the Nuclear Regulatory Commission's Food Pathway Dose Model* (ISSN 0017-9078 - Volume 62), and are based on 10 CFR 50, Appendix I rates for the MEI. The average rate for ingestion of drinking water listed in those sources is 370 L/yr (1 L/day). These publications consider indirect ingestion of water but do not consider whether or not the water is bottled or comes from a community or commercial source.

EPA drinking water survey, estimates per capita ingestion of water using data from the combined 1994, 1995, 1996, and 1998 *Continuing Survey of Food Intakes by Individuals (CSFII)*, conducted by the USDA. This publication considers indirect ingestion of water from food with water added at the final phase of food preparation and reports water consumption from community water, bottled water, water from other sources, missing source, and total water. Summary data found in the Executive Summary of EPA-822-R-00-001 (pages vii-viii) provide a 337 L/yr water ingestion rate.

According to EPA, direct water is plain water ingested directly as a beverage and indirect water is water added to foods and beverages during final preparation at home, or by food service establishments such as school cafeterias and restaurants. An example of indirect water is water added to dry cake mix. Community water is tap water from the community water supply; bottled water is purchased plain water; other water is water obtained from a well or rain cistern (household's), spring (household's or public), or other source; and preparation water is water used to prepare foods and includes the water used to prepare foods at home and by local food service establishments (indirect water), as well as, water added by commercial food manufacturers. Missing water source indicates that a survey participant responded "don't know" or "not ascertained" to the survey question regarding the source of water and total water is the sum of direct and indirect water from all sources which includes community water, bottled water, other water and missing sources. [EPA-822-R-00-001]

The EPA drinking water survey reports the mean per capita total water ingestion is 1,233 mL/person/d (450 L/yr) when viewed across genders and all age categories with 75% from community water, 13% from bottled water, 10% from other sources (well, spring and cistern, etc.), and 2% from non identified sources. This yields a mean of 924 mL/person/d (337 L/yr) from community water and 12.3 mL/person/d (4.5 L/yr) from other sources (well water). [EPA-822-R-00-001]

A value of 337 L/yr is used as the nominal water ingestion rate for all MOP and inadvertent intruder pathway analysis. In the stochastic analyses of this parameter, the water ingestion rate range was assumed to be as high as 730 L/yr (2 L/d), which, as discussed above, is a maximum evaluation point provided by the NRC. [10 CFR 50, Reg. Guide 1.109] The lower range of the water ingestion rate range was set at 184 L/yr, the minimum recommended water ingestion rate is cut in half (e.g., water or other liquids from a clean source are used instead of drinking water from a contaminated source). A triangular distribution is used in the stochastic analysis which causes the mean value for this parameter to rise well above the most likely value (417 L/yr vs. 337 L/yr).

- **Crop Yields** A survey of local practices (WSRC-RP-91-17) surveyed 21 county extension agents in Georgia and South Carolina to estimate the average mass, in kg, of vegetation harvested in a typical square meter of garden or farmland within a 50 mile radius of SRS. Crop yields in kg/m2 were estimated for leafy vegetation (cabbage, lettuce and spinach) and other aboveground vegetables (broccoli, cauliflower, green peas, lima beans, and sweet corn). Average agricultural, garden, and pasture grass productivity for farms in the 50 mile region is estimated to be 0.7 kg/m2, 0.2 kg/m2 and 1.8 kg/m2, respectively. Because the garden productivity was estimated to be an order of magnitude lower than 10 cfr 50, Reg. Guide 1.109 default, WSRC-RP-91-17 assumed the garden productivity is to be equal to agricultural productivity. This report recommends use of the site-specific value of 0.7 kg/m2 as the expected value for garden productivity, and the 0.2 kg/m2 should be considered in the uncertainty range.

➢ **Fraction of Foodstuff Intake from Garden** The current assumption of the fractions of vegetables, milk, and meat intake that is from a local garden were based on 10 CFR 50, Guide 1.109, professional judgment, and *Data Collection Handbook To Support Modeling Impacts Of Radioactive Material In Soil*, considers the 0.5 fraction of vegetable intake to be a maximum value. Table 13-71 of EPA-600-P-95-002 provides regional values for vegetables, milk, and meat intake fractions and scenario specific values. This report recommends use of the values provided in this publication for households with gardens who raise animals for an all-pathways analysis and those for households who farm for an intruder analysis.

⇒ **Garden Size** The garden size of 100m2 for a family of four is assumed in SRS PAs, and is based on site specific evaluation of consumption needs and annual productivity. It is assumed that a well would not be drilled for a single individual but rather for a household that includes at least two adults. As discussed in Section 4.6.2, SRS report, WSRC-RP-91-17 estimated that a person within a 50 mile radius of SRS consumes 184 kg of vegetables annually. The crop yields discussion above discusses the average garden vegetable yield of 0.2 kg/m2, but recommends the use of the agricultural 0.7 kg/m2, as reported in WSRC-RP-91-17. A garden size of 260m2 would be required to support the annual consumption of 184 kg of vegetables for a household with two adults assuming all vegetables consumed by the adults are from their garden. Assuming that only 17% of a person's vegetables are from their home garden (EPA-600-P-95-002), roughly 100m2 would be required to feed a family of four. This report recommends use of the 100m2 garden size for vegetables only. However, this area is not large enough to graze livestock. ANL-EAIS-8 states that an area of 1 hectare (10,000m2) is required to graze a single milk cow. A triangular distribution using the 1,000m2 as a maximum, 100m2 as a minimum, and the most likely value (100m2) as the peak was utilized for garden size in the stochastic analysis.

➢ **Soil Exposure Time Period** For soil exposure time period to irrigation (buildup) SRS report, WSRC-STI-2006-00123 recommends 40 years to indicate the life time of a facility releasing radionuclide and 0.5 of a MEI lifetime assuming the MEI is exposed at that location for their lifetime. For the intruder and MOP scenario, it is assumed that the irrigation and harvesting of vegetables occur during the first year of residence, yielding the 183 day updated value.

➢ **Foodstuff Consumption** For the inadvertent intruder, vegetable, milk and beef consumption rates are taken from ISSN 0017-9078 - Volume 62. These values are based on county specific statistics provided by the counties within the states of South Carolina and Georgia that fall within a 50 mile radius of SRS. This report recommends continued use of WSRC-RP-91-17 as a reference for these values as they are based on a site-specific evaluation. However, this report recommends use of average values for PAs where the MEI values are currently used in some cases. Triangular distributions using values from

applicable literature as maximum and minimum values, and the most likely value as the peak was utilized for consumption rates in the stochastic analysis.

5.6.3.12 Saturated Zone Flow Modeling Parameters

As discussed in Section 4.4.2.1, the GoldSim FTF modeling domain begins at the top of the waste layer and extends to a hypothetical groundwater well located 100m from the FTF boundary. The flow profiles used in the GoldSim model to represent flow through the waste are extracted from the PORFLOW model, which allows for changes in the closure cap, tank top and tank grout. The model is one-dimensional with downward flow represented in the unsaturated zone and predominantly horizontal flow in the saturated zone. The unsaturated zone is represented as a column underlying each particular initial inventory location (i.e., tank, evaporator, etc.).

The water flow boundary condition for the saturated zone bulk flow is also provided by the PORFLOW model. Saturated zone modeling Base Case values were refined in the GoldSim model during the benchmarking effort to align the GoldSim model results with the PORFLOW model results, as explained in the GoldSim benchmarking discussion (Section 5.6.2). Two modeling parameters of particular importance are the Saturated Zone Thickness and the Saturated Zone Darcy Velocity, additional information for each of these parameters is provided below.

- **Saturated Zone Thickness** — In the GoldSim model, water leaving the unsaturated zone enters the saturated zone (i.e., the aquifer) as recharge, and this infiltrating water is mixed into the volume of aquifer water. The volume is determined by the flow rate and mixing volume (flow face area times flow velocity time) in the aquifer. The aquifer thickness is important to the model because the volume of water directly affects the concentration. The thickness of the aquifer is defined in the GoldSim model as SatThickness, and is assigned a Base Case value of 5m. For the stochastic modeling, the Base Case "most likely" value of 5m was assumed as the minimum aquifer thickness and 20m was selected as a reasonably bounding maximum thickness. A uniform distribution using these maximum and minimum values was utilized to determine the distribution range.

- **Saturated Zone Darcy Velocity** — In the GoldSim FTF model, the saturated zone Darcy Velocity is the primary reference for the velocity of water flowing in the aquifer. The Darcy Velocity is important to the model because it directly affects the concentration. The thickness of the aquifer is defined in the GoldSim FTF model as SatThickness and is assigned a Base Case value of 5m. The waste tank dependent Base Case values used in the model are either 25 ft/yr or 30 ft/yr. For the stochastic modeling, a normal distribution was utilized to determine the distribution range, with the Base Case value set as the distribution mean and 0.5 ft/yr as the standard deviation.

5.6.4 Uncertainty/Sensitivity Analysis using the FTF Probablistic Model

A special model was developed for performing the uncertainty and sensitivity analyses of the FTF PA calculations using the GoldSim systems analysis software. The model is not intended to predict future potential doses, rather the goal is to characterize the context of uncertainty and sensitivity surrounding the PA calculations.

The uncertainty analysis is concerned with how the uncertainty in model input parameters is propagated through the model to the selected model results, or endpoints. These model endpoints are potential radiological doses to hypothetical human receptors and aqueous concentrations of specific contaminants.

In contrast, the sensitivity analysis, discussed in section 5.6.6, is focused on determining which of the many input parameters (called explanatory variables, in statistical parlance) are most responsible for determining the endpoints.

The probabilistic results of the GoldSim model are used to characterize the uncertainty manifested in the model input distributions. Some of these distributions are parameter values, such as material properties or water flow rates. Others are more oriented toward model uncertainty, such as the stochastic that selects which waste tank failure configuration to choose for a given realization. Together, the distributions, defined as Stochastic elements in GoldSim, are intended to capture the overall uncertainty in the model. Thes probabilistic model uncertainty analysis is not intended to quantify conceptual model uncertainty. Identification of conceptual model areas of importance is primarily accomplished throught the combined sensitivity analyses (both stochastic and single parameter sensitivities). The sensitivity analyses highlight the portions of the conceptual model that most impact the model results (e.g., aquifer thickness, soil thickness, basemat thickness).

The FTF sensitivity/uncertainty analysis is based on inputs and results for the GoldSim FTF model with the file name "FTF v1.1 r1000.gsm". This model run contains the results of 1,000-realizations of the FTF model, version 1.1. The *Monte Carlo* analysis sampled the input distributions with Latin Hypercube Sampling and with a seed value of one.

The most direct way to communicate the uncertain nature of the model results is to show graphs of certain key model endpoints. Statistics for maximum values for doses and MCLs are summarized in Tables 5.6-11 and 5.6-12. Table 5.6-11 is based on the 5,000-realization sensitivity run, configured to provide as much data as possible for the sensitivity analysis, yet without recording time histories. Table 5.6-12 is based on the 1,000-realization uncertainty run, and is shorter than the sensitivity runs due to the additional data storage necessary for recording time histories. The difference in the statistical results is due to the number of realizations run. These results are quite similar, indicating that the 1,000-realization run is sufficient for uncertainty analysis.

The values in the tables focus on two wells. Well 6 typically has the highest concentrations of those wells that tap into groundwater bound for UTR. Well 33 typically has the highest concentrations of those wells that tap into groundwater destined for Fourmile Branch. The values in the table focus on maximum doses (and concentrations) at these wells. The values in the tables show the statistics (mean, median, and 95th percentile) on the maximum. This is not the same thing as the statistical time histories shown in the subsequent graphs, which summarize the dose values at each time step. Since the primary goal is the reasonable assurance that the maximum dose is within the performance objective, it is necessary to examine the statistics surrounding the 1,000 (or 5,000) maximum doses that are calculated.

Table 5.6-11: Summary Statistics from 5,000 Realizations for Selected FTF Endpoints

Endpoint	Mean	Median (50th Percentile)	95th Percentile
Maximum MOP dose at Well 6 within 10,000 years (mrem/yr)	8.9	2.7	35
Maximum MOP dose at Well 33 within 10,000 years (mrem/yr)	5.2	1.2	20
Maximum concentration Pu-239 at Well 6 within 50,000 years (pCi/L)	170	37	960
Maximum concentration Np-237 at Well 6 within 50,000 years (pCi/L)	5.5	1.6	31
Maximum concentration Ra-226 at Well 6 within 50,000 years (pCi/L)	2.2	0.69	9.7
Maximum concentration Tc-99 at Well 6 within 50,000 years (pCi/L)	2,000	660	9500

(from GoldSim model file *FTF v1.1 SA r5000.gsm*)

Table 5.6-12: Summary Statistics from 1,000 Realizations for Selected FTF Endpoints

Endpoint	Mean	Median (50th %ile)	95th %ile
Maximum MOP dose at Well 6 within 10,000 years (mrem/yr)	9.0	2.7	37
Maximum MOP dose at Well 33 within 10,000 years (mrem/yr)	5.6	1.2	22
Maximum conc. Pu-239 at Well 6 within 50,000 years (pCi/L)	170	35	940
Maximum conc. Np-237 at Well 6 within 50,000 years (pCi/L)	5.6	1.5	31
Maximum conc. Ra-226 at Well 6 within 50,000 years (pCi/L)	2.3	0.67	9.8
Maximum conc. Tc-99 at Well 6 within 50,000 years (pCi/L)	2,000	660	9,200

(from GoldSim model file *FTF v1.1 r1000.gsm*)

Figure 5.6-20 shows the uncertainty in the dose to the MOP, using the maximum concentrations of all the wells at a given time, within 10,000 years, based on 1,000-realizations. Figure 5.6-21 shows the same information, but for the time period following the evaluation period (10,000 to 50,000 years). It should be noted that 5th and 95th percentiles are one or two orders of magnitude below and above the median value. The mean value is also driven higher, more-or-less to the 75th percentile, by the input distributions. This indicates that the model has input distributions with long tails (as in the lognormal distributions in K_d) or exhibit other extreme skewness, like those triangular distributions that have one end as the most likely value. Such values can inflate the variance of the endpoint, which in turn, can cause difficulties for the sensitivity analysis, as discussed below. This makes it more difficult to investigate the statistical structure of the model, and the problem is exacerbated by the number of parameters in the model. The chances of getting spurious results, especially when input distributions have extreme variability, are increased with the number of wide distributions. Many distributions have been redefined since the initial GoldSim FTF model was created to relieve some of the variability.

In addition to the skewed distributions, there are are some uncertainty issues associated with model structure. For example, the saturated thickness of the aquifer (*SatThickness*) is sampled independently for each waste tank, from a uniform distribution (5 to 20m). This modeling simplification is somewhat aphysical, since for a given realization thickness of the regional aquifer for each waste tank is expected to vary in a dependant manner with the aquifer height affecting all waste tanks simultaneously.

It is important to note that the tables above and the graphs below do not present the same information. The tables show the statistics of the maximum doses achieved in the 10,000 years and 50,000 year time frames. These are means (and medians and 95th percentiles) of the maximum values in dose, no matter when that dose was achieved within the time frame. Each realization produces a single maximum dose value at Well 6, for example. The mean of these maxima is the mean of the maximum dose values averaged over all the realizations, and does not reflect the variability of the dose values at different time steps, only the maximum doses in the period evaluated.

The graphs show statistical summaries by time step of the dose based on the well of highest concentration at each time step. The maximum value of the mean dose within the period of performance occurs at year 10,000, with a value of about 7.2 mrem/yr. The maximum mean dose within 50,000 years is about 130 mrem/yr, occurring with a broad peak between year 21,000 and 25,000.

The tables and graphs are not comparable since the tables are examining the maximum values at particular wells, and the graphs display the statistics of time histories of doses (not just their maximum values) across all wells.

Figure 5.6-20: Statistical Summary of Time History of Total MOP Dose, at the Well of Maximum Concentration (0 to 10,000 yr)

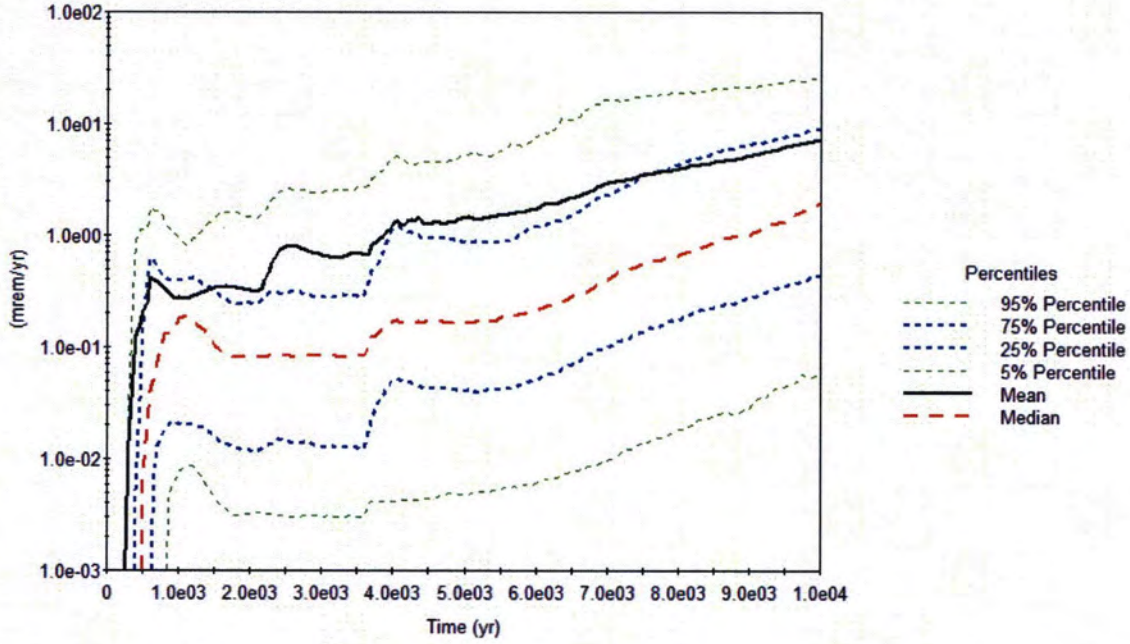

Figure 5.6-21: Statistical Summary of Time History of Total MOP Dose, at the Well of Maximum Concentration (10,000 to 50,000 yr)

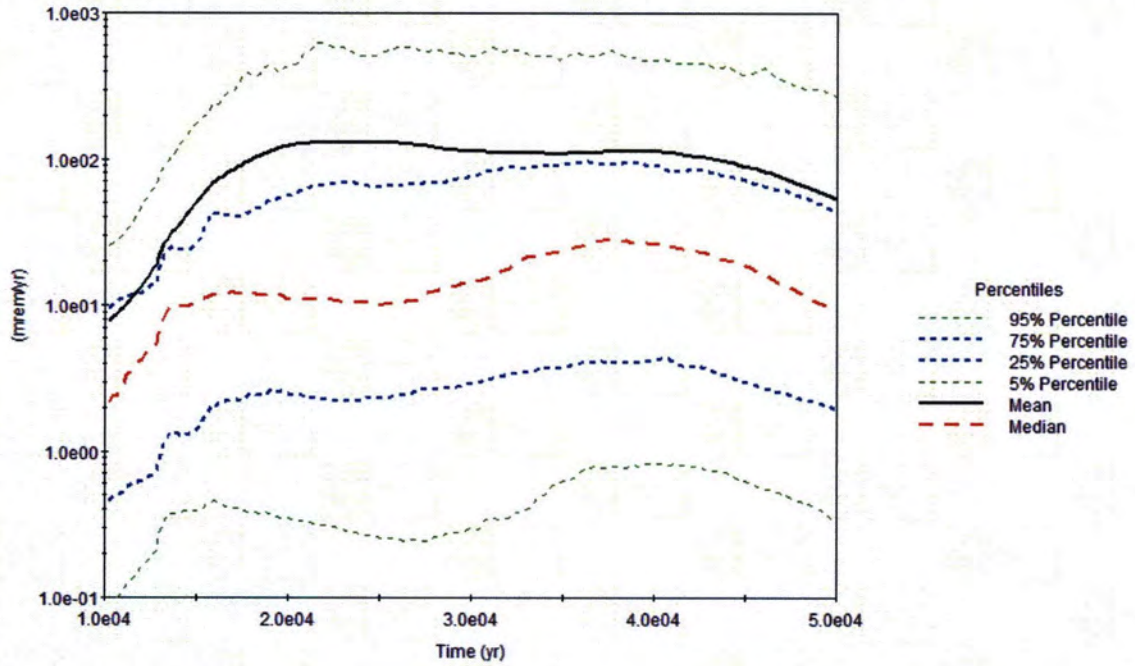

5.6.5 Variability in Dose Time Histories

In examining the results of a probabilistic analysis, the focus tends to fall upon the general statistics for a given result. For example, the mean time history of the total MOP dose at each well given 1,000-realizations is shown in Figure 5.6-22.

Figure 5.6-22: Mean Time History of Total MOP Dose by Well

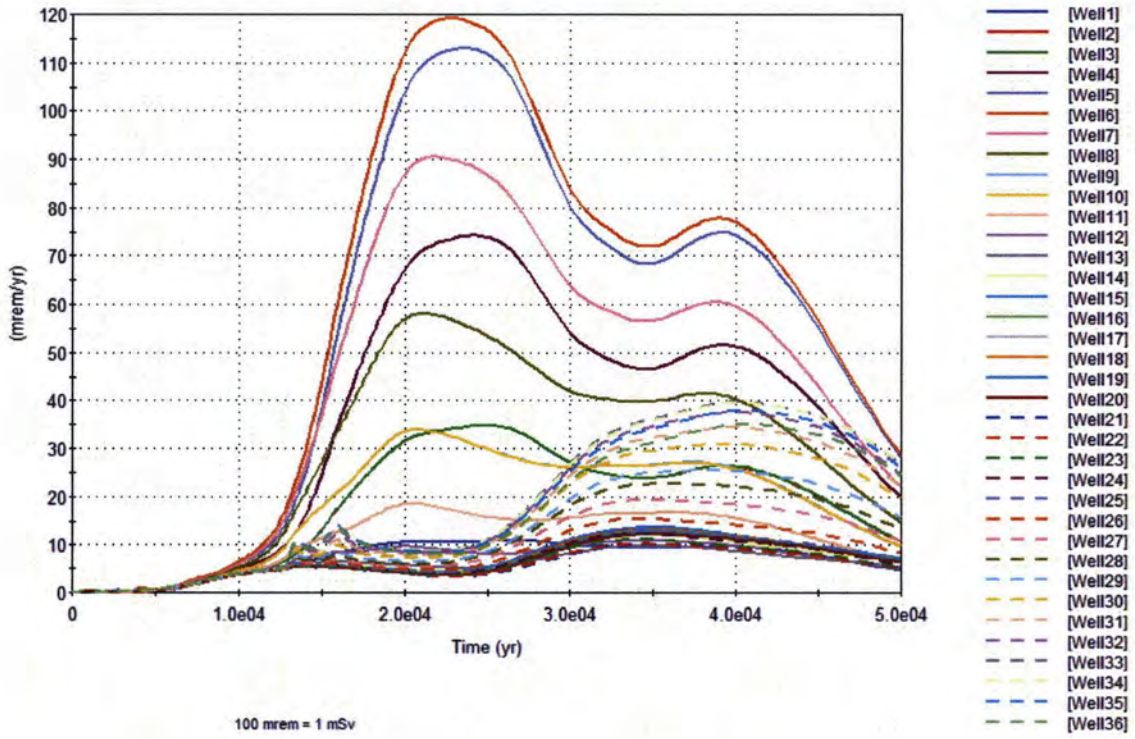

5.6.6 Sensitivity Analysis using the FTF Probabilistic Model

Given the uncertainties presented in Section 5.6.4, the next step was to identify those input parameters and other stochastic entities in the model that led to the uncertainties. Even in complex models, the results are often strongly dependent on only a handful of parameters. What is important for one result (e.g., the uranium concentration), may be insignificant for another, such as the maximum dose achieved within the 10,000-year period of performance. In fact, the maximum dose to the MOP will have different sensitivities at different times, since it is driven by the presence of different radionuclides. For example, a MOP dose may be dominated by Tc-99 at one time and by Pu-239 at another time, and these doses will be determined by different aspects of the model (different K_ds, DCFs, decay chains, etc.) Extracting the important model inputs for results of interest is the subject of the sensitivity analysis.

The results of the model output were analyzed using Gradient Boosting Models (GBM). The GBM modeling approach utilizes binary recursive partitioning algorithms that deconstruct a response into the relative influence from a given set of explanatory variables (stochastic model input parameters). This sensitivity analysis methodology identifies which stochastic model input parameters are most influential in determining the results, such as media concentrations or future potential doses.

The model was run using a *Monte Carlo* scheme, where each stochastic input parameter is sampled in different ways, and these are combined to produce many realizations, or equally probable outcomes. This sensitivity analysis is based on a run of 5,000-realizations.

5.6.6.1 Introduction to FTF Probabilistic Model Sensitivity Analysis

Complex modeling, such as the probabilistic modeling of the FTF, is needed to explore dynamics of systems where multiple variables interact in a nonlinear manner. The probabilistic simulation approach used in the GoldSim model propagates uncertainty regarding the explanatory variables (e.g., inputs such as physical soil properties or inventory mass) through the model to the predicted response (e.g., dose or concentration). Quantitative assessment of the importance of inputs is necessary when the level of uncertainty in the system response exceeds the acceptable threshold specified in the decision making framework. One of the goals of sensitivity analysis is to identify which variables have distributions that exert the greatest influence on the response.

Sensitivity analysis deals with estimating influence measures for input variables. Influence measures can be estimated in either a qualitative or quantitative context. A qualitative sensitivity analysis provides a relative ranking of the importance of input factors without incurring the computational cost of quantitatively estimating the percentage of the output variation accounted for by each input factor. For either approach the estimates can be obtained either locally or globally within the parameter space. A local sensitivity analysis involves varying one explanatory variable while holding all other explanatory variables constant and assessing the impact on the model response. This is local in the sense that only a minimal portion of the full explanatory variable space is explored (i.e., the point at which the explanatory variables are held constant). Although local sensitivity analysis is useful in some applications, the region of possible realizations for the model of interest is left largely unexplored. Global sensitivity analysis attempts to explore the possible realizations of the model more completely. The space of possible realizations for the model can be explored through the use of search curves or evaluation of multi-dimensional integrals using Monte Carlo methods. However, these approaches to global sensitivity analysis become more computationally intensive as the dimensionality of the model (i.e., the number of observations and explanatory variables) increases.

Because of the computational cost, sensitivity analysis of high-dimensional probabilistic models requires efficient algorithms for practical application. In this work, GBMs are used to perform a global sensitivity analysis that quantifies the importance of explanatory variables using sensitivity indices (SI), which are metrics based on the explained variance in the response. [ISSN 0885-6125 Vol 40 No 2, ISSN 0885-6125 Vol 24 No 2] The implementation of GBM used here comes from the *R* statistical package named GBM.

5.6.6.2 Model Fitting and Validation

This section presents detailed discussion of the statistical methods used in the sensitivity analysis. Global sensitivity is estimated here as the proportion of the variance of the response accounted for by each explanatory variable. This estimation is conducted by fitting GBM model predictions to realizations from the GoldSim model. Variance decomposition of the fitted GBM model is then used to estimate SIs. Under this decomposition approach, the goal is identify the most influential explanatory variables that are identified within a model. The necessary degree of model complexity is assessed using validation metrics based on comparison of model predictions with randomly selected subsets of the data. This approach uses the "deviance" of the model as a measure of goodness of fit. The concept of deviance is fundamental to classical statistical hypothesis tests (e.g., the common t-test can be derived using a deviance-based framework) and guides the model selection process applied here.

The GBM model fitting approach is based on finding the values of each explanatory variable that result in the greatest difference in means for the corresponding subsets of the response. For example, if there were only a single explanatory variable, the GBM would identify the value of the explanatory variable that corresponds to a split of the response into two parts such that no other split would result in corresponding groups of the response variable with a greater difference in means. When multiple explanatory variables are present, these multiple splits are referred to as "trees" and each tree results in an estimate (e.g., prediction) of the response. As multiple potential trees are evaluated, they are compared to the observed data using a loss function. The selection of the loss function is an influential aspect of the GBM process and depends on the distribution of the response variable. For data that are sufficiently skewed (e.g., non-normal), the absolute error loss function tends to produce more reliable results.

There is a trade-off that exists when considering which loss function to use. The squared-error loss function tends to result in better fitting models but can do so at the expense of introducing spurious variables into the model selection process when the response distribution is sufficiently skewed. The absolute error loss function tends to produce model predictions with more variability but is less likely to result in the selection of spurious variables into the model. For this application, the focus has been on using a deviance-based method to obtain models that identify the most important explanatory variables with respect to the observed variability in the response. To this end, the squared-error function was used in these applications.

Once a GBM model is constructed, each of the explanatory variables that exist in the model can be assigned an SI. The SI is obtained through variance decomposition and can be interpreted as the percentage of variability explained in the model by a given explanatory variable. The sum of the SIs across the entire set of explanatory variables in the model will approximately equal the R^2 of the linear regression of the GoldSim output versus the GBM predictions. The R^2 values for this version of the FTF model are quite low, indicating the high degree of difficulty encountered in getting the GBM to fit the GoldSim model.

In order to assess the relationship between an individual explanatory variable and the response of interest, partial dependence plots are used (these are presented below for each endpoint of interest). A partial dependence plot shows the distribution of the explanatory variable (shaded green), and the partial dependence curve (blue line) shows changes in the response as a function of the explanatory variable. The partial dependence is obtained through the integration across the joint density to obtain a marginal distribution. The integration is performed using a "weighted tree traversal" measure that is analogous to more common integration procedures performed with Riemann or Lebesgue measures. The vertical axis of the partial dependence plot shows the change in the response variable as a function of the changes in the explanatory variable of interest. With standard linear regression techniques, it is assumed that the relationship between the response and the explanatory variable is a constant (e.g., the parameter estimates in the linear model). With the GBM approach, this relationship is not constrained by assumptions of linearity and the partial dependence plots show the data-based estimate of the relationship between the response and the explanatory variable. This is especially useful for understanding the influence of changes in a single explanatory variable on the response, when integrating across all other explanatory variables.

5.6.6.3 Summary Statistics for Endpoints

The GoldSim model that was run for this sensitivity analysis has the file name "FTF v1.1 SA r5000.gsm". This model utilizes v1.1 of the model, set for 5000-realizations, with Latin Hypercube Sampling enabled and a seed value of one. The exporting of results follows the simple procedure outlined in the model, in the *SensitivityAnalysis* container, wherein the tabulated raw data contents of the element *Endpoints_SA* are exported to the file "FTF v1.1 SA r5000.gsd" (note the different extension, .gsd, for "GoldSim data") a 46 MB tab-delimited text file.

For each endpoint, as shown in Table 5.6-13, the four most significant parameters identified by the sensitivity analysis are presented, along with the SI for each. Relatively simple models characteristically have only a few dominant parameters, so each parameter contributes to a larger fraction of the variation in the model. For simple models, single parameters can typically impact 40% or more of the model, and occasionally 80% for some endpoints. The SI values displayed in the FTF sensivitity analysis are lower, meaning the influences are spread out over more parameters. These lower SI values are due to the FTF model being inherently complex, with sudden releases of large quantities of radionuclides at different times. The FTF model has multiple parameters that have the potential to greatly influence radionuclide release (e.g., liner failure date, solubility transition time, key radionuclide solubility values, key radionuclide K_d values) such that system behavior can be erratic. The SI values for the FTF model are generally lower than would be expected for a less complex model. These lower values are due in part to the distributions used to bound parameters for which a wide range of values are being evaluated. The lower SI values are also due to the FTF chaotic system behavior. While the sensitivity analysis SI values may be improved if the parametric distributions were revised to evaluate a smaller range of outcomes, it is not possible to eliminate the chaotic system behavior fundamental to the complex FTF model.

Following Table 5.6-13 is a series of figures (Figures 5.6-23 through 5.6-38), showing the partial dependence of each of the top four SI for each endpoint.

Table 5.6-13: Identification of the Most Sensitive Parameters for the Endpoints of Interest

Endpoint	SI Rank	Input Parameter	Sensitivity Index
Max. MOP dose at any well within 10,000 years	1	Saturated thickness of the aquifer	7.3
	2	Sandy soil K_d for Pu	5.5
	3	Tank 34 failure configuration selector	3.7
	4	Unsaturated zone (UZ) thickness beneath the Transfer Lines	3.1
Max. MOP dose at any well within 50,000 years	1	Saturated thickness of the aquifer	10
	2	Clayey soil K_d for Pu	8.9
	3	Aquifer Darcy velocity for Tank 46	2.2
	4	Sandy soil K_d for Pu	1.3
Max. MOP dose at Well 6 within 10,000 years	1	Sandy soil K_d for Pu	11
	2	UZ thickness beneath the Transfer Lines	6.8
	3	Saturated thickness of the aquifer	6.4
	4	Clayey soil K_d for Pu	4.9
Max. MOP dose at Well 6 within 50,000 years	1	Saturated thickness of the aquifer	20
	2	Clayey soil K_d for Pu	16
	3	Sandy soil K_d for Pu	3.2
	4	UZ thickness beneath Tank 18	3.1
Max. MOP dose at Well 33 within 10,000 years	1	Tank 34 failure configuration selector	11
	2	UZ thickness beneath the Transfer Lines	5.6
	3	Sandy soil K_d for Pu	4.9
	4	Saturated thickness of aquifer beneath the Transfer Lines	4.4

Table 5.6-13: Identification of the Most Sensitive Parameters for the Endpoints of Interest (Continued)

Endpoint	SI Rank	Input Parameter	Sensitivity Index
Max. MOP dose at Well 33 within 50,000 years	1	Saturated thickness of the aquifer	32
	2	Sandy soil K_d for Pu	4.4
	3	Well water consumption rate	1.7
	4	UZ thickness beneath Tank 33	1.5
Max. chronic Inadvertent Human Intruder (IHI) dose within 10,000 years	1	Saturated thickness of the aquifer	11
	2	Oxidizing young concrete K_d for Th	8.9
	3	TypeIV Tank Configuration Timing for Cases A&B	7.7
	4	UZ thickness beneath Tank 17	3.3
Max. chronic IHI dose within 50,000 years	1	Saturated thickness of the aquifer	26
	2	Aquifer width beneath Tank 17	3.0
	3	Longitudinal / vertical dispersivity ratio	2.9
	4	Natural infiltration rate	2.8
Max. conc. Pu-239 at Well 6 within 50,000 years	1	Saturated thickness of the aquifer	17
	2	Clayey soil K_d for Pu	12
	3	UZ thickness beneath Tank 18	2.8
	4	Sandy soil K_d for Pu	2.4
Max. conc. Ra-226 at Well 6 within 50,000 years	1	Saturated thickness of the aquifer	24
	2	TypeIV Tank Configuration Timing for Cases A&B	7.1
	3	Average waste thickness in Tank 4	1.9
	4	Oxidizing old concrete K_d for Pu	1.2
Max. conc. Np-237 at Well 6 within 50,000 years	1	Saturated thickness of the aquifer	2.8
	2	Saturated zone thickness beneath Tank 4	1.5
	3	Average waste thickness in Tank 4	1.3
	4	Oxidizing old concrete K_d for Np	1.0

Table 5.6-13: Identification of the Most Sensitive Parameters for the Endpoints of Interest (Continued)

Endpoint	SI Rank	Input Parameter	Sensitivity Index
Max. conc. Tc-99 at Well 6 within 50,000 years	1	Saturated thickness of the aquifer	9.2
	2	Average waste thickness in Tank 4	4.7
	3	Oxidizing middle-aged concrete K_d for Tc	2.2
	4	UZ thickness beneath Tank 20	2.0
Max. conc. Pu-239 at Well 33 within 50,000 years	1	Saturated thickness of the aquifer	16
	2	Sandy soil K_d for Pu	6.7
	3	UZ thickness beneath Transfer Lines	2.5
	4	Pore water volumes to transition from oxidizing middle-aged to oxidizing old concrete (second transition)	1.9
Max. conc. Ra-226 at Well 33 within 50,000 years	1	Saturated thickness of the aquifer	18
	2	Aquifer width beneath Tank 28	2.8
	3	Natural infiltration rate	2.2
	4	UZ thickness beneath Transfer Lines	1.9
Max. conc. Np-237 at Well 33 within 50,000 years	1	Saturated thickness of the aquifer	18
	2	Oxidizing old concrete K_d for Np	8.4
	3	Aquifer width beneath Tank 28	3.3
	4	Aquifer width beneath Tank 47	2.2
Max. conc. Tc-99 at Well 33 within 50,000 years	1	Saturated thickness of the aquifer	26
	2	Natural infiltration rate	4.1
	3	Aquifer width beneath Tank 28	2.6
	4	Aquifer width beneath Tank 46	2.3

The partial dependence plots shown in Figure 5.6-23 identify the four most significant model input parameters in determining the maximum dose to a MOP at any well within 10,000 years. The dose is driven by radionuclide concentrations in water drawn from a well, and in this case, the MOP is exposed to the worst concentration in any well at any given time. The most significant parameter is Saturated Thickness: the thickness of the aquifer, or saturated zone. Since the aquifer dilutes the radionuclides introduced to it, the dose from well water use depends highly on this parameter.

The blue lines indicate the part of the range of each variable that has the greatest influence. For aquifer thickness, then, the most significant influence is in its lower range. Since it is inversely related to dose, the roughly hyperbolic shape is to be expected.

Following the aquifer thickness in importance is the K_d of plutonium in sandy soil. Since the MOP dose is dominated by Pu-239, the role of K_d in retarding the transport of Pu-239 aids in delaying the dose peak past 10,000 year and thereby reducing its maximum at 10,000 years.

The probabilistic GoldSim FTF model includes a discrete distribution determining which of six tank failure configurations (summarized in Table 5.6-2) to assume for a given realization. As the green image of the underlying distribution shows, configuration 1 (Configuration A in this PA) is the most likely to occur, followed by 2 (Configruation B) and so on. The difference between Configurations A and B is further seen to be negligible in determining dose, as implied by the flat blue line. Since these configurations have very different properties, in terms of failure times and modes, configuration selection is an important stochastic variable.

The fourth-ranked variable, the unsaturated zone thickness, also helps in delaying the transport of radionuclides to the point of exposure at the well. This is also most sensitive in the lower half of its range (2m to 7m).

Figure 5.6-23: Partial Dependence Plot for Maximum MOP Dose (mrem/yr) from any Well within 10,000 Years

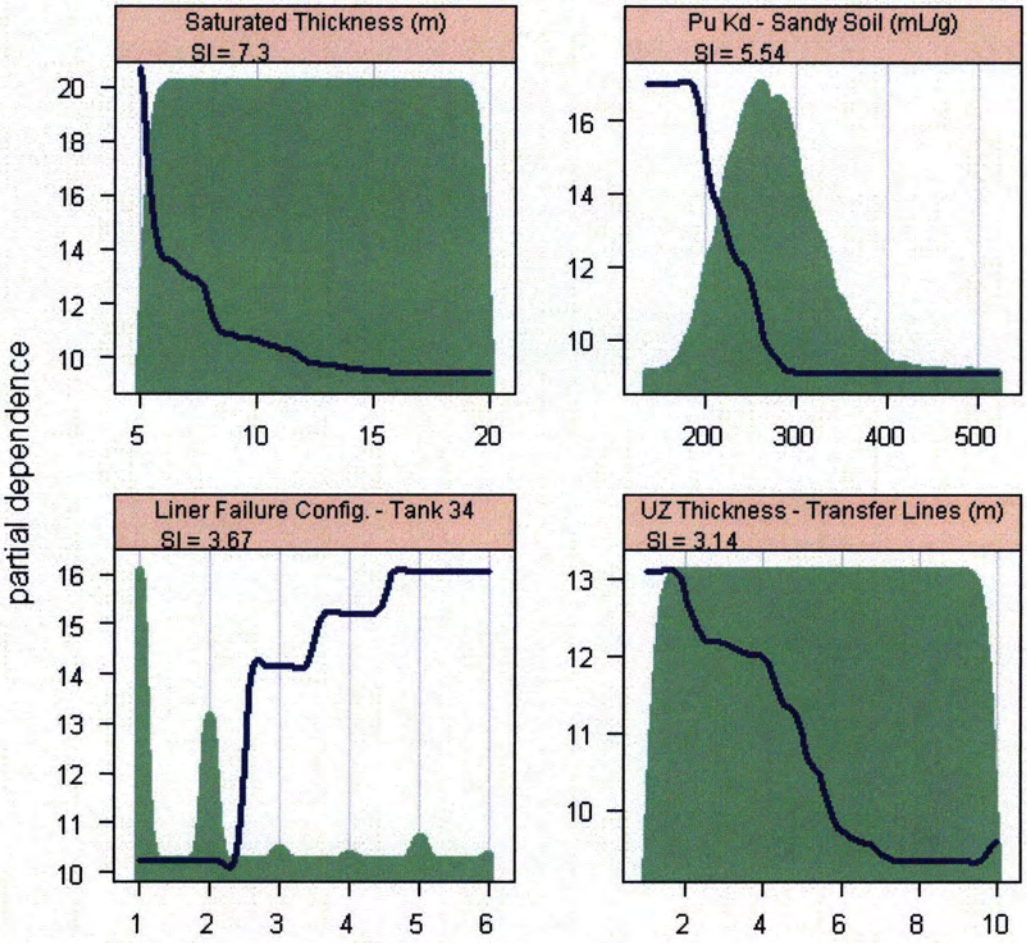

Figure 5.6-24 shows SI plots for the maximum dose to a MOP from any well occurring any time before 50,000 years. Again, the significance of aquifer thickness is dominant, with the related aquifer Darcy velocity (associated with Tank 46) ranked third. The K_d of Pu in natural soils, both sandy and clayey, also has a significant role.

Figure 5.6-24: Partial Dependence Plot for Maximum MOP Dose (mrem/yr) from any Well within 50,000 Years

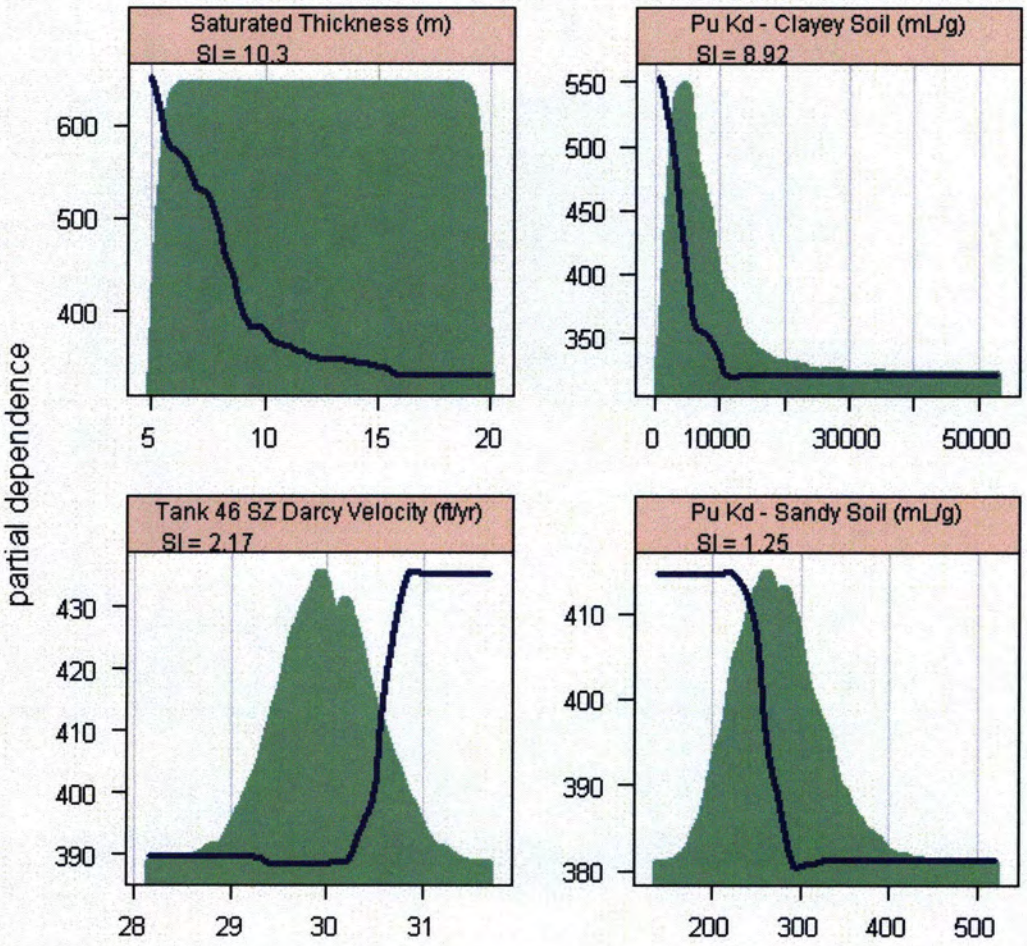

The results for the MOP dose from Well 6 within 10,000 years (Figure 5.6-25) identify sensitive parameters similar to those in the doses from any well (Figures 5.6-23 and 5.6-24), meaning whichever well has the highest concentration. The fact that the same parameters are sensitive to these endpoints is as expected, since the well with the highest concentrations is typically Well 6.

The transfer lines (in the second parameter) have some Pu inventory that is released relatively early due to the assumption that transfer line failure will occur sooner than the waste tank liner failure.

Figure 5.6-25: Partial Dependence Plot for Maximum MOP Dose from Well 6 within 10,000 Years

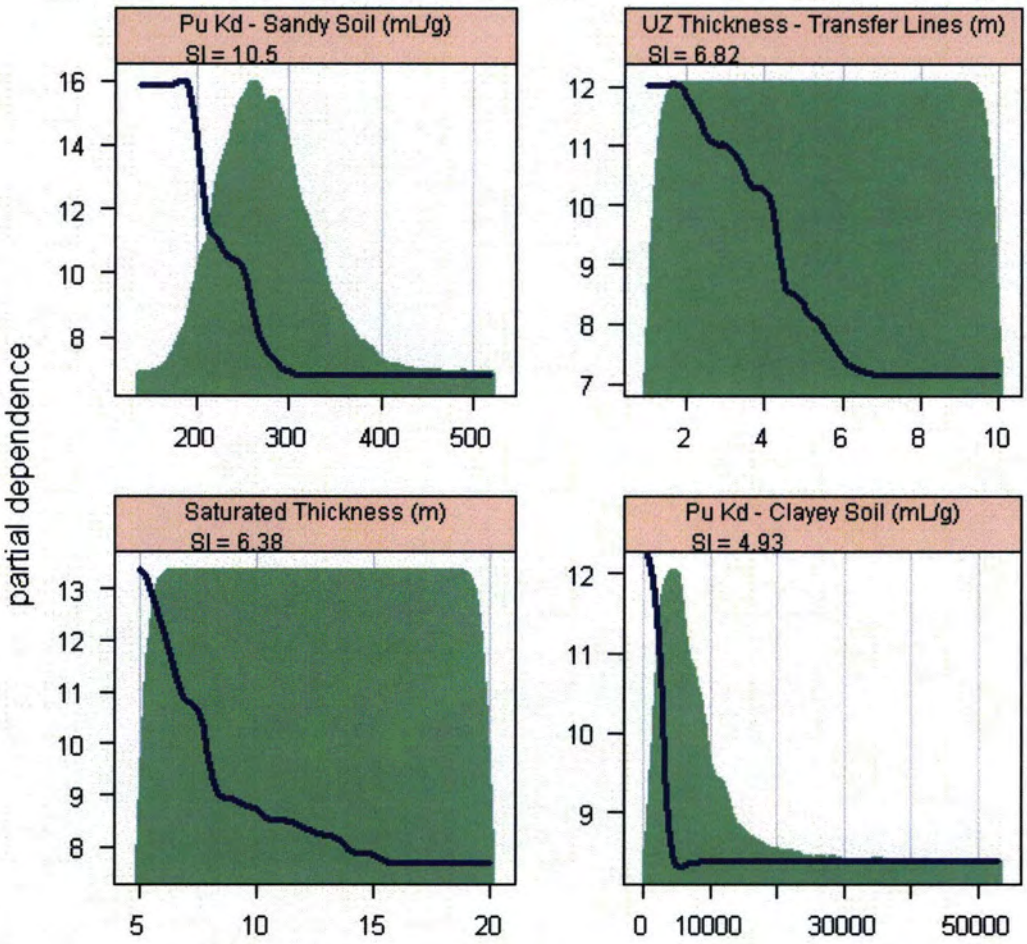

In Figure 5.6-26, the same four parameters appear, with the exception that the unsaturated zone thickness is under Tank 18 rather than the transfer lines. Since the dose examined here is within 50,000 years, the much larger inventory of Tank 18 relative to the transfer line is relevant because waste tank failure becomes more probable after 10,000 years.

Figure 5.6-26: Partial Dependence Plot for Maximum MOP Dose from Well 6 within 50,000 Years

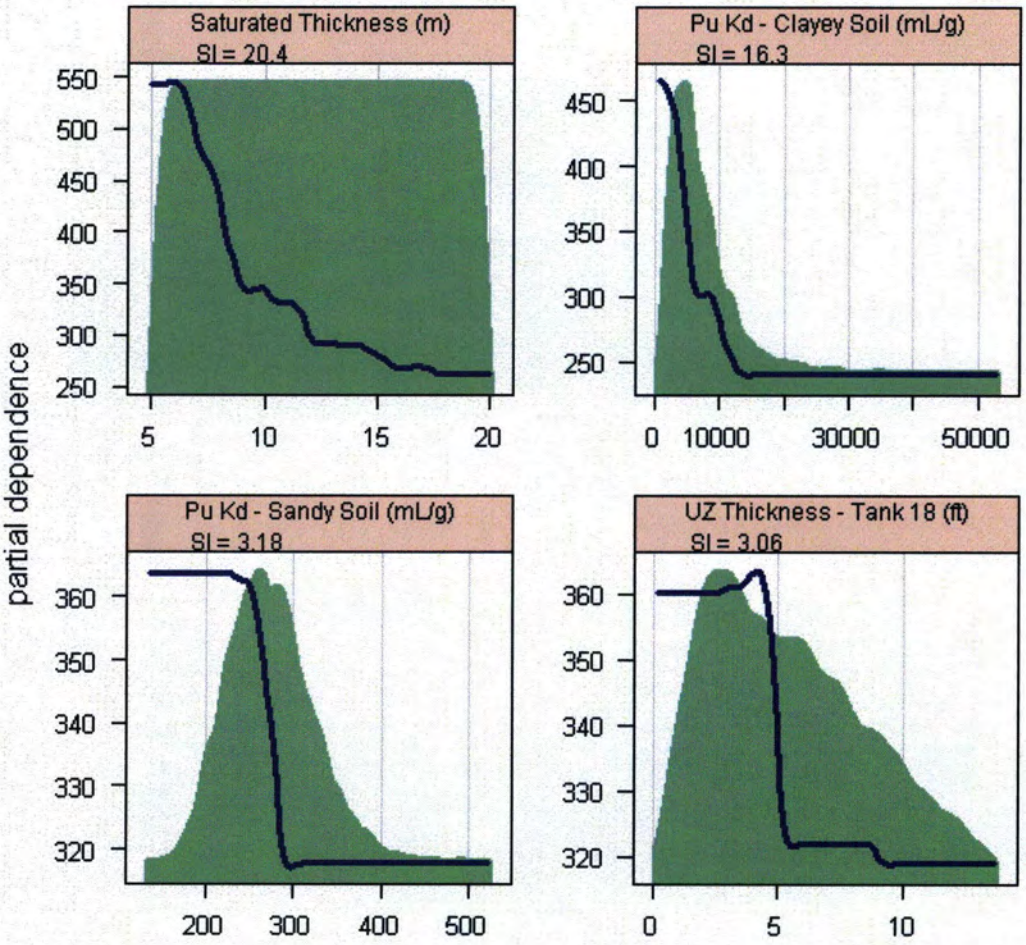

The MOP dose at Well 33 within the period of performance is sensitive to parameters governing the behavior of Tanks 33 and 34, which lie upstream (Figure 5.6-27). The failure configuration selector for Tank 34 is ranked first, followed by the unsaturated zone thickness under Tank 33. This is followed by the K_d for Pu, and the aquifer thickness associated with the transfer lines.

Figure 5.6-27: Partial Dependence Plot for Maximum MOP Dose from Well 33 within 10,000 Years

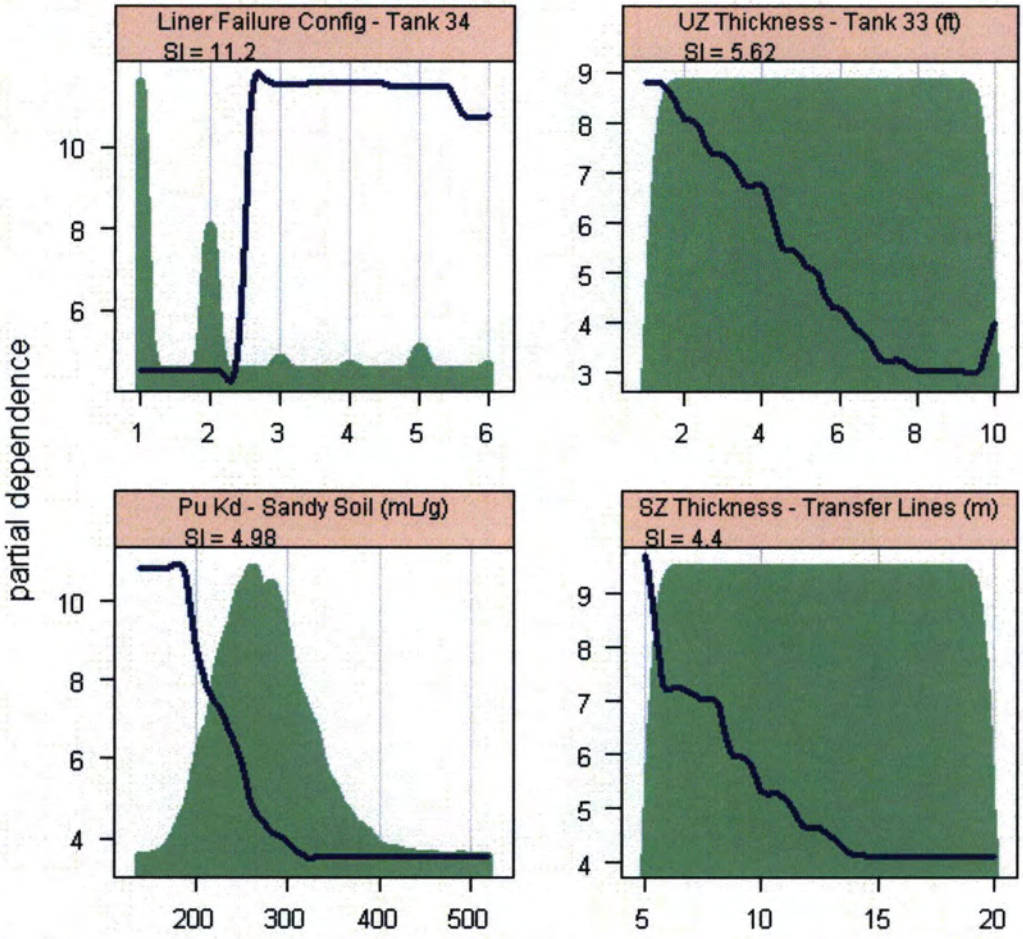

The MOP dose at Well 33 is dominated by the ingestion of Pu-239 in water, largely from Tank 33. All aspects of this pathway are seen in these plots shown in Figure 5.6-28: aquifer thickness, the K_d of Pu in sandy soil, the drinking water consumption rate, and the thickness of the unsaturated zone beneath Tank 33.

Figure 5.6-28: Partial Dependence Plot for Maximum MOP Dose from Well 33 within 50,000 Years

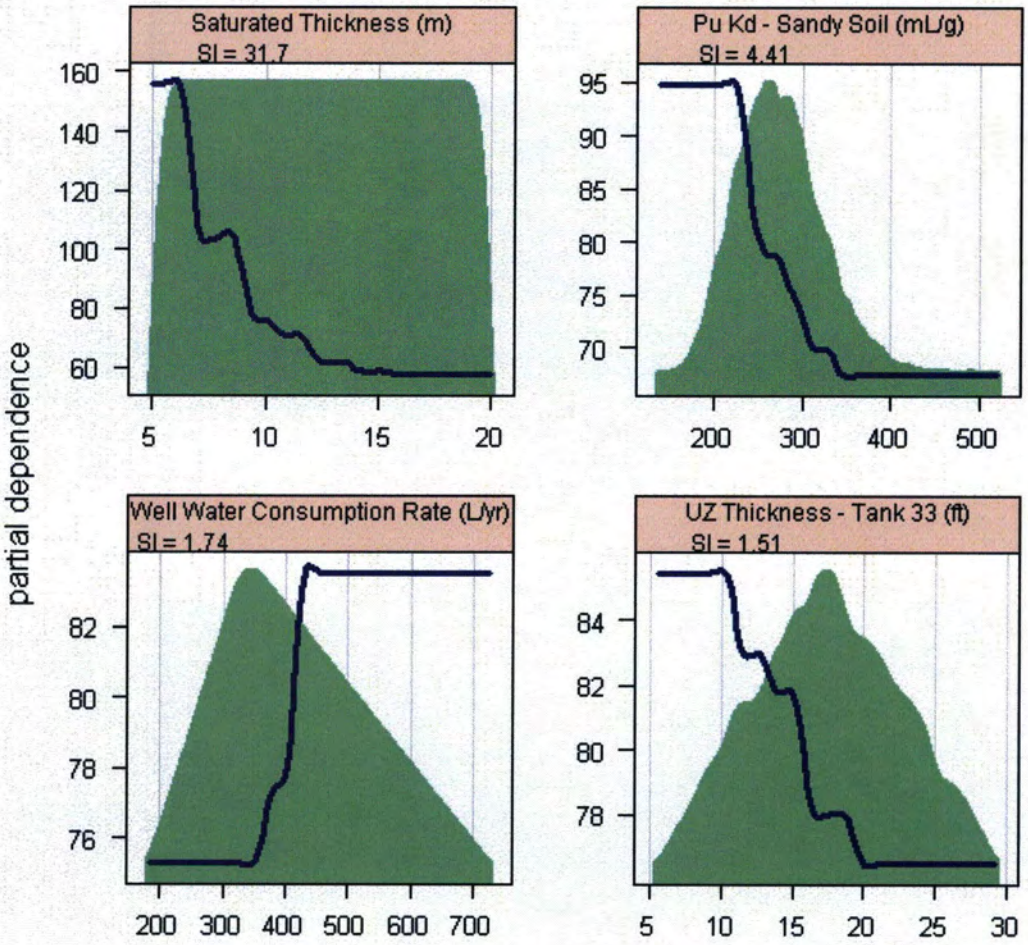

The parameters most influential to the chronic IHI dose within the period of performance are shown in Figure 5.6-29. The aquifer thickness is very significant, with an SI of 11. The the K_d for thorium in oxidizing young concrete also exhibits some influence. The third-ranked parameter is the time at which Type IV tanks fail, under Configurations A and B (as presented in Table 5.6-2. The fourth parameter is the thickness of the unsaturated zone beneath Tank 17.

Figure 5.6-29: Partial Dependence Plot for Maximum Inadvertent Human Intruder Chronic Dose within 10,000 Years

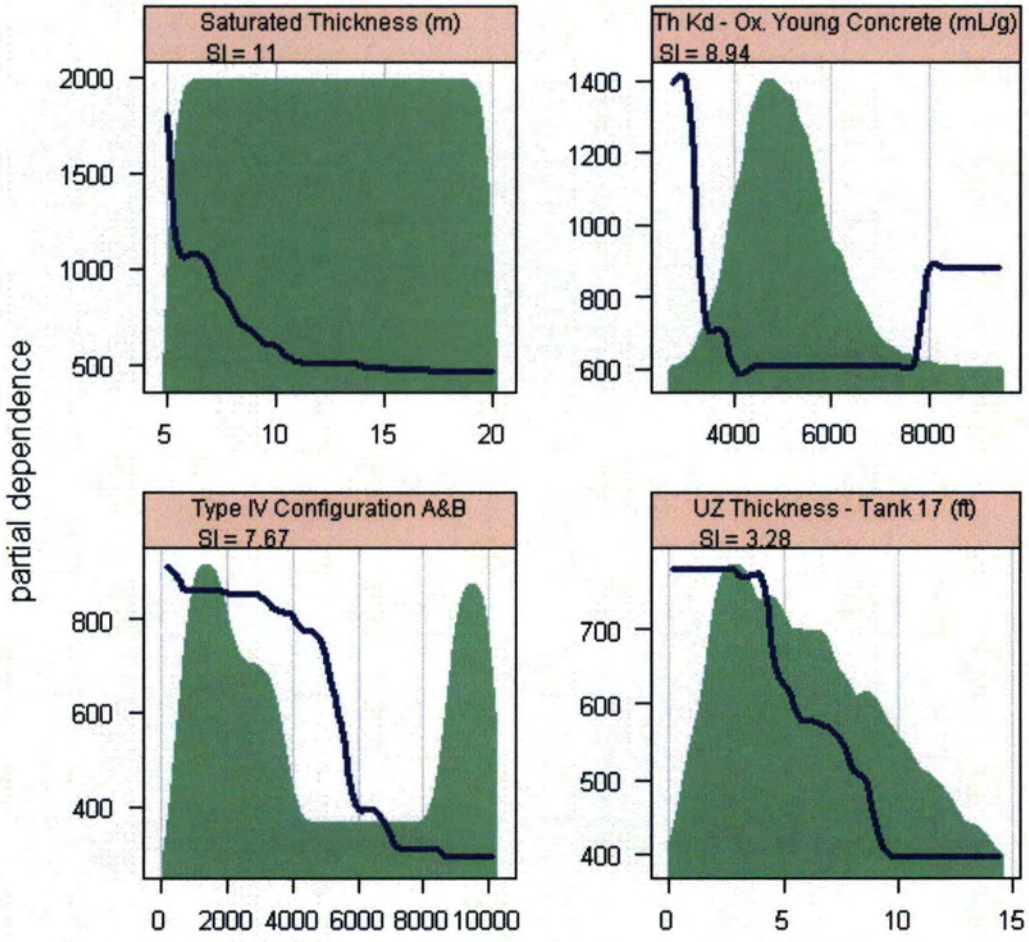

When extending the analysis from 10,000 to 50,000 years, the chronic IHI dose has some similarities (aquifer thickness and the width of the aquifer beneath Tank 17) and some new sensitivities as shown in Figure 5.6-30. The longitudinal-to-vertical dispersivity ratio is a groundwater hydraulic parameter governing the amount of vertical dispersion in the aquifer, in addition to the numerical dispersion inherent in modeling the aquifer as a single fully-mixed layer. The natural infiltration rate also exhibits some influence.

Figure 5.6-30: Partial Dependence Plot for Maximum Inadvertent Human Intruder Chronic Dose within 50,000 Years

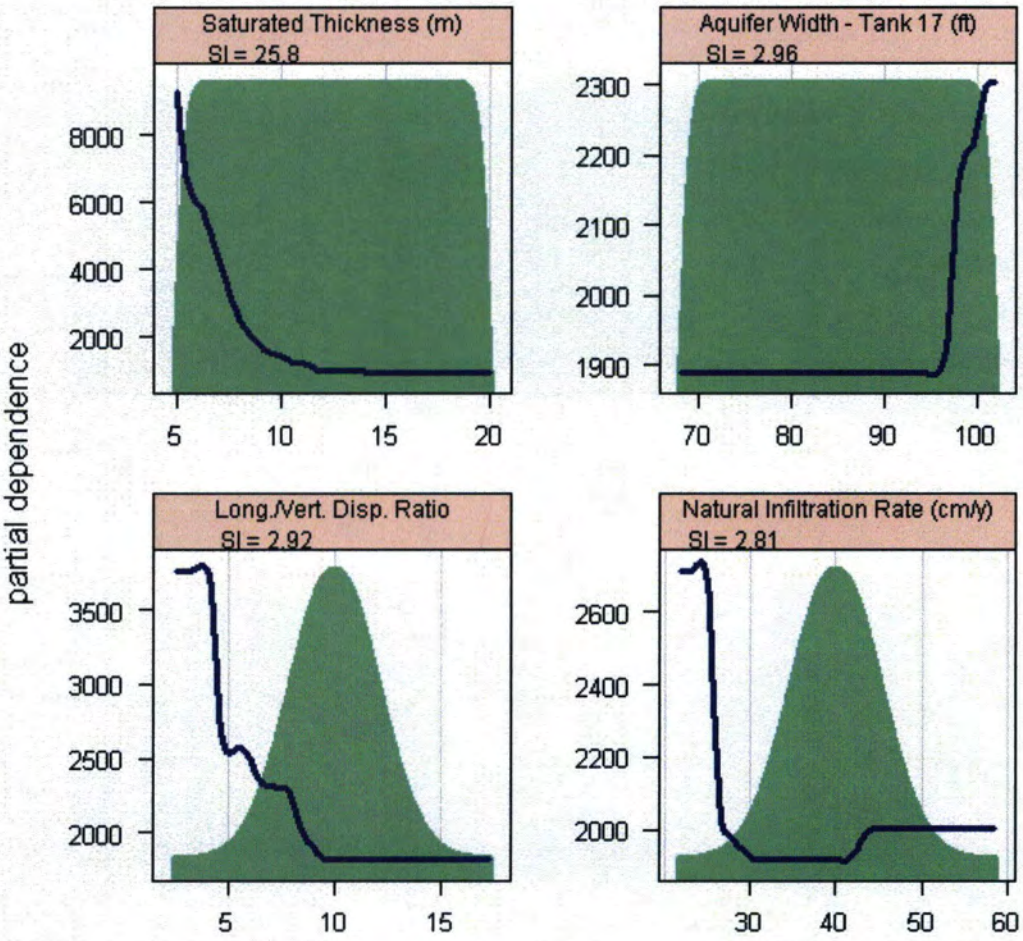

In addition to estimating doses to future receptors, there is interest in evaluating the maximum aqueous concentrations of various radionuclides at the point of exposure. A sensitivity analysis of such endpoints reveals the influence of contaminant fate and transport phenomena in isolation from dose parameters. Having examined the results from the perspective of dose, the most significant wells are found to be Wells 6 and 33. The most

significant radionuclides are Pu-239, Ra-226, Np-237, and Tc-99. Using these same endpoints helps in the comparison of sensitivities with and without the dose parameters. It is true, however, that only one dose parameter was found to be significant: the consumption rate of well water.

The first of the aqueous concentration analyses is focused on Pu-239 at Well 6, shown in Figure 5.6-31. These parameters are all clearly related to contaminant transport, and further identify Tank 18 as a significant contributor, since the thickness of the vadose zone beneath it is found to be sensitive.

Figure 5.6-31: Partial Dependence Plot for Maximum Aqueous Concentration of Pu-239 at Well 6 within 50,000 Years

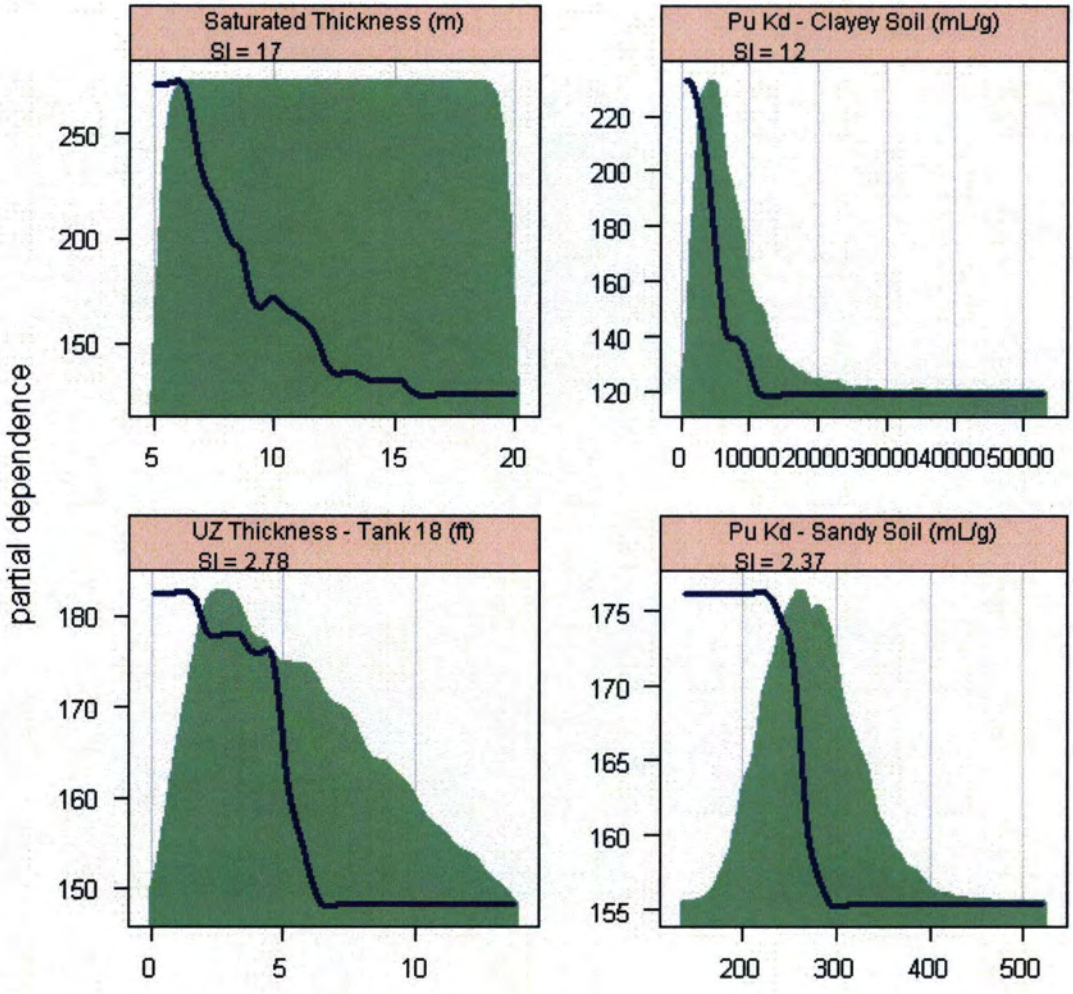

The parameters determining the concentration of Ra-226 at Well 6 are of many types, as seen in Figure 5.6-32. Aquifer thickness again has the highest SI, followed by the timing of tank failure in Configurations A and B. The average waste thickness in Tank 4 is next, showing that the most sensitive part of the range is between 0.20 and 0.25 inches. Finally, the K_d of Pu in oxidizing old concrete, illustrating how the influence of the Pu-238 parent is carried through to the progeny to Ra-226.

Figure 5.6-32: Partial Dependence Plot for Maximum Aqueous Concentration of Ra-226 at Well 6 within 50,000 Years

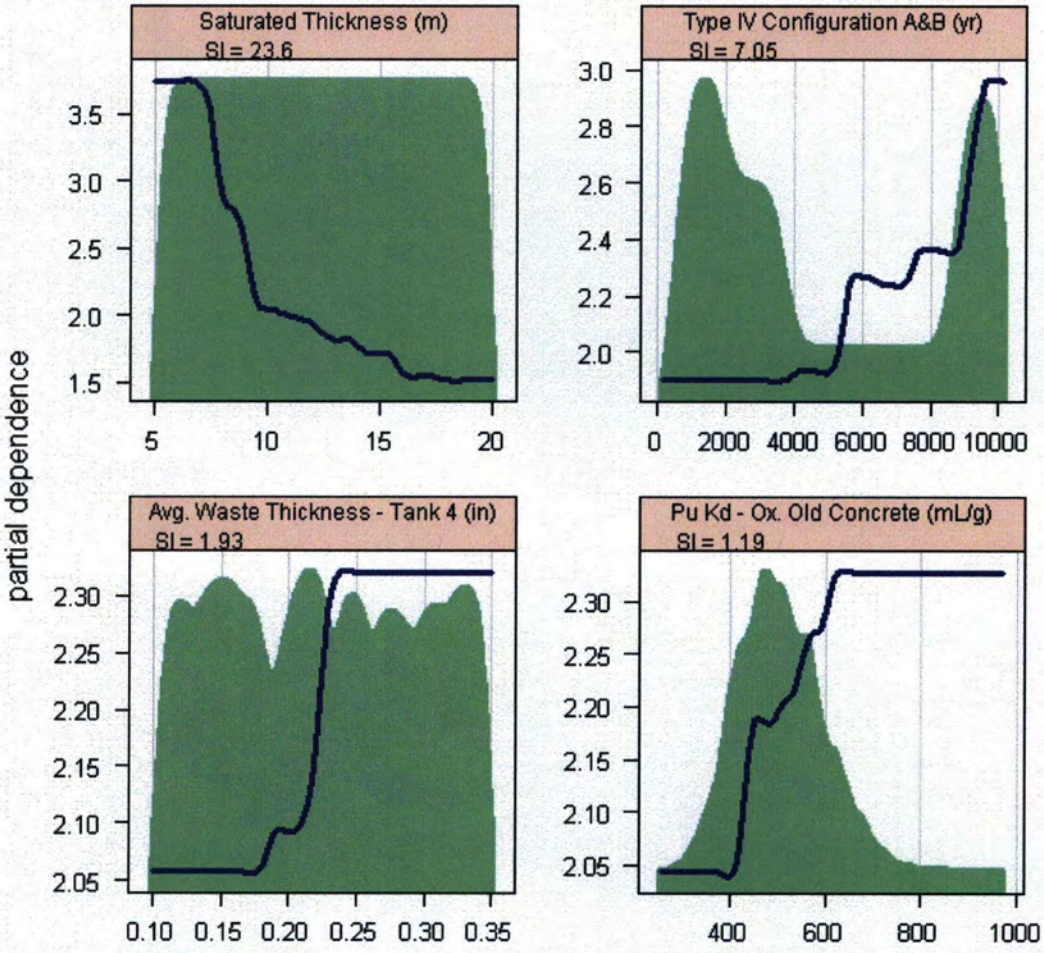

The variables influencing the aqueous concentration of Np-237 at Well 6 are as seen previously. Figure 5.6-33 shows the two most important parameters are aquifer thickness (defined as a global variable in the FTF model) and a separate incarnation of aquifer thickness, associated with only the transfer lines, part of the ancillary equipment at FTF. These are followed by the average waste thickness in Tank 4, and the K_d of Np in oxidizing old concrete.

Figure 5.6-33: Partial Dependence Plot for Maximum Aqueous Concentration of Np-237 at Well 6 within 50,000 Years

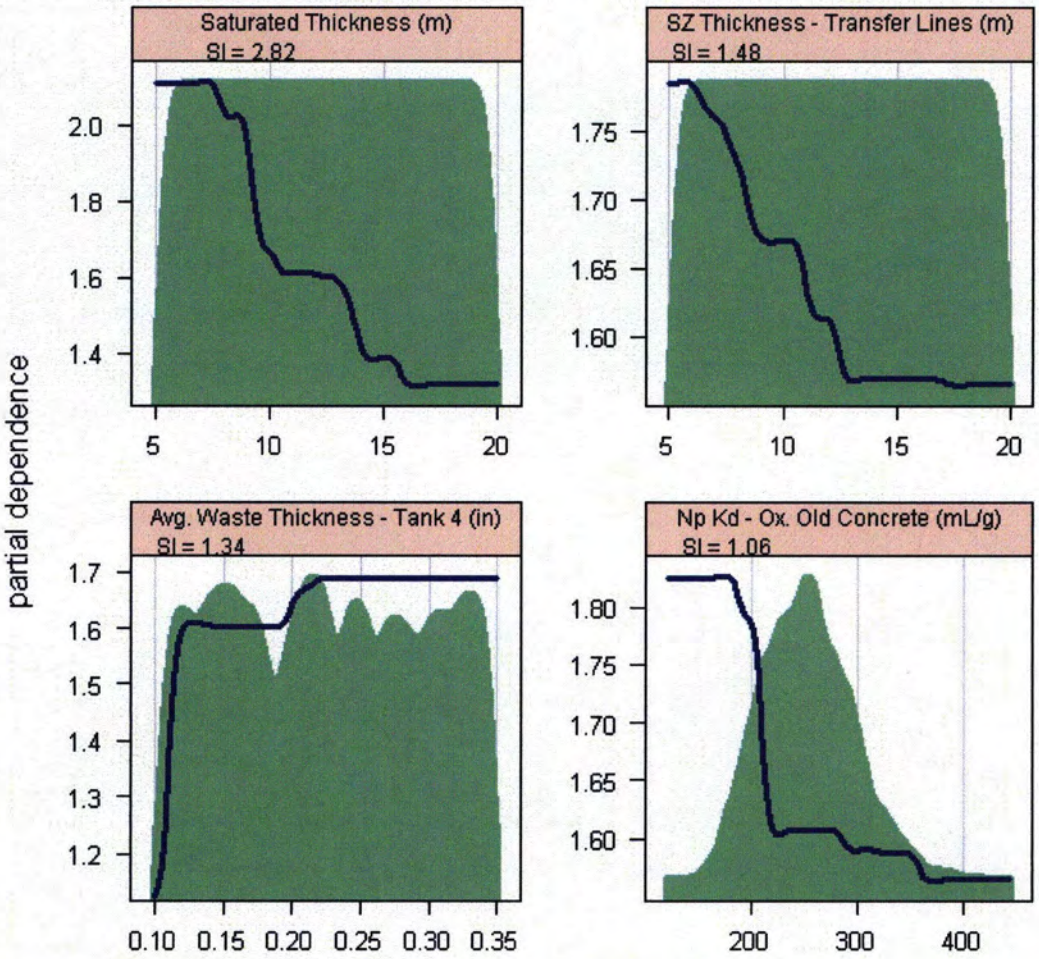

The sensitive parameters for the aqueous concentration of Tc-99 at Well 6 are shown in Figure 5.6-34. Aquifer thickness is the parameter of most importance, followed by the average waste thickness in Tank 4, the K_d of Tc in oxidizing middle-aged concrete, and the vadose zone thickness beneath Tank 20.

Figure 5.6-34: Partial Dependence Plot for Maximum Aqueous Concentration of Tc-99 at Well 6 within 50,000 Years

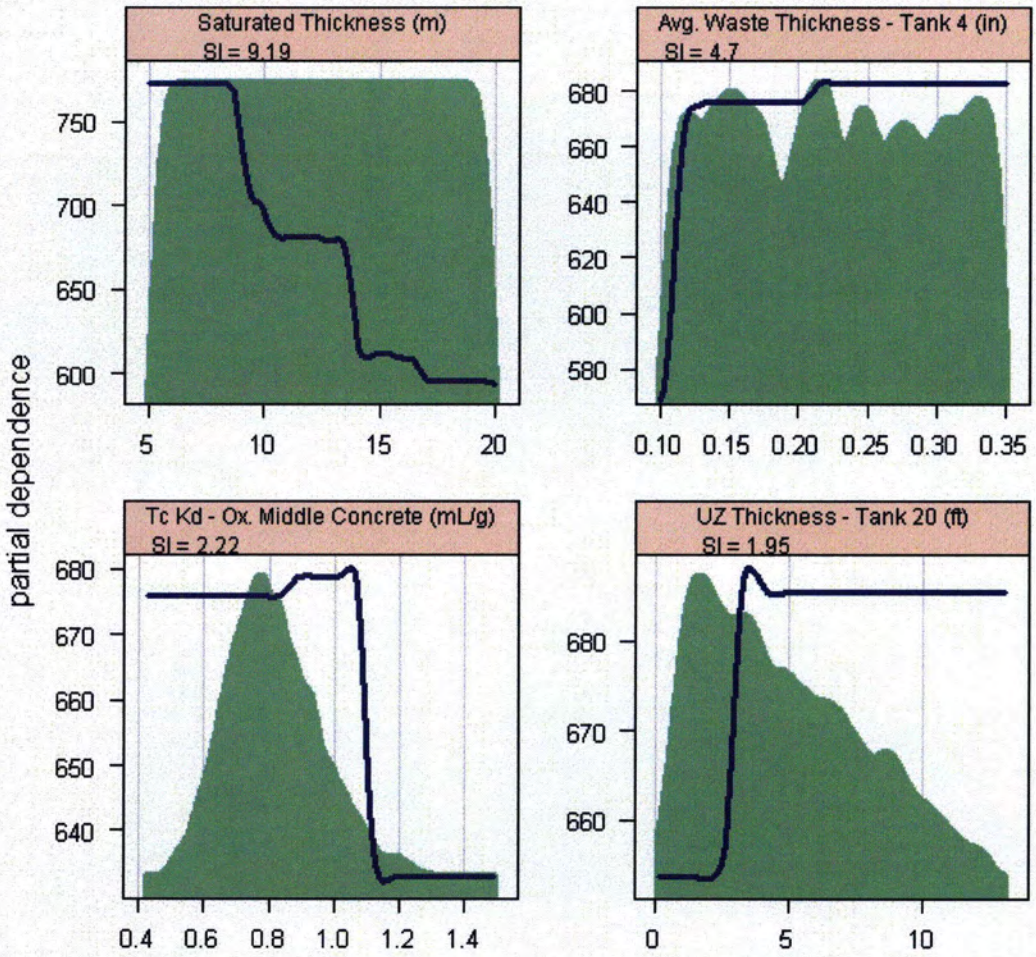

Figure 5.6-35 presents the sensitive parameters for the aqueous concentration of Pu-239 at Well 33. The first three parameters of importance are aquifer thickness, the K_d of Pu in sandy soil, and the vadose zone thickness beneath the transfer lines. The fourth is the number of pore volumes of water needed to make the second chemical transition in tank grout, which is associated with large changes in chemical solubilities and partition coefficients (K_ds), including those for Pu.

Figure 5.6-35: Partial Dependence Plot for Maximum Aqueous Concentration of Pu-239 at Well 33 within 50,000 Years

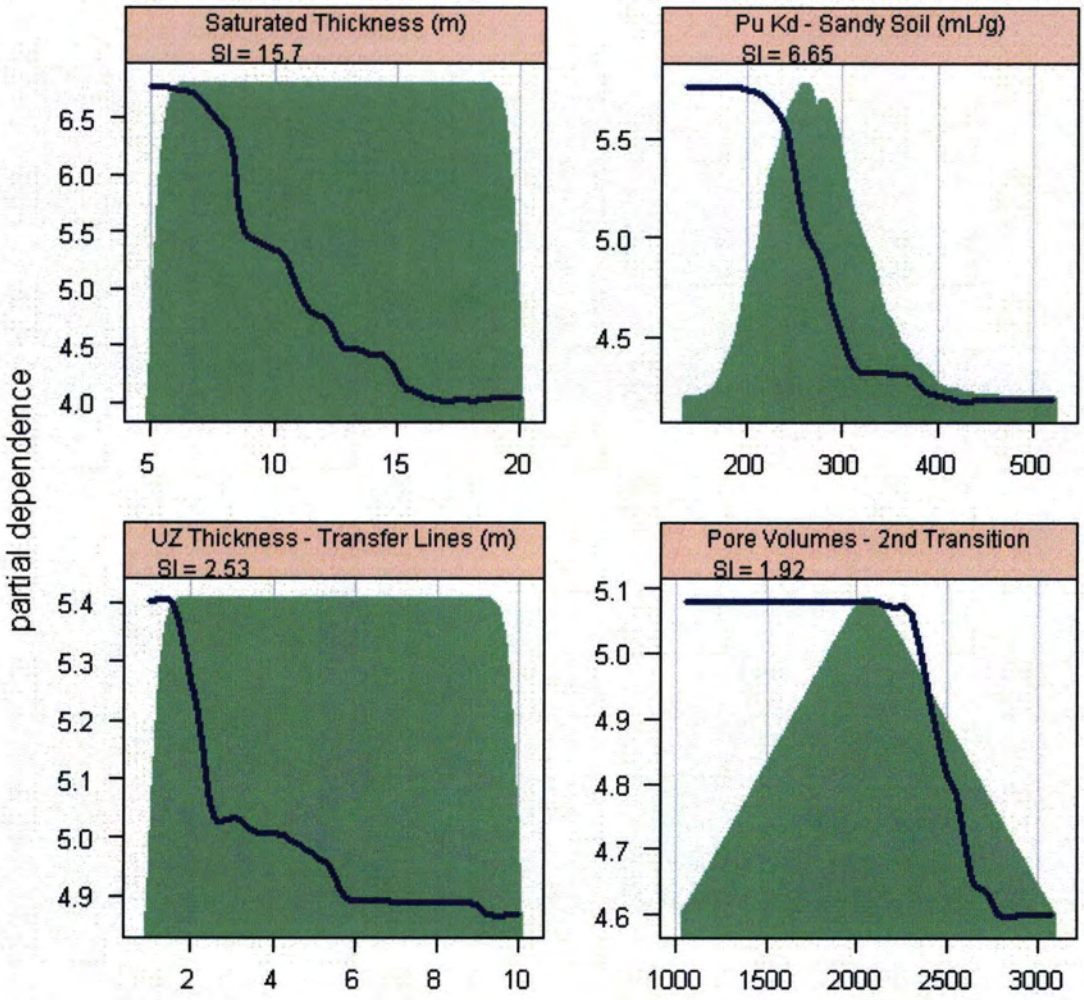

The results of the sensitivity analysis of the maximum aqueous concentration of Ra-226 at Well 33 are shown in Figure 5.6-36. The four most significant variables are all related to waterborne porous medium transport are the aquifer thickness, the width of the aquifer beneath Tank 28 (a contributor to Well 33), the natural infiltration rate of water above the FTF, and the assumed vadose zone thickness beneath the transfer lines.

Figure 5.6-36: Partial Dependence Plot for Maximum Aqueous Concentration of Ra-226 at Well 33 within 50,000 Years

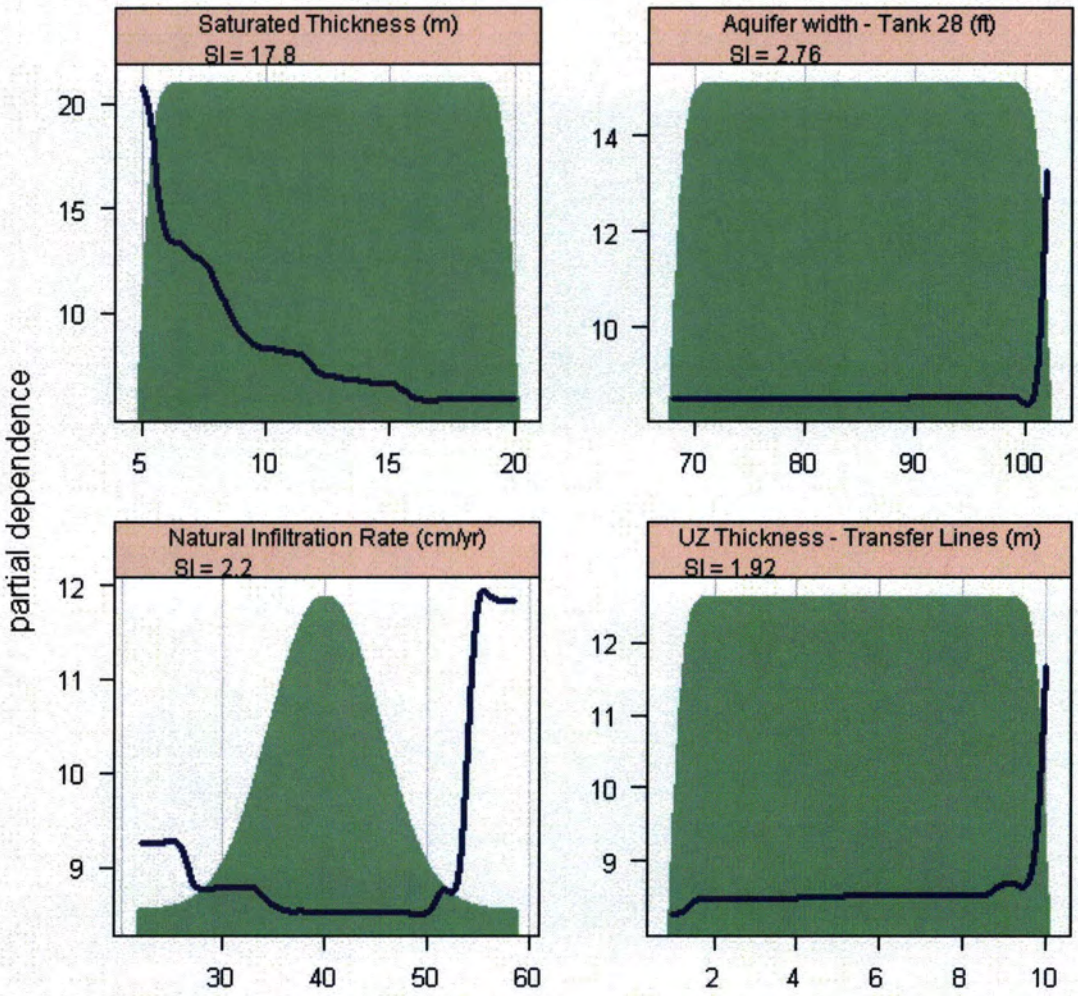

The maximum aqueous concentration of Np-237 is sensitive to the parameters identified in Figure 5.6-37. Aquifer thickness is followed by the K_d for Np in oxidizing old concrete, and the assumed aquifer width beneath Tanks 28 and 47.

Figure 5.6-37: Partial Dependence Plot for Maximum Aqueous Concentration of Np-237 at Well 33 within 50,000 Years

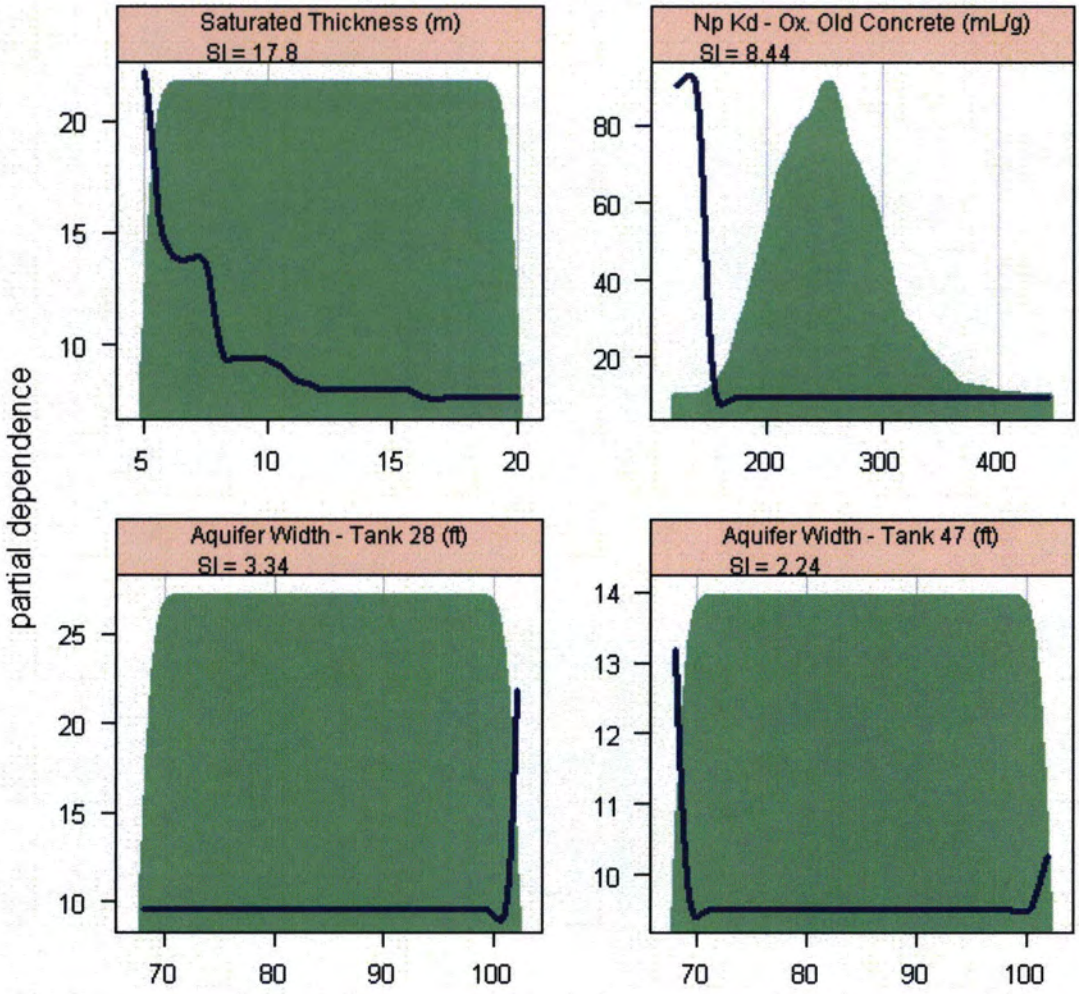

The maximum aqueous concentration of Tc-99 is also sensitive to waterborne transport parameters, as shown in Figure 5.6-38. In comparison to the plots for Ra-226 and Np-237, these show more variation in the partial dependence of the result on the variables of interest. The four most significant parameters for this endpoint are the aquifer thickness, natural infiltration rate, aquifer width beneath Tanks 28, and aquifier width beneath Tank 46.

Figure 5.6-38: Partial Dependence Plot for Maximum Aqueous Concentration of Tc-99 at Well 33 within 50,000 Years

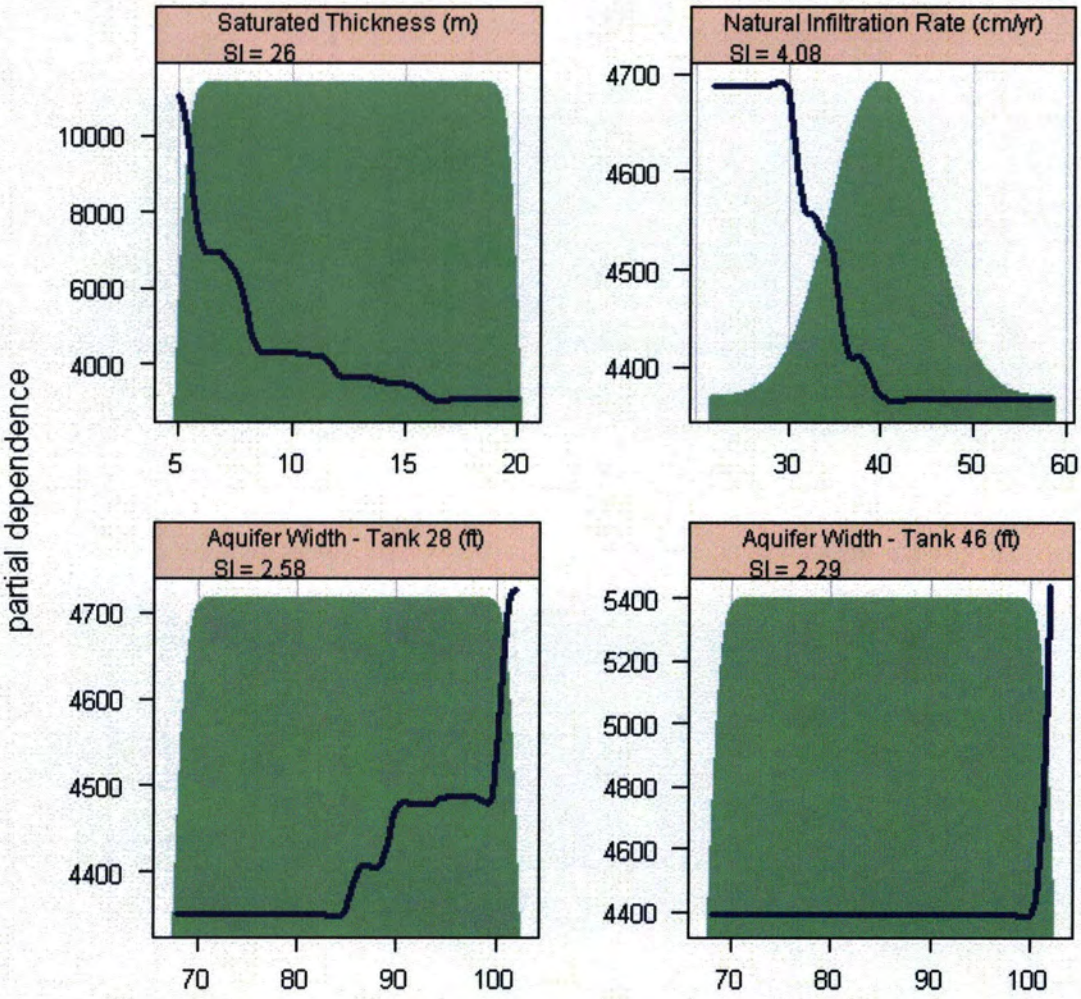

5.6.6.4 Summary of the FTF Probabilistic Model Sensitivity Analysis

The sensitivity analysis of the GoldSim FTF model v1.1 is complicated by the complexity of the FTF model and the wide ranges of some input distributions, as discussed in Section 5.6.6.3, and indicated by the relatively low SI. However, several recurring themes appeared in the sensitivity analysis:

- The generally low values of the SI indicate that there is some degree of uncertainty (at a minimum variability), as discussed in Section 5.6.5. Future refinement of distributions would be expected to further reduce model uncertainty.
- K_d values are quite significant, though the sensitivity may in part be due to the long tails from the lognormal distributions.
- Dose and concentration are sensitive to the dimensions and flow rates in the unsaturated and saturated zones. This is to be expected in a model dominated by waterborne transport processes.
- The timing and geochemical and hydraulic attributes associated with tank degradation are also important in determining radionuclide transport and subsequent dose.

Some parameters, such as unsaturated and saturated zone thickness were expected due to the depth of the Type IV tanks in relation to the upper aquifer. Based on these results, any future work would concentrate on these parameters identified as being important. Deterministic sensitivity cases for single parameter analyses (e.g., choice of tank configuration, tank inventories) have been conducted to supplement the probabilistic assessment, as discussed elsewhere in this Section.

5.6.7 Single Parameter Sensitivity Analyses

The purpose of this section is to consider the impact varying a single parameter might have on the FTF deterministic model, so that the sensitivity of the models to changes in select parameters of concern might be discovered.

5.6.7.1 Inventory Sensitivity Analysis using the PORFLOW Deterministic Model

The waste tank inventory sensitivity analysis results are provided in this section. Using the PORFLOW FTF Base Case presented in Section 4.4, the release rates (fluxes) for key radionuclides were calculated with increased and decreased inventories for Tanks 5, 6, 18 and 19. For Tanks 18 and 19, the low case is 0.8X the Base Case, and the high case is 1.2X the Base Case. For Tanks 5 and 6, the low case is 0.5X the Base Case, and the high case is 1.5X the Base Case. The results of these sensitivity analyses, showing the maximum flux in 20,000 years for the Base Case and sensivitity cases are presented in Tables 5.6-14 through 5.6-17. The results show that for most of the radionuclides, the flux essentially varies linearly with inventory. The exceptions (e.g., Pu-239, Pu-240, Tc-99, and U-238) are those radionuclides that are solubility controlled through iron co-precipitation and are present in a significant enough quantity for solubility control to have an effect.

Appendix J contains data curves showing the flux (Ci/year) leaving Tanks 5, 6, 18 and 19 for the inventory sensitivity cases. The flux is provided for the key radionuclides.

Table 5.6-14: Tank 5 Inventory Sensitivity Results

Nuclide	Base Case PeakFlux (Ci|kg/yr)	Higher Inventory PeakFlux (Ci|kg/yr)	Higher Inventory factor	Lower inventory PeakFlux (Ci|kg/yr)	Lower Inventory Factor
C-14	1.96E-06	2.94E-06	1.50	9.79E-07	0.50
Np-237	9.50E-06	1.48E-05	1.56	4.65E-06	0.49
Pa-231	4.76E-08	7.09E-08	1.49	2.44E-08	0.51
Pb-210	8.45E-08	1.27E-07	1.50	4.22E-08	0.50
Pu-239	1.59E-06	1.59E-06	1.00	1.59E-06	1.00
Pu-240	3.61E-06	3.61E-06	1.00	3.46E-06	0.96
Pu-242	1.27E-08	1.92E-08	1.51	6.31E-09	0.50
Ra-226	3.28E-05	4.92E-05	1.50	1.64E-05	0.50
Tc-99	5.82E-06	5.82E-06	1.00	5.82E-06	1.00
Th-229	3.74E-07	5.49E-07	1.47	1.92E-07	0.51
Th-230	2.64E-08	3.89E-08	1.47	1.36E-08	0.51
U-233	5.17E-06	7.64E-06	1.48	2.68E-06	0.52
U-234	2.99E-06	4.40E-06	1.47	1.55E-06	0.52
U-236	9.36E-08	1.39E-07	1.49	4.81E-08	0.51
U-238	1.13E-08	1.13E-08	1.00	1.13E-08	1.00

Table 5.6-15: Tank 6 Inventory Sensitivity Results

Nuclide	Base Case PeakFlux (Ci|kg/yr)	Higher Inventory PeakFlux (Ci|kg/yr)	Higher Inventory factor	Lower Inventory PeakFlux (Ci|kg/yr)	Lower Inventory Factor
C-14	1.60E-06	2.41E-06	1.50	8.02E-07	0.50
Np-237	5.00E-06	7.54E-06	1.51	2.49E-06	0.50
Pa-231	3.72E-08	5.53E-08	1.49	1.90E-08	0.51
Pb-210	1.04E-07	1.56E-07	1.50	5.21E-08	0.50
Pu-239	1.59E-06	1.59E-06	1.00	1.59E-06	1.00
Pu-240	3.61E-06	3.61E-06	1.00	3.39E-06	0.94
Pu-242	1.06E-07	1.22E-07	1.14	4.27E-08	0.40
Ra-226	4.04E-05	6.06E-05	1.50	2.02E-05	0.50
Tc-99	5.82E-06	5.82E-06	1.00	5.82E-06	1.00
Th-229	1.08E-07	1.61E-07	1.49	5.42E-08	0.50
Th-230	3.23E-08	4.75E-08	1.47	1.66E-08	0.51
U-233	1.52E-06	2.26E-06	1.49	7.64E-07	0.50
U-234	3.65E-06	5.40E-06	1.48	1.89E-06	0.52
U-236	1.05E-07	1.56E-07	1.49	5.36E-08	0.51
U-238	1.13E-08	1.13E-08	1.00	1.13E-08	1.00

Table 5.6-16: Tank 18 Inventory Sensitivity Results

Nuclide	Base Case PeakFlux (Ci|kg/yr)	Higher Inventory PeakFlux (Ci|kg/yr)	Higher Inventory factor	Lower inventory PeakFlux (Ci|kg/yr)	Lower Inventory Factor
C-14	3.14E-05	3.76E-05	1.20	2.51E-05	0.80
Np-237	1.52E-05	1.68E-05	1.11	1.47E-05	0.97
Pa-231	8.34E-08	1.00E-07	1.20	6.68E-08	0.80
Pb-210	1.21E-08	1.44E-08	1.20	9.75E-09	0.81
Pu-239	4.97E-06	4.97E-06	1.00	4.97E-06	1.00
Pu-240	1.50E-05	1.50E-05	1.00	1.50E-05	1.00
Pu-242	3.44E-07	3.44E-07	1.00	3.44E-07	1.00
Ra-226	4.60E-06	5.52E-06	1.20	3.72E-06	0.81
Tc-99	4.35E-06	4.35E-06	1.00	4.35E-06	1.00
Th-229	1.69E-05	2.11E-05	1.25	1.31E-05	0.77
Th-230	1.43E-06	1.71E-06	1.20	1.16E-06	0.81
U-233	1.36E-04	1.71E-04	1.26	1.00E-04	0.74
U-234	5.41E-05	6.90E-05	1.28	4.08E-05	0.75
U-236	2.27E-06	2.68E-06	1.18	1.72E-06	0.75
U-238	1.23E-08	1.23E-08	1.00	1.23E-08	1.00

Table 5.6-17: Tank 19 Inventory Sensitivity Results

Nuclide	Base Case PeakFlux (Ci|kg/yr)	Higher Inventory PeakFlux (Ci|kg/yr)	Higher Inventory factor	Lower Inventory PeakFlux (Ci|kg/yr)	Lower Inventory Factor
C-14	6.29E-05	7.55E-05	1.20	5.03E-05	0.80
Np-237	9.60E-07	1.16E-06	1.20	7.66E-07	0.80
Pa-231	1.41E-08	1.69E-08	1.20	1.13E-08	0.80
Pb-210	9.69E-10	1.16E-09	1.20	7.75E-10	0.80
Pu-239	4.97E-06	4.97E-06	1.00	4.97E-06	1.00
Pu-240	1.50E-05	1.50E-05	1.00	1.50E-05	1.00
Pu-242	3.44E-07	3.44E-07	1.00	3.44E-07	1.00
Ra-226	3.71E-07	4.45E-07	1.20	2.96E-07	0.80
Tc-99	4.35E-06	4.35E-06	1.00	4.35E-06	1.00
Th-229	1.02E-05	1.20E-05	1.18	8.37E-06	0.82
Th-230	1.15E-07	1.38E-07	1.20	9.17E-08	0.80
U-233	7.06E-05	8.93E-05	1.26	5.36E-05	0.76
U-234	3.57E-06	4.29E-06	1.20	2.85E-06	0.80
U-236	3.35E-07	4.05E-07	1.21	2.67E-07	0.80
U-238	1.23E-08	1.23E-08	1.00	1.23E-08	1.00

5.6.7.2 K_d Sensitivity Analysis using the PORFLOW Deterministic Model

The purpose of this section is to present the K_d sensitivity analysis results for selected waste tanks. Using the PORFLOW FTF Base Case presented in Section 4.4, the release rates (fluxes) for Tc-99 and Pu-239 were calculated with increased and decreased K_d values assigned to the associated basemat and soil for Tanks 5, 18 and 34. These three tanks were selected for analysis because they represent one of each tank type, and therefore have different characteristics.

In addition to the Base Case K_d value, four separate PORFLOW runs were made for each nuclide (Pu-239 and Tc-99). The four cases are elevated basemat K_d, lower basemat K_d, elevated soil K_d, and lower soil K_d. The soil and basemat K_d values were varied similar to the procedure used for the probabilistic distributions (Section 5.6.3.4): if the K_d value is greater than 1,000, then the lower bound is five times less and the upper bound five times higher, and if the K_d value is less than 1,000, then the lower bound is two times less, and the upper bound is two times higher. The results of the K_d sensitivity runs, showing the maximum flux in 20,000 years for the Base Case, and four different cases, are presented in Tables 5.6-18 and 5.6-19 (the four cases are identified in the tables as: CaseA_*, where * represents "base_high", "base_low", "soil_high", "soil_low"). The soil K_d change was for the sandy soil, which includes the area below the tank and much of the aquifer. The results show that the Tc-99 flux is relatively unaffected by K_d changes, while the Pu-239 flux can be significantly impacted, especially when the material layer is thick (e.g., the Type III and Type I basemats).

Appendix I contains data curves showing the flux (Ci/year) leaving Tanks 5, 18, and 34 for the K_d sensitivity cases. The flux is provided for the Tc-99 and Pu-239.

Table 5.6-18: Tc-99 K_d Sensitivity Results

Nuclide	Case	Tank	Peak Flux (Ci|kg/yr)	Ratio to Base Case
Tc-99	CaseA	Tank05	5.82E-06	N/A
Tc-99	CaseA_base_high	Tank05	5.82E-06	1.00
Tc-99	CaseA_base_low	Tank05	5.82E-06	1.00
Tc-99	CaseA_soil_high	Tank05	5.82E-06	1.00
Tc-99	CaseA_soil_low	Tank05	5.82E-06	1.00
Tc-99	CaseA	Tank34	9.09E-06	N/A
Tc-99	CaseA_base_high	Tank34	1.02E-05	1.12
Tc-99	CaseA_base_low	Tank34	8.34E-06	0.92
Tc-99	CaseA_soil_high	Tank34	8.83E-06	0.97
Tc-99	CaseA_soil_low	Tank34	9.24E-06	1.02
Tc-99	CaseA	Tank18	4.35E-06	N/A
Tc-99	CaseA_base_high	Tank18	4.54E-06	1.04
Tc-99	CaseA_base_low	Tank18	4.35E-06	1.00
Tc-99	CaseA_soil_high	Tank18	4.44E-06	1.02
Tc-99	CaseA_soil_low	Tank18	4.35E-06	1.00

Table 5.6-19: Pu-239 K_d Sensitivity Results

Nuclide	Case	Tank	Peak Flux (Ci|kg/yr)	Ratio to Base Case
Pu-239	CaseA	Tank05	1.59E-06	N/A
Pu-239	CaseA_base_high	Tank05	2.20E-07	0.14
Pu-239	CaseA_base_low	Tank05	3.05E-06	1.92
Pu-239	CaseA_soil_high	Tank05	5.04E-08	0.03
Pu-239	CaseA_soil_low	Tank05	4.08E-06	2.56
Pu-239	CaseA	Tank34	3.72E-09	N/A
Pu-239	CaseA_base_high	Tank34	6.33E-12	1.70E-03
Pu-239	CaseA_base_low	Tank34	1.15E-07	30.89
Pu-239	CaseA_soil_high	Tank34	1.55E-12	4.16E-04
Pu-239	CaseA_soil_low	Tank34	6.38E-07	171.65
Pu-239	CaseA	Tank18	4.97E-06	N/A
Pu-239	CaseA_base_high	Tank18	5.18E-06	1.04
Pu-239	CaseA_base_low	Tank18	5.11E-06	1.03
Pu-239	CaseA_soil_high	Tank18	4.90E-06	0.98
Pu-239	CaseA_soil_low	Tank18	5.15E-06	1.04

5.6.7.3 Sensitivity Analyses using the GoldSim Deterministic Model

The purpose of this section is to present single parameter sensitivity analysis results obtained using the GoldSim FTF model. Select parameters within the GoldSim FTF model have been changed to assess the impact on the all-pathways dose. A discussion of the individual parameters modeled in the GoldSim FTF model is provided in Section 5.6.3.

- **Base Case Parameters with Configuration A**

Figures 5.6-39 and 5.6-40 show the peak all-pathways dose for Wells 6 and 33, the two wells with the highest peak doses within 20,000 years (Well 6 is along the flow path to UTR, Well 33 is along the flow path to Fourmile Branch). These dose curves were produced using the GoldSim FTF model (version 1.099) in deterministic mode using the Base Case input parameters and Configuration A. These dose curves differ slightly from the PORFLOW FTF model peak dose curves (e.g., Figure 5.5-2) due to the inherent differences between the models (discussed in the benchmarking section). However, magnitude and timing of the peak doses are similar such that valid sensitivity trends can be analyzed using only the GoldSim FTF model.

Figure 5.6-39: GoldSim FTF Model Baseline Parameters, All-Pathways Dose for Well 6

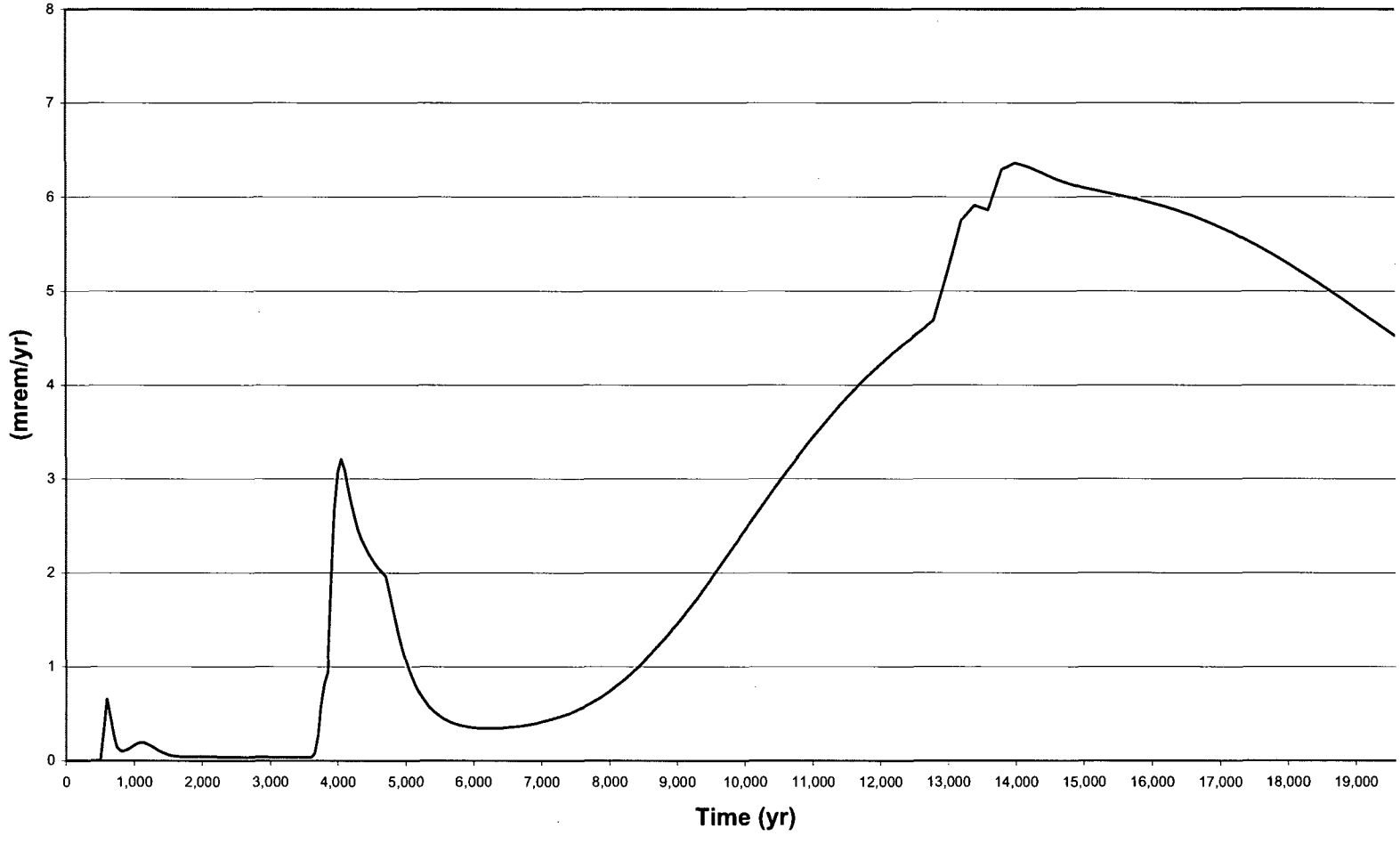

Figure 5.6-40: GoldSim FTF Model Baseline Parameters, All-Pathways Dose for Well 33

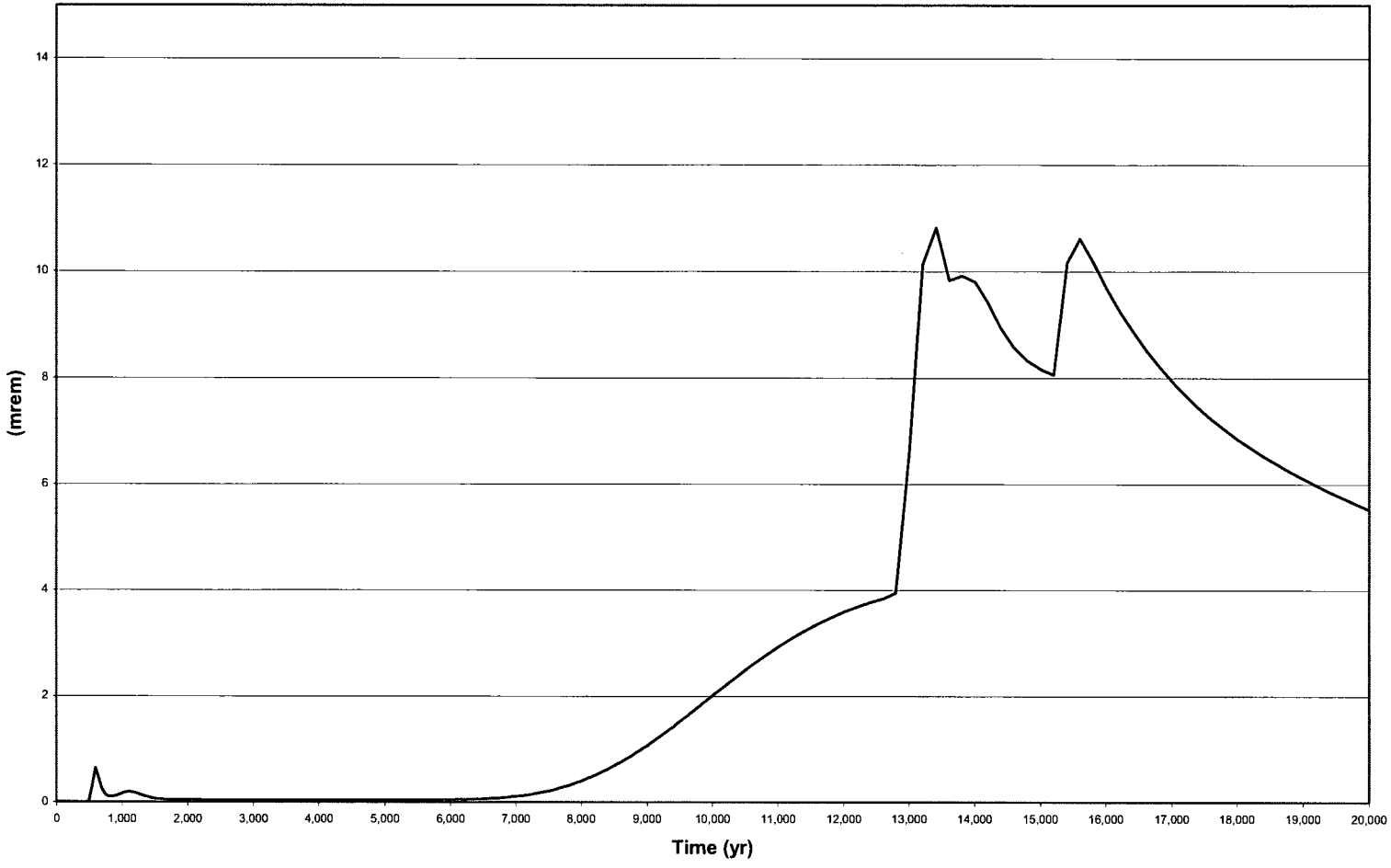

- **Base Case Parameters with Configuration A and a Bypass Fraction of 25%**

To investigate the effect of the tank basemat having reduced adsorptive properties, the "BypassFraction" deterministic value for all waste tanks was increased from 0.0 to 0.25. This change allows a full 25% of the flow from the waste to travel past the basemat without the basemat K_d having any effect. This sensitivity analysis conservatively bounds the impact of flow through a cracked basemat. Allowing the basemat to effectively have flow channels that penetrate over 25% of the basemat, with no adsorptive properties bounds any expected basemat degradation which would likely take the form of cracks. Figures 5.6-41 and 5.6-42 show the peak all-pathways dose for Wells 6 and 33 for 20,000 years with the 25% bypass fraction change in place. As can be seen from Figure 5.6-41, the 25% bypass fraction change has only a minor effect for Well 6, with the timing and magnitude of the dose peaks changing slightly. The 25% bypass fraction change has more effect for Well 33 (Figure 5.6-42), with the magnitude of the dose peaks increasing by about 20%-40%. The results are expected to vary for the two wells, since the Well 6 dose is dominated by Type IV Tanks, which have very thin basemats, while the Well 33 dose is dominated by Type III Tanks, which have very thick basemats.

Figure 5.6-41: GoldSim FTF Model Baseline Parameters with 25% Bypass, All-Pathways Dose for Well 6

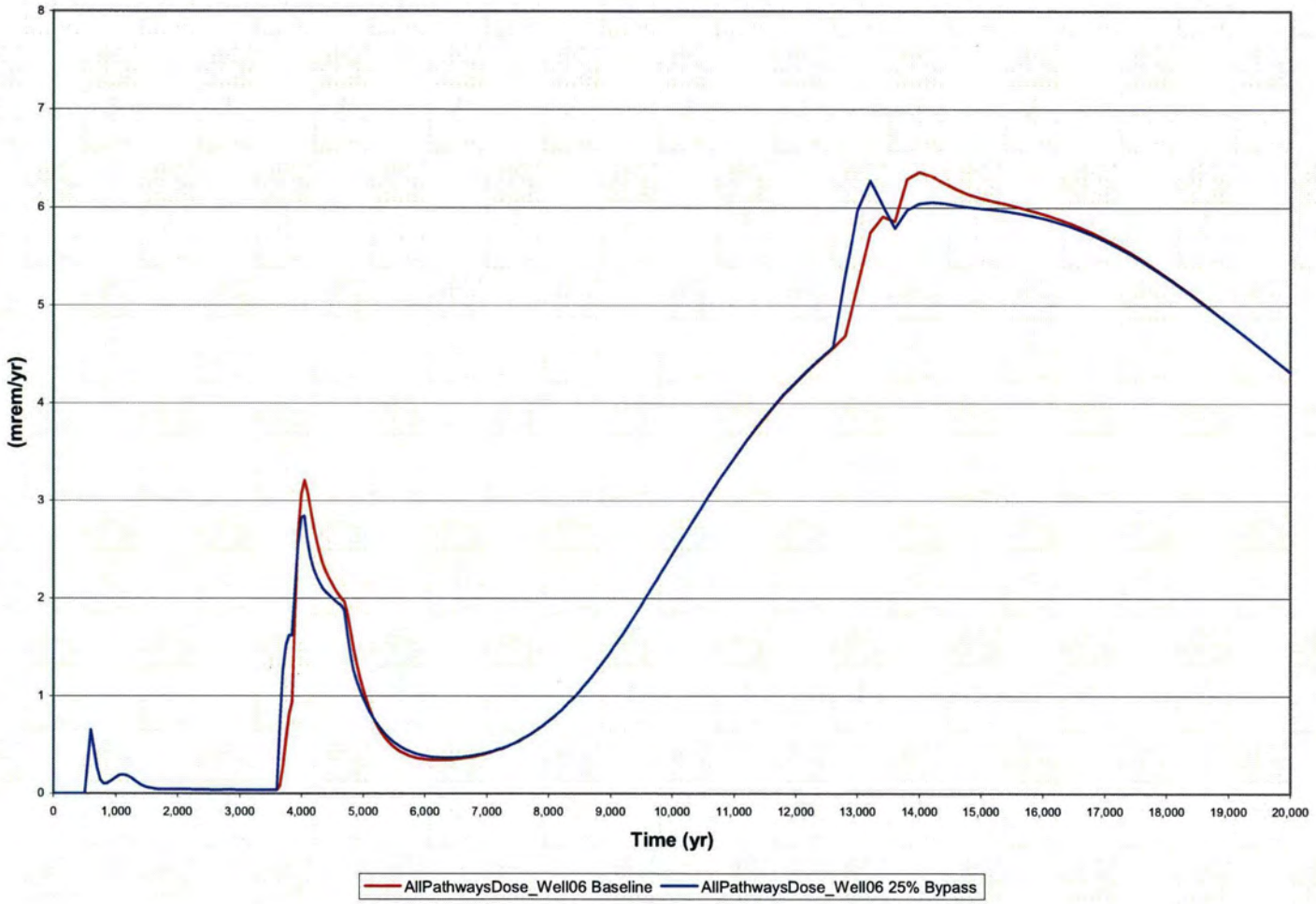

Figure 5.6-42: GoldSim FTF Model Baseline Parameters with 25% Bypass, All-Pathways Dose for Well 33

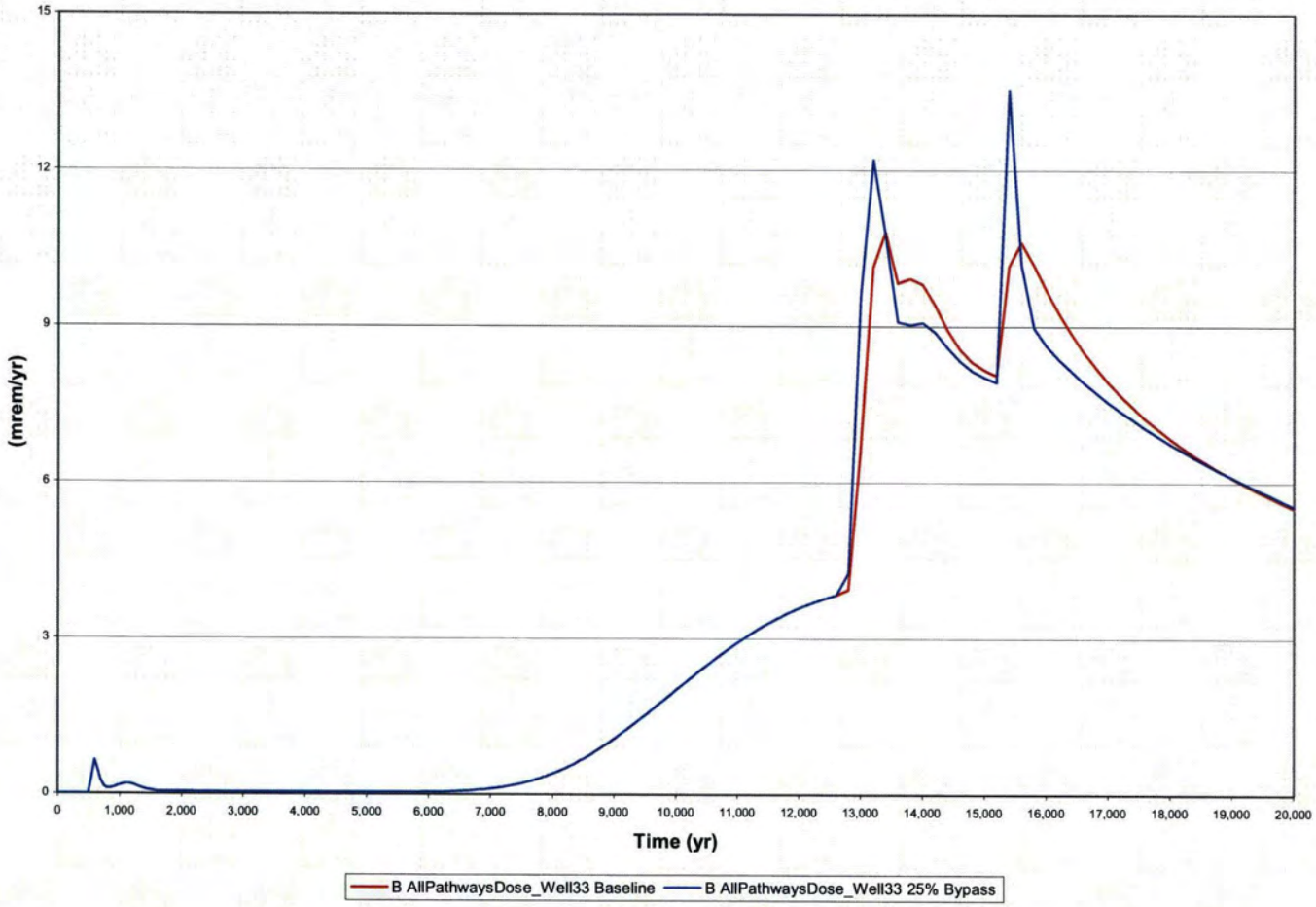

- **Base Case Parameters with Configuration D Flows and Failure Times**

To investigate the effect of the waste tank material properties degrading faster, the GoldSim FTF model was run with the flow profile and waste tank failure dates associated with Configuration D. This was accomplished in the model by redefining the configuration used for each waste tank to "4" (which is equivalent to Configuration D). The flow used in Configuration D was derived from the PORFLOW model for that configuration (discussed in Section 4.4.2.4). As discussed in Section 5.6.3, the parameters affected by Configuration D are liner failure time (75 years for Type IV, 1,140 years for Type I, and 2,077 years for Types III/IIIA), and time of complete degradation of the basemat (occurs at 501 years for all waste tanks). This sensitivity analysis reasonably represents the impact that accelerated materials degradation might have on the model results.

Figures 5.6-43 and 5.6-44 show the peak all-pathways dose for Wells 6 and 33 for 20,000 years with the configuration change. As can be seen from Figure 5.6-43 and 5.6-44, the configuration change has only a minor effect on magnitude of the dose peaks within 20,000 years. There is a significant change in the timing of the early peaks associated with Np-237 which shows a direct relationship to the change in the liner failure date. Since the release rate of the other radionclides most affecting dose (e.g., Tc, Pu, U) are solubility limited, their contribution to the peak doses are not greatly impacted by the change to Configuration D.

Figure 5.6-43: GoldSim FTF Model Baseline Parameters with Configuration D, All-Pathways Dose for Well 6

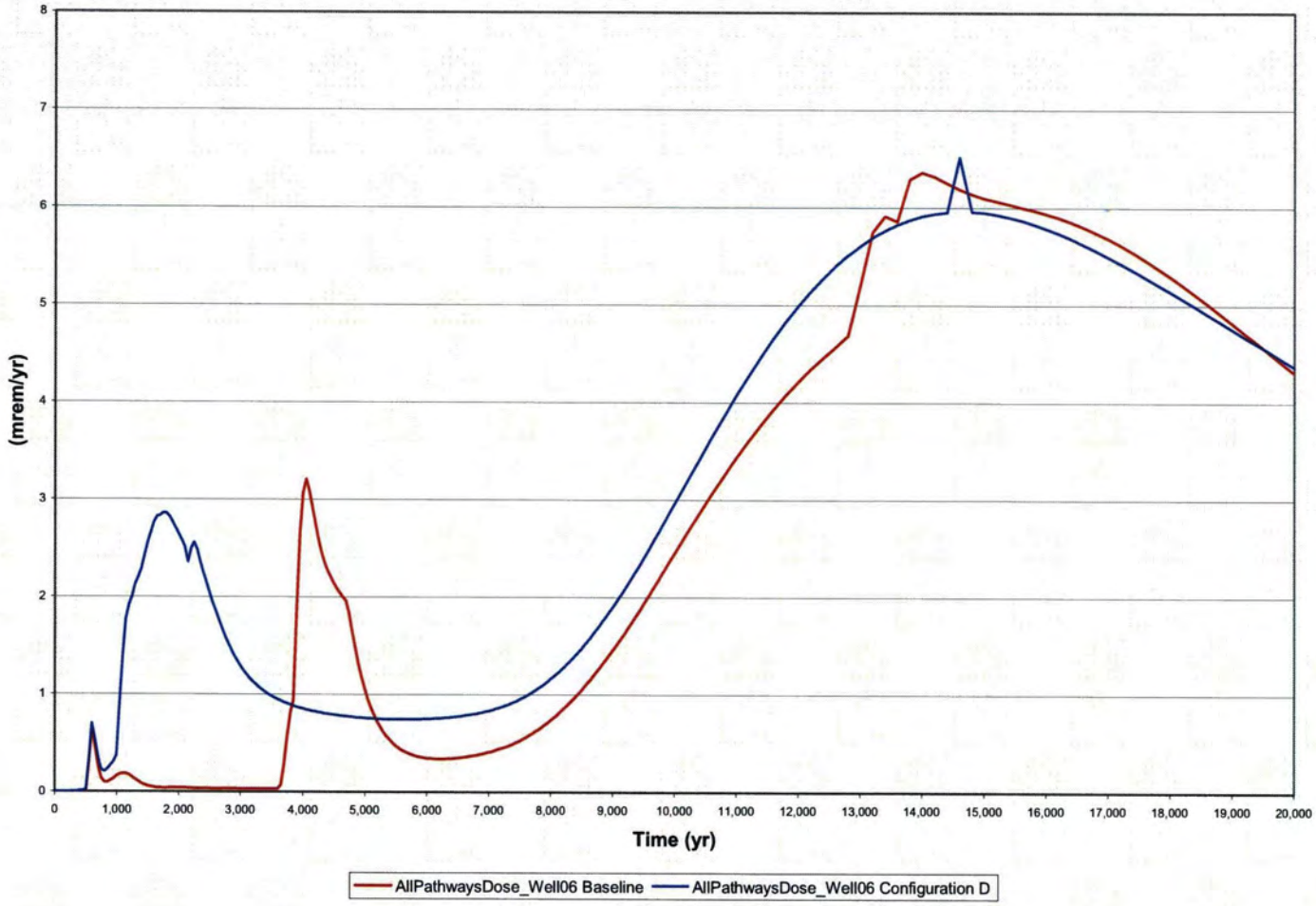

Figure 5.6-44: GoldSim FTF Model Baseline Parameters with Configuration D, All-Pathways Dose for Well 33

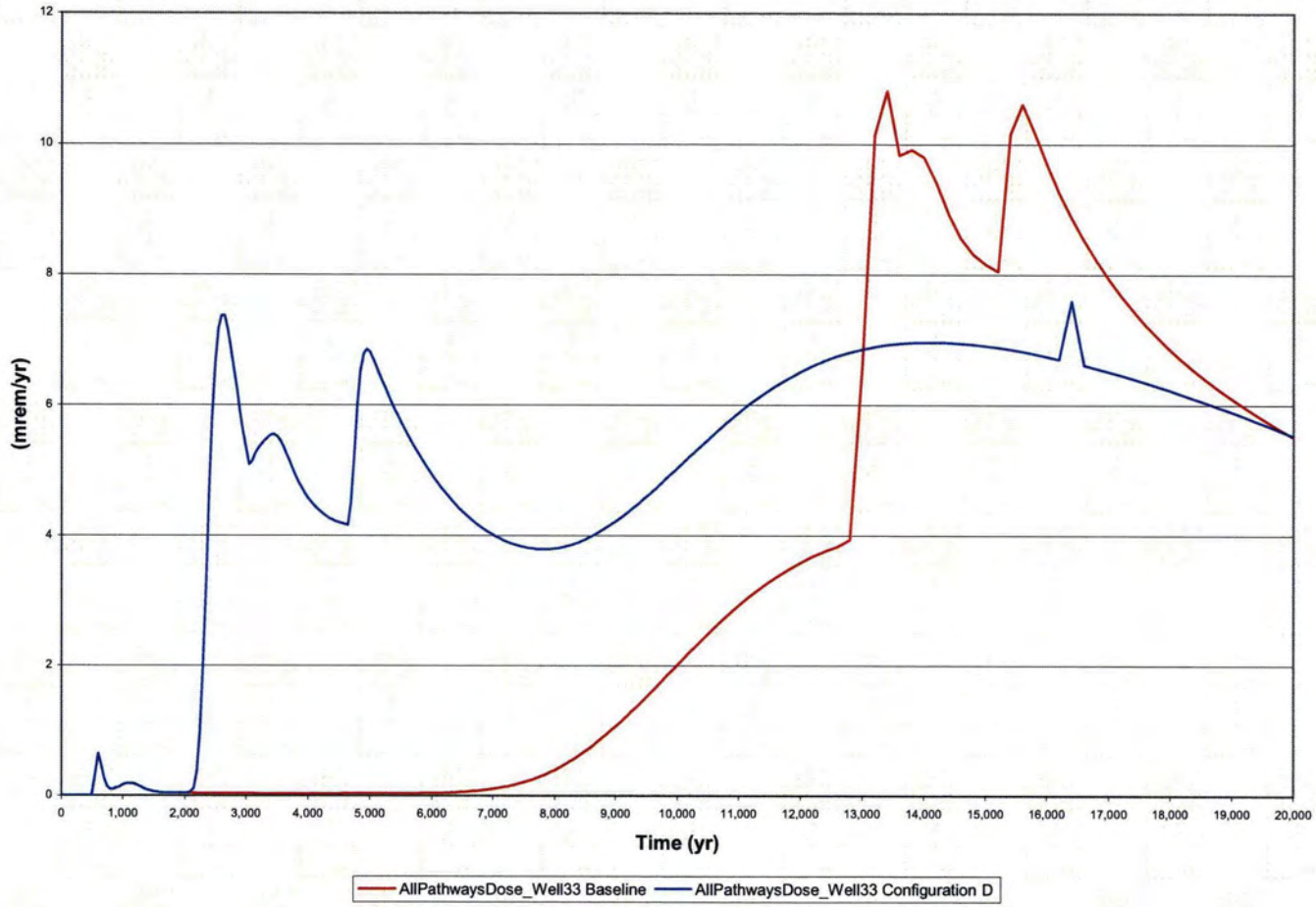

- **Base Case Parameters with Configuration D Flows and Failure Times and Rapid Transition to Oxidized Region III**

A final GoldSim sensitivity analysis on an incredible scenario was performed to investigate the effect of the waste tank material properties degrading faster and rapid transition of the pore water from reducing to oxidizing, the GoldSim FTF model was run with the flow profile and tank failure dates associated with Configuration D and with essentially instantaneous transition Oxidized Region III. This was accomplished by redefining the configuration as discussed in the previous sensitivity and by revising the transition times between chemical states values described in Section 5.6.3.8. In the model, the parameters "flush_1st" and "flush_2nd", which determine how many pore water volumes are required to pass through the waste tank before the CZ transitions from a reducing state to an oxidizing state, were changed. The transition from Reduced Region II to Oxidized Region II was changed from 371 to 0.01 pore volumes, and the transition from Oxidized Region II to Oxidized Region III was changed from 2,063 to 0.02 pore volumes. The waste tank inventories were reduced to 10% of the Base Case to reflect the fact that the CZ impacted under these conditions is expected to be only a fraction of that impacted under the Base Case.

This sensitivity effectively demonstrates what happens if flow is increased and the liner fails very early (75 years for Type IV, 1,140 years for Type I, and 2,077 years for Types III/IIIA), while at the same time the grout reducing properties are not transferred to the porewater, affecting the CZ solubility control. This sensitivity bounds what could be expected to occur if porewater was able to flow down the waste tank interior side walls and mobilize the waste tank wall inventory. The model allows only 10% of the waste tank inventory to be available for transport. The reduced inventory is reasonable since it is not credible that a fast flow path would develop down the side of a waste tank impacting all of the available waste tank inventory (causing the grout reducing properties to have no effect).

Figures 5.6-45 and 5.6-46 present the peak all-pathways dose for Wells 6 and 33 for 20,000 years with the configuration and solubility transition time changes in place. As can be seen from Figure 5.6-45 and 5.6-46, the configuration change has an effect on the timing and magnitude of the dose peaks within 20,000 years. The instantaneous transition to Oxidized Region III in conjunction with the extremely high Pu solubility assumed for Oxidized Region III waste (5.7E-05) places no solubility limit on Pu (in particular Pu-239) release. The effect of this change is more pronounced on the Well 6 dose because that dose is dominated by Type IV tanks, which have very thin basemats and short travel distances in soil to the aquifers, while the Well 33 dose is dominated by Type III tanks, which have very thick basemats and longer travel distances in soil to the aquifers. Since Pu has a relatively high K_d in both soil and concrete, the much faster release of Pu caused by the instantaneous transition to Oxidized Region III is mitigated for the Type III tanks by the Pu being held up in the basemat and soil below the tanks.

Figure 5.6-45: GoldSim FTF Model Baseline Parameters with Configuration D and Rapid Solubility Transition, All-Pathways Dose for Well 6

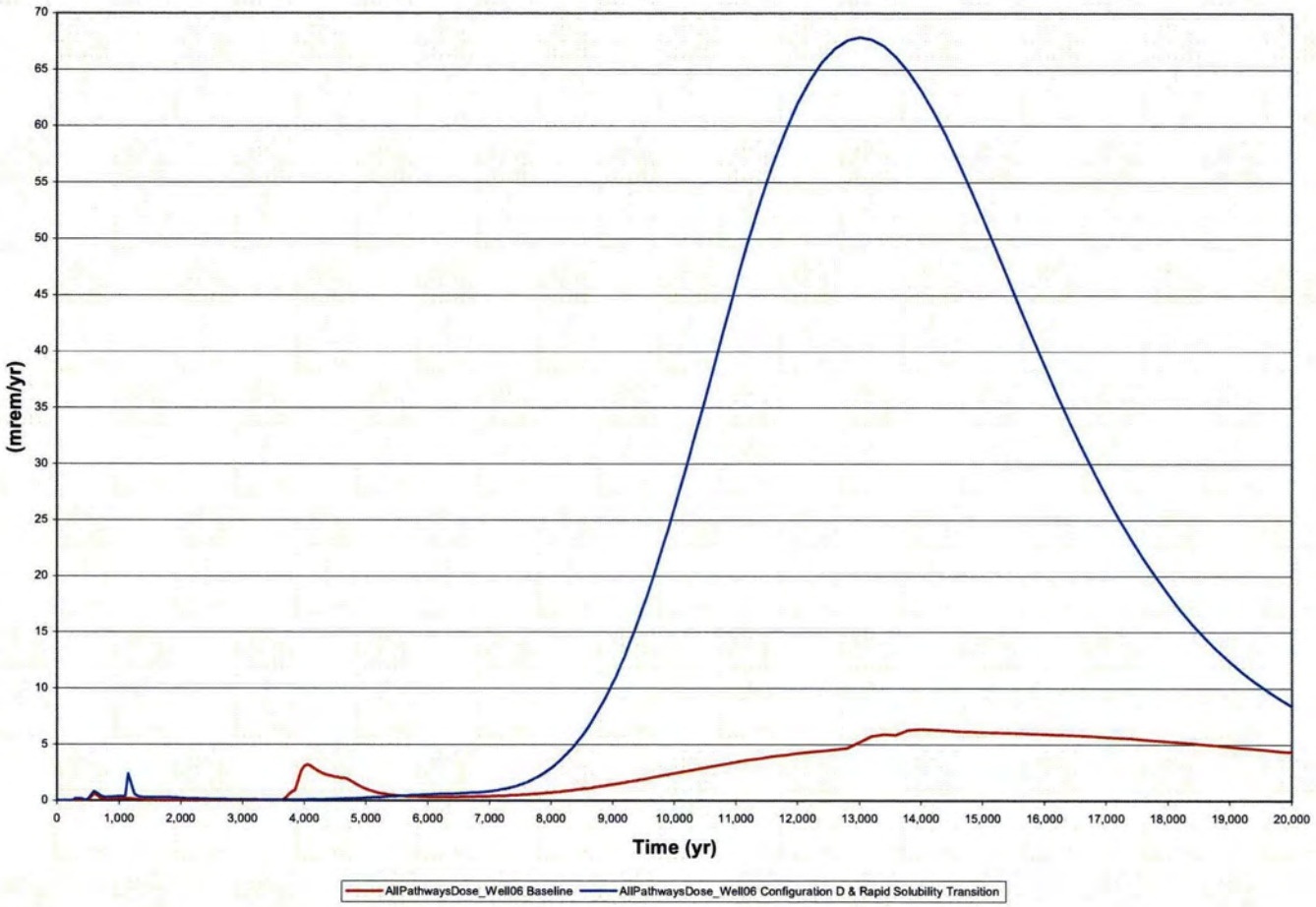

Figure 5.6-46: GoldSim FTF Model Baseline Parameters with Configuration D and Rapid Solubility Transition, All-Pathways Dose for Well 33

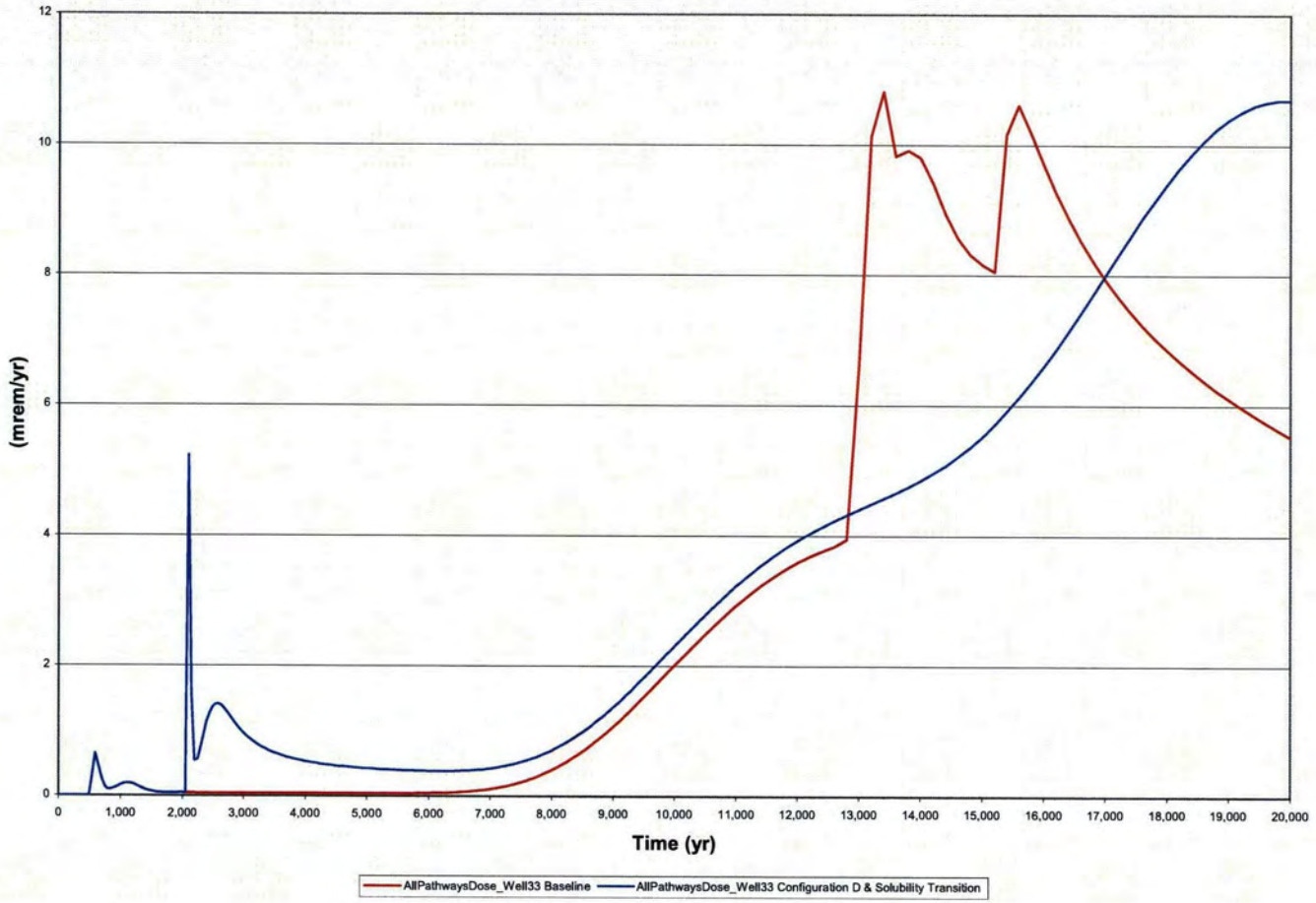

5.7 RCRA/CERCLA Risk Analysis

The RCRA/CERCLA risk assessment for the FTF closure follows the SGCP protocols for human health and ecological risk assessments. [ERD-AG-003] Based on available characterization data and estimated volume of residual material expected to remain in each of the waste tanks and ancillary equipment, the chemical and radiological inventory used for PA modeling has been calculated for FTF as discussed in Section 3.3. As discussed in Section 4.8, the placement of a low-permeability closure cap with at least 10 feet of clean backfill soil will ensure that the surface soils (0 to 1 foot) and the subsurface soils (1 to 4 feet) will not be contaminated and that there is no pathway for human health or ecological risk. The potential receptors of contamination include:

1. The industrial worker excavating deep soil containing PTSM
2. The resident who will be exposed to groundwater (ingestion and dermal contact)

Modeling was conducted to determine the peak concentrations of the non-radiological and radiological contaminants in the groundwater over the next 10,000 years.

5.7.1 Principal Threat Source Material

Principal Threat Source Materials are those materials that include or contain hazardous substances, pollutants or contaminants that act as a reservoir for migration of contamination to groundwater, surface water or air, or that act as a source for direct exposure. The USEPA defines PTSM as those sources materials considered to be highly toxic or mobile that generally cannot be reliably contained or would present a significant risk to human health or the environment should exposure occur. [OSWER 9380.3-06FS]

The FTF waste tanks and ancillary equipment will contain a heel of highly contaminated material that would present a significant risk should exposure occur, so they are, by definition, PTSM. The tanks and the heels remaining in the tanks will be stabilized and then covered as part of tank closure. This approach is consistent with SGCP remediation of reactor seepage basins which contain highly contaminated soils determined to be PTSM. No additional evaluation will be made to determine that the source material is PTSM.

5.7.2 Contaminant Migration Constituents of Concern

Contaminant Migration Constituents of Concern were identified through a system that is consistent with both the SGCP protocols and the PA. CMCOCs were identified by modeling the release of contaminants and their travel through the vadose zone. The same model used for the PA to meet 10 CFR 61 requirements is the basis of the CMCOC evaluation. The concentrations of contaminants that are modeled to reach the water table are compared to MCL or PRG or other appropriate standards in cases where the constituent does not have an MCL. Any constituents that are predicted to exceed these standards (i.e., fraction greather than 1.0) in the groundwater directly beneath FTF (1m from boundary) are identified as CMCOCs as shown in Table 5.7-1 and 5.7-2. The CMCOCs identified using the described protocols are Np-237, Pu-239, Pu-240, Th-229, U-233, U-234, and U-236.

Table 5.7-1: Groundwater Radionuclide Concentrations at 1m from FTF

Radionuclide	MCL (pCi/L)	Residential Tap Water PRG** (pCi/L)	Peak Concentration (pCi/L) 1 to 10,000 Years	Fraction of MCL or PRG at 1m
Ac-227	N/A	2.37E-01	4.03E-05	1.70E-04
Al-26	N/A	2.75E+00	9.58E-04	3.48E-04
Am-241	N/A	4.58E-01	4.86E-06	1.06E-05
Am-242m	N/A	6.74E-01	2.83E-19	4.20E-19
Am-243	N/A	4.62E-01	4.53E-08	9.81E-08
Ba-137m*	N/A	Cs-137 daughter	3.92E-11	N/A
Bk-249	N/A	3.84E-01	<1.0E-30	<1.0E-30
C-14	2,000	MCL used	3.87E+01	1.94E-02
Ce-144	N/A	1.35E+00	<1.0E-30	<1.0E-30
Cf-249	N/A	3.75E-01	1.26E-30	3.36E-30
Cm-242	N/A	1.24E+00	<1.0E-30	<1.0E-30
Cm-243	N/A	5.03E-01	<1.0E-30	<1.0E-30
Cm-244	N/A	5.70E-01	<1.0E-30	<1.0E-30
Cm-245	N/A	4.58E-01	6.15E-10	1.34E-09
Cm-247	N/A	4.79E-01	5.24E-20	1.09E-19
Cm-248	N/A	1.02E-01	1.19E-20	1.17E-19
Co-60	100	MCL used	<1.0E-30	<1.0E-30
Cs-134	N/A	1.13E+00	<1.0E-30	<1.0E-30
Cs-135	900	MCL used	2.01E-01	2.23E-04
Cs-137	200	MCL used	4.08E-11	2.04E-13
Eu-152	200	MCL used	<1.0E-30	<1.0E-30
Eu-154	60	MCL used	<1.0E-30	<1.0E-30
Eu-155	N/A	2.51E+01	<1.0E-30	<1.0E-30
Gd-152	N/A	1.60E+00	7.19E-17	4.49E-17
H-3	20,000	MCL used	1.92E-08	9.60E-13
I-129	1	MCL used	2.38E-02	2.38E-02
Na-22	N/A	4.95E+00	7.89E-25	1.59E-25
Nb-94	N/A	6.13E+00	2.05E+00	3.34E-01
Ni-59	N/A	1.74E+02	7.62E+01	4.38E-01
Ni-63	N/A	7.11E+01	2.50E-01	3.52E-03
Np-237	N/A	7.71E-01	1.08E+01	1.40E+01
Pa-231	N/A	2.75E-01	5.35E-02	1.95E-01
Pb-210	N/A	5.41E+02	1.09E-02	2.01E-05
Pm-147	N/A	2.82E+01	2.40E-16	8.51E-18
Pr-144	N/A	5.88E+02	<1.0E-30	<1.0E-30
Pu-238	N/A	3.64E-01	8.71E-20	2.39E-19

Table 5.7-1: Groundwater Radionuclide Concentrations at 1m from FTF (Continued)

Radionuclide	MCL (pCi/L)	Residential Tap Water PRG** (pCi/L)	Peak Concentration (pCi/L) 1 to 10,000 Years	Fraction of MCL or PRG at 1m
Pu-239	N/A	3.53E-01	2.20E+00	6.23E+00
Pu-240	N/A	3.53E-01	7.20E+00	2.04E+01
Pu-241	N/A	2.71E+01	2.68E-09	9.89E-11
Pu-242	N/A	3.72E-01	1.60E-01	4.30E-01
Pu-244	N/A	3.48E-01	3.01E-04	8.65E-04
Ra-226 + Ra-228	5.00E+00	MCL used	4.22E+00	8.44E-01
Rh-106*	N/A	Ru-106 daughter	2.86E-27	N/A
Ru-106 + D	N/A	1.13E+00	2.86E-27	2.53E-27
Sb-125	N/A	1.09E+01	<1.0E-30	<1.0E-30
Sb-126	N/A	4.29E+00	<1.0E-30	<1.0E-30
Sb-126m	N/A	7.15E+02	<1.0E-30	<1.0E-30
Se-79	N/A	6.53E+00	2.85E-01	4.36E-02
Sm-147	N/A	1.27E+00	2.19E-12	1.72E-12
Sm-151	1,000	MCL used	3.40E-25	3.40E-28
Sn-126	N/A	1.86E+00	5.12E-04	2.75E-04
Sr-90	8	MCL used	4.01E-05	5.01E-06
Tc-99	900	MCL used	2.05E+03	2.28E+00
Te-125m	N/A	1.43E+01	<1.0E-30	<1.0E-30
Th-228	N/A	4.45E-01	3.98E-08	8.94E-08
Th-229	N/A	2.13E-01	2.86E+00	1.34E+01
Th-230	N/A	5.23E-01	1.75E-01	3.35E-01
Th-232	N/A	4.71E-01	3.32E-08	7.05E-08
U-232	N/A	1.63E-01	1.45E-19	8.90E-19
U-233	N/A	6.63E-01	4.62E+01	6.97E+01
U-234	N/A	6.74E-01	2.25E+01	3.34E+01
U-235	N/A	6.84E-01	9.79E-02	1.43E-01
U-236	N/A	7.11E-01	8.55E-01	1.20E+00
U-238	N/A	7.44E-01	2.48E-02	3.33E-02
Y-90*	N/A	Sr-90 daughter	4.01E-05	N/A

* Daughters are assumed to be in equilibrium with the parent nuclide.

** Residential tap water PRGs are calculated at *http://epa-prgs.ornl.gov/radionuclides/*, based on a target cancer risk of 1.0E-06.

N/A = Not Available

Table 5.7-2: Groundwater Chemical Concentrations at 1m from FTF

Chemical	MCL (μg/L)	Residential Tap Water PRGs* (μg/L)	Peak Concentration (μg/L) 1 to10,000 Yrs	Fraction of MCL or PRG at 1m
Sb	6.00E+00	MCL used	5.28E-06	8.80E-07
As	1.00E+01	MCL used	2.52E-01	2.52E-02
Ba	2.00E+03	MCL used	1.38E+00	6.90E-04
Cd	5.00E+00	MCL used	4.75E+00	9.50E-01
Total Chromium	1.00E+02	MCL used	1.42E+00	1.42E-02
Cu	N/A	1.50E+03	2.75E+00	1.83E-03
F	N/A	2.20E+03	4.56E+01	2.07E-02
Fe	N/A	1.10E+04	9.53E+01	8.66E-03
Pb	1.50E+01	MCL used	5.40E-03	3.60E-04
Mn	N/A	8.80E+02	8.41E+01	9.56E-02
Hg	2.00E+00	MCL used	4.40E-02	2.20E-02
Ni	N/A	7.30E+02	4.01E+00	5.49E-03
NO_2+ NO_3	1.00E+04	MCL used	2.48E+03	2.48E-01
Se	5.00E+01	MCL used	3.92E-02	7.84E-04
Ag	N/A	1.80E+02	4.19E+00	2.33E-02
U	3.00E+01	MCL used	1.43E-01	4.77E-03
Zn	N/A	1.10E+04	2.70E+00	2.45E-04

* Residential tap water PRGs are calculated at *http://epa-prgs.ornl.gov/radionuclides/*, based on a target cancer risk of 1.0E-06.

N/A = Not Available

5.7.2.1 Neptunium-237

Neptunium-237 does not have an MCL so the peak concentration of 10.8 pCi/L at 1m is compared to the calculated PRG of 0.771 pCi/L. [*http://epa-prgs.ornl.gov/radionuclides/*] This peak concentration occurs 6,036 years following the assumed 100-year active control period. As shown in Table 5.7-3, the peak concentration drops to 2.16 pCi/L at 100m, and drops to 0.5224 pCi/L at the UTR seepline, which is below the PRG value.

5.7.2.2 Plutonium-239 and 240

Both of these plutonium isotopes have calculated PRGs of 0.353 pCi/L. [*http://epa-prgs.ornl.gov/radionuclides/*] The peak concentration for Pu-239 of 2.2 pCi/L at 1m occurs 10,000 years following the assumed 100-year active control period. As shown in Table 5.7-3, the peak concentration drops to 0.0137 pCi/L at 100m, which is below the PRG value.

The peak concentration for Pu-240 of 7.2 pCi/L at 1m occurs 10,000 years following the assumed 100-year active control period. As shown in Table 5.7-3, the peak concentration drops to 0.0376 pCi/L at 100m, which is below the PRG value.

5.7.2.3 Technetium-99

Technetium-99 has a peak concentration of 2,050 pCi/L at 1m compared to the MCL of 900 pCi/L. This peak concentration occurs approximately 600 years following the assumed 100-year active control period. As shown in Table 5.7-3, the peak concentration drops to 420 pCi/L at 100m, and drops to 1.56E-02 pCi/L at the UTR seepline.

5.7.2.4 Thorium-229

Thorium-229 does not have an MCL so the peak concentration of 2.86 pCi/L at 1m is compared to the calculated PRG of 0.213 pCi/L. [*http://epa-prgs.ornl.gov/radionuclides/*] This peak concentration occurs 10,000 years following the assumed 100-year active control period. As shown in Table 5.7-3, the peak concentration drops to 0.115 pCi/L at 100m, which is below the PRG value.

5.7.2.5 Uranium-233

Uranium-233 does not have an MCL so the peak concentration of 46.2 pCi/L at 1m is compared to the calculated PRG of 0.663 pCi/L. [*http://epa-prgs.ornl.gov/radionuclides/*] This peak concentration occurs 10,000 years following the assumed 100-year active control period. As shown in Table 5.7-3, the peak concentration drops to 4.29 pCi/L at 100m, and drops to 2.61E-06 pCi/L at the UTR seepline.

5.7.2.6 Uranium-234

Uranium-234 does not have an MCL so the peak concentration of 22.5 pCi/L at 1m is compared to the calculated PRG of 0.674 pCi/L. [*http://epa-prgs.ornl.gov/radionuclides/*] This peak concentration occurs 10,000 years following the assumed 100-year active control period. As shown in Table 5.7-3, the peak concentration drops to 1.59 pCi/L at 100m, and drops to 2.79E-10 pCi/L at the UTR seepline.

5.7.2.7 Uranium-236

Uranium-236 does not have an MCL so the peak concentration of 0.855 pCi/L at 1m is compared to the calculated PRG of 0.711 pCi/L. [*http://epa-prgs.ornl.gov/radionuclides/*] This peak concentration occurs 10,000 years following the assumed 100-year active control period. As shown in Table 5.7-3, the peak concentration drops to 0.0493 pCi/L at 100m, which is below the PRG value.

Table 5.7-3: Groundwater Concentrations of CMCOCs at 100m and Seepline

Radionuclide	MCL (pCi/L)	Residential Tap Water PRG (pCi/L)	Peak Concentration at 100m (pCi/L) 1 to 10,000 Yrs	Fraction of MCL or PRG at 100m	Peak Concentration at UTR Seepline (pCi/L) 1 to 10,000 Yrs	Fraction of MCL or PRG at UTR Seepline
Np-237	N/A	7.71E-01	2.16E+00	2.80E+00	5.24E-02	6.80E-02
Pu-239	N/A	3.53E-01	1.37E-02	3.88E-02	3.92E-15	1.11E-14
Pu-240	N/A	3.53E-01	3.76E-02	1.07E-01	7.22E-15	2.05E-14
Tc-99	900	N/A	4.20E+02	4.67E-01	1.56E+01	1.73E-02
Th-229	N/A	2.13E-01	1.15E-01	5.40E-01	1.64E-07	7.70E-07
U-233	N/A	6.63E-01	4.29E+00	6.47E+00	2.61E-06	3.94E-06
U-234	N/A	6.74E-01	1.59E+00	2.36E+00	2.79E-10	4.14E-10
U-236	N/A	7.11E-01	4.93E-02	6.93E-02	9.15E-12	1.29E-11

5.7.3 Evaluation of Results

CMCOCs are often addressed by the placement of a low permeability cap such as is planned for the FTF closure and described in Section 3.2.4. As described in Sections 2.4.2 and 2.4.3, the *SRS Long Range Comprehensive Plan* (PIT-MISC-0041_OUO) is founded on the following:

- The entire site will be owned and controlled by the federal government in perpetuity,
- The property will be used only for industrial purposes,
- Site boundaries will remain unchanged, and
- Residential use will not be allowed onsite.

Therefore, a scenario in which an individual establishes a residence on the FTF and obtains drinking water from the water table below is very unlikely. A more probable location for the MEI would be at the UTR seepline located approximately one mile from the FTF. As discussed previously, all isotopes meet the PRGs or MCLs at the UTR seepline.

5.8 ALARA Analysis

DOE's approach to radiation protection for LLW disposal units is based on the performance objectives listed in DOE O 435.1, which specify maximum doses for various pathways, and on the ALARA principle, which requires doses to be maintained "*As Low As Reasonably Achievable*". The ALARA requirement states in DOE O 435: "*Performance assessments shall include a determination that projected releases of radionuclide to the environment shall be maintained as low as reasonably achievable (ALARA).*"

The goal of the ALARA process is attainment of the lowest practical dose level after taking into account social, technical, economic, and public policy considerations. SRS has a well documented ALARA program and processes established in company level policies and procedures.

For the FTF PA modeling, a 100m buffer zone surrounding FTF and the seepline were evaluated after an institutional control period of 100 years. Conservatisms in the PA modeling are summarized in Section 7.2. In addition, the SRS land use plans indicate that that the current SRS boundaries will remain unchanged. Under this plan, the land will remain under the ownership of the federal government, consistent with the site's designation as a NERP. Thus, no MOP would have unrestricted access to the FTF. Because the FTF is a much greater distance (approximately five miles) from the site boundary than 100m, and groundwater potentially affected by releases from the FTF is completely intercepted by UTR and Fourmile Branch, the PA modeling results provide protection of the public to a much greater degree than the performance measures require. Considerable more dispersion of any radionuclides released to groundwater or air would occur if the closest access point to the disposal facility is the SRS site boundary.

DOE Manual 435.1-1, Chapter IV, P(2)(f) states:

> "Performance assessments shall include a demonstration that projected releases of radionuclides to the environment shall be maintained as low as reasonable achievable (ALARA). DOE G435.1-1 provides additional guidance on meeting this requirement. The Guide states in part that the goal of the ALARA process is not the attainment of a particular dose level (or, in this case, level of release), but rather the attainment of the lowest practical dose level after taking into account social, technical, economic, and public policy considerations. The PA should include assessments that focus on alternatives for LLW disposal. ALARA is meant to provide a documented answer to the question: "Have I done all that I can reasonably do to reduce radiation doses or releases to the environment?"

In addition, 10 CFR 61, Section 61.41, *Protection of the General Population from Releases of Radioactivity*, states:

> "Reasonable effort should be made to maintain releases of radioactivity in effluents to the general environment as low as is reasonable achievable."

DOE's approach to radiation protection is based on meeting the performance objectives identified in DOE M 435.1-1 and 10 CFR 61. These documents specify maximum doses for various pathways based upon the ALARA principle. The annual performance objectives for DOE M 435.1-1 are: 25 mrem all pathways; 4 mrem groundwater; and 10 mrem air pathway. The annual performance objective for 10 CFR 61 is 25 mrem all pathways.

Section 3.2.3 credits the EIS for tank closure for performing the alternative disposal analysis in regards to ALARA. [DOE-EIS-0303] In May 2002, DOE issued the EIS on tank cleaning and stabilization alternatives. DOE studied five alternatives:

1. Empty, clean and fill with grout,
2. Empty, clean and fill with sand
3. Empty, clean and fill with saltstone
4. Empty, clean and remove tanks, and
5. No action.

The EIS concluded the fill with grout option was the preferred option with the best approach to minimize human health and safety risks associated with closure of tanks. [DOE-EIS-0303]

In addition, the NDAA Section 3116, and DOE M 435.1-1 require that highly radioactive radionuclides be removed to the maximum extent practical. [NDAA_3116] This basic ALARA principle is accomplished through the cleaning of the waste tanks prior to closure. Section 3.3.2 delineates the estimations of waste tank inventory after tank cleaning.

At this time, it is inappropriate to do an in-depth ALARA cost-benefit analysis, because the cost of new technology and personnel exposures will not be available until following final waste tank cleaning and sampling operations. In-depth ALARA analysis will be completed as part of the NDAA Section 3116 Waste Determination and state-required Closure Modules.

The analysis of alternative disposal techniques; the application of cleaning the waste tanks to the maximum extent practical; the stabilization of the remaining inventory with grout; and meeting the performance objectives of DOE M 435.1-1 and 10 CFR 61 are evidence of the application of ALARA in limiting the release of radionuclides into the environment. Furthermore, an additional ALARA analysis will be performed following closure of FTF to support the CERCLA closure, including the final design considerations for the closure cap to evaluate opportunities to further reduce environmental releases. Therefore, the principle of ALARA is satisfied. [http://www.access.gpo.gov/uscode/title42/chapter103_.html]

6.0 INADVERTENT INTRUDER ANALYSIS

This section of the PA presents the analyses of the doses to a hypothetical individual who inadvertently intrudes into the FTF closed systems after the period of institutional control has ended.

The purpose of this section is to present the inadvertent intruder results for the analyses described in Section 4 of this PA.

Section 6.1 presents peak 1m groundwater concentrations for the radionuclides and chemicals discussed in the Source Term Screening Section of the PA (Section 4.2.1).

Section 6.2 and 6.3 presents the individual biotic pathway formulas used to calculate the dose to the acute and chronic intruder.

Section 6.4 presents acute and chronic Dose Analyses.

Section 6.5 presents Inadvertent Intruder Sensitivity and Uncertainty Analysis.

6.1 Groundwater Concentrations at 1m

The purpose of this section is to present the 1m groundwater concentrations for all of the radionuclides and chemicals discussed in the source term screening section of the PA (Section 4.2.1). Maximum groundwater concentrations are given for the modeling cell adjoining the analyzed source terms. Results are presented for the three distinct aquifers modeled (the UTR-UZ, the UTR-LZ, and Gordon aquifer).

The groundwater concentrations at 1m are calculated using the PORFLOW FTF model for the Base Case modeling configuration discussed in Section 4.4. A summary of the key parameters used in the baseline PORFLOW FTF modeling configuration are provided in Table 5.2-1. The PORFLOW 1m concentrations are provided for four sectors as shown on Figure 5.2-5, with results provided for the three aquifer depths of concern (i.e., UTR-UZ, UTR-LZ and Gordon aquifer). Dividing the results into sectors allows variability in peak concentration for different areas of the FTF to be more easily seen. The four sectors are searched for each radionuclide and chemical to find the maximum groundwater concentrations at 1m from the FTF.

Tables 6.1-1 through 6.1-3 show the peak 1m radionuclides concentrations for the three aquifers in the 10,000 year evaluation period. These radionuclide concentrations reflect the peak concentrations for each radionuclide in the highest sector. These values are conservatively high for the radionuclides present in multiple decay chains because the totals are simply the sum the individual peaks within that sector for a given radionuclide, without regard to location within the sector (as explained in Section 5.2.1). Tables 6.1-4 through 6.1-6 show the peak 1m chemical concentrations for the three aquifers in the 10,000 year evaluation period. These chemical concentrations also reflect the peak concentrations for the highest sector.

The 1m radionuclide and chemical concentration curves (for 20,000 years) associated with the four sectors and three aquifers for the Base Case, as described in Section 4.4.2, are captured in Appendix G.

Appendix G.1 – UTR-UZ for Sectors A through D at 1m.

Appendix G.2 – UTR-LZ for Sectors A through D at 1m.

Appendix G.3 - Gordon Aquifer for Sectors A through D at 1m.

Table 6.1-1: Radiological 1m Concentrations for UTR-UZ

Radionuclide	Sector A		Sector B		Sector C		Sector D	
	Concentration (pCi/L)	Year Peak Contribution Occurs	Concentration (pCi/L)	Year Peak Contribution Occurs	Concentration (pCi/L)	Year Peak Contribution Occurs	Concentration (pCi/L)	Year Peak Contribution Occurs
Ac-227	8.87E-08	1,776	6.22E-07	6,106	4.03E-05	6,090	3.24E-09	1,770
Al-26	1.75E-25	10,000	3.85E-08	10,000	9.58E-04	10,000	1.13E-16	10,000
Am-241	3.49E-25	10,000	8.73E-12	10,000	4.86E-06	8,762	2.73E-18	10,000
Am-242m	<1.0E-30	8,332	1.34E-24	7,078	2.83E-19	6,544	<1.0E-30	8,064
Am-243	4.76E-23	10,000	4.48E-13	10,000	4.53E-08	10,000	2.32E-16	10,000
Ba-137m	*	*	*	*	*	*	*	*
Bk-249	*	*	*	*	*	*	*	*
C-14	1.34E+00	556	2.21E+00	556	3.87E+01	3,754	5.02E-02	554
Ce-144	*	*	*	*	*	*	*	*
Cf-249	<1.0E-30	10,000	<1.0E-30	9,828	1.26E-30	8,900	1.26E-41	10,000
Cm-242	*	*	*	*	*	*	*	*
Cm-243	<1.0E-30	1,838	<1.0E-30	1,306	<1.0E-30	1,226	<1.0E-30	1,420
Cm-244	3.56E-81	1,298	<1.0E-30	978	<1.0E-30	922	<1.0E-30	1,050
Cm-245	1.95E-25	10,000	7.74E-15	10,000	6.15E-10	10,000	6.44E-19	10,000
Cm-247	<1.0E-30	10,000	5.48E-25	10,000	5.24E-20	10,000	<1.0E-30	10,000
Cm-248	<1.0E-30	10,000	1.24E-25	10,000	1.19E-20	10,000	<1.0E-30	10,000
Co-60	*	*	*	*	*	*	*	*
Cs-134	*	*	*	*	*	*	*	*
Cs-135	2.14E-03	7,122	8.30E-03	5,504	2.01E-01	4,726	7.84E-05	6,714
Cs-137	1.25E-24	1,922	1.16E-14	926	4.08E-11	790	2.03E-21	1,046
Eu-152	*	*	*	*	*	*	*	*
Eu-154	*	*	*	*	*	*	*	*
Eu-155	*	*	*	*	*	*	*	*
Gd-152	<1.0E-30	10,000	6.95E-22	10,000	7.19E-17	10,000	9.99E-28	10,000

Table 6.1-1: Radiological 1m Concentrations for UTR-UZ (Continued)

Radionuclide	Sector A		Sector B		Sector C		Sector D	
	Concentration (pCi/L)	Year Peak Contribution Occurs	Concentration (pCi/L)	Year Peak Contribution Occurs	Concentration (pCi/L)	Year Peak Contribution Occurs	Concentration (pCi/L)	Year Peak Contribution Occurs
H-3	7.10E-12	552	2.14E-11	202	1.92E-08	196	2.77E-12	158
I-129	8.24E-04	576	1.41E-03	578	2.38E-02	3,788	3.79E-05	536
Na-22	*	*	*	*	*	*	*	*
Nb-94	1.24E+00	556	2.05E+00	556	1.85E+00	556	4.64E-02	554
Ni-59	1.58E+00	1,796	2.98E+00	7,278	7.62E+01	7,126	5.79E-02	1,706
Ni-63	4.32E-03	1,380	7.63E-03	1,178	2.50E-01	1,058	1.64E-03	1,102
Np-237	1.52E-01	1,580	2.61E-01	1,582	1.08E+01	6,036	5.57E-03	1,570
Pa-231	1.17E-04	1,744	8.23E-04	6,054	5.35E-02	6,034	4.27E-06	1,738
Pb-210	4.92E-04	1,600	9.01E-04	1,598	1.09E-02	10,000	1.87E-05	1,636
Pm-147	*	*	*	*	*	*	*	*
Pr-144	*	*	*	*	*	*	*	*
Pu-238	3.69E-28	4,688	2.59E-20	6,370	8.71E-20	2,268	3.54E-24	4,162
Pu-239	3.27E-04	10,000	8.76E-03	10,000	2.20E+00	10,000	2.10E-03	10,000
Pu-240	5.57E-05	10,000	2.18E-02	10,000	7.20E+00	10,000	2.42E-04	10,000
Pu-241	1.05E-24	10,000	3.58E-14	10,000	2.68E-09	10,000	3.28E-18	10,000
Pu-242	1.29E-06	10,000	6.61E-04	10,000	1.60E-01	10,000	8.14E-07	10,000
Pu-244	6.20E-10	10,000	2.29E-06	10,000	3.01E-04	10,000	3.76E-09	10,000
Ra-226	1.90E-01	1,576	3.47E-01	1,574	4.22E+00	10,000	7.58E-03	996
Ra-228	3.36E-11	10,000	2.23E-08	10,000	6.84E-06	10,000	2.90E-11	10,000
Rh-106	*	*	*	*	*	*	*	*
Ru-106	*	*	*	*	*	*	*	*
Sb-125	*	*	*	*	*	*	*	*
Sb-126	*	*	*	*	*	*	*	*
Sb-126m	*	*	*	*	*	*	*	*
Se-79	2.17E-19	10,000	1.22E-05	10,000	2.85E-01	10,000	1.42E-12	10,000

Table 6.1-1: Radiological 1m Concentrations for UTR-UZ (Continued)

Radionuclide	Sector A		Sector B		Sector C		Sector D	
	Concentration (pCi/L)	Year Peak Contribution Occurs	Concentration (pCi/L)	Year Peak Contribution Occurs	Concentration (pCi/L)	Year Peak Contribution Occurs	Concentration (pCi/L)	Year Peak Contribution Occurs
Sm-147	7.75E-28	10,000	3.73E-17	10,000	2.19E-12	10,000	9.26E-25	10,000
Sm-151	<1.0E-30	5,970	<1.0E-30	2,704	3.40E-25	2,442	9.33E-40	3,380
Sn-126	1.58E-29	10,000	2.39E-10	10,000	5.12E-04	10,000	2.53E-19	10,000
Sr-90	6.44E-08	954	4.28E-07	958	4.01E-05	898	1.83E-07	912
Tc-99	2.99E+02	586	5.01E+02	588	2.05E+03	578	1.11E+01	582
Te-125m	*	*	*	*	*	*	*	*
Th-228	1.95E-13	10,000	1.30E-10	10,000	3.98E-08	10,000	1.69E-13	10,000
Th-229	1.39E-05	10,000	3.88E-02	10,000	2.86E+00	10,000	5.11E-06	10,000
Th-230	1.18E-06	10,000	2.72E-04	10,000	1.75E-01	10,000	1.43E-06	10,000
Th-232	1.24E-13	10,000	1.03E-10	10,000	3.32E-08	10,000	1.42E-13	10,000
U-232	<1.0E-30	3,840	9.23E-25	1,782	1.45E-19	1,460	1.66E-28	3,428
U-233	6.71E-04	10,000	1.11E+00	10,000	4.62E+01	8,656	1.37E-04	10,000
U-234	5.62E-04	10,000	8.21E-02	10,000	2.25E+01	8,634	2.96E-04	10,000
U-235	5.54E-06	10,000	1.07E-03	10,000	9.79E-02	10,000	4.44E-06	9,812
U-236	1.10E-05	10,000	5.48E-03	10,000	8.55E-01	9,002	5.98E-06	10,000
U-238	2.62E-04	10,000	1.12E-03	10,000	2.48E-02	10,000	1.95E-04	9,806
Y-90	*	*	*	*	*	*	*	*

*Short-lived radionuclides decayed prior to liner failure. PORFLOW does not track short-lived radionuclides during transport modeling, but the DCFs do include the equilibrium progeny.

Table 6.1-2: Radiological 1m Concentrations for UTR-LZ

Radionuclide	Sector A		Sector B		Sector C		Sector D	
	Concentration (pCi/L)	Year Peak Contribution Occurs	Concentration (pCi/L)	Year Peak Contribution Occurs	Concentration (pCi/L)	Year Peak Contribution Occurs	Concentration (pCi/L)	Year Peak Contribution Occurs
Ac-227	3.01E-08	1,784	2.87E-07	6,110	1.73E-05	6,094	1.19E-08	1,780
Al-26	3.46E-30	10,000	5.61E-12	10,000	7.88E-08	10,000	1.86E-14	10,000
Am-241	1.68E-29	10,000	3.51E-15	10,000	2.11E-09	10,000	2.51E-16	10,000
Am-242m	<1.0E-30	9,200	2.41E-29	8,014	8.82E-25	7,516	<1.0E-30	7,878
Am-243	2.20E-27	10,000	1.80E-16	10,000	5.68E-11	10,000	7.18E-17	10,000
Ba-137m	*	*	*	*	*	*	*	*
Bk-249	*	*	*	*	*	*	*	*
C-14	4.45E-01	558	1.22E+00	560	1.23E+01	3,754	1.47E-01	558
Ce-144	*	*	*	*	*	*	*	*
Cf-249	<1.0E-30	10,000	<1.0E-30	10,000	<1.0E-30	10,000	<1.0E-30	10,000
Cm-242	*	*	*	*	*	*	*	*
Cm-243	<1.0E-30	2,002	<1.0E-30	1,536	<1.0E-30	1,382	<1.0E-30	1,500
Cm-244	<1.0E-30	1,416	<1.0E-30	1,122	<1.0E-30	1,026	<1.0E-30	1,098
Cm-245	9.02E-30	10,000	3.41E-18	10,000	4.23E-13	10,000	4.25E-20	10,000
Cm-247	<1.0E-30	10,000	2.42E-28	10,000	7.25E-23	10,000	9.54E-29	10,000
Cm-248	<1.0E-30	10,000	5.47E-29	10,000	1.65E-23	10,000	2.17E-29	10,000
Co-60	*	*	*	*	*	*	*	*
Cs-134	*	*	*	*	*	*	*	*
Cs-135	7.24E-04	7,652	3.72E-03	5,980	6.25E-02	5,170	4.60E-04	3,458
Cs-137	4.62E-27	2,026	6.64E-17	1,036	7.84E-14	952	1.23E-19	1,016
Eu-152	*	*	*	*	*	*	*	*
Eu-154	*	*	*	*	*	*	*	*
Eu-155	*	*	*	*	*	*	*	*
Gd-152	<1.0E-30	10,000	3.07E-25	10,000	9.94E-20	10,000	1.31E-25	10,000

Table 6.1-2: Radiological 1m Concentrations for UTR-LZ (Continued)

Radionuclide	Sector A		Sector B		Sector C		Sector D	
	Concentration (pCi/L)	Year Peak Contribution Occurs	Concentration (pCi/L)	Year Peak Contribution Occurs	Concentration (pCi/L)	Year Peak Contribution Occurs	Concentration (pCi/L)	Year Peak Contribution Occurs
H-3	2.06E-12	554	1.01E-11	164	3.81E-09	200	1.65E-11	158
I-129	2.79E-04	578	8.02E-04	582	7.49E-03	3,788	2.30E-04	536
Na-22	*	*	*	*	*	*	*	*
Nb-94	4.11E-01	558	1.12E+00	560	1.08E+00	560	1.35E-01	558
Ni-59	5.32E-01	1,876	1.51E+00	1,976	2.76E+01	7,210	3.15E-01	1,172
Ni-63	8.71E-04	1,446	4.42E-03	1,214	5.29E-02	1,104	9.46E-03	1,108
Np-237	5.15E-02	1,584	1.49E-01	1,592	4.40E+00	6,042	2.41E-02	678
Pa-231	3.96E-05	1,752	3.79E-04	6,058	2.30E-02	6,038	1.57E-05	1,750
Pb-210	1.61E-04	1,734	4.88E-04	1,648	4.64E-03	10,000	9.71E-05	1,030
Pm-147	*	*	*	*	*	*	*	*
Pr-144	*	*	*	*	*	*	*	*
Pu-238	<1.0E-30	5,094	2.29E-23	6,828	9.44E-20	6,548	1.26E-25	6,758
Pu-239	8.56E-06	10,000	4.25E-04	10,000	1.68E-01	10,000	5.40E-03	10,000
Pu-240	1.46E-06	10,000	1.03E-03	10,000	5.73E-01	10,000	6.30E-04	10,000
Pu-241	5.07E-29	10,000	1.68E-17	10,000	1.95E-12	10,000	2.07E-19	10,000
Pu-242	3.39E-08	10,000	3.19E-05	10,000	1.24E-02	10,000	2.20E-06	10,000
Pu-244	1.62E-11	10,000	1.08E-07	10,000	2.46E-05	10,000	1.02E-08	10,000
Ra-226	6.22E-02	1,622	1.87E-01	1,626	1.79E+00	10,000	3.97E-02	10,00
Ra-228	2.28E-12	10,000	2.83E-09	10,000	1.44E-06	10,000	2.07E-10	10,000
Rh-106	*	*	*	*	*	*	*	*
Ru-106	*	*	*	*	*	*	*	*
Sb-125	*	*	*	*	*	*	*	*
Sb-126	*	*	*	*	*	*	*	*
Sb-126m	*	*	*	*	*	*	*	*
Se-79	1.61E-23	10,000	1.77E-08	10,000	7.36E-04	10,000	1.42E-10	10,000

Table 6.1-2: Radiological 1m Concentrations for UTR-LZ (Continued)

Radionuclide	Sector A		Sector B		Sector C		Sector D	
	Concentration (pCi/L)	Year Peak Contribution Occurs	Concentration (pCi/L)	Year Peak Contribution Occurs	Concentration (pCi/L)	Year Peak Contribution Occurs	Concentration (pCi/L)	Year Peak Contribution Occurs
Sm-147	3.94E-30	10,000	1.62E-20	10,000	1.42E-15	10,000	1.22E-22	10,000
Sm-151	<1.0E-30	6,582	<1.0E-30	3,354	2.12E-30	2,910	<1.0E-30	3,258
Sn-126	<1.0E-30	10,000	3.30E-15	10,000	1.11E-08	10,000	6.70E-17	10,000
Sr-90	9.21E-09	986	1.60E-07	986	5.48E-06	926	9.35E-07	928
Tc-99	1.00E+02	588	2.85E+02	592	1.11E+03	582	3.88E+01	548
Te-125m	*	*	*	*	*	*	*	*
Th-228	1.32E-14	10,000	1.64E-11	10,000	8.34E-09	10,000	1.20E-12	10,000
Th-229	1.03E-06	10,000	4.88E-03	10,000	6.97E-01	10,000	5.11E-05	10,000
Th-230	7.75E-08	10,000	3.06E-05	10,000	3.71E-02	10,000	9.01E-06	10,000
Th-232	7.97E-15	10,000	1.16E-11	10,000	6.82E-09	10,000	9.77E-13	10,000
U-232	1.00E-35	4,150	9.68E-28	2,130	4.76E-23	1,778	9.12E-30	2,076
U-233	5.26E-05	10,000	2.09E-01	10,000	1.79E+01	10,000	1.64E-03	10,000
U-234	4.22E-05	10,000	1.35E-02	10,000	8.35E+00	10,000	2.16E-03	10,000
U-235	4.15E-07	10,000	1.62E-04	10,000	2.31E-02	10,000	2.73E-05	10,000
U-236	8.18E-07	10,000	9.15E-04	10,000	3.17E-01	10,000	4.88E-05	10,000
U-238	1.97E-05	10,000	3.06E-04	10,000	6.48E-03	10,000	1.18E-03	9,984
Y-90	*	*	*	*	*	*	*	*

*Short-lived radionuclides decayed prior to liner failure. PORFLOW does not track short-lived radionuclides during transport modeling, but the DCFs do include the equilibrium progeny.

Table 6.1-3: Radiological 1m Concentrations for Gordon Aquifer

Radionuclide	Sector A		Sector B		Sector C		Sector D	
	Concentration (pCi/L)	Year Peak Contribution Occurs	Concentration (pCi/L)	Year Peak Contribution Occurs	Concentration (pCi/L)	Year Peak Contribution Occurs	Concentration (pCi/L)	Year Peak Contribution Occurs
Ac-227	8.13E-13	10,000	2.58E-11	10,000	3.23E-10	10,000	3.01E-12	10,000
Al-26	<1.0E-30	10,000	2.66E-26	10,000	6.23E-22	10,000	1.87E-26	10,000
Am-241	<1.0E-30	10,000	1.17E-30	10,000	8.71E-25	10,000	1.63E-29	10,000
Am-242m	<1.0E-30	10,000	<1.0E-30	9,328	<1.0E-30	8,650	<1.0E-30	9,116
Am-243	<1.0E-30	10,000	<1.0E-30	10,000	9.13E-26	10,000	4.69E-30	10,000
Ba-137m	*	*	*	*	*	*	*	*
Bk-249	*	*	*	*	*	*	*	*
C-14	9.54E-06	612	2.34E-04	610	9.59E-04	3,884	2.86E-05	602
Ce-144	*	*	*	*	*	*	*	*
Cf-249	<1.0E-30	10,000	<1.0E-30	10,000	<1.0E-30	10,000	<1.0E-30	10,000
Cm-242	*	*	*	*	*	*	*	*
Cm-243	<1.0E-30	2,292	<1.0E-30	1,824	<1.0E-30	1,664	<1.0E-30	1,782
Cm-244	<1.0E-30	1,598	<1.0E-30	1,300	<1.0E-30	1,200	<1.0E-30	1,274
Cm-245	<1.0E-30	10,000	<1.0E-30	10,000	2.03E-28	10,000	<1.0E-30	10,000
Cm-247	<1.0E-30	10,000	<1.0E-30	10,000	<1.0E-30	10,000	<1.0E-30	10,000
Cm-248	<1.0E-30	10,000	<1.0E-30	10,000	<1.0E-30	10,000	<1.0E-30	10,000
Co-60	*	*	*	*	*	*	*	*
Cs-134	*	*	*	*	*	*	*	*
Cs-135	4.85E-10	10,000	1.22E-08	10,000	2.97E-08	10,000	1.96E-09	10,000
Cs-137	<1.0E-30	2,288	4.93E-29	1,248	3.08E-26	1,168	7.43E-30	1,206
Eu-152	*	*	*	*	*	*	*	*
Eu-154	*	*	*	*	*	*	*	*
Eu-155	*	*	*	*	*	*	*	*
Gd-152	<1.0E-30	10,000	<1.0E-30	10,000	<1.0E-30	10,000	<1.0E-30	10,000

Table 6.1-3: Radiological 1m Concentrations for Gordon Aquifer

Radionuclide	Sector A		Sector B		Sector C		Sector D	
	Concentration (pCi/L)	Year Peak Contribution Occurs	Concentration (pCi/L)	Year Peak Contribution Occurs	Concentration (pCi/L)	Year Peak Contribution Occurs	Concentration (pCi/L)	Year Peak Contribution Occurs
H-3	8.09E-18	576	3.70E-16	184	8.02E-15	222	1.14E-16	178
I-129	5.55E-09	746	1.37E-07	726	2.84E-07	4,068	1.69E-08	712
Na-22	*	*	*	*	*	*	*	*
Nb-94	8.86E-06	612	2.17E-04	610	2.09E-04	608	2.52E-05	604
Ni-59	3.62E-06	6,948	1.03E-04	9,536	4.55E-04	10,000	1.11E-05	5,968
Ni-63	3.19E-11	1,748	8.17E-10	1,560	1.33E-09	1418	3.52E-10	1,378
Np-237	3.88E-07	7,738	1.01E-05	7,008	6.12E-05	10,000	1.19E-06	6,508
Pa-231	1.01E-09	10,000	3.28E-08	10,000	4.08E-07	10,000	3.87E-09	10,000
Pb-210	1.21E-09	10,000	3.13E-08	9,860	8.98E-09	2,826	4.06E-09	9,498
Pm-147	*	*	*	*	*	*	*	*
Pr-144	*	*	*	*	*	*	*	*
Pu-238	<1.0E-30	5,886	<1.0E-30	7,556	<1.0E-30	7,198	<1.0E-30	7,424
Pu-239	4.84E-18	10,000	6.16E-16	10,000	2.14E-13	10,000	1.27E-14	10,000
Pu-240	8.24E-19	10,000	7.79E-16	10,000	7.24E-13	10,000	1.84E-15	10,000
Pu-241	<1.0E-30	10,000	<1.0E-30	10,000	8.58E-28	10,000	<1.0E-30	10,000
Pu-242	1.91E-20	10,000	2.44E-17	10,000	1.61E-14	10,000	1.11E-17	10,000
Pu-244	9.18E-24	10,000	7.40E-20	10,000	3.74E-17	10,000	5.03E-20	10,000
Ra-226	4.61E-07	10,000	1.19E-05	9,828	3.44E-05	10,000	1.55E-06	9,466
Ra-228	1.57E-21	10,000	3.62E-18	10,000	3.25E-15	10,000	5.06E-18	10,000
Rh-106	*	*	*	*	*	*	*	*
Ru-106	*	*	*	*	*	*	*	*
Sb-125	*	*	*	*	*	*	*	*
Sb-126	*	*	*	*	*	*	*	*
Sb-126m	*	*	*	*	*	*	*	*

Table 6.1-3: Radiological 1m Concentrations for Gordon Aquifer

Radionuclide	Sector A		Sector B		Sector C		Sector D	
	Concentration (pCi/L)	Year Peak Contribution Occurs	Concentration (pCi/L)	Year Peak Contribution Occurs	Concentration (pCi/L)	Year Peak Contribution Occurs	Concentration (pCi/L)	Year Peak Contribution Occurs
Se-79	<1.0E-30	10,000	2.29E-21	10,000	1.41E-16	10,000	3.20E-21	10,000
Sm-147	<1.0E-30	106	<1.0E-30	10,000	<1.0E-30	10,000	<1.0E-30	10,000
Sm-151	<1.0E-30	7,440	<1.0E-30	4,222	<1.0E-30	3,762	<1.0E-30	4,086
Sn-126	<1.0E-30	10,000	<1.0E-30	10,000	3.21E-25	10,000	4.99E-31	10,000
Sr-90	5.78E-17	1,090	4.97E-15	1,098	1.91E-14	1,058	7.37E-15	1,034
Tc-99	2.12E-03	682	5.26E-02	674	6.78E-02	668	6.44E-03	664
Te-125m	*	*	*	*	*	*	*	*
Th-228	9.11E-24	10,000	2.10E-20	10,000	1.88E-17	10,000	3.25E-20	10,000
Th-229	7.06E-11	10,000	1.85E-09	10,000	5.92E-09	10,000	2.31E-10	10,000
Th-230	7.68E-17	10,000	4.83E-14	10,000	1.17E-10	10,000	1.98E-13	10,000
Th-232	7.60E-24	10,000	1.74E-20	10,000	1.80E-17	10,000	2.68E-20	10,000
U-232	<1.0E-30	4,766	<1.0E-30	2,690	<1.0E-30	2,372	<1.0E-30	2,586
U-233	1.39E-09	10,000	3.38E-08	10,000	2.95E-07	10,000	4.31E-09	10,000
U-234	8.09E-14	10,000	4.94E-11	10,000	9.38E-08	10,000	1.52E-10	10,000
U-235	7.89E-16	10,000	5.41E-13	10,000	1.50E-10	10,000	6.30E-13	10,000
U-236	1.50E-15	10,000	3.31E-12	10,000	2.78E-09	10,000	3.95E-12	10,000
U-238	3.77E-14	10,000	2.66E-12	10,000	4.16E-11	10,000	2.31E-11	10,000
Y-90	*	*	*	*	*	*	*	*

*Short-lived radionuclides decayed prior to liner failure. PORFLOW does not track short-lived radionuclides during transport modeling, but the DCFs do include the equilibrium progeny.

Table 6.1-4: Chemical 1m Concentrations for UTR-UZ

Chemical	Sector A		Sector B		Sector C		Sector D	
	Concentration (μg/L)	Year Peak Contribution Occurs	Concentration (μg/L)	Year Peak Contribution Occurs	Concentration (μg/L)	Year Peak Contribution Occurs	Concentration (μg/L)	Year Peak Contribution Occurs
Ag	1.74E-03	6,924	1.13E-01	5,806	4.19E+00	4,642	6.47E-05	3,734
As	4.25E-05	10,000	1.15E-02	8,250	2.52E-01	7,006	1.62E-06	9,498
Ba	1.50E-02	1,586	1.01E-01	4,962	1.38E+00	4,774	6.05E-04	998
Cd	6.48E-02	1,266	1.08E-01	1,304	4.75E+00	7,140	2.40E-03	1,228
Cr	2.43E-02	1,266	8.52E-02	4,740	1.42E+00	4,688	8.99E-04	1,228
Cu	2.16E-03	5,296	6.85E-02	5,474	2.75E+00	4,514	8.55E-05	4,938
F	2.47E-01	556	3.83E+00	3,840	4.56E+01	3,836	9.28E-03	554
Fe	1.85E-03	10,000	5.56E-01	10,000	9.53E+01	10,000	2.84E-03	9,926
Hg	2.79E-18	10,000	6.50E-06	10,000	4.40E-02	10,000	3.71E-12	10,000
Mn	3.42E-02	4,774	1.72E+00	5,080	8.41E+01	4,856	3.71E-03	1,776
N	9.63E+00	556	1.31E+02	3,654	2.48E+03	3,650	3.62E-01	554
Ni	8.07E-01	1,802	1.37E+00	1,896	4.01E+00	1,126	3.73E-02	1,166
Pb	1.43E-26	10,000	1.38E-08	10,000	5.40E-03	10,000	6.01E-17	10,000
Sb	1.23E-33	10,000	2.79E-17	10,000	5.28E-06	10,000	1.70E-19	10,000
Se	2.22E-22	10,000	9.47E-06	10,000	3.92E-02	10,000	2.33E-14	10,000
U	8.56E-04	10,000	3.66E-03	10,000	1.43E-01	8,472	1.13E-03	9,804
V	5.48E-09	562	1.14E-02	558	5.54E-01	554	5.70E-07	558
Zn	1.57E-03	10,000	6.01E-02	7,930	2.70E+00	5,960	5.99E-05	9,498

Table 6.1-5: Chemical 1m Concentrations for UTR-LZ

Chemical	Sector A		Sector B		Sector C		Sector D	
	Concentration (µg/L)	Year Peak Contribution Occurs	Concentration (µg/L)	Year Peak Contribution Occurs	Concentration (µg/L)	Year Peak Contribution Occurs	Concentration (µg/L)	Year Peak Contribution Occurs
Ag	5.81E-04	7,532	5.08E-02	6,274	8.87E-01	5,294	3.91E-04	3,788
As	1.24E-05	10,000	4.25E-03	9,056	7.02E-02	7,832	8.06E-06	5,572
Ba	5.00E-03	1,636	4.80E-02	4,980	4.81E-01	4,910	3.66E-03	1,002
Cd	2.18E-02	1,310	6.02E-02	1,362	1.78E+00	7,162	1.34E-02	922
Cr	8.17E-03	1,310	3.66E-02	4,774	4.60E-01	4,722	5.00E-03	922
Cu	7.00E-04	5,794	3.14E-02	5,864	6.39E-01	4,960	3.19E-04	3,264
F	8.23E-02	558	1.83E+00	3,840	1.75E+01	3,838	3.03E-02	534
Fe	1.46E-04	10,000	4.67E-02	10,000	1.30E+01	10,000	1.73E-02	10,000
Hg	6.15E-22	10,000	1.96E-08	10,000	2.41E-04	10,000	3.03E-10	10,000
Mn	1.16E-02	4,920	7.58E-01	5,192	2.69E+01	4,978	2.25E-02	1,792
N	3.20E+00	558	5.14E+01	3,656	7.53E+02	3,652	1.18E+00	534
Ni	2.73E-01	1,880	7.76E-01	1,976	1.21E+00	1,166	2.26E-01	1,172
Pb	4.94E-31	10,000	6.47E-13	10,000	5.60E-07	10,000	1.29E-14	10,000
Sb	8.55E-39	10,000	1.16E-21	10,000	2.23E-10	10,000	5.17E-17	10,000
Se	1.65E-26	10,000	1.37E-08	10,000	4.97E-05	10,000	2.34E-12	10,000
U	6.43E-05	10,000	1.00E-03	10,000	3.75E-02	9,816	6.81E-03	9,982
V	3.43E-09	566	5.69E-03	560	2.99E-01	554	1.20E-05	558
Zn	4.59E-04	10,000	2.77E-02	8,702	6.03E-01	6,846	2.99E-04	5,576

Table 6.1-6: Chemical 1m Concentrations for Gordon Aquifer

Chemical	Sector A		Sector B		Sector C		Sector D	
	Concentration (μg/L)	Year Peak Contribution Occurs	Concentration (μg/L)	Year Peak Contribution Occurs	Concentration (μg/L)	Year Peak Contribution Occurs	Concentration (μg/L)	Year Peak Contribution Occurs
Ag	6.89E-10	10,000	9.52E-08	10,000	1.03E-06	10,000	3.40E-09	10,000
As	7.53E-13	10,000	7.19E-10	10,000	1.41E-08	10,000	1.66E-11	10,000
Ba	4.05E-08	4,600	2.70E-06	10,000	1.97E-05	10,000	1.26E-07	3,924
Cd	1.93E-07	3,160	4.80E-06	2,944	8.82E-05	10,000	5.99E-07	2,758
Cr	7.25E-08	3,160	2.77E-06	8,734	2.33E-05	9,320	2.27E-07	2,758
Cu	3.36E-09	10,000	2.54E-07	10,000	2.47E-06	10,000	1.46E-08	10,000
F	1.78E-06	612	2.99E-04	3,988	2.26E-03	3,980	5.40E-06	602
Fe	1.52E-13	10,000	2.90E-11	10,000	8.89E-09	10,000	1.75E-10	10,000
Hg	1.49E-35	10,000	7.67E-21	10,000	1.44E-16	10,000	1.78E-20	10,000
Mn	2.68E-08	10,000	1.20E-06	10,000	9.49E-06	10,000	1.19E-07	10,000
N	6.92E-05	612	1.70E-03	610	1.08E-02	3,708	2.11E-04	602
Ni	1.95E-06	7,246	4.83E-05	6,528	4.77E-05	6,364	6.03E-06	6,066
Pb	3.10E-47	10,000	6.66E-29	10,000	8.04E-23	10,000	3.25E-28	10,000
Sb	1.46E-55	10,000	9.27E-38	10,000	1.32E-25	10,000	8.13E-31	10,000
Se	8.17E-40	10,000	1.76E-21	10,000	1.00E-17	10,000	5.26E-23	10,000
U	1.23E-13	10,000	8.67E-12	10,000	2.39E-10	10,000	1.34E-10	10,000
V	1.08E-13	620	1.72E-07	606	7.13E-06	600	9.33E-09	600
Zn	2.79E-11	10,000	1.00E-08	10,000	2.67E-07	10,000	5.66E-10	10,000

6.2 Acute Exposure Scenarios

6.2.1 Acute Intruder Ingestion Dose Pathway – Ingestion of Resuspended Drill Cuttings

The drill cuttings ingestion exposure route assumes the drill cuttings from the well installation are distributed across the garden. The receptor in turn is exposed by ingesting dirt. The source of material is a transfer line that is assumed to be penetrated during well installation. Only the exposure from the drill cuttings is included in this calculation (i.e., this does not include any other ingestion sources). Unless otherwise noted, formulas were based on those used in LADTAP model, report WSRC-STI-2006-00123 or in the PA for Idaho Tank Farm, document DOE-ID-10966. While these documents were used as guides for the other formulas, ultimately the basis for all the formulas can be traced to 10 CFR 50, Reg. Guide 1.109. The dose is calculated using the following formula. Unit conversions are not explicitly stated in the equations, but are coded into GoldSim.

$$D = \frac{C_{Xfer} \times d_W \times c_W \times F_{DC} \times U_S \times DCF}{\frac{d_W^{\,2}}{4} \times \pi \times l_W \times \rho_{SS}}$$

where:

C_{Xfer}	=	transfer line surface radionuclide concentration (pCi/ft^2)
d_W	=	well diameter (ft) [0.667 ft]
c_W	=	transfer line circumference (ft) [0.803 ft (for 3 inch inner diameter)]
F_{DC}	=	fraction of time exposed to drill cuttings (unitless) [0.0023 equates to 20 hours]
DCF	=	ingestion dose conversion factor (rem/μCi), Table 4.7-1
U_S	=	human consumption rate of dirt (kg/year), Table 4.6-7
l_W	=	well depth (ft) [100 ft]
ρ_{SS}	=	density of sandy soil (g/cm^3)

6.2.2 Acute Intruder Inhalation Dose Pathway – Inhalation of Drill Cuttings

The drill cuttings inhalation route assumes the drill cuttings from the well installation are distributed across the garden. The receptor in turn is directly exposed during time spent in the garden. The source of material is a transfer line that is assumed to be penetrated during well installation. Only the exposure from the drill cuttings is included in this calculation (i.e., this does not include any other direct exposure sources). This formula was derived following the approach of the previous pathway calculations, whose bases are found in other PA methods. The dose is calculated using the following formula.

$$D = \frac{C_{Xfer} \times d_W \times c_W \times F_{DC} \times DCF \times U_A \times L_{SiA}}{\frac{d_W^{\,2}}{4} \times \pi \times l_W \times \rho_{SS}}$$

where:

C_{Xfer}	=	transfer line surface radionuclide concentration (pCi/ft^2)
d_W	=	well diameter (ft) [0.667 ft]
c_W	=	transfer line circumference (ft) [0.803 ft (for 3 inch inner diameter)]
F_{DC}	=	fraction of time exposed to drill cuttings (unitless) [0.0023 equates to 20 hours]
DCF	=	inhalation dose conversion factor (rem/μCi), Table 4.7-1
l_W	=	well depth (ft) [100 ft]
U_A	=	air intake (m^3/yr), Table 4.6-7
L_{SiA}	=	soil loading in air while working in a garden (kg/m^3), Table 4.6-6
ρ_{SS}	=	density of sandy soil (g/cm^3)

6.2.3 Acute Intruder Direct Exposure Dose Pathways – Direct Exposure to Drill Cuttings

The drill cuttings direct exposure route assumes the receptor is directly exposed to the drill cuttings during well drilling operations. The source of material is a transfer line that is assumed to be penetrated during well installation. Only the exposure from the drill cuttings is included in this calculation (i.e., this does not include any other direct exposure sources). This formula was derived following the approach of the previous pathway calculations, whose bases are found in other PA methods. The dose is calculated using the following formula.

$$D = \frac{C_{Xfer} \times d_W \times c_W \times F_{DC} \times DCF}{\frac{d_W^{\,2}}{4} \times \pi \times l_W}$$

where:

C_{Xfer}	=	transfer line surface radionuclide concentration (pCi/ft^2)
d_W	=	well diameter (ft) [0.667 ft]
c_W	=	transfer line circumference (ft) [0.803 (for 3 inch inner diameter)]
F_{DC}	=	fraction of time exposed to drill cuttings (unitless) [0.0023 equates to 20 hours]
DCF	=	external dose conversion factor, 15 cm (rem/yr per μCi/m^3), Table 4.7-1
l_W	=	well depth (ft) [100 ft]

6.3 Chronic Exposure Scenarios

The exposure pathways for the FTF intruder are discussed in detail in Section 4.2.4.2. The Chronic Intruder Agricultural (Post-Drilling) Scenario analyzed in this PA is graphically represented in Figure 4.2-30. Provided below are the individual elements of the Chronic Intruder biotic pathways that were identified for analysis and inclusion in the Chronic Intruder Agricultural (Post-Drilling) Scenario dose. The GoldSim computer code was used to calculate doses following the dose formulas provided below and utilizing the PORFLOW calculated 1m concentrations as inputs. Unless otherwise noted, formulas were based on those used in LADTAP model report WSRC-STI-2006-00123 or in the PA for Idaho Tank Farm, document DOE-ID-10966. While these documents were used as guides for the other formulas, ultimately the bases for all the formulas can be traced to 10 CFR 50, Reg. Guide 1.109. Unit conversions are not explicitly stated in the equations, but are coded into GoldSim.

All transfers times are assumed negligible due to the half lives of the radionuclides and the long term analysis of the PA.

6.3.1 Chronic Intruder Ingestion Dose Pathways

Ingestion of Water

The drinking water exposure route assumes the receptor uses a well located 1m from the tank farm tanks as a drinking water source. The incidental ingestion of water from showering and during recreational activities is assumed to be negligible when compared to ingestion of drinking water.

$$D = C_{GW} \times U_W \times DCF$$

where:

D	=	dose from 1 year's consumption of contaminated media; in this equation, groundwater (rem/year)
C_{GW}	=	radionuclide concentration in groundwater from a well located at 1m (pCi/L)
U_W	=	human consumption rate of water (L/year), Table 4.6-7
DCF	=	ingestion dose conversion factor (rem/μCi), Table 4.7-1

Ingestion of Beef and Milk

The beef and dairy exposure route assumes cattle drink contaminated water and the intruder in turn consumes the contaminated beef and milk from the cattle. Beef and milk are treated separately. The dose is calculated using

Beef:

$$D = T_B \times \left(FF_B \times C_f \times Q_{FB} + C_{GW} \times Q_{WB}\right) \times DCF \times U_B \times F_B$$

Milk:

$$D = T_M \times \left(FF_M \times C_f \times Q_{FM} + C_{GW} \times Q_{WM}\right) \times DCF \times U_M \times F_M$$

where:

T_B	=	beef transfer coefficient (d/kg), Table 4.6-3
T_m	=	milk transfer coefficient (d/L), Table 4.6-2
FF_i	=	beef or milk cattle intake fraction from irrigated field/pasture, Table 4.6-7
C_f	=	radionuclide concentration in fodder (pCi/kg)
Q_{Fi}	=	consumption rate of fodder by beef or milk cattle (kg/d), Table 4.6-7
C_{GW}	=	radionuclide concentration in groundwater from a 1m well (pCi/L)
Q_W	=	consumption rate of water by beef or milk cattle (L/d), Table 4.6-7
DCF	=	ingestion dose conversion factor (rem/μCi), Table 4.7-1
U_B	=	human consumption rate of beef (kg/year), Table 4.6-7
U_M	=	human consumption rate of milk (L/year), Table 4.6-7
F_B	=	fraction of beef produced locally (unitless), Table 4.6-5
F_M	=	fraction of milk produced locally (unitless), Table 4.6-5

Ingestion of Vegetables

The dose to humans from ingestion of contaminated leafy vegetables and produce is calculated assuming three contamination routes: (1) direct deposition of contaminated irrigation water on plants, (2) deposition of contaminated irrigation water on soil followed by root uptake by plants, and (3) deposition of contaminated drill cuttings in soil followed by root uptake by plants. Leafy vegetables and produce are treated separately. The dose is calculated using:

$$D_{IV} = D_{GW} \times D_{DC}$$

where:

D_{IV} = the intruder dose from vegetable intake

D_{GW} = the vegetable dose to intruder associated with using contaminated well water

D_{DC} = the vegetable dose to intruder associated with drill cutting in the garden soil

$$D = C_{GW} \times I \times (LEAF + ROOT) \times DCF \times (U_{LV} + U_{OV} \times k) \times FV \times e^{-\lambda_i t_t}$$

$$D_{DC} = C_{SD} \times \frac{T_{StV}}{\rho_S} \times DCF \times (U_{LV} \times k + U_{OV}) \times FV$$

$$LEAF = \frac{r \times \left(1 - e^{-\lambda_e t_V}\right)}{Y_V \times \lambda}$$

$$ROOT = \frac{T_{StV} \times \left(1 - e^{-\lambda_i t_b}\right)}{\rho_S \times \lambda_i}$$

$$\lambda_e = \lambda_i + \lambda_w$$

where:

C_{GW}	=	radionuclide concentration in groundwater from a 1m well (pCi/L)
I	=	irrigation rate (L/m^2-d), Table 4.6-6
$LEAF$	=	radionuclide concentration in the vegetable's leaves (m^{2}d/kg)
$ROOT$	=	radionuclide concentration in the vegetable's roots (m^{2}d/kg)
DCF	=	ingestion dose conversion factor (rem/μCi), Table 4.7-1
U_{LV}	=	human consumption rate of leafy vegetables (kg/year), Table 4.6-7
U_{OV}	=	human consumption rate of other vegetables (produce) (kg/year), Table 4.6-7
k	=	fraction retention of deposition on leaves (unitless) [1]
FV	=	fraction of leafy vegetables and produce produced locally (unitless), Table 4.6-5
r	=	fraction of material deposited on leaves that is retained (unitless), Table 4.6-6
λ_e	=	weathering and radiological decay constant (1/d)
λ_w	=	weathering decay constant (0.0495/d)
t_V	=	time vegetables are exposed to irrigation (d), Table 4.6-5
Y_V	=	vegetation production yield (kg/m^2), Table 4.6-5
T_{StV}	=	soil to vegetable ratio (unitless), Table 4.6-1
ρ_S	=	surface soil density (kg/m^2), Table 4.6-6
t_b	=	buildup time of radionuclides in soil, Table 4.6-1
λ_i	=	radiological decay constant (ln2/half life of radionuclide i – 1/d)
C_{SD}	=	concentration in soil due to drill cuttings (pCi/L)
t_t	=	transport time (d), assumed to be zero

Ingestion of Fish

The fish exposure route assumes fish are caught from a stream contaminated from the aquifer, diluted, and the receptor in turn consumes the contaminated fish. The dose is calculated using the following formula.

$$D = C_S \times U_F \times T_F \times DCF$$

where:

C_S = radionuclide concentration in groundwater at the seep line (pCi/L)

U_F = human consumption rate of finfish (kg/year), Table 4.6-7

T_F = fish bioaccumulation factor (L/kg), Table 4.6-4

DCF = ingestion dose conversion factor (rem/μCi) Table 4.7-1

Ingestion of Soil

The soil ingestion exposure route assumes soil is irrigated with groundwater from a well 1m from the tank farm and the receptor in turn consumes the contaminated soil.). This formula was derived following the approach of the previous pathway calculations, whose bases are found in other PA methods. The dose is calculated using the following formula.

$$\frac{D = (C_D + C_W) \times DCF \times U_S}{\rho_{SS}}$$

where:

C_D = radionuclide concentration in soil contaminated with drill cuttings (pCi/m^3)

C_W = radionuclide concentration in soil irrigated with water from a 1m well (pCi/m^3)

DCF = ingestion dose conversion factor (rem/μCi), Table 4.7-1

U_S = human consumption rate of dirt (kg/year), Table 4.6-7

ρ_{SS} = density of sandy soil (g/cm^3)

6.3.2 Chronic Intruder Direct Exposure Dose Pathways

Direct Exposure from Irrigated Soil

The irrigated soil direct exposure route assumes soil is 1) irrigated with groundwater from a well 1m from the tank farm, and 2)contaminated with drill cuttings. The receptor, in turn, is exposed during time spent caring for a garden. The dose is calculated using the following formula.

$$D = (C_D + C_W) \times F_G \times DCF$$

where:

C_D = radionuclide concentration in soil contaminated with drill cuttings (pCi/m^3)

C_W = radionuclide concentration in soil irrigated with water from a 1m well (pCi/m^3)

DCF = external dose conversion factor, 15cm (rem/yr per μCi/m^3), Table 4.7-1

F_G = fraction of time spent in garden (unitless), Table 4.6-7

Direct Exposure from Swimming

The swimming direct exposure route assumes the receptor receives dose from swimming in a stream contaminated from the aquifer. The dose is calculated using the following formula.

$$D = GF_S \times t_S \times C_{SW} \times DCF$$

where:

DCF = external dose conversion factor, water immersion (rem/yr per μCi/m^3), Table 4.7-1

GF_S = swimming geometry factor (unitless) [1]

t_S = time per year spent swimming (hr/yr), Table 4.6-7

C_{SW} = radionuclide concentration in water from the stream (undiluted aquifer) (pCi/L)

Direct Exposure from Fishing/Boating

The fishing/boating direct exposure route assumes the receptor receives dose from fishing or boating in a stream contaminated from the aquifer. The dose is calculated using the following formula.

$$D = GF_B \times t_B \times C_{SW} \times DCF$$

where:

DCF = external dose conversion factor, 15 cm (rem/yr per μCi/m^3), Table 4.7-1

GF_B = boating geometry factor (unitless) [0.5]

t_B = time per year spent boating (hr/yr), Table 4.6-7

C_{SW} = radionuclide concentration in water from the stream (undiluted aquifer) (pCi/L)

6.3.3 Chronic Intruder Inhalation Dose Pathways

Inhalation during Irrigation

The irrigation inhalation exposure route assumes soil is irrigated with groundwater from a well 1m from the tank farm and the intruder in turn is exposed by breathing while the garden is irrigated but only during the time spent caring for a garden. For simplicity and conservatism, the source material is the moisture contained within the air with equal concentrations as the groundwater. No resistance to vaporization (i.e., vapor pressure) was used. This formula was derived following the approach of the previous pathway calculations, whose bases are found in other PA methods. The dose is calculated using the following formula.

$$D = \frac{C_{GW} \times DCF \times U_A \times F_G \times C_{WA}}{\rho_W}$$

where:

C_{GW}	=	radionuclide concentration in groundwater from a 1m well (pCi/L)
DCF	=	inhalation dose conversion factor (rem/μCi), Table 4.7-1
U_A	=	air intake (m^3/yr), Table 4.6-7
F_G	=	fraction of time spent in garden exposed to soil irrigated with contaminated ground water (unitless), Table 4.6-7
C_{WA}	=	water contained in air at ambient conditions, (g/m^3) [10 g/m^3]
ρ_W	=	water density (g/ml)

Inhalation during Showering

The showering inhalation exposure route assumes receptor exposed by breathing humid air within the shower. The source of water for the shower is a well 1m from the tank farm. For simplicity and conservatism, the source material is the moisture contained within the air with equal concentrations as the groundwater. No resistance to vaporization (i.e., vapor pressure) was used, adding to the conservatism. For example, heavy elements would be greatly influenced by this assumption because they would be less likely to volatize. This formula was derived following the approach of the previous pathway calculations, whose bases are found in other PA methods. The dose is calculated using the following formula.

$$D = \frac{C_{GW} \times DCF \times U_A \times t_S \times C_{WS}}{\rho_W}$$

where:

C_{GW}	=	radionuclide concentration in groundwater from a well (pCi/L)
DCF	=	inhalation dose conversion factor (rem/μCi), Table 4.7-1
U_A	=	air intake (m^3/yr), Table 4.6-7
t_S	=	time spent in shower (min), Table 4.6-7 Note: GoldSim uses fraction of time [0.0069 = 10 min/day]
C_{WS}	=	water contained in air at shower conditions, (g/m^3) [41 g/m^3]
ρ_W	=	water density (g/ml)

Inhalation of Dust from Irrigated Soil

The irrigation soil inhalation exposure route assumes soil is irrigated with groundwater from a well 1m from the tank farm and the receptor in turn is exposed by breathing dust during time spent caring for a garden. This formula was derived following the approach of the previous pathway calculations, whose bases are found in other PA methods. The dose is calculated using the following formula.

$$D = \frac{U_A \times L_{SiA} \times C_D \times DCF \times F_G}{\rho_{SS}}$$

where:

U_A	=	air intake (m^3/yr), Table 4.6-7
L_{SiA}	=	soil loading in air while working in a garden (kg/m^3), Table 4.6-6
C_D	=	radionuclide concentration in soil irrigated with water from a well and contaminated with drill cuttings (pCi/m^3)
DCF	=	inhalation dose conversion factor (rem/μCi), Table 4.7-1
F_G	=	fraction of time spent in garden exposed to soil irrigated with contaminated ground water (unitless), Table 4.6-7
ρ_{SS}	=	density of sandy soil (g/cm^3)

Inhalation During Swimming

The swimming inhalation exposure route assumes a stream contaminated from the aquifer and the receptor inhales saturated air. For simplicity and conservatism, the amount of moisture contained in the inhaled air assumed to be stream water. This formula was derived following the approach of the previous pathway calculations, whose bases are found in other PA methods. The dose is calculated using the following formula.

$$D = \frac{U_A \times GF_S \times t_S \times C_{SW} \times DCF \times C_{WiA}}{\rho_W}$$

where:

U_A	=	air intake (m^3/yr), Table 4.6-7
GF_S	=	swimming geometry factor (unitless) [1]
t_S	=	time per year spent swimming (hr/yr), Table 4.6-7
C_{SW}	=	radionuclide concentration in water from the stream, (undiluted aquifer) (pCi/L)
DCF	=	inhalation dose conversion factor (rem/μCi), Table 4.7-1
C_{WA}	=	water contained in air at ambient conditions, (g/m3) [10 g/m^3]
ρ_W	=	water density (g/ml)

6.4 Intruder Analysis Results

The peak total intruder doses were calculated utilizing the pathways identified in Section 6.2 for the Acute Intruder Scenario and in Section 6.3 for the Chronic Intruder Agricultural (Post-Drilling) Scenario. The peak total doses were calculated using the maximum 1m concentrations identified in Section 6.1. A peak dose was identified for the 10,000 year performance period.

The peak dose for the Acute Intruder in the 10,000 year performance period was 1.60 mrem at year 100, which was primarily due to exposure to drill cuttings (Table 6.4-1). The Acute Intruder scenario was not tied to a groundwater contribution and therefore did not vary by FTF Sector. Figure 6.4-1 presents the peak doses over time during the performance period (10,000 years) for the Acute Intruder.

The peak doses for the four 1m sectors were calculated using the highest concentration for each radionuclide in the Sector (a discussion of how peak concentrations were determined by sector was provided in Section 6.1). These peak doses were the total dose associated with all the individual 1m well pathways identified in Sections 6.2 and 6.3. Tables 6.4-1 and 6.4-2 present the Acute and Chronic Intruder peak doses. In calculating the peak chronic intruder doses, the highest radionuclide concentration was used from the applicable aquifers.

Table 6.4-1: Acute Intruder Dose Contributors

Acute Intruder Pathway Contributors	Peak Contribution (mrem)	Principal Radionuclide Pathway Dose (%)
Drill Cuttings Direct Exposure	1.53	Cs-137/Ba-137m (94%)
Drill Cuttings Ingestion	0.02	Am-241 (50%)
Drill Cuttings Inhalation	0.05	Am-241 (70%)
Total	**1.60**	

Figure 6.4-1: Acute Intruder Dose Results within 10,000 Years

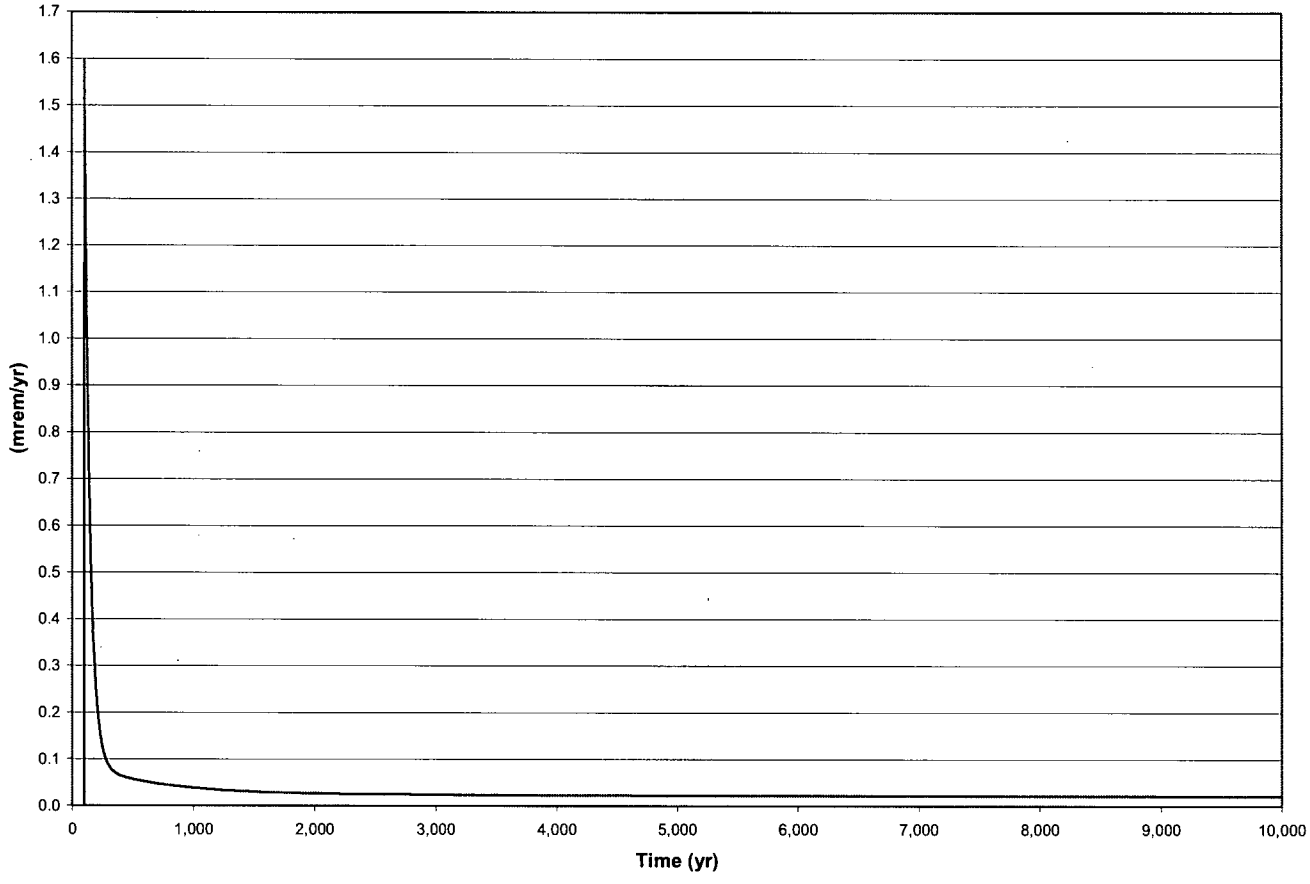

The peak dose for the Chronic Intruder scenario in the 10,000 year performance period was 72.8 mrem/yr. This peak dose was almost entirely due to ingestion of vegetables contaminated with drill cuttings, with 71.6 of the 72.8 mrem/yr being due to vegetable ingestion (Table 6.4-2). The principal radionuclide contributors to this vegetable dose were the short lived isotopes Sr-90/Y-90 and Cs-137/Ba-137m (Table 6.4-3). The Chronic Intruder scenario peak dose was not tied to a groundwater contribution and therefore does not vary by FTF Sector. Figure 6.4-2 presents a 1,000 year dose curve showing the peak dose during the performance period (10,000 years).

It should be noted that there are several conservatisms incorporated into the chronic intruder analysis. The chronic intruder scenario conservatively assumes that the intruder drills into a transfer line immediately after the end of the 100-year institutional control period. Since almost the entire dose comes from the short-lived isotopes, Sr-90/Y-90 and Cs-137/Ba-137m, even relatively small delay of 100 years in the timing of the intruder drilling would result in a significant reduction in the peak dose. No credit is taken for the fact that the intruder would have to drill through the steel transfer line or for some transfer line segments, the concrete encasement containing the transfer lines. The cross-sectional area of all of the transfer line segments from Table 3.2-3 is 11,400 ft^2 compared to the total FTF footprint of approximately 892,500 ft^2, so the opportunity for an intruder to drill into a transfer line exists for only about 1% of the total area of FTF.

Table 6.4-2: Chronic Intruder Peak Dose Contributors

Chronic Intruder Pathway Contributors	Contribution to Peak (mrem/yr)	Principal Radionuclide Pathway Dose (%)
Vegetable Ingestion	71.6	Sr-90 / Y-90 (56%) Cs-137 / Ba-137m (44%)
Soil Ingestion	0.7	Am-241 (43%) Sr-90 / Y-90 (35%)
Other Pathways	0.5	- - -
Total	**72.8**	

Table 6.4-3: Chronic Intruder Vegetable Ingestion Doses by Radionuclide

Radionuclide	Contribution to Peak (mrem/yr)
Sr-90/Y-90	39.9
Cs-137/Ba-137m	31.6
Others Nuclides	0.1
Total	**71.6**

The Chronic Intruder Dose values beyond the peak dose were impacted by groundwater contribution, and Figure 6.4-3 presents the Chronic Intruder doses within 20,000 years for the four 1m sectors. Sector C was the only sector that showed an appreciable dose during the performance period, which was due to this sector including the Type IV tanks.

Figure 6.4-2: Chronic Intruder Dose Results within 1,000 Years

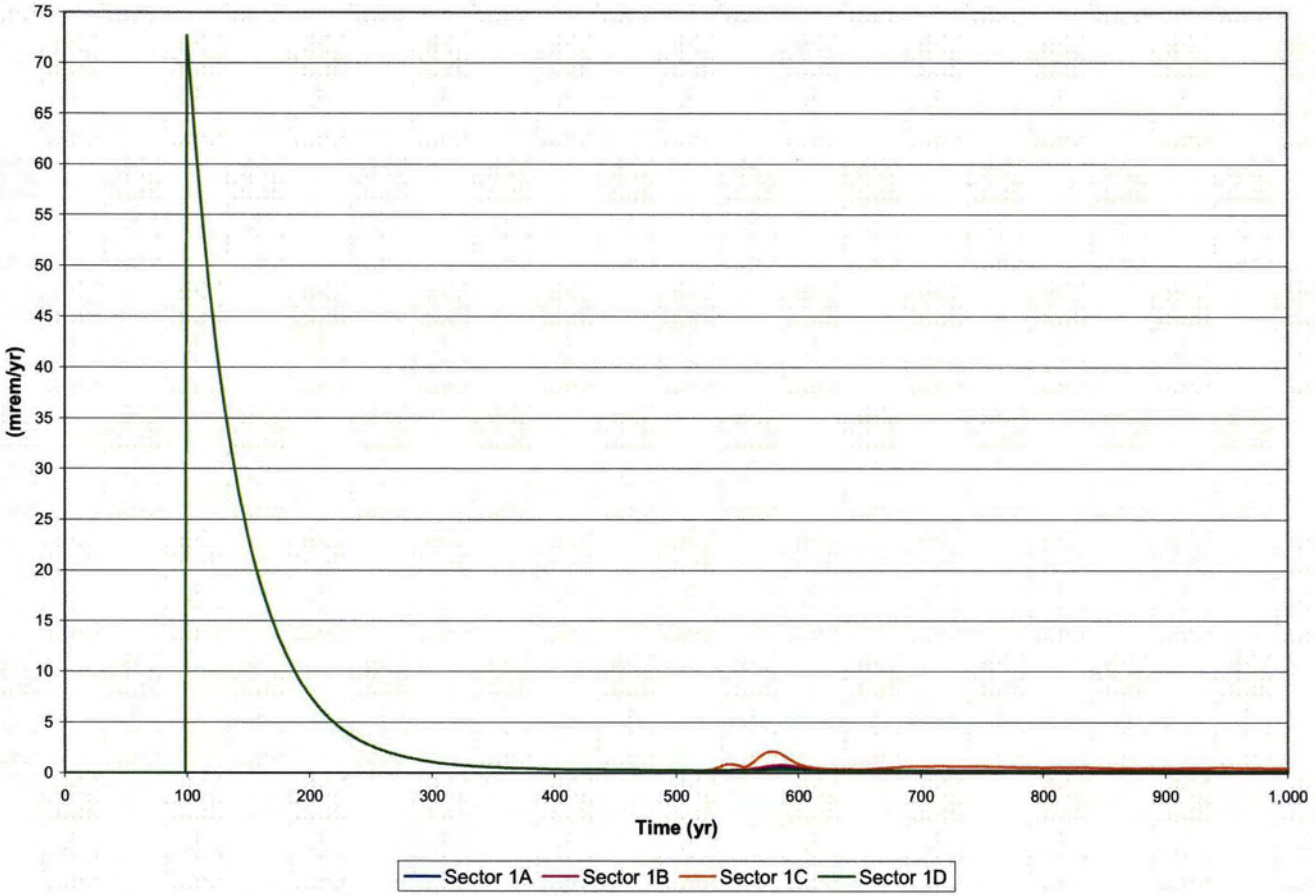

Note: 100-year peak is associated with all sectors.

Figure 6.4-3: Chronic Intruder Dose Results within 20,000 Years

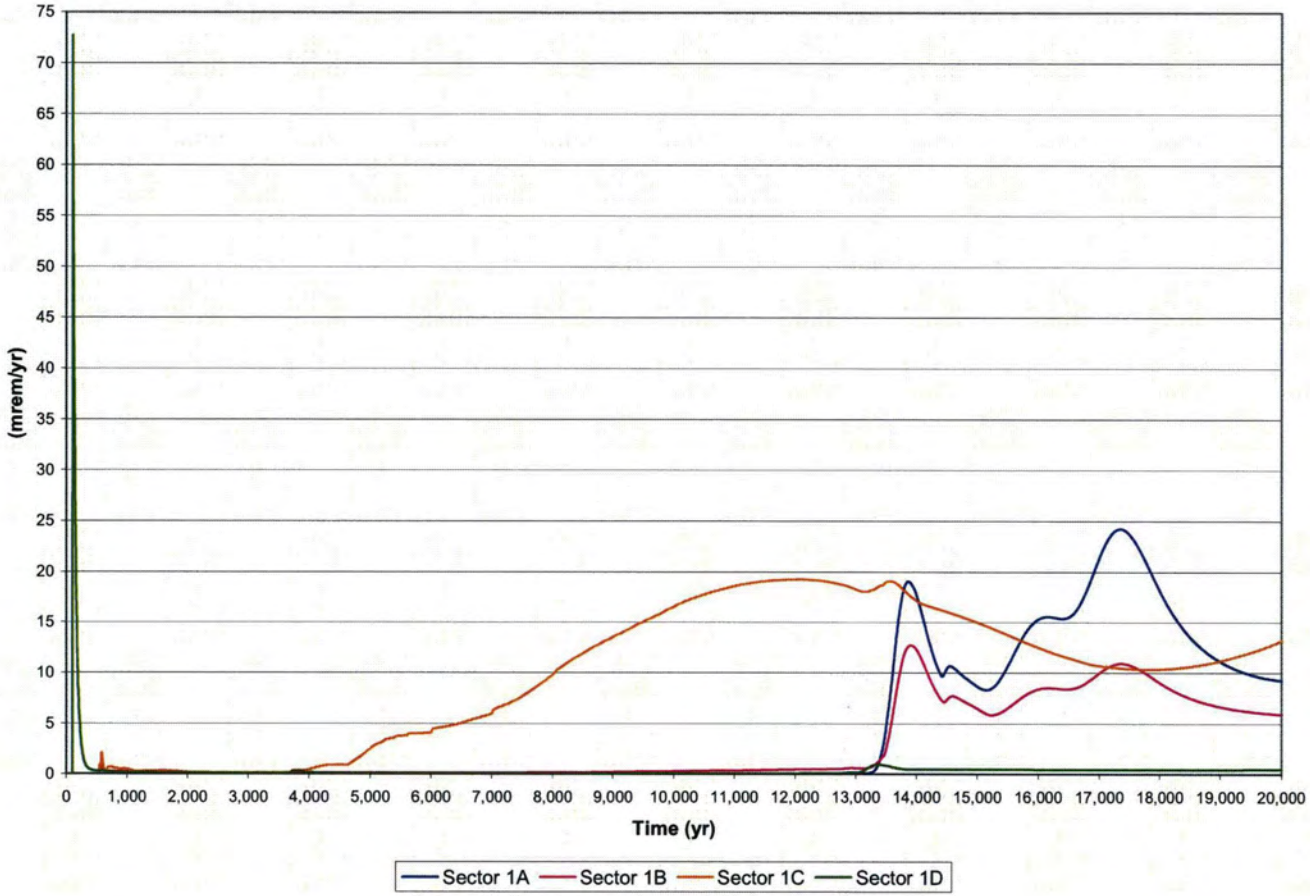

6.5 Intruder Sensitivity / Uncertainty Analysis

The purpose of this section was to consider the effects on the Intruder Analyses of uncertainties in the conceptual models used, and sensitivities in the parameters used in the mathematical models.

6.5.1 Intruder Probabilistic Sensitivity Analysis

A single sensitivity and uncertainty analysis was performed using the GoldSim FTF model (Section 5.6.6). This evaluation included inadvertent intruders as well as MOP. Intruder specific sensitivity analyses were performed for the maximum chronic intruder dose within 10,000 years (Figure 5.6-45) and within 20,000 years (Figure 5.6-46). The same parameters that influenced the public dose were impactive on the intruder dose. For example, the aquifer thickness is significant.

6.5.2 Intruder Single Parameter Deterministic Sensitivity Analyses

This purpose of this section is to present single parameter sensitivity analysis results obtained using the FTF Base Case model. The drill scenario inventories were modified to see the impact this parameter had on the chronic intruder scenarios.

6.5.2.1 Impact of Drilling into a 4 inch Transfer Line vs. a 3 inch Transfer Line

To investigate the effect of an intruder drilling into 4 inch transfer line vs. a 3 inch transfer line (which is not considered likely, since, as discussed in Section 4.2.4.2, only 0.24% of the FTF transfer lines are 4 inch lines), the transfer line inventory for a 4 inch line was substituted for the 3 inch transfer line inventory used in the Base Case modeling. All other parameters from the chronic intruder scenario were held constant. As presented in Figure 6.5-1, the 4 inch transfer line inventory change has an impact on the magnitude of the peak dose (the 125 mrem/yr peak is approximately 1.7 times the peak dose associated with drilling into a 3 inch transfer line).

6.5.2.2 Impact of Drilling into a Waste Tank vs. into a Transfer Line

To investigate the effect of an intruder drilling into a waste tank (which is not considered a credible scenario (Section 4.2.4.2), a conservative Tank 18 drilling inventory was substituted for the transfer line drilling inventory. Since the waste tank engineered barriers (e.g., closure cap erosion barrier, tank top concrete, and tank liner, where applicable), will prevent drilling into the waste inventory, this scenario was not considered to occur until 500 years after FTF closure. With the exception of the waste tank walls, all of the steel objects in the system will be encased by several feet of grout in the horizontal direction. All pumps, pipes, etc. that extend into the waste tank are suspended from the risers. The waste tanks are currently subject to a corrosion protection program that prevents corrosion of the walls by maintaining a high pH. [WSRC-TR-2002-00327] After placement of grout, the pH will remain high due to the properties of the grout. [WSRC-TR-97-0102, page 14] This will minimize the degradation effects on the carbon steel tank components and ensure the tank presents a credible drilling barrier, especially in the first 500 years. All other parameters from the acute intruder drilling scenario were held constant during the sensitivity run. Figure 6.5-2 shows the peak acute intruder dose for 20,000 years with the Tank 18 inventory change in place.

Figure 6.5-1: Chronic Intruder Dose Results Drilling into a 4 Inch Transfer Line

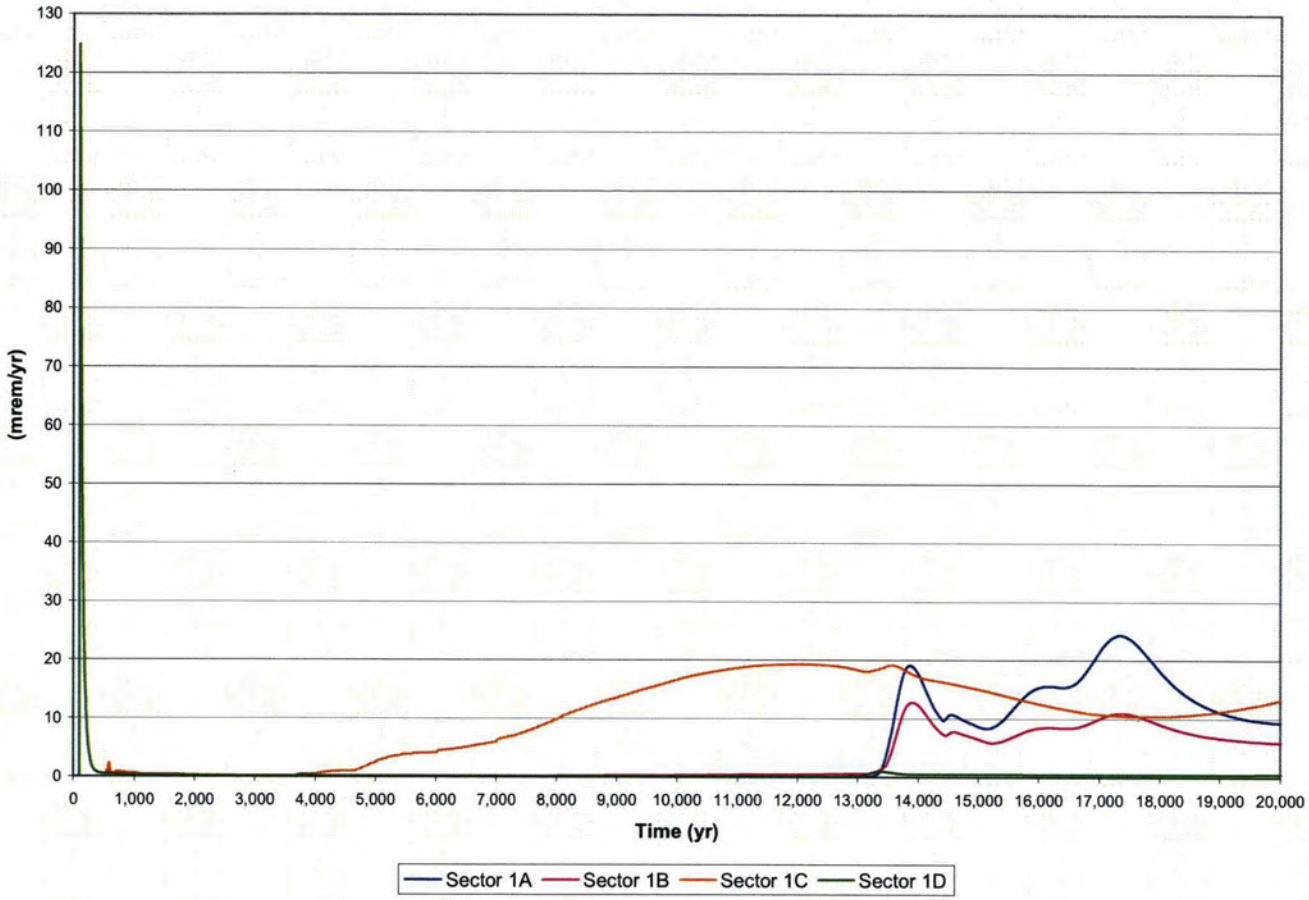

Figure 6.5-2: Acute Intruder Dose Results Drilling into Tank 18

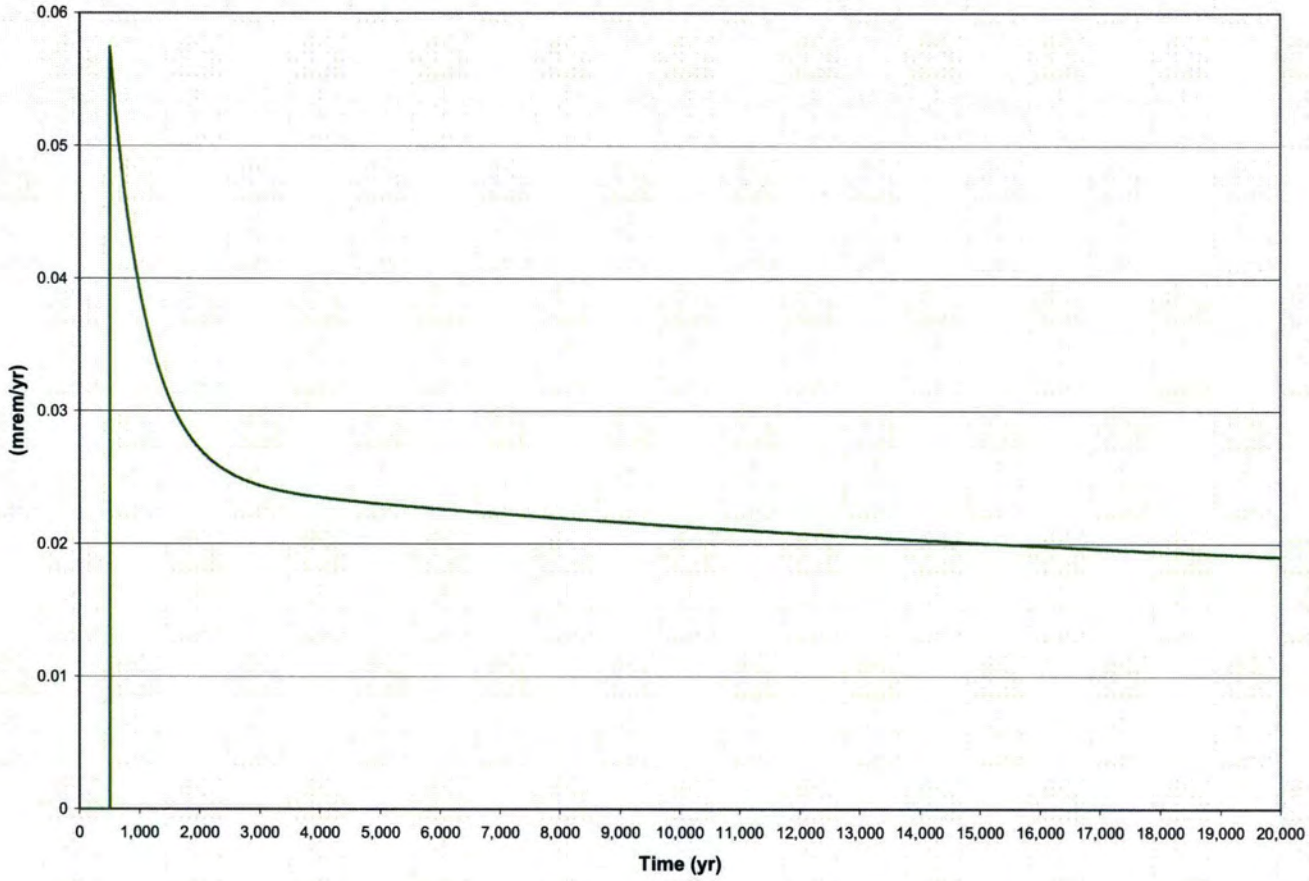

7.0 INTERPRETATION OF RESULTS

Summary for Section 7.0.

This section provides an interpretation of results presented in Sections 5 and 6.

Section 7.1 summarizes the results presented in Sections 5 and 6.

Section 7.2 summarizes the conservatisms used in modeling.

7.1 Performance Assessment Results

This section provides a summary and interpretation of the results presented in Section 5 and 6. Intrepretation of the results against 10 CFR 61 performance objectives shall be documented in DOE's Waste Determination documentation per NDAA Section 3116, and against the Industrial Wastewater Regulations in the Closure Plan. [NDAA_3116, SCDHEC_R.61-67]

7.1.1 Integrated System Behavior

Provided below is a short description of the impact that various segments of the integrated conceptual model have on dose results (the segments are discussed in some detail in Section 4.4.3).

7.1.1.1 Closure Cap

The Base Case liner failure dates are all after year 2500, so changes in the infiltration rate and corresponding changes in flow near the waste tanks does not significantly affect the flow model in the early years. Since the closure cap reaches the steady state flow values relatively quickly, the cap has a minimal effect on peak doses.

7.1.1.2 Tank Top

The timing of waste tank top concrete degradation affects the flow rate into the tank. Early concrete degradation, as modeled in some alternate configurations, allows the steady state flow values to be reached earlier, but doesn't appear to have as pronounced an impact on flow as other segments (e.g., liner failure, basemat bypass).

7.1.1.3 Tank Liner Top

Since the entire liner was modeled as failing simultaneously, isolated failure of the tank top liner was not studied. A discussion of the overall affect of the liner failure analyses and results is provided in Section 7.1.1.6.

7.1.1.4 Tank Grout

The timing of tank grout degradation affects the flow rate to the CZ. Early grout degradation, as modeled in some alternate configurations, allows the steady state flow values to be reached earlier, but doesn't appear to have as pronounced an impact on flow as other segments (e.g., liner failure, basemat bypass).

7.1.1.5 Contamination Zone

The CZ modeling segment has a significant impact on the peak dose results. The modeled solubility limits control the release rate of contaminants from the CZ, and higher solubility limits can cause increased release rate. The Section 5.6.7.1 sensitivity analysis results show that for most of the radionuclides, the waste release flux varies linearly with inventory, with the exceptions being those radionuclides (e.g., Pu-239, Pu-240, Tc-99, and U-238) that are solubility controlled through iron co-precipitation and are present in a significant enough quantity for solubility control to have an effect.

7.1.1.6 Tank Liner Sides and Bottom

In the probabilistic model, the waste tank liner was modeled utilizing different configurations, since independently moving the liner failure date forward tends to decrease the peak 20,000 year dose. As discussed in Section 5.6.7.3, early liner failure tends to allow the closure cap to reduce infiltration into the tank during release of radionuclides that are not significantly affected by either the waste release solubility limits and/or concrete/soil retardation (e.g., with low soil/concrete Kd values). The result is to spread the releases out over a longer time period. Early liner failure has only a minor effect on magnitude of the dose peaks within 20,000 years. There can be a significant change in the timing of the early peaks associated with some radionuclides, such as Np-237 which shows a direct relationship to the change in the liner failure date. Since the release rate of the other radionclides most affecting dose (e.g., Tc, Pu, U) are solubility limited, their contribution to the peak doses are not greatly impacted by early liner failure.

7.1.1.7 Basemat

As shown in the 5.6.7.3 GoldSim sensitivity studies, allowing contaminants to bypass the basemat has a minimal affect on tanks with thin basemats (Type IV tanks), but has a more appreciable affect when the waste tanks involved have a very thick basemat (e.g., Type I/III/IIIA tanks). This is due to the fact that bypassing the basemat removes both the flow restricting and K_d impacts of the basemat. The impact of the basemat can be very radionuclide specific depending on how high the K_d value of the concrete is for the applicable radionuclide. The Section 5.6.7.2 sensitivity analysis results show that the Tc-99 flux is relatively unaffected by K_d changes, while the Pu-239 flux can be significantly impacted, especially when the material layer is thick (e.g., the Type III and Type I basemats).

7.1.1.8 Vadose Zone Beneath Tank

The vadose zone beneath the waste tanks has a very similar radionuclide-specific effect to that of the basemat. The vadose zone depth can have a considerable affect if the vadose layer is thick or if the radionuclide in question has a high K_d in soil.

7.1.2 100m (Water from Well) Groundwater Pathways Doses

The peak 100m groundwater pathway doses in the 10,000 year performance period are in Sector E (1.3 mrem/yr) and Sector D (1.2 mrem/yr), as expected, because these sectors are closest to the Type IV tanks, which are the only tanks considered to have their liner fail in less than 10,000 years. The primary pathway contributors to the peak 100m groundwater dose are water ingestion and vegetable ingestion.

The 100m groundwater pathway dose during the 10,000 years evaluation period is primarily associated with Ra-226 and U-233. While there is very little Ra-226 in the Type IV tanks, the Ra-226 is a daughter product of U-238, of which there is an appreciable quantity in the Type IV tanks. The Ra-226 is a relatively fast moving (e.g., K_d < 20 units in soil) radionuclide so that it is capable of reaching the 100m location before it's parent. The U-233 is also a relatively fast moving (e.g., K_d = 300 units in soil) radionuclide which is present in the Type IV tanks.

The peak 100m groundwater pathway dose within 20,000 years is also in Sectors D and E. These sectors are close to the Type IV tanks and also begin to see the releases from the nearby Type I tanks within 20,000 years. While they do not contain the peak groundwater pathway doses, Sectors A and B begin to see noticeable 100m doses within 20,000 years due to releases from the Type III tanks (Tanks 33 and 34). Uncertainties of the results are discussed in Section 5.6.

7.1.3 Water at the Stream Groundwater Pathways Doses

The peak groundwater pathway dose at the stream in the 10,000 year performance period is associated with UTR. The MOP at the stream peak groundwater pathway dose in the 10,000 year evaluation period is 0.21 mrem/yr at year 3,788. UTR dose is higher than the Fourmile Branch dose because releases from the Type IV tanks (which are expected to have liner failure earlier than other tank types) will primarily go to UTR. The primary contributor (98% of the peak dose) to the UTR peak is fish ingestion, which is due to the large C-14 peak at year 3,788. Carbon is very fast moving (i.e., K_d = 0 in soil) and C-14 has a high fish uptake factor which allows the C-14 to predominate before other radionuclides appear at the stream.

The Fourmile Branch groundwater pathway stream doses are greater than the UTR doses within 20,000 years because the Type I and Type III/IIIA tank liners have failed and released material in the direction of Fourmile Branch by year 15,000. The primary contributors to the Fourmile Branch groundwater pathway stream dose at 14,468 years (the year of the peak dose) is finfish ingestion, with 97% of the dose from Ra-226.

7.1.4 All-Pathways Dose

The peak all-pathways annual dose for the MOP at 100m is calculated using the highest 100m groundwater pathway dose results during the 10,000 year performance period in combination with the air pathway results. The peak all-pathway annual dose for the MOP is 1.4 mrem/yr and is associated with Sector E at 100m. The all-pathways dose was dominated by the groundwater pathway with a dose of 1.3 mrem/yr 100m from the FTF. The airborne dose adds an additional 0.14 mrem/yr to the MOP.

7.1.5 Intruder Dose

The peak dose for the Acute Intruder in the 10,000 year performance period was 1.60 mrem, which was primarily due to exposure to drill cuttings. The Acute Intruder scenario did not include a groundwater contribution and therefore did not vary by FTF Sector.

The peak dose for the Chronic Intruder scenario in the 10,000 year performance period was 73 mrem/yr. This peak dose was almost entirely due to ingestion of vegetables contaminated with drill cuttings, with 72 of the 73 mrem/yr being due to vegetable ingestion. The principal radionuclide contributors to this vegetable dose were the short lived isotopes Sr-90/Y-90 and Cs-137/Ba-137m. The Chronic Intruder scenario peak dose was not driven by the groundwater contribution and therefore does not vary by FTF Sector.

7.1.6 Airborne Dose

The annual dose from airborne releases resulted in a total dose 0.14 mrem/yr (principally from Sn-126) at 100m from the FTF. These results were very conservative because the flux rates were based on simplified models as described in Section 4.5.

7.1.7 Radon Flux

These simplified models also resulted in a peak flux of radon at the ground surface of 9.3E-08 $pCi/m^2/sec$.

7.2 Conservatisms Included in the FTF Performance Assessment

Much conservatism was used in conducting the FTF PA as discussed in previous sections. Cumulative effects of the conservatisms are addressed through probabilistic modeling. A summary of those conservatisms are discussed below.

7.2.1 Inventory

Inventory estimates are based on sample analysis and the WCS. WCS generated values are generally conservative because of two main factors. First, each reactor spent fuel assembly that was reprocessed is assumed to have received the maximum burnup possible and, therefore, the amounts of actual fission products contained in an assembly were actually less than those entered into WCS. Second, some of the residual material characterized as fission product bearing PUREX Low Heat Waste actually originated as cladding waste or other low radionuclide bearing wastes that contain relatively small amounts of fission products. [LWO-PIT-2007-00025] Another factor expected to provide additional conservatism is the likelihood that actual concentrations for some constituents in the residual sludge on the waste tank bottoms after tank cleaning will be significantly less than the concentrations for dried

sludge currently given in the WCS. This condition is expected to result from various flushing that will take place and the use of OA to clean the tanks.

Analyses of samples from Tanks 5, 18, and 19 indicate that the predicted inventory modeled values are conservative compared to sample analysis values for most (approximately 75 %) of the constituents (Figure 3.3-3).

Using the estimated sludge concentrations for the characterization of ancillary equipment inventory also provides conservatism in the results.

The sorption of uranium onto the waste tank walls, as discussed in WSRC-STI-2007-00684, was overestimated in the inventory calculations. The inventory on the tank walls is expected to be overestimated by one or two orders of magnitude.

7.2.2 Closure Cap

The following are some of the measures which were taken to try and ensure conservative HELP model infiltration results.

- The precipitation data utilized included maximum daily precipitation up to 6.7 inches (i.e., significant pulses of water).
- The maximum slope length of the closure cap (i.e., 585 feet) was utilized to determine both runoff and lateral drainage for the entire closure cap.
- A maximum evaporative zone depth of 22 inches, which is considered conservative due to the anticipated capillarity of the surficial soils, was utilized.
- The erosion barrier is assumed to be infilled with a sandy soil; the use of a less permeable infill would reduce infiltration.
- A saturated hydraulic conductivity was assigned to the intact portions of the HDPE geomembrane even though water transport through HDPE is a vapor diffusional process.
- It has been assumed that every HDPE geomembrane hole generated over time is penetrated by a pine root that subsequently penetrates the GCL. However the results of the probability based root penetration model demonstrate that this is not the case and that most of the HDPE geomembrane holes are not penetrated by roots over the time period of interest.

7.2.3 Integrated Site Conceptual Model

Several assumptions were made that introduced conservatism into the timing of release of radionuclides from the FTF.

- Prior to failure, steel is assumed to be essentially impermeable with respect to both advection and diffusion. After failure, the steel liner is assumed to be absent, or otherwise not a hindrance to advection and diffusion.
- Failure times for steel liners assume corrosion from both sides.
- Liner failures ignore concrete vaults, pipe jackets and other protection.
- All waste tanks of the same type were assumed to fail simultaneously.
- Tank dimensions default to the minimum. For example, if wall thickness or basemat thickness varied, the minimum dimension was used for the entire wall or basemat.

- Based on stainless steel corrosion calculations, the earliest failure of a stainless steel transfer line is predicted to occur 510 years after FTF closure under SRS soil conditions. [WSRC-STI-2007-00460] Failure is assumed after the first pit penetration of the transfer line wall. Predicted failure times are dependent on the thickness of the transfer lines.
- A fundamental part of establishing solubility controlled stabilized contaminant release rates for the waste tanks is selection of a solubility controlling phase for each radionuclide. For some of the radionuclides of interest there are studies that can guide selection, for others it is based on engineering judgment. For this reason, selection of solubility controlling phases is generally very conservative, meaning that where multiple phases of a radionuclide were possible, that with the highest solubility is selected.
- No solubility control is assumed for ancillary equipment inventory. The ancillary equipment inventory is immediately released to the soil after failure with no holdup in the CZ.
- In an equilibrium model, the assumption that solubility rather than adsorption controls stabilized contaminant release is conservative, resulting in faster overall release of radionuclides. This is because the maximum concentration that can desorb is controlled by solubility. In effect, if the K_d is low enough that a concentration is released that exceeds solubility, some of the radionuclide will precipitate bringing the concentration down to solubility. The stabilized contaminant release rate will drop below that dictated by solubility when the radionuclide inventory is depleted to where the concentration released is below solubility. At higher K_d values the concentration released at any given time will always be below the concentration dictated by solubility. Thus, time until complete release of a radionuclide using adsorption controls will always be longer than when only solubility controls are used.
- The assumption that radionuclide release is controlled by solubility of discrete radionuclide phases rather than co-precipitation is conservative if equilibrium prevails and the choice of solubility controlling minerals is biased towards those with high solubility.
- The waste release model does not credit any additional potential contaminant retardation mechanisms, such as retardation associated with iron oxides/hydroxides from the corroded waste tank lines.

7.2.4 Volatile Radionuclide and Radon Analysis

The following conservatisms were used in the airborne radionuclide and radon analysis that conservatively bound the flux of radionuclides from the contaminant zone to the surface.

- Boundary conditions were used that force all of the gaseous radionuclides to move upward from the stabilized CZ to the land surface. In reality, some of the gaseous radionuclides diffuse sideways and downward in the air-filled pores surrounding the stabilized CZ; hence ignoring this has the effect of increasing the flux at the land surface.
- The removal of radionuclides by pore water moving vertically downward through the model domain was ignored. This mechanism would likely remove some dissolved radionuclides, and therefore its omission had the effect of increasing the estimate of instantaneous radionuclide flux at the land surface in simulations conducted as a part of this investigation.
- The HDPE geomembrane, the GCL, and the primary steel liner of the waste tank were excluded in the modeling. Inclusion of these materials in the model would significantly reduce the gaseous flux at the land surface due to their material properties (i.e., low air-filled porosity).
- Cover materials above the erosion barrier (i.e., top soil and upper backfill layers) were excluded. Excluding these materials shortens the diffusion pathway and could increase the flux at the land surface.
- The stabilized contaminant layer, the reducing grout, and concrete roof were assumed to be dry. This makes the air-filled porosity equal to the total porosity. This maximizes diffusive transport through these materials since gaseous flux is through the air-filled porosity.
- Use of the Type I tanks and minimum closure cap thickness in the modeling provided the shortest pathway from the CZ to the surface.
- The entire estimated FTF residual inventory was concentrated into a 1 foot stabilized contaminant layer in one Type I tank to determine the maximum dose and flux.

7.2.5 Other Factors Affecting Results

Quantified analysis of some pathways, that have been qualitatively judged insignificant in other PAs, impacted the results. This resulted in contributions that are probably insignificant but are hard to quantify (e.g., showering).

As discussed in Section 5.2.1, the use of sectors in determining groundwater concentrations added conservatism to the peak dose results, since the peak concentrations are determined for each radionuclide independent of the location within the sector.

As discussed in Section 5.6.2.5, solubility control is implemented unnaturally in the PORFLOW FTF model, with isotopes being treated as separate radionuclides with independent solubilities. Modeling solubility control in this method tends to allow more of the contaminant into solution, causing peak doses to occur sooner, and with higher values.

8.0 PERFORMANCE EVALUATION

Summary for Section 8.0

Section 8 describes the application of the PA.

Section 8.1 describes how the PA will be used.

Section 8.2 describes future work to be done to support maintenance of the PA.

8.1 Use of Performance Assessment Results

This PA for SRS was prepared to support the eventual closure of the FTF underground radioactive waste tanks and ancillary equipment. This PA provides the technical basis and results to be used in subsequent documents to demonstrate compliance with pertinent requirements of DOE O 435.1, NDAA Section 3116, the Industrial Wastewater Regulations, and the SRS FFA, as well as final closure of the FTF consistent with the CERCLA. [NDAA_3116, SCDHEC_R.61-67, WSRC-OS-94-42, http://www.access.gpo.gov/uscode/title42/chapter103_.html] The key requirements from these documents necessitate development and calculation of the following for the FTF: potential radiological doses to a hypothetical MOP; potential radiological doses to a hypothetical inadvertent intruder; radiological dose to a human receptor via the air pathway; radon flux at the ground surface; and, water concentrations. All of these calculations were performed to provide results over a minimum of 10,000 years. The water concentrations were calculated for both radioactive and non-radioactive contaminants at multiple locations outside FTF.

The regulatory process to complete closure of the FTF requires the development of multiple detailed technical documents with reviews and approvals by multiple state and federal agencies. The documents involved include an FTF Section 3116 Basis Document which will be used to demonstrate compliance with the NDAA Section 3116 criteria. [NDAA_3116] The FTF Section 3116 Basis Document is reviewed and approved by DOE in consultation with the NRC. Approval of a Section 3116 Waste Determination by the Secretary of Energy is then required so that the residual waste in FTF can be classified as low-level radioactive waste. The Section 3116 criteria include 10 CFR 61, Subpart C. The FTF PA provides the technical basis that will be used to demonstrate compliance with 10 CFR 61.41 and 61.42 performance objectives in the FTF Section 3116 Basis Document. These performance objectives are used in lieu of the comparable performance objectives from DOE O 435.1. Compliance with the SCDHEC requirements will be demonstrated using two primary documents that are supported by the FTF PA. The first is the FTF Closure Plan which will establish the general protocols, requirements and processes for closure of FTF. The second document(s) are Tank-Specific Closure Modules that authorize the closure and grouting of a specific tank, group of tanks or ancillary equipment. Both the FTF Closure Plan and the FTF Tank-Specific Closure Modules are reviewed and approved by DOE, SCDHEC and the EPA. The FTF PA will also support the final closure of the FTF consistent with CERCLA. [http://www.access.gpo.gov/uscode/title42/chapter103_.html]

8.2 Further Work

Because this PA is considered a living document for the closure of the FTF, it will be reviewed as additional information and studies are conducted to verify that it still bounds the FTF model inputs. As additional data become available and the PA needs to be revised, additional modeling will be required. The following areas of future work are presented to facilitate discussion for improving the PA in future revisions.

Further work is planned focusing on model improvement, with areas of interest being co-dependencies of model parameters and refinement of flow modeling within the GoldSim FTF model. Additional work should be conducted related to expanding the current sensitivity/uncertainty analyses. Additional benchmarking between GoldSim and PORFLOW should be conducted with additional parametric changes (e.g., tank configurations, flow conditions), to provide added assurance to the validity of the sensitivity/uncertainty results. The stochastic distributions will be refined to improve the distributions as additional information is available. The analyses should consider examination of additional dose peaks other than just the highest peak in the evaluation period.

Future work is also planned in the area of input refinement and confirmation. For example, further work should be conducted to refine and confirm the existing radionuclide inventories that will be present in FTF at site closure. This work includes additional sampling and analysis of existing waste and refinement of potential waste estimates for unsampled areas, such as the piping and other ancillary equipment. Sampling of the waste tanks after cleaning and before grouting will be necessary to evaluate the inventory to ensure that the groundwater protection performance objectives are met. Future waste tank sampling will also take into account the waste release assumptions regarding iron co-precipitation and sampling plans will address the need to investigate not just total radionuclide inventories, but chemical compositions as well. As part of input refinement and confirmation, future materials testing will be performed as needed (e.g., validation of grout properties, site specific soil K_d testing). This future work will consider uncertainty in material properties due to biases in testing methods including laboratory versus field experiments, as well as techniques used to measure properties (e.g., centrifuge versus flexible wall permeameter, column based K_d testing).

9.0 PREPARERS

BIRK, MARCIA, WSRC/ Site Regulatory Integration and Planning

B.S. Chemical Engineering – University of Minnesota, Institute of Technology

Experience: Ms. Birk has over 17 years of experience at SRS in waste management engineering and environmental compliance. In her assignment in waste management engineering, she was responsible for radioactive and chemical characterization of mixed waste to meet offsite treatment facility waste acceptance criteria and Department of Transportation (DOT) requirements for radioactive waste shipments. She has also held responsibility for regulatory compliance and for the maintenance of RCRA permits for the Consolidated Incineration Facility and the Hazardous and Mixed Waste Storage Facilities.

Contributions: Primary development of sections related to air pathways/radon analysis and the CERCLA risk assessment. Ms. Birk also assisted in the preparation and review of various PA sections.

COFFIELD, TIMOTHY, WSRC/ Site Regulatory Integration and Planning

B.S. Mechanical Engineering – University of Pittsburgh
M.S. Manufacturing Systems – Carnegie Institute of Technology

Experience: Mr. Coffield has over 30 years experience in the nuclear industry both in the commercial and governmental sectors. The last fifteen years at SRS have primarily been in waste management and regulatory compliance during waste characterization, storage and disposal operations for radioactive and hazardous waste.

Contributions: Coordinator for document development and assisted in technical review.

DEAN, BEN, WSRC/ Site Regulatory Integration and Planning

B.S. Chemical Engineering – Clemson University

Experience: With over 10 years experience, four at SRS, Mr. Dean has primarily worked with characterization of waste within the tank farms. Prior to joining WSRC, Mr. Dean spent six years in the chemical industry (chlor-alkai and fiberglass) with experience in operations, process engineering and statistics.

Contributions: Assisted in development of the waste tank characterization and exposure pathway calculations.

DESHPANDE, RANJEET, WSRC/ Site Regulatory Integration and Planning

B.S. Mechanical Engineering – University of South Carolina

Experience: Mr. Deshpande has over 9 years experience in project engineering management, project & design authority, production and process engineering. Previous experience comprise: Responsible Engineer for various chemical / mechanical process units in the Mixed-Oxide (MOX) project. Recent responsibilities include cementitious material for HLW tank closure, nuclear waste tank cleaning, isolation and closure.

Contributions: Primary development of grout section and related information on cementitious material.

FLACH, GREGORY, Savannah River National Laboratory

Ph D. Mechanical Engineering – North Carolina State University
M.S. Mechanical Engineering - North Carolina State University
B.S. Mechanical Engineering – University of Kentucky

Experience: Dr. Flach is a Fellow Engineer at SRNL with 18 years of experience related to groundwater hydrology, computational simulation, and numerical code development. He has been the principal investigator on a number of groundwater modeling studies at SRS involving regional and local scale hydrology, contaminant migration from waste sites, and evaluation of environmental cleanup alternatives. Over the last decade his efforts have focused on PA and composite analysis related projects, and research involving dual-domain formulations of contaminant transport.

Contributions: Dr. Flach is one of the principal modeling investigators focusing on the PORFLOW modeling of groundwater pathways.

JORDAN, JEFFREY, Savannah River National Laboratory

M.S. Mechanical Engineering – Georgia Institute of Technology
B.S. Physics – Furman University
B.A. History – Furman University

Experience: Jeff is a Senior Engineer at SRNL. He has an M.S. in Mechanical Engineering with a concentration in computational simulation. He has several years of experience with computational modeling of engineered systems.

Contributions: Focused on developing and evaluating the vadose zone PORFLOW models.

LAYTON, MARK, WSRC/ Site Regulatory Integration and Planning

B.S. Nuclear Engineering – University of Cincinnati

Experience: Mr. Layton has over 17 years experience at SRS in various regulatory compliance organizations. The majority of this time was spent working on HLW regulatory compliance assignments and supporting various Safety Basis activities. Mr. Layton also provided safety basis support for numerous other facilities at SRS and across the DOE complex, including Sandia, Pantex, and Oak Ridge.

Contributions: Primary technical author and modeling coordinator of the PA and provided support to the GoldSim modeling.

MARTIN, BRUCE, WSRC/ Site Regulatory Integration and Planning

B.S. Mechanical Engineering – United States Military Academy

Experience: Mr. Martin has over 19 years experience at SRS in various organizations including project management, maintenance, and project and design authority engineering. Recent responsibilities have been associated with nuclear waste tank cleaning, isolation and closure under state and federal regulatory compliance programs.

Contributions: Author of sections related to residual tank farm inventory.

NEWMAN, JEFF, WSRC/ Site Regulatory Integration and Planning

M.S. Public Health - University of South Carolina
B.S Kutztown University – Public Administration

Experience: Mr. Newman has responsibility for regulatory compliance of high-level radioactive tank system closures. He was a primary author and the regulatory lead in obtaining approval for closure of the first high level radioactive waste tanks (SRS Tanks 17 and 20) in the United States DOE complex. Mr. Newman has 30 years of environmental experience with a broad background in regulatory interpretation and compliance. Mr. Newman formerly held a position in the Enforcement Section of the Bureau of Wastewater at the SCDHEC.

Contributions: Provided assistance as overall technical reviewer.

ROSENBERGER, KENT, WSRC/ Site Regulatory Integration and Planning

B.S. Nuclear Engineering – Pennsylvania State University

Experience: Mr. Rosenberger has 17 years of experience at the SRS primarily in the area of radiological controls. He has spent the last 3 years supporting tank closure and Saltstone regulatory documents including 3116 Waste Determination and performance objectives development. He previously has held positions in radiological engineering project and operations support and facility operational radiological control management. Mr. Rosenberger has considerable experience with the SRS HLW processes and facilities, in addition to experience with reactor, chemical separations, plutonium processing and storage, and laboratory facilities.

Contributions: Provided overall technical review and management assistance.

SHEPPARD, RICHARD, WSRC/ Site Regulatory Integration and Planning

M.S. Nuclear Science – University of Michigan
B.S. Mathematics – Michigan Technological University

Experience: Mr. Sheppard has 31 years experience within the Nuclear Industry with 14 years at the SRS and 17 years in the commercial nuclear industry. During his period of commercial nuclear industry experience his emphasis was on accident analyses and dose assessments for various commercial nuclear power plants and regulatory and licensing activities associated with construction and operation. During his period at SRS, Mr. Sheppard coordinated hazard and safety analyses for design projects at various SRS nuclear facilities. He has spent the past two years supporting the WD efforts associated with the Saltstone and the closure of waste Tanks 18 and 19.

Contributions: Conducted data verification for the development of the PA and input to PORFLOW and GoldSim computer simulations.

TAYLOR, GLENN, Savannah River National Laboratory

M.S. Mechanical Engineering – University of Texas at Austin
B.S. Engineering Physics – University of Louisville

Experience: Mr. Taylor has 28 years of experience in code development, modeling, and research. His primary emphasis has been non-equilibrium thermal-hydraulics and chemical process methods development and modeling. He has been involved with Probabilistic Risk Assessment-type analyses since the mid-1980s. He has been doing groundwater modeling and contaminant transport modeling for the past 3 years.

Contributions: One of the principal investigators that performed the GoldSim groundwater pathway transport. Glenn also provided technical oversight of the sensitivity and uncertainty analyses provided by Neptune and Company and the dose calculator provided by SRNL staff.

The editor would also like to acknowledge the following personnel for their contributions:

- Engineering support personnel responsible for document management, which included: the development, design, configuration management, graphics development, comment incorporation, production/publication, literature searches, editorial and consistency reviews:

Connie Dyer
Dorinda Fletcher

- Professional Engineers and Scientists who conducted FTF PA reviews, and/or contributed valuable resources, information, or technical data:

  Savannah River National Laboratory Technical Reviewer:
  Roger Seitz

  Portage Environmental Technical Reviewers:
  Nick Stanisich
  David Thorne

  Neptune and Company Technical Reviewer:
  Dr. John Tauxe– Senior Research Scientist

  SRS Site Personnel:

Kenneth Dixon	Karthik Submaranian	Margaret Millings	Patricia Lee
Christine Langton	Miles Denham	Len Collard	Tad Whiteside
Mark Phifer	Dan Kaplan	Robert Swingle	Larry Hamm
Sebastian Aleman	Bill Jones	Cathy Lewis	Dave Noffsinger
Bruce Wiersma	Eduarto Farfan	Elmer Wilhite	Amitava Ganguly

- Management personnel:

Virginia Dickert
Steve Thomas
Tom Robinson
Heather Burns
Ed Stevens

10.0 REFERENCES

Note 1: Reference numbers with an –OUO designator have been classified as: ***"Official Use Only, Exemption 2 -- Not Releasable to the Public or Foreign Nationals without prior approval from DOE-SR"*** by the WSRC Computer and Information Security (C&IS), Safeguards, Security & Emergency Services (SS&ES) Department.

Note 2: References identified as (Copyright) were used in the development of this FTF PA, but are protected by copyright laws. No part of the publication may be reproduced in any form or by any means, including photocopying or electronic transmittal in any form by any means, without permission in writing from the copyright owner.

02224-01-R, *Excavation and Backfill, Engineering Requirements*, Savannah River Site, Aiken, SC, Rev. 1, August 19, 1994.

10 CFR 50, Regulatory Guide 1.109, *Calculation of Annual Doses to Man From Routine Releases of Reactor Effluents for the Purpose of Evaluating Compliance with 10 CFR 50, Appendix I*, U. S. Nuclear Regulatory Commission, Washington, D.C., Rev. 1, October 1977.

10 CFR 61, *Licensing Requirements for Land Disposal of Radioactive Waste*, U. S. Code of Federal Regulations, Nuclear Regulatory Commission, Washington, D.C., November 18, 2005.

10 CFR 830, *Nuclear Safety Management*, U. S. Code of Federal Regulations, Nuclear Regulatory Commission, Washington, D.C., January 2005.

1Q Manual, *Quality Assurance Manual*, Savannah River Site, Aiken, SC, Rev. 4, Dec. 15, 2004.

40 CFR 141, *Protection of Environment, National Primary Drinking Water Regulations,* U. S. Nuclear Regulatory Commission, Washington, D.C., Rev. 05-16-07, May 16, 2007.

40 CFR 143, *National Secondary Drinking Water Regulations,* U.S. Nuclear Regulatory Commission, Washington, D.C., July 1, 2003.

40 CFR 61, Subpart H, *National Emission Standards for Emissions of Radionuclides other than Radon from Department of Energy Facilities*, Environmental Protection Agency, Washington D.C., May 6, 2008.

ACRi-1994, *Analytic & Computational Research, Inc, PORFLOW Validation*, Version. 2.5, Analytic and Computational Research, Inc., Bel Air, CA, March 31, 1994.

ACRi-2002, *Analytic & Computational Research, Inc. PORFLOW User's Manual,* Version 5.0, Analytic and Computational Research, Inc., Bel Air, CA, March 25, 2002.

ANL-EAD-4, Yu, C., et al., *User's Manual for RESRAD Version 6*, Argonne National Laboratory, Chicago, IL, July 2001.

ANL-EAIS-8, Yu, C., et al., *Data Collection Handbook to Support Modeling the Impacts of Radioactive Material in Soil*, Argonne National Laboratory, Chicago, IL, April 1993.

ASME NQA-1-2004 (Copyright), *Quality Assurance Program Requirements for Nuclear Facilities/with Addenda*, An American National Standard, The American Society of Mechanical Engineers, New York, NY, Rev. 2000, December 22, 2004.

ASME NQA-1a-2005 (Copyright), *Addenda to ASME NAQ-1-2004, Quality Assurance Program Requirements for Nuclear Facilities/with Addenda*, An American National Standard, The American Society of Mechanical Engineers, New York, NY, May 3, 2006.

ASME NQA-1b-2007 (Copyright), *Addenda to ASME NAQ-1-2004, Quality Assurance Program Requirements for Nuclear Facilities/with Addenda*, An American National Standard, The American Society of Mechanical Engineers, New York, NY, June 1, 2007.

ASTM A 106-A 106M (Copyright), *Standard Specification for Seamless Carbon Steel Pipe for High-Temperature Service,* ASTM International, West Conshohocken, PA, Rev. A, October 2006.

ASTM A 53-A53M-07 (Copyright), *Standard Specific for Pipe, Steel, Black and Hot-Dipped, Zinc-Coated, Welded and Seamless*, ASTM International, West Conshohocken, PA. September 2007.

ASTM A285-A285M-03 (Copyright), *Standard Specification for Pressure Vessel Plates, Carbon Steel, Low – and Intermediate –Tensile Strength* Vol. 01.04, ASTM International, West Conshohocken, PA, September 10, 2003.

ASTM A516-A516M-06 (Copyright), *Standard Specification for Pressure Vessel Plates, Carbon Steel, for Moderate-and Lower-Temperature Service*, Vol. 01.04, ASTM International, West Conshohocken, PA, March 1, 2006.

ASTM A537-A537M-06 (Copyright), *Standard Specification for Pressure Vessel Plates, Heat-Treated, Carbon-Manganese-Silicon Steel*, Vol. 01.04, ASTM International, West Conshohocken, PA, March 1, 2006.

ASTM D 1586-99 (Copyright), *Standard Test Method for Penetration Test and Split-Barrel Sampling of Soils*, ASTM International, West Conshohocken, PA, January 1999.

ASTM D 6092-97 (Copyright), *Guide for Specifying Standard Sizes of Stone for Erosion Control*, ASTM International, West Conshohocken, PA, 2003.

ASTM D 6103-04 (Copyright), *Standard Test Method for Flow Consistency of Controlled Low Strength Material (CLSM),* ASTM International, West Conshohocken, PA, November 2004.

BPF-212512-Sh 1, *Pump Tank*, Industrial Alloy Fabricators, Inc., Rev. A, July 22, 1976.

B-SQP-H-00041, Bui, H., *Closure Business Unit LWDP Waste Characterization System Software Quality Assurance Plan,* Savannah River Site, Aiken, SC, Rev. 2, June 2007.

CAP-88, Beres, D. A., *The Clean Air Act Assessment Package – 1988 (CAP-88) A Dose and Risk Assessment Methodology for Radionuclide Emissions to Air Volume 1 User's Manual*, U.S. Environmental Protection Agency, Washington, D.C., October 1990.

CBU-LTS-2004-00078, Dixon, E. N., Ph.D., *Characterization of Residual Waste Remaining in 242-F Evaporator System,* Savannah River Site, Aiken, SC, SUPERSEDED Rev. 0, July 12, 2005.

CBU-PIT-2004-00010, Martin, B. A., *Tanks 17 and 20 Closure Errata,* Savannah River Site, Aiken, SC, Rev. 0, December 17, 2004.

CBU-PIT-2005-00040, Hutchens, G. J., *Estimate of Actinide Concentration by Radioactive Decay,* Savannah River Site, Aiken, SC, Rev. 0, March 15, 2005.

CBU-PIT-2005-00099, Hamm, B. A., *Tank Farm Zeolite Historical Review and Current Inventory Assessment,* Savannah River Site, Aiken, SC, Rev. 0, June 10, 2005.

CBU-PIT-2005-00120, Caldwell, T. B., *Ancillary Equipment Residual Radioactivity Estimate To Support Tank Closure Activities for F-Tank Farm,* Savannah River Site, Aiken, SC, Rev. 0, June 16, 2006.

CBU-PIT-2005-00146, Rosenberger, K., et al., *Saltstone Performance Objective Demonstration Document,* Savannah River Site, Aiken, SC, Rev. 0, June 16, 2005.

CBU-PIT-2005-00228, Hamm, B. A., *Savannah River Site High-Level-Waste Tank Farm Closure Radionuclide Screening Process (First-Level) Development and Application,* Savannah River Site, Aiken, SC, Rev. 0, November 7, 2006.

CBU-PIT-2006-00013, Smith, S. A., *3116 Determination Scoping Document for the 242-F Evaporator System and Tanks 17 – 20 Related Transfer Lines,* Savannah River Site, Aiken, SC, Rev. 0, January 24, 2006.

C-CLC-G-00364, Phillips, J. J., *Type I and II Tank Cooling Coil to Tank Volume Ratios and Area Ratios,* Calculation, Savannah River Site, Aiken, SC, Rev. 0, March 2, 2007.

CDC-2005, *Risk Based Screening of Radionuclide Releases from the Savannah River Site,* Center for Disease Control, Atlanta, GA, Rev. 1, March 2005.

C-ESR-F-00043, Wiersma, B., *Calculation of the Amount of Corrosion Product on the Wall of Tank 19,* Savannah River National Laboratory, Aiken, SC, Rev. 0, November 15, 2007.

C-SPP-F-00047, Huizenga, D. J., *F Tank Farm, Tank 18F and Tank 19F, Furnishing and Delivery of Tank Closure Mixes,* Savannah River Site, Aiken, SC, Rev. 2, April 2003.

D116001, *Savannah River Plant, 200 Area Building 241-F&H Bottom Cooling Coils for Waste Storage Tank,* Savannah River Operations Office, Aiken, SC, Rev. 10, July 21, 1955.

D116048, *Savannah River Plant, 200 Area Building 241-F&H Vertical Cooling Coils for Waste Storage Tank,* Savannah River Operations Office, Aiken, SC, Rev. 37, September 8, 1955.

D116850, *Pump Tank 12' Diameter X 8' 6",* Savannah River Operations Office, Aiken, SC, Rev. 24, December 4, 1985.

D146352, *Diversion Box #3, Detail Sheet 1,* Savannah River Operations Office, Aiken, SC, Rev. 47, June 7, 1979.

D181085, *Building 241-H Tank 4, 5, 6, 7, & 8 Waste Transfer Facilities Valve Box*, Savannah River Operations Office, Aiken, SC, Rev. 59, December 13, 2000.

D187892, *Waste Transfer Facilities Valve Box Details, Tank 4, 5, 6, 7 & 8*, Savannah River Operations Office, Aiken, SC, Rev. 20, October 12, 2000.

D199421, *Salt Removal Type III Phase 1 Single Valve Box Details, Sheet 1*, Savannah River Operations Office, Aiken, SC, Rev. 23, March 22, 1991.

D199424, *Salt Removal Type III, Phase 1 Three Valve, Valve Box Plan, Sheet 1,* Savannah River Operations Office, Aiken, SC, Rev. 31, June 7, 2006.

D199425, *Salt Removal Type III, Phase 1 Single Valve Box Details, Sheet 5*, Savannah River Operations Office, Aiken, SC, Rev. 26, February 2, 1988.

D199430, *Salt Removal Type III, Phase 1 Three Valve Valve Box, Sheet 2*, Savannah River Operations Office, Aiken, SC, Rev. 22, May 26, 1988.

DOE Format Guide_OUO, DRAFT *Format and Content Guide for U.S. Department of Energy Low-Level Waste Disposal Facility Performance Assessments and Composite Analyses*, U.S. Department of Energy, Washington, D.C., Rev. 1, May 11, 2007. (Draft Document - Not Approved for Public Release)

DOE M 435.1-1, *Radioactive Waste Management Manual,* Chg. 1, U.S. Department of Energy, Washington, D.C., June 2001.

DOE O 414.1B, *Quality Assurance*, U.S. Department of Energy, Washington, D.C., April 29, 2006.

DOE O 435.1, *Radioactive Waste Management*, Chg. 1, U.S. Department of Energy, Washington, D.C., August 28, 2001.

DOE O 5400.5, *Radiation Protection of the Public and the Environment*, Chg. 2, Department of Energy, Washington, D.C., January 1993.

DOE_02-09-2006, Rispoli, J. A., *Compliance with DOE M 435.1-1 Waste Incidental to Reprocessing Requirements and Implementation of Section 3116(a) of the National Defense Authorization Act for Fiscal Year 2005 (NDAA)*, Department of Energy, Washington, D.C., Rev. 0, February 9, 2006.

DOE-EIS-0303 ROD, *High Level Waste Tank Closure Final Environmental Impact Statement Record of Decision*, Savannah River Operations Office, Aiken, SC, Rev. 0, August 19, 2002.

DOE-EIS-0303, *High-Level Waste Tank Closure Final Environmental Impact Statement*, Savannah River Site, Aiken, SC, Rev. 0, May 2002.

DOE-ID-10966, *Performance Assessment for the Tank Farm Facility at the Idaho National Engineering Environmental Laboratory, Final*, Idaho National Laboratory, Idaho Falls, ID, Rev. 1, April 2003.

DP-478, Daniel, A. N., *Underground Storage of Low Level Radioactive Wastes at the Savannah River Site,* Engineering Considerations, Atomic Energy Department, Wilmington, DE, Rev. 0, June 1960.

DPSP-80-17-23, West, B., *Tank 16 Demonstration – Water Wash and Chemical Cleaning Results*, Savannah River Site, Aiken, SC, Rev. 0, December 16, 1980.

DPSPU-82-11-10_OUO, McNatt, F. G., *History of Waste Tank 20, 1959 through 1974,* Savannah River Plant, Aiken, SC, Rev. 0, July 1982.

DPST-80-424, Granaghan, J. T., *Analysis of Tank 20 Salt Cake,* Savannah River Site, Aiken, SC, Rev. 0, June 16, 1980.

DPST-81-441, Fowler, J., *Radiochemical Analyses of Samples from Tank 16 Cleanout*, Savannah River Site, Aiken, SC, Rev. 0, May 18, 1981.

EPA-402-R-93-081, *Federal Guidance Report No. 12, External Exposure to Radionuclides in Air, Water, and Soil*, Environmental Protection Agency, Washington, D.C., September 1993.

EPA-402-R-99-001, *Federal Guidance Report No. 13, Cancer Risk Coefficients for Environmental Exposure to Radionuclides,* Environmental Protection Agency, Washington, D.C., September 1999.

EPA-520-1-88-020, *Federal Guidance Report No. 11, Limiting Values of Radionuclide Intake and Air Concentration and Dose Conversion Factors for Inhalation, Submersion and Ingestion*, Environmental Protection Agency, Washington, D.C., September 1988.

EPA-600-2-87-049, Schroeder, P. R., Payton, R. L, *Verification of the Lateral Drainage Component of the HELP Modeling Using Physical Models*, Hazardous Waste Engineering Research Laboratory, Cincinnati, OH, July 1987.

EPA-600-2-87-050, Schroeder, P. R.,et al., *Verification of the Hydrologic Evaluation of Landfill Performance (HELP) Model Using Field Data*, Hazardous Waste Engineering Research Laboratory, Cincinnati, OH, July 1987.

EPA-600-P-95-002, *Exposure Factors Handbook*, U.S. National Center for Environmental Assessment, Environmental Protection Agency, Washington, D.C., August 1997.

EPA-600-R-94-168a, Schroeder, P. R., et al., *The Hydrologic Evaluation of Landfill Performance (HELP) Model: User's Guide for Version 3,* Hazardous Waste Engineering Research Laboratory, Cincinnati, OH, September 1994.

EPA-600-R-94-168b, Schroeder, P. R., et al., *The Hydrologic Evaluation of Landfill Performance (HELP) Model: Engineering Documentation for Version 3,* Hazardous Waste Engineering Research Laboratory, Cincinnati, OH, September 1994.

EPA-822-R-00-001, *Estimated Per Capita Water Ingestion and Body Weight in the United States – An Update, Based on data Collected by the United States Department of Agrilculture's 1994 – 1996 and 1998 Continuing Survey of Food Intakes by Individuals*, Environmental Protection Agency, Washington, D.C., Rev. 0, October 2004.

ERD-AG-003, *Environmental Restoration Division Regulatory Document Handbook, Evaluating Hydrogeological and Hydrochemical P.8.1 Data for Groundwater Modeling*, Savannah River Site, Aiken, SC, Rev. 9, December 1998.

G-SQA-A-00011, Swingle, R., *Software Quality Assurance Plan for GoldSim*, Savannah River National Laboratory, Aiken, SC, Rev. 0, August 2006.

GTG-2006a, *GoldSim User's Guide, Version 9.20. Volumes 1 & 2*, GoldSim Technology Group LLC. Issaquah, WA, Rev. 0, January 2006.

GTG-2006b, *Verification Plan: GoldSim Version 9.21*, GoldSim Technology Group LLC, Issaquah, WA, Rev. 0, April 2006.

G-TR-G-00002, Whiteside, T., *Software Testing and Verification for PORFLOW Version 6.10.3*, Savannah River National Laboratory, Aiken, SC, Rev. 0, October 2007.

HLW-STE-99-0023, Caldwell, T. B., *Tank 8F Waste Removal: Pump Tank Concentrations During Dilution Operations,* Savannah River Site, Aiken, SC, Rev. 0, January 27, 1999.

HNF-SA-3181-FP, Barney, G. S., Delegard, C. H., *Chemical Species of Plutonium in Hanford Radioactive Tank Waste*, Pacific Northwest National Laboratories, Richland, WA, Rev. 0, March 1997.

http://el.erdc.usace.army.mil/products.cfm?Topic=model&Type=landfill, *Hydrologic Evaluation of Landfill Performance (HELP)*: Computer Program for Landfill Confined Disposal Facility (CDF) Design, Version 3.

http://en.wikipedia.org/wiki/Geometric_mean, Geometric Mean, Wikipedia.

http://epa-prgs.ornl.gov/radionuclides/, *Preliminary Remediation Goals for Radionuclides* Information Homepage.

http://epw.senate.gov/water.pdf, *Clean Water Act* (original title: Federal Water Pollution Control Amendments of 1972, [As amended through P.L. 107-303, November 27, 2002], 33 U.S.C. 1251 et seq., U.S. Environmental Protection Agency.

http://factfinder.census.gov/home/saff/main.html?_lang=en, *Population Estimates*, American Fact Finder, U.S. Census Bureau. 2007.

http://www.access.gpo.gov/uscode/title42/chapter103_.html, *Comprehensive Environmental Response, Compensation, and Liability Act (CERCLA) of 1980*, Title 42, United States Code (U.S.C.) §§ 9601 et seq., as amended by the Superfund Amendments and Reauthorization Act of 1986, Pub. L. 99-499, U.S. Environmental Protection Agency.

http://www.acricfd.com/software/porflow/, *Computational Fluid Dynamics (CFD) tool by Analytic & Computational Research, Inc.* (software demo download and purchasing information).

http://www.epa.gov/epaoswer/osw/laws-reg.htm#regs, *Resource Conservation and Recovery Act (RCRA)*, Federal law of the United States contained in Title 42 U.S.C. §§6901-6992k, enacted in 1976.

http://www.epa.gov/radiation/heast.html *Radionuclide Carcinogenicity Slope Factors: HEAST*, U.S. Environmental Protection Agency.

http://www.epa.gov/region09/waste/sfund/prg/index.html, *Preliminary Remediation Goals*, Region 9, Superfund Homepage, U.S. Environmental Protection Agency.

http://www.epa.gov/safewater/sdwa/index.html, *Federal Safe Drinking Water Act*, United States Environmental Protection Agency, Washington, D.C.

http:/www.goldsim.com, *GoldSim Technology Group Home Page.*

IAEA-364 (Copyright), *Handbook of Parameter Values for the Prediction of Radionuclide Transfer in Template Environments, Produced in Collaboration with the International Union of Radioecologists, International Atomic Energy Agency, Technical Reports Series 364*, International Atomic Energy Agency, Vienna, July 29, 1957.

ICRP-72 (Copyright), *Radiation Protection: ICRP Publication 72 – Age-Dependent Doses to Members of the Public from Intake of Radionuclides: Part 5 Compilation of Ingestion and Inhalation Dose Coefficients*, International Commission on Radiological Protection, Didcot, Oxfordshire, September 1995.

ISSN 0017-9078 Vol. 62 No. 2, Hamby, D. M., *Site-Specific Parameter Values for the Nuclear Regulatory Commission's Food Pathway Dose Model*, Health Physics Radiation Protection Journal, Charleston, SC, Rev. 0, February 1992.

ISSN 0885-6125 Vol. 24 No. 2, Breiman, L., *Bagging Predicators*, Machine Learning, Springer Netherlands, Rev. 0, August 1994.

ISSN 0885-6125 Vol. 40 No. 2, Dietterich, T. G., *An Experimental Comparison of Three Methods for Constructing Ensembles of Decision Trees: Bagging, Boosting, and Randomization*, Machine Learning, Vol. 40, No. 2 Springer Netherlands, Rev. 0, 2000.

ISSN 1019-0643, Bradbury, M. H. and Sarott, F., *Sorption Databases for the Cementitious Near-Field of a L/ILW Repository for Performance Assessment*, Paul Scherrer Institut, Labor für Entsorgung, Villigen PSI, Switzerland, Rev. 0, March 1995.

K-CLC-F-00073, William, T. L., *Static Settlement of F-Area Waste Storage Tanks 18 and 19,* Calculation, Savannah River Site, Aiken, SC, Rev. 2, June 20, 2006.

K-CLC-G-00077, Martinson, D., *Radionuclide Preliminary Remediation Goals (RAD PRGs),* Engineering Calculation Sheet, Savannah River Site, Aiken, SC, Rev. 1, July 24, 2003.

LWO-LWE-2007-00104, Baughman, T. C., *Tanks 5 & 6 Closure Sequence of Events*, Savannah River Site, Aiken, SC, Rev. 1, October 17, 2007.

LWO-PIT-2006-00066, Vemulapalli, R., *Tanks 5 and 6 Oxalic Acid Aided Heel Removal Flowsheet,* Savannah River Site, Aiken, SC, Rev. 2, December 10, 2007.

LWO-PIT-2006-00069, Tran, H. Q., *Projected F-Tanks Radionuclide Concentrations at Closure,* Savannah River Site, Aiken, SC, Rev. 0, April 17, 2007.

LWO-PIT-2007-00025, Hill, P. J., *Response to the NRC's Request for Additional Information Comment #15,* Savannah River Site, Aiken, SC, Rev. 0, March 6, 2007.

LWO-PIT-2007-00045, Tran, H. Q., *Projected F-Tanks Chemical Concentrations at Closure,* Savannah River Site, Aiken, SC, Rev. 0, April 17, 2007.

LWO-PIT-2007-00062, Chew, D. P., et al., *Life-Cycle Liquid Waste Disposition System Plan: An Integrated System at the Savannah River Site*, Savannah River Site, Aiken, SC, Rev. 14, October 2007.

M-CLC-H-02820, Wong, H., *Volume and Surface Area Percentages of the Cooling Coils in Type III and Type IIIA Tanks,* Calculation, Savannah River Site, Aiken, SC, Rev. 0, April 17, 2007.

ML071550458, Camper, L. W. (NRC) to Marcinowski, F. (DOE), *Enhanced Consultation Process for Waste Determination activities conducted under the Ronald W. Reagan National Defense Authorization Act for Fiscal Year 2005*, U.S. Department of Energy, Washington, D.C., Rev. 0, June 15, 2007.

M-M6-F-3289, *F-Area Old Hill Valve Boxes Waste Transfer System P&ID Drawing*, Savannah River Site, Aiken, SC, Rev. 14, March 5, 2008.

NCRP-123 (Copyright), *Screening Models for Releases of Radionuclides to Atmosphere, Surface Water, And Ground, Vol. I and II*, National Council on Radiation Protection and Measurements, Bethesda, MD, January 22, 1996.

NDAA_3116, Public Law 108-375, *Ronald W. Reagan National Defense Authorization Act for Fiscal Year 2005",* Section 3116, *Defense Site Acceleration Completion*, Department of Energy, Washington, D.C., October 28, 2004.

NRMP-2005, *Natural Resources Management Plan (NRMP) for the Savannah River Site,* Department of Agriculture & Forestry Service, Savannah River Site, Aiken SC, Rev. 0, May 2005.

NUREG-0782, *Draft Environmental Impact Statement on 10 CFR Part 61" Licensing Requirements for Land Disposal of Radioactive Waste"*, U.S. Nuclear Regulatory Commission, Washington, D.C., April 2006.

NUREG-0945, *Final Environmental Impact Statement on 10 CFR 61 "Licensing Requirements for Land Disposal of Radioactive Waste", Summary and Main Report, Vol. 1*, U.S. Nuclear Regulatory Commission, Washington, D.C., November 2005.

NUREG-1573, *A Performance Assessment Methodology for Low-Level Radioactive Waste Disposal Facilities*, U.S. Nuclear Regulatory Commission, Washington, D.C., March 2005.

NUREG-1623, Johnson, T.L., *Design of Erosion Protection for Long-Term Stabilization*, Nuclear Regulatory Commission, Washington, D.C., September 2002.

NUREG-1854, *NRC Staff Guidance for Activities Related to U.S. Department of Energy Waste Determinations, Draft Final Report for Interim Use*, U.S. Nuclear Regulatory Commission, Washington, D.C., August 2007.

NUREG-CR-1759, Clancy, J. J., Gray, D. F., and Oztunali, O. I., *Data Base for Radioactive Waste Management - Impacts Analyses Methodology Report, Vol. 1, 2 & 3*, Nuclear Regulatory Commission, Washington, D.C., August 1981.

NUREG-CR-3620, (PNL-4054), *Intruder Dose Pathway Analysis for the Onsite Disposal of Radioactive Wastes: The ONSTIE MAXI1 Computer Program*, U.S. Nuclear Regulatory Commission, Washington, D.C., October 1984.

NUREG-CR-5512, (PNL-7994), Kennedy, W. E., Jr., et al., *Residual Radioactive Contamination From Decommissioning, Technical Basis for Translating Contamination Levels to Annual Total Effective Dose Equivalent, Final Report, Vol. 1*, Pacific Northwest Laboratory, Richland, WA, October 1992.

ORNL-5786, Baes, C. F., III, et al., *A Review and Analysis of Parameters for Assessing Transport of Environmentally Released Radionuclides through Agriculture*, Oak Ridge National Laboratory, Oak Ridge, TN, Rev. 0, September 1984.

OSWER 9380.3-06FS, A *Guide to Principal Threat and Low Level Threat Wastes*, U. S. Environmental Protection Agency, Washington, D.C., November 1991.

PIT-MISC-0002_OUO, *Industrial Wastewater Closure Module for the High-Level Waste Tank 20 System,* Savannah River Site, Aiken, SC, Rev. 1, January 8, 1997.

PIT-MISC-0004, *Industrial Wastewater Closure Module for the High-Level Waste Tank 17 System,* Savannah River Site, Aiken, SC, Rev. 2, August 26, 1997.

PIT-MISC-0041_OUO, *Discussion Draft, SRS Long Range Comprehensive Plan*, Savannah River Site, Aiken, SC, Rev. 0, December 2000.

PIT-MISC-0054, Kane, W. F., *Savannah River Site High Level Waste Tank Closure: Classification of Residual Waste as Incidental,* Nuclear Regulatory Commission, Washington, D.C., Rev. 0, June 30, 2000.

PIT-MISC-0072, Tuli, J. K., *Nuclear Wallet Cards*, *Seventh Edition*, National Nuclear Data Center, Brookhaven National Laboratory, Upton, NY, April 2005.

PIT-MISC-0089_OUO, *Savannah River Site End State Vision*, Savannah River Site, Aiken, SC, July 26, 2005.

PIT-MISC-0091, *U.S. Nuclear Regulatory Commission Review of the Department of Energy at Savannah River High-Level Waste Tank Closure Methodology,* Nuclear Regulatory Commission, Washington, D.C., Rev. 0, June 2000.

PIT-MISC-0104, *Soil Survey of Savannah River Plant Area, Parts of Aiken, Barnwell, and Allendale counties, South Carolina,* U.S. Department of Agriculture, Columbia, SC, Rev. 0, June 1990.

PIT-MISC-0108, *South Carolina Pollution Control Act*, South Carolina Code Ann., Section 48-1-10, et seq., South Carolina Legislative Council, Columbia, SC, 2004.

PIT-MISC-0109, Chapman, J. W., *Partial Permit to Operate F and H Area High Level Radioactive Waste Tank Farms Construction Permit No.: 17,424-IW,* South Carolina Department of Health and Environmental Control, Columbia, SC, Rev. 0, March 3, 1993.

PIT-MISC-0112, Aadland, R., et al., *Hydrogeologic Framework of West-Central Savannah River Area, South Carolina and Georgia, Report 5,* South Carolina Department of Natural Resources, Columbia, SC, Rev. 0, 1995.

PNNL-13421, Staven, L. H., et al., *A Compendium of Transfer Factors for Agricultural and Animal Products.*, Pacific Northwest Laboratory, Richland, WA, Rev. 0, June 2003.

Q-SQA-A-00005, Phifer, M. A., *Software Quality Assurance Plan for the Hydrologic Evaluation of Landfill Performance (HELP) Model,* Savannah River National Laboratory, Aiken, SC, Rev. 0, October 2006.

Q-SQP-A-00002, Jannik, G. T., *Software Quality Assurance Plan for Environmental Dosimetry,* Savannah River National Laboratory, Aiken, SC, Rev. 1, September 2006.

Q-SQP-G-00003, Flach, G., *Software Quality Assurance Plan for Aquifer Model Refinement Tool (MESH3D),* Savannah River National Laboratory, Aiken, SC, Rev. 0, February 2007.

SB-10-U, *Concrete Floor Finishing and Types of Finish,* Concrete Standard Engineering Specification, Savannah River Site, Aiken, SC, November 1983.

SB-5-A, *Building Materials, Concrete, Laboratory and Testing,* Standard Engineering Specifications, Savannah River Site, Aiken, SC, 24, Rev. 0, May 1949.

SB-6-A, *Building Materials, Concrete, Proportioning, Batching and Mixing,* Standard Engineering Specifications, Savannah River Site, Aiken, SC, December 1951.

SB-9-U, *Placing Concrete,* Concrete Standard Engineering Specification, Savannah River Site, Aiken, SC, April 1984.

SC-4-E, Fill, *Standard Compaction,* Civil Standard Engineering Specification, Savannah River Site, Aiken, SC, November 1983.

SC-5-E, *Fill, Test-Controlled Compaction,* Civil Standard Engineering Specification, Savannah River Site, Aiken, SC, August 1987.

SCDHEC_R.61-58, *State Primary Drinking Water Regulation,* South Carolina, Department Of Health and Environmental Control, Columbia, SC, October 27, 2006.

SCDHEC_R.61-67, *Standards for Wastewater Facility Construction,* South Carolina, Department Of Health and Environmental Control, Columbia, SC, May 24, 2002.

Spec-3019, Christy, W. O., *Supplement No. 4 to Project Specification 3019: Building Materials and Plumbing,* Savannah River Site, Aiken, SC, Rev. 0, May 5, 1960.

Spec-3206_OUO, *Specifications for Waste Disposal Tanks Buildings 241F and 241H,* Savannah River Site, Aiken, SC, Rev. 7, March 13, 1953.

Spec-3552, Endriss, R. J., *Specification No. 3552 for 1,300,000 Gal. Capacity Waste Storage Tanks, 200 Area – Bldg. 241-F,* Savannah River Site, Aiken, SC, Rev. 0, September 27, 1957.

Spec-6797, *Specification 6797: Primary and Secondary Steel Liner Tanks for Project 9S1493, Waste Storage Tanks, 200 Area – Bldg. 241-14F, Savannah River Plant,* Savannah River Site, Aiken, SC, Rev. 0, April 28, 1976.

Spec-7100, *Specification 7100: Primary and Secondary Steel Tanks for Project 9S1747, Waste Storage Tanks, 200 Area – Bldg. 241-54F, Savannah River Plant,* Savannah River Site, Aiken, SC, Rev. 32, March 14, 1977.

SRNL-ESB-2007-00001, Millings, M., et al., *Summary of the Quality Review Process for General Separations Area Aquifer Model Database*, Savannah River National Laboratory, Aiken, SC, Rev. 0, January 2007.

SRNL-ESB-2007-00008_OUO, Jones, W., et al., *F-Area Tank Farm Vadose Zone Material Property Recommendations,* Savannah River National Laboratory, Savannah River Site, Aiken, SC, Rev. 0, February 27, 2007.

SRNL-ESB-2007-00034, Phifer, M. A., et al., *Recommended Effective Diffusion Coefficient for FTF Base Mat Surrogate and Tank Grouts*, Savannah River National Laboratory, Aiken, SC, Rev. 0, October 18, 2007.

SRNL-ESB-2007-00035, Millings, M., et al., *Addendum to Integrated Hydrogeological Modeling Report of the General Separations Area (GSA),* Savannah River National Laboratory, Aiken, SC, Rev. 0, October 14, 2007.

SRNL-RPA-2007-00006, Kaplan, D., *Distribution Coefficients for Various Elements of Concern to the Tank Waste Performance Assessment*, Savannah River National Laboratory, Aiken, SC, Rev. 0, July 10, 2007.

SRNL-SCS-2007-00011, Shine, G., *Preliminary Guidance for the Distribution of Cs, SR, and U Geochemical Input Terms to Stochastic Transport Models,* Savannah River National Laboratory, Savannah River Site, Aiken, SC, Rev. 0, April 26, 2007.

SRS-REG-2007-00008, Cloessner, E.A., *Chemical Inventory Comparison (CIC) between the Waste Characterization System (WCS) and Savannah River National Laboratory (SRNL) Reports for Tanks 5, 18 and 19*, Savannah River Site, Aiken, SC, Rev. 0, August 10, 2007.

SRS-REG-2007-00027, Deshpande, R., *Tank Farm Grout and Concrete Degradation*, Savannah River Site, Aiken, SC, Rev. 0, November 19, 2007.

SRS-REG-2007-00029, Birk, M. B., *General Separations Area Well Drilling Probabilities*, Savannah River Site, Aiken, SC, Rev. 0, November 21, 2007.

SRS-REG-2007-00036, *Documentation of Personal Communication Between Kaplan, D. I. to Newman, J. L., September 9, 2007*, Savannah River Site, Aiken, SC, Rev. 0, November 13, 2007.

SRT-ESB-2007-00046, Flach, G., *Design Checks on PORFLOW Modeling to Support the F-Tank Farm PA,* Savannah River National Laboratory, Aiken, SC, Rev. 0, December 11, 2007.

SRT-EST-2003-00134, Jannik, T., *Cesium-137 Bioconcentration Factor for Freshwater Fish in the SRS Environment*, Savannah River National Laboratory, Aiken, SC, Rev. 0, July 15, 2003.

SRT-MTS-2002-20004, Wiersma, B. J., *Calculation of the Amount of Corrosion Product in HLW Tank 19,* Savannah River Site, Aiken, SC, Rev. 1, February 8, 2002.

SRT-WED-2002-00016, Cook, J., *Estimation of the Potential Contamination on Corrosion Products in Tank 19*, Savannah River National Laboratory, Aiken, SC, Rev. 3, April 6, 2005.

SRT-WPT-2005-00049, Cook, J., *Estimation of the Potential Contamination of Corrosion Products in Tank 18,* Savannah River National Laboratory, Aiken, SC, Rev. 0, April 21, 2005.

S-TSR-G-00001, *Concentration, Storage, and Transfer Facilities*, Technical Safety Requirements, Savannah River Site, Aiken, SC, Rev. 19, July 2005.

SW10.6-SVP-5, Section 7.2, *Pressure Testing of Waste Line Jackets,* Savannah River Site, Aiken, SC, Rev. 4, May 30, 2006.

T-CLC-F-00373, Macaraeg, E., *Tanks 18 and 19 Closure Structural Calculation (U),* Calculation, Savannah River Site, Aiken, SC, Rev. 0, May 2006.

T-CLC-F-00421, Carey, S. A., *Structural Assessment of F-Area Tank Farm After Final Closure*, Savannah River Site, Aiken, SC, Rev. 0, December 18, 2007.

U-TR-F-00005, Thomas, J. L., *Characterization of Tank 18 Residual Waste,* Savannah River Site, Aiken, SC, Rev. 2, August 2005.

W145225, *200 Area Waste Storage Tanks – 241 F & H,* Design of Concrete Tank Concrete, Savannah River Site, Aiken, SC, Rev. 4, September 1993.

W145293, *200 Area Waste Storage Tanks 241 F & H, Bottom Slab – Plan, Sections & Details Concrete,* Savannah River Site, Aiken, SC, Rev. 16, August 17, 1989.

W145367, *200 Area Waste Storage Tanks – 241 F & H Steel Pan Plate Details Steel,* Savannah River Site, Aiken, SC, Rev. 1, 1989.

W145379, *200 Area Type I Tanks 1 – 8 and 9 – 12 Waste Storage Tanks 241 F & H 75'-0" Dia. Steel Tank Details, Steel,* Savannah River Site, Aiken, SC, Rev. 4, April 2004.

W145491, *200 Area Waste Storage Tanks 241 F Excavation – Plan & Sections, Civil,* Savannah River Site, Aiken, SC, Rev. 6, July 1951.

W145573, *200 Area Type 1 Tanks 1 – 8 and 9 – 12 Waste Storage Tanks 241-H General Arrangement & Construction Details, Concrete and Steel,* Rev. 29, April 5, 2004.

W146075, *200 Area Building 241-F Encasement of Catch Tank Plan & Sections, Concrete,* Savannah River Site, Aiken, SC, Rev. 28, August 27, 1974.

W146968, *Diversion Box No. 1 General Arrangement & Construction Details*, Savannah River Site, Aiken, SC, Rev. 40, April 30, 1976.

W163941, *200 Area Bldg. 241F Additional Waste Storage Tanks 85'-0" DIA. Steel Tank - Plan & Details Steel,* Savannah River Site, Aiken, SC, Rev. 55, April 21, 1969.

W166430, *200 Area Tanks: 17, 18, 19, & 20 - Plot & Grading Plan,* Savannah River Site, Aiken, SC, Rev. 58, October 28, 1993.

W167477, *Additional Waste Storage Tanks Dome Plan and Details,* Savannah River Site, Aiken, SC, Rev. 21, January 24, 2002.

W167482, *Additional Waste Storage Tanks Bottom Slab Plan & Details,* Savannah River Site, Aiken, SC, Rev. 22, July 3, 1958.

W167486, *Tanks 17 – 20, Type IV, Additional Waste Storage Wall Details, Concrete Rod & Turnbuckle Design*, Savannah River Site, Aiken, SC, Rev. 9, April 26, 2004.

W167801, *Additional Waste Storage Tanks Riser & Plug Details Concrete,* Savannah River Site, Aiken, SC, Rev. 25, March 4, 1983.

W167808, *Additional Waste Storage Tanks General Arrangement and Construction Details*, Savannah River Site, Aiken, SC, Rev. 3, July 3, 1958.

W230843, *Building 242-F Equipment & Piping Arrangement-Plans*, Savannah River Site, Aiken, SC, Rev. 109, October 2, 1991.

W236676, *Inter-Area Waste Transfer Line Pumping Pit, Piping Arrangement*, Savannah River Site, Aiken, SC, Rev. 70, July 11, 2000.

W238154, *Waste Storage Tanks Excavation Plan and Details,* Savannah River Site, Aiken, SC, Rev. 16, December 4, 1969.

W238160, *Cooling Slots Plan and Details*, Savannah River Site, Aiken, SC, Rev. 3, June 9, 1971.

W238161, *Waste Storage Facilities Secondary Liner Plan & Details*, Savannah River Site, Aiken, SC, Rev. 2, February 23, 1971.

W238163_OUO, *Waste Storage Facilities, General Arrangements & Construction*, Savannah River Site, Aiken, SC, Rev. 10, May 15, 1975.

W238167, *Waste Storage Facilities, Wall and Column Sections & Details*, Savannah River Site, Aiken, SC, Rev. 4, December 5, 1969.

W238168, *Waste Storage Facilities Liner Plate Attachments*, Savannah River Site, Aiken, SC, Rev. 26, June 8, 1971.

W238169, *High Level Waste Storage Facilities Base Slab Plan,* Savannah River Site, Aiken, SC, Rev. 2, February 23, 1971.

W238875, *Building 241-11F Waste Storage Tanks Grading Plan*, Savannah River Site, Aiken, SC, Rev. 5, October 15, 2002.

W700283_OUO, *Building 241-14F Additional Waste Storage Tanks Excavation Plan*, Savannah River Site, Aiken, SC, Rev. 33, July 21, 1978.

W700321, *Additional Waste Storage Tanks Primary Liner Plans & Details*, Savannah River Site, Aiken, SC, Rev. 64, July 18, 1979.

W700324_OUO, *Additional Waste Storage Tanks General Arrangement,* Savannah River Site, Aiken, SC, Rev. 16, March 22, 1988.

W700325, *Additional Waste Storage Tanks Liner Plate and Attachments*, Savannah River Site, Aiken, SC, Rev. 94, May 27, 1977.

W700339, *Additional Waste Storage Tanks Cooling Slots Plan & Details*, Savannah River Site, Aiken, SC, Rev. 32, March 14, 1977.

W700598, *Building 241-F Additional Waste Storage Tanks Excavation Plan FY77*, Savannah River Site, Aiken, SC, Rev. 17, July 21, 1978.

W700839, *Waste Storage Facilities, FY75 PP2 & 3, and FDB4 Process Arrangement, Sheet 2*, Savannah River Site, Aiken, SC, Rev. 41, February 17, 1987.

W701330, *Additional Waste Storage Tanks Grading Plan*, Savannah River Site, Aiken, SC, Rev. 62, December 4, 1995.

W701347, *Waste Storage Facilities FY75 P.P. s & 3 & FDB4 Process Piping Arrangement*, Savannah River Site, Aiken, SC, Rev. 63, February 16, 1987.

W701904, *Additional Waste Storage Tanks Plans & Details, Liner Pump Pits & DB4*, Savannah River Site, Aiken, SC, Rev. 109, December 27, 1977.

W702275, *Waste Storage Facilities, TY76 FDB6 Equipment Arrangement, Sheet 1*, Savannah River Site, Aiken, SC, Rev. 47, August 3, 1979.

W702452, *Waste Storage Facilities FDB5 Equipment Arrangement*, Savannah River Site, Aiken, SC, Rev. 57, August 1996.

W702756, *Waste Storage Facilities, Underground Thermocouples*, Savannah River Site, Aiken, SC, Rev. 32, April 21, 1997.

W702976, *Waste Management Improvements Modified Leak Detection Box, Process & Instrumentation, Building 241-F-H*, Savannah River Site, Aiken, SC, Rev. 52, December 21, 1998.

W703133, *Additional Waste Storage, Tanks Base Slab Reinforcing,* Savannah River Site, Aiken, SC, Rev. 7, March 1978.

W703786, *Tanks 44 thru 47, Additional Waste Storage Tanks Leak Detection System*, Savannah River Site, Aiken, SC, Rev. 6, February 1978.

W703793, *Superior Evaporator in Bldg. 242-F, Piping & Arrangement, Plan & Sections*, Savannah River Site, Aiken, SC, Rev. 0, March 21, 1977.

W704824, *Additional Waste Storage Tanks Grading & Drainage Plan*, Savannah River Site, Aiken, SC, Rev. 51, June 2, 1987.

W704922, *Additional Waste Storage Tanks Top Slab Reinforcement*, Savannah River Site, Aiken, SC, Rev. 6, March 23, 1978.

W705828, *Waste Storage Facility, FY77 Cooling Coil Leads in Slab Tank 47 Process*, Savannah River Site, Aiken, SC, Rev. 1, April 1980.

W715343, *Waste Storage Facilities Leak Detection*, Savannah River Site, Aiken, SC, Rev. 10, September 12, 1980.

W717008_OUO, *Tank #17, 18, & 19 Waste Removal Facilities Transfer Line*, Savannah River Site, Aiken, SC, Rev. 48, April 2, 1993.

W819641, *W238 F-Area Salt Removal Type III, Phase 1 Three Valve, Valve Box*, Savannah River Site, Aiken, SC, Rev. 9, March 1988.

WSRC 1-01, MP 4.2, *Manual WSRC 1-01, Management Policies, Section 4.2, Quality Assurance*, Savannah River Site, Aiken, SC, Rev. 4, January 13, 2005.

WSRC E7 Manual, 2.31, *Conduct of Engineering Manual, Engineering Calculations*, Savannah River Site, Aiken, SC, Rev. 10, September 27, 2007.

WSRC E7 Manual, 2.60, *Conduct of Engineering Manual, Technical Reviews*, Savannah River Site, Aiken, SC, Rev. 11, September 27, 2007.

WSRC-IM-2004-00008, *DSA Support Document - Site Characteristics and Program Description*, Savannah River Site, Aiken, SC, Rev. 1, June 2007.

WSRC-MS-92-513, Cook, J., *Selection and Cultivation of Final Vegetative Cover for Closed Waste Sites at the Savannah River Site, SC*, Savannah River National Laboratory, Aiken, SC, Rev. 0, August 23, 2005.

WSRC-MS-95-0524, Hiergesell, R., A., *Regional Water Table Map of the Savannah River Site, 1Q-95,* Savannah River National Laboratory, Aiken, SC, Rev. 0, 1995.

WSRC-OS-94-42, *Federal Facility Agreement for the Savannah River Site,* http://www.srs.gov/general/programs/soil/ffa/ffa.pdf, Savannah River Site, Aiken, SC.

WSRC-RP-2001-00410, Swingle, R. F., et al., *Data Report: Tank 19 F NE Riser Zeolite Mound Sample Analysis*, Savannah River Site, Aiken, SC, Rev. 0, April 17, 2001.

WSRC-RP-2005-01674, Kaplan, D., et al., *Estimated Duration of the Reduction Capacity within a High-Level Waste Tank*, Savannah River National Laboratory, Aiken, SC, Rev. 0, August 3, 2005.

WSRC-RP-2005-01675, Langton, C. A., *HLW Tank Intruder Deterrent Grout*, Savannah River National Laboratory, Aiken, SC, Rev. 0, April 26, 2005.

WSRC-RP-2005-01684, Langton, C. A., *Grout Placement Requirements for SRS Class C Tank Residual Waste Forms*, Savannah River National Laboratory, Aiken, SC, Rev. 0, April 5, 2005.

WSRC-RP-2007-01122, Kaplan, D., et al., *Concrete Kd Values Appropriate for the Tank Closure Performance Assessment*, Savannah River National Laboratory, Aiken, SC, Rev. 0, October 11, 2007.

WSRC-RP-91-17, Hamby, D. M., *Land and Water-Use Characteristics in the Vicinity of the Savannah River Site*, Savannah River Site, Aiken, SC, Rev. 0, March 1991.

WSRC-RP-92-1360, Garrett, T. C., *Radiological Performance Assessment for the Z-Area Saltstone Disposal Facility*, Savannah River Site, Aiken, SC, Rev. 0, October 14, 1998.

WSRC-RP-92-225, *Quality Assurance Management Plan*, Savannah River Site, Aiken, SC, Rev. 18, August 30, 2007.

WSRC-RP-92-450, Strom, R., *SRP Baseline Hydrogeologic Investigation: Aquifer Characterization, Groundwater Geochemistry of the Savannah River Site and Vicinity*, Savannah River Site, Aiken, SC, Rev. 0, March 1992.

WSRC-RP-93-1174, Hamby, D. M., *IRRIDOSE: An Electronic Spreadsheet Designed to Calculate Ingestion Dose Resulting from Irrigating with Savannah River Water*, Savannah River Site, Aiken, SC, Rev. 0, October 1, 1993.

WSRC-RP-94-0218, Cook, J. R., et al, *Radiological Performance Assessment for the E-Area Vaults Disposal Facility*, Savannah River Site, Aiken, SC, Rev. 1, March 29, 2000.

WSRC-SQP-A-00028, Collard, L., *Software Quality Assurance Plan for the PORFLOW Code*, Savannah River National Laboratory, Aiken, SC, Rev. 0, September 30, 2002.

WSRC-STI-2006-00123, Jannik, G. T., et al., *LADTAP-PA: A Spreadsheet for Estimating Dose Resulting from E-Area Groundwater Contamination at the Savannah River Site*, Savannah River National Laboratory, Aiken, SC, Rev. 0, August 2006.

WSRC-STI-2006-00159, Crapse, K., et al., *Atmospheric Pathway Screening Analysis for the E-Area Low-Level Waste Facility*, Savannah River National Laboratory, Aiken, SC, Rev. 0, September 5, 2006.

WSRC-STI-2006-00198, Phifer, M., et al., *Hydraulic Property Data Package for the E-Area and Z-Area Soils, Cementitious Materials, and Waste Zones*, Savannah River National Laboratory, Aiken, SC, Rev. 0, September 2006.

WSRC-STI-2007-00004, Lee, P. L., et al., *Baseline Parameter Update for Human Health Input and Transfer Factors for Radiological Performance Assessments at the Savannah River Site*, Savannah River Site, Aiken, SC, Rev. 4, June 2008.

WSRC-STI-2007-00061, Subramanian, K., *Life Estimation of High Level Waste Tank Steel for T-Tank Farm Closure Performance Assessment*, Savannah River National Laboratory, Aiken, SC, Rev. 2, June 2008.

WSRC-STI-2007-00184_OUO, Phifer, M., *FTF Closure Cap Concept and Infiltration Estimates,* Savannah River National Laboratory, Aiken, SC, Rev. 2, October 15, 2007.

WSRC-STI-2007-00192, Hay, M., et al., *Characterization and Actual Waste Test with Tank 5F Samples*, Savannah River National Laboratory, Aiken, SC, Rev. 1, August 2007.

WSRC-STI-2007-00343, Farfan, E., *Air Pathway Dose Modeling for the F-Area Tank Farm*, Savannah River National Laboratory, Aiken, SC, Rev. 0, August 6, 2007.

WSRC-STI-2007-00355_OUO, Dixon, K., et al., *Air and Radon Pathway Modeling for the F-Area Tank Farm*, Savannah River National Laboratory, Aiken, SC, Rev. 0, September 2007.

WSRC-STI-2007-00369, Dixon, K., et al., *Hydraulic and Physical Properties of Tank Grouts and Base Mat Surrogate Concrete for FTF Closure*, Savannah River National Laboratory, Aiken, SC, Rev. 0, October 2007.

WSRC-STI-2007-00460, Subramanian, K., *Life Estimation of Transfer Lines for Tank Farm Closure Performance Assessment,* Savannah River National Laboratory, Aiken, SC, Rev. 0, October 2007.

WSRC-STI-2007-00544, Denham, M. E., *Conceptual Model of Waste Release from the Contaminated Zone of Closed Radioactive Waste Tanks,* Savannah River National Laboratory Aiken, SC, Rev. 0, November 2007.

WSRC-STI-2007-00607, Langton, C. A., *Chemical Degradation Assessment of Cementitious Materials for the HLW Tank Closure Project*, Savannah River National Laboratory, Aiken, SC, Rev. 0, September 14, 2007.

WSRC-STI-2007-00641, Langton, C. A., et al., *Grout Formulations and Properties for the F-Tank Farm Closure Project,* Savannah River National Laboratory, Aiken, SC, Rev. 0, November 12, 2007.

WSRC-STI-2007-00684, Kaplan, D. I., *Suggested Sorption Parameters for Uranium onto the Walls of High-Level Waste Tanks*, Savannah River National Laboratory, Aiken, SC, Rev. 0, December 2006.

WSRC-TR-2000-00454_OUO, Wyatt, D. E., *Natural Phenomena Hazards (NPH) Design Criteria and Other Characterization Information for the Mixed Oxide (MOX) Fuel Fabrication Facility at Savannah River Site,* Savannah River Site, Aiken, SC, Rev. 0, November 2000.

WSRC-TR-2002-00052, Thomas, J., *Characterization of Tank 19 Residual Waste,* Savannah River Site, Aiken, SC, Rev. 3, August 17, 2005.

WSRC-TR-2002-00107, Swingle, R., *Characterization of the Tank 19F Closure Grab and Core Samples and the Tank 18F Dip Sample*, Savannah River National Laboratory, Aiken, SC, Rev. 0, March 6, 2002.

WSRC-TR-2002-00327, Fox, L., *CSTF Corrosion Control Program*, Savannah River Site, Aiken, SC, Rev. 3, November 22, 2004.

WSRC-TR-2002-00445, Weber, A. H., *Summary of Data and Steps for Processing the 1997-2001 SRS Meteorological Database*, Savannah River Site, Aiken, SC, Rev. 0, November 2002.

WSRC-TR-2003-00048, Ledbetter, L. A., *Waste Characterization System Program Description Document*, Savannah River Site, Aiken, SC, Rev. 2, June 22, 2004.

WSRC-TR-2003-00250, Hiergesell, R. A., et al., *An Updated Regional Water Table of the Savannah River Site and Related Coverages*, Savannah River Site, Aiken, SC, Rev. 0, December 2003.

WSRC-TR-2003-00436, Phifer, M., et al., *Saltstone Disposal Facility Closure Cap Configuration and Degradation Base Case: Institutional Control to Pine Forest Scenario*, Savannah River National Laboratory, Aiken, SC, Rev. 0, September 22, 2003.

WSRC-TR-2004-00106, Flach, G., *Groundwater Flow Model of the General Separations Area Using PorFlow*, Savannah River National Laboratory, Aiken, SC, Rev. 0, July 14, 2004.

WSRC-TR-2004-00152, *Savannah River Site Groundwater Protection Program*, Savannah River Site, Aiken, SC, Rev. 0, March 2004.

WSRC-TR-2005-00131, Hiergesell, R. A., *Saltstone Disposal Facility: Determination of the Probable Maximum Water Table Elevation*, Savannah River National Laboratory, Aiken, SC, Rev. 0, April 2005.

WSRC-TR-2005-00201, Wike, L. D., et al., *SRS Ecology: Environmental Information Document*, Savannah River Ecology Laboratory, Aiken, SC, Rev. 0, March 2006.

WSRC-TR-2006-00004, Kaplan, D., *Geochemical Data Package for Performance Assessment Calculations Related to Savannah River Site*, Savannah River Site, Aiken, SC, Rev. 0, February 2006.

WSRC-TR-2007-00008, *Savannah River Site Environmental Report for 2006*, Savannah River Site, Aiken, SC, Rev. 0, September 2007.

WSRC-TR-2007-00094, Waltz, R., et al., *Annual Radioactive Waste Tank Inspection Program – 2006,* Savannah River Site, Aiken, SC, Rev. 0, June 19, 2007.

WSRC-TR-2007-00118, Kabela, E., et al., *Savannah River Site Annual Meteorology Report for 2006*, Savannah River National Laboratory, Aiken, SC, Rev. 0, April 20, 2007.

WSRC-TR-2007-00283, Millings, et al., *Hydrogeologic Data Summary in Support of the F-Area Tank Farm (FTF) Performance Assessment*, Savannah River Site, Aiken, SC, Rev. 0, July 2007.

WSRC-TR-93-304, Hamby, D. M., *Soil Concentration Guidelines for the Savannah River Site Using the DOE/RESRAD Methodology*, Savannah River Site, Aiken, SC, Rev. 0, June 1993.

WSRC-TR-95-0046, Denham, M., *SRS Geology & Hydrogeology*, Savannah River National Laboratory, Aiken, SC, Rev. 0, June 1999.

WSRC-TR-96-0231, Friday, G., *Radiological Bioconcentration Factors for Aquatic, Terrestrial, and Wetland Ecosystems at the Savannah River Site*, Savannah River National Laboratory, Aiken, SC, Rev. 0, December 1996.

WSRC-TR-96-0267, d'Entremont, P., et al., *Characterization of Tank 20 Residual Waste,* Savannah River Site, Aiken, SC, Rev. 0, March 17, 1997.

WSRC-TR-96-0399-Vol. 1, Flach, G., et al., *Integrated Hydrogeological Modeling of the General Separations Area, Vol. 1*, Savannah River National Laboratory, Savannah River Site, Aiken, SC, Rev. 0, August 1997.

WSRC-TR-96-0399-Vol. 2, Flach, G., et al., *Integrated Hydrogeological Modeling of the General Separations Area, Vol. 2*, Savannah River National Laboratory, Savannah River Site, Aiken, SC, Rev. 1, April 1999.

WSRC-TR-97-0066, d'Entremont, P. et al., *Characterization of Tank 17 Residual Waste,* Savannah River Site, Aiken, SC, Rev. 1, September 22, 1997.

WSRC-TR-97-0102, Caldwell, T., Tank *Closure Reducing Grout*, Savannah River Site, Aiken, SC, Rev. 0, April 18, 1997.

WSRC-TR-97-0171, Mamatey, A., et al., *Savannah River Site Environmental Report for 1996*, Savannah River Site, Aiken, SC, Rev. 0, 1981.

WSRC-TR-98-0045, Hiergesell, R., *The Regional Water Table of the Savannah River Site and Related Coverages*, Savannah River National Laboratory, Aiken, SC, Rev. 0, October 26, 1998.

WSRC-TR-98-271, Langton, C. A., *Laboratory and Field Testing of High Performance-Zero Bleed CLSM Mixes for Future Tank Closure Applications*, Savannah River Site, Aiken, SC, Rev. 0, March 1998.

WSRC-TR-99-00369, Chen, K. F., *Flood Hazard Recurrence Frequencies for C-, F-, E-,S-, H-, Y-, and Z-Areas*, Westinghouse Savannah River Company, Aiken, SC, Rev. 0, September 1999.

X-CLC-F-00440, Wiersma, B., *Estimate of the Corrosion Product on the Walls of Tank 18*, Calculation, Savannah River National Laboratory, Aiken, SC, Rev. 1, December 13, 2007.

11.0 GLOSSARY

A

Absorption — Entering of particles of one phase into a different bulk phase by penetrating a surface.

Accuracy — Closeness of the result of a measurement to the true value of the quantity.

Actinide — Group of elements of atomic number 89 through 103. Laboratory analysis of actinides by alpha spectrometry generally refers to the elements plutonium, americium, uranium, and curium but may also include neptunium and thorium.

Adsorbtion — The enrichment or agglomeration of particles on a surface or interface.

Air Content — Amount of air incorporated into the grout as the result of mixing and placement.

Air Pathway — Exposure pathway to radioactive material dispersed in the air in the form of dusts, fumes, particulates, mists, vapors, or gases.

ALARA — As Low As Reasonably Achievable - making every reasonable effort to maintain exposures to radiation as far below the dose limits as is practical consistent with the purpose for which the licensed activity is undertaken, taking into account the state of technology, the economics of improvements in relation to state of technology, the economics of improvements in relation to benefits to the public health and safety, and other societal and socioeconomic considerations.

Amorphous — Latin meaning without form. Non-crystalline structure.

Ancillary Equipment — Ancillary equipment associated with the waste storage tanks, such equipment as transfer line piping, pump tanks, evaporators, that are used to distribute or control the transfer of waste, from one storage point to another storage point.

Annulus The annulus also referred to as the secondary containment of a waste tank. The secondary containment surrounds the primary tank shell of Types I, II, III, and IIIA waste tanks, providing a location for collection of any leakage from the primary tank shell.

Aquifer Saturated, permeable geologic unit that can transmit significant quantities of water under ordinary hydraulic gradients.

Aquitard Geologic unit that inhibits the flow of water.

Argillaceous Containing, made of, or resembling clay; clayey.

Atomic Energy Commission Federal agency created in 1946 to manage the development, use, and control of nuclear energy for military and civilian application. It was abolished by the Energy Reorganization Act of 1974 and succeeded by the Energy Research and Development Administration. Functions of the Energy Research and Development Administration eventually were taken over by the U.S. Department of Energy and the U.S. Nuclear Regulatory Commission.

Axisymmetric Having symmetry around an axis.

B

Background Radiation Naturally occurring radiation, fallout, and cosmic radiation. Generally, the lowest level of radiation obtainable within the scope of an analytical measurement, i.e., a blank sample.

Base Case Tank Configuration A, scenario in which the closure cap is assumed in place and no fast flow path exists from outside the waste tank system, through the tank, and exiting the system. It was assumed that the concrete that makes up the walls, the tank grout, and basemat concrete degrades over time (with these changes simulated by increasing hydraulic conductivity).

Basemat Concrete pad upon which the waste tank is constructed. The pad has close tolerances for leveling of tank and the concrete is quality controlled to ensure the structural integrity to tank foundation. The basemat is also referred to as floor slab or foundation.

Bioaccumulation Factor Calculations that define parameters used to calculate contaminant concentrations via a variety of environmental mechanisms.

Biotic Transport (Pathway) Amounts and rates of radionuclides transported by living components (i.e., animals, plants or bacterial life) of an ecosystem.

Blackwater Stream Waterways that contain high concentrations of naturally occurring tannic acid that gives the water a tea color.

Bleed Water Water that separates from the grout as the result of solids settling.

C

Carbonation The reaction of CO_2 gas with the hydrated phases of the Portland cement in the grout blocking the pores in the grout.

Cementitious Like or relevant to or having the properties of cement.

Central Savannah River Area (CSRA) Eighteen-county area in Georgia and South Carolina surrounding Augusta, Georgia. The Savannah River Site is included in the Central Savannah River Area. Counties are Richmond, Columbia, McDuffie, Burke, Emanuel, Glascock, Jenkins, Jefferson, Lincoln, Screven, Taliaferro, Warren, and Wilkes in Georgia and Aiken, Edgefield, Allendale, Barnwell, and McCormick in South Carolina.

CERCLA Comprehensive Environmental Response, Compensation, and Liability Act (CERCLA), commonly known as Superfund, was enacted by Congress on December 11, 1980. This law provides to clean up uncontrolled or abandoned hazardous-waste sites as well as accidents, spills, and other emergency releases of pollutants and contaminants into the environment. Through the Act, EPA was given power to seek out those parties responsible for any release and assure their cooperation in the cleanup.

Chromated Cooling Water Coolant comprised of choromate-inhibited water that circulates through the cooling coils of waste tanks to remove radioactive decay heat and other sources of heat (i.e., steam heat loads, ventilation heat loads, or mechanical heat loads from pumping/mixing operations).

Citizens Advisory Board (CAB)	The Savannah River Site Citizens Advisory Board is composed of 25 individuals from South Carolina and Georgia. The board members are chosen to reflect the cultural diversity of the population affected by SRS. The Board provides advice and recommendations to the U.S. Department of Energy (DOE) on environmental remediation, waste management and related issues. All meetings are open to the public and public participation is encouraged. Public comment periods are offered at various times throughout the meetings.
Clean Water Act	The Clean Water Act is the cornerstone of surface water quality protection in the United States. (The Act does not deal directly with groundwater nor with water quantity issues.) The law employs a variety of regulatory and non-regulatory tools to sharply reduce direct pollutant discharges into waterways, finance municipal wastewater treatment facilities, and manage polluted runoff.
Closure Plan	Plan that presents the environmental regulatory standards and guidelines pertinent to the closure of the tanks and describes that process for evaluating and selecting the closure configuration (i.e., residual inventory and form.)
Compressive Strength	Force per unit area required to break an unconfined grout or concrete sample.
Concentration	Amount (e.g., in grams or moles) per volume of a substance.
Conductivity Probes	The conductivity probe is a simple electrical device that works on the principle that liquids conduct electricity more readily than air. If a liquid comes in contact with the probe it will complete an electrical circuit and send a signal for indication or alarm purposes of a waste leak in ancillary equipment.
Cone Penetration Test	The cone penetration test (CPT) is an in-situ testing method used to determine the geotechnical engineering properties of soils and delineating soil stratigraphy. The CPT is one of the most used and accepted in-situ test methods for soil investigation. The test method consists of pushing an instrumented cone, tip first, into the ground at a controlled rate.
Consumption Rates	Physical human health exposure parameters used for evaluating pathway-specific dose.

Controlled Low Strength Material — CLSM (Controlled Low Strength Material) is a cementitious flowable fill that is used as backfill or infill and has soil-like properties. It is self compacting and consequently does not required mechanical compaction to achieve design density. CLSM typically contains sand, fly ash and less than 100 pounds of hydraulic material per cubic yard of fill.

Cooling coils — Cooling coils are installed in the tanks to remove the decay heat that is generated by the waste in the tanks. Arrangements and designs of cooling coils differ, depending on the type of tank. Type I and II tanks, in addition to having vertical cooling coils, also have cooling coils across the bottom of the tank to provide a means for cooling the bottom of the tank.

Co-Precipitation — Co-precipitation as defined here is the incorporation of an element into the crystal structure of a solid phase that is predominantly made of other elements or the trapping of an element within the bulk mass of a phase made up of other elements, but not necessarily within the crystal lattice.

Core pipe — Internal pipe of transfer line that comes into contact with the waste materials. The core pipe is usually located within a jacket pipe.

Cretaceous — The geological time period between 140 and 65 million years ago.

Curie — A unit of radioactivity; the quantity of nuclear material that has 3.7E+10 disintegrations per second.

D

Darcy Velocity — Formula for measuring velocity and flow of groundwater.

De-Passivation — Deterioration of steel that has been covered with a passivating product (ex., concrete) as a result of the introduction of too much chloride.

Desorption — The opposite process to adsorption meaning the removal of aggregated particles from a surface.

Deterministic — When fixed parameters are used in calculations versus a distribution of values (probabilistic).

Diffusion	Movement of contaminants from an area of higher concentration to an area of lower concentration.
Diffusion Coefficient	The rate of diffusion of particles, depending on the particle size, viscosity and temperature.
Dip Tubes	Dip Tubes are used to provide an estimate of the rate of leakage into the annulus and to serve as a backup for the conductivity probes. Dip tubes operate by relying on the hydrostatic pressure (height) of the liquid column to cause a backpressure on the dip tube.
Dispersivity	Equal to the dispersion coefficient divided by the velocity.
Distribution Coefficient (K_d)	The quantity of a solute sorbed by a solid, per unit weight of solid, divided by the quantity of the solute dissolved in the water per unit volume of water.
Diversion Box	Diversion box is a shielded reinforced concrete structure containing transfer line nozzles to which jumpers are connected in order to direct waste transfers to the desired location.
Dolomitic	A magnesia-rich sedimentary rock resembling limestone.
Dose Conversion Factor	A factor used to convert radionuclide concentrations in environmental media to doses. Factors are used for inhalation, ingestion, immersion and external exposure.
Dose Limits	The permissible upper bounds of radiation doses.

E

Effective Diffusion Coefficient (D_e)	The diffusion coefficient of a species through a saturated porous medium taken over the pore area of the medium through which diffusion occurs under steady-state conditions.
Effective Dose Equivalent	The sum of the products of the dose equivalent to the organ or tissue (H_T) and the weighting factors (W_T) applicable to each of the body organs or tissues that are irradiated ($H_E = \Sigma W_T H_T$).
E_h	The symbol for redox potential in millivolts.

Erosion Barrier	The layer within a multi-part closure cap made of rock (riprap) and filler materials designed to prevent riprap movement during a Probable Maximum Precipitation event and therefore forms a barrier to further erosion and gully formation (i.e., provide closure cap physical stability). It will be used to maintain a minimum 10 ft of clean material above the tanks and significant ancillary equipment to act as an intruder deterrent. It will also act to preclude burrowing animals from access to underlying closure cap layers. It also provides minimal water storage for the promotion of evapotranspiration.
Escarpment	A steep slope or long cliff caused by erosion or faulting separating two level areas of differing heights.
Ettringite	Ettringite is hexacalcium aluminate trisulfate hydrate. Ettrigite is found in hydrated Portland cement system as a result of the reaction of calcium aluminate with calcium sulfate, both present in Portland cement.
Evaporator	Steam-heated, water-cooled system installed in the tank farms to concentrate underground waste storage tank contents, in order to reduce the liquid waste volume.
Evapotranspiration	Evapotranspiration (ET) is a term used to describe the sum of evaporation and plant transpiration from the earth's land surface to atmosphere. Evaporation accounts for the movement of water to the air from sources such as the soil, canopy interception, and waterbodies.
Exposure	Being exposed to ionizing radiation or to radioactive material.
Exposure Pathway	The means by which humans are exposed to contaminants. The key exposure pathways are air and water, with most exposures via drinking water, crops, other foods, inhalation and direct radiation.
External Dose	That portion of the dose equivalent received from radiation sources outside the body.

F

Federal Facility Agreement (FFA)

Agreement between EPA, DOE and SCDHEC that directs the comprehensive remediation of the Savannah River Site (SRS). It contains requirements for (1) site investigation and remediation of releases and potential releases of hazardous substances, and (2) interim status corrective action for releases of hazardous wastes or hazardous constituents.

Fick's Second Law of Diffusion

Movement of contaminants from an area of higher concentration to an area of lower concentrations, where the concentrations are changing over time.

Flow

Ability of the grout to spread evenly without vibration (self-level).

Flux

The time rate of change or concentration. For example, curies per year leaving the CZ.

Fly Ash

Fly ash is a mineral admixture used in grout to enhance finishing characteristics, make the mix more economical, and to improve pumping. It is finer in consistency than cement, and its particles are round. These fine particles make the mix finish easier, and pump easier.

G

General Separations Area

Centralized area of SRS including, E, F, H, S and Z Areas that are the heavily industrialized areas of SRS.

Geosynthetic Clay Liner

A woven fabric-like material primarily used for the lining of landfills. It is a kind of geomembrane and geosynthetic which incorporates a bentonite or other clay, which has a very low hydraulic conductivity.

GoldSim

A simulation software program designed to dynamically model the release and transport of radioactive constituents. The fundamental output consists of predicted mass fluxes at specified locations within a system, and predicted concentrations within environmental media (e.g., groundwater, soil, air).

Goethite — Red or yellow or brown mineral; an oxide of iron that is a common constituent of rust found in soil and other low temperature environments.

Gradient Boosting Model — Modeling approach that utilizes binary recursive partitioning algorithms that deconstruct a response into the relative influence from a given set of explanatory variables (stochastic model input parameters).

Grahams Law — Grahams Law states that the rate of diffusion of a gas is inversely proportional to the square root of its molecular weight.

Groundwater Flow — The rate of groundwater movement through the subsurface.

Grout — A cement mixture, sufficiently fluid, which can be pumped into equipment cavities creating a watertight bond, and increasing the strength of the existing structural foundation. Capable of slowing the vertical movement or migration of water.

H

Hematite — A widely distributed mineral which is an important iron ore, occurring in crystalline, massive, or granular form, and reddish-brown when powdered.

Herpetofauna — Term used that refers to reptiles and amphibians, collectively.

Homogenous — Similar or uniform structure or composition throughout.

Hydraulic Conductivity — Velocity of water flow through saturated materials (e.g., concrete, grout, soil)

Hydrostratigraphy — A geologic framework consisting of a body of rock having considerable lateral extent and composing a reasonably distinct hydrologic system.

I

Igneous Rock — An aggregate of interlocking silicate minerals formed by cooling and solidification of magma or lava. Igneous rocks are formed by volcanic processes.

Indurated — Hard or thickened.

Institutional Control — A 100-year period in which DOE retains ownership and control of FTF such that FTF facility maintenance and controls will be performed to prevent inadvertent intrusion and protect public health and the environment.

Interfluvial — The region of higher land between two rivers that are in the same drainage system.

Internal Dose — That portion of the dose equivalent received from radioactive material taken into the body.

J

Jurassic — The geological period between 210 and 140 million years ago.

K

Kelco-Crete — A special viscosity modifying admixture. Kelco-Crete is included in the mix design to enhance physical stability of the grout (minimizing segregation) and achieve a robust mix.

L

Lacustrine Sediments — A type of deposit that comes from lakes which previously occupied the area. They are fine-grained soils that have settled through the water and accumulated on the lake bottom, typically leaving them in a soft condition.

Latin Hypercube Sampling — A form of sampling that can be applied to multiple variables. The method is commonly used to reduce the number or runs necessary for a Monte Carlo simulation to achieve a reasonably accurate random distribution.

Leachate — Leachate is the liquid that drains or 'leaches' from a closure system. It can contain both dissolved and suspended material.

Leaching — Leaching occurs when infiltrating water seeps into the closure system and transports contaminants out of the system.

Leak Detection Boxes — Leak detection boxes provide for the collection and detection of leakage from the transfer lines.

Line Encasement (Sealed Concrete Trench) — Enclosed core pipes in a covered reinforced concrete encasement below ground. Any core pipe leakage into the encasement and in-leakage of groundwater into the encasement will gravity drain to catch tank.

Lithified Terrigenous Sediment — Sediments derived from the erosion of rocks on land.

Lithology — The description of rocks, especially in hand specimen and in outcrop, on the basis of such characteristics as color, mineralogic composition, and grain size.

M

Macroinvertebrate — Any nonvertebrate organism that is large enough to be seen without the aid of a microscope.

Maximally Exposed Individual (MEI)	A hypothetical individual who, because of proximity, activities, or living habits, could potentially receive the maximum possible dose of radiation or of a hazardous chemical from a given event or process.
Maximum Contaminant Level (MCL)	The highest level of a contaminant that is allowed in drinking water, below which there is no known or expected risk to health. MCLs are EPA enforceable standards.
Mesozoic	An area of geologic time, from the end of the Paleozoic to the beginning of the Cenozoic, or from about 225 million years to about 65 million years ago.
Metamorphosed Sedimentary Rock	Rock that is formed by the consolidation of sediment particles or of the remains of plants and animals.
Miocene-age	Middle of Tertiary Period, dating back 13-25 million years.
Molar	Relating to a solution that contains X moles of solute per liter of solution, where X is a number.
Monte Carlo Analysis	An analytical technique in which a large numbers of simulations are run using random quantities for uncertain variables and looking at the distribution of results to infer which values are most likely.

N

National Pollutant Discharge Elimination System	As authorized by the Clean Water Act, the National Pollutant Discharge Elimination System (NPDES) permit program controls water pollution by regulating point sources that discharge pollutants into waters of the United States. Point sources are discrete conveyances such as pipes or man-made ditches.

NDAA Section 3116

The Ronald W. Reagan National Defense Authorization Act for Fiscal Year 2005 Section 3116 was passed by Congress on October 9, 2004 and signed by the President on October 28, 2004. Section 3116 of the NDAA specifies that the term "high-level radioactive waste" does not include radioactive waste that results from reprocessing spent nuclear fuel if the Secretary of Energy determines, in consultation with the NRC, that the waste meets certain criteria.

O

Occupational Dose

The dose received by an individual in the course of employment in which the individual's assigned duties involve exposure to radiation or to radioactive material. Occupational dose does not include doses received from background radiation or from any medical administration the individual has received.

Operable Unit

Operable Unit is discrete action that comprises an incremental step toward comprehensively addressing site CERCLA problems. This discrete portion of a remedial response manages migration, or eliminates or mitigates a release, threat of release, or pathway of exposure. The remediation of a site is divided into a number of operable units, depending on the complexity of the problems associated with the site. Operable units will not impede implementation of subsequent actions, including final action at the site. FTF is a part of the GSA Western Groundwater Operable Unit.

Operational Period

Period of time during which tanks are in operation, waste is removed from the waste tanks and ancillary equipment, the systems are grouted, and a closure cap is installed in accordance with FFA requirements.

Outcrop

Also referred to as seepline, it is the location where groundwater from the upper aquifers is discharged to the surface.

Oxalic Acid

Oxalic acid is a relatively strong organic acid, being about 10,000 times stronger than acetic acid.

Oxidation Potential

The measure of a material to oxidize or lose electrons.

Oxidized Combined with or having undergone a chemical reaction with oxygen.

P

Paleozoic The geological period between 600 to 230 million years ago.

Par Pond A lake constructed at Savannah River Site in 1958 to provide cooling water for P-Reactor and R-Reactor.

Perennial Stream A perennial stream has flowing water year-round during a typical year. The water table is located above the stream bed for most of the year. Groundwater is the primary source of water for stream flow. Run-off from rainfall is a supplemental source of water for stream flow.

Permeability Capability of a material to let pass other molecules or particles.

pH A measure of the acidity or alkalinity of a solution, numerically equal to 7 for neutral solutions, increasing with increasing alkalinity and decreasing with increasing acidity.

Phosphatic Pertaining to, or containing, phosphorus, phosphoric acid, or phosphates; as, phosphatic nodules.

Pitting Localized corrosion of a metal surface, confined to a point or small area that takes the form of cavities.

Plume A body of contaminated groundwater eminating from a specific source.

Pore Hole in a material.

PORFLOW	A comprehensive Comprehensive Fluid Dynamics (CFD) simulation software program developed to accurately solve problems involving transient or steady state fluid flow, heat, salinity and mass transport in multi-phase, variably saturated, porous or fractured media with dynamic phase change. The porous/fractured media may be anisotropic and heterogeneous, arbitrary sources (ex., wells) may be present and, chemical reactions or radioactive decay may take place. It accommodates alternate fluid and property relations and complex and arbitrary boundary conditions.
Porosity	Grout porosity is generally defined as the percentage of total volume of cured grout that is not occupied by the starting cementitious materials and the products that result from reaction of these cementitious materials with water.
Potable Water	Water that is safe for human consumption.
Precambrian	An informal term to include all geologic time from the beginning of the Earth to the beginning of the Cambrian period 570 million years ago.
Preliminary Remediation Goal (PRG)	Health-based chemical concentration in an environmental media associated with a particular exposure scenario. PRGs may be developed based on exposure scenarios evaluated prior to or as a result of a baseline risk assessment.
Primary Tank	The primary tank, sometimes referred to as the "shell," is the component of the tank that actually contains the liquid waste. The primary tank is contained within the secondary containment, if any, and also houses the support equipment for the tank.
Principal Threat Source Material (PTSM)	When a distribution of values are used in calculations versus fixed parameters (deterministic).
Probabalistic	A model that assigns a likelihood to events or data within a population, as expressed by a ranked numerical value or an estimate of best case, worst case or most likely.
Probable Maximum Precipitation	Theoretically, the greatest depth of precipitation for a given duration that is physically possible over a given size storm area at a particular geographical location at a certain time of the year.
Progeny	Decay products or descendants of specific radionuclides.

Public Dose — The dose received by a member of the public from exposure to radiation. Public dose does not include occupational dose or doses received from background radiation or from any medical administration the individual has received.

Pump Pit — Pump Pits are shielded reinforced concrete structures located below grade at the low points of transfer lines, contain pump tanks and are usually lined with stainless steel.

Pump Tank — All pump pits house a pump tank with the pump pits providing secondary containment for pump tanks. The pump tanks have a nominal capacity of 8,000 gallons each. The pump tanks installed in FTF are all of the same basic size (8.5 feet tall, 12 feet in diameter).

R

RCRA — The Resource Conservation and Recovery Act (RCRA) is the public law that creates the framework for the proper management of hazardous and nonhazardous solid waste.

Redox — Redox (shorthand for oxidation/reduction reaction) describes all chemical reactions in which atoms have their oxidation number (oxidation state) changed.

Remedial Investigation Process — The mechanism for collecting data to characterize site conditions, determine the nature of the waste, or assess risk to human health and the environment as overseen by the EPA.

Residual Radioactivity — Radioactivity in structures, materials, soils, groundwater, and other media at a site remaining after closure.

Riemann or Lebesgue Measures — Statistical method of ingegration

Riser — The risers through the tank tops provide for access to the tank and annulus interiors. Risers are used primarily to provide for the installation of equipment such as pumps and cooling equipment, instrumentation such as level probes and leak detection, and ventilation, and to provide access to the tank interior for sampling, depth measurement, and inspection.

S

Saltcake — Saltcake located in waste tanks consists of crystallized salts with interstitial void space and entrained soluble solids (assumed to be partially sludge solids).

Saltstone — A process in which low-activity salt solution is mixed with dry chemicals (cement, slag, and fly ash) to form a homogeneous grout mixture.

Saturated zone — The saturated zone encompasses the area below ground in which all interconnected openings within the geologic medium are completely filled with water.

Screeded — Screeding is leveling and smoothing the top layer of a material that is poured, such as concrete, so the material is the same height as the forms, or guides, that surround it.

Secondary Containment — The secondary containment also referred to as annulus, of a waste tank. The secondary containment surrounds the primary tank shell of Types I, II, III, and IIIA waste tanks, providing a location for collection of any leakage from the primary tank shell.

Sector — A logical division or grouping.

Seepline — Also referred to as outcrop or far field, it is the location where groundwater from the upper aquifers is discharged to the surface.

Segregation — Separation of sand from binder as the result of impact, and separation of water from grout as the result of gravity settling of the solids from the grout slurry.

Set time — Time after mixing at which the grout responds as a solid.

Shotcrete — Shotcrete is a substance applied via pressure hoses. Shotcrete is usually concrete conveyed through a hose and pneumatically projected at high velocity onto a surface. Shotcrete undergoes placement and compaction at the same time due to the force with which it is projected from the nozzle. Shotcrete was used in the construction of Type IV tanks.

Shrinkage	Percent length change of grout samples cured at 73°F as a function of curing time in saturated and drying environments.
Silica fume	Silica fume, also known as microsilica, is a byproduct of the reduction of high-purity quartz with coke in electric arc furnaces in the production of silicon and ferrosilicon alloys. Silica fume is used as an addition in Portland cement concretes to improve properties. It has been found that silica fume improves compressive strength, bond strength, and abrasion resistance. Addition of silica fume also reduces the permeability of concrete to chloride ions, which protects concrete's reinforcing steel from corrosion.
Slag	Slag was introduced into the design mixes which in addition to its hydraulic activity, also provides chemical reducing power to the mix. Slag has been shown to possess chemically reducing properties that are favorable for technetium reduction and for plutonium and selenium.
Slug test	A slug test is a particular type of aquifer test where water is quickly added or removed from a groundwater well, and the change in hydraulic head is monitored through time, to determine the near-well aquifer characteristics. It is a method used by hydrogeologists to determine the transmissivity and storativity of the material the well is completed in.
Solubility	Mixture of at least two liquid components or of at least one solid and a liquid component.
Source Term	The amount and type of radioactive material released into the environment.
Spalling	Destruction of a surface by frost, heat, corrosion, or mechanical causes.
Stabilized Contaminant	Grouted waste remaining in the waste tanks or ancillary equipment after system closure.
Stated Mean Sea Level	The reference point used as a standard for determining terrestrial and atmospheric elevation or ocean depths and is calculated as the average of hourly tide levels measured by mechanical tide gauges over extended periods of time.
Stochastic	A probabilistic distribution of parameters.

Stoichiometry Calculation of the quantitative relationships between the amounts of reactants and products formed during a chemical reaction.

Supernate Liquid salt solution found above the sludge layer after settling of solids in waste tanks has occurred as a result of a liquid waste transfer to one of the waste processing facilities or receipt tanks.

T

Thermodynamic The science of heat and temperature and of the laws governing the conversion of heat into mechanical, electrical, or chemical energy.

TNX TNX Area Operable Unit consists of four major subunits: the New TNX Seepage Basin, the TNX Burying Ground, the Old TNX Seepage Basin, and the TNX Groundwater.

Tortuosity A geometrical parameter which intervenes in the description of the inertial effects between the fluid filled porous material and its structure at high frequency range.

Total Effective Dose Equivalent (TEDE) The sum of the deep-dose equivalent (for external exposures) and the committed EDE (for internal exposures).

Tracer An amount of material introduced into a system model in order to follow the behavior of some component of that system.

Triassic The period of geological time between 248 and 213 million years ago.

U

Udorthents Well drained soils that formed in heterogeneous materials, which are the spoil or refuse from excavations and major construction operations.

Underliner Sump An underliner sump collects any leakage through the concrete or stainless steel liners beneath waste tanks.

Unit Weight Weight of a unit volume, typically one cubic foot.

V

Vadose Zone The unsaturated zone located between the ground surface and the water table or saturated zone.

Van der Waals Force In physical chemistry, the name van der Waals force refers to the attractive or repulsive forces between molecules (or between parts of the same molecule) other than those due to covalent bonds or to the electrostatic interaction of ions with one another or with neutral molecules.

Valve Boxes Transfer valve boxes facilitate specific waste transfers that are conducted frequently. The valves are generally manual ball valves in removable jumpers with flush water connections on the transfer piping. The valve boxes provide containment of and access to the valves.

Vault Term used to describe the underground concrete floor, walls and roof that enclose the steel primary liner of the waste tank.

Viscosity Rheological quality of fluids describing the resistance to flow.

Volatilization The transport of a liquid substance by vaporization.

W

Waste Characterization System Computer based system designed to integrate historical information, current sample data, and physical properties of constituents to develop predictions of concentrations and inventory.

Waste Inventory Residual contaminants remaining in the radioactive waste tanks and associated ancillary equipment.

Working Slab

Concrete surface usually placed to create a level construction surface. This concrete is normally lower quality without reinforcement and is either broken up after or cracked during construction activities between the tanks, thus is not considered a barrier to vertical water migration.

Young's Modulus

Young's modulus (E) is a measure of the stiffness of a given material. It is also known as the modulus of elasticity, elastic modulus or tensile modulus. It is defined as the ratio, for small strains, of the rate of change of stress with strain.